UNIVERSITY OF CALIFORNIA

Santa Barbara

Herding is Risky Business: Agropastoral Strategies in Neolithic Northern Dalmatia

A dissertation submitted in partial satisfaction of the requirements for the degree Doctor of Philosophy in Anthropology

by

Nicholas Peter Triozzi

Committee in charge:

Professor Sarah B. McClure, Chair

Professor Douglas J. Kennett

Professor Amber M. VanDerwarker

Professor Gregory D. Wilson

December 2024

The dissertation of Nicholas Peter Triozzi is approved.

Douglas J. Kennett

Amber M. VanDerwarker

Gregory D. Wilson

Sarah B. McClure, Committee Chair

December 2024

Herding is Risky Business: Agropastoral Strategies in Neolithic Northern Dalmatia

by

Nicholas Peter Triozzi

DEDICATION

To my parents Peter and Nancy and to my grandma and favorite teacher Rosalie Triozzi.
Thank you for supporting me and encouraging me to see this through.

ACKNOWLEDGMENTS

First and foremost, I want to express my gratitude to my partner and soulmate, Lucija, who stood by me in the home stretch of this long and difficult journey. I am deeply grateful to my mother Nancy, sisters Kirstin and Kelsey, and brother Michael; you cheered me on, encouraged me, and kept me motivated to stay the course.

I am truly indebted to members of my committee, especially my advisor, mentor, and now colleague, Sarah McClure who, along with Douglas Kennett have provided invaluable academic, professional, and personal guidance. I can say with complete certainty that I would not be where I am today without the enduring support and unbridled empathy of these two individuals.

I am sincerely grateful to all who facilitated the collection, sampling, and processing of archaeological materials related to this work. I would like to highlight the contributions of Professor Kristina Horvat Oštrić of University of Zadar's Department of Archaeology. Professor Horvat Oštrić served as the faculty sponsor coordinating my institutional affiliation with the university during my Fulbright Fellowship, facilitated access to archaeological assemblages curated at the university and local museums, and invested her time, money, and energy into collaborating on excavations and publications. I am grateful to Emil Podrug of the Šibenik City Museum who assisted me with fieldwork at several hillfort sites near Šibenik and later introduced me to Prof. Horvat Oštrić, getting me established in the broader community of archaeologists focusing on prehistory in Dalmatia. Thank you to the Croatian students and professionals comprising the excavation teams, especially Mia Mandarić, Martin Keretić, Luka Bogdanić, Enzo Gabrijelić, Marijan Aničić, Marina Šimičić, Luka Rožek, Dominik Kelava, and Miroslav Klarić. Special thanks to Maja Grgurić Srzentić for assisting me with bone identification in the lab. Access to curated assemblages was made possible by Natalija Čondić (Zadar Archaeological Museum) and Marin Ćurković (Benkovac Local Heritage Museum). I would also like to acknowledge Doris Vidas and Kelly Reed of Oxford University for taking the lead on processing flotation samples and conducting archaeobotanical analysis.

My appreciation extends to those who helped me process samples, especially Kira Williams-Wates, Dr. Gina Buckley, and Dr. Claire Ebert. I also am profoundly grateful to Dr. Richard George for offering me his expertise in stable isotope analysis and radiocarbon dating in the lab and for allocating his time to review drafts of my work. Thank you to Amanda Strom for assisting me with FTIR analysis in the Material Research Lab at UCSB. Additionally, I want to thank the UC Santa Barbara Department of Archaeology, especially David Lawson for arranging financial support during the terminal phases of my degree.

Finally, I am grateful to the following sources of funding that made this research possible: the Doctoral Dissertation Research Improvement Grant from the National Science Foundation (NSF Grant No. 2131489); the Fulbright U.S. Scholar Program which is sponsored by the U.S. Department of State and the Croatian Ministry of Science and Education; Archaeological Specialty Dating Grant, Register of Professional Archaeologists; Leal Anne Kerry Mertes Grant, UC Santa Barbara Department of Geography; and the Archaeological Institute of America, Orange County Society.

VITAE OF NICHOLAS PETER TRIOZZI
DECEMBER 2024

EDUCATION

2024	Ph.D., Anthropology, University of California Santa Barbara, Department of Anthropology
2019	M.A., Anthropology, The Pennsylvania State University, Department of Anthropology
2017	Advanced Certificate, Geographic Information Science, City University of New York - Hunter College, Department of Geography
2014	M.A., Anthropology, *with distinction*, Monmouth University, Department of Anthropology
2011	B.S., Evolutionary Anthropology, Rutgers University, Department of Anthropology

ACADEMIC APPOINTMENTS

2021-2022	GIS Consultant/Research Assistant **Center for Restorative Environmental Work** Global Studies Dept., UCSB *Designed a series of StoryMaps using ArcGIS Online web application development platform; Created narrative and visual content focused on decommissioning of gas and oil infrastructure in California and the challenges of achieving environmental justice in Chile.*
2020	Research Assistant **Mediterranean Prehistory and Paleoecology Laboratory** Dept. of Anthropology, UCSB *Assisted with data collection and visualizations for Dalmatian Neolithic research. Created maps and models for paleoecology datasets; produced figures for publications; stable isotope analysis.*
2020	Database Architect **California Archaeological Repository** Dept. of Anthropology, UCSB *Developed a relational database to store information associated with archaeological materials curated by the Repository; Designed customized applications for data access and entry.*
2019	Technician / Research Assistant **Primate Functional Morphology Lab** Dept. of Anthropology, Penn State University *Analysis of CT scans of human hand bones recovered from Late Archaic period sites in Lowland Belize. Data processing was performed using Avizo software; 3D morphometric analyses completed using scripting procedures executed in R.*

2018	Technician / Research Assistant **Human Paleoecology and Isotope Geochemistry Lab** Dept. of Anthropology, Penn State University *Analysis of CT scans of shell beads from the Northern Channel Islands, CA. Processing tasks involved 3D manipulation of images and statistical analysis of data (Principal Components Analysis and Multivariate Statistical Analysis)*
2018	Research Assistant **GeoSyntheSES Lab** Dept. of Geography, Penn State University *Integrated human survey data and geospatial data to calculate distance between residences and family-owned cultivation plots in Huanuco, Peru. Developed scripts to generate a network analysis of various transportation options based on least cost paths in rugged terrain of the Central Andes Mountains.*
2018	GIS Consultant **Mesoamerican Economy and Archaeology Lab** Dept. of Anthropology, Penn State University *Digitization of paper maps of standing architecture associated with the Teotihuacan archaeological site. Work involved extensive georeferencing and feature creation towards the production of geodatabase using ArcGIS.*
2017-2018	Consultant / Research Assistant **Computational Anthropology Research Lab** Dept. of Anthropology, Penn State University *Reimagined and redesigned graduate student computer laboratory to better accommodate research needs; Customized machine hardware and software purchasing and installation; provided technical support to graduate researchers and department faculty.*
2017	Research Assistant **Matson Museum of Anthropology** Dept. of Anthropology, Penn State University *Develop and manage relational database to store accession records of a vast collection of archaeological and ethnographic materials. Organized and cataloged hominin cast teaching collections, mentored volunteer undergraduates in inventory and 3D scanning techniques.*

LABORATORY EXPERIENCE

2021	Stable Isotope Paleoecology Laboratory, Dept. of Anthropology, UC Santa Barbara (*Tooth enamel and bone collagen sample preparation for stable isotope analysis and AMS dating*)
2018	Human Paleoecology and Isotope Geochemistry Lab. Dept. of Anthropology, The Pennsylvania State University

2018	Center for Quantitative Imaging. Dept. of Anthropology, The Pennsylvania State University
2017	Matson Museum of Anthropology, Dept. of Anthropology, The Pennsylvania State University
2011-2017	Nels Nelson North American Archaeology Lab, American Museum of Natural History, New York City, NY
2012	Presidio Archaeology Lab, The Presidio Trust of San Francisco, CA
2011	Sedimentology Lab Assistant, Rutgers University, New Brunswick, NJ

PROFESSIONAL WORK

2013-2017 GIS and Photography Specialist, Nels Nelson North American Archaeology Lab, American Museum of Natural History, New York City, NY

Directed collection and curation of all geospatial and photographic data pertaining to archaeological research on St. Catherines Island, Georgia (USA); mentored undergraduate interns; generated 3D models of artifacts and in situ archaeological features; developed innovative data management solutions; created visual content for publications; presented research at professional conferences.

TEACHING EXPERIENCE

2020-21	Teaching Assistant, Introduction to Archaeology (ANTH 3); Dept. of Anthropology, UCSB
2020	Teaching Assistant, Introductory Biosocial Anthropology (ANTH 7); Dept. of Anthropology, UCSB
2020	Teaching Assistant, Introductory Biological Anthropology (ANTH 5); Dept. of Anthropology, UCSB
2019	Teaching Assistant, Human Growth and Development (ANTH 161); Dept. of Anthropology, UCSB
2018	Teaching Assistant, World Archaeology; Dept. of Anthropology, Penn State University
2018	Teaching Assistant, Forensic Anthropology; Dept. of Anthropology, Penn State University
2018	Teaching Assistant, First Farmers; Dept. of Anthropology, Penn State University

GRANTS, FELLOWSHIPS, AND AWARDS

Grants

2021-24	National Science Foundation Doctoral Dissertation Improvement Grant; $31,000
2021	Archaeological Specialty Dating Grant, Register of Professional Archaeologists; $1,000
2021	Leal Anne Kerry Mertes Grant, UC Santa Barbara Dept. of Geography; $2,500
2021	Archaeological Institute of America, Orange County Society; $2,000

2018	Lewis and Clark Fund for Exploration and Field Research, American Philosophical Society; $5,000
2018	Hill Fellowship Training Award, Penn State Anthropology; $1,500
2018	Center for Landscape Dynamics Graduate Research Award, Penn State Earth and Mineral Sciences/Anthropology; $1,500
Fellowships	
2021-22	Fulbright Student Research Fellowship, Zadar, Croatia, $30,000
2018-19	NASA Pennsylvania Space Grant Consortium Graduate Fellow, $5,000
2017-18	Matson Fellow, AIA membership award
2016	Social Media Fellowship, Spatial Ecology; €200
2015-16	Fredrick M. Warburg Scholarship, American Museum of Natural History; $1200
2011	New Brunswick Winter Session Scholarship, Rutgers University Financial Aid Office; $500.
Awards	
2018	Matson-Benson Award, Matson Museum of Anthropology, Penn State; $1,025
2017-18	Graduate Assistantship, Department of Anthropology, The Pennsylvania State University; $19,035
2016	Honorarium, REU Site: Immersive Research in the Bioarchaeology of Greek Colonization, for talk presented to REU students; $150
2015	Conference Travel Award, Graduate Student Association, Hunter College; $800
2010-11	Henry Rutgers Scholar Award, for outstanding School of Arts and Sciences Interdisciplinary Honors research achievement; $1300
2011	2nd Annual Anthropology Research Symposium Award, Rutgers University Anthropology Dept., sup. voted best honors research project by faculty; $200.
2010	Bigel Endowment Award for Undergraduate Research in Anthropology, Rutgers University Anthropology Dept.; $335.45.
2010-11	Jerome and Lorraine Aresty Research Scholarship, Aresty Research Grants and Conference Funding for undergraduate honors research, "Energetics of Pounding, Foraging, and Chewing in Modern Homo sapiens"; $1000.
2010	Rutgers University SAS Dean's List
2009	Rutgers University SAS Dean's List
2008	Rutgers University SAS Dean's List

PUBLICATIONS

Forthcoming	Horvat Oštrić, K., **Triozzi, N**., McClure, S. B., Reed, K. and Vidas, D. Rezultati Probnog Arheološkog Istraživanja Neolitičkog Nalazišta Pod Jarugom. *Archeol. Adriatica*
Forthcoming	McClure, S. B., Podrug, E., Ebert, C., Buckley, G., Jović, J., Moore, A.,

Triozzi, N., Welker, M. H., Zavodny, E., Freeman, K. and Kennett, D. J., Intensified dairying and transhumance in the Adriatic documented at 7200 cal. BP by oxygen isotopes in sheep and goat teeth. Sci. Adv.

2024 Horvat Oštrić, K. and **Triozzi, N.**, Probna istraživanja neolitičkog nalazišta u Islamu Grčkom. *In Situ* 1: 46–51.

2024 Horvat Oštrić, K. and **Triozzi, N.**, Neolitičko nalazište Pod Jarugom. *In Situ* 1: 72–76.

2023 Partridge, T., Barandiaran, J., **Triozzi, N.** and Toni Valtierra, V. Decommissioning: another critical challenge for energy transitions. *Glob. Soc. Challenges J.* **2**: 188–202.

2022 McClure, S. B., Podrug, E., Jović, J., Monroe, S., Radde, H. D., **Triozzi, N.**, Welker, M. H. and Zavodny, E., The Zooarchaeology of Neolithic farmers: Herding and hunting on the Dalmatian coast of Croatia. *Quat. Int.* 634: 27–37.

2022 Welker, M.H., Zavodny, E., McClure, S.B., Podrug, E., Jovic, J., **Triozzi**, **N.**, Kennett, D., A Wolf in Sheep's Clothing: The Development of Livestock Guarding Dogs in the Adriatic Region of Croatia., Journal of Archaeological Science: Reports

2018 MacEachren, A. M., Caneba, R., Chen, H., Cole, H., Domanico, E., **Triozzi, N**., Xu, F. and Yang, L., Is This Statement About A Place? Comparing two perspectives. GIScience 1–6.

PROFESSIONAL PRESENTATIONS

2024 Tooth Enamel $\delta^{13}C$ and $\delta^{18}O$ Reveal Diverse Ovicaprid Husbandry Strategies during the Neolithic on the Dalmatian Coast, Croatia. European Association of Archaeologists 30th Annual Meeting, Rome, Italy, 28 – 31 August.

2022 Herding is Risky Business: Investigating agropastoral resource management in Northern Dalmatia 8-6 kya. Research and methods overview presented to University of Zadar students Monday 6 August.

2018 A model for identifying corridors of ecological niche construction from transhumance in Northern Dalmatia. Paper given, European Association of Archaeologists 24th Annual Meeting, Barcelona, Spain 5-8 September. Co-authors: Sarah B. McClure, Emil Podrug

2018 Competing with the Crown: Early Spanish Mission Settlement Decisions in a Human Behavioral Ecology Model, Paper given, Society for American Archaeology 83rd Annual Meeting,, Washington DC, 12 April

2017 GIS and Mapping Techniques in Archaeology, Talk for undergrads, University of Alabama Archaeological Field School, St. Catherines Island, GA, May

2017 Causes and consequences of pre- and proto-historic social network connectedness in coastal Georgia. Poster presentation, Society for American Archaeology 82nd Annual Meeting, Vancouver, BC, CAN. 29 March – 2 April; Co-authors: Anna M. Semon and Thomas O. Blaber

2017 From the East Coast to the Great Basin, Using RTI to highlight subtle artistic

features Lightning talk, Illumination of Material Culture: Computational Photography and Reflectance Transformation Imaging (RTI), The Metropolitan Museum of Art, New York City, NY; March. Co-author: David Hurst Thomas.

2016 Reconstructing stratigraphy at Cannatello: GIS, Photogrammetry, and 3D Modeling Techniques Talk for CUNY Hunter Central Mediterranean Archaeology Program, San Leone, Sicily, IT, July.

2016 Mapping the Fallen Tree Mortuary Complex: GIS, Photogrammetry, and 3D Modeling Techniques Talk for REU students, REU Site: Immersive Research in the Bioarchaeology of Greek Colonization, Campofelice de Roccella, Sicily, IT, June.

2015 Buried at Morning Light: A GIS analysis of skeleton orientations at the Fallen Tree Mortuary Complex, St. Catherines Island, GA Poster, Southeastern Archaeology Conference, Nashville, TN, November.

2015 More than a Rusty Nail: Archaeometric Analysis of Wrought Iron Nails from Fallen Tree, St. Catherines Island, GA Talk, Society of American Archaeology 80th Annual Meeting, San Francisco, CA, April. Co-authors: Henry Towbin and Glen Keeton.

2014 A Vessel to the Next World: Examining an Urn Burial from St. Catherines Island, GA and others on the Georgia Coast Talk, Southeastern Archaeology Conference, Greenville, SC, November. Co-author: Anna M. Semon.

2013 Butchery tool choice at Mission Santa Catalina de Guale, St. Catherines Island, Georgia Talk, Southeastern Archaeology Conference, Tampa, FL, November.

2011 Energetics of Pounding, Foraging, and Chewing in Modern Homo sapiens Undergraduate Honors Thesis, Rutgers University, May 2011

ARCHAEOLOGICAL FIELDWORK

Domestic (United States)

2018 Katmai National Park, AK. *"Following in the footsteps of the National Geographic Society's original Katmai expeditions,"* National Geographic Society

2017 Creighton Island, GA. *University of Alabama*

2011-2017 St. Catherines Island, GA, *St. Catherines Archaeological Project, American Museum of Natural History, NY*

2013 Delaware Water Gap Recreation Area, NJ, PA. *E2 Project Management, LLC, Rockaway, NJ*

2012 Presidio of San Francisco, CA. *Presidio Trust*

Abroad (Outside U.S.)

2021-2022 Zadar County, Croatia, Islam Grčki and Lisičić

2018 Donje Polje, Šibenik County, Croatia

2018 Bekes 103, Vésztő, Hungary. *Bronze Age Körös Off-Tell Archaeology (BAKOTA)*

2016 Cannatello, Sicily, IT. *Sapienza Università di Roma and Hunter*

	College, CUNY
2013	Fort Charles, St. Kitts and Nevis. *Nevis Archaeological Field School, Monmouth University, NJ*
2010	Koobi Fora, Lake Turkana, Kenya. *Field School in Paleoanthropology, Rutgers University Study Abroad*

SYNERGISTIC ACTIVITIES

Committees

2019-21	Treasurer, Anthropology Graduate Student Association, UCSB
2019-21	Fundraising Committee Chair, Anthropology Graduate Student Association, UCSB
2018-19	Treasurer, Anthropology Graduate Student Association, Penn State
2018-19	Penn State Anthropology Colloquium Committee Member
2018	Pete Triozzi Memorial Scholarship Fund, Inc., Trustee and co-founder
2009-11	President, Rutgers Undergraduate Anthropology Club

Outreach

2020	AGSA's First Annual Chili Cook-Off (organizer of fundraising event to support UCSB Anthropology graduate student conference participation; raised >$1k)
2018	Primate Perspectives: A Crash Course on Our Closest Living Relatives; i-STEAM workshop for K-8 teachers
2018	Haunted-U; science activities for K-12
2018	Envision: STEM Career Day for Girls
2018	TEDxPSU Volunteer

TRAINING

2022	Fourier Transform Infrared Spectroscopy, *Materials Research Laboratory, UC Santa Barbara*
2022	Laboratory Safety, *Environmental Health and Safety, UC Santa Barbara*
2019	Geospatial Applications of Unmanned Aerial Systems (UAS). *World Campus, Penn State University, State College, PA*
2018	Chemical Safety. *Environmental Health and Safety, Penn State University*
2018	Emergency Preparedness. *Environmental Health and Safety, Penn State University*
2018	Introduction to Laboratory. *Environmental Health and Safety, Penn State University*
2018	Laboratory Waste Disposal and Management. *Environmental Health and Safety, Penn State University*
2018	Computational modelling, network science, semantic technology. *Summer School in Digital Archaeology, Universitat de Barcelona, ES*
2018	Backcountry Operations, *Katmai National Park, King Salmon, AK*
2018	Wildlife Firearms and Safety, *Katmai National Park, King Salmon, AK*
2018	CPR and First Aid, *Katmai National Park, King Salmon, AK*

2018 Swiftwater crossing and rescue, *Katmai National Park, King Salmon, AK*
2018 Aviation Safety (A-100, A-312), *Katmai National Park, King Salmon, AK*
2018 Advanced Cyber Infrastructure Seminar Series, Penn State High-Performance Computing, *Institute for Cyber Science, State College, PA*
2016 Spatio-temporal data Analysis using Free and Open Source Software. *Spatial Ecology, Universitá Basilicata, Matera, IT*
2016 Hands-on Open Source Drone Mapping and High-Performance Computing for Big Geo-Data. *Spatial Ecology, Universitá Basilicata, Matera, IT*

AFFILIATIONS

2014-21 Register of Professional Archaeologists: **28578352**
2018-21 Federal Aviation Administration Part 107 – sUAS Remote Pilot Number: **4279174**

Current Professional and Academic Memberships

2012 Society of American Archaeology
2017 Archaeological Institute of America
2018 European Association of Archaeologists
2018 Complex Systems Society
2011 Phi Beta Kappa Society

REFERENCES AVAILABLE ON REQUEST

Sarah B. McClure
Professor
Department of Anthropology
University of California, Santa Barbara

Douglas J. Kennett
Professor
Department of Anthropology
University of California, Santa Barbara

Tristan Partridge
Lecturer: Global Studies
Coordinator: Center for Restorative Environmental Work
University of California, Santa Barbara

ABSTRACT

Herding is Risky Business: Agropastoral Strategies in Neolithic Northern Dalmatia

by

Nicholas Peter Triozzi

Beginning around 9,000 years ago, Neolithic farming societies originating in Anatolia began to disperse into Europe. Within 1,000 years, domesticated plants and animals arrived to coastal areas of the Central Mediterranean Basin including the Adriatic Sea. The colonization of Eastern Adriatic islands and coastal areas such as the Dalmatian Coast of Croatia by agropastoralists dramatically altered endemic plant ecologies and biodiversity. This was primarily due to the heavy reliance on herds of sheep and goats for subsistence and associated animal husbandry systems.

Three consecutive cultural phases, Impresso, Danilo, and Hvar, are recognized via the appearance of distinct ceramic traditions. Archaeological evidence indicates Impresso agricultural settlements were established in Dalmatia for about 500 years before a suite of technological, economic, and social changes arrived alongside Danilo ceramics. By approximately 7000 cal. BP (calibrated calendar years before present), Hvar ceramics appear in open-air village contexts. The appearance of Danilo cultural material distinguishes the Early (8000-7400 cal. BP) from the Middle Neolithic (~7500-7000 cal. BP) in Northern Dalmatia and the development of the Hvar cultural phase marks the beginning of the Late Neolithic. The Impresso-Danilo transition is well-documented archaeologically but the

transformative effects on livestock husbandry strategies during this period marked by important changes to food production are not well understood. Over the 2,000-year duration of the Neolithic in Dalmatia subsistence was based primarily on a combination of intensive crop cultivation and small-scale livestock husbandry. However, it is unclear whether broader social and technological developments that occurred from the Early to the Middle Neolithic were accompanied by changes in livestock management.

I address this gap in our knowledge of this critical period of the spread and development of agriculture in Europe through a comprehensive exploration of Neolithic livestock management practices in Dalmatia. This research employs several methodological approaches to investigate how ancient herders optimized livestock production goals, maintained herd size and viability, and managed animal diet, mobility, and breeding. These aspects of herd management are examined using a combination of traditional zooarchaeological techniques, population projection modeling, and stable isotope analysis of ancient livestock tissues. Additionally, I interpret the data within the theoretical framework of risk minimization, which is an effective approach towards understanding human decision making when faced with uncertainty in the outcome of subsistence behaviors.

The results of my work demonstrate that Neolithic herders on the Dalmatian Coast of Croatia engaged in a variety of strategies that were not exclusive to any one cultural-temporal phase, thus reflecting short-term solutions oriented around minimizing risk of subsistence failure. Key strategies of managing animal diet include provisioning herds with fodder and the exploitation of both local and non-local grazing and browsing environments. Moreover, the data suggest herders occasionally engaged in vertical transhumance, taking advantage of abundant mountain pastures in response to low quality grazing in the summertime.

Additionally, the results of birth seasonality modeling presented here suggest that herders manipulated animal breeding rhythms to extend birthing seasons according to whether production goals were dairy or meat focused. This work also contributes new radiocarbon dates for four Neolithic sites in Dalmatia: Islam Grčki - Graduša Lokve, Pograđe - Pod Jarugom (i.e., Lisičić), Smilčić-Barice, and Zemunik Donji. By integrating insights gleaned from multiple analytical perspectives, this research contributes a new and nuanced view of how ancient agropastoral communities balanced and mitigated the risks associated with maintaining livestock viability to meet subsistence needs.

TABLE OF CONTENTS

LIST OF TABLES

LIST OF FIGURES

I. Introduction

The development and spread of agriculture into Europe from the Near East was complex and multifaceted. Agriculture dispersed swiftly out of Anatolia along coastal routes of the Mediterranean basin, reaching the Atlantic coast in less than 3,000 years (Fernández et al. 2014; Zeder 2008). The Neolithization of Europe involved the transfer of domesticated plants, livestock, and human populations along coastal and inland routes (Hofmanová et al. 2016; Lacan et al. 2011; Pilaar Birch et al. 2019; Zeder 2008). The earliest farming societies to colonize southeastern Europe tailored their crop cultivation and livestock management strategies to local ecologies (Gaastra et al. 2019; Gaastra and Vander Linden 2018; Manning et al. 2013; McClure 2013).

The Eastern Adriatic is a critical region for examining localized adaptations that facilitated the spread and intensification of agriculture into the Mediterranean basin and for understanding the processes underlying the Neolithization of Europe. Beginning around 8000 cal. BP Neolithic farming societies began to transport cultigens and livestock to the Adriatic coast via maritime routes (Fernández et al. 2014; Forenbaher et al. 2013; Forenbaher and Miracle 2014; Hofmanová et al. 2016; Larson et al. 2007; Olalde et al. 2015; Pilaar Birch 2017). On the Dalmatian Coast of Croatia the Neolithic period (8000-6000 cal. BP) is represented by an increasing number of open-air and cave sites. In Dalmatia, the Neolithic is separated into Early (8000-7500 cal. BP), Middle (~7400-7000 cal. BP), and Late (7000-

6000 cal. BP), corresponding to the *Impresso*, *Danilo*, and *Hvar* stylistic pottery sequences, respectively (Batović 1966; Forenbaher et al. 2013; Forenbaher and Miracle 2005; McClure et al. 2014; McClure and Podrug 2016).

Throughout southeast Europe Neolithic subsistence was primarily based on an intensive mixed farming model characterized by high labor inputs per unit land area, modest numbers of livestock, and food production sufficient for household subsistence needs (Bogaard 2004; 2005). Einkorn (*Triticum monococcum*), emmer (*Triticum dicoccum*), and barley (*Hordeum vulgare*), in addition to flax (*Linum usitatissimum*), grass pea (*Lathyrus sativus*) and a range of wild fruit species were typical of Neolithic plant economies in Dalmatia (Moore et al. 2019; Reed 2016; Reed and Colledge 2016; Reed and Podrug 2016). The proportions of domesticated animal species represented at archaeological sites remained relatively stable throughout the Neolithic in the region. Faunal assemblages are dominated by caprines (i.e., sheep and goats), with cattle, pig, and wild game and fish representing a smaller proportion of animal bone recovered (McClure et al. 2022; McClure and Podrug 2016; Moore et al. 2019; Schwartz 1988; 1996).

Domesticated animals were extremely important contributors to subsistence. Livestock are a form of "live storage," buffering risk of starvation during crop failure (Flannery 1969) as well as broadening the array of risk minimization strategies available to subsistence agropastoralists (Halstead 1990; Halstead and Jones 1989). Within this context, caprines likely played a key role in the rapid dispersal of Neolithic communities throughout the Mediterranean (Manen et al. 2019; Sierra et al. 2023) and facilitated the colonization of Dalmatia's island and coastal environments (Pilaar Birch 2018). In contrast to Neolithic sites associated with the spread of agriculture into central Europe via the Pannonian Plain and the

Danube river corridor where faunal assemblages are dominated by cattle bones, sites along the Adriatic coast are characterized by higher proportions of sheep and goat (Orton et al. 2016). For pioneering Neolithic groups prospecting the viability of farming along Mediterranean coastal areas, sheep and goat husbandry was an effective means to buffer risk of food shortages arising from cropping in tenuous environments (Halstead 2006).

Preference for sheep and goats in the Mediterranean is likely due to a range of behavioral and biological traits compatible with relocating and adapting to new environments. Relative to cattle and pigs, sheep and goats have better mobility in uneven karst terrain and exhibit greater dietary flexibility and drought resistance (Leppard and Birch 2016; Munro and Stiner 2015). Additionally, caprines are lighter and more prolific relative to other livestock species, plus the variety of products they provide and the docile nature of sheep in particular would have been extremely advantageous to Neolithic communities organizing seaward migrations (Broodbank and Strasser 1991; Sierra et al. 2023). Moreover, the accumulation of manure through small-scale sheep and goat husbandry would have complemented intensive crop cultivation by replenishing soils in fields with important nutrients (Bogaard 2005; Halstead 2006). Nonetheless, herders likely faced new challenges as they adapted livestock feeding strategies to the novel grazing and browsing environments of the Mediterranean.

Livestock management entails careful and economical allocations of herder time and labor into the plant and animal resources (Russell 1988). As a result, herder decisions directly influence the capacity of livestock to meet human subsistence goals, and stewards of herds often must adapt to spatial and temporal variation in resources (Halstead 1998b; Halstead and Jones 1989; Halstead and O'Shea 1989; Redding 1981). Understanding the strategies that

Neolithic farmers employed to maximize the dietary and environmental adaptability of sheep and goats is of particular importance to ongoing research on the dispersal of agriculture into Europe.

This dissertation examines the development of livestock management strategies within the intensive mixed farming systems that characterize Neolithic subsistence in the Eastern Adriatic. I focus largely on sheep and goat husbandry and investigate the decisions herders made within the theoretical framework of risk minimization. I employ a range of methods to assess how herders managed animal diet, breeding, mobility, and herd demography. I draw on new and previous archaeological research spanning the 2,000-year period of the Neolithic on the Dalmatian Coast of Croatia. Dalmatia is a key region of the Eastern Adriatic where evidence for agricultural intensification is clear, but the particularities of sheep and goat husbandry remain under-defined. This gap in knowledge obscures our understanding of how farming developed and spread throughout Europe. To address this lack of clarity my research contributes new insight into how herders balanced the risks associated with caprine management and their own subsistence needs. Through this research, a nuanced perspective emerges of the initial dispersal of farming throughout the Mediterranean and subsequent development of *in situ* agricultural economies.

A. Theoretical Orientation

Risk mitigation provides a useful explanatory framework for understanding intensification processes and how certain strategies are employed among a variety of alternatives. From an evolutionary perspective, individuals should aim to minimize risk, which can be understood as probabilistic variance in returns or more plainly, chance of loss

(Goland 1993a,b; Halstead and Jones 1989; Winterhalder 1986; 1990; Winterhalder et al. 1999). In agricultural subsistence economies, farmers can pursue a variety of strategies that are broadly characterized as either intensification or diversification (Marston 2011; 2021). Intensification strategies aim to increase crop yields or animal products per unit land and buffers the risk of failing to meet subsistence requirements via overproduction (Morrison 1994). Diversification buffers this risk by spreading investments across a broader range of resource types, resource patches, or return rates (Marston 2011). Additionally, intensification and diversification strategies can be used in combination and may vary between communities facing similar subsistence challenges (Halstead and O'Shea 1989; Marston 2021). In addition to milk, meat, and fiber, livestock produce manure which can be used to improve crop yields as an intensification strategy (Bogaard et al. 2007; Kanstrup et al. 2011). Herders can also accumulate "animal capital" as a means of navigating various social, economic, and political transactions (e.g., dowry, barter, inheritance, etc.); in this respect keeping livestock is a way of spreading risk across a broad range of activities and subsistence (Halstead 1989; 1996).

Although risk is often applied to economic problems, it has been adapted by archaeologists pursuing research framed in behavioral ecological terms (Halstead and Jones 1989; Marston 2011; 2021; Winterhalder 1986; 1990). Within this theoretical framework, individuals make decisions intended to reduce the chances that a particular food production strategy will result in returns that are insufficient to meet subsistence needs (i.e., subsistence failure). The survival of goat and sheep herds relies on the diligence of shepherds; and the looming threat of unpredictable catastrophic losses (e.g., arising from drought or disease) serves as a strong impetus for herders to develop ways of ensuring herds are resilient.

But how can risk minimization strategies be distinguished from routine practices

inherent to a particular herding system, and can such decisions be identified archaeologically? It is generally assumed that the scale of production in Europe during the Neolithic remained at the subsistence level and was focused near settlements (i.e., intensive mixed farming). Current archaeological data from the study area indicate livestock production emphasized meat during the Impresso and Hvar phases of the Early and Late Neolithic (respectively) while milk was prioritized by Danilo groups during the Middle Neolithic (McClure et al. 2022; Radović 2011). Based on evidence for alternative livestock production goals corresponding with different cultural phases of the Neolithic in Dalmatia, it is hypothesized that different herding and risk minimization strategies were employed in response to changes to the social and economic value of livestock and the relative importance of various livestock products for subsistence. To evaluate this overarching hypothesis, I address three thematic assumptions about risk minimization within herding systems:

(1) Herding decisions during the Neolithic were sensitive to changes in herd size and demography and shepherds employed alternative breeding and slaughtering regimes to minimize risk of failing to meet subsistence needs.

(2) Neolithic herders employed a variety of strategies to ensure the nutritional requirements of herds were met which included the incorporation of fodder into livestock diet.

(3) An alternative to foddering was the exploitation of non-local pastures via vertical transhumance (i.e., seasonal movement between high and low altitude pastures) and this extensive strategy was effective towards minimizing risk within small-scale intensive herding systems.

The research presented here explores these assumptions using archaeological data from

multiple contemporary sites associated with three distinct cultural phases of the Neolithic in Dalmatia. As will be shown, risk minimization strategies should be identifiable as variation among contemporary herding systems with similar production goals. Furthermore, it will be argued that the long-term effects of strategies that successfully minimized risk contributed to the development of agricultural economies in the study area. These developments should be observable as diachronic changes in livestock management. In the following section I outline how this dissertation is organized to tackle these research themes.

B. Organization of Dissertation

The following chapter describes the theoretical framework of this research in greater detail and draws on ethnographic and archaeological examples of how agropastoral risk is minimized in various environmental and cultural contexts. In Chapter Three of this dissertation, I provide an overview of what is currently understood about the Neolithic period in the Eastern Adriatic based on previous archaeological research on the Dalmatian Coast of Croatia. I describe the main archaeological sites and recovery of the zooarchaeological materials sampled for radiocarbon dating, stable isotope analysis, and reconstruction of caprine (i.e., sheep and goats) culling patterns. Chapter Three concludes with a detailed review of paleoclimate and paleo-ecological research to contextualize the environmental setting in which important developments in agricultural production occurred during the Neolithic period in the study area. In Chapter Four I focus on chronology, reporting both published and new radiocarbon dates associated with sites described in Chapter Three.

In Chapter Five I present the results of new zooarchaeological analyses of sheep and goat mandibles. This chapter provides an overview of the methodology and interpretive

framework associated with mortality profiles. I first describe how age-at-death data are obtained from sheep and goat mandibular tooth wear and how these data are used to approximate the production goals of past herding economies. Interpretations of culling strategies and production goals are proposed, which provide important context to inferences made later in this work, which combine insight into other aspects of herding such as birth seasonality.

I dedicate Chapter Six to herd demography. Building on the research presented in the preceding chapter, I examine various theoretical strategies of livestock management inferred by survivorship profiles. A population projection model is used to evaluate the viability of sheep and goat herds under different herd culling strategies. The implications of both theoretical and empirical harvest profiles are considered within the context of risk minimization.

In Chapter Seven, I provide detailed explanations of stable isotope analysis of enamel bioapatite and bone collagen and justify the utility of these approaches for reconstructing past livestock management strategies. The results of stable isotope analysis are introduced in Chapter Nine, but the discussion of these data is focused exclusively on implications for management of sheep and goat diet. I present stable isotope results from animal bone collagen demonstrating a variety of animal husbandry strategies were in use by Impresso and Danilo period herders on the Dalmatian Coast of Croatia. I interpret the $\delta^{13}C$ and $\delta^{15}N$ values of archaeological animal bone collagen as direct lines of evidence for strategies of livestock diet management and describe how these data indicate shifts in landscape use through time. I then shift the discussion towards the results of intra-tooth stable isotope analysis of caprine enamel bioapatite. Compared to bone collagen the intra-tooth stable isotope data offer a

higher-resolution perspective of herding decisions made within a single year. At a broader level, inter-site comparisons of these data indicate different dietary spaces among herds from different sites and highlight the variability of herd management among contemporary Neolithic villages.

Chapter Nine deals with herd mobility. As I describe in Chapter Seven, changes in the environment in which an individual ingests water can be observed in the oxygen isotope profiles obtained via intra-tooth stable isotope analysis of enamel bioapatite. Specifically, I use this approach to investigate evidence for vertical transhumance, a herding strategy entailing seasonal movements between low and high elevation pastures. I provide an overview of the historical background of this strategy in the study area and describe why we might expect the origins of this practice to date to the Neolithic. I then weigh the evidence, focusing on specific examples within the data that suggest that seasonal visitation of upland pastures may have been practiced on a small scale during the Neolithic as a means of minimizing risk.

Chapter Ten is prefaced with a discussion of sheep and goat reproduction and how herders can navigate or manipulate natural breeding rhythms. I then describe how oxygen isotope ratios obtained from incrementally sampled tooth enamel are used to model season of birth of individual sheep and goats. The discussion of the modeling results centers around how manipulating lambing and kidding birth seasonality during the Neolithic in Dalmatia could have minimized risk of reduced milk production in nursing females. I also explore how these strategies potentially relate to herd culling decisions.

The concluding chapter weaves together the insights obtained from stable isotope analysis, demographic modeling, and herd culling strategies. I also suggest future research

directions into under-explored aspects of the data. Finally, I highlight the key contributions of this research and explore some of the broader implications of trends in the data.

II. Risk in Agropastoral Subsistence Systems

Agropastoralism is the integration of herding animals and crop cultivation. Farming and herding subsistence activities are commonly classified as *intensive* or *extensive*, though, as will be discussed, these approaches are not mutually exclusive. Under the intensive farming model, returns are high per unit of cultivated land or livestock and sufficient for domestic consumption, and farmers exploit the functional interdependence of livestock and plants (Bogaard 2005; Flannery 1969; Jones 2005; van der Veen 2005). Intensively managed livestock are grazed or penned close to the settled area and recycle nutrients into the system by depositing dung, fertilizing soil, and promoting crop growth (Bogaard 2005; Choi et al. 2003). Crop byproducts such as straw, leaves and stalks, and hulls and shells that are unpalatable, inedible, or poorly digested by humans complement the diet of intensively managed livestock (Halstead 1990; Halstead et al. 1998; Jones and Halstead 1995). Livestock are an essential source of labor for tillage, plowing, and transport of seed and crops between cultivation, processing, and consumption areas (Greenfield 2010; Halstead and Jones 1989; Sherratt 1983). Intensive farming is also associated with mixed herding of different livestock species. Inter-species differences in dietary needs and high labor costs of collecting or producing fodder restrict the scale of animal husbandry to household subsistence needs (Halstead 1996).

Extensive farming and herding are more decentralized than intensive agropastoralism because crops and livestock are managed at large geographic scales, often drawing on the labor of extended kin to lower investment per capita and per unit of land (Bogaard 2005; Jones 2005). Extensive animal husbandry achieves greater efficiency when herds are large and herders are specialized in a single species (Bogaard 2005; Dyson-Hudson and Dyson-Hudson 1980; Halstead 1996). However, large, single-species herds are at greater risk of succumbing to drought or disease than are mixed-species herds. Due to the reliance on non-local grazing areas, extensive animal husbandry is incompatible with manuring (Bogaard 2005).

Research has shown that intensive and extensive farming are not mutually exclusive (Guillet 1987; Halstead 1998b; 2006; Johnston 2003; Makarewicz and Tuross 2006; Marston 2011; Marston and Miller 2014; Morrison 1996; Perišić 1940; Scarry and Scarry 2005; Stone and Downum 1999) but alternating between intensive and extensive systems entails significant restructuring of social and economic organization at both the household and community scales (Bogaard 2005; Flannery 2002; Halstead 1987). Limited archaeological evidence of intensive or extensive strategies does not necessarily signal system-wide reconfigurations of prevailing modes of agropastoral food production—these processes are seldom unidirectional and take time (Morrison 1994; Tucker 2006).

Humans dependent on intensive agropastoral food production must effectively manage resources to sustain the interdependence of livestock and plants. Today, people practice agropastoralism in many different environments and have adapted how plants and animals are suited to various habitats. Ecological, cultural, and social factors shape how humans leverage the interdependence between crops and livestock to satisfy their subsistence

needs (Schutkowski 2006). These factors result in immense variation within and between agropastoral subsistence systems through time and space. Much research has been directed towards understanding this variability in the context of the introduction and spread of agriculture into Europe ca. 8000 years ago. The archaeological record is rife with evidence of how humans adapted farming to unfamiliar environments. In this context, I use human behavioral ecology, a theoretical framework based on evolutionary theory that is well-equipped for addressing how humans cope with risk in unpredictable environments using archaeological data (Bird and O'Connell 2006).

I begin the following sections of this chapter with a brief overview of human behavioral ecology. Next, I discuss how behavioral models dealing with risk and uncertainty offer promising heuristic devices for understanding human decision-making about agropastoral subsistence strategies. This discussion is critical to articulating the concepts of risk and uncertainty with human decisions about allocating resources and, crucially, establishing clear definitions of risk and related concepts. To effectively utilize risk as an explanatory framework to address the present research questions, it is necessary to explore agropastoral subsistence from a cross-cultural anthropological perspective. To this end, I describe strategies that minimize risk in specific environmental and ecological conditions. This step is crucial for grasping how various ecological, social, and cultural factors—often poorly comprehended due to the limitations of incomplete archaeological data—may have influenced the decisions surrounding small-stock husbandry in historical contexts. Understanding these elements will provide deeper insights into the complexities of past agricultural practices and the interplay of environmental conditions and human choices. In order to gain a comprehensive understanding of the archaeological data that will be analyzed

in the following chapters of this dissertation, it is essential to explore both theoretical models and ethnographic research that focus on the concepts of risk and uncertainty. This exploration will provide valuable context and insight, helping to inform my interpretations and conclusions throughout the study.

A. Human Behavioral Ecology

Human behavioral ecology (HBE) is the study of the trade-offs and fitness-related outcomes of the behaviors of individuals within particular environments (Bird and O'Connell 2006: 144). The goal of HBE is to understand the variability in social and behavioral traits by employing theory to deduce under what social and ecological conditions particular traits or behaviors will emerge and persist in a population as a result of individual decision-making (Krebs and Davies 1997; Smith and Winterhalder 1992; Winterhalder and Smith 2000). In this perspective, human behavior is viewed as a phenotypic adaptation that has evolved in response to various environmental stimuli. Accordingly, human behaviors are shaped by the principles of natural selection, which involves several key processes: phenotypic (i.e., behavioral) variation among individuals, the inheritance of these variations from one generation to the next, and the differential survivorship and reproductive success that arise from these heritable traits. Behaviors that improve survival and reproduction can become more common over time, highlighting the dynamic interaction between humans and their environments (Codding and Bird 2015: 9).

By assuming that the function of any phenotypic trait (i.e., including behavior) is to maximize an individual's fitness, HBE approaches focus on explaining *why* there is variability in behavior. Designing research at this ultimate level of explanation (*sensu*

Tinbergen 1963) researchers aim to understand individual decision-making (e.g., why target prey type A and not types B or C?) while setting aside equally important but non-competing explanations for *how* that behavior was acquired (e.g., whether the preference for prey type A is instinctual or learned) for alternative lines of inquiry (Richerson and Boyd 1992: 62). Underlying this assumption, dubbed the "phenotypic gambit" (Grafen 1984) is that variability in human behavior is a result of how individuals interact with their environment and natural selection favors phenotypic traits that confer fitness advantages irrespective of mechanisms of inheritance (Smith and Winterhalder 1992: 33).

HBE researchers employ formal optimality models to generate predictions about human behavior to be tested empirically. The premise of such models is an optimization rule or goal in which the outcome of a behavior will maximize an individual's fitness (Maynard Smith 1978). Conflicting needs of different parts of an organism, such as its shape, eating habits, and past experiences, limit perfect optimization. Additionally, there is a time gap between what an individual does and the selection pressures affecting the population. Environmental uncertainty also plays a role in these constraints (Foley 1985). By focusing only on the fitness-level consequences of a particular behavior the immediate value of one subsistence activity can be weighed relative to others and formalized as an ecological model to predict decision-making within a set of habitat-specific constraints (Winterhalder and Kennett 2006: 13). In this respect, optimal foraging models (Bettinger 2009; Charnov 1976; Macarthur and Pianka 1966) have been used to investigate the wide range of conditions under which individuals make decisions about food production.

Optimal foraging models assume humans make decisions (e.g., about diet, foraging location and time) to maximize the rate of net energy gain (Bettinger et al. 2015: 92). Hunter-

gatherer subsistence decisions have been investigated using variations of the diet breadth model such as the prey and patch choice models and the patch residence time model (Bird et al. 2009; Broughton et al. 2011; Hawkes et al. 1982; O'Connell and Hawkes 1984; Thomas 2014). The diet breadth model focuses on momentary decisions a forager makes about which prey items will be incorporated into their diet when the relative abundance, nutritional value, and pursuit costs are known (Macarthur and Pianka 1966).

The diet breadth model and its variants (e.g., prey and patch choice models and central place models) are 'deterministic' models because they assume central tendency in an individual's behavior and environment (Winterhalder et al. 1999: 303). Concerning the diet breadth model, energy and time investments and net gains for any particular prey type are constant, higher valued prey items have priority, and a forager's preference over one or another prey is binary (Bettinger et al. 2015: 92). Short-term variation is negligible in deterministic models which, depending on the research question, may be an oversimplification of forager behavior. For example, when the return rate of a highly valued prey item reduces due to a seasonal decrease in abundance or increase in pursuit costs, the diet breadth model predicts that a forager will increasingly target prey types with lower nutritional values. The result is that lower-ranked resources will constantly move into and out of the optimal diet, which could consist of an infinite number of very low-ranked foods as long as net gains are equal to or greater than zero. Moreover, there is no assumption in deterministic optimization models that the positive net gains achieved by a seemingly desperate forager will be sufficient to satisfy a minimum return rate necessary for their survival (Winterhalder et al. 1999).

In reality, the mean and variance of returns from subsistence behaviors factor into forager decisions (Caraco et al. 1980; Houston et al. 1988; Stephens and Charnov 1982). This real-world problem of variation in resource availability raises essential questions about food production strategies in stochastic environments. The problem is especially relevant to the transition from hunter-gatherer subsistence to an agricultural way of life (Kennett and Winterhalder 2006; Winterhalder and Goland 1997). Human behavioral ecologists have turned to more sophisticated risk-sensitive foraging models (Caraco et al. 1980) to address how humans deal with unpredictable resource variance (Cashdan 1985; Henrich and McElreath 2002; Kuznar 2001; Mace 1990; Mace and Houston 1989; Winterhalder et al. 1999). In the upcoming section, I will offer a comprehensive definition of risk and explore, in greater detail, the various strategies humans employ to navigate the uncertainties posed by their environment, particularly within the context of mixed-farming subsistence systems. This discussion will delve into how individuals and communities adapt to the unpredictable nature of their surroundings, balancing agricultural practices with the need for sustainability and resilience.

B. Definitions of Risk and Uncertainty

Risk and uncertainty are two related but distinct concepts. One definition of risk is the probability that returns from a subsistence activity will be below a desired or necessary threshold (Winterhalder 1986: 374). In agricultural decision-making, risk is commonly equated with chance of loss (Goland 1993b; Halstead and Jones 1989). Risk is also conceptualized in foraging theory as variance in returns (Winterhalder et al. 1999). Uncertainty refers to incomplete or no knowledge of outcome probabilities and affects risk

sensitivity when individuals face rapidly changing environmental variables (Winterhalder et al. 1999). Several varieties of decision-making models allow organisms to overcome uncertainty through learning (Roumasset 1979; Stephens 1987; 1989), but stochasticity makes it impossible to predict any particular outcome of a behavior accurately; no amount of experience can overcome risk since outcomes cannot be foretold, only assigned odds (Winterhalder et al. 1999: 303).

Risk-sensitive behavioral models are a special variant of optimization models in which the environmental constraints on behavior (e.g., prey abundance, pursuit, handling costs, patch residence time) are subject to stochastic variation (Stephens and Charnov 1982; Winterhalder et al. 1999). They are particularly useful for understanding behavioral variation in agropastoral subsistence economies because humans have adapted this mode of production to a wide range of environments, each presenting unique sources of risk. Risk is operationalized in formal modeling approaches as outcome probability distributions such that risk-prone (i.e., high-variance) and risk-averse (i.e., low-variance) strategies can be compared based on the degree to which returns are above some measurable threshold (e.g., minimum amount of profit, livestock acquired, destitution, or starvation; Caraco 1981; 1982; Caraco et al. 1980; Mace 1990; Mace and Houston 1989; Marston 2011; Stephens and Charnov 1982; Winterhalder et al. 1999).

Future discounting models, for example, help understand how individuals make risk-sensitive decisions when resources are uncertain or rewards are delayed (Winterhalder et al. 1999). These models consider how time may constrain an individual's perception of outcome probabilities associated with alternative subsistence options with varied outcome values and the delay one must endure before realizing gains. Future discounting models have been used

to model human decision-making leading to the transition from foraging to farming (Winterhalder and Goland 1997) in various contexts (e.g., Barlow 2006; Thomas 2008; Tucker 2006).

Varieties of future discounting models are an elaboration of the Z-score model (Winterhalder 1999; Figure 2.1). The Z-score model allows for the comparison of different subsistence strategies with different outcome probabilities and predicts that individuals who choose among strategies where the mean return from each is above a starvation threshold will select the one with the lowest variance (Marston 2011: 191; Winterhalder et al. 1999; Winterhalder and Goland 1997). Ideally, applying the Z-score model will compare probability distributions of different strategies to make predictions about which strategy should be chosen. But the underlying principles of the model allow for its use as a heuristic device provided the researcher has a reasonable understanding of how alternative strategies affect outcome probabilities (i.e., is a particular strategy known to increase mean of returns through overproduction or reduce variance by diversifying the base of subsistence). Risk minimization tactics used by farmers are broadly categorized as intensification and diversification strategies (Marston 2011). In the following section, I describe these concepts in greater depth before discussing how agropastoralists minimize the chance of subsistence failure in various social and environmental contexts.

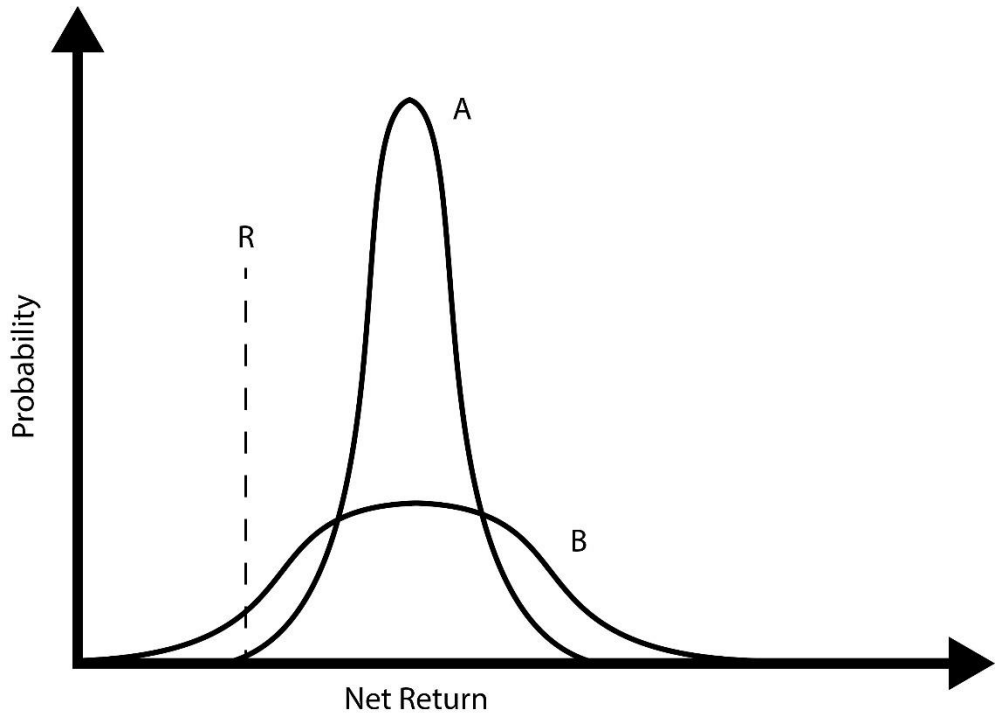

Figure 2.1. A comparison of the Z-score model for a low-variance strategy (A) and high-variance strategy (B). Returns for both options are above the starvation threshold (R) so the low-variance strategy should be preferred. Diagram reproduced following Marston (2011, Fig. 1).

C. Risk Minimization Strategies: Intensification and Diversification

Intensification and diversification are two distinct approaches to minimizing the chance of subsistence failure (i.e., risk) in agropastoral systems (Marston 2011: 191). *Intensification* strategies reduce variance in returns through overproduction; increased investment per unit of land is a premium paid to lower the chances that a household will succumb to starvation during unpredictable food shortages. Examples of intensification strategies include overproduction and irrigation. Overproduction of agricultural resources is achieved either by increasing the land used to grow crops or increasing the labor investment in a fixed area of land. Surplus occurs when there is more crop production than needed, but this only happens if farmers can store the crops after harvesting. This storage helps reduce

the chances of food shortages in future seasons. Therefore, storage technology or techniques that prevent surplus grains from spoiling or being attacked by pests is a necessary component of overproduction.

On the other hand, livestock are often used as a form of "live storage" of surplus production (Flannery 1969) when farmers provision surplus grains to animals as fodder. Fodder permits animals to maintain productivity across periodic resource scarcity and is often a complementary source of livestock diet in intensive farming systems. Another intensification strategy is maximizing herd size, which, as will be discussed, is an approach herders use to generate a surplus of animal products to diversify their subsistence base through exchange networks or participation in market economies.

Diversification strategies reduce variance in returns by spreading investment in subsistence more broadly. Diversification strategies that minimize risk include crop, spatial, and temporal diversification (Marston 2011). Crop diversification reduces variance in returns by focusing on crops with varied time to maturity, environmental sensitivities, and flexibility in how farmers use the crop and its byproducts (Walker and Jodha 1986: 20). Spatial diversification involves averaging yields from a range of growing environments which may require cycles of seasonal or annual mobility, or permanent resettlement (Marston 2011). Temporal diversification can take the form of food storage when the primary crop is harvested annually and rationed between harvests or can involve manipulating animal breeding cycles to stagger milking seasons within the annual cycle. Pastoralists cope with temporal and spatial variability of drought through prevention and response. Preventative strategies take the form of insurance against losses, while farmers deploy responsive

measures when preventative measures, if at all implemented, fail (VanDerwarker et al. 2013: 71–72; Walker and Jodha 1986).

Transhumance is a special variety of spatial diversification available to pastoralists. This approach entails the movement of domesticated herding animals to pastures in different microhabitats that may vary in productivity on a seasonal basis. Transhumant herders generally rotate between two or more settlement locations on a seasonal basis, whereas residence is more flexible among nomadic herders (Dyson-Hudson and Dyson-Hudson 1980). Mobile herding can be horizontal (i.e., between pastures occurring within a restricted range of altitudes) or vertical (i.e., between pastures in different elevations). Vertical transhumance is common in many southern European pastoral groups (Arnold and Greenfield 2006; Bartosiewicz and Greenfield 1999; Bindi 2022). Mobility also reduces grazing pressure on pastures, lowering the risk of overgrazing (Zervas 1998).

Mixed- or multi-species herding is analogous to crop diversification. Different livestock species have different reproduction and growth rates, and some are less vulnerable to drought than others. Multi-species herding minimizes the risk of a herder losing all of their animals. Additionally, due to differences in feeding behaviors and forage preferences, mixed-species grazing improves biodiversity, increases pasture carrying capacity, and breaks parasite life cycles (Anderson et al. 2012; McClure 2015; Rocha et al. 2008; Walker 1994).

Intensification and diversification strategies can become systemic through routine use, and a subsistence farming economy can be based on both intensive and extensive farming models. But these strategies can also serve as *ad hoc* solutions to minimize risk within either intensive or extensive farming systems and farmers often implement them simultaneously. It is important to note, however, that intensive and extensive farming models

involve different degrees of plants-animals inter-dependence and contributions to subsistence, different technologies, food production techniques, different measures of and ways to deal with surplus, and therefore different labor inputs and production outputs across nearly every step of the subsistence process (Halstead 1987: 84).

The different ways humans allocate resources to production within intensive and extensive farming systems have implications for which risk-buffering strategies are best suited to minimize the chance of subsistence failure. A purely economic approach to understanding risk-sensitive behaviors, however, may not always be appropriate because socially acquired strategies, preferences, and beliefs about which practices are associated with success in particular cultural arenas also shape how humans perceive and respond to risk (Henrich and McElreath 2002; Kuznar 2001). These perspectives are generally not accessible to archaeologists. On the other hand, risk buffering strategies can be more effectively predicted by understanding the temporal structure (frequency and duration of the operant risk), spatial structure (geographic extent and prevalence of variability from one habitat to the next), and relative intensity (variation of resource scarcity severity) of the source of variability affecting outcome probabilities (Halstead and O'Shea 1989: 3).

Social factors may present unique, non-environmental risks for herders (e.g., the probability of theft cannot be fully known). However, more research is needed to know about whether and how Neolithic villages in Dalmatia interacted with one another. For this research, the primary sources of risk considered are environmental, focusing on livestock diet as a critical aspect of herd management directly shaped by decisions made by individuals, households, and communities. Keeping this narrow perspective of risk, I aim to examine how agropastoralists cope with similar environmental challenges across time and space.

Small-stock herders in many parts of the world feel the influence of precipitation and temperature variability on pasture quality. Unpredictable precipitation is a considerable risk faced by pastoralists who rely on small-stock such as sheep and goats. In many environments, rainfall is closely linked to pasture quality (Martins-Noguerol et al. 2023; Sloat et al. 2018). Low pasture quality can be a severe constraint on the metabolic demands of pregnant and nursing sheep and goats and negatively impacts the survival of young (Dahl and Hjort 1976; Galina et al. 1995; Mellado et al. 2006). The seasonality of sheep and goat reproduction is an adaptation to seasonal cycles in pasture quality, which is largely a product of daylength, precipitation, and temperature rhythms (Rosa and Bryant 2003; Thimonier 1981; Yeates 1949). Therefore, in mixed-farming systems heavily reliant on caprine production, herders must know how to integrate various and sometimes overlapping farming and herding activities into an annual productivity cycle. To cope, herders dynamically employ various strategies such as controlling reproduction, rotational grazing, seasonal movement, provisioning of fodder, and, when possible, communal labor networks. As discussed in the following sections, buffering risk often entails a combination of strategies not merely attuned to environmental variability but shaped by social, economic, and cultural factors that may have deep historical roots.

D. A Cross-Cultural Perspective of Agropastoral Risk Buffering Strategies

In the remainder of this chapter, I focus on ethnographic examples of risk-buffering strategies in agropastoral systems. This review will highlight the diversity of risk coping strategies through space and time, broadening the context of my research on how ancient Dalmatia herders managed risk. In the second part of my analysis, I explore the various

strategies used to manage risk and examine its different *sources*. This analysis will also uncover the various economic, climatic, and social influences that play a crucial role in shaping individuals' perceptions and reactions to uncertainty in livestock husbandry. These influences can be viewed as distinct sets of dependent variables, from which various combinations of intensification and diversification strategies arise. By examining these factors in depth, we can gain a clearer understanding of how they interact and contribute to the decision-making processes of those involved in livestock farming.

1. Semi-Arid East Africa

In the arid and semi-arid environments of the Rift Valley of Eastern Africa, specialized pastoralist communities such as the Maasai, Turkana, Somali, and Borana must cope with drought that has increased in severity amidst the desertification of the region over the last century (Hogg 1987; Johnson 1993). For example, in the low-lying Rift Valley region of Ngisonyoka, there is little seasonal variation in the mean annual temperature of 30°C. At the same time, high-intensity but infrequent rainfall events are concentrated in the 2-3 month wet season, bringing 150-600 mm of rain (Coughenour et al. 1985: 620). Despite linguistic and cultural differences, diverse East African pastoralist groups employ similar risk-buffering strategies, including mobility, mixed-species herding, control over animal breeding, and tapping into exchange networks.

There are many reasons why pastoralists should choose to be mobile, and anthropologists have struggled to identify commonalities among the diversity of nomadic groups in pursuit of a generalizable theory (Dyson-Hudson 1980; Dyson-Hudson and Dyson-Hudson 1980). Mobility is and has historically been a critical component of pastoral subsistence and has played a key role in shaping migration and settlement patterns and social

organization of modern cultural and linguistic groups in East Africa (Dyson-Hudson 1980; Dyson-Hudson and Smith 1978; Galaty 2021). Pastoral mobility solves seasonal pasture limitations, and movement patterns and herding decisions vary with inter-annual differences in precipitation. For instance, the localization of rainstorms could mean that a herder travels thousands of kilometers in one year and only a few hundred kilometers in the next (Dyson-Hudson and Dyson-Hudson 1969).

During an extremely severe drought from 1979 to 1981, only 150 mm of rain fell. This situation made some Turkana cattle herders take more risks in certain aspects of herding while being more cautious in others. In response, Turkana herders were observed driving herds into enemy territories (i.e., increasing the risk of theft) and expelling individuals from the community (reducing labor availability) but reduced grazing pressure by dividing livestock into smaller herd sizes (Dyson-Hudson and McCabe 1985). Herder movement patterns also reflect the degree to which communities rely on agriculture and the availability of labor. In eastern Uganda, the Karimojong people have specific roles for men and women. Men are responsible for herding animals, while women mostly handle farming. Women prefer to stay close to settlements, especially when pregnant because moving long distances with herds can be challenging. Staying near homes also helps protect them from violent encounters with neighboring tribes (Dyson-Hudson and Dyson-Hudson 1969).

Another strategy used among some Rift Valley pastoralist groups is mixed-species herding, and herders decide about herd compositions based on the different advantages of keeping camels, cattle, and caprines. Due to the spatial and temporal variability of precipitation in the Rift Valley, camels are highly valued among some pastoralist groups because they are less susceptible to drought conditions. During the severe drought from

1979-1981 camel losses were much smaller cattle and caprines (McCabe 1987). Additionally, camels primarily consume shrubs and woody plants, which retain green biomass longer into the dry season than the types of forage consumed by caprines and cattle. Camels are, therefore, more capable of providing a steady source of milk throughout the year. For example, 80% of the food energy obtained by the Ngisonyoka people of the Turkana tribe in northwest Kenya annually comes from milk, and more than half of that is camel milk (Coughenour et al. 1985). Cattle milk, on the other hand, is only available during the wet season when herbaceous plants are growing, but meat and blood obtained from goats and camels provide a vital source of energy when milk is in short supply (Coughenour et al. 1985: 622).

To understand how East African herders make decisions about herd composition to cope with uncertainty stemming from the frequency and severity of drought, Mace and Houston (1989) devised a stochastic dynamic programming model to predict the proportion of goats and camels expected to minimize the risk of a household failing to meet its subsistence needs. The simulation assumed that the optimal mix is the one that promotes the household's long-term viability. Based on empirical data on the effects of drought on different livestock species (McCabe 1987), the model parameters aimed to treat small-stock as the risk-prone option since goats have high reproduction rates but are more susceptible to drought (high variance, high mean) and camels as the risk-averse alternative with slower reproduction and growth rates but higher drought resistance (low variance, low mean; Mace and Houston 1989). The simulations reveal that the optimal herd composition depends on household wealth, with impoverished households preferring to accumulate risk-prone small-stock before exchanging these animals for risk-averse camels. In contrast, more wealthy

households focus more heavily on low-variance large-stock. The accuracy of these simulations was demonstrated in the herd structures of pastoral communities in Somalia, Niger, Mali, Sudan, and Kenya (Mace 1990).

Mace then used the same approach in a different model, considering whether to invest household wealth into cultivation and whether to maintain wealth as the number of cattle held, stored grain, or some combination thereof (Mace 1993a: 365). Despite crop yields being unpredictable from one year to the next and more susceptible to drought than cattle, impoverished households are more likely to recover by investing resources towards cultivation than focusing only on herding; combining farming and herding enables longer-term survival (Mace 1993a). Thus, lacking the means to implement preventative strategies, impoverished households are expected to rely on responsive measures to minimize risk. In the case of East African pastoralist communities, response to loss takes the form of greater dependency on a triangular exchange network of herders, farmers, and hunter-foragers that developed over millennia (Galaty 2021).

Another risk buffering strategy East African pastoralist groups employ is restricting sheep and goat breeding activity. In northern Kenya, the Gabbra, a pastoralist community, deliberately restrict male access to female sheep, a practice deeply intertwined with notions of wealth and social status within their culture. Conversely, when it comes to goats—animals known for their remarkable resilience to drought—this careful management of breeding is rarely observed (Mace 1993b: 330). Unrestricted breeding in goats may be less of a liability because of a tendency for larger litter sizes and higher drought tolerance (Dahl and Hjort 1976).

Strategies for controlling breeding could involve grazing males and females separately and dividing sexes into different enclosures (as practiced by the Gabbra; Mace 1993b) or using contraceptive devices. For example, the Masai in east Africa fit males with an apron and the Targui in north and west Africa use a 'kunan' to restrict the function of the male apparatus (Wilson 1989). A side effect of controlling breeding is that primiparous females can physiologically mature before experiencing metabolically high costs of pregnancy and nursing (Wilson 1989), which may reduce the risk of abortion (Mellado et al. 2006).

Aside from ensuring herd nutritional demands will not exceed pasture resources, controlling sheep breeding by keeping females separate until they are close to giving birth can increase the interbirth interval by up to four months (Dahl and Hjort 1976; Wilson 1985). Delaying the time to re-impregnation may also extend the length of lactation (Mace 1993b: 330) to the benefit of herders focused on dairy production. On the other hand, Wilson (1989) notes that total lifetime production of goats is better than sheep; control over breeding restricts the reproductive potential of small-stock, which comes at the expense of overall herd productivity in the near-term. Mace (1993b) found that among the Gabbra, poor herders permitted unrestricted sheep breeding while wealthy herders opted for the risk-averse option of limiting sheep breeding. Conversely, the Karimojong maintain significant herds of both male and female cattle, placing greater importance on obtaining blood and milk rather than focusing on meat production. Additionally, retaining unproductive animals, such as barren females, helps to transform the available forage into food for human consumption (Dyson-Hudson and Dyson-Hudson 1969).

To summarize, pastoralist communities like the Maasai, Turkana, Somali, and Borana in East Africa face increasing drought and desertification, driving them to adopt strategies like mobility, herd diversification, and managing herd growth to survive. Mobility is a spatial and temporal diversification strategy East African pastoralists use to minimize the risk of losing herds to seasonal pasture shortages. However, the spatial scale of herder mobility and movement patterns can fluctuate depending on the severity of conditions, availability of labor, and the extent to which extensive herding is compatible with the goals of other subsistence activities (i.e., farming). In the arid Rift Valley, pastoralists value camels for their drought resilience and ability to provide milk year-round, unlike cattle, which are productive only in wet seasons. Decisions about herd composition often balance short-term advantages of high-risk, fast-reproducing animals like goats and slower-growing but drought-resistant camels to minimize subsistence risk. Some groups also practice controlled breeding to ensure long-term herd stability and optimize resource use for dairy and blood production, though this may reduce immediate productivity. Such preventative strategies lower risk but may only be accessible to wealthy (Mace 1990; 1993a; Mace and Houston 1989). Conversely, maximizing herd size increases the risk of straining resources, but herders could slaughter caprines or sell off high-value camels in response to an unpredictably severe drought. This action would lower the household's wealth and restrict its ability to recover from losses. However, poorer households may then turn to farming as a viable means to reduce variance and slowly recover from destitution even when livestock productivity is limited.

2. The Andes Mountains

The Andes mountains exhibit a pronounced environmental gradient, with distinct micro-climates in isolated valleys that span significant altitude variations. Rainfall and

temperature, pest infestations, theft, and crop diseases vary in severity and are unpredictable from one micro-environment to the next (Brush 1976). Additionally, land privatization and development projects arising from rural population growth have increased water consumption and land fragmentation, leading to severe overgrazing in parts of the Central Andes (Browman 1987; Verzijl and Quispe 2013). These anthropogenic modifications to natural hydrological systems have exacerbated the effects of receding glaciers in the tropical Peruvian Andes over the last 40 years by delaying the start of the rainy season and increasing drought frequency (Mark et al. 2010). Andean herders and farmers employ diversification strategies to cope with spatial and temporal variability. For farmers, these strategies include crop diversification and field scattering, while herders have the advantage of being mobile.

Andean farmers utilize various cultivars specially adapted to a range of altitude zones and use their knowledge of how various crops will perform under different conditions to adapt to micro-environmental variability dynamically (Guillet 1981). For example, small-holder subsistence farming communities of Cuyo Cuyo in the Peruvian Andes cultivate at least 65 varieties of potatoes in addition to maize, beans, squash, and other crops across nearly 500 individual fields, which effectively reduces variance in yields despite higher travel and transportation costs (Goland 1993a,b). This approach is known as field scattering and entails the use of spatially distributed cultivation areas, which may vary based on their size, suitability for one or more cultigens, and distance from the settlement (Bentley 1987; Goland 1993b; Halstead and O'Shea 1989; McCloskey 1976; 1991).

Farmers integrate this spatial diversification strategy into a complex sectoral fallowing system prevalent in the eastern and Central Andes (Orlove and Godoy 1986). Fallowing refers to leaving a field open and free of cultivation to let the soil recover from

nutrient loss to crops. In the context of Andean agriculture, there are four main advantages to fallowing: (1) regrowth of native plants in the fields protects them from erosion; (2) deep-rooted perennial grasses draw nutrients from deeper in the soil to the surface, making them more accessible to shallow-rooted crops; (3) reincorporation of organic matter into the soil improves water retention potential; and (4) when herders use fallow fields for grazing, animal dung deposits nutrients from fields and pastures located in different elevations Andes (Orlove and Godoy 1986: 178). Therefore, the fallow field system in the Andes is a preventative strategy that provides farmers with some insurance that soil health will be maintained while also supporting the mutual dependence of agriculturalists and pastoralists.

In the Central Andes, specialized camelid herding is primarily practiced above 3,700 masl in the highlands known as the *puna* or *altiplano* and has historically been the most important region for pastoralism in South America (Westreicher et al. 2007). The domestication of South American camelids began approximately 6,000 years ago, leading to the emergence of societies specialized in herding llamas and alpacas (Diaz-Maroto et al. 2021; Wheeler 1995). In the 17th century A.D., the Spanish introduced sheep, goats, and cattle. However, these species are not well-adapted to high altitudes, and productivity is generally lower than when caprines and cattle are herded in lowland areas (Westreicher et al. 2007).

Variations in the rates of reproduction, product output, and adaptability of different animal species to various elevation zones in the Andean environment significantly influence the choices that individual herders make concerning the species and their proportions in husbandry. For example, Kuznar (1991) examined optimal herd composition among the indigenous Chinchillape community of Aymara-speaking herders in southern Peru, located in

the high *puna* zone (4500 masl). The model predicted that herds should be dominated by alpacas and a smaller number of llamas and sheep and cattle were so unproductive under the constraints that they should be excluded. Kuznar also determined that a family raising only 75 alpacas could survive by selling wool and dung, while the poorest Chinchillape households owned an average of 123 animals. This discrepancy suggests that Aymara herders pursue a maximizing strategy, allowing for surplus production. Additionally, the Aymara herders also rely on sheep and cattle despite their low productivity, which suggests that the benefits of mixed-species grazing for pastures (Anderson et al. 2012; Rocha et al. 2008; Walker 1994) may be realized in the *punas* (Browman 1997).

Transhumance is a vital aspect of pastoralism in the Central Andes, and llama and alpaca herders have exploited high-altitude grasslands (i.e., *punas* or *altiplano*) on a seasonal basis for centuries. This form of vertical transhumance alternates between perrenial grasses in the lowlands during the rainy season (November to March) and permanent pastures in upland areas in the dry season (April-October; Westreicher et al. 2007: 94). These permanent upland pastures located in the *altiplano/puna* elevation zone are found in highly productive wetland patches known as *bofedales.*

Development projects rerouting *bofedal* spring water and climate change, leading to increased freezing events and greater seasonal variability, threaten herding communities dependent on these productive upland oases (Mark et al. 2010; Verzijl and Quispe 2013). To minimize the risk of *bofedal* deterioration and, by extension, lower herd productivity, pastoral communities organize access and share the responsibility of constructing and maintaining irrigation canals to ensure *bofedales* remain productive (Browman 1987: 184; Verzijl and Quispe 2013). Herding communities carefully schedule access to *puna* grasslands

to prevent overgrazing, reducing pasture productivity variance. Meanwhile, irrigation of *bofedales* is an intensification strategy in which increased investment in the land serves as a preventative measure to buffer against periodic drought (Guillet 1987).

Transhumant herders based in the high-sierra elevation zone (i.e., below the *altiplano*) of the Asana Valley focus primarily on goat husbandry in addition to smaller numbers of sheep and cattle (Kuznar 1991). The schedule of movements is similar to that of camelid herders in the *altiplano*, but the livestock grazed at lower elevations. The primary hazard faced by Asana Valley herders is unpredictable precipitation, followed by theft and predation (Kuznar 1991). Asana herders have reported losses of 60% of the herd to severe drought and up to 20% of the herd to theft. To mitigate these risks, herders (1) prefer goats owing to their high prolificacy and flexible diet; (2) move herds to different grazing areas; and (3) use a specialized slaughter strategy. This strategy generally aims to maximize herd sizes during years when precipitation levels are normal. When herders perceive reduced rainfall as evidence of a drought, they increase the culling rate to reduce the size of the herd (sometimes up to 50%) to a level sustainable by the grazing resources available to the household. Under this approach, excess forage only occurs when the herd size is recovering from destocking (Kuznar 1991: 102).

Aside from transhumance, another diversification strategy employed by Andean households is integrating market-oriented with subsistence-oriented production (López-i-Gelats et al. 2015; Valdivia et al. 1996). Dung is an essential resource in the harsh *altiplano* environment. Dung improves the aeration and moisture of poor soils to promote crop growth and provides a highly efficient fuel source for cooking and heating (Winterhalder et al. 1974). For many Andean herders, selling milk, meat, hides, and dung from sheep, goats,

llamas, and alpacas is vital for accumulating wealth and acquiring agricultural products (Valdivia et al. 1996). Selling these animal products is a way of diversifying for Andean pastoralists but is contingent on maximizing the number of animals in their herds (Browman 1997: 30).

Within the integrated farmer-herder exchange network in the Central Andes, the ways in which households minimize risk depend on access to land, labor, and livestock (López-i-Gelats et al. 2015). For example, Kuznar (2001) examined risk-sensitive decision making among two Aymara herding communities: one in the high-sierra (2500-3800 masl) focused on raising goat, sheep, and cattle primarily for meat production, and a second in the *puna* (3800-4500 masl) concentrated on alpacas and llamas. Each community faces different challenges. Herds in the high-sierras are vulnerable to theft, and rainfall predictability is 50%. Conversely, snow is the most significant hazard for the *puna* community, which utilizes domestic camelids for transportation and for meat and wool, which herders exchange for agricultural produce. Kuznar observed that high-sierra herders were much more risk-averse than the *punas* herders and attributed this difference to greater environmental variability in the high-sierra zone (2001: 438).

It is important to recognize that the risk-buffering strategies used by Andean herders and farmers are often complementary. For example, in the village of Uchucmara in the Peruvian Andes, production is at sufficient levels for the community to be self-sustaining, but a minority of households have direct access to all production zones, and reciprocity networks are therefore critical for enduring times of scarcity (Brush 1976; 1982). While integrating market-oriented strategies does provide a means for households to diversify (López-i-Gelats et al. 2015), the ability to do so is often conditioned by the household's access to land, labor,

and livestock (Kuznar 2001; Valdivia et al. 1996). For some, such as the Cuyo Cuyo community, the efficacy of such alternative measures of reducing risk (e.g., via exchange or external sources of income) is limited, may only be effective in the short-term, and can be made inaccessible by the same environmental hazards individuals or households are trying to cope with (Goland 1993b: 335). Overall, these examples of Andean diversification strategies illustrate how transhumance may be an integral component of broader social and economic relationships between agriculturalists and pastoralists.

3. The Balkans

The remaining examples of risk-minimization strategies reference herding and farming communities in the Balkans, with particular attention paid to agropastoral adaptations in Greece and transhumant pastoralists on Croatia's Dalmatian Coast. These regions have a sub-mediterranean climate with hot, dry summers and cold, rainy winters. Drought conditions are prevalent in the summertime and unpredictable with respect to severity and duration (Chapman et al. 1996; Halstead 1990).

Ethnographic research in the late 20th century on farming and herding communities in Greece has provided anthropologists with valuable insight into risk minimization strategies used within traditional agropastoral subsistence systems (Halstead 1987; 1990; Halstead et al. 1998; Koster 1977). Pastoralism in Greece today takes the form of both intensive husbandry and transhumance. Production is oriented towards selling meat and milk, with changes in market value driving the emphasis on either product (Halstead 1998b; Koster 1977; Ragkos 2022). Frost and dry wind are among the main hazards faced by farmers. However, drought is the most prevalent concern throughout Greece, including the semi-arid lowland regions in the south and east of the country as well as for agropastoralists in high altitude zone of the

Pindos mountains located in the wetter northwest (Halstead 1990: 147). To cope with the patchiness of drought and other hazards, farmers in Greece engage in a variety of diversification strategies such as sowing multiple types of crops (i.e., crop diversity) and cultivating within a dispersed tenure field system (i.e., field scattering; Halstead 1990; Halstead and Jones 1989; Jones and Halstead 1995).

On the islands of Amargos and Karpathos, farmers use field scattering as a partial defense against pest infestations, which vary in severity from one field to the next (Halstead and Jones 1989). Agricultural production relies heavily on animals for the transport of labor, seed, and harvested yields, as well as for plowing (Halstead 1987: 84). On these islands, farmers also plant a range of crops with different schedules of water and human labor requirements. This approach distributes resources along a broader temporal range (Halstead and Jones 1989). These spatial and temporal strategies are complemented by sowing wheat-barley and common vetch-grass pea maslins (i.e., deliberate grain mixtures). Maslins reduce the risk of loss in two important ways. First, sowing wheat-barley maslins exploits the opposing optimal growing conditions of wheat (a drought-sensitive crop) and barley (a drought-resistant crop) such that limited production in one grain often accompanies superb results for the other (Jones and Halstead 1995: 111). Secondly, maslins allow for flexibility in how farmers use yields. Vetch-pea maslins combine livestock preference for grass pea with the pest resistance found in common vetch. Barley mainly serves as feed for livestock, yet bread created from a wheat-barley maslin can be eaten without breaching cultural standards regarding acceptable human food (Halstead and Jones 1989: 51; Jones and Halstead 1995: 111). Maslins are, therefore, multi-purpose, functioning to reduce the risk of

human and livestock starvation and provide an excellent example of how livestock convert agricultural yields to "live storage" (Flannery 1969).

The history of pastoralism in Greece is deeply rooted, evolving from early nomadic and semi-nomadic practices to today's modern (i.e., post-World War II era) transhumant systems (Gidarakou and Apostolopoulos 1995). A distinction can be made between these classifications of pastoralism. Nomadism involves the continual movement of herds with residential flexibility, whereas transhumance refers to seasonal movements between two or more fixed areas of habitation (Moudopoulos-Athanasiou et al. 2022). Nomads generally specialize in herding and depend on exchange systems, but agriculture tends to be more integrated into subsistence in transhumant systems (Chang 1993). Initially, Neolithic sheep and goat herding was intensive and closely integrated with agricultural production at a scale sufficient for household subsistence (Halstead 1989; 1996). With the rise of city-states, nomadic and semi-nomadic tribes dominated but later shifted to extensive grazing during the Byzantine period (ca. 1,600 - 600 years ago). Under Ottoman rule (ca. 600 – 250 years ago), nomadic and semi-nomadic herders migrated freely throughout the entire Balkan region, and the *tsiflikia* system provided large estates with grazing fallow fields in crop rotations (Gidarakou and Apostolopoulos 1995). Seasonal migrations between the Pindos mountains and lowland areas became common at this time. Nomadic pastoralism declined sharply after the *tsiflikia* system ended in 1922, reducing winter pastures and forcing herders to reduce flock sizes (Hadjigeorgiou 2011). World War II further limited grazing land, and many herders responded by purchasing land and establishing permanent residences near lowland fields (Gidarakou and Apostolopoulos 1995; Halstead 1998a; Koster 1977). Social, cultural, and economic pressures such as population growth, land ownership changes, and

administrative policies shaped the development of various herding systems (Hadjigeorgiou 2011).

Within the context of modern agropastoralism in Greece (i.e., intensive mixed-farming and seasonal transhumance), some communities cope with economic uncertainty stemming from the milk and meat market and persistent climatological risks (i.e., drought and frost) by integrating traditional strategies within modern production systems. This was demonstrated among 20th-century agropastoralists in the village of Didyma in the Argolid region of Peloponnese in northeastern Greece. Farmers there divided individually owned fields into two sectors, one used to plant crops and the other left fallow, used for grazing by sheep and goats. This practice, similar to the segmentation of land under the *tsiflikia* system, concentrates dung deposition into fields and provides a cost-effective alternative to chemical fertilizers (Koster 1977: 166).

The winter period (October 1 through May 31) is the most critical season for sheep and goat herders in Greece because during this period, ewes and does have recently mated, and herders must ensure that their animals have enough food during gestation and lactation (Koster 1977; Nitsiakos 1985). At the onset of the winter period, Didyma herders and their animals descend from the Pindos mountains. Some herders build enclosures at different altitudes. Herds are moved between these structures to exploit several micro-environments that vary with respect to pasture quality and the severity of cold, wet, and sometimes windy winter conditions (Koster 1977: 176–178). These structures were vital to protecting animals from the cold, which can negatively impact milk production (Halstead 1998b; Koster 1977).

The abolishment of *tsiflikia* drove many nomadic and semi-nomadic herders to relocate to lowland habitations and rely on Pindos mountain vegetation only during the

summer (Gidarakou and Apostolopoulos 1995). However, some Pindos communities remained and adapted the husbandry of their modestly sized livestock herds to overwintering the challenging mountain environments. One example is the village of Plikáti located 1240 masl on the southern slope of Mt. Grámmos. Some households abandoned transhumance after land reforms made it difficult for herders to access lowland winter grazing areas (Halstead 1998a). Plikáti herders downscaled herding activities and intensified crop production. The limited scale of cultivation was sufficient for the household's needs but restricted the amount of fodder produced (Halstead 1998a). In response to cultivation activities centered close to residences and the pressure of becoming more sedentary, Plikáti herders became more sedentary, keeping their animals in stalls from January to April rather than moving animals to lowland pastures that were, until recently, reserved for their community's herds. In the winter, up to 1.5 m of snow covers mountain pasture grasses. To keep their animals from starving during the winter, Plikáti villagers collected grassy hay from nearby pastures during the summer, and leafy hay from drought-resistant tree species found in the surrounding sub-montane forests as well as deciduous oaks (e.g., *Quercus sp.*) from lower altitudes (Halstead 1998a; Halstead et al. 1998).

Not all nomadic communities in Greece completely abandoned mobile strategies, however. The Sarakatsani and Vlach are the only two remaining transhumant or nomadic sheep and goat herding communities to have endured the major social and economic restructuring of the 20th century (Chang 1993; Nitsiakos 1985). Sheep milk is a major source of income for Vlach pastoralists and much of the preparations for the milking season occur during the winter period aim to maximize milk yields. Vlach herders benefit from concentrating the lambing season for a short period because milking is a labor-intensive

activity. Herders aim to control breeding to ensure that most lambs are born over a few days, but often, two lambing seasons result from early females failing to mate successfully. Shepherds capitalize on this by marketing the sale of lambs at both Christmas and again at Easter (Nitsiakos 1985: 38).

Contemporary herders in Dalmatia faced similar hazards. Sheep and goat herding was the region's economic backbone from as early as the Roman period into modern history (Belaj 2004; Forenbaher 2007). The earliest prehistoric evidence for transhumance in Dalmatia comes from archaeological research of Late Bronze Age settlements in Lika, the hinterlands immediately east of the Velebit mountain range (Forenbaher 2007; 2022; Zavodny et al. 2019). Until the mid-20th century, this form of pastoralism was central to Dalmatia's economy, social organization, and household subsistence. For example, at its peak in the second half of the 19th century, as many as 100,000 sheep and goats grazed the pastures of the Velebit (Forenbaher 2007).

Differences in the timing of herd movement, settlement structure, and division of labor existed between three groups depending on the location of fixed bases (Marković 1980; 1987; Nimac 1940; Perišić 1940). For example, Lowland Dalmatians inhabited the plains of the Ravni Kotari, a peninsular landmass of the northern Dalmatian Coast and organized companies that were internally hierarchical and mostly comprised of men (Nimac 1940). In the summer, the companies organized by Lowland Dalmatians ferried their herds north and eastward across deep Adriatic inlets to the shores below the Velebit and then drove the animals directly to the summit, where they remained until fall (Marković 1980; Vinšćak 1981).

Meanwhile, littoral shepherds and their families who lived at the base of the Velebit on the coast during the winter made short, step-wise movements to higher-altitude pastures beginning in the spring. Littoral groups also made use of rudimentary structures called *bunja* and caves to protect their animals from the elements during their ascension and descent in the spring and late summer, respectively (Marković 1980). Shepherds from the littoral had three permanent settlements. One was close to the sea, occupied during the winter months. A second village approximately 800 masl was used from spring to autumn where littoral communities cultivated barley and potatoes and collected hay to fodder their animals (Belaj 2004). Finally, a third, summer settlement was located under the peaks of the Velebit (Belaj 2004). Domiciles at high altitudes were comparable in structural quality to those at the Velebit's base (Nandris 1999). When it was time to move from the base up to their houses up the Velebit, the entire household would make the trip carrying everything they needed for the summer (Perišić 1940). Some of the littoral group's herds reached the summit by late summer only to descend in early September at which point they carried hay collected from the mountain down to their winter residences (Belaj 2004).

Finally, shepherds based to the east of the Velebit range, in Lika, inhabited highlands of approximately 600 masl. Lika does not experience the same drought conditions as Dalmatia. For these populations, transhumance was primarily motivated by the need to protect crops from animals during the summer, during which time they collected mountain hay (Marković 1980; Vinšćak 1981). The journey to the Velebit was much shorter in distance and duration for the people of Lika, allowing them to bring only necessities. When the Lika herders departed high pastures in mid-summer, those pastures became available to littoral groups (Marković 1980). The scheduling of these groups' use of high-altitude pastures was

not always an organic or coincidental coordination of pasture use without conflict. Instead, these pastoralists followed a system set up by the Austro-Hungarian authorities in the 19th century AD that detailed how to use the land to avoid arguments over grazing access (Belaj 2004; Vinšćak 1981).

Risk-minimization strategies in the Balkans are closely tied to agropastoral practices, especially in Greece and along Croatia's Dalmatian Coast. In Greece, farmers contend with drought and other climatic challenges through crop diversification and field scattering, which reduce risk by spreading investment in agricultural activities across varied landscapes (i.e., lowland and mountain areas) and crop types. On islands like Amorgos and Karpathos, farmers sow maslins to balance different crop needs and nutritional outputs, benefiting both humans and livestock. Historically, pastoralism in Greece and Dalmatia adapted to social and political changes. These traditional risk-management techniques, influenced by environmental and political contexts, showcase the resilience of agropastoral communities in the Mediterranean.

E. Summary

This chapter began by defining the theoretical framework of risk used in the present research to understand prehistoric pastoral strategies. Additionally, this chapter provides a review of farming and herding strategies used by various agropastoral societies across a range of environments. The diversity of risk-buffering tactics shown in these cases relates to the species of livestock managed, the various strategies employed, and the differing perspectives of risk. Although camelid, cattle, and caprine pastoralists discussed have adapted to unique conditions in East Africa, Andes, Greece, and Dalmatia, herders in these

regions have in common the ability to diversify in response to environmental hazards and to prevent losses amidst expected seasonal fluctuations in precipitation and temperature.

Two opposing perspectives of risk stemming from resource availability and herd size were presented. Among the Gabbra, managing herd sizes prevents the overuse of limited dietary resources, and risk-averse strategies limit the extent to which livestock dietary resources *might* be strained by curtailing their herds' growth. In the Andes, Greece, and Dalmatia, this is achieved through mobility, though fodder is also critical for maintaining livestock diet in Greece. Andean pastoralists also aim to maximize herd size to maximize capital from livestock products but rely on social and economic networks, leveraging reciprocity and redistribution to pool land, labor, and resources during times of scarcity (Cashdan 1985; 1990; Winterhalder 1986). These practices, often supported by communal systems of resource sharing, help maintain food security despite fluctuating environmental conditions.

In Greece, agropastoralists engage in diversification strategies to mitigate risks from frost, drought, and pests, which are commonly employed as a means to combat pests, suppress weeds, resist lodging and frost, and stabilize yields (McAlvay et al. 2022). For example, the sowing maslins on Amorgos and Karpathos (Halstead and Jones 1989; Jones and Halstead 1995) was also used in Greece during the Bronze Age at the site of Assiros in Macedonia in the form of a combination of emmer wheat and spelt (Jones et al. 1986). Different types of maslins have been recognized as part of farming practices in 27 nations across Eurasia (e.g., Spain, France, Georgia, Pakistan, India and others) and northern Africa (e.g., Ethiopia and Eritrea; McAlvay et al. 2022). Sowing maslins is a flexible preventative strategy because both humans and livestock can consume yields.

Foddering animals with maslins or crop byproducts or permitting animals to graze on stubble from harvested crops or in fallow fields is an essential aspect of mixed-farming subsistence systems. The use of fodder effectively converts agricultural investment into livestock productivity (Halstead 1990). Although this strategy is typically associated with intensive animal husbandry, transhumant pastoralists benefit from penning and foddering their animals during critical periods in the annual cycle of productivity. Examples of this semi-extensive approach were provided (e.g., the Vlach shepherds and goat herders of Didyma). Foddering can also take the form of collecting forage resources that farmers can reserve for periods of scarcity. Winter foddering was a common practice at Plikati in Greece (Halstead 1998a; Halstead et al. 1998), among mixed-herding peasant communities in 19th century Sweden (Slotte 2001), and contemporary shepherds in the desert-steppe of the Gobi Desert in Mongolia (Makarewicz 2014). Foddering of livestock has also been identified archaeologically across a variety of Neolithic cultures within a wide range of environmental contexts, from the Chasséen in France (Balasse et al. 2012a), to the Pfyner culture in Switzerland (Rasmussen 1989), to the Linearbandkeramik phase in Germany (Berthon et al. 2018).

Transhumance is a common feature of Mediterranean pastoral systems (Bindi 2022). Various forms of pastoral mobility have been practiced in the southern and Balkans for thousands of years (Gidarakou and Apostolopoulos 1995; Halstead 1987; Isaakidou et al. 2019; 2022). Even as its prevalence has waned in recent decades, its continued practice is a testament to its efficacy as a risk-buffering strategy and its resilience to changing social and political conditions. The resilience of transhumant pastoralism may be credited to the organization of communities around the economic and subsistence goals shared among

households. Traditional systems of grazing land partnerships such as the *tsegliata* in Greece (Gidarakou and Apostolopoulos 1995) and self-organized use of common pastures among different, sometimes rivaling herding communities in the Velebit mountains (Belaj 2004; Marković 1987; Vinšćak 1981) allowed for coordinated movement between mountain pastures and lowland fields. Though primarily shaped by herders adapting to environmental hazards, these systems were also shaped by government policies that designated specific regions for pasture use. While social contracts such as these may be invisible to archaeologists, evidence of highly mobile pastoral strategies is not. Transhumance was practiced by Neolithic groups in Italy (Varkuleviciute et al. 2021), the Pyrenees (Knockaert et al. 2018), and Turkey (Makarewicz et al. 2017). The highly mobile nature of transhumance suggests that inter-group arrangements, conflicts, and exchange networks were fundamental components of ancient herding communities, as they have been in the recent past.

This chapter highlights how environmental, social, and political factors interact in traditional pastoralist risk-sensitive decision making. The primary focus of this chapter was to demonstrate various strategies for diversification and intensification in agropastoral systems. The examples presented in this section are restricted to a limited set of diversification strategies most pertinent to the current research. These include strategies for controlling herd size, integrating livestock grazing into cultivation areas, provisioning and collecting fodder, and mobility. These tactics are distinct in how they are exercised across cultures but are generally employed to respond to and prevent subsistence failure. In the following chapter, I describe the environmental and archaeological context in which similar herding strategies are expected to have developed in Dalmatia 8,000 years ago.

III. Archaeological and Environmental Setting

A. Overview of the Neolithic in Southeast Europe and the Eastern Adriatic

Agriculture originated in the Near East (i.e., the region comprising Mesopotamia, Anatolia, and the Levant) following processes of domestication of key founder crop (emmer, einkorn, and pulses) and livestock species (sheep, goats, pigs, and cattle) beginning around 11,500 cal. BP (Zeder 2011). A well-developed knowledge of seafaring technology and navigation, evidenced by 10,500 year-old villages on Cyprus resembling construction techniques associated with aceramic Neolithic phases in Anatolia (Vigne et al. 2012) and long-distance import of central Anatolian obsidian into Crete (Şevketoğlu 2008), facilitated the introduction of agriculture into Europe. Multiple competing mechanisms of diffusion have been proposed to explain this process (Bocquet-Appel et al. 2009; Bocquet-Appel and Naji 2006; Özdoğan 2011; Zvelebil 2001). However, current archaeological evidence indicates the colonization of the Aegean islands and continental Greece by agricultural societies emanating from southern Anatolia was completed through a piecemeal, step-wise process (Horejs et al. 2015; Perles 2003; Reingruber 2011).

Neolithic groups arrived to the southern Balkans by both land and sea from ca. 8600 cal. BP and integrated with indigenous hunter-gatherer populations (Battaglia et al. 2009; Özdoğan 2011; Perles 2003). The southern Aegean islands (e.g., Crete) received the first

agriculturalists, followed by Thessaly as early as 8500 cal BP, as evidenced by radiocarbon dated deposits from Franchthi Cave in the Argolid region of Greece (Perlès et al. 2013) and the deepest strata of the tell at Dikili Tash in eastern Macedonia (Lespez et al. 2013). These communities settled throughout the Peloponnese, Thessaly, Greek Thrace, and other parts of the southern Balkans that featured a sub-Mediterranean climate preferrable to the pioneering farming societies (Krauß et al. 2018). Neolithic settlements in Greece, Macedonia, Kosovo, and Bulgaria resemble those in Anatolia and include tells clustered around floodplains in river valleys with highly productive soils for agriculture (Raczky 2015). The earliest farmers in the southern Balkans initially adapted to the new terrain by exploiting a broad range of crops and raising mixed-species herds (i.e., diversification; Ivanova et al. 2018). Further subsistence adaptations are observed following the onset of harsh Balkan winters during a rapid climate change event lasting approximately 500 years (Krauß et al. 2018; Weninger et al. 2014). This included the abandonment of leguminous crops and increased importance of cattle relative to sheep, goats, and pigs, which some authors suggest was a facultative prerequisite for eventual northward migrations into the Pannonian and Carpathian Basins (Ivanova et al. 2018).

Within a few centuries of colonizing the Aegean and southern Balkans, human populations and the agricultural way of life dispersed further into Europe. Some authors suggest this subsequent period of human migration was driven by rapid climate deterioration (i.e., the 8.2 ka event), characterized by a 2-3°C drop in mean annual temperature and pronounced aridity beginning around 8200 cal. BP (Berger and Guilaine 2009; Weninger et al. 2006; 2009). The diffusion of Neolithic groups from the Aegean and southern Balkan peninsula followed two routes into Europe: the *continental* route whereby societies navigated

along the Danube river and its tributaries, and the *maritime* route associated with the *Impressa/Cardial* cultures that colonized Mediterranean coastlines (Bocquet-Appel et al. 2009; Rowley-Conwy 2011).

Farming groups originating in the Thessalian plains of northern Greece followed the continental route into Europe and rapidly advanced northward through the Struma and Vardar river valleys (Kotsakis 2014; Krauß et al. 2018). Radiocarbon dated sites in the Central Balkans indicate these early Neolithic groups penetrated the southern parts of the Great Hungarian Plain in as little as 150 years (Biagi et al. 2005). By around 8000 cal. BP Neolithic agropastoralists associated with the Starčevo-Criş-Körös (SCK) cultural complex settled a vast expanse of southeast and central Europe with epicenters in the Iron Gates (i.e., the section of the Danube River Valley forming the border between Romania and Serbia), Transylvania (Romania), the Tisza valley in the Great Hungarian Plain, and central Serbia (Biagi et al. 2005; Bonsall 2007; Whittle et al. 2005).

SCK subsistence economy resembles some aspects of Early Neolithic cultures in northern Greece and Macedonia but with distinct economic and stylistic differences. For example, SCK farmers cultivated the same cereals that were domesticated in the Near East but abandoned some Mediterranean pulses such as grass pea and chickpea (Bogaard and Halstead 2015). Additionally, while animal husbandry focused more on goats and sheep than cattle, most of the meat consumed was obtained from the latter species (Gronenborn 1999: 145). Milk fats and degraded fatty acids detected in the fabric of SCK ceramics indicates herders relied on processed (i.e., heated) milk on a small scale (Craig et al. 2005). Avoidance of hunting large wild mammals appears to be a characteristic cultural preference of Early Neolithic communities in southeastern Europe (Bartosiewicz 2005; Bogaard and Halstead

2015). Compared to the more permanent and higher-density settlements of the southern Balkans, SCK settlements were more diffuse and expansive (Bogaard and Halstead 2015). Residences were constructed with enough distance between them to allow space for intensive cultivation, and the dispersed settlement pattern was conducive to different and adaptive degrees of mobility (Raczky 2015).

The SCK phase of the Early Neolithic persists until 7500 cal. BP, at which point it is gradually replaced by the Vinča and Linearbandkeramik (LBK) cultures (Gronenborn and Dolukhanov 2013). The Vinča and LBK cultures appear to have evolved out of the later phase of the Starčevo culture in the Transdanubian region, in which significant economic and social changes occurred, largely attributed to population growth (Chapman 1981; Gronenborn 1999). Additionally, interactions between the SCK cultures and indigenous Mesolithic populations led to the adoption and adaptation of farming by local hunter-gatherers, potentially contributing to the development of the LBK (Nikitin et al. 2019; Zvelebil 2001). Vinča sites are generally distributed throughout Serbia, eastern Croatia, and as far north as Lake Balaton in the Carpathian Basin while early LBK sites initially occupy the Transdanubian region and rapidly expand northwest deep into central Europe via the Rhine valley 7300 cal. BP (Dolukhanov et al. 2005; Jakucs et al. 2016). A second expansion of LBK introduced agriculture as far west as the Paris Basin by 6800 cal. BP (Dolukhanov et al. 2005). Vinča and LBK exhibit distinct pottery and settlement traditions. Vinča sites large, more numerous, and are often associated with tells (Chapman 1981; Greenfield 2014; Gronenborn 1999; Raczky 2015) and LBK settlements are generally flat and comprised of post-lined long-houses residences (Gronenborn 1999).

The LBK and Vinča cultural phases are associated with significant changes in

subsistence. Compared to the Early Neolithic, the number of cattle herded increased as did the contributions from hunted large wild game (Bartosiewicz 2005; Bogaard and Halstead 2015). Herding was focused more heavily on cattle than sheep and goats during this Middle Neolithic phase of continental Europe (Orton et al. 2016). This reconfiguration of the pastoral component of subsistence may be a result of herders adapting to the more temperate central European forested environments which are better suited to the browsing behaviors of cattle. Cattle were exploited for both meat and milk, which is reflected by a shift in herder decisions to keep older animals in their herds, leading to higher levels of investment in livestock (Gillis et al. 2017). Additionally, LBK groups began to produce cheese and yogurt, evidenced by the presence of milk lipids on ceramic sieves (Bogucki 1984; Salque et al. 2013).

Around 8100 cal. BP, seafaring agriculturalists from the Aegean followed the maritime route into Europe, and arrived to both coasts of the Adriatic (Bass 1998; Forenbaher et al. 2013). The spread of agriculture in this region is not well understood. However, some of the earliest dated archaeological contexts containing Impresso pottery and domesticated animals come from sites in southeast Italy and southern and central Dalmatia (Forenbaher and Kaiser 2000; Forenbaher and Miracle 2014; McClure et al. 2014; Miracle and Forenbaher 2005; Skeates 1994). The Impresso culture is found widely throughout the Mediterranean basin (Binder et al. 2017; Capelli et al. 2017; Kačar 2019; Manen et al. 2019). In Italy, dense concentrations of Impresso settlements are found in Apulia along coastlines of the Adriatic and Ionian seas (Whitehouse 1970) but only appear north of the Pescaro River after a delay of approximately 1000 years (Pluciennik 1998). On the opposite coast, open-air villages were progressively established in prime agricultural zones, particularly on the Ravni

Kotari coastal plain of Northern Dalmatia (Figure 3.1; Forenbaher and Miracle 2005; 2014). Radiocarbon dated sites spanning the Eastern Adriatic suggest that this process of initial colonization and settling in open-air contexts lasted approximately 500 years (Forenbaher et al. 2013).

Impressed-ware pottery is decorated with indentations made by fingers, fingernails, marine shell (*Cardium*), and other objects but there are inter-regional differences in style such that the Dalmatian and Italian traditions can be distinguished. Evidence for trans-Adriatic contact between both coasts exists as the presence of Liparian obsidian and Tavoliere flint in Dalmatia, though pottery was undoubtedly produced locally (Spataro 2002). This exchange network made use of an archipelago of islands stretching across the southern Adriatic (Bass 1998; Della Casa et al. 2009). Radiocarbon dated cave and open-air village sites associated with Impresso ceramics span from approximately 8000 to 7400 cal. BP (Forenbaher and Miracle 2005; 2014; McClure et al. 2014).

Within 400-500 years of the arrival of Impresso communities, the Danilo ceramic tradition appeared in Dalmatia, marking ~7400 cal. BP as the beginning of the Middle Neolithic in this region (Batović 1966; Korošec 1958; Legge and Moore 2011; McClure et al. 2014; McClure and Podrug 2016; Spataro 2002; 2009). Hvar type pottery appears around 7000 cal. BP and although approximately 30 Late Neolithic open-air sites have been identified, only two have been excavated (Batović 1966; Horvat Oštrić and Triozzi 2024b; McClure et al. 2014; McClure and Podrug 2016; Podrug 2010).

Neolithic communities in Dalmatia practiced intensive mixed-farming involving small-scale herding of primarily sheep and goats (Legge and Moore 2011; McClure et al. 2022; McClure and Podrug 2016; Sierra et al. 2023), cultivation of einkorn (*Triticum*

monococcum), emmer (*Triticum dicoccum*), barley (*Hordeum vulgare*), flax (*Linum usitatissimum*), grass pea (*Lathyrus sativus*) and collection of wild fruits (Moore et al. 2019; Reed 2016; Reed and Colledge 2016; Reed and Podrug 2016). On rare occasions, millet (*Panicum miliaceum*) has also been recovered (Moore et al. 2019). Sheep and goat remains dominate zooarchaeological assemblages while cattle and pig bones comprise a smaller proportion (McClure and Podrug 2016; Moore et al. 2019) of domesticated species, which is a pattern typical of coastal Mediterranean Neolithic sites (Orton et al. 2016). Roe and red deer, hare, wild boar, and chamois were also hunted but wild game and fish contributed minimally to subsistence (Guiry et al. 2017; McClure et al. 2022; Radović 2009; 2011; Schwartz 1988).

Analysis of lipids on Impresso ceramics indicate Impresso groups exploited sheep and goats for milk (McClure et al. 2018). A long-enduring tradition of milk production originating in Anatolia from 9000 cal. BP (Evershed et al. 2008) was likely critical for the successful maritime-driven colonization of the Adriatic coasts by Impresso groups who emanated from the area (Rowley-Conwy 2011). Recent work has determined that herders at two of the earliest open-air *Impresso* settlements in Dalmatia, Crno Vrilo and Tinj-Podlivade specialized in sheep husbandry (Sierra et al. 2023). The preference for sheep over goat may be related a combination of the animal's social value, higher nutritional values of the species relative to goats, environmental suitability, and ease of transport (Sierra et al. 2023). Sheep, in addition to goat husbandry was nonetheless central to subsistence at other Impresso and Danilo period open-air sites such as Pokrovnik and Smilčić (McClure and Podrug 2016; Moore et al. 2019; Moore and Menđušić 2019; Schwartz 1988). Although less is known about subsistence at Late Neolithic open-air settlements, caprines continue to dominate Hvar

period faunal assemblages (McClure et al. 2022). Wild and weedy plant species recovered from burnt dung in Hvar period contexts at Turska Peć suggest farmers also sowed fields for grazing in addition to growing fodder crops (Reed 2015; 2016).

Impresso and Danilo ceramics have long been reliable markers for distinguishing Early (8000-7400 cal. BP) from Middle Neolithic (~7500-7000 cal. BP) archaeological deposits (Batović 1966; Spataro 2002; 2009). The Early-Middle Neolithic transition occurred gradually, with Danilo ceramic vessels slowly replacing Impresso wares in Dalmatia over the course of about a century (Forenbaher et al. 2013; Forenbaher and Miracle 2005; Horvat 2017; Korošec 1958; Legge and Moore 2011; McClure et al. 2014; Spataro 2002). This transition is not well understood. However, differences between Early and Middle Neolithic subsistence economies have recently come to light via lithic (Mazzucco et al. 2018) and ceramic functional analyses (McClure et al. 2018) and comparative zooarchaeological research (McClure et al. 2022). Moreover, this evidence suggests agricultural production intensified (i.e., increased yields per unit land farmed and per livestock raised) with the arrival of the Danilo culture.

In the Danilo Neolithic sharper, more durable and efficiently maintained stone sickle blades gradually phase out single-use lithics associated with the earlier Impresso period (Mazzucco et al. 2018). Experimental data suggest that advanced sickle blades enable more efficient grain harvesting and overall increase in yield per investment in pre-industrial subsistence farming systems (Russell 1988; Simms and Russell 1997). The Danilo ceramic industry introduced a proliferation of vessel types that replaced Impresso wares in Dalmatia over the course of about a century (Forenbaher et al. 2013; Forenbaher and Miracle 2005; Legge and Moore 2011; McClure et al. 2014). These vessels include decorated and

undecorated carinated and hemispheric bowls and pedestalled vessels, and *figulina* which are red or brown and red painted wares in the form of deep cylindrical cups, jars, and bowls decorated with geometric motifs on the exterior (Spataro 2002: 31). The Danilo period is also associated with the appearance of *rhyta* which are bowl-like vessels with four legs, sometimes with zoomorphic features (Biagi 2003) or anthropomorphic depictions of women giving birth (Mlekuž 2007). Analysis of preserved lipids recovered from *figulina*, *rhyta*, and ceramic sieves, indicate these specialized wares functioned to produce or store milk and fermented dairy products such as cheese and yogurt (McClure et al. 2018). Although *figulina* wares are associated with the Danilo period in Dalmatia, in southern Italy they are manufactured somewhat earlier and are associated with the Early Neolithic Impresso culture (Whitehouse 1970). In contrast to other, "ordinary" pottery types, *figulina* were likely distributed among regional exchange networks potentially through centralized redistribution sites on both sides of the Adriatic (Spataro 2002: 191).

Little is known about the social organization of Neolithic communities in Dalmatia. Human burials are rarely encountered and often poorly preserved with very limited material culture. Villages are flat and extended and found in fertile valleys but are not clustered together as is the case for Neolithic settlements in the Central Balkans (Bogaard and Halstead 2015). It also appears that villages were largely self-sufficient. Pottery appears to have been produced using local materials and there is no support for inter-village ceramic distribution (Teoh et al. 2014), but an exception may be *figulina* which may have been exchanged between Danilo period villages in Dalmatia (Spataro 2002: 191). Another aspect of life that is unknown is the division of labor, so it is unclear which members of society were responsible for herding, farming, pottery production, hunting, and other subsistence

activities.

Recent age-at-death assessments of ovicaprid (i.e., sheep and/or goat) elements from Pokrovnik and Velištak show prioritization of meat during the Early Neolithic shifted to a focus on milk production in the Middle Neolithic, then to a strategy emphasizing meat and possibly fiber in the Late Neolithic (McClure et al. 2022). That study demonstrated a decrease in juvenile roe deer elements from Early to Middle Neolithic contexts at Pokrovnik, suggesting a reallocation of labor away from opportunistic hunting by Impresso groups towards a focus on seasonal sheep and goat breeding activities during the Danilo period (McClure et al. 2022). Additionally, stable isotope analyses of caprine, cattle, and pig bone collagen recovered from Neolithic sites in Dalmatia indicate Impresso, Danilo, and Hvar period herders engaged in different strategies of managing livestock diet (Zavodny et al. 2014; 2015). Collectively, these studies point to changes in food production at the Impresso-Danilo transition c. 7500-7400 cal. BP and that multiple intensification processes were occurring in parallel during the Middle Neolithic in Dalmatia. Therefore, the appearance of novel food production technologies during the Danilo phase of the Neolithic in Dalmatia potentially marks a critical economic development in sheep and goat herding.

The importance of dairy products during the Neolithic is not exclusive to Dalmatia (Bogucki 1984; Budja 2013). The earliest production of fermented dairy foods such as cheese and yogurt in Europe represents an important turning point in human history. Lactase persistence, or the ability to digest lactose into adulthood, evolved independently in multiple parts of the world in populations with long dairying histories (Tishkoff et al. 2007). Today, about 30% of adults worldwide can consume large amounts of milk without experiencing abdominal pain, diarrhea, flatulence, or bloating (Lomer et al. 2007). These individuals

possess the genetic variant of an allele that enables the production of the milk sugar lactose-digesting enzyme called lactase to continue into adulthood while the vast majority of the world's population cease lactase production after they are weaned off breast milk (Budja 2013; Herring et al. 1998; Lomer et al. 2007). Ancient DNA studies show that lactase persistence is a relatively recent development, emerging in the Bronze Age (ca. 3100 cal. BP) and becoming more widespread in later periods (Burger et al. 2007; Gamba et al. 2014; Itan et al. 2009). However, archaeological evidence for dairying during the Neolithic in Europe predates the emergence of lactase persistence in European populations by thousands of years (Marciniak and Perry 2017). The significant effects of dairy technology on development of pre-industrial economies are worth exploring in greater depth.

Processed dairy foods can be stored for longer than milk and can be more easily transported. Additionally, fermented dairy foods provide important nutritional benefits that are not obtained from raw milk and are easier to digest (Feulner et al. 2012; Gerbault et al. 2011; Itan et al. 2009). Incorporation of dairy products into agropastoral subsistence economies would have been an effective risk-buffering strategy during times of food scarcity (Cook and Al-Torki 1975; Gerbault et al. 2011; O'Brien and Bentley 2015; Rowley-Conwy 2011: S436).

Neolithic farmers in Dalmatia were among the earliest cheese producers in the Mediterranean (McClure et al. 2018). Moreover, good preservation of archaeological deposits containing large quantities of domesticated faunal remains in the Ravni Kotari region makes this area particularly well-suited to provide deep diachronic perspective into technology-related changes to food production.

A central argument presented in this research is that the novel use of milk gave new

meaning to livestock husbandry and permanently changed the dynamics of human-animal interactions. Advantages of intensified dairying may have incentivized Neolithic herders to adjust caprine herd management to maximize milk production, as was the case for cattle husbandry by Linearbandkeramik groups in continental Europe (Gillis et al. 2017). This can be achieved in several ways. Slaughtering young animals is one such approach since humans are in direct competition with infant lambs and kids for milk (Halstead 1998b). In modern sheep and goat herds, the nutritional value and volume of milk that can be attained is limited by the quality of nursing female diet (Dahl and Hjort 1976; Halstead 1998b). A constant supply of milk might only be achieved when there were no limitations on pasture or labor because the nutritional requirements of the herd would be greater due to the physiological demands of lactation (Halstead 1998b). This could be problematic in environments where the availability of grazing or browsing resources vary seasonally unless herders intensified crop production to generate a surplus for use as fodder when pasture quality is low. Herders might therefore benefit from moving their animals to areas with quality forage or collecting and storing fodder for periods of low pasture productivity.

Additionally, since ewes and does produce milk only after giving birth, herders can aim to minimize the length of time between births by breeding animals more frequently or strategically extend the milking season by delaying the slaughter of animals until they are weaned (Halstead 1998b). Alternatively, herding milking females, non-productive animals (i.e., males and young or barren females), and weaned lambs separately can maximize milk production (Halstead 1996; 1998b: 10; Koster 1977) at the expense of reallocating labor investments (Nitsiakos 1985). Increasing milk production via this route may be more feasible in transhumant pastoralist systems, whereby animals are driven to locations where seasonal

stress on pastures is less extreme, such as in high elevation mountain ranges (Budja 2013; Nimac 1940; Perišić 1940).

Throughout the Mediterranean region, seasonal visitation of caves located in higher elevations played an important role in sheep and goat breeding and safeguarding cultivation areas during the Neolithic (Martín and Tornero 2023). On the Dalmatian Coast, large-scale vertical transhumance developed in response to seasonal cycles of pasture quality in the Ravni Kotari lowlands (Forenbaher 2007). Modern Dalmatian summers experience high temperatures and low precipitation whereas cooler temperatures and wetter conditions are found in mountain ranges located in the nearby Dinaric Alps. Velebit and Dinara mountain pastures located at altitudes >1000 masl were frequented by coastal sheep and goat herders since the Bronze Age beginning around 2400 cal. BP (Forenbaher 2007). Reduced pasture quality in lowland areas due to seasonality or periodic drought during the mid-Holocene could have motivated Neolithic herders to drive livestock into mountain pastures. However, there is currently no evidence linking Neolithic open-air sites with contemporary cave deposits in these mountains (Forenbaher 2007).

The archaeological data on which this research is based derives exclusively from open-air sites in Northern Dalmatia (Figure 3.1). The sampling strategy aimed to assess whether the evidence for agricultural intensification reviewed above spurred adaptations to livestock management. To this end, the sites considered span the Early, Middle, and Late Neolithic, with special attention paid to contexts corresponding temporally to the Impresso-Danilo transition. These sites are described in detail in the following section.

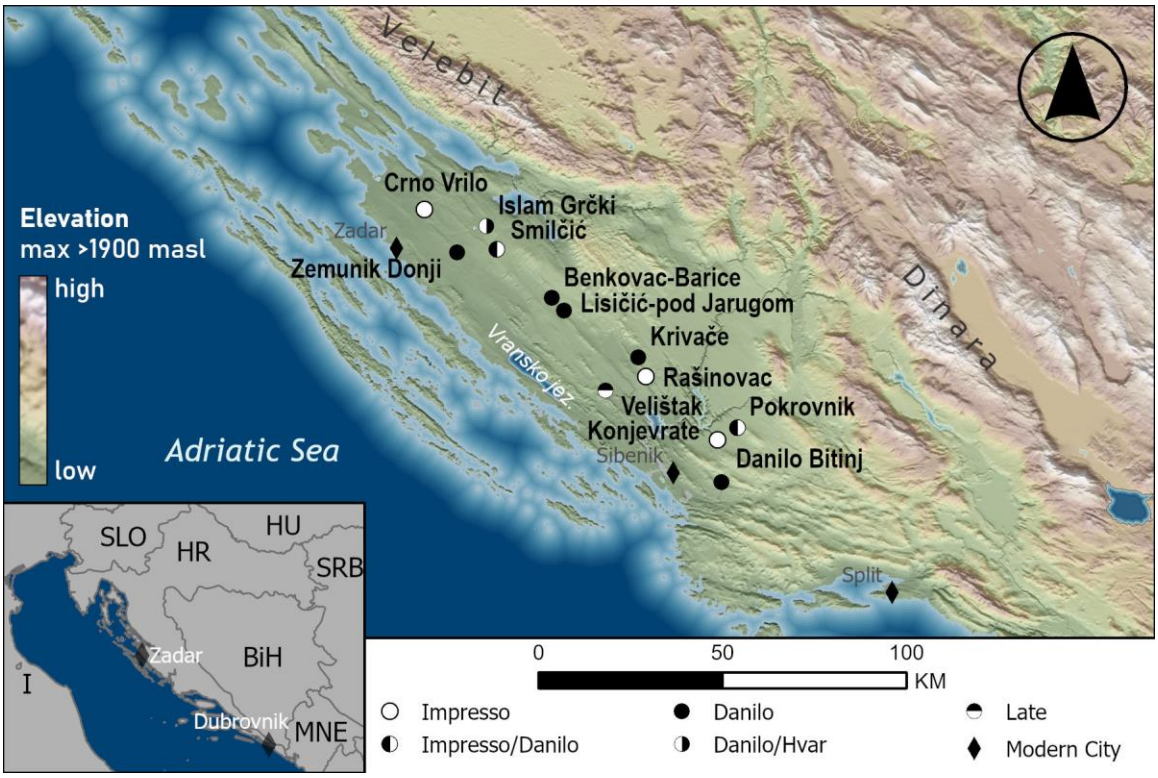

Figure 3.1 Map of Dalmatia and archaeological sites discussed.

B. Archaeological Sites

This research explores agropastoral management strategies during the Neolithic using archaeological data from Impresso, Danilo, and Hvar period sites Northern Dalmatia (Figure 3.1). In this section I provide an overview of the research completed by other investigators at Benkovac-Barice, Crno Vrilo, Danilo-Bitinj (Danilo), Konjevrate, Krivače, Pokrovnik, Rašinovac, Smilčić-Barice (Smilčić), Velištak, and Zemunik Donji. Additionally, I briefly describe new excavations at Islam Grčki - Graduša Lokve and Podgrađe - Pod Jarugom (Lisičić) which were completed as part of this dissertation research (Horvat Oštrić et al. forthcoming; Horvat Oštrić and Triozzi 2024a,b). Unless specified otherwise, all dates refer to 2σ calibrated radiocarbon age ranges obtained using the IntCal20 calibration curve (Ramsey 2008; Reimer et al. 2020).

1. Previously Excavated Sites

1.1. Benkovac-Barice (7250-7000 cal. BP)

Benkovac-Barice is situated approximately 31 km southeast of Zadar in the modern city of Benkovac (Figure 3.1). The site was identified by farmers who encountered concentrations of Impresso, Danilo, and Hvar pottery encountered on the surface (Batović 1990). Limited excavations were initially carried out by Batović who observed that plowing had destroyed much of the later deposits (Batović 1990). The area containing a concentration of Danilo materials was later excavated in 2012 by the University of Zadar Department of Archaeology (Marijanović 2012). A 225 m^2 area was investigated in which a 0.90-0.95 m thick cultural deposit contained parts of at least six residential structures containing compact floors and wall trenches reinforced with stone foundations. Three major occupational horizons were observed with superimposed structural features that indicate extended site occupation and renewal. Chipped stone tools (arrows, blades, and knives), polished stone axes, bone tools and jewelry, and Danilo ceramics including *rhyton* fragments were recovered (Vujević and Horvat 2012). A preliminary unpublished faunal analysis completed by Radović indicates sheep and goats represent over 75% of NISP followed by cattle, bird, and pig; wild fauna accounts for less than 1% of NISP and mortality profiles reflect exploitation of caprines for meat (Horvat 2017: 61). No archaeobotanical sampling was conducted.

Two radiocarbon dates from the beginning and end of stratum II place Benkovac-Barice in the Middle (Beta-327216, 7160-6950 cal. BP) and Late (Beta-327215, 6790-6660 cal. BP) Neolithic (Marijanović 2012) although the artifacts analyzed are typical of the Danilo period (Vujević and Horvat 2012). Two additional bone samples were dated as part of

the current research (see Table 4.1 in Chapter Four), yielding dates of 7245-7015 cal. BP (UCI-280714) and 7160-7000 cal. BP (UCI-280715), which correspond with the later part of the Danilo phase in Dalmatia (McClure et al. 2014). Zooarchaeological materials curated at the Benkovac Local Heritage Museum were accessed as part of this dissertation research. Sampling of faunal materials focused mainly on ovicaprid mandibles for the construction of a mortality profile and stable isotope analyses.

1.2. Crno Vrilo (7750-7550 cal. BP)

The Neolithic site of Crno Vrilo is located in Dračevac-Ninski, a municipality 12 km northeast of Zadar on the southern face of a low (63 masl) limestone ridge close to a freshwater spring (Figure 3.1). Archaeologists from University of Zadar excavated 550 m^2 of the site from 2001-2005 (Marijanović 2009a,b). Several residential structures were encountered, some of which featured baked mud floors, hearths, and ovens and it is estimated that the entire settlement was 6750-7500 m^2 (Marijanović 2009a). Analyses of the lithic assemblage identified multiple Gargano chert artifacts indicating the residents of Crno Vrilo were in some way connected to a pan-Adriatic raw materials distribution network (Kačar 2019; Kačar and Philibert 2022). Crop cultivation is evidenced by einkorn and emmer wheat, barley, and pulses recovered from flotation samples (Šoštarić 2009). Caprine elements comprise over 95% of the terrestrial faunal remains that included domesticated cattle and pigs and a few wild species (Radović 2009). Other animal taxa are represented including 23 species of birds, mussels, oysters, and fish.

The inhabitants of Crno Vrilo specialized in sheep husbandry and exploitation of herds for meat but likely also for milk (Radović 2009; 2011; Sierra et al. 2023). Stable carbon and oxygen analyses of lower M3 molars of sheep indicate most animals were born in

the early winter, pointing to a breeding period at the end of summer or in the early autumn (Sierra et al. 2023). Marijanović estimated the site was occupied only for 100 years (Marijanović 2009a: 228) and concluded based on comparison of six radiocarbon dates that the site dates to 7750-7550 cal. BP corresponding to the Early Neolithic Impresso period. Faunal materials accessed for this research were curated at the Archaeological Museum in Zadar.

1.3. Danilo Bitinj (7250-6850 cal. BP)

Danilo Bitinj (i.e., Danilo) is situated in the Danilo Valley, approximately 18 km east of Šibenik (Figure 3.1). Following a test probe of the area in 1951 (Korošec 1952), an area of 2500 m^2 was excavated in the summers of 1953 and 1955 by Korošec, who encountered pottery unique to the known varieties in the Eastern Adriatic and named the new assemblage Danilo (Korošec 1958). A second limited rescue excavation (60 m^2) was completed in 1992 by Menđušić (1993). Most recently, from 2003-2006 the site was again investigated via a series of five 25 m^2 trenches (Legge and Moore 2011; Moore et al. 2007b; Moore and Menđušić 2004). The distribution of surface finds indicates a densely occupied village spanning over 9 ha. Residents subsisted on the typical variety of Neolithic crops (i.e., einkorn and emmer wheat, barley), pulses, and wild fruits, and products from herding sheep, goats, and cattle (Moore and Menđušić 2019). Radiocarbon dates show the site was occupied for several centuries spanning 7250 to 6850 cal. BP (McClure et al. 2014).

1.4. Konjevrate (7170-6980 cal. BP)

Konjevrate is located under a modern churchyard cemetery approximately 11 km northeast of Šibenik (Figure 3.1). The site was initially excavated by Menđušić as a salvage

operation during the construction of new graves in the 1980s and 1990s (Menđušić 1988; 1998; 1999; 2005). Recovered materials include Impresso style pottery, stone tools and faunal remains. AMS analysis of two sheep bones returned dates of 7580 to 7480 cal. BP (KON-2/PSU-5291/UCIAMS-116203) and 7170 to 6980 cal. BP (KON-4/PSU-5557/UCIAMS-119838; McClure et al. 2014). The later date (KON-4) is likely a sample associated with an intrusive feature considering the absence of ceramics from later period (Korić and Horvat 2018; McClure et al. 2014; McClure and Podrug 2016).

1.5. Krivače (7260-7000 cal. BP)

The Neolithic site known as Krivače is in the Bribir-Ostrovica Valley 22 km north-northwest of Šibenik (Figure 3.1). The site was identified by surface pottery finds associated mainly with the Danilo and Hvar periods (Korošec and Korošec 1974). Subsequent excavation of a 90 m^2 area was completed 2001-2004 by Menđušić (Podrug 2013), confirming the site was a Middle Neolithic open-air village. More recent explorations of Krivače by Podrug and McClure in 2013 recovered additional Danilo style pottery including *rhyta* and *figulina*, chert and obsidian tools, and faunal remains among various structural features (i.e., ditches, pits, hearths, house floors; McClure et al. 2014; McClure and Podrug 2016). Radiocarbon dates obtained from human and animal bone collagen samples span from 7260 to 7000 cal. BP (McClure et al. 2014; McClure and Podrug 2016) and demonstrate the recently excavated part of the site was only occupied during the Middle Neolithic, Danilo phase.

1.6. Pokrovnik (7970-7000 cal. BP)

Pokrovnik is located 15 km northeast of Šibenik in Drniš county below a hill where

the modern church Sveti Mihovil and a prehistoric hillfort are located (Figure 3.1). The site was discovered in 1979 during the plowing of vineyards and was promptly investigated via a series of trenches covering an area of 114 m^2 (Brusić 1979; 2008; Moore and Menđušić 2019). Subsequent excavations of four trenches ranging 25-40 m^2 were completed in 2006 under the direction of Moore and Menđušić (Moore et al. 2007a) and two more trenches totaling to 188 m^2 were excavated from 2010 to 2011 and in 2013 by Marijanović (2017).

Collectively the archaeological investigations at this site documented multiple residential structures reinforced with stone wall foundations, pits, and hearths (Marijanović 2017; Moore et al. 2019). Large quantities of both Impresso and Danilo style ceramics, stone tools, animal bone, and archaeobotanical remains were recovered (Horvat and Vujević 2017; McClure and Podrug 2016; Moore et al. 2007a). Archaeobotanical remains include wheat, barley, oat, grass pea, lentil, flax, and broomcorn millet (Karg and Müller 1990; Legge and Moore 2011; Moore et al. 2019; 2007a; Reed and Colledge 2016). The faunal assemblage is dominated by caprines, especially sheep, with smaller proportions of cattle and pig present (Legge and Moore 2011; McClure et al. 2022; Moore et al. 2019). Hunting of wild roe and red deer, and other small mammals resulted in a smaller proportion of wild animals relative to domesticates. The presence of hare (*Lepus europaeus*) led Legge and Moore (2011) to suspect the area around the site was relatively open. Recent zooarchaeological analyses have determined that Impresso period exploitation of caprines emphasized meat while milk was prioritized by Danilo period herders during the Middle Neolithic (McClure et al. 2022). AMS radiocarbon dates obtained from bone and carbonized seeds recovered during the 2006 excavations demonstrated the site was occupied as early as 7970-7850 cal. BP (PSUAMS-5293/UCIAMS-116205) and was inhabited for approximately 900 years (McClure et al.

2014). A Bayesian analysis of a suite of AMS radiocarbon dates from the site indicates Pokrovnik was occupied throughout the Early and Middle Neolithic and that Impresso wares continued to be used for up to 300 years after the arrival of Danilo ceramics to the region (McClure et al. 2014).

1.7. Rašinovac (7950-7850 cal. BP)

This site is situated 19 km north of Šibenik between the villages of Piramatovci and Ždrapanj (Figure 3.1). The presence of Neolithic settlements in this area was long suspected based on reports of Impresso and Danilo period surface finds (Podrug et al. 2018). The site was discovered in 2013 during a surface survey and subsequently tested with a 2 x 2 m trench which recovered Impresso style pottery, Early Neolithic stone tools and animal bone (Podrug et al. 2013). Analysis of the lithic assemblage identified cherts sourced locally as well as Gargano cherts originating in Italy (Podrug et al. 2018). Two radiocarbon dates (PSUAMS-5612/UCIAMS-127394 and PSU-6492/UCIAMS-158546) indicate the site was occupied from 7950 to 7850 cal. BP making this site one of the earliest known open air Neolithic village locations in Dalmatia (McClure et al. 2014; Podrug et al. 2018).

1.8. Smilčić (7840-6850 cal. BP)

Smilčić is located 20 km east of Zadar (Figure 3.1). A 1150 m^2 area of the site was initially excavated by Batović from 1956 to 1959 and in 1962 (Batović 1958; 1966). In 2016-2017 a 700 m^2 area of the site was excavated in four trenches by Marijanović (2022). Ceramics recovered during the excavations were mainly of the Impresso and Danilo types but the site is unique for various reasons:

1) the disproportionate number of cattle in the faunal assemblages compared to other

contemporary sites in Dalmatia (McClure and Podrug 2016; Schwartz 1988);

2) Danilo phase *figulina* pottery production involved techniques distinct from those used at contemporary sites (Teoh et al. 2014);

3) residential structures appear to be oval shaped, in contrast to rectangular layouts seen elsewhere in Dalmatia (Batović 1958; 1979);

4) the site features three large, concentric semi-circular ditches spaced 18-50 cm apart each filled with materials from different phases of the Neolithic (Batović 1958; 1979; McClure and Podrug 2016); and

5) several human burials and a dozen isolated human skulls were found in various parts of the site associated with different Neolithic phases (Batović 1966; Janković et al. 2020; Marijanović 2022).

One of the burials (Grave 2) featured a relatively complete skeleton of an adult male which showed signs of violent trauma (Janković et al. 2020). Two AMS radiocarbon dates have been reported for humans in Grave 1 and Grave 2 (Marijanović 2022). These dates show the Impresso occupation began as early as 7675-7580 cal. BP (Beta-471103) and likely endured through the transition to the Danilo period around 7560-7420 cal. BP (Beta-471104). No botanical remains were collected at the time of excavation, but indirect evidence for farming is supported by milling stones and crop harvesting use-wear on lithics (Horvat 2017). The faunal assemblages resulting from both excavation campaigns are currently curated at the Zadar Archaeological Museum. These collections were accessed to sample faunal materials associated with contexts containing Impresso and Danilo ceramics. AMS radiocarbon dates for an additional four bone samples were obtained from the assemblage recovered during excavations from 2016 to 2017 to confirm the chronology of ovicaprid

mandibles examined as part of research presented in later chapters (see Table 4.1 in Chapter Four).

1.9. Velištak (6950-6650 cal. BP)

Velištak is located 19 km northwest of Šibenik (Figure 3.1). The site has been the focus of systematic excavations since 2007 by the Šibenik City Museum, with work continuing today (McClure and Podrug 2016; Podrug 2010; 2013). Until recently, the site was the only open-air Late Neolithic settlement excavated in Dalmatia (see description of Islam Grčki, section 2.1 below). Evidence of the site's continued use and renewal over time include hardened and burnt clay floors, dwellings, and round or oval pits intruding into one another at different levels within the 0.60 m cultural deposit (Podrug 2013). Pits were filled with Hvar style pottery, animal bones, soot and ash suggesting their use as refuse deposits from household activities and stone tools were recovered in large quantities (Podrug 2010; 2013). Age at death data indicate sheep and goat herding was oriented towards wool production (McClure et al. 2022). The assemblage of archaeobotanical remains obtained via flotation was rich in barley grains (93%), while emmer and einkorn wheat grains, lentils, bitter vetch, peas, and flax, and wild fruits and grasses were also present in smaller numbers (Reed and Podrug 2016). According to AMS radiocarbon dates from several contexts, the village was occupied for 200-300 years between 6950 and 6650 cal. BP (McClure et al. 2014; Podrug 2010).

1.10. Zemunik Donji (7560-7010 cal. BP)

Zemunik Donji is positioned 11 km east of Zadar on the edge of a hilltop that was used as a fortified position beginning in the Iron Age (c. 2800-2100 cal. BP) (Figure 3.1).

The site was partially destroyed during prehistoric fortification of the area and likely was impacted later in time by repeated use of the site from the Roman period (2100-1450 cal. BP) present day (Čelhar and Borzić 2016). In 2014 a 250 m^2 area was excavated by Marijanović and University of Zadar archaeologists (Marijanović and Horvat 2016). Excavators identified the partial remains of two rectangular structures with the skeletal remains of a human child discovered between them. The site was likely established during the Early Neolithic on the basis of a limited quantity of Impresso ceramics recovered during excavations. However, a larger and richer assemblage of artifacts representing the Danilo period including polished stone axes, projectile points, bone tools, and *figulina* and *rhyton* fragments point to a Middle Neolithic occupation. One goat metacarpal and one cattle metatarsal were dated using Accelerator Mass Spectrometry as part of this work (see Chapter Four). The goat bone was dated to 7565-7430 cal. BP (UCIAMS-271230) while the cattle bone dates to 7240-7010 cal. BP (UCIAMS-271231; see Table 4.1 in Chapter Four). These dates indicate the site was in use during the transition from the Impresso to Danilo cultures that occurred in Dalmatia around 7500 cal. BP, and Neolithic farmers continued to occupied the hilltop for several centuries. Faunal materials accessed for this research are curated in the Archaeology Laboratory at the University of Zadar.

2. New Excavations

2.1. Islam Grčki - Graduša Lokve (7250-7000 / 6880-6660 cal. BP)

The site of Graduša Lokve is in the modern village of Islam Grčki 17 km east-northeast of Zadar (Figure 3.1). A rich collection of Danilo and Hvar period artifacts were collected throughout the 1960s and 1970s on the surface of cultivated fields covering an area

of approximately 200 m by 150 m (Batović 1985; 1987; Batović 1970). Among the finds were Danilo and Hvar period pottery, faunal remains, milling stones, groundstone axes, and chert and obsidian stone tools fashioned from raw material sources in Italy (Batović 1985; 1987). No excavations were completed at the site until 2021 and 2022 as part of this dissertation research in coordination with Professor Kristina Horvat Oštrić (University of Zadar). These excavations are discussed in greater detail elsewhere (Horvat Oštrić and Triozzi 2024b) so I only summarize the work here.

In October 2021 the first of two exploratory trenches, Sonda A, was placed in a section of the field at Graduša Lokva where tilled soil was extremely dark and numerous ceramics found on the surface. Sonda A was a 4 x 4 m unit excavated in Fall 2021 and January 2022 to a depth of 2 m below surface. Numerous pits were encountered in the fill of a linear trench running north-south. Large quantities of Danilo period wares such as *rhyta* and ceramic sieves were recovered, as well as chipped stone blades. A single adult human fibula was also recovered in SJ53 but no other human skeletal elements were identified by excavators. Soil was dry-screened through 1 cm wire mesh and 48 flotation samples collected.

Sonda B was a 2 x 3 m trench excavated in June 2022 approximately 30 m south of Sonda A. A wide trench running east-west was observable 30 cm below the surface. The investigation of this feature revealed a complex series of filling episodes of pits intruding into one another, each containing Hvar period pottery, lithics, and animal bones. The trench was excavated to a maximum depth of 2.2 m below surface. At the very bottom of the trench was SJ47, a narrow strip of dark grey sandy loam soil that contained a large quantity of charred seeds and a few ceramics. Much of this feature was set aside as one of the 24 flotation

samples collected from Sonda B. Immediately beneath SJ47 was SJ48, a brown, orange-yellow soil that contained a large, perforated cervid mandible and a T-shaped antler. Analysis of these artifacts is ongoing but for now, the significance of Sonda B is that most of the pottery can be attributed to the Late Neolithic, Hvar style, making this site the second of its kind in Dalmatia to be excavated.

Archaeobotanical and zooarchaeological analyses of the materials collected from both trenches are ongoing. However, numerous wheat, barley, and other seeds were identified during flotation of samples collected from both trenches. Goat, sheep, and cattle bones were present in the dry screened material (0.5 cm mesh). Ovicaprid mandibles and humeri from this site were analyzed in the Archaeology Laboratory at The University of Zadar using comparative materials to aid in species determination (see Chapter Five).

A series of AMS radiocarbon dates were obtained from bone and carbonized plants collected during excavations (see Chapter Four). The human fibula recovered from Sonda A returned a date of 7250 to 7020 cal. BP (UCIAMS-280709), which coincides with the earliest AMS radiocarbon dates obtained from other features in this excavation trench. A charred barley seed recovered from one of the deepest features encountered in Sonda B (SJ47) was dated to 6780 to 6660 cal. BP (UCIAMS-271173). These dates confirm the site was in use during the Middle and Late Neolithic but there is a 250-year difference between the youngest dates of Sonda A and the oldest of Sonda B. Further excavations are required to determine whether the site was occupied continuously or if there was a hiatus lasting several centuries.

2.2. Podgrađe - Pod Jarugom (Lisičić; 7160-7000 cal. BP)

This site is located approximately 3 km southeast of the modern city of Benkovac and the site of Barice described above (Figure 3.1). Batović, who discovered the site in 1976

initially described its location in relation to the neighboring village Lisičić (Batović 1990: 27). The modern village Lisičić settlement is quite far from the site itself, which Batović additionally connected with the toponym Pod Jarugom as a spatially more precise description of the site's location. The site is in fact closer to the modern village of Podgrađe. In this dissertation, Lisičić is used to refer to this site which is officially named Podgrađe - Pod Jarugom (Horvat Oštrić and Triozzi 2024a).

In March 2022 a 1 x 3 m trench was excavated as part of this dissertation research and in collaboration with Professor Kristina Horvat Oštrić (University of Zadar) to evaluate the potential of the site for future work (Horvat Oštrić and Triozzi 2024a). The excavation recovered Middle Neolithic ceramics of the Danilo style, including *rhyton* fragments, polished bone tools, stone tools, and animal bone. Analysis of archaeobotanicals collected in 10 flotation samples (Horvat Oštrić et al. forthcoming) identified emmer (*Triticum dicoccum*), einkorn (*Triticum monococcum*), a few grains of free-threshing wheat (*Triticum aestivum/durum*) and barley (*Hordeum sp.*), lentils (*Lens culinaris*) and one chickpea (*Cicer arietinum*). Faunal analysis was completed by Dr. Sarah B. McClure in the Mediterranean Prehistory and Paleoecology Laboratory at UC Santa Barbara. Most animal bone recovered was identified as ovicaprid, with smaller proportions of cattle, dog, hare, rodents, bird and fish species (Horvat Oštrić et al. forthcoming). One carbonized wood sample was AMS radiocarbon dated to 7160-7000 cal. BP (UCIAMS-271164; see Chapter Four), corresponding to the later part of the Middle Neolithic, Danilo period in Dalmatia.

C. Environmental Context

The region of Dalmatia includes the islands and coastal plains of the Eastern Adriatic

littoral between the modern Croatian cities of Zadar and Dubrovnik (Figure 3.1). Northern Dalmatia refers to the Croatian municipalities of Zadar and Šibenik-Knin counties which encompass the wide peninsular coastal plain known as the Ravni Kotari. The Ravni Kotari attracted Neolithic seafaring farmers because it features some of the best farming land in the Eastern Adriatic (Forenbaher and Miracle 2014). Fertile areas are at or below sea-level and are segmented by series of parallel, small amplitude (maximum 200 m) karstic ridges that run north-west to south-east and rarely extend for more than 20 km (Chapman et al. 1996).

The modern vegetation is a result of human activity beginning in the Iron Age (Grüger 1996). Shrubby drought-resistant maquis (i.e., dense evergreen shrubs and small trees <5 m tall) and garrigue (i.e., shrubs <1m tall) cover most of coastal Croatia and are vital sources of sheep and goat forage (Rogosic et al. 2006). *Quercus ilex* forests dominate the immediate coast and adjacent islands while further inland are deciduous oak-hornbeam forests comprised of *Carpinus, Ostrya, Fraxinus*, and *Quercus* species (Horvat et al. 1974). Inland vegetation grades with increasing altitude into *Fagus*, *Abies alba*, and *Picea* species characteristic of the montane and sub-Alpine environments of the Dinarides mountain system also known as the Dinaric Alps (Grüger 1996; Horvat et al. 1974). The sub-Mediterranean climate of the Dalmatian coast terminates at the central belt of the Dinaric Alps which includes the Velebit and Dinara mountain ranges (Figure 3.1).

The sub-Mediterranean climate of the Ravni Kotari lowlands is characterized by hot and dry summers and cold, rainy winters (Figure 3.2). From 1961 to 2021, mean annual precipitation was 912 mm, mean annual temperature was 15.4°C, and ranged from 7.4°C in the coldest month (January) to 24.3°C in the warmest month (July; Lawrimore et al. 2016). Within this 60-year period, average precipitation during the winter (November-March) was

430 mm and 138 mm during the summer (June-August). Precipitation steadily declines in the spring reaching the lowest levels in July. Plentiful autumn and winter rainfall and seasonal freshwater streams and springs provide ample water for farming but summer drought restricts growth of non-irrigated crops and places seasonal limitations on pasture quality (Chapman et al. 1996). In contrast, relief from high temperatures and drought conditions are found in the Velebit and Dinara mountains where summer precipitation levels are more than twice those of Northern Dalmatia (Marković 1980; 1987). Monthly rainfall recorded at the Zavižan station (1594 masl) in the Velebit range of the Dinarides is consistently higher than the lowlands (Figure 3.2).

Paleoenvironmental reconstructions for the central Mediterranean basin indicate wet winters and dry summers prevailed from 9000 to 7800 cal. BP (Peyron et al. 2011; Sadori et al. 2011). At around 8200 cal. BP temperatures dropped by 1-3°C as rapid climatic deterioration of the Northern Hemisphere (i.e., the 8.2 ka event; Berger and Guilaine 2009; Weninger et al. 2009) had variable effects on regional environments (Kačar 2021; Peyron et al. 2011). Palynological data from sections of lake core samples taken from Bokanjačka blato spanning the early Holocene show a decline in *Juniperus,* expansion of deciduous tree forests (i.e., *Quercus ilex*; Grüger 1996) and evidence of high sediment input (Ilijanić et al. 2018), collectively indicating higher levels of precipitation and erosion at the onset of the Neolithic c. 8000 cal. BP. Analysis of ostracods (i.e., small, bi-valved crustaceans) obtained from lake cores in Vrankso jezero in Northern Dalmatia (Figure 3.1) indicate that between 8100 and 5200 cal. BP Dalmatia's climate experienced pronounced temperature variations amidst a relatively warm and humid climate (Hajek-Tadesse et al. 2018). Cores from the Adriatic Sea and the Italian Peninsula indicate several major cooling/drying events occurred throughout

the early Holocene, including three during the Neolithic period, at 7700, 7000, and again at 6400 cal. BP (Combourieu-Nebout et al. 2013). These reconstructions of regional paleoclimate events are corroborated by lake cores taken from paleolake sites in northern Dalmatia, including the Bokanjačka blato karst polje, Vransko jezero, and the Bribir-Ostrovica polje (Hajek-Tadesse et al. 2018; Ilijanić et al. 2018).

At Vransko jezero cool-dry oscillations at 8100 cal. BP precede the interruption of sapropel S1 formation from 7900 to 7400 cal. BP signaling drier conditions lasted approximately 500 years (Bakrač et al. 2018). Increased *Juniperus* and *Pistacia* and declining *Quercus* and *Corylus* pollen in the interrupted S1 horizon (Bakrač et al. 2018) points to opening of wooded areas (Combourieu-Nebout et al. 2013; Grüger 1996; Jahns and van den Bogaard 1998). At around 7700 cal. BP a brief cooling period and higher summer rainfall characterized the central Mediterranean (Combourieu-Nebout et al. 2013). In Dalmatia, a pluvial period is observed from 7600 to 6900 cal. BP, indicated by higher sediment detrital input into the Bokanjačka blato basin near Zadar (Ilijanić et al. 2018). Continuation of sapropel S1 formation at Vransko Jezero after 7400 cal. BP (Bakrač et al. 2018) corresponds with sea sediment cores signaling warming temperatures and peak precipitation in the Adriatic between 7500 and 7000 cal. BP (Combourieu-Nebout et al. 2013), and coincides with the appearance of Danilo ceramic styles in Dalmatia from 7400 cal. BP (McClure et al. 2014).

Another brief period of aridity in the East Adriatic is also observed at around 7100 cal. BP based on the sharp decline of freshwater phytoplankton species detected in lake cores obtained from Malo Jezero on the island of Mljet in southern Dalmatia (Wunsam et al. 1999). From 7000 cal. BP summer precipitation steadily decreases while *Quercus* again declines

signaling continued opening of forests (Combourieu-Nebout et al. 2013). In summary, the paleoclimatic data suggest mostly dry conditions during most of the Early Neolithic were followed by higher temperatures and peak summer precipitation in the Middle Neolithic, and a gradual approach towards the modern Mediterranean climate by the Late Neolithic.

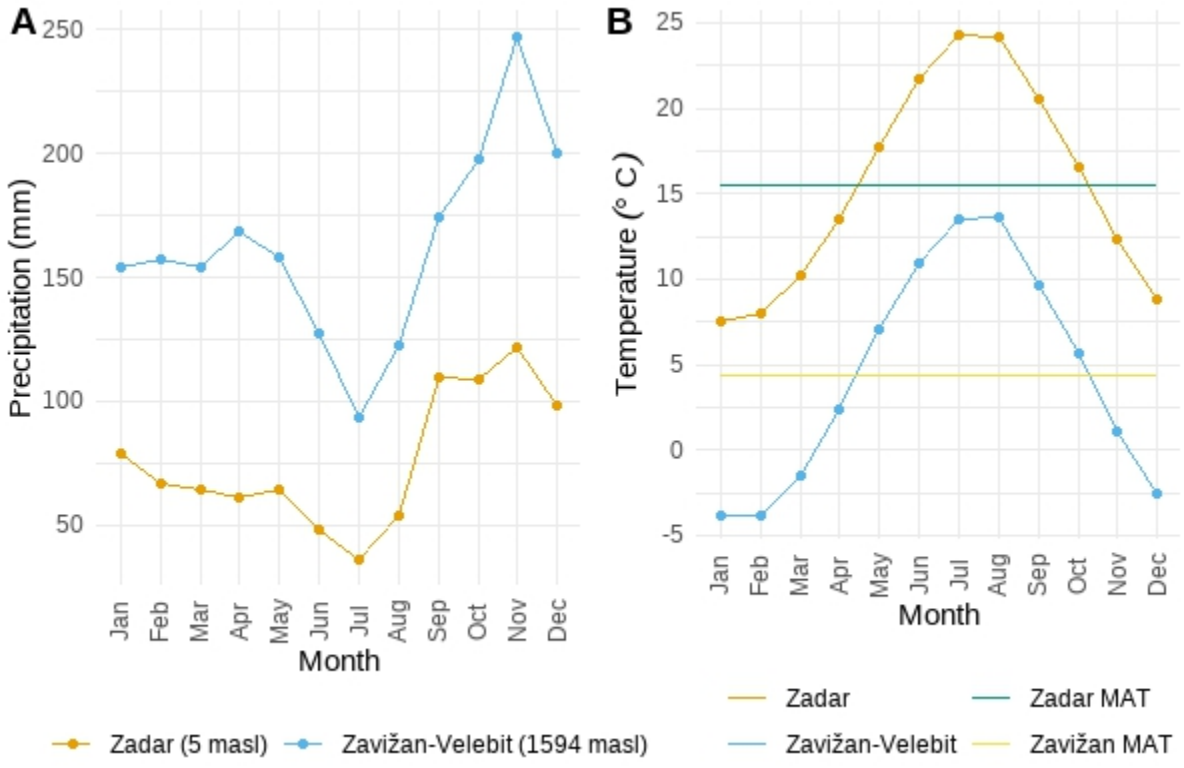

Figure 3.2 (A) Average amount of rainfall and (B) average monthly temperatures recorded by weather monitoring stations at Zadar and Zavižan mountain in the Velebit range from 1961-2021. Data source: Global Summary of the Month (GSOM) Version 1 (Lawrimore et al. 2016).

IV. Chronology of Neolithic Sites in Northern Dalmatia

In this chapter I discuss the temporal phases of the Neolithic in Northern Dalmatia and describe the methods and materials used to generate a suite of new radiocarbon dates. The significance of the new dates is considered in the final section. All dates refer to 2σ calibrated radiocarbon age ranges in years before present (i.e., cal. BP) obtained using the IntCal20 calibration curve (Ramsey 2008; Reimer et al. 2020), unless specified otherwise.

A. Preface

Three phases of the Neolithic period in Dalmatia (Impresso/Early, Danilo/Middle, and Hvar/Late) are distinguished by stylistic and functional differences in ceramic wares (Batović 1966; Korošec 1952; McClure et al. 2014; McClure and Podrug 2016; Spataro 2002). The earliest farming groups to settle in Dalmatia by 8000 cal. BP are recognized archaeologically by the presence of ceramics associated with the Impresso cultural group (Forenbaher et al. 2013; Forenbaher and Miracle 2005; 2014; McClure and Podrug 2016; Spataro 2002). These ceramics are decorated with impressions of fingernails, fingers, *Cardium* shell, and other tools (Spataro 2002: 24–25). In Dalmatia, the Early Neolithic is synonymous with the Impresso phase and lasts approximately 400-500 years (Forenbaher et al. 2013; Forenbaher and Miracle 2014; McClure et al. 2014; McClure and Podrug 2016).

At around 7500-7400 cal. BP, a gradual replacement of Impresso wares begins with the arrival of a new cultural phase associated with Danilo style pottery (Korošec 1952; 1958; McClure et al. 2014; Spataro 2002). The Danilo ceramic tradition is characterized by a wider variety of vessel types and decorations, including incised patterns and paint (Forenbaher et al. 2004; 2013; McClure and Podrug 2016; Spataro 2002). In Dalmatia, the Middle Neolithic refers to the Danilo cultural phase because radiocarbon dates from contexts bearing Danilo ceramics are preceded by the chronology of the Impresso ware phase (Spataro 2002: 30). However, Vlaška pottery, which resembles Danilo wares, are associated with the earliest archaeological evidence of agriculture in the Northern Adriatic (e.g., Istria) leading some to hypothesize that this region was not settled by farmers prior to the Middle Neolithic in Dalmatia (Biagi 2003; Biagi and Spataro 2001; Forenbaher et al. 2013; Forenbaher and Kaiser 2006; Forenbaher and Miracle 2006; 2014).

The Hvar cultural phase (Novak 1955) appears in Dalmatia c. 7000 cal. BP marking the beginning of the 1,000-year period of the Late Neolithic in this region. This cultural phase is assumed to be a derivation of the Danilo culture based on similarities in pottery, site distribution, and because the absolute chronology follows the Danilo period (Forenbaher and Kaiser 2000). Currently only two open-air sites attributed to the Hvar period have been excavated in Northern Dalmatia: Velištak (Podrug 2010) and Graduša Lokve in Islam Grčki (Figure 3.1; Horvat Oštrić and Triozzi 2024b).

The Neolithic period in Dalmatia is relatively well-dated (Chapman et al. 1996; Forenbaher et al. 2013; McClure et al. 2014). In this chapter I present 21 new radiocarbon dates for five of the sites described in the previous chapter: Benkovac-Barice, Islam Grčki-Graduša Lokve, Smilčić-Barice, Lisičić-pod Jarugom, and Zemunik Donji.

B. Materials and Methods

As indicated in Chapter Two, most of the sites discussed in this research have been radiometrically dated. The sampling strategy for bone samples from Smilčić, Benkovac-Barice, and Zemunik Donji was intended to obtain dates of contexts associated with ovicaprid mandibles and M2 molars that were prepared for stable isotope analysis of enamel bioapatite although Benkovac-Barice and Smilčić had been previously been dated (Marijanović 2012; 2022). Samples from Islam Grčki Sonda A were collected from various contexts to better understand the chronological relationships between the multiple pits and horizons encountered during excavations (Horvat Oštrić and Triozzi 2024b). Among the bone samples from Sonda A was one adult human fibula recovered from SJ53. For Islam Grčki Sonda B, bone, carbonized wood, and carbonized seeds were collected during excavation from upper strata and the deepest feature encountered (SJ47). A single carbonized wood fragment was collected from Sonda A, SJ3 during excavations at Lisičić (Horvat Oštrić and Triozzi 2024a) for AMS dating.

Preparation of bone, carbonized wood, and carbonized seed for accelerator mass spectrometry (AMS) radiocarbon dating was completed in the Paleoecology and AMS Radiocarbon Research Laboratory at UC Santa Barbara. Sample information is provided in Table 4.1. Bone collagen preparation for carbon and nitrogen isotope analysis was completed using a modified Longin method with ultrafiltration (Brown et al. 1988; Kennett et al. 2017; Longin 1971; McClure et al. 2010). Between 300 and 800 mg of dry bone was sampled from each specimen after manually scraping away a thin layer of bone with a scalpel to remove superficial contaminants. Samples were then crushed into small pieces to maximize surface area to improve demineralization. Crushed bone was demineralized in 0.5N HCl at 5°C for

24 to 72 hours, then subjected to three 20-minute NanoPure water rinses. Demineralized bone samples were gelatinized on a heat block at 110°C in 0.05N HCl for 24 hours, then lyophilized in a thick-walled culture tube. The collagen was dissolved with NanoPure H_2O and pipetted into >30kD ultrafilters, centrifuged three times for 30 minutes, diluted with more NanoPure water, followed by another three centrifuge cycles to desalt the solution. Ultrafiltered collagen was then lyophilized and weighed to determine collagen yield. High-yield samples were sent to Yale Analytical Stable Isotope Center for stable isotope analysis of carbon and nitrogen.

From the bone collagen samples, approximately 2.5 mg of collagen was combusted with CuO and Ag wire at 900°C for three hours in vacuum-sealed quartz tubes. The combusted samples were sent to UC Irvine's W.M. Keck Carbon Cycle Accelerator Mass Spectrometry Facility (KCCAMS), where sample CO_2 was converted to graphite at 500°C with H_2 and a Fe catalyst as reaction water was removed with $Mg(ClO_4)_2$ (Santos et al. 2004) and packed into aluminum capsules for AMS analysis. $\delta^{13}C$ measurements were used to correct ^{14}C ages for mass dependent fractionation (Stuiver and Polach 1977) and compared to internal lab standards for calibration.

Charcoal and carbonized seed samples collected from excavation Sonda A and Sonda B at Islam Grčki and Sonda A at Lisičić-pod Jarugom were pretreated using an acid-base-acid procedure to remove contaminants. The process was repeated until the acid solution was clear. Samples were dried on a heat block overnight at 100-degrees C. Carbon samples were combusted with CuO and Ag wire at 900 degrees C in vacuum-sealed quartz tubes and sent to KCCAMS for analysis. Radiocarbon ages were calibrated in R Statistical Software (v4.3.1; R Core Team 2023) using the "oxcAAR" package (version 4.4.4; Martin et al. 2021)

interface to the OxCal Radiocarbon Calibration program (Bronk Ramsey 2009) and IntCal 20 calibration curve (Reimer et al. 2020). Table 4.1 provides the calibrated AMS radiocarbon dates shown in Figure 4.1.

C. Results: New AMS Radiocarbon Dates

In Figure 4.1 and Table 4.1 I present new and previously published radiocarbon dates for sites considered in this research. The results of AMS radiocarbon dating of Islam Grčki confirm the suspected chronologies of Sonda A and Sonda B indicated by the recovery of Danilo and Hvar period ceramics (respectively) during excavations (Horvat Oštrić and Triozzi 2024b). The AMS radiocarbon dates from Sonda A range from 7250 to 7000 cal. BP, corresponding with the later part of the Middle Neolithic in Dalmatia. The date range for Sonda B is from 6880 to 6660 cal. BP, during the Late Neolithic (Table 4.1). The date range from 7160 to 7000 cal. BP obtained for Lisičić (i.e., Podgrađe - Pod Jarugom) corroborates the assumptions of a Middle Neolithic occupation inferred by the presence of *rhyton* fragments and other Danilo period ceramics (Horvat Oštrić et al. forthcoming; Horvat Oštrić and Triozzi 2024a). Additionally, the limited number of Impresso ceramics found at Zemunik Donji amidst the apparently more intensive Danilo phase occupation suggests that the site was occupied at the transition from the Early to the Middle Neolithic (Marijanović and Horvat 2016). The new AMS radiocarbon dates spanning 7565 to 7010 cal. BP indeed confirm this suspicion as the appearance of Danilo ceramic in Northern Dalmatia begins around 7500-7400 cal. BP (McClure et al. 2014).

New AMS radiocarbon dates were obtained for two sites that were previously dated radiometrically (Benkovac-Barice and Smilčić). The purpose of obtaining new AMS

radiocarbon dates for these sites was to confirm the chronology of contexts that were sampled for stable isotope analysis. Additionally, while Batović recovered large quantities of Impresso and Danilo period ceramics during the earliest excavations at Smilčić (Batović 1958; 1974; 1990), the nature of the site's use during the Middle Neolithic has recently been disputed (Marijanović 2022). Marijanović contends that the relationship between Impresso and Danilo phase occupations was discontinuous, and calls into question Batović's (1958) interpretation of the site's expansion in the Middle Neolithic (Marijanović 2022). The new AMS radiocarbon dates from Smilčić appear to corroborate Marijanović's argument (2022). For example, the previously published AMS radiocarbon date of 7560-7430 cal. BP obtained for Grave 2 (Table 4.1) corresponds to the transitional phase between the Impresso and Danilo cultural phases shown elsewhere (McClure et al. 2014). The two new dates (UCIAMS-280713 and UCIAMS-280710) range from 7840 to 7610 cal. BP, which corresponds to the date previously obtained from Grave 1 (Beta-471013; Marijanović 2022), confirming an Impresso period use of the site (Figure 4.1). Furthermore, two other new dates for this site (UCIAMS-280711 and UCIAMS-280712) span 7160 to 6850 cal. BP, potentially due to either a hiatus of several centuries or because Danilo period activity was concentrated in another part of the site. These new dates differentiate Early and Middle Neolithic samples used for analyses presented in later chapters of this dissertation.

The new dates obtained for Benkovac-Barice were also instrumental in this regard since one of the previously reported dates (Beta-327215) corresponds to the Late Neolithic, Hvar period. These dates range from 7250 to 7000 cal. BP, confirming that contexts from which multiple samples were used to reconstruct Middle Neolithic husbandry strategies for Benkovac-Barice can be confidently considered in terms of Danilo period subsistence.

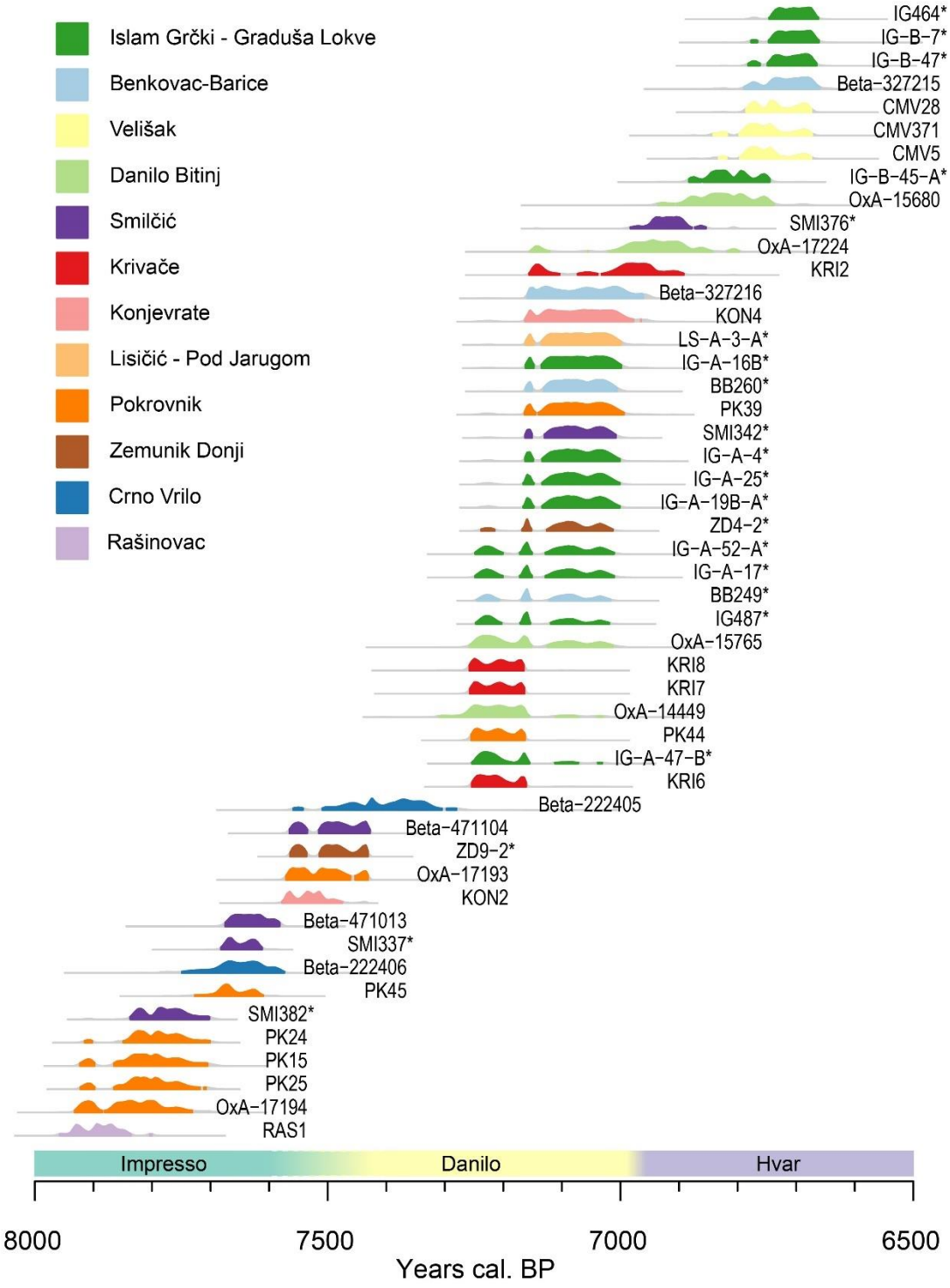

*Figure 4.1. Radiocarbon dates for sites in northern Dalmatia, calibrated with OxCal version 4.4.4 (Bronk Ramsey 2009) with IntCal20 atmospheric curve (Reimer et al. 2020) in R Statistical Software v4.3.1 (R Core Team 2023) using "oxcAAR" package (Martin et al. 2021). See Table 4.1 for sample details. * = new date reported in this study.*

Table 4.1. Calibrated AMS radiocarbon dates obtained from samples associated with sites in this study. Radiocarbon dates for sites in central and northern Dalmatia, calibrated with OxCal version 4.4.4 (Bronk Ramsey 2009) with IntCal20 atmospheric curve (Reimer et al. 2020) in R Statistical Software v4.3.1 (R Core Team 2023) using "oxcAAR" package (Martin et al. 2021).

Sample ID	Provenience	Sample Material	^{14}C Age BP	2σ cal. BP	Reference
UCIAMS-280715					
BB260	Benkovac-Barice, Kv. B3, SJ49	Bone collagen (humerus) (*Capra hircus*)	6190±15	7161 to 7149 (6.12%) 7131 to 7003 (89.33%)	This study
Beta-327215					
	Benkovac-Barice, SJ26 Level 1 (Stratum II end)	Bone collagen	5900±30	6789 to 6658 (95.45%)	Marijanović (2012)
Beta-327216					
	Benkovac-Barice, SJ35 Podnica 2A (Stratum II begin)	Bone collagen	6160±30	7158 to 6957 (95.45%)	Marijanović (2012)
UCIAMS-280714					
BB249	Benkovac-Barice, Kv. B2, SJ49	Bone collagen (humerus) (*Ovis aries*)	6225±15	7121 to 7015 (57.36%) 7245 to 7205 (22.54%) 7169 to 7151 (15.55%)	This study
Beta-222406					
	Crno Vrilo, A/IA/Zdravica (lower part of cultural layer)	Bone collagen	6820±50	7749 to 7573 (95.45%)	Marijanović (2009:113)
Beta-222405					
	Crno Vrilo, A/IA/1 (upper part of cultural layer)	Bone collagen	6500±60	7297 to 7279 (2.43%) 7559 to 7540 (3%) 7509 to 7304	Marijanović (2009:112)

Sample ID	Provenience	Sample Material	^{14}C Age BP	2σ cal. BP	Reference
				(90.02%)	
OxA-14449					
	Danilo Bitinj, A/17	Bone collagen (*Ovis musimon;* sheep)	6284±40	7041 to 7027 (1.12%) 7310 to 7154 (89.85%) 7111 to 7069 (4.48%)	Moore et al. (2007)
OxA-15765					
	Danilo Bitinj, E/14	charred grain (*Triticum monococcum;* einkorn)	6245±39	7258 to 7150 (58.45%) 7127 to 7009 (37%)	Moore et al. (2007)
OxA-17224					
	Danilo Bitinj, C/15	charred seed (*Rosa sp.;* wild rose)	6083±35	6817 to 6795 (2.94%) 7021 to 6840 (84.26%) 7060 to 7051 (0.58%)	McClure et al. (2014)
OxA-15680					
	Danilo Bitinj, B/21	charred grain (*Triticum monococcum;* einkorn)	5987±35	6935 to 6736 (95.45%)	Legge and Moore (2011)
OxA-17224					
	Danilo Bitinj, C/15	charred seed (*Rosa sp.;* wild rose)	6083±35	7153 to 7119 (7.67%)	McClure et al. (2014)
UCIAMS-271172					
IG-B-45-A	Islam Grčki, Sonda B, SJ45	charcoal	5980±20	6883 to 6743 (95.45%)	This study

Sample ID	Provenience	Sample Material	^{14}C Age BP	2σ cal. BP	Reference
UCIAMS-271173					
IG-B-47	Islam Grčki, Sonda B, SJ47	seed (*Hordeum vulgare*)	5900±20	6781 to 6760 (8.69%) 6749 to 6663 (86.76%)	This study
UCIAMS-271174					
IG-B-7	Islam Grčki, Sonda B, SJ7	seed (*Hordeum vulgare*)	5890±20	6779 to 6763 (3.86%) 6747 to 6659 (91.59%)	This study
UCIAMS-280708					
IG464	Islam Grčki, Sonda B, SJ20	Bone collagen (metacarpal) (*Bos taurus*)	5890±15	6745 to 6661 (95.45%)	This study
UCIAMS-280709					
IG487	Islam Grčki, Sonda A, SJ53	Bone collagen (fibula) (*Homo sapiens*)	6230±15	7247 to 7201 (33.86%) 7171 to 7153 (17.23%) 7119 to 7018 (44.35%)	This study
UCIAMS-271171					
IG-A-52-A	Islam Grčki, Sonda A, SJ52	charcoal	6225±25	7248 to 7198 (23.61%) 7172 to 7149 (12.67%) 7129 to 7009 (59.17%)	This study
UCIAMS-271170					
IG-A-47-B	Islam Grčki, Sonda A, SJ47	charcoal	6250±20	7113 to 7069 (7.83%) 7041 to 7027	This study

Sample ID	Provenience	Sample Material	^{14}C Age BP	2σ cal. BP	Reference
				(1.64%)	
UCIAMS-271169					
IG-A-25	Islam Grčki, Sonda A, SJ25	charcoal	6200±20	7165 to 7147 (8.23%) 7133 to 6999 (87.22%)	This study
UCIAMS-271170					
IG-A-47-B	Islam Grčki, Sonda A, SJ47	charcoal	6250±20	7253 to 7154 (85.98%)	This study
UCIAMS-271168					
IG-A-19B-A	Islam Grčki, Sonda A, SJ19B	charcoal	6200±20	7133 to 6999 (87.22%) 7165 to 7147 (8.23%)	This study
UCIAMS-271167					
IG-A-17	Islam Grčki, Sonda A, SJ17	charcoal	6225±25	7248 to 7198 (23.61%) 7172 to 7149 (12.67%) 7129 to 7009 (59.17%)	This study
UCIAMS-271166					
IG-A-16B	Islam Grčki, Sonda A, SJ16B	charcoal	6185±20	7134 to 6999 (88.82%) 7161 to 7147 (6.63%)	This study
UCIAMS-271165					
IG-A-4	Islam Grčki, Sonda A, SJ4	charcoal	6195±20	7163 to 7147 (7.45%) 7134 to 6999 (88%)	This study

Sample ID	Provenience	Sample Material	^{14}C Age BP	2σ cal. BP	Reference
PSUAMS-5557/UCIAMS-119838					
KON4	Konjevrate, III.O.S	Bone collagen (*Ovis aries*)	6175±30	7163 to 6977 (95.07%) 6966 to 6963 (0.38%)	McClure et al. (2014)
PSUAMS-5291/UCIAMS-116203					
KON2	Konjevrate, I.O.S	Bone collagen (*Ovis aries*)	6655±25	7578 to 7473 (95.45%)	McClure et al. (2014)
PSUAMS-5615/UCIAMS-127397					
KRI8	Krivače, 1/SJ20	Bone collagen (*Homo sapiens*)	6290±20	7257 to 7163 (95.45%)	McClure et al. (2014)
PSUAMS-5558/UCIAMS-119839					
KRI2	Krivače, III/A2	Bone collagen (*Sus scrofa;* pig)	6115±30	7156 to 7100 (20.99%) 7073 to 6890 (74.46%)	McClure et al. (2014)
PSUAMS-5613/UCIAMS-127395					
KRI6	Krivače, 1/SJ22	Bone collagen (*Homo sapiens*)	6270±20	7254 to 7159 (95.45%)	McClure et al. (2014)
PSUAMS-5614/UCIAMS-127396					
KRI7	Krivače, 1/SJ24	Bone collagen (*Homo sapiens*)	6285±20	7255 to 7163 (95.45%)	McClure et al. (2014)
UCIAMS-271164					
LS-A-3-A	Lisičić, Sonda A, SJ3	Charcoal	6185±20	7161 to 7147 (6.63%) 7134 to 6999 (88.82%)	This study
OxA-17194					
	Pokrovnik, D/21	charred grain (*Triticum dicoccum;* emmer)	6999±37	7932 to 7729 (95.45%)	Legge and Moore (2011)

Sample ID	Provenience	Sample Material	^{14}C Age BP	2σ cal. BP	Reference
PSUAMS-5618/UCIAMS-127400					
PK25	Pokrovnik, D/23	Bone collagen (*Ovis aries*)	6975±25	7921 to 7897 (8.98%) 7864 to 7717 (86.47%)	McClure et al. (2014)
PSUAMS-5617/UCIAMS-127399					
PK24	Pokrovnik, D/23	Bone collagen (Ovicaprid)	6965±20	7915 to 7900 (3.35%) 7849 to 7699 (92.1%)	McClure et al. (2014)
PSUAMS-5556/UCIAMS-119837					
PK15	Pokrovnik, D/23	Bone collagen (*Ovis aries*)	6975±30	7923 to 7896 (9.9%) 7865 to 7703 (85.55%)	McClure et al. (2014)
PSUAMS-4960/UCIAMS-106477					
PK44	Pokrovnik, D/9	Bone collagen (*Ovis aries*)	6280±20	7254 to 7162 (95.45%)	McClure et al. (2014)
OxA-17193					
	Pokrovnik, D/11	charred grain (*Triticum dicoccum;* emmer)	6625±36	7571 to 7429 (95.45%)	McClure et al. (2014)
PSUAMS-4961/UCIAMS-106478					
PK45	Pokrovnik, D/11	Bone collagen (*Ovis aries*)	6840±25	7729 to 7609 (95.45%)	McClure et al. (2014)
PSUAMS-5294/UCIAMS-116206					
PK39	Pokrovnik, D/10	Bone collagen (*Bos taurus*)	6190±25	7163 to 6992 (95.45%)	McClure et al. (2014)
PSUAMS-5612/UCIAMS-127394					
RAS1	Rašinovac, 1/SJ3	Bone collagen (*Bos taurus*)	7060±25	7958 to 7834 (94.62%) 7803 to 7799	McClure et al. (2014)

Sample ID	Provenience	Sample Material	^{14}C Age BP	2σ cal. BP	Reference
				(0.83%)	
Beta-471104					
	Smilčić, Grave 2	Bone collagen (*Homo sapiens*)	6600±30	7513 to 7427 (71.7%) 7565 to 7533 (23.75%)	Marijanović (2022)
Beta-471013					
	Smilčić, Grave 1	Bone collagen (*Homo sapiens*)	6790±30	7675 to 7580 (95.45%)	Marijanović (2022)
UCIAMS-280713					
SMI382	Smilčić, Sonda D, Kv. N6, SJ52	Bone collagen (humerus) (*Capra hircus*)	6955±15	7837 to 7698 (95.45%)	This study
UCIAMS-280710					
SMI337	Smilčić, Sonda B, Kv. N2, SJ22	Bone collagen (humerus) (*Capra hircus*)	6820±15	7683 to 7609 (95.45%)	This study
UCIAMS-280711					
SMI342	Smilčić, Sonda C, Kv. P10, SJ41	Bone collagen (humerus) (*Capra hircus*)	6195±15	7162 to 7149 (6.58%) 7130 to 7006 (88.87%)	This study
UCIAMS-280712					
SMI376	Smilčić, Sonda D, Kv. L6, SJ56	Bone collagen (humerus) (*Ovis aries*)	6065±15	6983 to 6853 (95.45%)	This study
PSUAMS-5289/UCIAMS-116201					
CMV5	Velištak, F/3	Bone collagen (*Ovis aries*)	5935±20	6795 to 6673 (92.5%) 6829 to 6818 (2.95%)	McClure et al. (2014)
PSUAMS-3702/UCIAMS-78156					
CMV28	Velištak, A/3	Bone collagen (Ovicaprid)	5920±15	6785 to 6673 (95.45%)	Podrug (2010)

Sample ID	Provenience	Sample Material	^{14}C Age BP	2σ cal. BP	Reference
PSUAMS-2045					
CMV371	Velištak,	seed	5935±25	6841 to 6816 (7.23%) 6797 to 6671 (88.22%)	McClure et al. (2014)
UCIAMS-271231					
ZD4-2	Zemunik Donji, Kv.9, SJ43A	Bone collagen (metatarsal) (*Bos taurus*)	6215±15	7238 to 7213 (7%) 7167 to 7150 (11.84%) 7125 to 7011 (76.61%)	This study
UCIAMS-271230					
ZD9-2	Zemunik Donji, Kv.9/8, SJ47	Bone collagen (metacarpal) (*Capra hircus*)	6605±20	7565 to 7533 (26.31%) 7513 to 7429 (69.14%)	This study

D. Summary

The chronology of Neolithic Northern Dalmatia is divided into three phases: Impresso (Early), Danilo (Middle), and Hvar (Late) which are primarily distinguished by changes in ceramic styles. This chapter contributes 21 new AMS radiocarbon dates for five Neolithic sites in the study area. The results confirm that (1) habitation of Smilčić began during the Impresso period and endured to the later part of the Danilo phase; (2) the Danilo period occupation of Zemunik Donji began as early as the Impresso-Danilo transition around 7500 cal. BP; (3) the presence of an open-air village at Islam Grčki during the Danilo and Hvar phases; (4) Lisičić-pod Jarugom was inhabited as early as the Danilo phase; and (5) the excavated component of Benkovac-Barice represents an open-air village inhabited during the Danilo phase. The sampling strategy, targeting bone and charcoal for AMS radiocarbon dating in combination with ceramics recovered from these sites supports the identification of phase-specific occupations. The contexts represented by the new and previously reported dates discussed in this chapter are associated with bone and tooth samples selected for stable isotope analyses (see Chapter Seven), allowing for greater accuracy in the interpretation of herding strategies through time.

V. Insight into Herd Culling Strategies at four Neolithic Sites in Dalmatia

A. Preface

The production goals (e.g., prioritizing meat, milk, or fiber) of past herding economies are often inferred from analysis of zooarchaeological assemblages. Most commonly this is achieved by estimating age-at-death of individual animals and constructing and interpreting mortality profiles (Greenfield 2005; Helmer et al. 2007; Payne 1973; Price et al. 2016). Mortality profiles provide insight into the age-related culling (i.e., slaughtering) rates of animals in a managed herd.

Age-at-death data are typically presented as mortality profiles showing the frequency distributions of raw counts for each age class or as survivorship probabilities which are calculated as the inverse cumulative distributions of the frequency distributions (Price et al. 2016: 158). Various aspects of livestock management emerge from survivorship curves including a herd's age structure and economic goals. Models that link survivorship curves to the subsistence or economic goals of pastoralists have been developed which continue to serve as references for inferring the production goals of past agropastoral economies (Figure 5.1).

Three of the most widely used models were developed by Payne (1973) based on observations of slaughtering patterns among modern pastoralists in Turkey. Generally, when

the goal of herding is to maximize the quantity of meat produced from a flock of goats or sheep, the kill-off pattern will exhibit preferential slaughter of young males when the optimum point of weight gain is reached between 18 and 30 months. With male goats yielding higher live meat weight earlier in life (Dahl and Hjort 1976; Payne 1973; Redding 1981), survivorship curves for models of meat-focused production will exhibit a sharp decline in the first two years of life for males, while female survivorship will drop more steadily since they are valuable for reproduction. Under a system that aims to maximize the availability of milk for human consumption, herders will act to ensure that females who survive to the age of sexual maturity will have sufficient access to food so they may lactate effectively (Dahl and Hjort 1976; Halstead 1998b). Payne's (1973) milk optimization model entails preferentially slaughtering pre-weaning males to maximize the availability of milk for human consumption. In contrast to a meat-focused system, the proportion of males to females under a wool-focused model will be more equitable and kill-off patterns will reflect a bias towards older adult animals.

Redding (1981) devised two alternative models that differentiate between optimization of energy production via meat and milk and ensuring herd security. The energy optimization model is realized as a kill-off pattern favoring the slaughter of young males between 12 and 18 months, when the rate of weight gain slows. The security model predicts the goal of herders is to minimize fluctuations in herd size that could result in reduced annual returns. This is achieved by delaying the slaughter of younger animals until the following lambing/kidding season to avoid losses from unexpected increases in mortality (e.g., due to drought) in the interim.

Several additional models developed by Vigne and Helmer (2007) and Helmer et al.

(2007) account for multiple culling patterns converging on the same priorities (see also Helmer and Vigne 2004). These refined models distinguish two culling patterns associated with meat and two patterns associated with milk. Mortality profiles approximating the Meat type A strategy are recognizable by high frequencies of caprines in age classes B (2-6 months), C (6-12 months), and D (1-2 years) with class C being over-represented. This strategy prioritizes tender meat of younger animals. Meat type B mortality profiles are characterized by high frequencies of individuals in age classes C, D, and EF (2-4 years), with class D being the peak. Meat type B allows time for younger animals to fatten and maximizes meat quantity, whereas smaller animals culled under the Meat type A strategy may be better suited for household level subsistence needs. The two strategies for dairying are referred to as Milk type A, involving the preferential culling of pre-weaned lambs and kids in age class A (0-2 months), and Milk type B, where peak mortality rates are expected for age class EF when milk production purportedly decreases. The profile of Milk type B may be challenging to distinguish from a strategy focused on Fleece in which there are unusually high percentages of animals from age classes G (4-6 years) and particularly HI (6 years and older). The Fleece strategy may only be recognizable when practiced on a large scale (Helmer et al. 2007).

Marom and Bar-Oz (2009) configured survivorship probabilities for each of the ten theoretical harvest profiles described above, standardizing survivorship rates using bins fitting both Payne's (1973) and Vigne and Helmer's (2007) age class systems. These probabilities associated with different culling profiles are depicted as survivorship curves in Figure 5.1. Caprine mortality data has already been published for Pokrovnik, Velišstak, (McClure et al. 2022), Danilo-Bitnj (Moore and Menđušić 2019), Crno Vrilo, and Tinj

(Radović 2011; Sierra et al. 2023) but not for Smilčić, Zemunik Donji, Islam Grčki, or Benkovac-Barice. In this chapter I present new mortality data of caprines representing these four Neolithic sites in northern and central Dalmatia. These data are used to infer culling strategies, providing important context for understanding the decision making of Neolithic herders in Dalmatia.

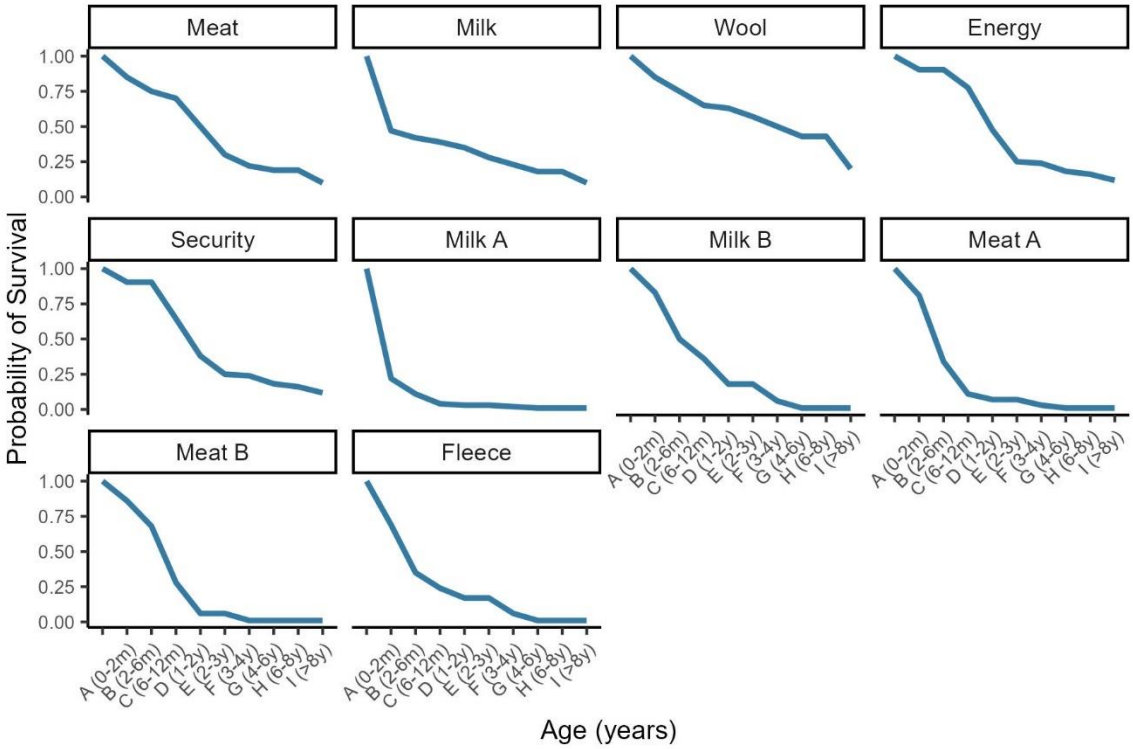

Figure 5.1. Survivorship curves from theoretical culling strategies devised by Payne (1973), Redding (1981), and Vigne and Helmer (2007).

B. Culling Profile Reconstruction Methods and Data

Culling profiles are constructed using well-established osteological and odontological indices of age and sex to estimate the age at death of individual animals (Helmer et al. 2007; Payne 1973; Reitz and Wing 2008; Vigne and Helmer 2007; Wilson et al. 1982; Zeder 2006). Four stages of epiphyseal fusion broadly correspond to the first four years of life but the timing of fusion varies depending on the bone and for males, fusion time can be affected by

castration (Moran and O'Connor 1994; Zeder 2006). Age determinations made by epiphyseal fusion analysis are therefore broad and limited to four categories: infant, juvenile, sub-adult, and adult. Additionally, the use of post-cranial elements for age determination has been criticized for being inaccurate and subject to unpredictable bias stemming from differential preservation of skeletal elements through time (Vigne and Helmer 2007: 17). Higher-resolution age determinations can be achieved via analysis of mandibular tooth eruption and wear (Grant 1982; Payne 1973; Zeder 2006; Zeder and Lapham 2010; Zeder and Pilaar 2010). However, it should be noted that high infant mortality rates and poor preservation of neonate skeletal material may complicate interpretations of mortality profiles (Budja 2013: 63). Nonetheless, this approach is used here because it provides useful insight into herd management.

Mortality profiles for ovicaprids have been reported for Crno Vrilo (Radović 2009; 2011; Sierra et al. 2023), Impresso and Danilo period Pokrovnik (McClure et al. 2022; Moore et al. 2019), and Hvar period Velištak (McClure et al. 2022). An unpublished, partial analysis of the zooarchaeological assemblage from Benkovac-Barice[1] indicates that herders raised sheep and goats for meat production (Horvat 2017). A more complete age-at-death analysis using all ovicaprid mandibles recovered in excavations of Benkovac-Barice (Marijanović 2012) is presented here. Additionally, zooarchaeological analysis of the Smilčić assemblage resulting from Batović's (Batović 1963; 1966) excavations could not assess caprine culling patterns based on age and sex, citing small sample sizes (Schwartz 1988). Therefore, mandibles recovered from Impresso and Danilo contexts excavated at Smilčić

1. Analysis by Dr. Siniša Radović, research associate at the Institute for Paleontology and Quaternary Geology, of the Croatian Academy of Sciences and Arts.

(Batović 1963; Marijanović 2022) were sampled and analyzed. All ovicaprid mandibles recovered during excavations at Islam Grčki and Zemunik Donji were also analyzed.

Age-at-death estimations were completed via the analysis of sheep and goat mandibles recovered from Impresso (n=44) and Danilo (n=58) period contexts at Smilčić, and Danilo period contexts at Zemunik Donji (n=33), Benkovac-Barice (n=77), and Islam Grčki (Danilo: n=37 and Hvar: n=10). Descriptions of these sites and excavations are provided in Chapter Two. Analysis was completed at The University of Zadar Archaeology Laboratory and in the Mediterranean Prehistory and Paleoecology Laboratory at UC Santa Barbara. Using comparative materials and criteria for distinguishing between *Ovis* and *Capra* using dental and mandibular morphological traits (Zeder and Pilaar 2010), mandibles were attributed to goat, sheep, or ovicaprid when a specimen could not be attributed to either sheep or goat. Osteological measurements were recorded following von den Driesch (1976). All data were entered into a relational database using File Maker Pro 19 software.

Age-at-death for each mandible specimen was estimated using a modified version of Payne's (1973) dental wear classification system (Zeder 2006). The revised classification system differentiates between sheep and goat occlusal wear stages and was applied appropriately. Specimens identified only as ovicaprid were assigned an age category using the sheep classification system (Zeder 2006). Age-at-death was estimated for 238 out of 251 mandibles analyzed (Appendix A). In some cases, a specimen was assigned to multiple age classes if there were teeth missing from the mandible, but the dentition present met criteria for more than one age class. These individuals were proportionally allocated to absolute frequencies of each age class represented. For example, specimen BB.B1.SJ6.188 from Benkovac-Barice was assigned to age classes E, F, and G, so 0.33 was added to the absolute

frequencies of these age classes for this site and context. Frequency distributions for each age class were calculated using R Statistical Software (v4.3.1; R Core Team 2023). The mortality profiles shown in Figure 5.2 present these data as percentages of the cumulate frequency distributions. All data processing procedures are documented in Appendix B.

C. Mortality Profiles for Smilčić, Benkovac-Barice, Zemunik Donji, and Islam Grčki

Mortality profiles constructed from dental wear analysis of mandibles from Smilčić, Benkovac-Barice, Zemunik Donji, and Islam Grčki are shown as percentages of cumulative frequency densities in Figure 5.2. The results of wear analysis are provided in Appendix A.

1. Smilčić mortality profiles

In the mortality profile created from the Impresso phase assemblage at Smilčić (n=44), age classes B (2-6 months) and C (6-12 months) represent 71% of the cumulative frequency distribution (CFD). The youngest age group represented (age class B) is overrepresented relative to animals aged 1-2 years (age class D) and animals over two years (age classes EF, G, and HI), representing 23% and 5% of the CFD, respectively. Infants in age class A (younger than 2 months) are not represented.

For Danilo period Smilčić (n=57) animals younger than 1 year account for 43% of the CFD, which includes 10% from age class A (0-2 months), 21% from age class B, and 12% from age class C. There is a high representation (40%) of the CFD slaughtered in age class D (12-24 months) compared to other adult age classes representing animals over 2 years of age. The main difference between Impresso and Danilo mortality profiles is the conspicuous absence in the Early Neolithic of animals younger than 2 months, an age at which many herders wean infants (Halstead 1998b). In the Middle Neolithic, more animals were

slaughtered before 2 months of age and more survived to age class D.

2. Benkovac-Barice mortality profile

Two peaks in the mortality profile for Danilo period Benkovac-Barice are observed. The first peak reflects 30% of the CFD slaughtered in age class B (2-6 months) while the combination of the two youngest age classes (A: 0-2 months and B: 2-6 months) accounts for 38% of the CFD. The second peak in age class D (12-24 months) represents 31% of the CFD. Animals older than 2 years represent 27% of the mortality profile (age classes EF: 13%; age class G: 13%, age classes HI: 1%).

3. Zemunik Donji mortality profile

Most animals at Zemunik Donji were slaughtered between 2 and 6 months of age (age class B), representing 39% of the CFD. A second peak in the mortality profile is observed for age class D (12-24 months) accounting for 32% of the CFD. Animals older than 2 years only account for 10% of the CFD (age classes EF: 9%; age class G: 1%). No individuals older than 72 months were identified in the assemblage (age class HI). As was the case for Impresso period Smilčić, herders appear to have delayed slaughter until animals were weaned.

4. Islam Grčki mortality profiles

Animals in the youngest age class (n=6, age class A, 0-2 months) are overrepresented in the Danilo period assemblage from Islam Grčki (n=32) relative to older animals, accounting for 60% of the CFD. No mandibles were identified as age class B (2-6 months). Animals aged 6 to 24 months represent 31% of the CFD (age class C: 15%; age class D: 16%). Only 8% of the CFD was attributed to animals older than 2 years old.

Although there is a small sample size for the Late Neolithic assemblage from Islam Grčki (n=10), no animals younger than 12 months were identified. age class D (12-24 months) exhibits the highest frequency accounting for 48% of the CFD, and the remaining mandibles are split between age classes EF (24-48 months: 32%), G (48-72 months: 16%) and HI (older than 72 months: 4%).

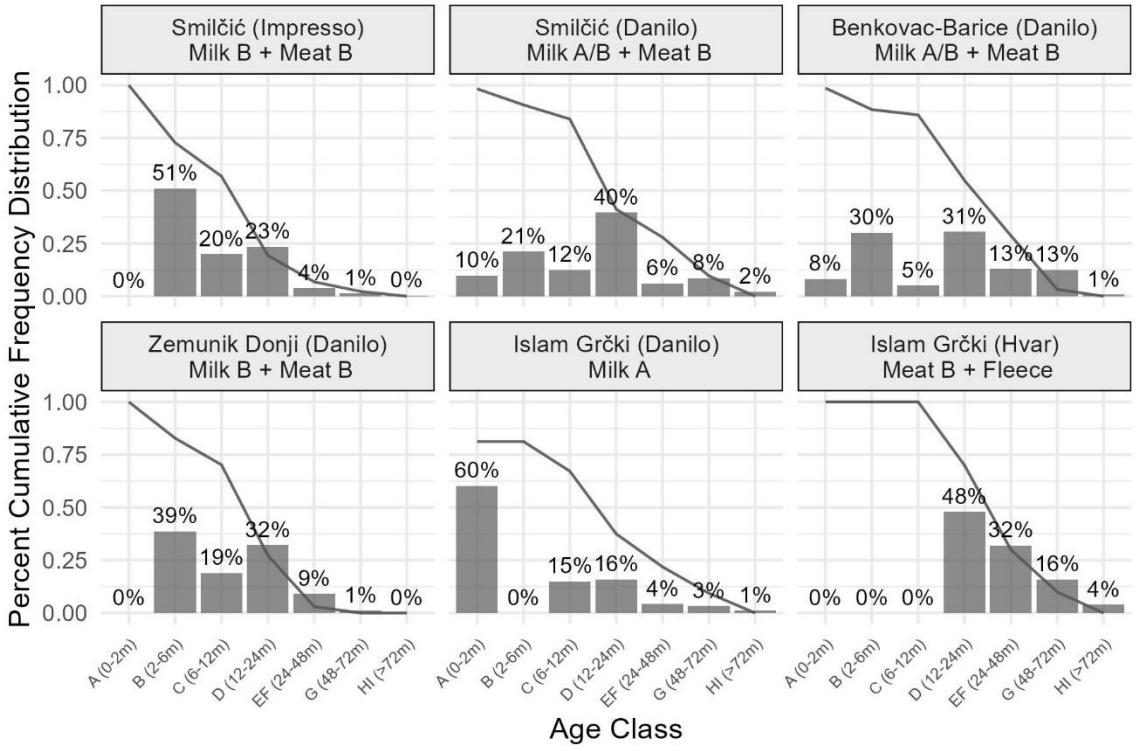

Figure 5.2. Mortality profiles and survivorship curves for ovicaprids from Smilčić, Benkovac-Barice, Zemunik Donji, and Islam Grčki. Columns show percent of cumulative frequency distributions weighted by age.

Table 5.1. Summary of age-at-death (in months) data including corrected absolute frequency (n), relative frequencies (n/total), frequency density (Rel. Freq. /bin width), and percent of frequency density (Freq. Density / sum of Freq. Density). Bin widths for age classes A through HI are 1/6, 1/3, 1/2, 1, 2, 2, and 4, respectively following Brochier (2013). See Appendix B for details on calculations.

Age Class	A (0-2m)	B (2-6m)	C (6-12m)	D (12-24m)	EF (24-48m)	G (48-72m)	HI (>72m)
Benkovac-Barice (Danilo)							
n	1.00	7.33	1.83	22.33	18.83	18.33	2.33
Rel. Freq.	0.01	0.10	0.03	0.31	0.26	0.25	0.03
Freq. Density	0.08	0.31	0.05	0.31	0.13	0.13	0.01
Proportion Freq. Density	0.08	0.30	0.05	0.31	0.13	0.13	0.01
Islam Grčki (Hvar)							
n	0.00	0.00	0.00	3.00	4.00	2.00	1.00
Rel. Freq.	0.00	0.00	0.00	0.30	0.40	0.20	0.10
Freq. Density	0.00	0.00	0.00	0.30	0.20	0.10	0.02
Proportion Freq. Density	0.00	0.00	0.00	0.48	0.32	0.16	0.04
Islam Grčki (Danilo)							
n	6.00	0.00	4.50	9.50	5.00	4.00	3.00
Rel. Freq.	0.19	0.00	0.14	0.30	0.16	0.12	0.09
Freq. Density	1.12	0.00	0.28	0.30	0.08	0.06	0.02
Proportion Freq. Density	0.60	0.00	0.15	0.16	0.04	0.03	0.01

Age Class	A (0-2m)	B (2-6m)	C (6-12m)	D (12-24m)	EF (24-48m)	G (48-72m)	HI (>72m)
Smilčić (Impresso)							
n	0.00	12.00	7.00	16.50	5.50	2.00	1.00
Rel. Freq.	0.00	0.27	0.16	0.38	0.12	0.05	0.02
Freq. Density	0.00	0.82	0.32	0.38	0.06	0.02	0.01
Proportion Freq. Density	0.00	0.51	0.20	0.23	0.04	0.01	0.00
Smilčić (Danilo)							
n	1.00	4.33	3.83	24.33	7.58	10.42	5.50
Rel. Freq.	0.02	0.08	0.07	0.43	0.13	0.18	0.10
Freq. Density	0.11	0.23	0.13	0.43	0.07	0.09	0.02
Proportion Freq. Density	0.10	0.21	0.12	0.40	0.06	0.08	0.02
Zemunik Donji (Danilo)							
n	0.00	5.67	4.17	14.17	8.00	1.00	0.00
Rel. Freq.	0.00	0.17	0.13	0.43	0.24	0.03	0.00
Freq. Density	0.00	0.52	0.25	0.43	0.12	0.02	0.00
Proportion Freq. Density	0.00	0.39	0.19	0.32	0.09	0.01	0.00

D. Insights into Sheep and Goat Slaughtering in Neolithic Dalmatia

Based on the culling profiles presented here, milk and meat were important end-products of sheep and goat husbandry during the first half of the Neolithic in Dalmatia. Upon closer examination of these mortality profiles, changes in culling strategies through time and variation between contemporary sites come to light.

Beginning with Smilčić, Impresso herders appear to have delayed the slaughter of young animals until they were at least two months old while a second peak in the mortality profile corresponds with age class D (12-24 months; Figure 5.2). In the Danilo period, herders continued to preferentially slaughter animals aged 1-2 years but began to cull animals at an earlier, pre-weaning age. Additionally, higher percentages of age classes >24 months (EF, G, and HI) are shown for the Danilo mortality profile relative to the Impresso profile for this site which may be related to culling animals that have passed peak reproductive ages (Vigne and Helmer 2007). The delay of slaughtering pre-weaning lambs and kids and higher mortality rates for animals older than 2 years resembles the Milk B strategy while high mortality rates associated with sub-adults of 1-2 years is characteristic of the Meat B type (Vigne and Helmer 2007). Using these criteria, Impresso slaughtering practices at Smilčić might best be characterized as a combined Milk B and Meat B culling strategy. Considering the increase of pre-weaning animals (i.e., age class A) slaughtered and relatively higher mortality rates for animals aged 2 years and older, the Danilo period strategy appears to have shifted towards Milk A/B and Meat B (Vigne and Helmer 2007).

Inter-site differences in culling strategies are shown in the Middle Neolithic. The age-distribution of mortality rates at Danilo period Benkovac-Barice resembles that of Danilo

period Smilčić indicating both herding groups engaged in a combination of Milk A/B and Meat B strategies. In contrast, a Milk B strategy is observed at Zemunik Donji as herders appear to have delayed slaughtering lambs and kids until they were weaned, and culled animals aged 2 years and up. Additionally, high mortality rates of 1-2 year old animals suggests the Milk B strategy was combined with Meat B type. In contrast, the strategy used by Danilo-period Islam Grčki herders was distinctly Milk type A, which is characterized by high mortality rates of pre-weaning animals (Vigne and Helmer 2007).

Vigne and Helmer (2007) discuss the implications of "truncated" mortality profiles reflected in the Danilo and Hvar period data from Islam Grčki. High infant mortality rates would prohibit herd survival and may indicate seasonal use of a site. It is therefore possible that the very high infant slaughter rate shown for Danilo period Islam Grčki reflects seasonal mobility. Seasonal movements between the Ravni Kotari coastal plain and the Velebit mountains by transhumant sheep and goat herders is well-documented (Marković 1975; 1980; 1987; Nimac 1940; Perišić 1940), but evidence of this type of herding has not yet been demonstrated for the Neolithic (Forenbaher 2007). Pending analyses of the faunal assemblage from the Danilo contexts of this site could shed light on whether Islam Grčki was occupied on a seasonal basis. For example, higher proportions of juvenile wild deer species may provide a signal of seasonal hunting activities (McClure et al. 2022).

During the Hvar period, the herding strategy appears to have changed considerably at Islam Grčki. During the Late Neolithic, the culling strategy at Islam Grčki is consistent with optimizing gains from meat and possibly wool as virtually no animals younger than 1-2 years were present in the Hvar period assemblage from this site. The restructuring of production priorities at Islam Grčki is also observed from the Middle Neolithic (Danilo/Vlaška) to the

Late Neolithic at the Northern Adriatic site of Pupićina Cave as an increase in the ratio of sheep to goats and a culling strategy that shifts from an emphasis on dairy to meat production (Miracle 2006). The Late Neolithic Pupićina Cave pattern is similar to what was observed at Hvar period Veliš̌tak (McClure et al. 2022). The Hvar period mortality profile for Islam Grčki is also truncated but the seasonal implications are not supported absent an assemblage from a complementary seasonally occupied site (Vigne and Helmer 2007: 42).

The mortality profiles offer important insight into the livestock production goals of these Neolithic contexts. However, potential problems with the interpretation of mortality data should be noted. First, absolute frequencies may be impacted by poor preservation of infant sheep and goat remains resulting from taphonomic processes (Munson and Garniewicz 2003). Differences in excavation and recovery methods may also have resulted in the over-representation of older animals. For example, Marijanović has commented on the difference between sampling strategies guiding previous, large-scale excavations (i.e., Batović 1963) and more recent, targeted and hypothesis-driven investigations of Smilčić (Marijanović 2022: 9). In particular, the lack of specification of recovery methods in published summaries of excavations, such as whether excavated soil was dry-screened, and the unfortunate tendency to avoid screening all together in exploratory investigations may contribute to sampling bias.

Furthermore, the use of culling profiles as a method for inferring economic priorities of past herding groups has been criticized. For example, Marom and Bar-Oz (2009) compared the survivorship probabilities depicted in Figure 5.1 and demonstrate that most of the profiles are statistically indistinguishable from one another. According to Vigne and Helmer (2007), the creation of frequency densities based on raw counts of specimens attributed to each age group should involve a correction algorithm that accounts for the span

of time individuals spend in each age class (e.g., 2 months for age class A, 24 months for age class G). However, as implemented by Vigne and Helmer (2007) the upwards correction of the number of mandibles attributed to the youngest age groups systematically over-estimates the frequencies of kids and lambs and under-estimates the frequencies of older individuals (Brochier 2013). To avoid inaccurate representations of the mortality rates, the data presented here corrected frequencies following Brochier (2013; see Appendix B).

Having appropriately corrected raw counts of specimens in each age class, the caveats and criticisms related to sampling, recovery, and interpretation are acknowledged and set aside. In the context of this dissertation, the culling profiles are interpreted as idealized models to describe the products these past herding systems *potentially optimized*, and not as indisputable empirical evidence of a specialized and rigid culling strategy (Halstead 1998b; 2024). As such, this research uses the culling profiles presented in this chapter as heuristic models to simplify the assumptions regarding Neolithic livestock production at various times and locations in the study area. In the next chapter, the results discussed above and the theoretical survivorship profiles presented in Figure 5.1 are considered with respect to the implications these strategies have for management of herd demography.

VI. Revisiting Having Herds: Application of Dynamic Population Modeling of Sheep and Goat Herds in Neolithic Dalmatia

A. Preface

Sheep and goats were critical to the subsistence base of the pioneering agriculturalists that colonized coastal areas of the Mediterranean Basin (Orton et al. 2016; Pilaar Birch 2018; Sierra et al. 2023). These livestock species exhibit a range of behavioral and biological traits that provide a greater capacity to relocate and adapt to new environments. In addition to being highly prolific, their smaller size comes with higher drought tolerance and better mobility in difficult terrain (Leppard and Birch 2016; Munro and Stiner 2015). But the survival of goat and sheep herds relies on the diligence of shepherds to the extent that management strategies are resilient to unpredictable threats to herd vitality. Careful management of grazing and browsing resources is therefore critical to ensuring herds remain viable contributors to the subsistence needs of humans. Managing these resources effectively may require herders to preferentially slaughter some animals in the herd based on age and sex (Dahl and Hjort 1976; Halstead 1996; 1998b; Payne 1973; Redding 1981).

The previous chapter alluded to how production focused on meat, milk, and fiber can entail distinct herd demographic structures and slaughtering practices. These production goals have implications for the decisions herders must make to sustain herd productivity while minimizing the chance of loss due to disease or drought. Some herd age and sex

structures may be more compatible with particular production goals. As a result, resource use may vary between livestock husbandry systems according to variation in herd demography. Achieving different goals therefore has implications for herd demography, reproduction, and the herd's dietary requirements.

Seeking insight into the production goals of ancient herding communities, archaeologists interpret mortality profiles through comparison with slaughtering patterns observed ethnographically (Payne 1973; Redding 1981; Vigne and Helmer 2007). However, zooarchaeological assemblages that have accumulated over centuries likely reflect an aggregation of multiple generations of contemporary herders who simultaneously employed diverse culling strategies oriented towards different production goals (Helmer et al. 2007). In the absence of tight chronological control over the source assemblage used to construct a mortality profile, the resulting survivorship profile may misrepresent multiple diverse production strategies as a cohesive and enduring economic system oriented towards the production of a single product. Summaries of aggregate datasets may well be appropriate to describe large-scale, extensive herding systems where specialization is facilitated by the production of a limited range of livestock products with high exchange value; but would be less expected in small-scale systems that rely on a broader variety of livestock products for domestic consumption (Halstead 1996).

Another caveat of using survivorship profiles to infer herd management is that the mortality rates associated with certain age classes may have a deleterious effect on herds in the long term. When offered as a representation of the production goal for a herding system spanning multiple concurrent occupations, survivorship profiles imply offtake (i.e., culling) rates are constant through time. But a stable slaughtering rate can only be achieved when

herd size is also stable through time (Negassa et al. 2015). Such a scenario may be ideal but unrealistic.

Stochastic environmental variation can lead to unexpected changes in the availability of graze or browse. Disease, predation, or theft can result in unexpected herd losses. The interaction of these factors with poor management decisions can further reduce production and potentially lead to rapid decimation of a herd. Pastoralists employ a range of preventative strategies to buffer risk (see Chapter Two). For example, over-stocking can lower the carrying capacity of the system and over-harvesting can inhibit the ability for herd numbers to recover when forage is unexpectedly reduced during a drought (Browman 1987; Mace 1990).

To minimize the risk of reductions in herd size or quality, many small-scale livestock holders prioritize maximizing the number of animals kept over the amount of meat obtained from slaughtering an animal. As was discussed in Chapter Two, increasing herd size allows herders in the Andes to maximize yields from other products such as milk, blood, and dung (Bradburd 1980; Browman 1997). Modifying age-structured slaughter regimes annually or seasonally can therefore be critical for both ensuring subsistence needs are met as well as maximizing the number of animals in the herd. In the long term, such decisions should allow for stable returns. Since culling profiles are essentially centennial-scale summaries of livestock culling rates, they cannot reflect nuanced decisions that may have been vital to the immediate subsistence needs of ancient herders. This is unfortunate since careful management of herd demography is a key aspect of navigating risk in small-scale livestock systems such as those in the Andes (Bradburd 1982; Browman 1987) and East Africa (Mace 1990; 1993b).

This chapter aims to understand flexibility in herd culling as a strategy to minimize the risk of rapid herd size decline. To this end, the development of a population projection model is presented that aims to address four questions: (1) Can survivorship profiles be used to model herd demography? (2) Do theoretical culling profiles commonly cited by archaeologists reflect sustainable herding strategies? (3) Can population models be used to assess the viability of slaughtering patterns for a given site? and (4) How does modifying harvest rates minimize risk in the short and long-term?

The approach used here involves projecting population dynamics when fertility and mortality rates vary stochastically while offtake rates remain constant to assess the sustainability of a given culling strategy. An optimization procedure is used to explore whether a herd can achieve a steady state by periodically adjusting offtake as conditions change. In the first part of this chapter, an overview of population projection matrix models is provided to demonstrate suitability of this approach to address the theoretical questions at hand. Next, key parameters of the model are described. To illustrate the implications that various theoretical culling strategies have on the survival of a herd, survivorship probabilities are parameterized as age-structured offtake probabilities. From these data, survivorship as a function of age provides key information about the age structure of a managed herd and the basis for projecting herd size changes through time. Lastly, the model is used to project herd demographic change using survivorship rates derived from Neolithic sites on the Dalmatian Coast of Croatia. Finally, the results are discussed in the context of risk minimization.

B. Modeling Herd Demography

A simplistic population model projects the change in the size of a population, n from

time t to $t+1$ as:

$$n_{t+1} = (n_t + B) - D \qquad (6.1)$$

where parameters B and D represent the number of births and deaths, respectively (Cummings and Morris 2022). Equation 6.1 models change in population size through time provided an initial population size and the population's fertility and mortality rates. In this simple model, an individual's chances of reproducing and dying are the same as the rest of the population, regardless of how many time-steps they survived and reproduced. In other words, fertility and mortality rates are constant irrespective of an individual's age or sex. Leslie and Lefkovitch population projection matrix models (Lefkovitch 1965; Leslie 1945) are more sophisticated and are commonly employed in studies of livestock population growth dynamics (Caswell 2001; Lesnoff 1999; Lesnoff et al. 2000; Negassa et al. 2015). These two matrix models are similar in structure but different in terms of their flexibility and assumptions.

The Leslie matrix (Leslie 1945) is primarily suitable for modeling populations where individuals are grouped into discrete, non-overlapping age classes. Each row of a Leslie matrix represents the fecundity (average number of offspring produced) of individuals in each age class, and the matrix is typically static across each time step (i.e., survival and fecundity remain constant over time). When using the Leslie matrix model only needs to know age- and sex-related fertility and mortality rates and the age distribution of the initial population. To simulate the growth of a population using a Leslie matrix, the difference between each age class must be equal to the time interval used to track the change in population size. In other words, if age classes are 0-10, 11-20, 21-30, 31-40, each time step must be a decade. Additionally, this approach assumes that every individual in the population

gives birth simultaneously with probability *f* and, if they survive, are expected to graduate to the next decadal age class at the same moment that every other member of the population graduates—or die at the same moment as every other individual who dies with probability *m*.

The Leslie matrix can sometimes be implemented towards simulating population dynamics amidst environmental variation. However, the rigid age-structure of the matrix is incompatible with mortality profiles constructed using zooarchaeological data which, for ovicaprids, uses age groups of different lengths (e.g., age class A = 0-2 months, age class B = 6-12 months). A recent application of the Leslie population projection matrix model to explore the introduction of domesticated cattle to British Isles by Neolithic groups simulated environmental stochasticity by varying annual birth and death rates within prescribed ranges (Cummings and Morris 2022). That study focused only on the exploitation of livestock for dairy products. But the age groups used to model cattle population dynamics were set at 1-year increments so the simulation could not account for different mortality rates of calves younger than 12 months, despite the potential for reconstructing higher resolution age groups for younger animals (McGrory et al. 2012).

By comparison, the Lefkovitch population projection matrix (Lefkovitch 1965) is more flexible because it can be 'stage-structured' so that mortality, growth, and fecundity rates are the same for all individuals in the same *stage class* and do not need to correspond with discrete *age classes*. This allows for probabilities of remaining in the current stage to be calculated based on the duration of stages, which may vary by age and sex (Crouse et al. 1987: 1413). These probabilities are entered into transition matrices to simulate changes in vital rates as individuals move through different life history stages, making the model adaptable to fluctuating environmental conditions. A Lefkovitch matrix can therefore be

created to track the population dynamics of a herd of livestock modeled using a demographic structure based on Payne's (1973) age class system (e.g., A = 0-2 months; B = 2-6 months; C = 6-12 months, etc.).

Structurally, the Lefkovitch transition matrix *A*, is a generalization of the Leslie matrix:

$$A = \left|\begin{array}{cccccc} 0 & 0 & 0.5F_a & 0 & 0 & 0 \\ G_{j,s} & P_{s,s} & 0 & 0 & 0 & 0 \\ 0 & G_{s,a} & P_{a,a} & 0 & 0 & 0 \\ \hline 0 & 0 & 0.5F_a & 0 & 0 & 0 \\ 0 & 0 & 0 & G_{j,s} & P_{s,s} & 0 \\ 0 & 0 & 0 & 0 & G_{s,a} & P_{a,a} \end{array}\right| \qquad (6.2)$$

The subdivision of the 6x6 matrix *A* in Equation 6.2 reflects the different stages for females (above dividing line) and males (below dividing line) in age groups *j, s,* and *a* representing juvenile, sub-adult, and adult, respectively. In the first row, F_a represents the fecundity of female adults calculated as the product of the parturition and net prolificacy rates, multiplied by the probability of giving birth to a female (Negassa et al. 2015). F_a in the fourth row of matrix *A* in Equation 6.2 is the male fertility rate which has a negligible effect on population size in female dominated population models (Caswell 2001). $G_{j,s}$ represents the probability of surviving and graduating from the juvenile stage to the sub-adult stage and $P_{s,s}$ reflects the probability of sub-adults surviving and persisting in the current stage. Parameters P_i and G_i are derived from the stage-specific survival probability, s_i and the duration of the stage, d_i (Crouse et al. 1987: 1415):

$$P_i = \left(\frac{1 - {p_i}^{d_i - 1}}{1 - {p_i}^{d_i}}\right) p_i \qquad (6.3)$$

and G_i is found by:

$$G_i = \frac{{p_i}^{d_i}(1 - p_i)}{1 - {p_i}^{d_i}} \qquad (6.4)$$

The probability that an individual survives is determined by the competing risks of offtake and mortality. For a given stage class, i, offtake (o_i) and mortality (m_i) rates are used to calculate the survival probability, s_i following Lesnoff (2000):

$$s_i = 1 - m_i - o_i \qquad (6.5)$$

These probabilities are supplied to the Lefkovitch matrix described earlier which is used to establish herd structure. Multiplying a vector consisting of the number of sub-adult, juvenile, and adult females and males in a herd at time t by the 6x6 transition matrix A, yields the number of animals in each sex and stage class at time $t+1$:

$$\begin{vmatrix} F_{j,t+1} \\ F_{s,t+1} \\ F_{a,t+1} \\ M_{j,t+1} \\ M_{s,t+1} \\ M_{a,t+1} \end{vmatrix} = \begin{vmatrix} 0 & 0 & 0.5F_a & 0 & 0 & 0 \\ G_{j,s} & P_{s,s} & 0 & 0 & 0 & 0 \\ 0 & G_{s,a} & P_{a,a} & 0 & 0 & 0 \\ 0 & 0 & 0.5F_a & 0 & 0 & 0 \\ 0 & 0 & 0 & G_{j,s} & P_{s,s} & 0 \\ 0 & 0 & 0 & 0 & G_{s,a} & P_{a,a} \end{vmatrix} \times \begin{vmatrix} F_{j,t} \\ F_{s,t} \\ F_{a,t} \\ M_{j,t} \\ M_{s,t} \\ M_{a,t} \end{vmatrix} \qquad (6.6)$$

Equation 6.6 is the long form of the discrete time first-order difference equation:

$$n_{t+1} = A \times n_t \qquad (6.7)$$

where n_{t+1} is the 6x1 vector of the number of individuals in the three female and three male stages on the left side of Equation 6.6. On the right side of Equation 6.7, matrix A is multiplied by n_t, the 6x1 vector of the number of animals in each group at time t on the far right of Equation 6.6.

The eigenvalues and eigenvectors of the transition matrix A are valuable for the analysis of a population's growth dynamics (Negassa et al. 2015). The dominant eigenvalue (λ) of the Lefkovitch matrix gives the population multiplication or growth rate (Crouse et al. 1987). The normalized eigenvector (w) associated with λ gives the proportions of individuals in each stage. The reproductive values of each stage are found as the standardized

eigenvectors (v) associated with λ. In other words, v indicates the relative contribution of each stage to long-term population growth (Negassa et al. 2015). In equilibrium (i.e., when w is stable through time) the projection matrix model can be simplified as:

$$Aw = \lambda \times w \qquad (6.8)$$

so that

$$n_{t+1} = \lambda \times n_t \qquad (6.9)$$

as shown by Negassa et al. (2015). Equation 6.9 can rewritten to solve for λ:

$$\lambda = \frac{n_{t+1}}{n_t} \qquad (6.10)$$

The value λ serves as an indicator of the population growth rate calculated as the ratio of n_{t+1} to n_t. When $\lambda < 1$, the population is in decline and when $\lambda > 1$, the population is growing. The population has reached a steady state when $\lambda = 1$, indicating the number of additions cancel out removals over a given time period. A steady-state is defined as a situation where $\lambda = 1$, meaning the population size is constant from t to the terminal time-step, T. This may be achieved when increases in the population (e.g., through the importation of new individuals from a different herd) counteract losses. Most populations for which there is no offtake will have $\lambda > 1$ (Lesnoff et al. 2000).

The model is said to be female-dominated since the multiplication rate λ depends on female demographics (Caswell 2001). The parameterization of stage-structured population projection models can therefore draw exclusively on female fertility and mortality figures but when the age and sex structure of a population is of interest, male mortality rates are needed.

When a steady state with constant offtake rates has been reached, offtake can be calculated as:

$$O_{i,j,t} = O_{i,i} \times n_0 \times w \qquad (6.11)$$

where $O_{i,j,t}$ is the offtake rate of the *i*-th sex in the *j*-th growth stage at time *t*, n_0 is the initial population vector of the number of animals in the *j*-th stage, and *w* is the normalized eigen vector (i.e., proportional stages of the population). In terms of livestock management, a constant offtake rate applied to each female age class implies that the slaughtering regime secures regular returns from the herd in the form of meat while keeping herd size stable.

Manipulating the transition matrix so that $\lambda = 1$ and using non-linear optimization to establish the set of sex and stage-linked offtake rates is one approach towards reaching a steady state (Lesnoff et al. 2014; Negassa et al. 2015). Since the model is female-dominated, increasing female offtake rates will decrease λ and reduce population growth. The intensity of the female offtake rate may be parameterized as φ such that for females:

$$O_{f,j,t} = \varphi \times O_{f,j} \qquad (6.12)$$

which implies that increasing φ would be expected to decrease λ. In the simulations presented here, risk minimization by way of reducing female offtake by a factor of φ is initiated when λ is below a threshold.

C. Population and Management Parameters

1. Mortality

As this chapter is focused on assessing the impacts of culling on herd growth, a distinction between deaths attributed to natural causes and slaughter must be made. Mortality rate is expressed as the number of deaths per unit of time attributed to disease, starvation or dehydration caused by extreme weather, predation, genetic disorders, and age-related health deterioration. Effective herd management may reduce mortality to the extent that the above factors can be mitigated. Some examples may include promptly removing sick animals from

the herd before disease can spread or before sick animals reproduce. Additionally, accumulating fodder and water reservoirs, and sheltering animals overnight or using dogs to deter predators can preemptively reduce herd mortality rate. Infants are particularly vulnerable to starvation, disease, and dehydration which can cause mortality rates to fluctuate with respect to environmental conditions (Awemu et al. 1999; Dahl and Hjort 1976; Debele et al. 2011; Debele and Duguma 2013).

In comparison to Redding's (1981) approach, which consolidated lamb and kid mortality into an age class of 0 to 1 year, the model presented here splits juveniles into three groups: 0-2 months, 2-6 months, and 6-12 months (Table 6.1). These groups reflect age classes A, B, and C (respectively) which are used in archaeological mortality profiles and allow for a more nuanced exploration of the demographic effects of mortality rates of young animals when they are most vulnerable to disease, starvation, and predation. The mortality rates used in this study (Table 6.1) are based on previous research described in this section.

Redding (1981) cautions that mortality rates used to model herd dynamics should be drawn from studies on sheep and goats raised under similar conditions to minimize the differences in disease prevalence and effects of climate in different livestock systems. Additionally, these data should be acquired from longitudinal studies so that mortality rates reflect inter-annual variations in environmental conditions. Redding's herd demography models draw mortality rates from studies of traditional pastoralists from the Middle East and Africa (1981). Modern management of sheep and goats has been improved by vaccines and other interventions to deter parasites and this is especially true in Europe where production is often commercial in scale (Dwyer et al. 2016). However, many modern agropastoralists situated in West and Central Africa continue to use traditional management techniques and

may have limited access to veterinary medicines. For these reasons, mortality rates used by Redding (1981) are employed here to initialize stochastic variation in mortality as part of the population projection simulations.

The average lifespan of sheep and goats in modern systems is typically five or six years but data reflecting mortality rates by age for adult animals are somewhat lacking. This is mainly because animals exhibiting problems with udder health and function, mobility, digestion, and reproductive disorders, and low productivity as a function of age are usually culled before succumbing to underlying diseases (Hoffman and Valencak 2020). Dahl and Hjort discuss several pastoral groups whose animals may live longer either for breeding purposes or when production is focused on wool (1976: 94), but very few studies report age-specific mortality rates for adult animals.

Herd productivity is heavily influenced by neonate mortality which is sensitive to how well the herd is managed (Debbarma and Sarkar 2021; Vostrý and Milerski 2013). As a result, there is a substantial body of research focused on genetic, environmental, and management factors associated with mortality of kids and lambs (i.e., referring to goats and sheep up to 12 months of age). Lamb and kid mortality (see Table C.6) may be further conditioned by the adaptability of different breeds to the environments in which they are raised (e.g., Mourad 1993; Mukasa-Mugerwa et al. 2000) and driven by interactions between season of birth, disease patterns, and management practices (Awemu et al. 1999).

The primary causes of death in lambs are pneumonia, digestive disorders, starvation (e.g., Mandal et al. 2007; Yapi et al. 1990), birth trauma, poor bonding between the lamb and ewe, and disease (Dwyer et al. 2016). Lamb mortality increases with increasing litter size (Kerslake et al. 2005) and decreases with increasing age of the ewe (Berhan and Van

Arendonk 2006). Mortality rates for lambs decline with age in the first year of life. Lambs are most vulnerable before they are weaned (Hatcher et al. 2008), which may occur in as little as five weeks after birth or delayed to six months (Redden and Thorne 2020). Green and Morgan (1993) report a mortality rate of 9.7% for lambs up to 10 weeks old weaned at five to seven weeks after birth. Mukasa-Mugerwa and colleagues (2000) found mortality rates for pre-weaning lambs up to three months was 20%, 18% for lambs 3-6 months, 10% at 6-9 months, and 5% at 9-12 months in herds comprised of Horro and Menz breeds under semi-intensive management. Muzaffarnagari lambs raised under similar conditions exhibited lower mortality rates: 7.5% for lambs up to three months, 2.7% for lambs 3-6 months, 1.6% at 6-9 months, and 1.2% at 9-12 months (Mandal et al. 2007). One study of 140 flocks of Awassi sheep raised under extensive and semi-extensive management in Jordan report a mortality rate for lambs 0-2 months of 18.6% (Abdelqader et al. 2017).

Reasons for mortality in kids are similar to lambs but disease seems to be more common, either as a consequence of increased susceptibility to infection or as a reflection of the tendency for studies to focus on goat management systems where vaccination programs are less common and veterinary resources are limited (Dwyer et al. 2016). Some studies indicate seasonal variation in kid mortality may be due to easier transport of pathogens during rainy seasons (Awemu et al. 1999; Debele et al. 2011; Debele and Duguma 2013), or related to climatic stress associated with fluctuating daily temperatures (Singh et al. 2011). However seasonal increases in mortality may be offset by improved feeding strategies, deworming, and sheltering (Hailu et al. 2006). A mortality rate of 22.4% for kids up to 12 months of age has been reported for Arsi-Bale goats raised by small-scale agropastoralists in the mid-Rift valley of Ethiopia (Debele et al. 2011; Debele and Duguma 2013). Pre-weaning

(0-3 months) survivability among Jamunapari goats raised under semi-intensive conditions in India was 82.25% (i.e., mortality rate of 17.75%), though mortality rates decline with increasing age: 11%, for kids 0-1 month of age and 3% for kids 1-2 and 2-3 months old (Singh et al. 2011). Among French Alpine and Zaraibi goats, pre-weaning (0-3 months) mortality was reported to be 16% and 13%, respectively (Mourad 1993). Studies reporting post-weaning mortality rates are scarce. A study of West African Dwarf goats and Dwarf-Red Sokoto hybrids which were weaned at one month reported kid mortality rates of 5.3% at 0-1 month and 19% for 2-3 months (Ebozoje and Ngere 1995).

As described above, recent studies suggest lambs and kids are more vulnerable early in life, with earlier weaning associated with higher mortality rates (Hatcher et al. 2008; Wilson et al. 1985). Earlier weaning might be desirable when production is focused on maximizing milk quantities whereas delayed weaning would contribute to faster weight gain and might be expected when livestock are exploited for meat (Halstead 1998b; Helmer et al. 2007). Assessing the effects of weaning age on herd growth is beyond the scope of this chapter, but data on pre-weaning mortality can be leveraged to more effectively track population dynamics in a model where lambs and kids are distributed into three age groups.

A review of reported mortality rates found that in arid and semi-arid regions of Kenya, pre-weaning mortality rates vary between 3% and 39% in lambs and 5% to 32% in goats, and is generally higher for goats than sheep, even in mixed herds (Peeler and Wanyangu 1998). In the studies reviewed, the average weaning time was five months and average lamb and kid mortality was 19.1% and 22.6%, respectively (Peeler and Wanyangu 1998). Redding used lamb and kid mortality rates of 32% and 45%, respectively but did not differentiate male from female lamb and kid mortality citing limited support for a significant

effect of sex on mortality (1981). Since then, many studies have reported significantly higher mortality rates for male versus female lambs and kids (e.g., Hailu et al. 2006; Mandal et al. 2007; Mukasa-Mugerwa et al. 2000; Singh et al. 2011). In the female-dominated model presented here, only females contribute to population growth so using different values for male and female lamb and kid mortality should not have a major effect on herd growth so long as harvest rates permit at least some males to survive to reproductive age.

Based on an assumption of higher susceptibility to disease and accounting for offtake of infertile females, Redding's model employed a mortality rate of 10% for ewes and does in age classes 1-2 and 2-3 years, a rate of 5% for age classes 3-4 and 4-5, and higher rates for animals older than five years (1981: 75). Redding also assumed lower adult mortality rates for males than females, and slightly higher mortality in bucks than rams. Low mortality for ages 2-6 years was assumed based on herders selecting for healthy males resistant to diseases, and slaughtering of males over six years of age results in a mortality rate of 100%.

These rates can be contrasted with those reported by one study in western France which aimed to determine reasons for removal of intensively raised Saanen and Alpine dairy goats from the herd and distinguished natural mortality rates from other reasons for exit (e.g., culling for health, infertility, or age; Malher et al. 2001). In that study, which did not distinguish between males and females, mortality of goats aged 1-2 years was 37.6%, and 19.5%, 13.6%, 12.1%, and 17.2% for goats aged 3, 4, 5, and >5 years, respectively. The average of these rates is 20%. The higher rates reported by Malher et al. (2001) may be related to intensively managed herds whereas Redding's (1981) model reflects studies of sheep and goats within traditional semi-extensive management systems. However, the reported mortality of the older aged goats from France (i.e., Malher et al. 2001) are

independent of offtake so they may be useful for isolating the effects of culling on herd demography.

The mortality rates used in the simulations presented here are provided in Table 6.1. These rates reflect Redding's assumptions regarding susceptibility to disease and drought but have been reduced for adult female age classes because in the present model mortality due to slaughter is parameterized separately, as age-structured offtake rates. Redding (1981) employed lamb and kid mortality rates of 32% and 45%, respectively. These rates are similar to the lamb and kid mortality rates of 30% and 48% (respectively) used by Upton to model dwarf sheep and goat productivity under a traditional management system (Upton 1984). Here, these rates are proportionally allocated across the three lamb and kid age classes (0-2 months, 2-6 months, and 6-12 months) based on the duration of each age class so that the youngest animals have the highest mortality probabilities (Table 6.1). For adult animals aged 1-7 years mortality rates of 10% and 15% are applied to male and females, respectively. Age-specific mortality rates for males are the lowest from 1-6 years of age and increase thereafter. For females aged 1-3 years higher mortality reflects susceptibility to disease and mortality related to first parturition, then decreases for ages 3-5 years before increasing thereafter. The mortality rates in Table 6.1 are baseline rates from which inter-annual variation in mortality is simulated by the program (described below).

2. Fertility

Increase in population size is contingent on fertility (i.e., reproductive output) exceeding net mortality (i.e., the number of individuals exiting the population). For domesticated species fertility is influenced by genetic as well as environmental factors which can be conditioned by herd management strategies affecting offtake and breeding. *Fecundity*

refers to the biological potential for reproduction and reflects life history factors such as when females become biologically capable of carrying pregnancies to term (i.e., age of first parturition) and the number of offspring expected per birth (i.e., prolificacy rate). Herd management practices such as delaying the age of first parturition by keeping males separate from females or ensuring nursing females have access to quality forage can positively affect fertility independent of fecundity. Fertility is parameterized in the present model as the interaction between prolificacy rates, parturition rate and the age of first parturition.

Prolificacy rate refers to the average number of live offspring delivered per birth (i.e., litter size, or lambing and kidding rate for sheep and goats, respectively). This number has been shown to vary depending on the adaptability of different breeds to environmental conditions (Mourad 1993), as well as the season of birth and parity in both sheep and goats (Wilson 1989). Multiple births are more common in goats than sheep (Dahl and Hjort 1976: 93). Redding utilized lambing and kidding rates based on Awassi ewes and Baladi goats (respectively) that were adjusted to account for unreported abortions (Redding 1981). Overall, the incidence of twinning and survival of both offspring is influenced by the nutritional status of the mother (Dahl and Hjort 1976; Mellado et al. 2006) but prolificacy has also been shown to increase with age and parity (Wilson 1989; Wilson et al. 1984; Wilson and Durkin 1983). A study of Improved Boer goats reported kidding rates increased from 18 months to 3.5 years of age and decreased from 4.5 years and older (Erasmus et al. 1985).

Parturition rate refers to the number of births per female over a specific time frame; typically, this time frame reflects a breeding season or year which varies with gestation length and the time it takes for estrus to re-occur after giving birth. Also referred to as the annual reproductive rate (*ARR*), this composite value considers the inter-birth interval and the

number of offspring expected per birth. *ARR* is calculated as:

$$ARR = \frac{l \times 365}{i} \qquad (6.13)$$

where l is the mean litter size (or mean prolificacy rate), and i is the inter-birth interval in days (Upton 1984; Wilson 1989).

Inter-birth intervals are limited by the gestation period which can be 140-160 days for sheep and can range from 120 to 180 days for goats (Dahl and Hjort 1976). Both sheep and goats experience seasonal variation in reproductive ability as the onset of estrous coincides with decreases in day length and ends when day length increases (Rosa and Bryant 2003; Thimonier 1981; Yeates 1949). The effect is more pronounced as one moves farther north or south of the equator as seasonal changes in day length become more extreme (Hafez 1952).

Seasonal variation in environmental conditions can also affect parturition rate. For example, a study of Mexican dairy goats found that fertility, conception, prolificacy, and kidding interval is positively associated with rainfall which is highest in the summer whereas the effect of photoperiod on reproduction was not significant (Galina et al. 1995). The seasonal breeding rhythm of some Mediterranean breeds that are physiologically capable of out-of-season breeding can be manipulated by herders so that lambing occurs in the autumn (Balasse et al. 2023; Todaro et al. 2015) but this has not yet been observed among Neolithic herders in Dalmatia (see Chapter Ten; Sierra et al. 2023). Manipulation of seasonal breeding rhythms may also reduce the inter-birth interval. For example, a herd of Alpine dairy goats raised in semi-arid Mexico that gave birth out-of-season, in the late spring, exhibited a kidding interval of 265 days compared to 362 days shown for does that kidded in autumn, the main lambing season (Silva et al. 1998). A review of goat and sheep reproductive traits within various environmental zones and management systems indicates a parturition interval

of 10 months is the norm but can be shorter or longer depending on whether breeding is controlled (Wilson 1989).

The age of first parturition is an important factor for herd growth because if animals can give birth earlier in life, the overall fertility rate and productivity of the herd will increase (Redding 1981: 59; Wilson et al. 1985; Wilson and Durkin 1983). However, higher risk of abortion observed for primiparous females (i.e., first time mothers) may indicate that physical development has greater physiological importance than reproduction (Mellado et al. 2006).

Delaying age of first parturition can be achieved by separating males from females or outfitting males with specialized contraceptive devices (Wilson 1989). Healthier and more productive offspring are expected from delaying the age of first conception to when ewes and does have fully developed physically (Erasmus et al. 1985). From a perspective of productivity, an earlier age of first parturition may be worth accepting an increased infant mortality rate because doing so would extend the total length of reproductive life of an individual and improve total flock productivity (Wilson and Durkin 1983). Whether or not herders should delay the age of first parturition is therefore a critical aspect of livestock breeding. Based on data collected from sheep and goat management systems within 10 countries in Africa south of the Sahara, the average age of first parturition for goats is 513 days or 17 months and 504 days or 16.5 months for sheep (Wilson 1989) but among different breeds raised under different conditions, this age may be as young as 14 ± 2 months (Galina et al. 1995).

In the model used here female fecundity is calculated as the product of the parturition rate (i.e., *ARR*, Equation 6.13) and the prolificacy rate for each stage class that includes

individuals who have reached the age of first parturition (Table 6.1). Although it is possible for female goats and sheep to become pregnant earlier than 12 months of age (Dahl and Hjort 1976), the model presented here sets 12 months as the age of first parturition. Prolificacy rates for each reproductive female are generated using a normal distribution function based on average sheep and goat prolificacy rates of 1.15 ± 0.122 (sd) and 1.49 ± 0.275 (sd), respectively based on a review of prolificacy among sheep and goats raised under traditional management systems throughout Africa (see Table 2 in Wilson 1989). The mean and standard deviation are used to generate a normal distribution of values corresponding to the number of age classes of reproductive females. The array is then re-arranged so that peak prolificacy rates are attained at the midpoint of these ages, in this case corresponding to the 3-4 year age class. An example of prolificacy based on this algorithm is provided in Table 6.1. In the model, parturition rates are calculated using Equation 6.13 for each time-step, where l is the mean of the stochastically generated prolificacy rates for that time-step and i is fixed at 300 days based on a 10-month inter-birth interval (Wilson 1989).

3. Herd Culling

One goal of this chapter is to assess whether archaeological culling profiles can be used in population projection models to understand the management decisions driving herd dynamics and to identify aspects of risk minimization related to herd demography. To this end, the demographic implications of theoretical culling strategies as well as culling strategies associated with Neolithic period sites excavated on the Dalmatian Coast of Croatia are examined.

Marom and Bar-Oz (2009) provide survivorship probabilities for each of the ten theoretical harvest profiles described in Chapter Five, standardizing survivorship rates using

bins fitting both Payne's (1973) and Vigne and Helmer's (2007) age class systems. The probabilities associated with these culling strategies were depicted as survivorship curves in Figure 5.1. Here, these probabilities are parameterized as age-specific offtake rates (Table 6.2) to examine the effect of these theoretical culling strategies on sheep and goat herds. Additionally, while Payne's (1973) wool and Vigne and Helmer's (2007) fleece strategies were devised to model sheep management, they are used to model the population effects of applying these culling rates to both sheep and goat herds. In Chapter Five age-at-death data for caprines recovered from Smilčić, Zemunik Donji, Benkovac-Barice, and Islam Grčki were used to construct mortality profiles (see Chapter Five, Figure 5.2). That procedure involved calculating frequency density from relative frequencies following Brochier (2013; see Appendix B). A slightly different method was used to calculate survival probabilities for each of these sites (excluding Hvar period Islam Grčki due to small sample size). Here, relative frequencies were calculated from absolute frequencies as before. The cumulative sum (Q_x) of the relative frequencies was then used to obtain survival probabilities for each age class, calculated as $1\text{-}Q_x$, following Price et al. (2016; see also Appendix B). The survival probabilities used to model empirical harvest strategies are therefore derived from the relative frequencies rather than the frequency densities shown in the mortality profiles (Figure 5.1).

The empirical survival probabilities are presented as survivorship curves using Payne's age groups in Figure 6.1. Survival probabilities for age class G (4-6 years) and H (6-8 years) were reallocated to ages 5 and 6, and 7 (respectively) to fit these empirical culling profiles to the age distribution used in the model (Table 6.1) using the formula:

$$x = 1 - \sqrt{1 - z} \qquad (6.14)$$

where x is the offtake rate of each age in age class G (or H), and z is the offtake rate of age class G (or H). This allocation assumes that, for age class G, the same offtake rate applies to individuals aged 4-5 years and individuals 5-6 years. The recalculated survival probabilities are presented in Table 6.3. In the simulations, the survivorship probability p for each age class i are converted to offtake rates as $o_i = 1 - p_i$.

Table 6.1. Parameters used in this study to construct Lefkovitch population projection matrix for sheep and goats. Parturition rates are calculated following Equation 6.13 and vary with respect to prolificacy rates. Prolificacy rate were generated based on average sheep and goat rates of 1.15 ± 0.122 and 1.49 ± 0.275 (respectively) reported by Wilson (1989). Mortality rates reflect Redding's (1981) assumptions of age-related vulnerability of adults. These are baseline rates from which inter-annual variation in mortality are simulated in the program.

Age	Parturition Rate		Prolificacy		Mortality	
(years)	Female	Male	Female	Male	Female	Male
Taxon: Goat						
0.17	0.00	0	0.00	0	0.225	0.225
0.50	0.00	0	0.00	0	0.150	0.150
1.00	0.00	0	0.00	0	0.075	0.075
2.00	1.82	0	1.00	0	0.100	0.050
3.00	1.82	0	1.15	0	0.100	0.050
4.00	1.82	0	1.43	0	0.050	0.050
5.00	1.82	0	1.94	0	0.050	0.050
6.00	1.82	0	1.39	0	0.100	0.150
7.00	1.82	0	1.12	0	0.500	0.250
Taxon: Sheep						
0.17	0.00	0	0.00	0	0.160	0.160
0.50	0.00	0	0.00	0	0.107	0.107
1.00	0.00	0	0.00	0	0.053	0.053
2.00	1.40	0	1.05	0	0.100	0.050
3.00	1.40	0	1.14	0	0.100	0.050
4.00	1.40	0	1.23	0	0.050	0.050
5.00	1.40	0	1.24	0	0.050	0.050
6.00	1.40	0	1.20	0	0.100	0.150
7.00	1.40	0	1.09	0	0.500	0.250

Table 6.2. Survivorship percentages for ten theoretical harvest profiles associated with different production strategies, as presented by Marom and Bar-Oz (2009). Survival probabilities derived from Redding (1981), Payne (1973), and Vigne and Helmer (2007).

Age	Energy[a]	Security[a]	Meat[b]	Milk[b]	Wool[b]	Meat A[c]	Meat B[c]	Milk A[c]	Milk B[c]	Fleece[c]
0.17	90.4	90.4	85	47	85	81	86	22	83	69
0.50	90.4	90.4	75	42	75	34	68	11	50	35
1.00	77.6	64.5	70	39	65	11	28	4	36	24
2.00	47.6	38.0	50	35	63	7	6	3	18	17
3.00	25.0	25.0	30	28	57	7	6	3	18	17
4.00	23.9	23.9	22	23	50	3	1	2	6	6
5.00	18.2	18.2	19	18	43	1	1	1	1	1
6.00	16.1	16.1	19	18	43	1	1	1	1	1
7.00	11.8	11.8	10	10	20	1	1	1	1	1

[a]Redding (1981); [b]Payne (1973); [c]Vigne and Helmer (2007);

Table 6.3. Survivorship probabilities derived from age-at-death data associated with the four Neolithic sites examined. Probabilities calculated following Price et al. (2016).

Age (years)	Smilčić EN	Smilčić MN	Benkovac-Barice MN	Islam Grčki MN	Zemunik Donji MN
0.2	100.0	98.2	98.6	81.2	100.0
0.5	72.7	90.6	88.4	81.2	82.8
1.0	56.8	83.9	85.9	67.2	70.2
2.0	19.3	41.2	54.9	37.5	27.3
3.0	13.6	37.4	39.6	28.1	21.2
4.0	6.8	27.9	28.7	21.9	3.0
5.0	2.3	9.6	3.2	9.4	0.0
6.0	0.0	2.2	0.0	6.2	0.0
7.0	0.0	0.0	0.0	0.0	0.0

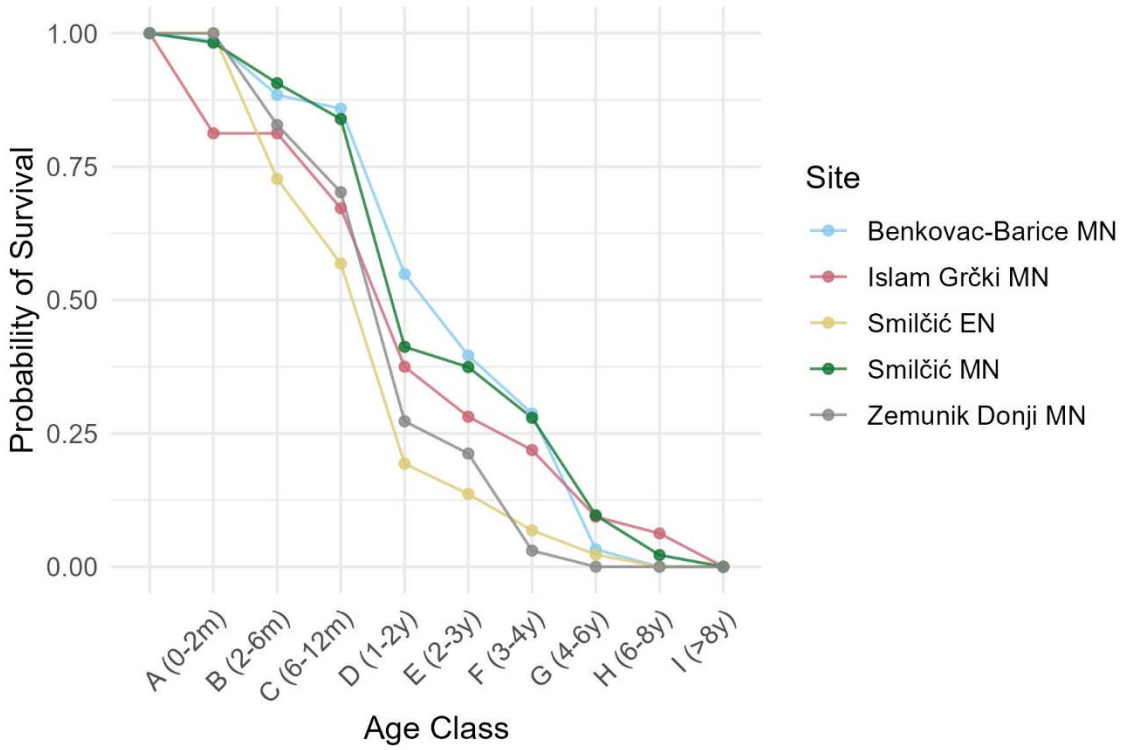

Figure 6.1. Survivorship curves from age-at-death data obtained from analysis of sheep and goat mandibles from Early (EN) and Middle (MN) Neolithic sites mentioned in text based on data presented in Table 6.3.

D. Simulating Stochastic Herd Growth Dynamics

The construction of Lefkovitch population projection matrix models and demographic simulations were performed in R Statistical Software (v4.3.1; R Core Team 2023) using the "mmage" package v2.4.2 (Lesnoff 2024). A step-by-step guide to the creation of the projection matrix, derivation of predictive indices of population states (e.g., λ, sex proportion, herd age structure), population projection simulations, and customized scripting procedures is provided in Appendix C.

Annual herd growth dynamics were projected over a 200-year period. An initial herd size of 150 animals was used based on an assumption that this was the number at which small-scale pastoral households might be self-sufficient (Bradburd 1980). Halstead suggests that a family of six would need at least 300 primitive, unimproved ovicaprids to survive assuming the herd was exploited for some combination of milk and meat (Halstead 1996: 34). Since this number may underestimate the importance of herder skill and luck (Moritz et al. 2017: 531) the program implemented here simulates environmental stochasticity. This is achieved by varying fertility and mortality rates from one time-step to the next by sampling from a normal distribution at each time-step. A normal distribution of 100 values based on prolificacy mean and standard deviation for goats (1.49 ± 0.275) and sheep (1.15 ±1.22). Six values from the distribution were then sampled at random and rearranged so that that peak prolificacy corresponds to the 3-4 year age class, consistent with observations on prolificacy rates as a function of parity (Erasmus et al. 1985; Wilson 1989; Wilson et al. 1984). The number of prolificacy rates used depends on the number of age classes containing reproductive females. In the present simulation, age of first parturition was set to age class D (1-2 years) and females surviving through age class I (>8 years) continue to reproduce unless

they die naturally or are slaughtered. A similar approach was used to vary infant and adult mortality rates using the mean and standard deviation of the values presented in Table 6.1. The values shown in Table 6.1 are but one possible outcome of this prolificacy and mortality rate generation procedure. For each time-step, the average of the six randomly sampled prolificacy rates (l) was used to calculate the parturition rate (ARR) following Equation 6.13.

Each unique combination of mortality and fertility rates represents the environmental conditions of a single year. Two separate sets of 200 years of environmental conditions were simulated (one for sheep and one for goats) to assess the performance of the two populations under each harvest strategy. Survival probabilities by age were derived from the five culling profiles and each of the 10 theoretical harvest models and supplied as offtake rates to the projections. An additional "Baseline" strategy was included which sets offtake rates for males and females of all age classes to zero to simulate herd population dynamics unconstrained by annual slaughter.

Projections were made for goats and sheep separately, resulting in 32 herd growth simulations with age-specific offtake rates differentiating population models from one another. The program assumes offtake rates primarily apply to males. Since herd growth is dependent on females, precluding females from offtake would prohibit the evaluation of each theoretical and empirical harvest strategy since herd survival would be influenced solely by stochastic variation in fertility and mortality. Assuming herders aim to maximize herd numbers, the applied female offtake rates were 15% of each strategy's rates. The net female offtake rate of 15% is based on a report indicating that 14.5% of intensively managed goats were culled due to infertility and a culling rate of 17.1% for infertile animals aged 1-2 years (Malher et al. 2001).

E. Results: Herd Population Structure and Growth

Even before running the simulation, two important demographic metrics with predictive value can be obtained from the mortality, fertility, and survivorship rates described above. The first metric is λ (i.e., the herd or population growth rate), which is obtained from the dominant eigenvalue of the Lefkovitch transition matrix (Equation 6.9; Crouse et al. 1987; Lesnoff et al. 2000; Negassa et al. 2015). When $\lambda > 1$, populations are expected to increase; $\lambda < 1$ predicts negative population growth; and a steady state is reached when $\lambda = 1$. The second metric is the proportions of females and males in herds which will vary under different fertility and mortality constraints. Since fertility and mortality rates vary at each time-step, λ and herd structure can vary as a result. After creating the 200-year environment, λ and proportion of females were obtained for each herd and strategy combination and bootstrapped estimates (n =1000) of the mean of each metric were calculated (Tables 6.4 and 6.5).

Overall, bootstrapped estimated mean λ (λ_{boot}) for goats is higher than sheep λ_{boot}, consistent with higher intrinsic population growth in goats relative to sheep shown by other demographic models for these species (Redding 1984; 1981; Upton 1984). This suggests that goats will tend to outperform sheep in terms of population growth under the variety of harvest strategies examined. Rapid and exponential population growth is predicted for the Baseline model, which is expected because the main constraint on population size, offtake was removed for this strategy (Lesnoff et al. 2000; Moritz et al. 2017). Importantly, the Baseline $\lambda_{boot} > 1$ for both goats and sheep; this confirms that the mortality and fertility rates are realistic. If fertility rates were too low or mortality rates too high such that the Baseline model $\lambda_{boot} < 1$, population decline would be inevitable for both species regardless of harvest

strategy. Additionally, Baseline λ_{boot} is 0.006 higher for goats than sheep while inter-species differences in λ_{boot} among the strategies examined varies between 0.001 and 0.004 (Table 6.4). For example, excluding the Baseline model, the largest difference between sheep and goat λ_{boot} is shown for Wool and the smaller differences are shown is for the Meat A, Meat B, and Milk B strategies; and λ_{boot} for goats is always higher. This suggests some culling strategies may have stronger effects on the growth of sheep than goat populations.

For six of the theoretical harvest profiles (Milk, Meat A and B, Milk A and B, and Fleece), $\lambda_{boot} < 1$ for both goats and sheep, indicating herd sizes will *decline* (Table 6.4). The Milk A harvesting strategy is associated with the lowest λ_{boot} estimates for both goat and sheep populations, predicting rapid decreases in herd size relative to other strategies. This is likely due to the very low survival probability of animals younger than 1 year under the Milk A survivorship profile (Table 6.2). In contrast, the Energy, Security, Meat, and Wool strategies each permit sheep and goat herd growth with $\lambda_{boot} > 1$. As for the empirical culling profiles associated with the four Neolithic sites, λ_{boot} predicts *unsustainable harvesting rates* for sheep and goats at Impresso period Smilčić, while harvest strategies identified for the Danilo-period sites (Smilčić, Benkovac-Barice, Islam Grčki, Zemunik Donji) are predicted to *maintain or increase herd sizes* (Table 6.5).

A significant negative correlation was found between λ_{boot} and the proportion of females in the herd (Pearson's product-moment correlation: $r = -0.902$, $t = -11.07$, $df = 28$, $p < 0.001$), indicating that high female-to-male ratios are associated with lower λ and therefore reduced or even negative population growth. This association is unexpected given the importance of females for reproduction. Traditional sheep and goat systems tend to have higher proportions of females in herds to limit resource consumption by non-reproductive

animals (e.g., males and infertile females; Dahl and Hjort 1976; Redding 1981; Wilson 1978). However, the strategy exhibiting the highest proportion of females and the lowest λ_{boot} is Milk A. Additionally, for each of the theoretical strategies where the proportion of females is greater than 0.70, $\lambda_{boot} < 1$ which predicts herd sizes will decline. At first glance, it might seem as if there is a threshold of the ratio of female-to-male animals that if surpassed will have a negative impact on herd reproductive potential. On the other hand, the estimated proportion of females under the Impresso period Smilčić strategy is 0.65 which is higher than the proportion of females under other empirical culling strategies for which $\lambda_{boot} > 1$ and herd growth is expected (i.e., Smilčić MN, Benkovac-Barice, and Zemunik Donji, Table 6.5). The negative association between female-to-male ratio and λ_{boot} may therefore be attributed to low survival probabilities of animals before they reach the age of first parturition. Animals younger than 2 years of age under the Milk A and Impresso period Smilčić strategies have the lowest survival rates relative to other theoretical and empirical culling strategies (respectively), which may account for the relatively low λ_{boot} estimates (Figure 6.1).

The initial age structure of herds under each strategy is shown in Figure 6.2. For each strategy the number of infant goats in age class 0-2 months exceeds that of sheep but the trend is reversed in subsequent age classes. This is likely a result of a combination of higher prolificacy rates of breeding does and higher mortality rates of kids. Higher kid than lamb mortality rates reduce number of goats relative to sheep that reach adulthood. The same effect is observed in the Baseline strategy suggesting that fertility and infant mortality rates play a non-trivial role in herd structure. Subtle differences in the age-structure of herds from one strategy to the next are therefore a reflection of offtake rates associated with particular production goals.

The results of the 200-year herd demography simulations are illustrated in Figure 6.3. As predicted by λ_{boot}, the numbers of sheep and goats decline rapidly for Payne's (1973) Milk profile and for the Vigne and Helmer's (2007) Meat A and B, Milk A and B, and Fleece models. Herds increase well above the initial population size under the Energy, Security, Meat, and Wool strategies. Both goat and sheep populations decline under the Early Neolithic (Impresso) Smilčić strategy, falling to less than 50 animals total after 200 years. Both sheep and goat populations increase dramatically over 200 years at Benkovac-Barice and Middle Neolithic (Danilo) Smilčić, but the goat population is more than twice the sheep population at the end of the simulation. The trajectories of sheep and goat populations are under the Zemunik Donji and Islam Grčki harvest strategies are indistinguishable; goat numbers gradually increase over the course of the simulation and sheep herd sizes remain relatively stable. Overall, in terms of population size, goats outperform sheep when age-structured culling rates are held constant through time.

The projections were replicated 10 times to assess whether the environments simulated for sheep were more hostile than the ones simulated for goats. Each replicate entailed the generation of a new set of 200 annual fertility and mortality rate combinations. The results of the replications involving the simulation of 10 new sets of environmental conditions for both goats and sheep are consistent with the original projection (Figure 6.4). These results suggest that the Milk (Payne 1973), Meat A and B, Milk A and B, and Fleece (Vigne and Helmer 2007) harvest strategies *are incompatible* with the assumed goal of maximizing the number of animals in the herd. These data also indicate that the Energy, Security (Redding 1981), Meat, and Wool (Payne 1973) strategies accommodate goat population growth whereas sheep population growth is more restricted. Furthermore, among

these four theoretical strategies as well as the Danilo period strategies, higher prolificacy rates in goats appear to compensate for higher kid mortality rates even when conditions may be periodically unfavorable.

Table 6.4 Bootstrapped (n=1000) means of predicted herd growth rate, λ (λ_{boot}), proportions of females and males in sheep and goat herds starting at 150 animals when survivorship probabilities derived from theoretical culling profiles (Payne 1973; Redding 1981; Vigne and Helmer 2007; Table 6.2) are parameterized as offtake rates in the Lefkovitch population projection matrix (Lefkovitch 1965). Values shown here reflect 200 years of variation in mortality and fertility rates given in Table 6.1.

	Energy	Security	Meat	Milk	Wool	Meat A	Meat B	Milk A	Milk B	Fleece	Baseline
Taxon: goat											
λ_{boot}	1.019	1.007	1.009	0.967	1.017	0.939	0.960	0.917	0.964	0.950	1.074
Proportion Female	0.63	0.64	0.68	0.79	0.68	0.75	0.71	0.84	0.73	0.76	0.49
Proportion Male	0.37	0.36	0.32	0.21	0.32	0.25	0.29	0.16	0.27	0.24	0.51
Taxon: sheep											
λ_{boot}	1.016	1.004	1.006	0.965	1.013	0.938	0.959	0.915	0.963	0.948	1.068
Proportion Female	0.64	0.65	0.69	0.81	0.69	0.77	0.72	0.86	0.75	0.79	0.47
Proportion Male	0.36	0.35	0.31	0.19	0.31	0.23	0.28	0.14	0.25	0.21	0.53

Table 6.5. Bootstrapped (n=1000) means of predicted herd growth rate, λ (λ_{boot}),), proportions of females and males in sheep and goat herds starting at 150 animals when survivorship probabilities derived from empirical culling profiles for one Early (EN) and four Middle (MN) Neolithic sites (Table 6.3) are parameterized as offtake rates in the Lefkovitch population projection matrix (Lefkovitch 1965). Values shown here reflect 200 years of variation in mortality and fertility rates given in Table 6.1.

	Benkovac-Barice MN	Islam Grčki MN	Smilčić EN	Smilčić MN	Zemunik Donji MN
Taxon: goat					
λ_{boot}	1.029	1.003	0.987	1.022	1.003
Proportion Female	0.60	0.68	0.65	0.60	0.62
Proportion Male	0.40	0.32	0.35	0.40	0.38
Taxon: sheep					
λ_{boot}	1.026	1.000	0.985	1.019	1.000
Proportion Female	0.60	0.69	0.67	0.60	0.64
Proportion Male	0.40	0.31	0.33	0.40	0.36

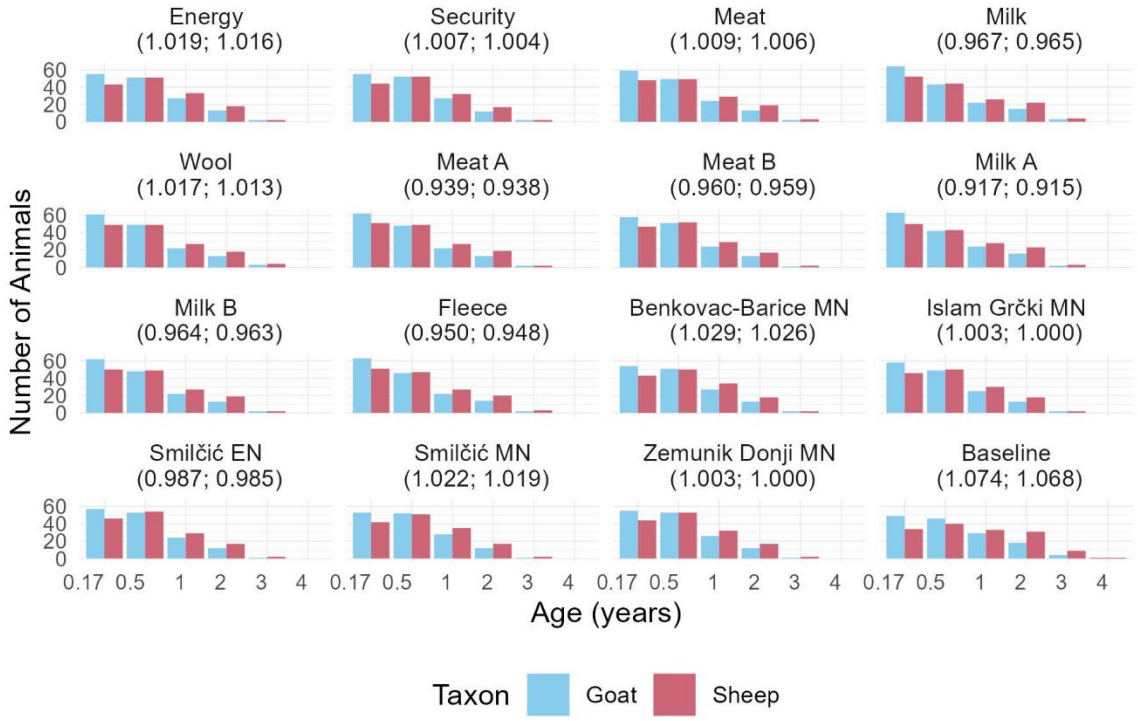

Figure 6.2. Initial age-structure (combined males and females) of herds of 150 goats and 150 sheep for each culling strategy examined. Age-structure generated using sex proportions in Tables 6.4 and 6.5. Graphs representing demographic simulations for Neolithic sites distinguish Impresso (EN) from Danilo (MN) period data. Values in parentheses are the predicted herd growth rates (λ_{boot}) for goats and sheep, respectively.

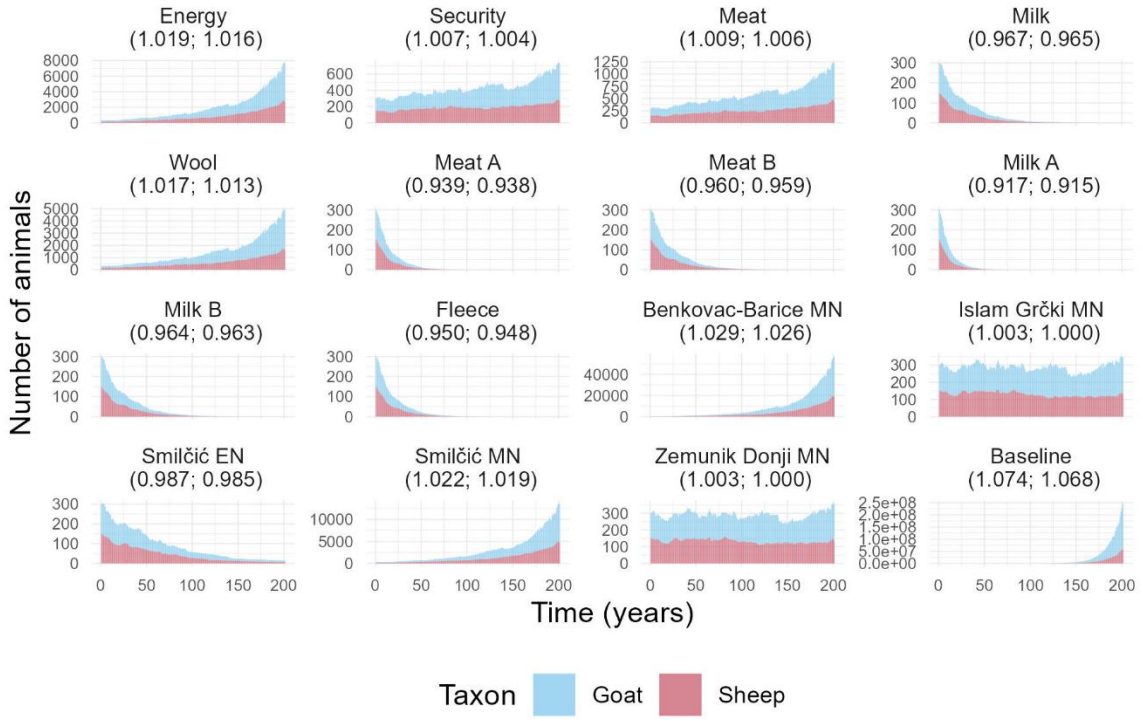

Figure 6.3 Simulation of goat and sheep population size changes over a 200-year period for each of the harvest profiles discussed above. The Baseline model projects herd population dynamics unconstrained by offtake rates. Herd sizes start at 150 sheep and 150 goats. Inter-annual variation in fertility and mortality was simulated separately for goats and sheep. Values in parentheses are the bootstrapped estimated herd growth rates (λ_{boot}) for goats and sheep (respectively) given in Tables 6.4 and 6.5. Herd size growth is predicted when $\lambda_{boot} > 1$, decline when $\lambda_{boot} < 1$, and steady state when $\lambda_{boot} = 1$. Projections demonstrate that goat population sizes grow faster than sheep for strategies where $\lambda_{boot} \geq 1$. Both sheep and goat populations decline rapidly and are virtually extinct within 25-50 years under six of the theoretical harvest strategies (Milk, Meat A and B, Milk A and B, and Fleece). Stable slaughtering strategies are shown for two of the Neolithic culling profiles (Zemunik Donji and Islam Grčki). Graphs representing demographic simulations for Neolithic sites distinguish Impresso (EN) from Danilo (MN) period data.

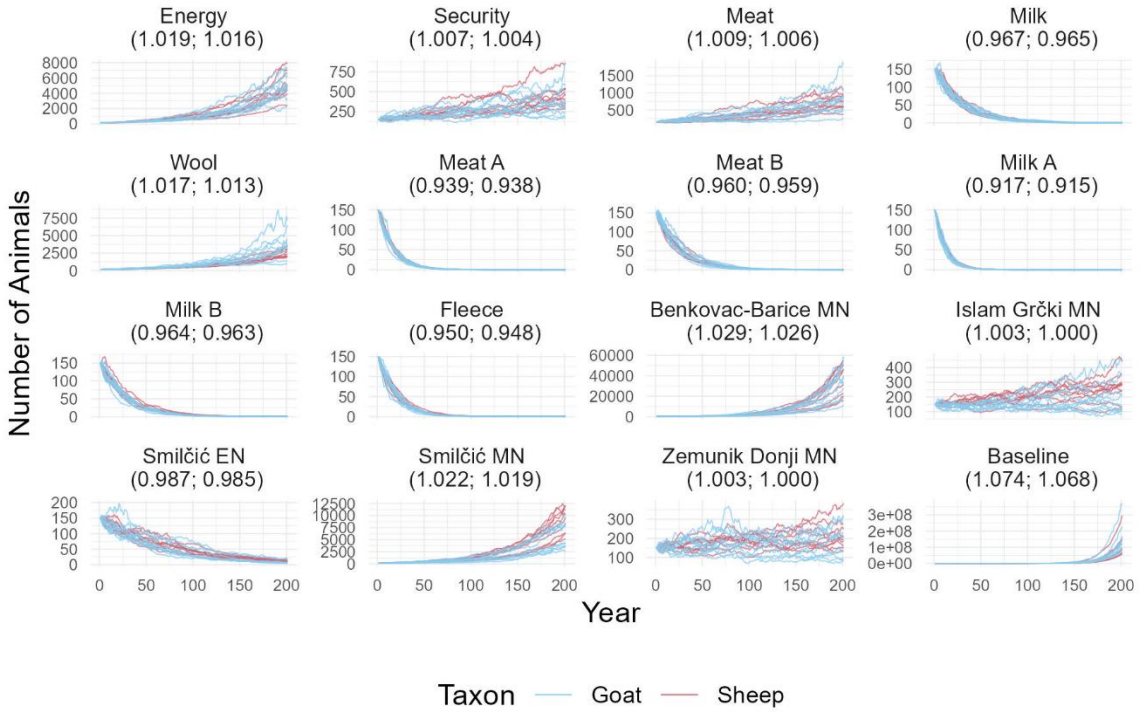

Figure 6.4. Results of 10 replications simulated goat and sheep population size changes over a 200-year period for each of the harvest profiles discussed above, starting with 150 sheep and 150 goats. The Baseline model simulates population dynamics unconstrained by offtake rates. Each replication utilized a unique set of inter-annual fertility and mortality rates, performed separately for goats and sheep. Values in parentheses are the bootstrapped estimated herd growth rates (λ_{boot}) for goats and sheep (respectively) given in Tables 6.4 and 6.5. Replications are consistent with the predictions associated with λ_{boot}: growth when $\lambda_{boot} > 1$, decline when $\lambda_{boot} < 1$, and steady state when $\lambda_{boot} = 1$.

F. Modeling Risk Minimization via Optimization of Offtake

Herd culling is a key aspect of livestock management that herders can directly control. One of the questions this chapter aims to address is whether population projection models can illuminate how culling strategies minimized risk within ancient agropastoral economies. The population projections presented above demonstrate the utility of λ as a predictor of herd size change when offtake rates are held constant. But during periods of low fertility or high mortality, herders may need to reduce offtake rates to allow for livestock herds sizes to remain stable or recover from losses. Conversely, a more aggressive culling

strategy may be required when the demands of an increasing herd size are constrained by available labor, pasturage, or sources of fodder. This section examines when and by what factor offtake rates must be adjusted so that a steady state can be achieved, assuming herders seek to maximize herd size when resources restrict the number of livestock to 150 sheep and 150 goats.

The initial projections assumed offtake rates were applied with an intensity rate, $\varphi = 1$, that was constant across all time-steps (Lesnoff 2024; Lesnoff et al. 2000). An optimization procedure was employed to identify the optimal intensity rate, φ_{opt}, by which the probability of offtake for females must be reduced such that $\lambda = 1$ (Lesnoff et al. 2000; 2014). In other words, an algorithm was written to identify a factor that when multiplied by the offtake rates, would result in herd sizes remaining unchanged from the current to the subsequent timestep.

The value φ_{opt} was found through an iterative process of minimizing $(\lambda - m)^2$ where m is the multiplication rate of a population in a steady state (Lesnoff 2024). Mathematically, the optimization goal was defined as $\lambda = m = 1$. The simulation described in the previous section was repeated but with an additional step. Before completing a projection from t to $t + 1$, the predicted growth rate, λ, was obtained from the current time-step's transition matrix. Since the model is female-dominated, female offtake probabilities were then adjusted by the optimal harvest intensity rate, φ_{opt}, if $\lambda < \lambda_{min}$ or if $\lambda \geq \lambda_{max}$. The threshold values of λ_{min} and λ_{max} were defined as the 25th and 75th percentiles (respectively) of the bootstrapped λ values summarized as λ_{boot} in Tables 6.4 and 6.5. Omitting λ estimates for the Baseline strategy, $\lambda_{min} = 0.954$ and $\lambda_{max} = 1.017$. A Levene's test for equality of variances was performed to determine whether optimizing offtake significantly reduced inter-annual variance in the

multiplication rates of sheep and goat herds for each strategy (Table 6.6).

*Table 6.6. Results of Levene's test for equality of variances comparing predicted annual herd growth rate (λ) under each strategy's unadjusted culling rates with actual annual herd multiplication rates (*m*) after culling rates were optimized. When $\lambda < \lambda_{min}$ (0.954) offtake rates were decreased and increased when $\lambda > \lambda_{max}$ (1.017) to achieve m = 1, such that herd size remained unchanged from one year to the next. Column λ_{boot} gives the mean of 1000 bootstrap estimates of λ (Tables 6.4 and 6.5). A pattern emerges from the significant ($p < 0.05$) results (in bold): optimization of sheep culling rates reliably reduces inter-annual variance of m while the significant reductions of variance in m for goats are only associated with strategies where $\lambda_{boot} > \lambda_{max}$.*

	goat		sheep	
strategy	**F**	**p-value**	**F**	**p-value**
Energy	5.559	**0.019**	7.171	**0.008**
Security	3.068	0.081	5.200	**0.023**
Meat	3.747	0.054	7.215	**0.008**
Milk	3.856	0.050	3.907	**0.049**
Wool	5.834	**0.016**	9.209	**0.003**
Meat A	1.023	0.312	6.186	**0.013**
Meat B	1.726	0.190	3.250	0.072
Milk A	3.235	0.073	16.171	**0.000**
Milk B	2.419	0.121	4.095	**0.044**
Fleece	2.330	0.128	8.323	**0.004**
Benkovac-Barice MN	6.623	**0.010**	9.557	**0.002**
Islam Grčki MN	2.609	0.107	6.380	**0.012**
Smilčić EN	1.863	0.173	3.657	0.057
Smilčić MN	5.694	**0.017**	5.603	**0.018**
Zemunik Donji MN	2.439	0.119	4.184	**0.041**
Baseline	0.000	1.000	0.000	1.000

The population projections and the mean number of goats and sheep over the 200-year period with optimized offtake are shown in Figure 6.5 and Figure 6.6, respectively. Figures 6.7 and 6.8 present the 10-year moving average of λ calculated from the unadjusted

offtake rates and the multiplication rate (m) following the φ_{opt}-adjusted (i.e., optimized) offtake rates for goats and sheep, respectively. In these figures, the frequency by which culling rates were adjusted can be ascertained by the amount of overlap between λ and m (i.e., less overlap reflects more frequent offtake adjustments). Additionally, the decrease in inter-annual variation of actual herd growth rates as a result of optimizing offtake is observable as reduced distortion of m relative to λ in Figures 6.7 and 6.8.

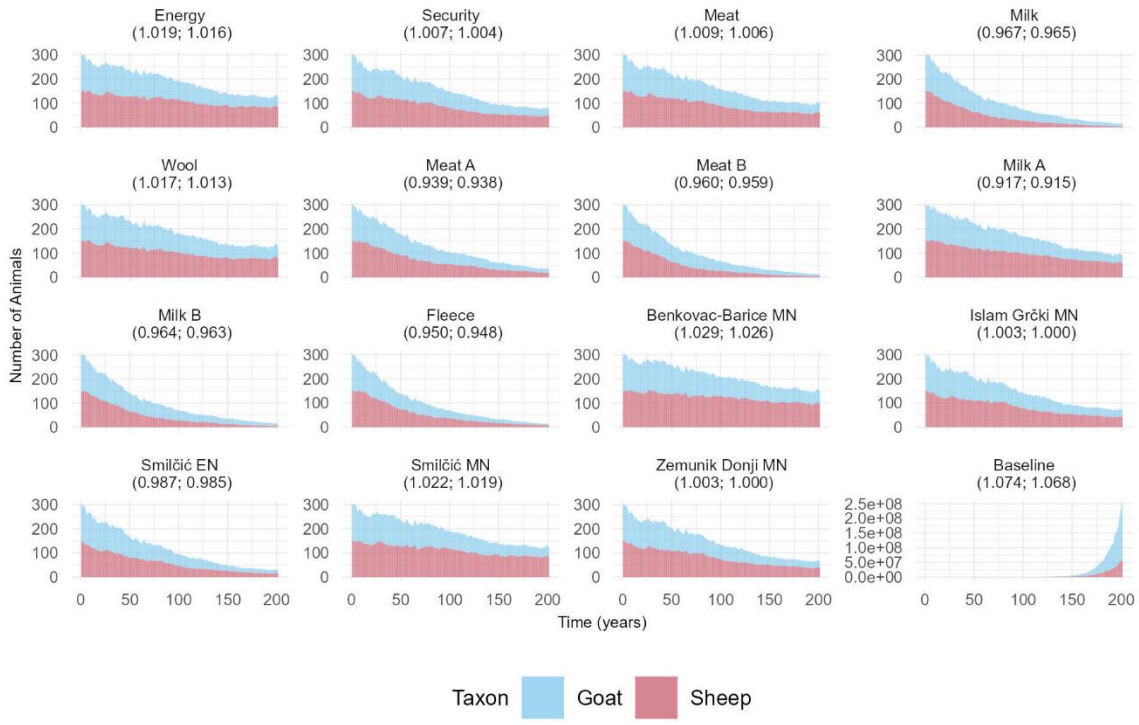

Figure 6.5. Reprojections of goat and sheep population size changes (starting with 150 sheep and 150 goats) within the same 200-year simulated environment used in the initial projection (Figure 6.3) but with optimized offtake rates. Optimization compared predicted annual herd growth rate (λ) to lower (λ_{min} = 0.954) and upper (λ_{max} = 1.017) thresholds. When $\lambda < \lambda_{min}$ offtake rates were decreased and increased when $\lambda > \lambda_{max}$, such that herd size remained unchanged from one year to the next (i.e., actual herd growth rate, m = 1). The Baseline model projects herd population dynamics unconstrained by offtake rates and remained unchanged from the initial simulation. Values in parentheses are the bootstrapped estimated herd growth rates (λ_{boot}) for goats and sheep (respectively) given in Tables 6.4 and 6.5. Optimization prolonged herd survival for all strategies where $\lambda_{boot} < 1$ and led to the decline in populations for strategies where $\lambda_{boot} > 1$.

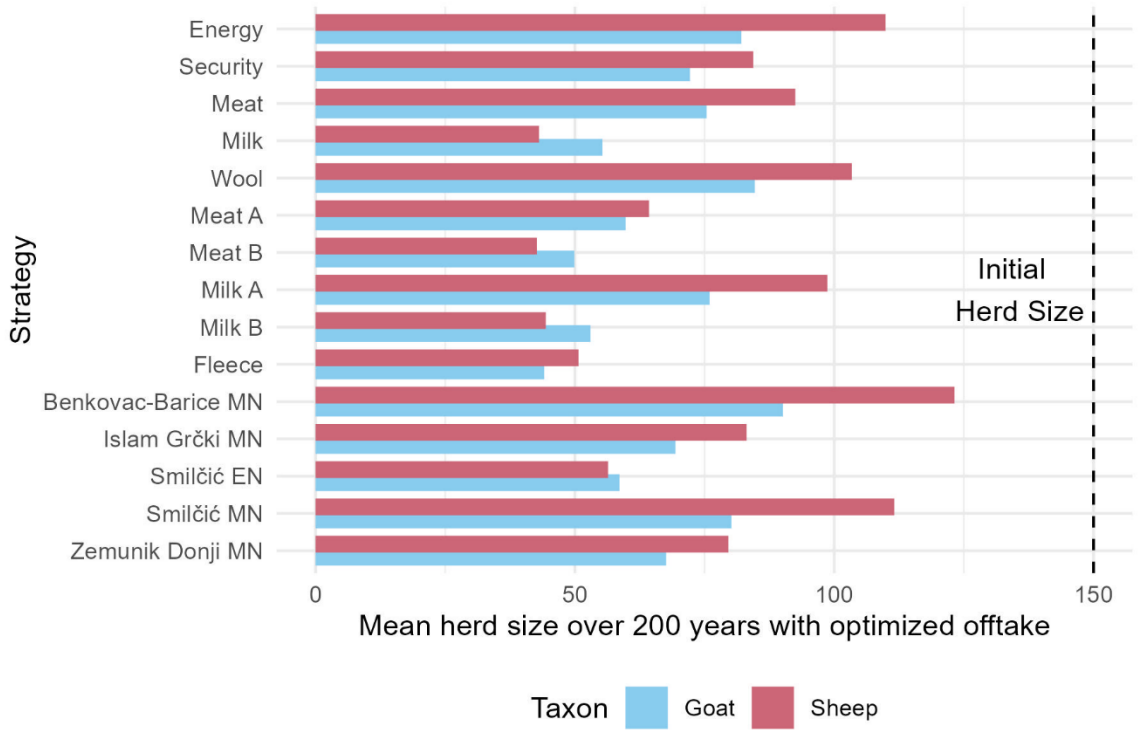

Figure 6.6. Mean herd size over the 200-year simulation of goat and sheep population size changes (starting with 150 sheep and 150 goats) within the same 200-year simulated environment used in the initial projection (Figure 6.3) but with optimized offtake rates. Mean number of sheep herd sizes are larger than goats for all strategies except for Payne's (1973) Milk and Vigne and Helmer's (2007) Meat B and Milk B strategies.

Several insights into the viability of the harvest profiles under consideration are revealed in the results of the optimization procedure. Overall, optimization of the female culling rate prolonged the survival of sheep and goat populations for strategies where herds were predicted to decline rapidly (Figure 6.5). Additionally, when offtake was optimized populations still declined under the six theoretical strategies where $\lambda_{boot} < 1$ (i.e., (Milk, Meat A and B, Milk A and B, and Fleece) but at a slower rate than the initial projections. Prior to the optimization simulation, sheep and goat herds went extinct within 25-50 years (Figure 6.3). When offtake was optimized, herd sizes after 200 years were small but not extinguished.

Recall that of all harvest profiles, sheep and goat populations were predicted to decline the fastest under the Milk A strategy based on the relatively low λ_{boot} estimate (Table 6.4). However, when offtake was optimized the Milk A strategy performed the best of the six unsustainable strategies in terms of both herd longevity (Figure 6.5) and average herd size (Figure 6.6). As a result of the annual predicted population growth rate (λ) being consistently lower than the threshold λ_{min}, offtake rates were frequently adjusted to achieve an actual herd multiplication rate of $m = 1$. In turn, inter-annual variation in herd growth rates was greatly reduced for the Milk A strategy, which is shown as lower distortion in the 10-year moving average of m relative to λ in Figures 6.7 and 6.8.

By comparison, herd sizes declined faster for the Meat A and B, Milk B, Fleece, and Milk strategies than for the Milk A strategy in the optimization simulation. For these strategies, estimated herd growth rates (λ_{boot}) were close to or even greater than the lower growth rate threshold ($\lambda_{min} = 0.954$) used to trigger the adjustment of offtake rates (Table 6.4). The optimization procedure was not initiated as frequently because for these models λ_{min} was too low a threshold. As a result, sheep and goat populations were fixed in a perpetual state of decline that was prolonged only by the occasional down-scaling of offtake rates which occurred any time-step where $\lambda > 1.017$. This prevented herds from sufficiently rebounding from previous losses.

Adjusting offtake rates curtailed the exponential population growth simulated among some strategies for which bootstrapped estimated herd growth (λ_{boot}) was greater than the upper threshold (λ_{max}) used to initiate the optimization procedure (i.e., when $\lambda_{boot} > 1.017$; Figure 6.5). The optimization procedure was designed to adjust offtake so that herd size remained stable from one timestep to the next. But increasing culling rates when the

predicted herd growth rate exceeded the upper threshold had a long-term negative impact on population sizes among the strategies where herd growth was expected (i.e., strategies where $\lambda_{boot} > 1$ in Tables 6.4 and 6.5). This situation explains why goat populations declined faster than sheep populations under the Energy, Wool, Benkovac-Barice, and Danilo Smilčić strategies.

The negative impact on herd size is perhaps most consequential for the Zemunik Donji and Islam Grčki strategies which were predicted to be sustainable (Table 6.5). For these strategies, sheep and goat population sizes were maintained over the initial 200-year simulation (Figure 6.3) and repeatedly shown to permit modest herd growth under a variety of fertility and mortality conditions (Figure 6.4). But optimizing offtake led to the gradual decline of sheep and especially goat populations for the Zemunik Donji and Islam Grčki strategies (Figure 6.5). The explanation for this is clearly related to the suitability of the thresholds used for initiating the optimization procedure. Predicted growth rates (λ) for these two strategies rarely dropped below the lower threshold (λ_{min}) of 0.954 (Figures 6.7 and 6.8) so for most of the simulated time, $\lambda_{min} < \lambda < 1$ and culling rates were not lowered. However, the increase of culling rates was triggered when the predicted growth rate exceeded the upper threshold (i.e., $\lambda > 1.017$) and appears to have occurred multiple times in the 200-year simulation for the Zemunik Donji and Islam Grčki strategies (Figures 6.7 and 6.8). Increasing offtake rates to restrict herd growth appears to have prevented both goat and sheep herds from rebounding from periods of low fertility and/or high mortality. The sustainability of the Zemunik Donji and Islam Grčki culling strategies demonstrated in the initial projections is likely attributed to intermittent but nonetheless essential periods of population growth. It appears, however, that these important episodes of rebounding herd size were nullified by the

optimization procedure.

Another insight of the optimization simulation is revealed in the lower average herd sizes of goats relative to sheep, even under strategies that permit population growth for both species (e.g., Benkovac-Barice and Danilo period Smilčić; Figure 6.6). Comparing goat and sheep herd growth rates under the Baseline model (Figures 6.7 and 6.8) suggests that goat population dynamics are more variable than sheep. Furthermore, with the exception of the Meat B and Early Neolithic (Impresso) Smilčić strategies, optimizing sheep offtake rates consistently reduced inter-annual variance in actual herd multiplication rates (*m*; Table 6.6). But for goats, this variance was significantly reduced only for strategies where bootstrapped estimated growth rate (λ_{boot}) was higher than the upper optimization threshold ($\lambda_{max} = 1.017$) used to initiate increased culling rates (i.e., Energy, Wool, Benkovac-Barice, and Middle Neolithic Smilčić; Table 6.6).

In the initial simulation higher prolificacy and parturition rates enabled goats to outperform sheep in terms of herd size within strategies where $\lambda > 1$ (Figure 6.3) even as a favorable year can immediately follow an unfavorable year. However, the optimized simulation restricts the reproductive capacity of goat populations such that if herd growth declines one year, and is predicted to be high the next year, the optimization procedure will increase culling rates so that herd sizes do not change from the first year. The implication of this observation is that there may be a key difference between goats and sheep in terms of the long-term impact of curbing herd growth by increasing slaughter rates. That is, despite overall higher growth rate, inter-annual variability in goat population dynamics cannot be reduced simply by increasing culling rates.

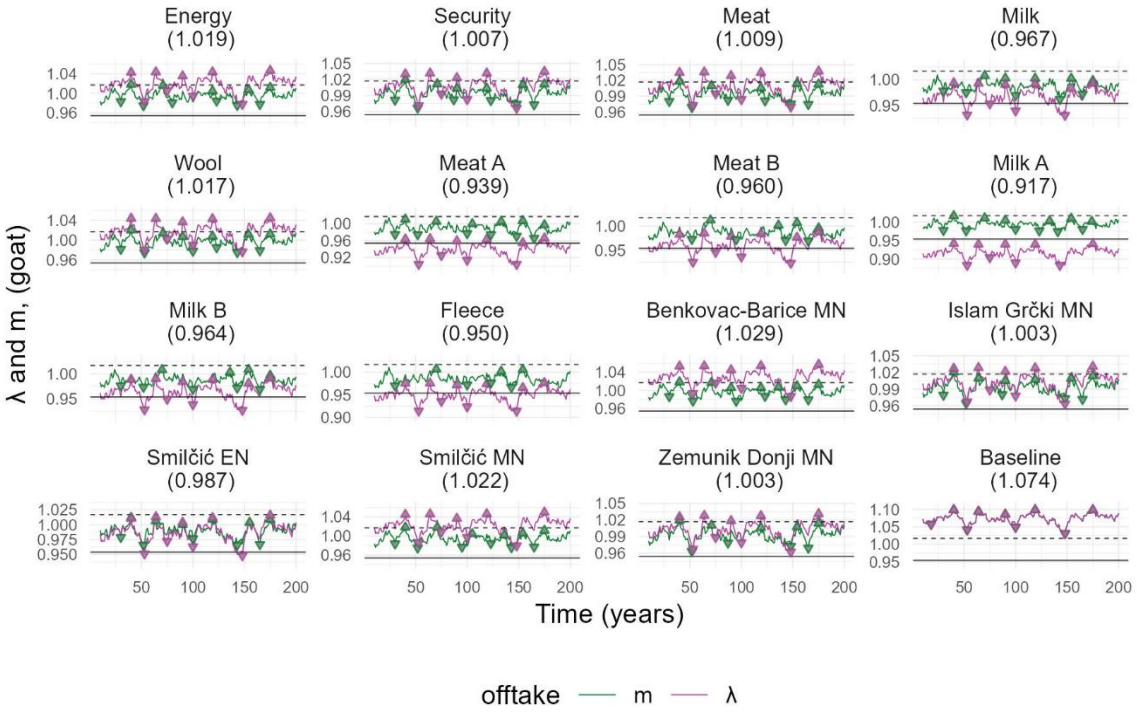

Figure 6.7. Annual goat population growth rate with unadjusted offtake rates (λ) versus actual population growth rate after optimization of offtake rates (m) summarized as 10-year moving average for easier visualization of trends. Values in parentheses are the bootstrapped estimated herd growth rates (λ_{boot}) given in Tables 6.4 and 6.5. Triangles and inverted triangles show high and low points, respectively. Solid and dashed lines refer to lower (λ_{min} = 0.954) and upper (λ_{max} = 1.017) thresholds used to initiate optimization of culling rates. The degree to which m and λ overlap is an indication of the frequency by which culling rates were adjusted. For example, no overlap is shown for Milk A since λ was almost always less than λ_{min}.

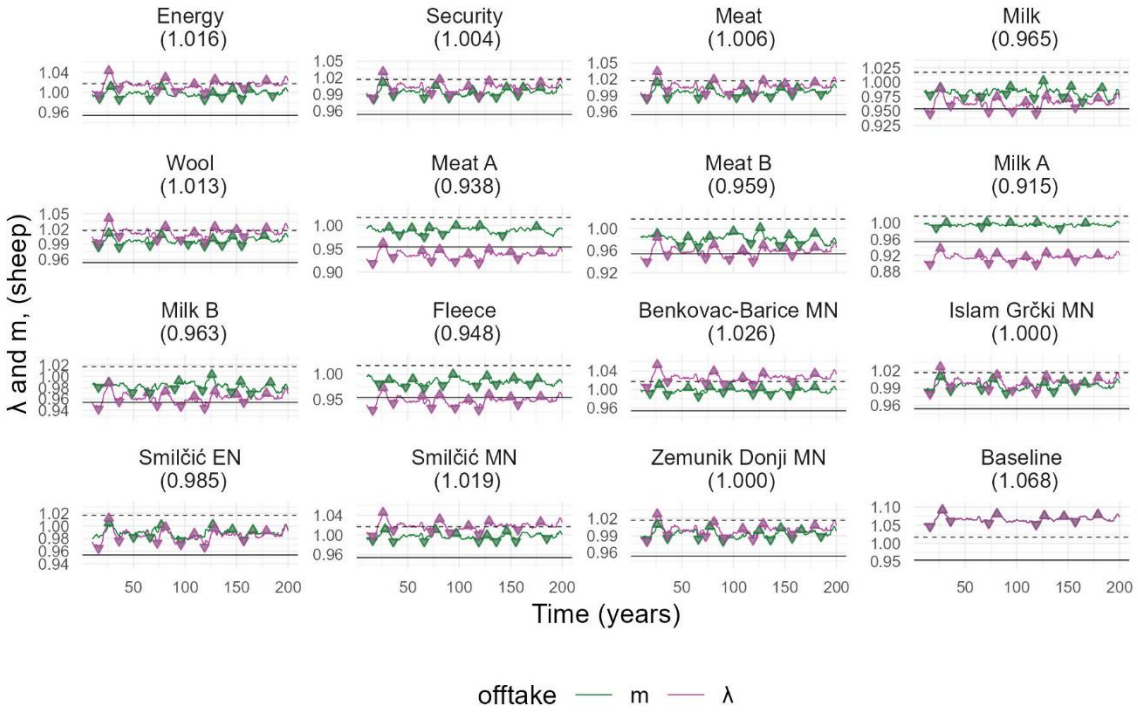

*Figure 6.8. Annual sheep population growth rate with unadjusted offtake rates (λ) versus actual population growth rate after optimization of offtake rates (*m*) summarized as 10-year moving average for easier visualization of trends. Values in parentheses are the bootstrapped estimated herd growth rates (λ_{boot}) given in Tables 6.4 and 6.5. Triangles and inverted triangles show high and low points, respectively. Solid and dashed lines refer to lower (λ_{min} = 0.954) and upper (λ_{max} = 1.017) thresholds used to initiate optimization of culling rates. The degree to which m and λ overlap is an indication of the frequency by which culling rates were adjusted. For example, no overlap is shown for Milk A and Meat A since λ was almost always less than λ_{min}.*

G. Discussion: Risk and Optimization of Herd Culling Rates

The projection model presented in this research is female dominated (i.e., population growth rates are derived from female fertility). In the model females of all age classes were subjected to reduced culling rates to differentiate between the demographic implications of the various harvest profiles examined. Female culling rates were 15% of the rates applied to males to account for the slaughter of infertile females (Malher et al. 2001). The population projection results show that applying culling rates to females even at this very reduced rate variably impacted livestock populations. For example, many of the theoretical culling

profiles in the literature used by archaeologists to interpret age-at-death data were shown to be unsustainable. The simulations projected rapid decimation of herds under strategies that have low survivorship probabilities associated with very young animals (e.g., Milk, Milk A, Meat A) and animals of reproductive age (e.g., Meat A and B, Milk B, Fleece).

The decimation of herds under the other strategies also highlights the relative importance of ensuring the survival of females. For example, population growth was projected for four of the theoretical models (i.e., Energy, Security, Meat, Wool) with the most forgiving culling rates for young animals and for age class C (1-2 years) in particular, which was parameterized as the age of first parturition (Table 6.1). For these four strategies animals aged 6-12 months have the highest probability of surviving relative to the other theoretical strategies considered (Figure 5.1). Additionally, for the Energy, Security, Meat, Wool strategies, greater numbers of females surviving to the age of first parturition resulted in higher annual birth rate relative to the other theoretical strategies. However, the advantage of higher birth rates was diminished when culling rates were optimized.

One likely explanation for why stable herd sizes are not achieved under some management models even with optimized offtake is that females from one or more age groups with high reproductive value were over-harvested. Age classes F (3-4 years) through I (>8 years) are associated with the lowest survival probabilities for six of the theoretical harvest strategies, but peak prolificacy is programmed to reflect the fourth parity, coinciding with age class G (4-6 years). This clearly explains the rapid demise of herds when offtake is unadjusted. But in the optimized offtake simulations, adjustment of harvest rates was contingent on the estimated herd growth rate (λ) falling outside of the arbitrarily defined thresholds (i.e., λ_{min} and λ_{max}). The efficacy of modifying offtake rates to ensure herd survival

is therefore dependent on the threshold at which this decision is made. If the lower threshold is too low, culling rates will not be reduced as frequently as they should be, and herd sizes may decline continuously. Likewise, if the upper threshold is too low, the maximum herd growth rate may never be achieved. Placing constraints on high fertility may drastically limit a population's capacity to rebound from periods of decline.

It is important to emphasize here that if the net female culling rate was set to zero, the population projections for each strategy would be identical to the projection made for the Baseline strategy with no offtake. In some traditional herding systems females were rarely slaughtered younger than 5 years unless they became unproductive (Hadjikoumis 2017). However, the age at which surplus female kids and lambs are slaughtered depends on whether herders are focused on meat, milk, or a combination of these products (Halstead 1998b). Adjusting the female culling rates in the optimization algorithm approximates these considerations to only a limited extent. In the model more animals are slaughtered not when there is a surplus, but when herd multiplication rates exceed an arbitrary threshold. But herders do not base such decisions on arbitrary demographic metrics. A combination of factors such as forage or fodder availability, the market value of livestock products, social obligations, and environmental conditions can influence how herders manage livestock and how slaughtering decisions are made (Browman 1987; 1997; Dahl and Hjort 1976; Halstead 1996; 1998b; Marković 1987; Nitsiakos 1985; Redding 1981).

The simulations also assessed the viability of slaughtering practices inferred from newly reported age-at-death data obtained from Neolithic contexts at Benkovac-Barice, Smilčić, Zemunik Donji, and Islam Grčki. In the simulations using these empirical mortality data, herds of sheep and goats endured longer under the Middle Neolithic strategies

examined, perhaps reflecting Danilo-period herders' goal of maximizing herd sizes. The Danilo period is associated with key technological innovations associated with agricultural intensification, including improved lithics used to harvest crops (Mazzucco et al. 2018), and the use of ceramic sieves and other pottery types for production of fermented dairy products such as cheese or yogurt (McClure et al. 2018). Although only one Early Neolithic profile was examined, incorporating other datasets associated with Impresso sites in Dalmatia could shed light on whether the differences observed between Early and Middle Neolithic Smilčić strategies are echoed elsewhere. Recent zooarchaeological analyses of Impresso and Danilo period assemblages from Pokrovnik, for example suggest production shifted from a focus on meat to a focus on dairying (McClure et al. 2022). But the failure of herds to thrive under several of the harvest models examined reflects how the models represent idealized culling rates for optimizing a single production goal (Halstead 1998b).

During the Neolithic culling decisions were likely oriented towards the exploitation of a combination of products rather than an emphasis on a single goal (Bogaard et al. 2016; Halstead 2024; Vigne and Helmer 2007). The simulations presented in this chapter did not examine the effect of using a combination of strategies. However, several of the mortality profiles presented in the previous chapter are consistent with some combination of Vigne and Helmer's (2007) Milk A, Milk B, Meat B, and Fleece models (Figure 5.2). The mortality profiles constructed for Impresso period Smilčić and Danilo period Zemunik Donji were both interpreted as a combination of the Milk B and Meat B strategies. Although both herding systems appear to emphasize the same production goals, the simulations show that the culling strategy as implemented by Impresso period herders at Smilčić was not sustainable (Figure 6.3). The key advantage for Zemunik Donji herds over Early Neolithic Smilčić may lie in the

slightly higher survival probability associated with animals aged 2-6 months (Figure 6.1). Furthermore, the decimation of herds during the Impresso period at Smilčić can be contrasted with the Danilo period strategy resembling a combination of Milk A/B and Meat B, for which projections indicated herd growth (Figure 6.3). The differences between the survivorship curves for these two strategies are somewhat subtle but animals under the Danilo strategy generally had higher survival probabilities across all age classes than animals under the Impresso strategy (Figure 6.1). In this respect, a shift in production is more clearly observed in the population projections than in the culling profiles.

Marom and Bar-Oz (2009) rightly criticize the use of established harvest models to infer production goals based on the inability of the survivorship probabilities to be distinguished statistically. The authors show how any survivorship curve produced from a zooarchaeological assemblage can fit more than one of the theoretical models examined here (Marom and Bar-Oz 2009). Indeed, the population projections presented in this study show that several theoretical culling strategies are associated with similar herd structure, herd growth rates, and sex proportions; these aspects of herd management can be observed only to a limited extent using traditional zooarchaeological methods. On the other hand, the demographic projections made using the empirical culling data provide useful insight into how strategies that appear to be very different based on mortality profile reconstructions were actually similar in terms of long-term herd survival. Additionally, the simulations reveal potential demographic implications of shifting livestock culling strategies through time. Population projection modeling can therefore be useful for comparing livestock culling strategies to better understand nuanced differences in mortality profiles.

The use of population projection models here offers a way to better distinguish

between past livestock production capabilities as well as insight into the challenges herders faced while maintaining the viability of their herds. An optimization procedure was used to understand how modifying offtake rates could have functioned to minimize risk of decimating herds. Periodically reducing female offtake rates prolonged survival of sheep and goat herds that would have otherwise been rapidly extinguished under six of the theoretical harvest profiles frequently used to interpret age-at-death profiles associated with archaeological assemblages. However, the optimization procedure also penalized herd growth, which restricted recovery from earlier periods of population decline. This effect was stronger on goat than sheep populations, indicating that high goat fecundity may not compensate for high kid mortality.

Adjusting offtake also had the effect of reducing inter-annual variation in herd growth but did not always result in stable herd sizes. These short-term reductions in meat production may not be reflected in culling profiles but could potentially be detected archaeologically as brief shifts in plant and animal species diversity as farmers may rely more heavily on other forms of subsistence (Halstead and Jones 1989). The simulations demonstrated that culling rates should be regarded as approximations of economic strategies oriented towards the optimization of a particular production goal (Halstead 1998b; 2024) rather than evidence of an enduring livestock system.

Population projection models are flexible enough to track population change on a seasonal basis which can shed light on whether age-at-death data reflect episodic butchering activities or reflect year-round occupation of a site. However, keeping the model focused only on culling strategies within simulated environmental variation was intended to address this frequently overlooked aspect of minimizing risk within livestock production systems.

Propagating herd numbers requires herders to be attuned to the reproductive capabilities of their animals and recognizing when to scale down or scale up culling rates. Moreover, this chapter illustrates how modeling stage-structured population dynamics of domesticated animals can be used to reveal meaningful differences between mortality profiles. In a more practical sense, the demographic implications afforded by these simulations provide a way to contextualize herd breeding strategies.

It was initially expected that goat populations with higher overall prolificacy would always out-number sheep (Dahl and Hjort 1976; Redding 1981; Wilson 1989) and that goat herds might have been better able to rebound from losses than sheep. Indeed, predicted population growth rates for goats were generally higher than sheep, consistent with other livestock demographic models (Redding 1984; 1981). It is therefore surprising that goat populations were less likely than sheep to thrive and that mean goat herd sizes were generally smaller than mean sheep populations when offtake rates were optimized. These results indicate high kid mortality is not compensated for by higher kidding rates and that goat herd longevity may be more susceptible to high culling rates of young animals than are populations of sheep with lower lamb mortality rates. This advantage may have been harnessed by some Impresso period herders that specialized in sheep production on the Dalmatian Coast (Sierra et al. 2023). Additionally, it is likely that different culling rates were applied to sheep and goats as herders may take advantage of differences in growth rates and nutritional quality of milk (Hadjikoumis 2017).

Higher slaughter rates lead to an increase of net mortality rates (i.e., the combination of intrinsic mortality and offtake probabilities) including rates for juvenile age groups which are already higher for goats than sheep (Table 6.1). Furthermore, this variability could be a

liability when goats are relied on for both dairy and meat since overharvesting animals for meat consumption could compromise the ability for goat herds to rebound from one or more years of herd losses. Recognizing this liability, Neolithic herders in Dalmatia (and elsewhere) might have opted to specialize in sheep herding (Sierra et al. 2023) or maintain herds comprised of both species (McClure et al. 2022; McClure and Podrug 2016; Redding 1984) as a means to minimize risk of compounded (and catastrophic) herd losses. From these observations it seems that counter-acting increased herd growth can have unexpected negative consequences for sheep and goat populations in later years. Increasing offtake in response to a period of very high fertility could therefore be problematic if herd growth rates are low in subsequent years. This proposition echoes the importance of maximizing herd size as a means to minimize risk expressed in the husbandry strategies of some modern pastoralists in the Central Andes (Browman 1987; 1997).

The population projections presented here provide useful insight into the demographic implications of archaeological age-at-death data. Nonetheless, the results of the simulations highlight aspects of the model that can be further developed. First, the comparison of sheep and goat population dynamics might be better served by synchronizing the stochastic variation of fertility and mortality. As is, there is no correspondence between annual sheep and goat herd growth rates in the model; any given year could be really good for one species and really bad for the other. Refining the program so that environmental variability has similar effects on goats and sheep would allow for a deeper exploration of herder decisions such as whether to modify the culling rates of one species based on the performance of the other (Redding 1984).

Additionally, the population projections used an initial herd size of 150 animals with

the initial vector containing the number of animals in each age-group based on proportional allocation of the initial population size. Increasing the initial herd size would result in a larger number of reproductive females in the initial population, increasing the number of parturitions in the subsequent time-step and potentially having a cumulative effect on population size. Moreover, the model assumes herders controlled breeding by delaying the age of first parturition to 12-24 months of age. An improvement of the optimization algorithm could involve conditionally setting the age of first parturition to the previous age class and keeping prolificacy low as studies suggest earlier parturitions should increase overall herd productivity at the expense of higher lamb and kid mortality rates (Redding 1981; Wilson 1989; Wilson and Durkin 1983).

Another point of future development pertains to the initialization of the herd structure itself. Although mortality profiles typically show agglomerated age classes (e.g., A, B, C, D, EF, G, HI), the model presented here underutilized a key advantage of the Lefkovitch matrix (i.e., stage-based versus age-based class divisions; Crouse et al. 1987; Lefkovitch 1965; Lesnoff et al. 2000). The age classes implemented in this study were structured to make the evaluation of the ten theoretical harvest profiles and comparison with the empirical data more practical. Although beyond the scope of this chapter, restructuring the population projection matrix to explore population dynamics with fewer age classes would be straightforward and could meaningfully expand the analytical potential of post-cranial epiphyseal fusion age-at-death data.

Finally, further development of the modeling program should take into consideration the above discussion pertaining to the suitability of the thresholds used to initiate the optimization of culling rates as well as the relative vulnerability of herds under different

management strategies to female culling rates. In this regard, future research would make effective use of a sensitivity analysis to assess how the vulnerability of herds under different management strategies is affected by initial population size, the slaughter of females as well as evaluate a range of optimization thresholds.

VII. Methods: Stable Isotope Analysis of Teeth and Bone

This chapter is devoted to the stable isotope analysis methodologies used to reconstruct livestock diet, breeding seasonality, and mobility during the Neolithic in Dalmatia. In the first section I provide a detailed explanation of how important aspects of domesticated animal management are investigated via stable isotope analysis of tooth enamel bioapatite. Therein I explain how the carbon and oxygen isotope ratios obtained by serially sampling the lower M2 molar of ancient caprines can be leveraged to determine an individual's season of birth, mobility, and diet. In the second section, I describe the methodological approach behind stable isotope analysis of animal bone collagen and discuss how the carbon and nitrogen composition of zooarchaeological bone reflects animal diet and, for livestock, a reflection of herd management decisions. In each section I provide information about the samples used.

A. Preface

The isotopic composition of domesticated species provides a unique perspective of human behaviors as livestock diet is under the control of herders (Pederzani and Britton 2019). The interpretation of carbon and nitrogen isotope ratios of bone collagen obtained from zooarchaeological remains of managed species has provided insight into how past

agropastoralists husbanded livestock (Guiry et al. 2017; Lightfoot et al. 2011; Welker et al. 2022; Zavodny et al. 2014; 2015; 2017; 2022). Since bone remodels very slowly relative to other organic tissues, the isotopic composition of bone collagen reflects the animal's diet over the last few years of life (Ambrose and Norr 1993; DeNiro and Epstein 1981). Therefore, stable isotope analysis of bone collagen may only provide a more generalized picture of how humans managed domesticated animal diet while short-lived interventions in feeding behaviors of herds are overlooked.

Alternatively, stable isotope analysis of sequential samples of enamel bioapatite can provide higher temporal resolution of variation in diet experienced during an individual's lifetime. Variation in carbon and oxygen isotopic ratios of plants comprising an animal's diet is subject to seasonal changes in the environment. Due to the incremental nature of enamel formation and timing of enamel mineralization (Hillson 1986), comparison of intra-tooth $\delta^{13}C_{apa}$ and $\delta^{18}O_{apa}$ values within an individual tooth offers insight into changes in the animal's diet (Figure 7.1) and when these data are compared between different individuals, season of birth can be estimated (Balasse 2002; Balasse et al. 2003; 2012b).

A diachronic perspective can provide critical insight into how sheep and goat husbandry may have changed over a 2,000-year period. At this temporal scale, it may be possible to shed light on how the allocation of time and energy into agricultural pursuits varied amidst broader changes in environmental conditions and food production technologies. Interpretations of the results are considered alongside hypothetical production goals inferred from mortality profiles reconstructed using mandibular tooth wear assessments for seven Neolithic settlements in the study area.

B. Stable carbon and oxygen isotope analysis of enamel bioapatite

Analysis of stable carbon and oxygen isotope ratios of ancient livestock tooth enamel bioapatite ($\delta^{13}C_{apa}$ and $\delta^{18}O_{apa}$) is a powerful investigative technique for reconstructing seasonal changes in diet, season of birth, and transhumance (Balasse et al. 2003; 2012a,b; Bernard et al. 2009; Berthon et al. 2018; Blaise and Balasse 2011; Henton 2012; Henton et al. 2010; 2014; Hermes et al. 2022; 2019; Lazzerini et al. 2021; Makarewicz 2017; Makarewicz et al. 2017; Makarewicz and Pederzani 2017; Tornero et al. 2013; 2016; 2018; Ventresca Miller et al. 2019; Zazzo et al. 2012). Like other skeletal tissues, the isotopic composition of enamel is closely linked to an individual's diet (Fry and Arnold 1982; Trayler and Kohn 2017). Unlike bone, the timing and duration of tooth growth and enamel maturation is fixed within species (Hillson 1986). Additionally, enamel has higher crystallinity making it more resistant to diagenesis than bone collagen (Gage et al. 1989). Enamel formation begins early in life and remains biologically inert once mineralization is complete (Dean 1987). During enamel formation, variation in the isotopic composition of diet is incorporated into the bioapatite matrix and serial sampling along the growth axis of the tooth enables a time-series reconstruction of an animal's diet during the period in which the tooth was forming (Figure 7.1; Balasse et al. 2003; Zazzo et al. 2010). These properties are why enamel samples of fossil and archaeological teeth are taken to obtain paleoclimatic and palaeoecological information (Fricke and O'Neil 1996; Kohn et al. 2002; Pederzani et al. 2021; Pellegrini et al. 2008).

The most mineralized tissue in mammals is enamel, which is composed almost entirely of bioapatite mineral, referring to the carbonate-rich, hydroxyl-deficient mineral component of skeletal tissues (Elliott 2002; Trayler and Kohn 2017). The carbonate

component of bioapatite archives the carbon and oxygen isotope composition of body water (Trayler and Kohn 2017). Amelogenesis (i.e., enamel formation) progresses from the tip of the crown to the tooth root in two stages: “matrix production” and “enamel maturation” (Allan 1967; Hillson 1986).

During the first stage (i.e., apposition) an organic matrix of apatite crystals is secreted by ameloblast cells and deposited on a surface parallel to the enamel-dentine junction (EDJ; Adserias-Garriga and Visnapuu 2019; Passey and Cerling 2002). During apposition mineralization of the apatite crystals begins immediately, accounting for 25-30% of the total mineral content in fully-formed enamel while the apatite’s isotopic composition reflects that of the individual’s body water (Hoppe et al. 2004; Passey and Cerling 2002). As tooth length increases, the appositional surface inclines relative to the EDJ causing each successive layer of newly deposited enamel matrix to orient at a sharp angle (~5-15°) to the tooth growth axis (Hoppe et al. 2004; Kierdorf et al. 2012; 2013). The remaining 75% of mineral in enamel is formed during the subsequent maturation stage when crystals infill the matrix, coarsen, and reduce organic content (Suga 1982).

The main influx of oxygen in skeletal tissues such as collagen and enamel bioapatite is body water which is obtained through food (i.e., leaf water) and drinking water for ruminant species (Daniel Bryant et al. 1996a; Kohn et al. 1996; 1998; Longinelli 1984; Luz et al. 1984; Podlesak et al. 2008; Trayler and Kohn 2017). During the maturation stage, enamel re-equilibrates the oxygen isotopic composition of appositional enamel such that enamel bioapatite samples represent the isotopic composition of body water with high fidelity (Trayler and Kohn 2017).

It is important to note that the length of time needed for the enamel within a particular

segment of a tooth to mature (i.e., enamel maturation rate l_m) varies between species and not all teeth mineralize at the same rate or at a constant rate (Balasse 2002; Balasse et al. 2012b; Fricke and O'Neil 1996; Kohn 2004; Passey and Cerling 2002; Zazzo et al. 2010). Longer enamel maturation rates result in greater attenuation of the isotopic signal of the environment (Passey and Cerling 2002). This is because for slower rates of deposition and mineralization, successive layers of enamel matrix have isotopic compositions representing a greater period of time, potentially spanning seasonal variability in the animal's diet (Kohn 2004; Passey and Cerling 2002). Hence, small bovids (e.g., sheep, goats, antelope) with enamel maturation length scale (l_m) of 2-3 mm per month are better suited for seasonality studies than large-bodied bovids (e.g., cattle, bison) and equids with l_m of approximately 25 mm per month (Balasse 2002; Kohn 2004). Furthermore, the duration of enamel mineralization is longer than that of enamel matrix formation.

For sheep molars, maturation accounts for two-thirds of the total enamel development time (Suga 1982), estimated to be approximately four months for the lower second molar (Zazzo et al. 2012) meaning the duration of enamel development for this tooth is about six months (Balasse et al. 2012b). A 5-6 month shift of the environmental signal results from this delayed maturation time causing the earliest isotopic inputs from the environment to correspond with the animal's diet when it reaches approximately 6 months old (Balasse et al. 2012b; Zazzo et al. 2010). Dampening of the environmental signal will also be affected by the residence time of oxygen in the body which can range from 3 to 6 days in small mammals (Podlesak et al. 2008) to several weeks in large herbivores (Kohn et al. 2002) but adjusting the sampling procedure can minimize attenuation (Passey and Cerling 2002).

Sampling tooth enamel to reconstruct a time-series of the isotopic composition of

bioapatite carbonates is performed by drilling a series of equally-spaced, linear pits, or bands perpendicular to the length of the axis of tooth growth (Ventresca Miller et al. 2018). Due to the oblique orientation of enamel layers relative to the face of the enamel dentine junction, sampling bands crosscut multiple overlapping layers so that the isotopic composition of the sample reflects a time-averaged signal of isotopic inputs from an individual's diet (Passey and Cerling 2002). Because each sampling pit drills through and collects enamel from multiple appositional surfaces that mineralized at the rate of l_m, a practicable pit length (i.e., measured parallel to tooth growth axis) no greater than $0.5*l_m$ is sufficient for obtaining a record of the isotopic composition of the animal's body water during the period of enamel maturation (Passey and Cerling 2002). For sheep and goats with an enamel maturation rate of 2-3 mm per month, sample pit lengths of 1-2 mm with maximum 2 mm between samples across a 30-40 mm long tooth should produce, with monthly resolution, an isotopic record that is attenuated by as little as 10% relative to the environmental signal (Kohn 2004: 404). This approach yields a time-series of bioapatite carbonate samples, from which seasonal variation in $\delta^{13}C$ and $\delta^{18}O$ values can be tracked over the period of tooth growth (Figure 7.1; Balasse 2002; Pederzani and Britton 2019; Zazzo et al. 2012).

In sheep, the lower M2 molar forms completely during the first year of life (Milhaud and Nezit 1991; Upex and Dobney 2012; Weinreb and Sharav 1964; Zazzo et al. 2010) with a six-month enamel maturation period (Balasse et al. 2012b; Blaise and Balasse 2011; Zazzo et al. 2010). Sequential measurements of the $^{13}C/^{12}C$ and $^{18}O/^{16}O$ isotopic ratios of M2 enamel bioapatite ($\delta^{13}C_{apa}$ and $\delta^{18}O_{apa}$) in ovicaprids can be used to examine seasonal changes in diet. Although both elements have been used to identify seasonal reproduction patterns and diet (Balasse et al. 2003; 2009; 2012a; Bernard et al. 2009; Blaise and Balasse

2011; Bocherens et al. 2015; Gillis et al. 2013; Henton 2012; Makarewicz et al. 2017; Makarewicz and Tuross 2012; Sierra et al. 2023; Tornero et al. 2013; Ventresca Miller et al. 2019; 2020), some researchers prefer to work with the M3 over the M2 because it erupts later and will experience less occlusal wear, potentially allowing for more enamel samples to be collected (Balasse et al. 2023). Additionally, the M2 can be misidentified as an M1 molar unless the tooth is extracted directly from a mandible. However, reduced inter-individual variability of enamel maturation rate has been shown for the lower M2 compared to the lower M3, which begins to develop later in life and is completely formed after the animal has aged two years (Blaise and Balasse 2011; Lazzerini et al. 2021; Tornero et al. 2013; Zazzo et al. 2012). Therefore, the M2 is preferable for reconstructing season of birth than the M3 (Zazzo et al. 2010).

1. Carbon

C_3 and C_4 plants differ in their photosynthetic pathways, their carbon isotope fractionation patterns, and the environments they are adapted to. Due to the divergent carbon fixation processes that occur during photosynthesis C_3 and C_4 plants can be distinguished isotopically. The C_3 pathway involves greater discrimination against the heavier carbon isotope (^{13}C) than the C_4 pathway and results in preferential incorporation of the lighter carbon isotope (^{12}C) and lower $\delta^{13}C$ values in C_3 plants (Farquhar et al. 1989). The average $\delta^{13}C$ value of the majority of C_3 plants in modern open habitats is -27.0‰, ranging from -29 to -25‰ while values lower than -31.5‰ are exclusive to understory plants that grow in dense forests (Kohn 2010). Lower carbon discrimination of C_4 plants allows for the incorporation of a higher ratio of ^{13}C to ^{12}C which results in more positive $\delta^{13}C$ values that average between -14 and -12.5‰ and range from -16 to -9‰ (van der Merwe and Medina

1991; O'Leary 1988; Sharp 2007). Applying a +1.5‰ correction for the fossil fuel effect (Freyer and Belacy 1983), the $\delta^{13}C$ ranges of pre-industrial C_3 and C_4 plants is estimated to be -27.5 to -23.5‰ and -14.5 to -7.5‰, respectively.

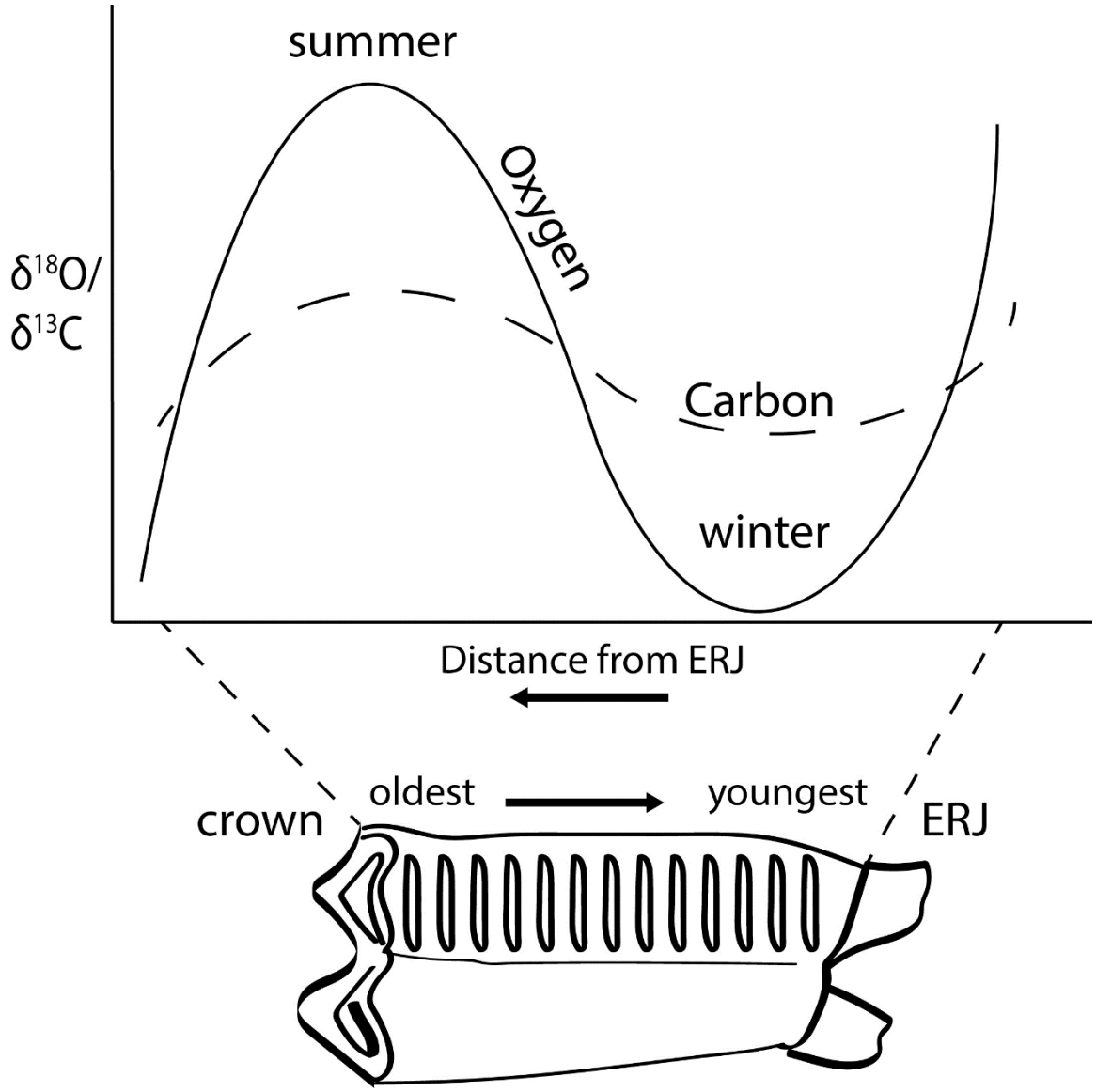

Figure 7.1. Expected seasonal variation of intra-tooth $\delta^{18}O_{apa}$ and $\delta^{13}C_{apa}$ in enamel samples taken along the tooth growth axis of a lower M2 ovicaprid molar. ERJ refers to the enamel-root junction associated with the most recently formed enamel.

C_4 plants (e.g., subtropical grasses, maize, millet) thrive under conditions of low stomatal conductance, which is an adaptation to minimize water loss in hot and arid environments, while C_3 plants include all trees, woody shrubs, and grasses found in forests in temperate climates including most of Europe (van der Merwe 1982; van der Merwe and Medina 1991; Sharp 2007; Tieszen 1991). C_4 vegetation is well-adapted to dry climates so water-stress induced variation in $\delta^{13}C$ is negligible compared to C_3 plants whose $\delta^{13}C$ values are more sensitive to environmental factors (Tieszen 1991). Reduction of stomatal conductance minimizes water loss as an adaptation to increased temperature and aridity in both C_3 and C_4 plants (Tieszen 1991). Increased water-use efficiency subdues discrimination against the heavier carbon isotope leading to ^{13}C-enrichment (Farquhar et al. 1989). As a result, wetter conditions are associated with more negative $\delta^{13}C$ values in C_3 plants while hot and dry conditions lead to more positive $\delta^{13}C$ values (Kohn 2010; Stewart et al. 1995).

C_3 plants are found in a wide variety of environments so seasonal fluctuations in $\delta^{13}C$ are more pronounced than C_4 plants that are primarily found in arid conditions (Smedley et al. 1991). In high altitudes a lower ratio of internal to external partial pressure of carbon dioxide in leaves of C_3 plants enables greater efficiency of CO_2 uptake resulting in 1.2‰ enrichment of ^{13}C per 1000 m gain in elevation (Körner et al. 1988; 1991). Compared to grasses found in open C_3 biomes, lower $\delta^{13}C$ values occur in understory plants in forests due to the ^{12}C-enriched CO_2 released during leaf litter decay (i.e., the canopy effect; Broadmeadow et al. 1992; van der Merwe and Medina 1991) and $\delta^{13}C$ values less than -31.5‰ has been proposed as a threshold for identifying understory plants (Kohn 2010).

Environmental influences can lead to differences in $\delta^{13}C$ values of C_3 plants by 2-3‰ (Tieszen 1991) and potentially enable changes in foraging habitat to be identified in

sequential enamel bioapatite samples of ruminant dentition (Balasse et al. 2009; Berthon et al. 2018; Henton et al. 2014). The $\delta^{13}C$ values of mammalian skeletal tissues, including enamel bioapatite are directly related to the carbon isotope composition of the diet (Cerling and Harris 1999; Lee-Thorp and van der Merwe 1991). Controlled feeding experiments have shown inter-species variation in ^{13}C-enrichment of enamel bioapatite (Ambrose and Norr 1993; Howland et al. 2003; Jim et al. 2004; Passey et al. 2005; Tieszen and Fagre 1993) and that intra-tooth variation in $\delta^{13}C_{apa}$ values can signal a switch between C_3 and C_4 diets (Balasse 2002; Zazzo et al. 2010). ^{13}C-enrichment of enamel bioapatite for sheep under controlled diet (Zazzo et al. 2010) ranged between c. 11‰ and 15‰ and similar to the c. 14‰ enrichment for cattle (Balasse 2002; Passey et al. 2005) and wild ruminants (Cerling and Harris 1999).

Intra-species variation in ^{13}C-enrichment can be as large as 3-4‰ when diet is exclusively C_3 or C_4 plants (Zazzo et al. 2010). Furthermore, animals whose diets are primarily C_4 plants may potentially result in lower ^{13}C-enrichment (c. +12‰) than C_3 plants (c. +15‰) despite the fact that C_4 plants have higher $\delta^{13}C$ values (Balasse 2002; Zazzo et al. 2010). Additionally, out of season foddering such as the use of hay collected during the summer for over-wintering (Halstead et al. 1998) may be observable as intra-tooth $\delta^{13}C_{apa}$ values that are inversely related to a corresponding seasonal signal seen in the profile of oxygen isotope ratios (Balasse et al. 2012a; Ventresca Miller et al. 2020). Foddering may also lead to lower $\delta^{13}C_{apa}$ if animals were provisioned with vegetation collected from forested environments (Berthon et al. 2018) or obscure the seasonal variation of plant $\delta^{13}C$ (Chase et al. 2014).

Based on the range of pre-industrial C_3 and C_4 $\delta^{13}C$ values (-27.5 to -23.5‰ and -14.5

to -7.5‰), the influence of altitude and aridity on these values, and the c. 14‰ enrichment of ruminant enamel bioapatite in ^{13}C relative to dietary carbon, the expected intra-tooth $\delta^{13}C$ ranges can be modeled. Enamel bioapatite $\delta^{13}C$ ranges for individuals whose diet was exclusively C_3 open biome vegetation may be between -13.5 and -9.5‰ and between -0.5 and 6.5‰ for individuals that consume only C_4 grasses. A mixed C_3/C_4 diet might be expected to produce $\delta^{13}C$ values somewhere between these ranges especially if the C_4 contributions were substantial.

For individuals that grazed in high altitudes, a C_3 diet may be enriched in ^{13}C by approximately 1.2‰ for every 1000 m difference in elevation (Körner et al. 1988). Switching between pure C_3 and pure C_4 diets should also be observable if the new diet was sustained for a period of approximately 6 months (Zazzo et al. 2010). C_4 plants are found in extremely low abundance in southeastern Europe (Collins and Jones 1985; Pyankov et al. 2010) so it is expected that livestock in Neolithic Dalmatia mainly consumed C_3 plants. There is at least one example of the cultivation of millet, a C_4 crop, during the Neolithic at Pokrovnik (Moore et al. 2007a) but millet does not appear to have been a staple crop until the Bronze Age in Dalmatia (Reed 2016).

2. Oxygen

Temperature is a key factor in the fractionation of oxygen isotopes in meteoric water. Due to the temperature dependence of isotopic fractionation during the condensation of precipitation surface-air temperature is positively associated with precipitation $\delta^{18}O$ in middle and upper latitudes (Rozanski et al. 1992). Preferential evaporation of the lighter oxygen isotope, ^{17}O leaves water bodies enriched in the heavier isotope, ^{18}O (Dansgaard 1964). However, when temperatures are high, the strength of evaporation is increased and the

heavier oxygen isotope, ^{18}O is removed as water vapor at a higher rate. This enriches cloud masses formed during the summer in ^{18}O. During condensation, the heavier isotope is preferentially removed in the form of precipitation, depleting cloud moisture of ^{18}O-enriched water (Gat 1996). Evaporation in colder temperatures is less effective at removing the heavier isotope so cloud masses are relatively depleted in ^{18}O. Intra-annual cycling of meteoric water $\delta^{18}O$ therefore reflects seasonal variation in air temperature such that rainfall is ^{18}O-enriched in the summer and ^{18}O-depleted in the winter (Gat 1996; Kohn and Welker 2005; Rozanski et al. 1992; 2013).

Fractionation is also influenced by altitude, continentality, quantity of rainfall, humidity, and seasonality (Dansgaard 1964; Gat 1996; Poage and Chamberlain 2001; Rozanski et al. 2013; Yang et al. 2019). Reduced $\delta^{18}O$ of meteoric water is linked to altitude with ^{18}O-enriched water preferentially and progressively removed from clouds (i.e., the rain out effect) with increasing distance from the coast and elevation where air temperature is lower (Gat 1996; Gonfiantini et al. 2001; Poage and Chamberlain 2001). This relationship causes more negative precipitation $\delta^{18}O$ in high altitudes and more positive $\delta^{18}O$ values at low altitudes.

Due to the highly predictable relationship between meteoric water $\delta^{18}O$, temperature, and altitude, the ratio of heavy (^{18}O) to light (^{17}O) oxygen isotopes in archaeological animal tissues can be used for palaeoecological reconstructions and the identification of seasonal herding practices such as transhumance and breeding (Pederzani and Britton 2019). The main source of oxygen in skeletal tissues is body water obtained via drinking or food water, which are sourced primarily from precipitation (Podlesak et al. 2008). The $\delta^{18}O$ values of skeletal tissues such as bioapatite carbonate ($\delta^{18}O_{apa}$) are therefore closely linked to the $\delta^{18}O$ values

of environmental water ($\delta^{18}O_{ew}$) (Daniel Bryant et al. 1996a,b; Kohn et al. 1996; Longinelli 1984).

Construction of a time-series of the isotopic composition of sources of water in an animal's diet can be realized through serial sampling enamel along the tooth growth axis (Balasse 2002; Kohn 2004; Passey and Cerling 2002). Because temperature varies seasonally, intra-annual fluctuations in the ^{18}O-enrichment of meteoric water is observable as sinusoidal variation in sequential $\delta^{18}O_{apa}$ values (Balasse et al. 2012b; Bernard et al. 2009; Henton 2012; Pederzani et al. 2021). Seasonal variation in $\delta^{18}O_{ew}$ over one or more annual cycles is most clearly observed when a sufficient number of regularly spaced enamel samples are collected from a tooth specimen. When a full year is represented, the $\delta^{18}O_{apa}$ of a series of enamel bioapatite will exhibit maximum and minimum values that correspond to fluctuations in precipitation $\delta^{18}O_{ew}$ associated with seasonal changes in temperature (Figure 7.1).

Due to constant tooth growth rates within species, seasonal variation in $\delta^{18}O_{apa}$ will be reflected in samples taken at the same distance from the enamel root junction in individuals born at the same time of year (Balasse et al. 2003; Tornero et al. 2016). Elimination of inter-individual differences in tooth eruption and enamel formation rates can be achieved by normalizing the distance between the location along the tooth growth axis where each sample was taken and the enamel root junction (i.e., ERJ; Balasse et al. 2012b; Blaise and Balasse 2011). Using this approach it is possible to determine when in the annual cycle animals were born, providing insight into husbandry practices involving, for example, extended breeding seasons or out-of-season lambing (Balasse et al. 2003; 2020; 2023; Fabre et al. 2023; Sierra et al. 2023; Tornero et al. 2016).

Time-series reconstruction of water sources in an animal's diet also allows for the

detection of migratory patterns of wild species (Julien et al. 2012; Pellegrini et al. 2008; Pilaar Birch et al. 2016) and transhumance in domesticated species (Henton et al. 2010; Knockaert et al. 2018; Lazzerini et al. 2021; Makarewicz et al. 2017; Tejedor-Rodríguez et al. 2021). Transhumance is a common strategy among pastoralists in marginal environments involving the movement of livestock in response to seasonal changes in resource availability or to avoid climatic extremes (Forenbaher 2007; Greenfield 1999; Halstead 1987; Pederzani and Britton 2019). Summer migration to environments characterized by cooler temperatures either in higher latitudes (i.e., horizontal transhumance) or higher altitudes (i.e., vertical transhumance) can result in the incorporation of meteoric water with lower $\delta^{18}O_{ew}$ values (Bowen and Wilkinson 2002; Dansgaard 1964; Rozanski et al. 1992). This practice may result in reduced amplitudes of intra-tooth $\delta^{18}O_{apa}$ variation relative to intensively managed animals that did not experience large changes in altitude (Britton et al. 2009; Henton 2012; Henton et al. 2010; Lazzerini et al. 2021; Pellegrini et al. 2008; Pilaar Birch et al. 2016). Amplitudes of variation of intra-tooth $\delta^{18}O_{apa}$ have been shown to range from 1‰ (Britton et al. 2009) in migratory species and range from 2-4‰ in non-migratory caprids (Balasse et al. 2002).

Dampened amplitudes of $\delta^{18}O_{apa}$ variation may also result from residing near springs fed by various sources that would lead to averaging of $\delta^{18}O_{ew}$ values and indicate restricted mobility (Balasse et al. 2009; Henton 2012; Pellegrini et al. 2008). Since various surface and sub-surface sources may contribute to discharge, the isotopic composition of river water may not reflect seasonal variation of precipitation $\delta^{18}O$ except where surface run-off is the primary input (Fritz 1981). The isotopic composition of meteoric groundwater (i.e., subsurface waters derived directly from rainfall via recharge through an unsaturated soil

zone) typically resembles the average composition of precipitation over the catchment area (Gat 1981a: 223–224). Karst systems like the Dinaric karst spanning the Dalmatian coast are porous and highly productive, which means aquifers are recharged by meteoric groundwater (Bonacci et al. 2019). Spring and well water $\delta^{18}O$ in Dalmatia is in line with the regional meteoric water line established using precipitation $\delta^{18}O_{VSMOW}$ (Brkić et al. 2020; Vreča et al. 2006). The $\delta^{18}O_{VSMOW}$ values of water sampled from various ponds, wells, and springs at elevations below 500 masl in the study area are consistent with annual precipitation $\delta^{18}O_{VSMOW}$ estimates for each sampling location (Appendix D).

For non-obligate drinking herbivores (e.g., caprines) that are adapted to arid environments body water is mainly obtained through leaf water (Dunson 1974). Leaf water tends to be enriched in ^{18}O relative to precipitation as a consequence of evapotranspiration, which returns water vapor to the atmosphere and the strongest evaporative effects are associated with warm arid conditions (Farquhar et al. 1989; Luz et al. 2009). This enriching effect of evapotranspiration on oxygen isotope composition of plant water is particularly evident in grasses, but less pronounced in broad-leafed vegetation (Helliker and Ehleringer 2000).

Sheep and goats require water more frequently in the summer but goats tend to be better able to withstand dehydration than sheep (Dahl and Hjort 1976; Silanikove 1987). When conditions are extremely dry, attenuation of the summer environmental signal in $\delta^{18}O_{apa}$ may therefore be due to herders relocating animals to mountain pastures or to areas with access to lake, spring, well, or pond water (Henton et al. 2014). These water sources are better shielded from the temperature dependent fractionation effects of surface waters and tend to have more negative $\delta^{18}O$ values (Gat 1981b). Herding decisions made in response to

uncharacteristic environmental conditions may produce inter-individual differences in oxygen isotope profiles of serially sampled teeth. For example, inter-individual variation in $\delta^{18}O_{apa}$ has been proposed as an indication of transhumance resulting from increased access to non-local sources of water (Mashkour 2003), while others have suggested that non-migratory behaviors will reduce intra-group differences (Julien et al. 2012). The amplitude of $\delta^{18}O_{apa}$ variation may therefore be a less reliable measure of movements across a landscape than it is for the characterization of seasonal changes in precipitation and temperature (Hermes et al. 2017).

3. Materials and Methods for Stable Isotope Analysis of Enamel Bioapatite

Sheep and goat lower M2 molars from seven Neolithic period sites were selected for enamel bioapatite sampling (Table 7.1). Descriptions of the sites in Table 7.1 are found in Chapter Two. Stable isotope analysis was also performed on four modern teeth. Three modern specimens (DIN5, DIN6, and DIN7) were extracted from mandibles collected in 2006 from unspecified pastures in the Dinara mountain range. One modern specimen (VRL481) was obtained from a sheep raised in Maovice, a village situated on the northern slope of Svilaja mountain near Vrlika, approximately 43 km north of Split (Figure 7.2). The lambing season for the Maovice flock extends from late-winter to early spring and the animal was slaughtered in early May of 2022. Sheep freely graze on grasses around Maovice between 750 and 975 masl. In the winter the flock's diet is supplemented with maize, oats, and barley but summer diet is primarily grass. Based on dental wear, the individual was estimated to be between 5 and 6 years old when slaughtered.

A total of 77 sheep and goat lower M2 molars were sampled for stable isotope analysis including the four modern specimens. Each mandible was assigned an individual

catalog number corresponding to the item's provenience. Specimens were weighed and photographed, and mandibles and teeth were measured following von den Driesch (1976). All data was entered into a FileMaker Pro relational database. Analysis was completed at The University of Zadar and at the Mediterranean Prehistory Lab at UC Santa Barbara using comparative materials. Information about individual specimens including taxon, tooth side, position, wear, and estimated age are provided in Appendix E. Samples chosen for stable isotope analysis of enamel bioapatite reflect species-specific minimum number of individuals (MNI) for each context within a site. Lower second molars that were well-preserved were extracted from mandibles for enamel sampling using a Dremel to cut through bone where necessary.

Each tooth was sonicated for 1-2 h in NanoPure water to remove debris and sediment and air-dried overnight. Remaining debris and calculus was removed using a Dremel equipped with a disposable sanding disc. Enamel sampling followed the protocol described by Ventresca Miller et al. (2018). Sequential sampling of the buccal side of the posterior loph was performed perpendicular to the axis of growth from the enamel root junction to the tooth crown. The procedure resulted in the collection of 3-37 mg of enamel powder from 5-16 sampling bands spaced approximately 2 mm apart for each tooth. Enamel powder was collected into pre-weighed 2.0 mL microcentrifuge tubes using a 1 mm diamond-tipped drill bit fitted onto a Dremel. Sampling was completed in a fume hood which was cleaned with methylhydroxide between each sample band. The distance of each sample from the enamel-root junction (ERJ) was measured using digital calipers.

Enamel powder was soaked for 24 h in 1 mL of 30% H_2O_2 per 10mg of sample, centrifuged for 10 minutes at 13,500 x g, and superstrate H_2O_2 was discarded. Ventresca-

Miller et al. (2018) caution that the use of an oxidizing agent (e.g., 30% H_2O_2) can potentially alter the stable carbon and oxygen isotopes of a sample and that the use of reagents is unnecessary. However, because some samples from Pokrovnik were prepared for a different study which used the H_2O_2 soak, I followed the same protocol to ensure that results were comparable. Following the hydrogen peroxide soak, samples were subjected to three cycles of NanoPure water rinse and centrifuging. Samples were then soaked in 1 mL of 0.1 N Acetic Acid per 10 mg of initial sample for 4 hours, then subjected to three more cycles of water washing and centrifuging, until neutrality of the solution was confirmed by testing the pH. Superstrate water was removed and samples were dried on a heating block at 70°C for 24 hours. Dried samples weights were 1.2-18 mg, and the preparation resulted in mean sample loss of 68 ± 6.4%.

Fourier Transform Infrared Spectrometry (FTIR) was used to determine whether the tooth enamel was affected by diagenesis and to confirm that the isotopic composition of samples was not altered during pretreatment. Samples from each tooth were analyzed on a Thermo Nicolet is10 FTIR Spectrometer equipped with a Smart Diamond ATR accessory accessed within the shared facilities of the National Science Foundation (NSF) Materials Research Science and Engineering Center at UC Santa Barbara, DMR-1720256. The UCSB MRSEC is a member of the Materials Research Facilities Network (www.mrfn.org). The FTIR analyses resulted in the exclusion of eight samples (PK94, PK96, PK98, PK100, PK102, PK104, VEL30, and VEL31) whose phosphate crystallinity indexes (PCI) and B-type carbonate to V_3 phosphate (C/P) ratios were outside of the range recommended for well-preserved enamel (Appendix F).

Analysis of $\delta^{13}C$ and $\delta^{18}O$ values was performed at the Yale Analytical Stable Isotope

Center (YASIC). Dried carbonate was analyzed with a KIEL IV Carbonate device connected to a Thermo MAT253 IRMS. The reaction temperature was 70°C. Results are expressed in permille along the Vienna Pee-Dee Belemnite scale (‰$_{VPDB}$). The $\delta^{13}C_{apa}$ and $\delta^{18}O_{apa}$ values each tooth sample are provided in Appendix G.

Table 7.1. Summary of sites and number of teeth and isotope samples processed for this study.

Site	Tooth Specimens	Total Isotope Samples
Early Neolithic (Impresso)		
Crno Vrilo	11	83
Pokrovnik	8	85
Smilčić	6	63
Middle Neolithic (Danilo)		
Benkovac-Barice	6	62
Islam Grčki	6	65
Pokrovnik	6	56
Smilčić	4	45
Zemunik Donji	7	69
Late Neolithic (Hvar)		
Islam Grčki	6	65
Velištak	5	41
Modern		
Dinara	3	18
Vrlika	1	10
Total	**69**	**662**

C. Stable carbon and nitrogen isotope analysis of bone collagen

Stable isotope analysis has been widely applied to address questions about past human behavior and relationships between humans, plants, and animals (Lelli et al. 2012;

Lightfoot et al. 2015; Stevens et al. 2006). Dietary reconstructions are based on the principle that isotopic signatures are transferred up the food chain from prey to predator (i.e., including plants to herbivores; DeNiro 1985; DeNiro and Epstein 1978; 1981; Hedges and Reynard 2007; van der Merwe 1982; van der Merwe and Vogel 1978; Pearson et al. 2007; Schoeninger and DeNiro 1984). This relationship is known as the trophic level effect and results in $\delta^{13}C$ and $\delta^{15}N$ values that are 3 to 5‰ more positive in animal tissues over animal diets (DeNiro and Epstein 1978; 1981; Stevens et al. 2006).

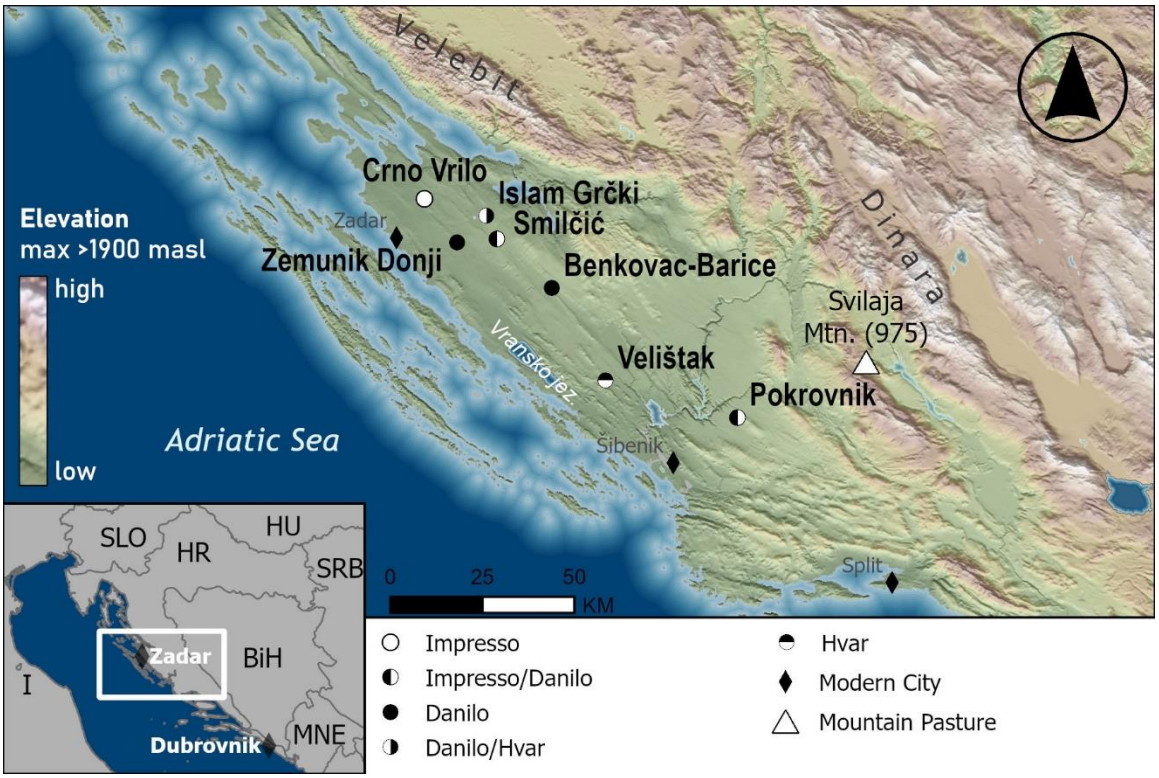

Figure 7.2. Map showing locations of sites sampled for stable isotope analysis of enamel bioapatite.

The isotopic composition of an individual's diet is incorporated into the skeleton as new tissue forms (Fry and Arnold 1982). Bone remodeling involves the removal and replacement of old with new bone and occurs continuously over the course of an individual's lifetime (Eriksen 2010). The rate of bone turnover for some bones is faster than the rate of

other bones (Fahy et al. 2017) and additional factors such as age, sex, health, and activity contribute to inter-individual variation in remodeling rates (Burr 2002; Hedges et al. 2007; Martin and Seeman 2008; Pfeiffer et al. 2006). The continuous nature of bone tissue formation and variation in bone turnover rates results in the isotopic composition of bone collagen samples reflecting time-averaged dietary inputs spanning anywhere from a few years to decades (Copley et al. 2004; Hedges et al. 2007; Manolagas 2000).

A critical aspect of animal husbandry is management of livestock diet. Stable isotope analysis of ancient bone collagen of domesticated sheep, goats, cattle, and pigs therefore provides direct insight into prehistoric livestock management practices (Bocherens et al. 2015; Doppler et al. 2017; Isaakidou et al. 2022; Jones and Mulville 2018; Makarewicz and Tuross 2006; Zavodny et al. 2014; 2017; 2019). The reliability of paleodiet reconstructions is often challenged by the effects that environmental variables have on plant isotopic composition and the effect behavioral variability has on the isotopic composition of animal bone collagen.

Plants produce carbon during photosynthesis which is assimilated in successive stages in the food chain resulting in the ^{13}C-enrichment of bone collagen (i.e., an increase in the stable carbon isotope ratio, $\delta^{13}C$) of approximately 5‰ from plant to consumer (Ambrose and Norr 1993; DeNiro and Epstein 1978). C_3 and C_4 plants utilize different photosynthetic pathways causing them to be isotopically distinct (Farquhar et al. 1989). C_4 plants are more enriched in ^{13}C (mean $\delta^{13}C$ -14 to -12.5‰) than C_3 plants (mean $\delta^{13}C$ -27‰) (Kohn 2010; O'Leary 1988) and the habitual consumption of C_4 plants will lead to $\delta^{13}C$ values that are 10-15‰ more positive in the skeletal tissues of C_4 plant browsers relative to C_3 grazers (DeNiro and Epstein 1978; Vogel 1978).

Most of Europe's climate is characterized as temperate with predominately C_3 plants including all trees, most shrubs, and grasses, whereas C_4 plants are typically found in more arid environments with little to no shade (van der Merwe 1982). Some domesticated plant species that follow the C_4 photosynthetic pathway, such as millet are known to have been cultivated in later prehistory in Dalmatia but such crops were not heavily relied upon during the Neolithic despite their presence at some localities (i.e., Pokrovnik; Moore et al. 2019; 2007a).

Aridity, rainfall, and temperature can also influence the isotopic composition of plants. For example, increased rainfall will cause $\delta^{13}C$ and $\delta^{15}N$ values of C_3 plants to decrease (Hartman and Danin 2010). Differential exposure to sunlight can influence the relative enrichment of ^{13}C in C_3 plants resulting in $\delta^{13}C$ values that are 2-5‰ lower in plants found in dense forested areas than grasses and trees found in open C_3 biomes (Broadmeadow et al. 1992; van der Merwe and Medina 1991; Tieszen 1991). The depletion of ^{13}C in closed habitat vegetation has been linked to more negative $\delta^{13}C$ values in bone collagen of animals consuming forest plants exclusively (Drucker et al. 2008). The canopy effect (Bonafini et al. 2013; van der Merwe and Medina 1991) enables the identification of dietary input from forest vegetation (Berthon et al. 2018; Drucker et al. 2008; Sykut et al. 2021). Depleted $\delta^{13}C$ ratios in ancient livestock tissues has also been associated with the practice of winter leaf foddering, whereby farmers provision animals with leafy vegetation collected from forests (Balasse et al. 2012a; Berthon et al. 2018).

Plants absorb nitrogen from the soils in which they are grown but environmental variables can also influence $\delta^{15}N$ values. For example, soil and plants exhibit increasing $\delta^{15}N$ values with decreasing mean annual precipitation (Aranibar et al. 2004; Austin and Vitousek

1998) and increasing mean annual temperature (Amundson et al. 2003; Martinelli et al. 1999). Different plant parts may vary in the relative enrichment of ^{15}N. For example, grains from manured crops will tend to have higher $\delta^{15}N$ values than rachis (Bogaard et al. 2007). Additionally, other crop by-products such as plant shoots and stems that are often used to fodder livestock are generally enriched in ^{15}N relative to the leaves and grains set aside for human consumption (Szpak 2014).

Anthropogenic influences on soil can also lead to changes in the availability of nitrogen to plants. Manure replenishes agricultural fields with nutrients after they have become fallow, or nutrient-depleted, and improves crop yields (Bayliss-Smith 1982; Crate 2008; Halstead and Jones 1989; Winterhalder et al. 1974). Intensively manured plants become enriched in ^{15}N leading to higher $\delta^{15}N$ values (Bogaard et al. 2007; Kanstrup et al. 2011; Szpak and Chiou 2020). These higher $\delta^{15}N$ values are passed up the food chain to herbivores provisioned with crops and crop by-products grown in improved soils (Bogaard et al. 2013; Choi et al. 2003; Styring et al. 2016). Because nitrogen contained in plants is passed up the food chain to their consumers, the bone collagen of animals consuming nitrogen-enriched fodder should exhibit higher $\delta^{15}N$ values relative to wild herbivores. For livestock, nitrogen values of bone collagen can be enriched by 1-3‰ when foddered with crops treated with manure (Bogaard et al. 2007; 2013) while animals fed domestic refuse (e.g., pigs) can exhibit $\delta^{15}N$ value increases on the order of 3-5‰ (Schoeninger and DeNiro 1984).

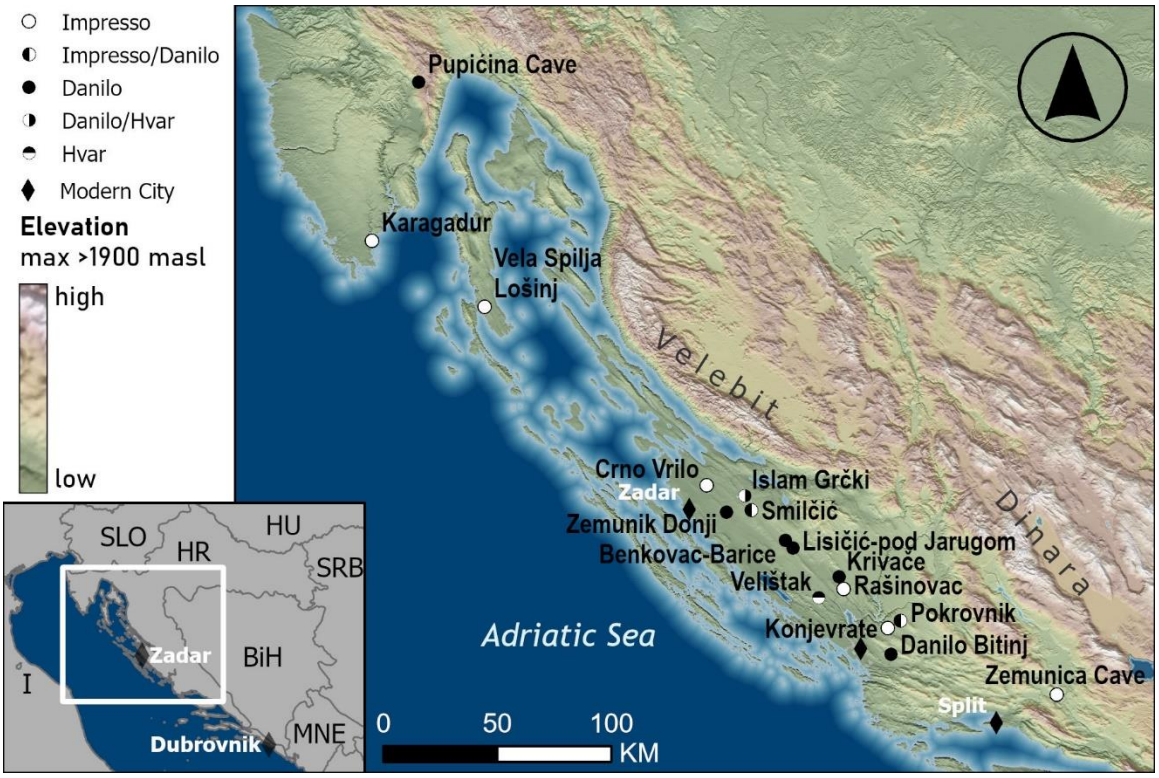

Figure 7.3. Neolithic sites represented in the stable isotope analysis of bone collagen.

1. Materials and Methods for Stable Isotope Analysis of Animal Bone Collagen

The faunal samples used in this study were collected from Early, Middle, and Late Neolithic period sites in Northern Dalmatia representing the Impresso, Danilo, and Hvar cultural phases, respectively (Table 7.2; Figure 7.3). Animal bone samples were selected from assemblages resulting from older excavations stored at the Šibenik City Museum (Konjevrate and Krivače), Zadar Archaeological Museum (Crno Vrilo and Smilčić; Marijanović 1993; 2009a,b; 2022), University of Zadar (Zemunik Donji; Marijanović and Horvat 2016; Marijanović and Vujević 2013), and the Benkovac Local Heritage Museum (Benkovac-Barice; Marijanović 2012; Vujević and Horvat 2012). Additional samples were obtained via recent excavations at Velištak, Pokrovnik, Krivače, and Rašinovac (McClure et al. 2014; McClure and Podrug 2016) and new excavations at Islam Grčki-Graduša Lokve and

Pograđe-pod Jarugom near Lisičić (Horvat Oštrić and Triozzi 2024a,b). Excavations and recovery methods used at all sites have been reported elsewhere and are summarized in Chapter Three.

Species and element determinations for materials collected from Islam Grčki, Lisičić, Zemunik Donji, Crno Vrilo, Benkovac-Barice, and Smilčić were completed in the University of Zadar Archaeology Laboratory and with the assistance of Dr. Sarah B. McClure at the Mediterranean Prehistory Laboratory at UC Santa Barbara using comparative materials. The materials from Velištak, Pokrovnik, Krivače, Danilo-Bitinj, and Rašinovac were analyzed by Dr. McClure and colleagues at the Šibenik City Museum and the Penn State Zooarchaeology Laboratory (McClure et al. 2022). Distinguishing between sheep (*Ovis aries*) and goat (*Capra hircus*) elements was performed following established criteria (Zeder and Lapham 2010; Zeder and Pilaar 2010). When sheep-goat distinctions could not be made an element was identified as "ovicaprid". Collagen was extracted from 113 faunal skeletal elements from Impresso/Early (EN), Danilo/Middle (MN), and Hvar/Late Neolithic (LN) archaeological assemblages of 12 Neolithic open-air villages in Dalmatia (Figure 7.3). Table 7.2 contains the number of samples from each site and period, including 34 specimens reported by Zavodny et al. (2014). Species and element determinations are reported in Appendix H with the results of stable isotope analysis.

Sample preparation for carbon and nitrogen isotope analysis was completed using a modified Longin method (Brown et al. 1988; Longin 1971) at the Penn State Isotope Paleoecology Lab and at the UC Santa Barbara Paleoecology and Accelerator Mass Spectrometry (AMS) Radiocarbon Research Laboratory. Bone collagen samples were prepared for analysis following the same procedures as Zavodny et al. (2014), whose data I

examine alongside new results.

Between 300 and 1400 mg of dry bone was sampled from each specimen after manually scraping away a thin layer of bone with a scalpel to remove superficial contaminants. Samples were then crushed into small pieces to maximize surface area to improve demineralization. Crushed bone was demineralized in 0.5N HCl at 5°C for 24 to 72 hours, then subjected to three 20-minute NanoPure water rinses. Demineralized bone samples were gelatinized on a heat block at 110°C in 0.05N HCl for 24 hours, then lyophilized in a thick-walled culture tube. The collagen was dissolved with NanoPure H_2O and pipetted into >30kD ultrafilters, centrifuged three times for 30 minutes, diluted with more NanoPure water, followed by another three centrifuge cycles to desalt the solution. Ultrafiltered collagen was then lyophilized and weighted to determine collagen yield. Purified collagen was packed in tin capsules and sent to Yale Analytical and Stable Isotope Center with a Thermo Delta Advantage analyzer equipped with a Costech ECS 4010 Elemental Analyzer with a Conflo III interface.

$\delta^{13}C$ and $\delta^{15}N$ values are reported in standard ‰ notation with respect to VPDB and atmospheric nitrogen (AIR) in Appendix H. Samples were screened for quality by %C, %N, and C:N ratios before further analysis, excluding samples outside the C:N range of 2.9-3.6 (see Appendix H). Samples with C:N ratios less than 2.9 or greater than 3.6 may exhibit unreliable $\delta^{13}C$ values due to the sample having been affected by poor collagen preservation or contamination, respectively (DeNiro 1985; van Klinken 1999). A subset of the purified collagen samples was set aside for AMS analysis, as described in Chapter Four.

Table 7.2. Bone collagen sample numbers for each site by period. Tallies include new and previously unpublished data and specimens reported by Zavodny et al. (2014).

Site	N Collagen Samples
Impresso	
Crno Vrilo	13
Konjevrate	7
Pokrovnik	35
Rašinovac	6
Smilčić	2
subtotal	**63**
Danilo	
Pokrovnik	20
Smilčić	2
Benkovac-Barice	2
Danilo-bitnj	8
Islam Grčki	2
Krivače	21
Lisičić	2
Zemunik Donji	8
subtotal	**65**
Hvar	
Islam Grčki	2
Velištak	17
subtotal	**19**
Total	**147**

The following chapter presents the results of the two methodological approaches described here. Integrating these approaches enables the interpretation of both short- and long-term herding strategies. The close relationship between the carbon and nitrogen isotopic composition of diet and the $\delta^{13}C$ and $\delta^{15}N$ values of animal tissues can be leveraged to assess variation in animal diet. Stable carbon and nitrogen isotope analysis of wild and domesticated

animal bone collagen is used here to evaluate change or stability in livestock diet during the Neolithic in Dalmatia. Differences in livestock diet would indicate that different feeding strategies were employed during these two time periods. Given what is known about Impresso and Danilo phase subsistence farming in Dalmatia, it might be expected that the stable isotope results will be generally consistent with feeding strategies associated with intensively managed livestock that were largely foddered and penned versus extensively grazed (Bogaard 2004; 2005; Bogaard et al. 2013; Halstead 2006). Furthermore, it is predicted that livestock bone collagen will be enriched in ^{15}N relative to wild herbivores. Additionally, I anticipate greater ^{13}C-enrichment in domestic than wild species, consistent with the prediction that animals were grazing more frequently in open-air contexts and provisioned with crops grown in open fields. These broader trends in management of livestock diet should be discernable in inter-species and diachronic comparisons of bone collagen stable isotope data.

Higher temporal resolution of management strategies will be evident in the isotopic composition of intra-tooth enamel bioapatite which provides idiosyncratic records of intra-annual changes in diet and mobility. If the importance of dairying during the Danilo period was impacted by the appearance of fermentation technology (e.g., ceramic sieves) it might be expected that some aspects of herding such as the degree of mobility or breeding seasonality will be distinct from Impresso period strategies. For example, increased labor demands of milking animals during the Danilo period may have constrained herders' ability to procure fodder, potentially increasing their reliance on extensive grazing or incentivizing them to rotate between pastures seasonally (i.e., transhumance). Adjustments to the natural breeding rhythms of sheep and goats to extend the milking season may also be expected where

dairying is critical to meeting subsistence needs (Halstead 1996; 1998b). Comparison of these data with broader trends in livestock diet evidenced by stable isotope values of bone collagen can reveal nuanced, short-term modifications to conventional herding strategies and expose the variety of risk minimization strategies used in Neolithic Dalmatia.

VIII. Strategies for Managing Livestock Diet

A. Preface

One of the most important aspects of livestock management is animal diet. Previous research has demonstrated that for about 2,000 years the proportions of domesticated animal species exploited by Dalmatia's earliest subsistence farmers changed very little despite the appearance of novel food production technologies during the Impresso-Danilo transition c. 7500-7400 cal. BP (McClure et al. 2022; McClure and Podrug 2016). However, culling strategies inferred from age-at-death data for sheep and goats suggest variability in how Neolithic herders in Dalmatia managed livestock through time and space (McClure et al. 2022; see Chapter Five).

Currently, only a handful of studies use stable isotope analysis of wild and domesticated animal bone collagen to address livestock husbandry during the Neolithic in the Eastern Adriatic (Guiry et al. 2017; Lightfoot et al. 2011; Welker et al. 2022; Zavodny et al. 2014; 2015). Stable carbon and nitrogen isotope data for wild and domestic species have been reported for Neolithic contexts at three sites in Istria (Kargadur, Pupićina Cave, and Vela Spila on Lošinj; Lightfoot et al. 2011), four sites in Northern Dalmatia (Konjevrate, Pokrovnik, Danilo, Krivače, and Čista-Mala – Velištak; Zavodny et al. 2014), and one site in central Dalmatia (Zemunica Cave; Guiry et al. 2017).

Zavodny et al. (2014) examine diachronic changes in Neolithic livestock management throughout the Adriatic and compare data from Northern Dalmatia with datasets representing Neolithic period sites in Italy, Slovenia, and the region of Istria in Croatia (Lightfoot et al. 2011). That work determined that diet of cattle, caprines, and pigs was largely similar throughout the Neolithic across the Adriatic and the authors suggest farmers provisioned animals with fodder as one possible explanation for a relatively uniform diet (Zavodny et al. 2014; 2015). More recently, Guiry et al. (2017) examined dietary changes occurring at the onset of the Neolithic period in Dalmatia, concluding domesticated animals that were grazed in areas with a higher baseline $\delta^{15}N$ provided the majority of dietary protein to humans despite an abundance of aquatic resources.

For this research, I expanded the sample size for each of the four Dalmatian sites discussed by Zavodny et al. (2014), and broadened the geographical coverage to an additional eight Neolithic period sites in Northern Dalmatia (Figure 7.3). The expanded dataset allows for a more robust inter-species and diachronic comparative analysis for Northern Dalmatia. I draw on stable isotope data for wild cervids from the three sites in Istria and the wild cervids and ovicaprids from one site in Central Dalmatia to evaluate the Northern Dalmatian findings within the context of the broader Eastern Adriatic region.

As discussed in Chapter Seven, stable isotope analysis of bone collagen can provide useful insight into past animal diet (Lelli et al. 2012; Lightfoot et al. 2015; Stevens et al. 2006). But the temporal resolution of these data is constrained by the continuous nature of bone remodeling (Eriksen 2010). As a result, the stable isotope composition of a bone collagen sample reflects an individual's diet over several years or even decades (Copley et al. 2004; Hedges et al. 2007; Manolagas 2000).

To explore changes in diet within the lifetime of individual animals, I employed a serial sampling technique on teeth to obtain a sub-annual record of the diet of ovicaprids managed by Neolithic herders in Dalmatia. In this chapter I present an analysis of the carbon and oxygen isotopic composition of enamel bioapatite and discuss the utility of short-term dietary variation for minimizing risk of herd starvation. After presenting the results of stable isotope analysis of bone collagen and enamel bioapatite, I discuss the broader patterns borne in these data and reflect on the implications for subsistence developments in Neolithic Dalmatia.

B. Results and analysis of stable isotope analysis of animal bone collagen

Comparisons of Impresso and Danilo period cattle and ovicaprid $\delta^{13}C$ and $\delta^{15}N$ values were made using Welch's Student's tests (i.e., t-tests assuming unequal variance). Welch's t-test is more robust against type I and type II errors when combined sample sizes are small, unequal, and population variance is unknown (Ruxton 2006). The small sample sizes also justify the use of the Kruskal-Wallis test, a non-parametric statistical test used to compare two or more groups. Where Kruskal-Wallis tests identified a significant difference between groups, Dunn's post-hoc test provided adjusted p-values using Holm's method (Holm 1979) to identify significance in pair-wise group comparisons.

Results of stable carbon and nitrogen isotope analysis of the 113 new samples along with the 34 samples reported by Zavodny et al. (2014) are provided in detail in Appendix H and discussed here. Table 8.1 summarizes the results by period. Four specimens (KON-1, DA-4, DA-5, and DA-14) were omitted from statistical analyses because their C:N ratios were outside of the acceptable range. Below, I discuss the results by period.

Table 8.1. Summary of bone collagen stable isotope results by period. Summarized data includes new and previously reported results (Zavodny et al. 2014) associated with sites in Northern Dalmatia (see Appendix H).

Species	Mean $\delta^{13}C$ (‰$_{VPDB}$)	Mean $\delta^{15}N$ (‰$_{AIR}$)	N
Early Neolithic (Impresso)			
Bos taurus (cattle)	-20.2 ± 0.3	5.9 ± 0.8	8
Capra hircus (goat)	-20.2 ± 0.5	6.6 ± 1.0	16
Capreolus capreolus (roe deer)	-20.1 ± 0.3	5.8 ± 0.4	4
Cervus elaphus (red deer)	-20.7	5.5	1
Lepus europaeus (hare)	-20.9	6.8	1
Ovicaprid (sheep/goat)	-20.0 ± 0.7	6.9 ± 1.1	12
Ovis aries (sheep)	-20.2 ± 0.6	6.3 ± 0.9	20
Middle Neolithic (Danilo)			
Bos taurus (cattle)	-19.7 ± 0.6	5.4 ± 0.9	16
Capra hircus (goat)	-19.9 ± 0.5	5.6 ± 0.8	8
Capreolus capreolus (roe deer)	-19.9 ± 1.1	6.0 ± 1.1	7
Cervus elaphus (red deer)	-21.0 ± 0.7	5.3 ± 1.1	3
Lepus europaeus (hare)	-22.4	4.4	1
Ovicaprid (sheep/goat)	-20.1 ± 0.5	5.7 ± 0.9	6
Ovis aries (sheep)	-20.0 ± 0.9	6.2 ± 1.0	17
Sus domesticus (pig)	-19.8 ± 0.8	5.7 ± 0.7	4
Late Neolithic (Hvar)			
Bos taurus (cattle)	-19.0 ± 0.9	5.7 ± 0.6	5
Capra hircus (goat)	-19.9 ± 0.1	5.0 ± 0.0	2
Capreolus capreolus (roe deer)	-19.3	6.6	1
Cervus elaphus (red deer)	-18.4 ± 1.8	6.6 ± 1.6	2
Lepus europaeus (hare)	-22.2 ± 1.9	5.3 ± 0.6	2
Ovis aries (sheep)	-20.8	4.8	1
Sus domesticus (pig)	-20.3 ± 0.6	6.3 ± 0.7	5
Sus scrofa (wild boar)	-20.3	7.4	1

1. Early Neolithic Impresso (8000-7400 cal. BP)

Sixty-two wild and domesticated faunal samples represent five Impresso period sites: Crno Vrilo, Konjevrate, Rašinovac, including the Early Neolithic components of Smilčić and Pokrovnik (Figure 8.1; Appendix H). The $\delta^{13}C$ values of domesticated animals from this period (n=56) range from -21.6 to -18.1‰ and $\delta^{15}N$ values range from 4.3 to 9.2‰. Early Neolithic cattle (n=8) $\delta^{13}C$ values range from -20.6 to -19.7‰ and exhibit $\delta^{15}N$ values ranging from 4.3 to 6.9‰. The $\delta^{13}C$ and $\delta^{15}N$ values of goats (n=16) range from -21.4 to -19.6‰ and 5.3 to 9.1‰, respectively. Sheep collagen samples (n=20) produced $\delta^{13}C$ values between -21.6 and -19.3‰ and $\delta^{15}N$ values from 4.8 to 8.3‰. Ovicaprids, a group consisting of either goats or sheep (n=12) exhibit $\delta^{13}C$ values ranging from -20.6 to -18.1‰ and $\delta^{15}N$ values between 5.5 and 9.2‰.

Wild fauna representing the Early Neolithic include roe deer (*Capreolus capreolus*; n=4) and red deer (*Cervus elaphus*; n=1) from Pokrovnik, and hare (*Lepus europaeus*; n=1) from Rašinovac. Roe deer $\delta^{13}C$ values range from -20.4 to -19.8‰ and exhibit $\delta^{15}N$ values between 5.6 and 6.3‰. The red deer sample $\delta^{13}C$ and $\delta^{15}N$ values are -20.7‰ and 5.5‰, respectively while the Rašinovac hare exhibited a $\delta^{13}C$ value of -20.9‰ and a $\delta^{15}N$ value of 6.8‰. Overall, the $\delta^{13}C$ values for wild and domesticated species are within the range expected for an environment dominated by C_3 vegetation.

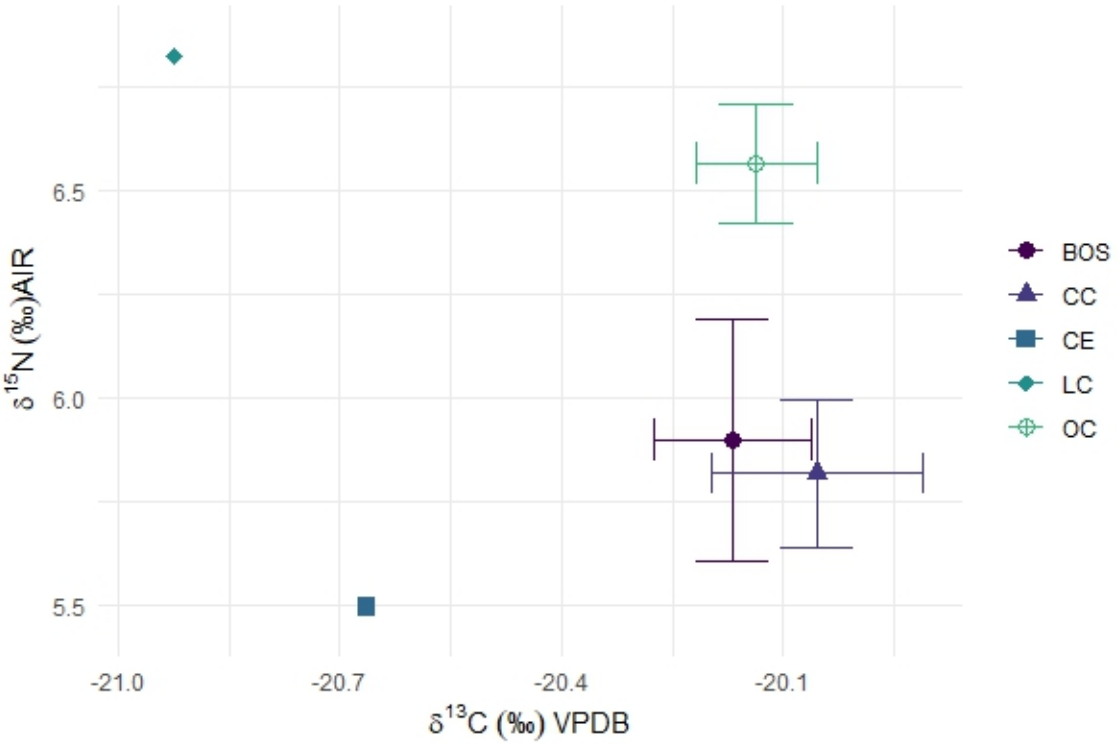

Figure 8.1. Mean and standard error of $\delta^{13}C$ and $\delta^{15}N$ bone collagen stable isotope values for Impresso (Early Neolithic) cattle (BOS), roe deer (CC), red deer (CE), hare (LC), and ovicaprid (OC) samples.

2. Middle Neolithic Danilo (c. 7500-7000 cal. BP)

Sixty-two faunal samples were tested representing eight Danilo period sites: Zemunik Donji, Lisičić-pod Jarugom, Benkovac-Barice, Danilo-Bitinj, Krivače, including the Middle Neolithic components of Islam Grčki, Smilčić, and Pokrovnik (Figure 8.2; Appendix H). Domesticated faunal samples recovered from Middle Neolithic contexts at these sites (n=51) exhibit $\delta^{13}C$ values ranging from -21.4 to -17.4‰ while $\delta^{15}N$ values are between 4.0 and 8.4‰. Cattle from this period (n=16) exhibit $\delta^{13}C$ values between -20.6 and -18.4‰ and $\delta^{15}N$ values from 4.0 to 7.1‰. Goat (n=8) $\delta^{13}C$ values were between -20.4 and -19.0‰ and $\delta^{15}N$ values between 4.8 and 6.9‰ while sheep (n=17) show a wider range of both $\delta^{13}C$ and $\delta^{15}N$ values ranging from -21.4 to -17.4‰ and 4.3 to 8.4‰, respectively. Ovicaprid (i.e., specimens identified as either goat or sheep; n=6) $\delta^{13}C$ and $\delta^{15}N$ values range between -20.5

to -19.3‰ and 4.9 to 6.9‰, respectively. Four pig specimens (two each from Krivače and Pokrovnik) have $\delta^{13}C$ values between -20.5 and -18.7‰ and $\delta^{15}N$ values from 4.8 to 6.5‰.

Wild fauna from this period (n=11) include roe deer (*Capreolus capreolus*; n=7), red deer (*Cervus elaphus*; n=3), and hare (*Lepus europaeus;* n=1). As a group, Middle Neolithic wild fauna present $\delta^{13}C$ values between -22.4 and -18.2‰ and $\delta^{15}N$ values from 4.1 to 7.9‰. Roe deer $\delta^{13}C$ values are between -21.1 and -18.2‰ and $\delta^{15}N$ values are from 4.4 to 7.9‰. Red deer $\delta^{13}C$ and $\delta^{15}N$ values are more restricted than the roe deer, ranging from -21.6 to -20.3‰ and 4.1 to 6.2‰, respectively. The single hare specimen recovered from Krivače exhibits a $\delta^{13}C$ value of -22.4‰ and a $\delta^{15}N$ value of 4.4‰ (Zavodny et al. 2014).

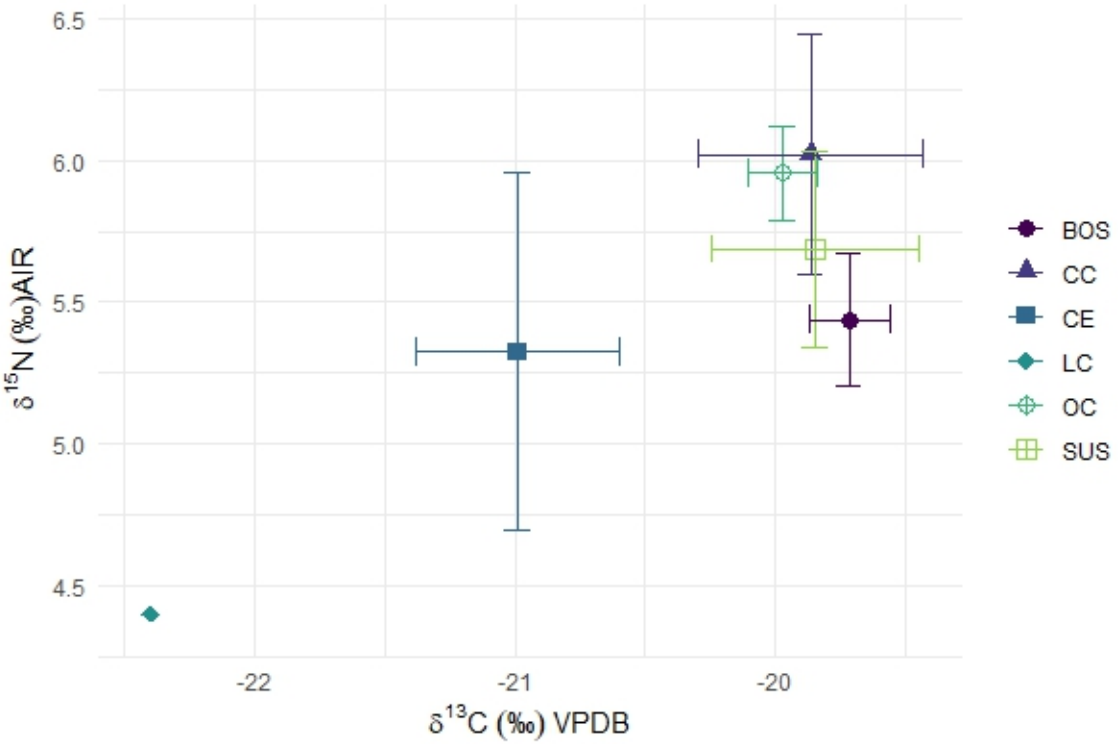

Figure 8.2. Mean and standard error of $\delta^{13}C$ and $\delta^{15}N$ bone collagen stable isotope values for Danilo (Middle Neolithic) cattle (BOS), roe deer (CC), red deer (CE), hare (LC), ovicaprid (OC), and domestic pig (SUS) samples.

3. Late Neolithic Hvar (7000-8000 cal. BP)

A total of 19 faunal samples were analyzed from Hvar period contexts at Islam Grčki (n=2) and Velištak (n=17; Figure 8.3; Appendix H). Domesticated faunal samples (n=13) exhibit $\delta^{13}C$ values between -21.2 and -17.6‰ and $\delta^{15}N$ values from 4.8 to 7.0‰. Late Neolithic cattle (n=5) $\delta^{13}C$ values range from -20.0 to -17.6‰ while $\delta^{15}N$ values are between 4.8 and 6.3‰. Ovicaprids are represented by two goat and one sheep which have a $\delta^{13}C$ value range of -20.8 to -19.9‰ while $\delta^{15}N$ values are between 4.8 and 5.0‰. Domesticated pigs (*Sus domesticus,* n=5) exhibit $\delta^{13}C$ and $\delta^{15}N$ values ranging between -21.2 to -19.8‰ and 5.4 to 7.0‰, respectively.

All Late Neolithic wild fauna (n=6) were recovered from Velištak and exhibit $\delta^{13}C$ values between -23.5 and -17.1‰ while $\delta^{15}N$ values range from 4.9 to 7.8‰. The single roe deer sample from the site has a $\delta^{13}C$ value of -19.3‰ and $\delta^{15}N$ value of 6.6‰. Two Late Neolithic red deer samples each exhibit more positive $\delta^{13}C$ and $\delta^{15}N$ values than earlier periods (VEL15: $\delta^{13}C$= -19.7‰, $\delta^{15}N$=5.5‰; VEL16: $\delta^{13}C$= -17.1‰, $\delta^{15}N$= 7.8‰). Sample VEL16 exhibits anomalously high $\delta^{13}C$ and $\delta^{15}N$ values when compared to red deer samples from other sites. The two hare samples exhibit similar $\delta^{13}C$ and $\delta^{15}N$ ranges to earlier periods (VEL20: $\delta^{13}C$=-23.5‰, $\delta^{15}N$=5.7; VEL21: $\delta^{13}C$=-20.9‰, $\delta^{15}N$=4.9‰). One wild boar sample (VEL19) from Velištak has a $\delta^{13}C$ value of -20.3‰ and a $\delta^{15}N$ value of 7.4‰.

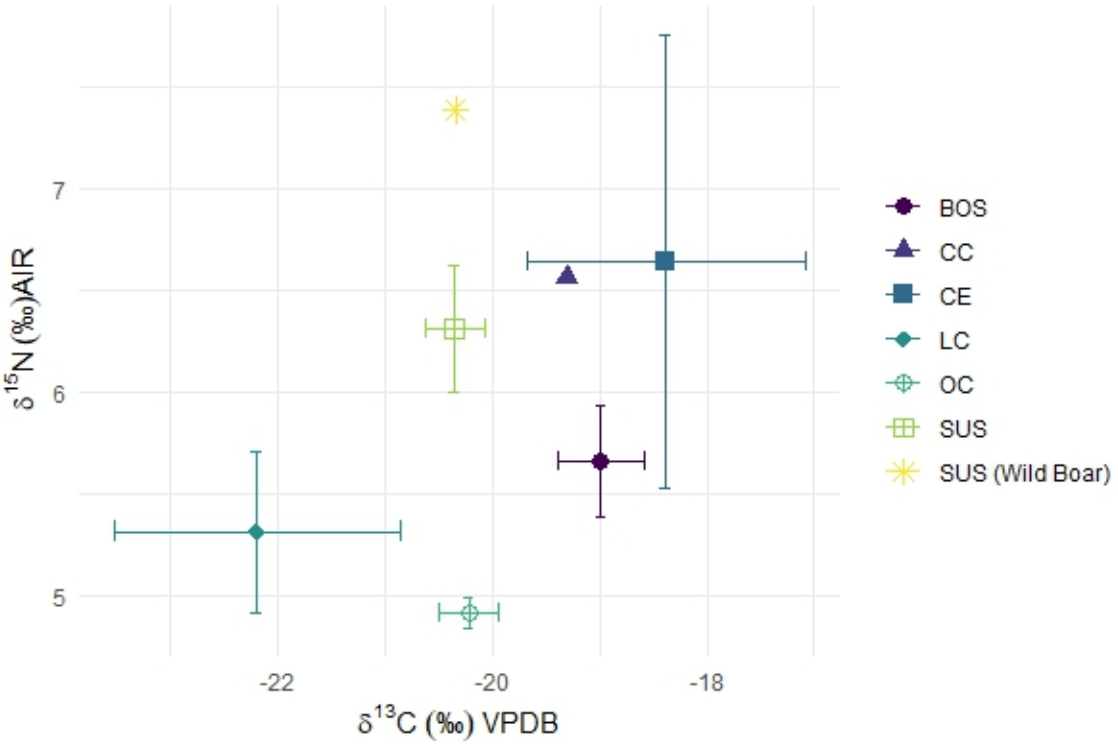

Figure 8.3. Mean and standard error of $\delta^{13}C$ and $\delta^{15}N$ bone collagen stable isotope values for Hvar / Late Neolithic cattle (BOS), roe deer (CC), red deer (CE), hare (LC), ovicaprid (OC), domestic pig (SUS), and wild boar samples.

4. Impresso versus Danilo Caprine and Cattle Dietary Management

Zooarchaeological analysis of caprine bones identified 16 goats, 20 sheep, and 12 ovicaprids (i.e., either goats or sheep) from the Impresso (Early Neolithic) phase contexts, and eight goats, 17 sheep, and six ovicaprids from Danilo (Middle Neolithic) contexts. T-tests for inter-species comparisons of mean $\delta^{13}C$ and $\delta^{15}N$ values address whether livestock species were managed differently within these periods. Mean $\delta^{13}C$ values of Impresso sheep (-20.2‰ ± 0.5) were nearly identical to goat (-20.2‰ ± 0.6) but the mean of goat $\delta^{15}N$ values is slightly higher in goats (6.7‰ ± 1.0) than sheep (6.3‰ ± 0.9). The mean $\delta^{13}C$ value is only slightly more negative for Danilo sheep (-20.0‰ ± 0.9) than goats (-19.9‰ ± 0.5). Mean $\delta^{15}N$ values are also somewhat higher for Danilo sheep (6.2‰ ± 1.0) relative to goats (5.6‰ ± 0.8) but the difference is not significant (t-test assuming unequal variance; p=0.18). Based

on these assessments, goat and sheep diet was uniform within both the Impresso and the Danilo phases of the Neolithic.

With respect to differences between caprine and cattle diet (Figure 8.4), mean $\delta^{13}C$ for Early Neolithic cattle (-20.2‰ ± 0.3; n = 8) is similar to caprine mean $\delta^{13}C$ (-20.1‰ ± 0.6; n = 47). Caprine mean $\delta^{15}N$ (6.6‰ ± 1.0) is higher relative to cattle (5.9‰ ± 0.8) but the difference is not significant (t-test assuming unequal variance; p = 0.064). The mean $\delta^{13}C$ for Middle Neolithic (Danilo period) cattle (-19.7‰ ± 0.6) is slightly more positive than in caprines (-20.0‰ ± 0.7), while caprine mean $\delta^{15}N$ (6.0‰ ± 0.9) is slightly higher relative to cattle (5.4‰ ± 0.9). These differences are not significant (t-tests assuming unequal variance for $\delta^{13}C$ p = 0.215; $\delta^{15}N$ p = 0.082). Small sample sizes for the Hvar period preclude determination of statistically significant inter-species differences in the stable isotope results of Late Neolithic assemblages.

Having determined that the $\delta^{13}C$ and $\delta^{15}N$ values indicate that caprine and cattle diet was similar during both the Early and Middle Neolithic, I then explored whether the stable isotope data support diachronic changes in diet for both caprines and cattle. My aim was to assess whether Impresso livestock diet was different from Danilo livestock diet, and the data confirms this prediction. Significant livestock dietary changes are evident from the Early to the Middle Neolithic based on comparison of mean $\delta^{13}C$ and $\delta^{15}N$ for both cattle and caprines (Figure 8.4). Mean $\delta^{13}C$ for Early Neolithic cattle bone collagen samples (-20.2‰ ± 0.3; n=8) is significantly more negative than the mean of Middle Neolithic (-19.7‰ ± 0.6; n=16) cattle specimens (t-test assuming unequal variance, p=0.026). Additionally, Early Neolithic cattle are slightly more enriched in ^{15}N (mean $\delta^{15}N$=5.9‰ ± 0.8) than Middle Neolithic specimens (mean $\delta^{15}N$=5.4‰ ± 0.9) but the difference is not significant (t-test

assuming unequal variance, p=0.233).

Mean $\delta^{13}C$ for Early Neolithic caprines (-20.1‰ ± 0.6, n=48) is very similar to mean $\delta^{13}C$ for Middle Neolithic specimens (-20.0‰ ± 0.7, n=31). However, Impresso caprine mean $\delta^{15}N$ is significantly higher at 6.6‰ ± 1.0 compared to the Danilo caprine average of 6.0‰ ± 0.9. A t-test assuming unequal variance indicates that the ^{15}N enrichment in Early versus Middle caprine diet is significant ($p<0.01$). Interestingly, Impresso and Danilo sheep mean $\delta^{13}C$ and $\delta^{15}N$ are not significantly different, but this is not the case for goats. Mean $\delta^{13}C$ is slightly more negative for Early relative to Middle Neolithic goats while mean $\delta^{15}N$ is significantly higher in the former (6.7‰ ± 1.0) than the latter (5.6‰ ± 0.8) based on a t-test assuming unequal variance (p=0.02). These data indicate that Impresso herders may have been provisioning their sheep and goats with fodder cultivated in manure-enriched soils, or grazing herds in restricted areas such as fallow fields where plant $\delta^{15}N$ values were increased by high concentrations of dung. Danilo herders seem to have not restricted grazing to the extent that soils would have been significantly enriched in ^{15}N. The higher $\delta^{13}C$ values shown for Middle Neolithic cattle suggests that Danilo herders were exploiting more open habitats for grazing or fodder collection.

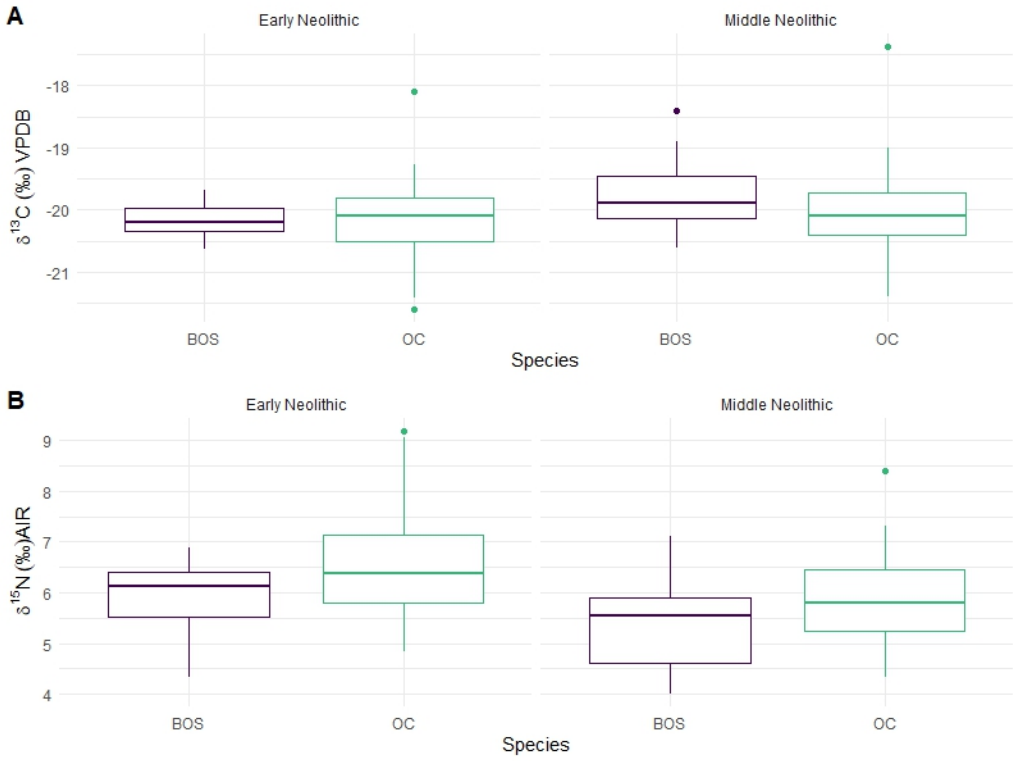

Figure 8.4 Comparison of $\delta^{13}C$ (A) and $\delta^{15}N$ (B) bone collagen stable isotope data of Impresso (Early Neolithic) and Danilo (Middle Neolithic) cattle (BOS) and ovicaprids (OC).

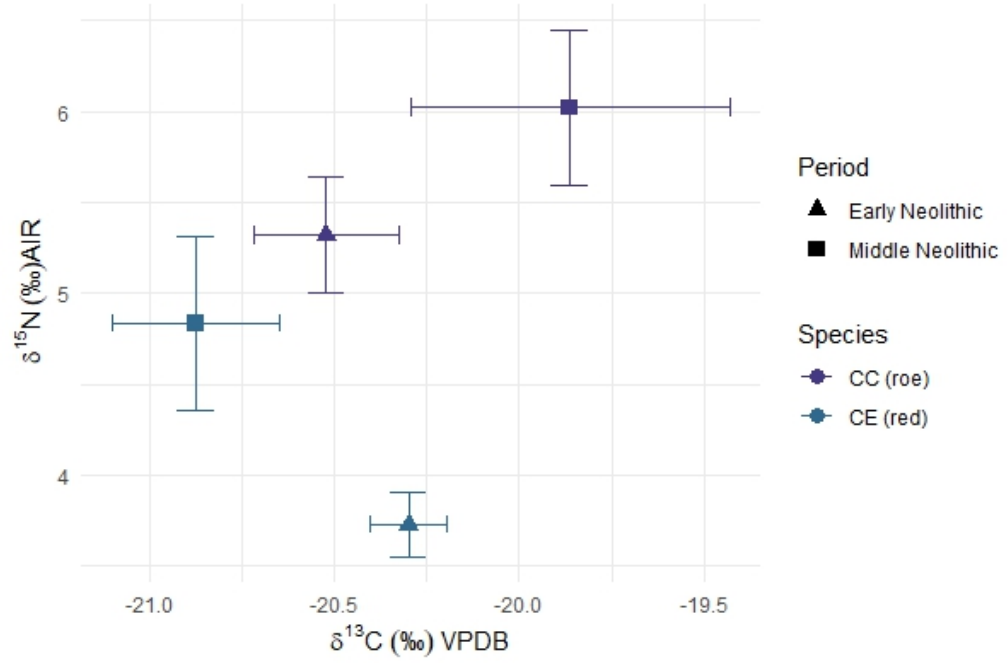

Figure 8.5. Mean and standard error of $\delta^{13}C$ and $\delta^{15}N$ bone collagen stable isotope values for Impresso (Early Neolithic) and Danilo (Middle Neolithic) roe and red deer samples.

5. Domesticated versus wild fauna

Roe (*Capreolus capreolus*) and red deer (*Cervus elaphus*) are two large herbivore species that frequently occur in Neolithic faunal assemblages as a result of opportunistic hunting (McClure et al. 2022). Red deer are widespread in Europe and consume a range of vegetation types including trees, shrubs, herbs, sedges, and grasses (Gebert and Verheyden-Tixier 2001). Roe deer are smaller than red deer and are found in deciduous, coniferous and Mediterranean forests, shrublands and moorlands (Drucker et al. 2008).

Bone collagen $\delta^{13}C$ values in red and roe deer and other large herbivores have been linked to the degree of closure of feeding habitats. More negative $\delta^{13}C$ values are typical for populations feeding in dense forests while more positive $\delta^{15}N$ values have been associated with lower density forests, increased mean annual temperature, and proximity to marine environments (Drucker et al. 2008; Hofman-Kamińska et al. 2018; Sykut et al. 2021). Variation in $\delta^{13}C$ values within populations of red deer may also occur in regions where both closed and open habitats are available for grazing (Stevens et al. 2006). Identifying shared diet spaces between livestock and wild herbivore species could indicate how Neolithic herders were managing their herd's diets.

Here, I combine stable isotope results of bone collagen of roe and red deer with published data for these species representing other sites in the Eastern Adriatic (Table 8.2) to establish baselines for expected isotopic signatures of large herbivore diets that were unmanaged. These sites include Early Neolithic / Impresso deposits at Kargadur (6760 ± 60 BP or 5710 – 5630 1-sigma cal. BC, Beta-188924; Komšo 2006), Vela Spilja Lošinj (7134 ± 37 or 6050 – 5985 1-sigma cal. BC, OxA-18118; Forenbaher and Miracle 2014), and Zemunica Cave (7120 ± 40 or 6030 – 5930 1-sigma cal. BC, Beta-225630; Radović 2011),

and Middle Neolithic / Danilo material from Pupićina Cave (6680 ± 100 or 5670 – 5480 1-sig. cal. BC Beta-131625; Miracle and Forenbaher 2005). Red and roe deer samples from the Late Neolithic site of Velištak are omitted from the following analysis for two reasons. First, the two red deer samples exhibit anomalously high $\delta^{13}C$ and $\delta^{15}N$ values which would skew summary statistics of the Early and Middle Neolithic Eastern Adriatic deer. Second, Late Neolithic cattle and caprine sample sizes are too small for inter- and intra-species comparisons. This analysis therefore compares Early and Middle Neolithic cattle and caprines with Early and Middle Neolithic roe and red deer (Figure 8.5).

Omitting the Hvar period samples, Eastern Adriatic roe deer $\delta^{13}C$ values fall between -22.3 and -18.2‰ (range= 4.1‰, mean=20.3‰ ±0.9, n=22). Red deer have a smaller range exhibiting $\delta^{13}C$ values between -21.6 and -18.9‰ (range=2.7‰, mean=-20.4‰ ±0.6, n=34). Roe deer exhibit a slightly wider range of $\delta^{15}N$ values, from 3.6 to 7.9‰ (range=4.3‰, mean=5.5‰ ±1.2) than red deer with $\delta^{15}N$ values between 2.3 and 6.3‰ (range=4.0‰, mean=3.9‰ ±1.0). Eastern Adriatic roe deer bone collagen samples are significantly more enriched in ^{15}N than red deer samples (t-test assuming unequal variance; $p<0.01$) while there is no statistical difference in mean $\delta^{13}C$. Red and roe deer show no significant intra-species differences when $\delta^{13}C$ and $\delta^{15}N$ values were compared between Impresso and Danilo specimens. However, $\delta^{15}N$ values for both species are higher in the Danilo than the Impresso period (Figure 8.5). Failing to reject the null hypothesis that Early and Middle Neolithic red and roe deer $\delta^{13}C$ and $\delta^{15}N$ values are from the same populations provides a basis for grouping the cervid data by species for comparison with Impresso and Danilo livestock.

Kruskal-Wallis tests were used to compare Impresso and Danilo cattle and caprines with roe and red deer. When the Kruskal-Wallis test detected significant inter-species

differences in either $\delta^{13}C$ or $\delta^{15}N$ values, Dunn's post-hoc test was used to make pairwise comparisons using the Holm p-value adjustment method to minimize type I and type II error risk (Holm 1979). Statistical tests were performed using the R Statistical Software v4.3.1 (R Core Team 2023). The results of these tests, summarized below, are provided in Table 8.3 and depicted graphically in Figure 8.6.

The Kruskal-Wallis tests confirm that no significant differences are observed between cattle and caprine $\delta^{13}C$ and $\delta^{15}N$ values, both within and between Neolithic phases. However, compelling differences are observed between the stable isotope composition of these livestock and that of wild cervids. Neither Impresso cattle nor caprine $\delta^{13}C$ values are significantly different from both red and roe deer (chi-squared=5.71, df=3, p=0.13). Inter-species differences are observed between $\delta^{15}N$ values of wild cervids and Early Neolithic livestock (chi-squared=59.35, df=3, $p<0.01$). Specifically, Early Neolithic cattle $\delta^{15}N$ values are significantly different from red deer (Z=3.29, $p_{adj}<0.01$) while caprine $\delta^{15}N$ values are significantly different from both red (Z=-7.67, $p_{adj}<0.01$) and roe deer (Z=-2.63, $p_{adj}=0.03$). Interspecies differences are also observed between wild cervids and Danilo phase domesticated animals ($\delta^{13}C$: chi-squared=14.59, df=3, $p<0.01$; $\delta^{15}N$: chi-squared=43.65, df=3, $p<0.01$). Danilo period cattle $\delta^{13}C$ values are significantly different from both roe (Z=2.76, $p_{adj}=0.03$) and red deer (Z=3.37, $p_{adj}<0.01$) while caprine $\delta^{13}C$ values cannot be distinguished from red and roe deer at the 95% confidence level. However, in the Danilo period both cattle and caprine $\delta^{15}N$ values are significantly different from red deer only ($p_{adj}<0.01$).

These assessments indicate that during the Impresso period, cattle diet was similar to that of roe deer in terms of ^{13}C and ^{15}N enrichment but more enriched in ^{15}N than plants

consumed by red deer. Meanwhile, caprine diet was more enriched in ^{15}N than both red and roe deer during the Early Neolithic. Feeding strategies appear to have changed in the Danilo period, as the diet of cattle became more dissimilar (i.e., enriched in ^{13}C) from both wild cervid species while remaining more enriched in ^{15}N than red deer. While cattle diet appears to have shifted away from the dietary space of roe and red deer in the Middle Neolithic, caprine diet appears to do the opposite, with lower $\delta^{15}N$ values that enter the range of roe deer values but remaining significantly more enriched in ^{15}N than red deer. These results indicate that Impresso and Danilo herders generally herded caprines and cattle together but were exploiting different grazing and foraging habitats.

Table 8.2 Summary of mean and standard deviation of $\delta^{13}C$ and $\delta^{15}N$ bone collagen stable isotope values from Kargadur, Vela Spilja Lošinj, Pupićina Cave (Lightfoot et al. 2011), and Zemunica Cave (Guiry et al. 2017).

	Mean $\delta^{13}C$ (‰$_{VPDB}$)	Mean $\delta^{15}N$ (‰$_{AIR}$)	N
Early Neolithic			
Karagadur†			
Cervus elaphus (red deer)	-20.8 ± 0.3	5.1 ± 1.1	3
Ovicaprid (sheep/goat)	-20.7 ± 0.2	6.8 ± 0.3	3
Ovis aries (sheep)	-18.8 ± 2.8	7.1 ± 2.1	2
Vela Spilja Lošinj†			
Capreolus capreolus (roe deer)	-20.1 ± 0.5	6.7 ± 1.0	4
Lepus europaeus (hare)	-21.0 ± 0.5	6.4 ± 1.0	5
Ovicaprid (sheep/goat)	-20.4 ± 0.9	7.4 ± 1.7	5
Sus sp. (pig)	-20.5	6.8	1
Zemunica Cave‡			
Bos sp. (cattle)	-20.3 ± 0.5	4.6 ± 0.9	5
Capreolus capreolus (roe deer)	-21.0 ± 0.7	4.2 ± 0.4	7
Cervus elaphus (red deer)	-20.2 ± 0.5	3.5 ± 0.7	25
Ovicaprid (sheep/goat)	-19.9 ± 0.2	5.3 ± 1.1	9
Rupicapra rupicapra (wild goat)	-20.1	7.9	1
Sus scrofa (wild boar)	-20.9 ± 0.7	4.5 ± 1.2	6
Sus sp. (pig)	-19.8 ± 0.3	5.0 ± 0.5	4
Middle Neolithic			
Pupićina†			
Bos sp. (cattle)	-20.5 ± 0.6	5.0 ± 0.2	3
Capra hircus (goat)	-19.9 ± 1.3	5.3 ± 0.7	2
Cervus elaphus (red deer)	-20.7 ± 0.0	4.1 ± 0.6	2
Ovis aries (sheep)	-20.2 ± 0.1	5.3 ± 0.2	5
Sus sp. (pig)	-19.4 ± 0.3	6.9 ± 1.3	5

†Lightfoot et al. (2011); ‡Guiry et al. (2017)

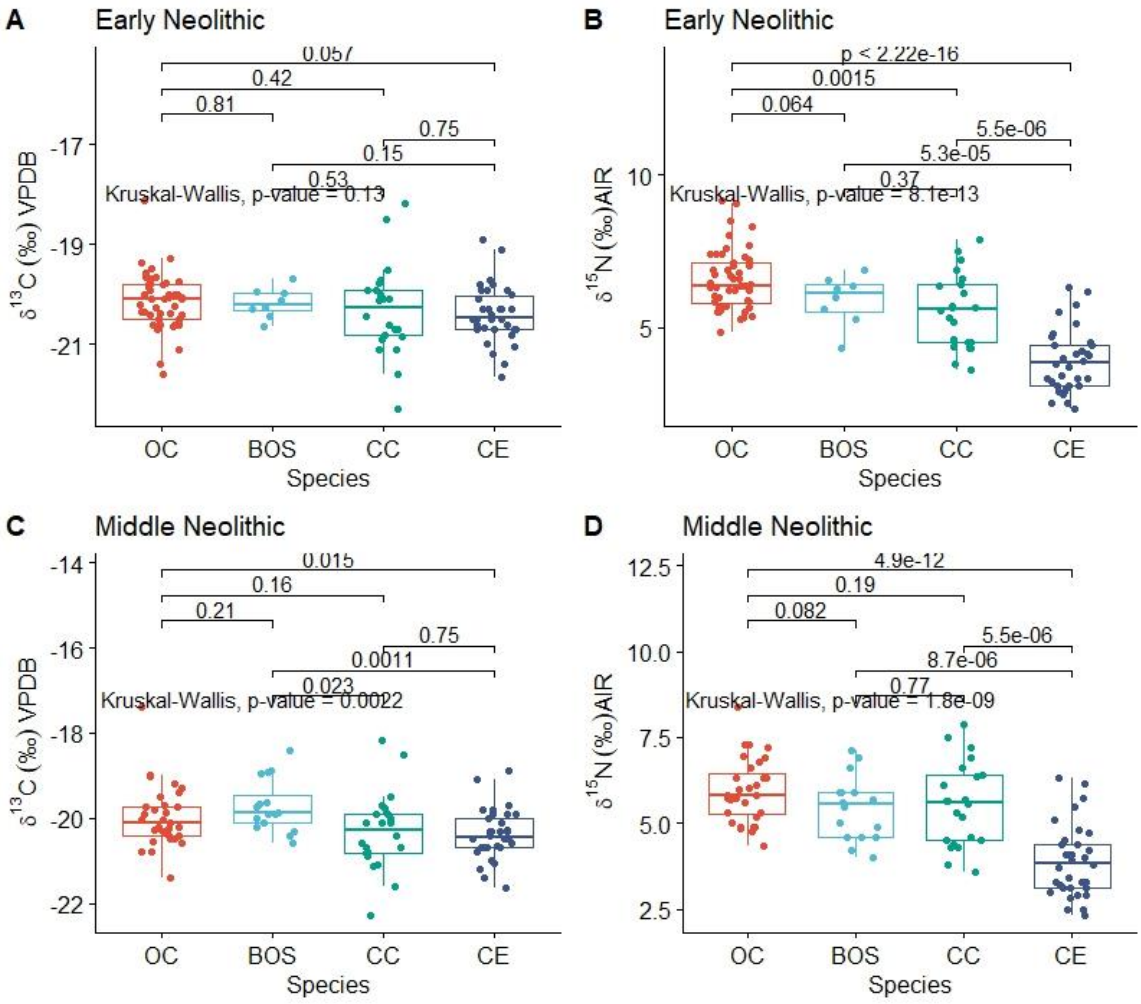

Figure 8.6. Boxplots showing $\delta^{13}C$ and $\delta^{15}N$ values, Kruskal-Wallis p-values, and p-values of pairwise t-tests comparing Early and Middle Neolithic ovicaprids (OC), cattle (BOS) from Northern Dalmatia and Eastern Adriatic roe deer (CC) and red deer (CE).

Table 8.3. Results of Kruskal-Wallis and Dunn's pair-wise comparison test of inter-species differences in $\delta^{13}C$ and $\delta^{15}N$ values of bone collagen. Bold values indicate significance at 95% confidence. BOS = cattle, CC = roe deer, CE = red deer, OC = ovicaprid.

Early Neolithic						
	$\delta^{13}C$			$\delta^{15}N$		
Kruskal-Wallis Result	X2=5.713, df=3, p=0.13			X2=59.347, df=3, p=0		
Species Compared	**Z**	**p**	**p-adjusted**	**Z**	**p**	**p-adjusted**
BOS - CC	0.825	0.409	1.000	0.606	0.544	0.544
BOS - CE	1.123	0.261	1.000	3.285	0.001	**0.004**
CC - CE	0.368	0.713	1.000	3.803	0.000	**0.001**
BOS - OC	-0.134	0.894	0.894	-1.119	0.263	0.526
CC - OC	-1.522	0.128	0.640	-2.631	0.009	**0.026**
CE - OC	-2.197	0.028	0.168	-7.665	0.000	**0.000**
Middle Neolithic						
	$\delta^{13}C$			$\delta^{15}N$		
Kruskal-Wallis Result	X2=14.588, df=3, p=0			X2=43.649, df=3, p=0		
Species Compared	**Z**	**p**	**p-adjusted**	**Z**	**p**	**p-adjusted**
BOS - CC	2.763	0.006	**0.029**	-0.133	0.894	0.894
BOS - CE	3.372	0.001	**0.004**	3.784	0.000	**0.001**
CC - CE	0.419	0.676	0.676	4.353	0.000	**0.000**
BOS - OC	1.360	0.174	0.348	-1.322	0.186	0.558
CC - OC	-1.755	0.079	0.238	-1.303	0.193	0.385
CE - OC	-2.431	0.015	0.060	-6.259	0.000	**0.000**

Table 8.4. Results of Kruskal Wallis and Dunn's pairwise comparison tests of inter-site differences for ovicaprids from Impresso-period sites. Bold values indicate significance at 95% confidence.

	$\delta^{13}C$			$\delta^{15}N$		
Kruskal-Wallis Result	X2=9.716, df=2, p=0.01			X2=19.037, df=2, p=0		
Site Comparison	Z	P.unadj	P.adj	Z	P.unadj	P.adj
Crno Vrilo - Pokrovnik	-2.269	0.023	**0.047**	3.060	0.002	**0.004**
Crno Vrilo - Zemunica Cave	-3.026	0.002	**0.007**	4.272	0.000	**0.000**
Pokrovnik - Zemunica Cave	-1.403	0.161	0.161	2.109	0.035	**0.035**

6. Assessing inter-site variation in Impresso livestock diet

Due to limited sample sizes, inter-site comparisons of sheep and goat diet are restricted to three Impresso sites: Crno Vrilo, Pokrovnik, and Zemunica Cave. Radiocarbon dates indicate that these three sites were inhabited contemporaneously in the Early Neolithic

(Forenbaher and Miracle 2014; Marijanović 2009a; McClure et al. 2014; Moore et al. 2007a; Radović 2011). For each of these sites, the number of caprine samples was at least eight, the minimum sample size appropriate for estimating the population mean (Pearson and Grove 2013). Mean $\delta^{13}C$ values for caprines from Crno Vrilo, Pokrovnik, and Zemunica Cave are -20.6 ± 0.6‰, -20.1 ± 0.5‰, and -19.9 ± 0.2‰, respectively and mean $\delta^{15}N$ values are 7.1 ± 0.6‰, 6.1 ± 0.8‰, and 5.3 ± 1.1‰, respectively. A Kruskal-Wallis test was used to perform site-wise comparisons of caprine $\delta^{13}C$ and $\delta^{15}N$ values with a Dunn post-hoc test identifying site-wise differences with adjusted p-values. Figure 8.7 shows the results of the comparisons which are summarized in Table 8.4.

Differences in mean $\delta^{13}C$ values for ovicaprids are significant between Crno Vrilo and Pokrovnik, and between Crno Vrilo and Zemunica Cave. Additionally, significant differences in ovicaprid mean $\delta^{15}N$ are exhibited between all three sites. Crno Vrilo ovicaprid diet was significantly depleted in ^{13}C, and significantly more enriched in ^{15}N relative to both Pokrovnik and Zemunica Cave animals. The Zemunica Cave isotope data indicates ovicaprid diet was significantly depleted in ^{15}N relative to both Pokrovnik and Crno Vrilo.

These comparisons indicate at least three distinct approaches to managing caprine diet were in use in the Early Neolithic: (1) penning of animals on arable fields close to the settlement at Crno Vrilo; (2) semi-intensive management of livestock at Pokrovnik with lower stocking densities and less integrated with cultivation relative to Crno Vrilo; and (3) extensive or semi-extensive husbandry at Zemunica Cave characterized by movements between the cave and, presumably, a nearby village site. Guiry et al. (2017) point out that the mean $\delta^{15}N$ value for domestic herbivores (ovicaprid n=9, cattle n=5, 5.0 ± 1.0‰) was slightly higher than wild cervids (roe deer n=7, red deer n=25, 3.6 ± 0.7‰) and suggest as an

explanation anthropogenic influences on soil chemistry and plant communities. The very high $\delta^{15}N$ values of Crno Vrilo ovicaprids relative to Zemunica Cave suggests animals raised at the former site were likely consuming manured fodder crops (Bogaard et al. 2013; Isaakidou et al. 2022; Szpak 2014). An alternative but not mutually exclusive explanation is that caprine stocking density at Crno Vrilo was higher than at the two other sites. Increased stocking density has been suggested as a variable that could lead to ^{15}N enrichment of soil within animal pens (Szpak 2014). Herders appear to have supplemented Pokrovnik caprine diet with plants grown in nitrogen-rich soils while Zemunica Cave animals grazed plants that had overall lower $\delta^{15}N$ values.

Crno Vrilo caprine diet was also significantly depleted in ^{13}C relative to diet of animals raised at the two other sites. Low $\delta^{13}C$ values in bone collagen may result from feeding exclusively on vegetation sources from densely canopied habitats, either through grazing in those habitats or via collection of leafy understory vegetation for winter fodder (Balasse et al. 2013; Berthon et al. 2018; Bonafini et al. 2013; Drucker et al. 2008; Stevens et al. 2006). The animals raised at Pokrovnik may have occasionally accessed ^{13}C-depleted vegetation but to a lesser degree than the animals from Crno Vrilo. The lower $\delta^{13}C$ values observed in Crno Vrilo caprines relative to Pokrovnik and Zemunica Cave suggests the exploitation of different grazing habitats. A focus on understory plants, either grazed or collected as winter fodder may have been a strategy employed at Crno Vrilo but not at Pokrovnik and Zemunica Cave.

It appears that herders who utilized Zemunica Cave likely organized grazing in more open habitats where caprines accessed vegetation more enriched in ^{13}C, and perhaps only rarely consumed plants collected from forested areas. Grazing in more open habitats is

consistent with the relatively lower $\delta^{15}N$ values exhibited in the Zemunica Cave caprine samples. Herders at Zemunica Cave apparently did not provision their animals with nitrogen-rich plants such as fodder crops grown in soil augmented by manure. The use of manured fodder is associated with intensive animal management, whereby animals are typically penned and remain close to the household. While Zemunica Cave has been interpreted as part of an open-air settlement in the nearby Bisko-Poljanice valley (Šošić-Klindžić et al. 2015), my analyses indicate that the isotopic composition of caprine bone collagen from the site is not characteristic of animals raised at other open-air sites. The comparisons provided here support the suggestion that, unlike the open-air sites at Crno Vrilo and Pokrovnik, Zemunica Cave was primarily used for shelter by herders who engaged in a more extensive form of livestock management characterized by greater mobility (Guiry et al. 2017). The above comparisons also suggest that mobile pastoralism can be detected by comparing in the carbon and nitrogen stable isotope composition of herded animal bone collagen.

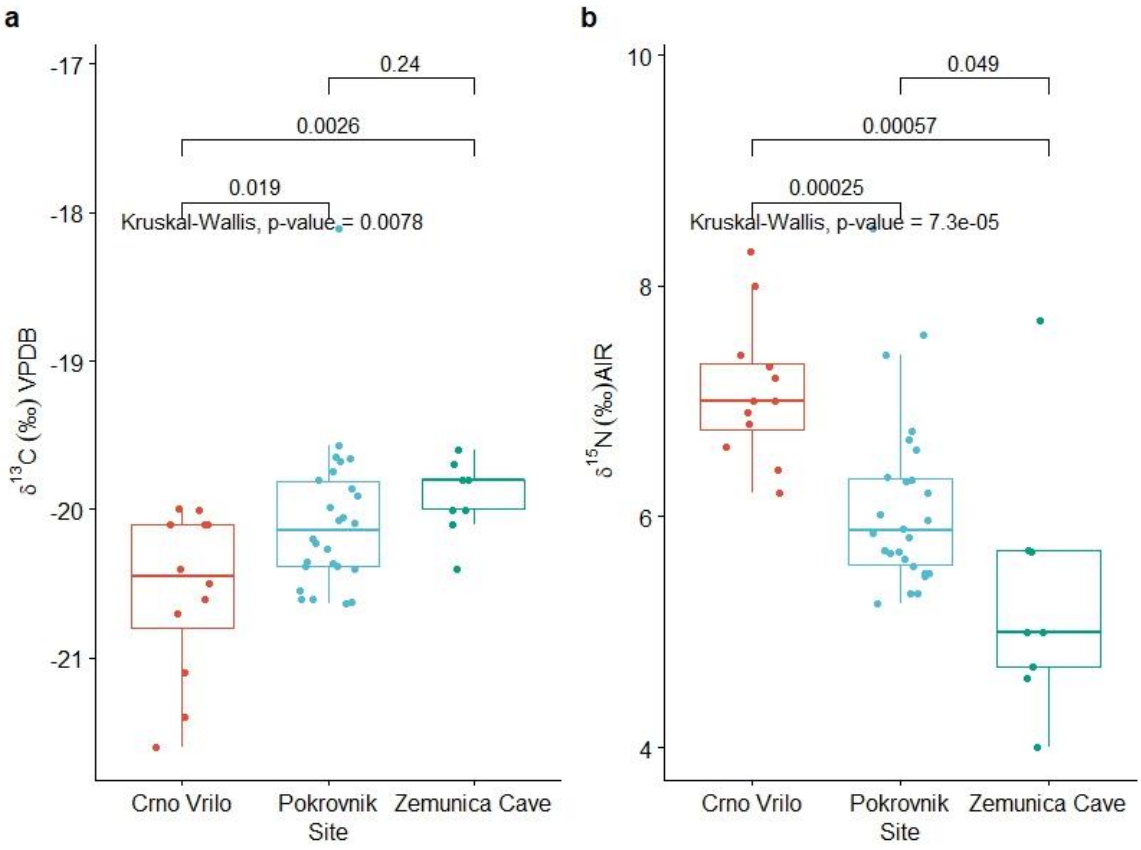

Figure 8.7. $\delta^{13}C$ and $\delta^{15}N$ values of bone collagen samples summarized as boxplots. Kruskal-Wallis p-values and p-values of pairwise t-tests comparing Impresso ovicaprid samples from three sites in Dalmatia. Data for Zemunica Cave reported by Guiry et al. (2017).

C. Results of stable isotope analysis of ovicaprid enamel bioapatite

In this section, I present the results of the carbon and oxygen isotope analysis completed for the 65 archaeological tooth specimens sampled for isotope analysis. Specimens include 20 goats and 31 sheep identified using comparative materials and established criteria for distinguishing species based on dental attributes (Zeder and Pilaar 2010). An additional 14 specimens were assigned to a catch-all, "ovicaprid" group. Between four and fourteen enamel bioapatite samples were collected from each tooth. The $\delta^{13}C_{apa}$ and $\delta^{18}O_{apa}$ values for Impresso, Danilo, and Hvar specimens are plotted in Figure 8.10, Figure 8.11, and Figure 8.12, respectively. Summaries of measured $\delta^{13}C_{apa}$ and $\delta^{18}O_{apa}$ values are

reported for each specimen in Table 8.5 and by site and period in Table 8.6 (full dataset is provided in Appendix G).

1. Carbon Isotope Ratios

Mean $\delta^{13}C_{apa}$ for all archaeological samples is -11.4 ± 0.7‰ and intra-tooth means range from -12.7 to -9.7‰ (Table 8.5). Mean intra-tooth $\delta^{13}C_{apa}$ values are similar across the three taxonomic groups (*C. hircus*: -11.7 ± 0.7‰; *O. aries*: -11.2 ± 0.8‰; ovicaprid: -11.4 ± 0.7‰). Factoring in 14‰ trophic level ^{13}C-enrichment from diet to enamel bioapatite carbonate for ruminants, sheep and goats consumed plants whose $\delta^{13}C$ values were in the range of -26.7 to -23.7‰, consistent with a predominately C_3 diet (Figure 8.8A).

The range of mean intra-tooth $\delta^{13}C_{apa}$ values for Impresso period goats is -12.7 to -11.6‰ (n=9) and -12.6 to -9.7‰ for sheep (n=14). The Danilo period goats exhibit intra-tooth mean $\delta^{13}C_{apa}$ from -12.5 to -10.6‰ (n=9) and for sheep the range is -11.7 to -10.1‰ (n=12). Mean $\delta^{13}C_{apa}$ values range from -11.1 to -10.4‰ and -11.5 to -10.0‰ among Hvar period goats (n=2) and sheep (n=5), respectively. Sheep and goats during the Impresso and Danilo phases exhibit statistically indistinguishable mean intra-tooth $\delta^{13}C_{apa}$ values (Kruskal-Wallis rank sum test for Impresso sheep versus goat: $X^2 = 2.2857$, df = 1, p-value = 0.1306; for Danilo sheep versus goat: $X^2 = 1.6364$, df = 1, p-value = 0.2008). Small sample sizes from the Hvar period preclude statistical comparisons of the results by species with other periods.

No significant differences in amplitude (max-min) of $\delta^{13}C_{apa}$ variation were found between goats and sheep for the Early or Middle Neolithic. Mean $\delta^{13}C_{apa}$ for Impresso goats is similar to Danilo goats. However, Danilo period sheep exhibit significantly more positive mean $\delta^{13}C_{apa}$ than Impresso sheep (Kruskal-Wallis rank sum test: X^2=4.4471, df = 1, p-value

< 0.05), and the same is true for the mid-range (max + min / 2; Kruskal-Wallis rank sum test: X^2=5.5979, df = 1, p-value < 0.05). Comparing species within periods reveals that $\delta^{13}C_{apa}$ mid-range of Danilo period sheep is significantly more positive than goats (Kruskal-Wallis rank sum test: X^2=6.5455, df = 1, p-value < 0.05). This could be a result of Danilo herders becoming more mobile resulting in the consumption of a broader diversity of plants, including some types of vegetation with very high $\delta^{13}C$ values.

The relatively higher $\delta^{13}C_{apa}$ values shown among Danilo specimens is reflective of caprine diet becoming more ^{13}C-enriched through time (mean $\delta^{13}C_{apa}$ for Impresso: -11.7 ±0.8‰; Danilo: -11.3 ±0.7‰; Hvar: -10.9 ± 0.5‰; Figure 8.8D) and these changes are significant (Kruskal-Wallis rank sum test: X^2=14.658, df=2, p<0.001). Pairwise comparisons of mean $\delta^{13}C$ values of Impresso, Danilo, and Hvar period teeth indicate statistically significant differences between Impresso and Danilo, and Impresso and Hvar specimens (adjusted p-value from Dunn's Kruskal-Wallis multiple comparisons test: Impresso-Danilo p_{adj}=0.014; Impresso-Hvar p_{adj}=0.001; Table 8.7). The intra-tooth $\delta^{13}C_{apa}$ amplitudes increase from the Impresso to the Hvar period and Impresso period amplitudes are significantly lower than in the Danilo period (p-value from Dunn's Kruskal-Wallis multiple comparisons test: Impresso-Danilo p_{adj}=0.022; Table 8.7). Impresso maximum $\delta^{13}C_{apa}$ is also significantly lower than both the Danilo and Hvar period (adjusted p-value from Dunn's Kruskal-Wallis multiple comparisons test: Impresso-Danilo p_{adj}=0.001; Impresso-Danilo p_{adj}=0.002; Table 8.7). No significant inter-site differences in $\delta^{13}C_{apa}$ were detected between Crno Vrilo and Impresso period Pokrovnik which are the only two groups with sample sizes large enough to permit statistical comparison (Pearson and Grove 2013).

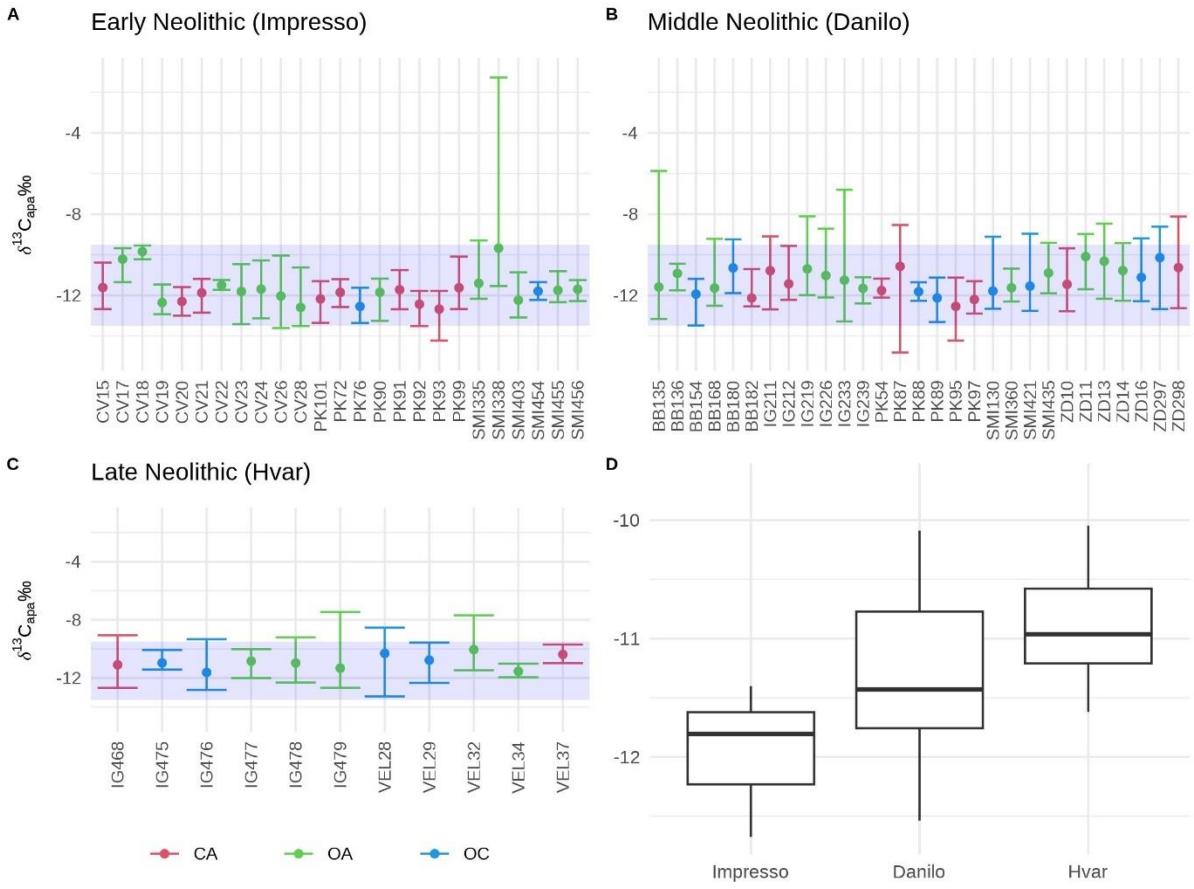

Figure 8.8. Comparison of intra-tooth $\delta^{13}C_{apa}$ mean and range for each specimen by period: (A) Early Neolithic – Impresso; (B) Middle Neolithic – Danilo; (C) Late Neolithic – Hvar. (D) Comparison of mean δ13Capa by period. Colors in A-C correspond to goat (CA), sheep (OA), and ovicaprid (OC) Site and sample numbers in Table 8.5. Blue shaded area represents the expected δ13C range of enamel bioapatite values for ruminants consuming an exclusively C3 diet after trophic enrichment of 14‰ (Passey et al. 2005; Zazzo et al. 2010), i.e., from -13.5‰ to -9.5‰.

Table 8.5. Summary of $\delta^{18}O_{apa}$ and $\delta^{13}C_{apa}$ by specimen (mean, standard deviation, minimum, maximum, amplitude of variation (A = max - min), and covariance obtained by Pearson's product moment correlation coefficient; p-value with bold values indicates significance at 95% confidence. Species abbreviations: CA = Capra hircus; OA = Ovis aries; OC = ovicaprid.

				$\delta^{18}O$‰				$\delta^{13}C$‰				covariance		
Specimen	**Species**	**Side**	**n**	**Mean**	**Min.**	**Max.**	**A**	**Mean**	**Min.**	**Max.**	**A**	**Pearson's R**	**df**	**p**
Crno Vrilo (Impresso)														
CV15	CA	R	8	-0.8 ± 1.2	-2.6	0.7	3.3	-11.6 ± 0.7	-12.7	-10.4	2.3	0.79	6	**0.019**
CV17	OA	L	7	-1.7 ± 1.3	-3.8	-0.2	3.7	-10.2 ± 0.6	-11.3	-9.7	1.7	0.53	5	0.217
CV18	OA	L	4	-2.8 ± 1.3	-4.3	-1.2	3.2	-9.8 ± 0.3	-10.2	-9.5	0.7	-0.34	2	0.658
CV19	OA	L	7	-1.9 ± 1.1	-3.0	0.1	3.0	-12.4 ± 0.5	-12.9	-11.5	1.5	0.81	5	**0.027**
CV20	CA	L	9	-2.2 ± 1.3	-3.9	-0.2	3.7	-12.3 ± 0.5	-13.0	-11.6	1.4	0.78	7	**0.014**
CV21	CA	L	9	0.1 ± 1.3	-1.9	1.7	3.5	-11.9 ± 0.6	-12.8	-11.2	1.7	0.63	7	0.069
CV22	OA	R	6	-0.8 ± 1.5	-3.4	0.3	3.7	-11.5 ± 0.2	-11.7	-11.2	0.5	0.01	4	0.983
CV23	OA	R	10	-1.2 ± 1.3	-3.1	0.3	3.4	-11.8 ± 1.1	-13.4	-10.5	3.0	0.76	8	**0.011**
CV24	OA	R	9	-1.3 ± 0.8	-2.8	-0.2	2.6	-11.7 ± 1.1	-13.1	-10.3	2.8	0.83	7	**0.005**
CV26	OA	R	8	-1.7 ± 1.2	-3.4	-0.5	2.9	-12 ± 1.5	-13.6	-10.0	3.6	0.24	6	0.565
CV28	OA	R	6	-2.1 ± 1	-3.2	-0.9	2.4	-12.6 ± 1	-13.5	-10.6	2.9	0.57	4	0.239
Pokrovnik (Impresso)														
PK101	CA	L	10	-0.9 ± 1.1	-3.2	0.4	3.6	-12.2 ± 0.8	-13.3	-11.3	2.0	-0.40	8	0.253
PK72	CA	L	10	-0.7 ± 1.2	-2.4	0.7	3.1	-11.8 ± 0.5	-12.6	-11.2	1.4	0.14	8	0.698
PK76	OC	R	11	-1.9 ± 1	-3.0	-0.3	2.7	-12.5 ± 0.6	-13.4	-11.6	1.7	0.79	9	**0.004**
PK90	OA	R	10	-1.5 ± 0.4	-2.0	-1.0	1.0	-11.8 ± 0.6	-13.2	-11.2	2.1	0.51	8	0.135
PK91	CA	L	10	-1.4 ± 1.7	-4.2	0.8	5.0	-11.7 ± 0.7	-12.7	-10.8	1.9	0.91	8	**0.000**

				δ18O‰				δ13C‰				covariance		
Specimen	**Species**	**Side**	**n**	**Mean**	**Min.**	**Max.**	**A**	**Mean**	**Min.**	**Max.**	**A**	**Pearson's R**	**df**	**p**
PK92	CA	R	10	-2.2 ± 0.7	-3.6	-1.4	2.2	-12.4 ± 0.5	-13.5	-11.8	1.7	0.70	8	**0.024**
PK93	CA	R	12	-2.8 ± 0.4	-3.5	-2.2	1.3	-12.7 ± 0.8	-14.2	-11.8	2.4	0.80	10	**0.002**
PK99	CA	L	12	-2.1 ± 1.2	-3.9	0.5	4.4	-11.6 ± 0.7	-12.7	-10.1	2.6	0.16	10	0.610
Smilčić (Impresso)														
SMI335	OA	L	10	-2.3 ± 1.7	-4.4	0.3	4.7	-11.4 ± 1	-12.2	-9.3	2.9	0.78	8	**0.007**
SMI338	OA	L	10	-2.3 ± 1.6	-4.1	0.4	4.4	-9.7 ± 3.1	-11.5	-1.3	10.3	-0.11	8	0.759
SMI403	OA	L	9	-1.4 ± 2	-3.5	1.4	5.0	-12.2 ± 0.8	-13.1	-10.9	2.2	0.90	7	**0.001**
SMI454	OC	L	11	-1.1 ± 1.1	-2.5	0.3	2.9	-11.8 ± 0.3	-12.2	-11.3	0.9	0.64	9	**0.032**
SMI455	OA	R	11	-1.4 ± 1	-3.0	-0.2	2.8	-11.7 ± 0.6	-12.3	-10.8	1.5	0.73	9	**0.012**
SMI456	OA	R	12	-2.2 ± 1.2	-3.8	-0.4	3.4	-11.7 ± 0.3	-12.3	-11.2	1.0	0.65	10	**0.022**
Benkovac-Barice (Danilo)														
BB135	OA	L	10	-3.3 ± 1.1	-4.4	-1.3	3.0	-11.6 ± 2.3	-13.2	-5.9	7.3	0.20	8	0.580
BB136	OA	R	9	-1.8 ± 2	-4.9	0.1	5.0	-10.9 ± 0.4	-11.7	-10.4	1.3	0.84	7	**0.004**
BB154	OC	L	10	-1 ± 1.6	-3.8	0.7	4.5	-11.9 ± 0.7	-13.5	-11.2	2.3	0.45	8	0.190
BB168	OA	R	11	-1.5 ± 1.1	-3.3	-0.3	3.0	-11.6 ± 1.1	-12.5	-9.2	3.3	0.54	9	0.089
BB180	OC	L	12	-1.3 ± 1	-3.3	-0.2	3.1	-10.6 ± 1	-11.9	-9.2	2.6	0.46	10	0.129
BB182	CA	L	10	-3.3 ± 1.2	-4.6	-1.1	3.5	-12.1 ± 0.6	-12.5	-10.7	1.8	0.87	8	**0.001**
Islam Grčki (Danilo)														
IG211	CA	L	12	-1.5 ± 1.2	-3.1	0.2	3.3	-10.8 ± 1.4	-12.7	-9.1	3.6	0.70	10	**0.011**
IG212	CA	L	10	-2.1 ± 1.2	-3.5	-0.2	3.3	-11.4 ± 0.9	-12.2	-9.6	2.7	0.91	8	**0.000**
IG219	OA	L	10	-2.6 ± 0.9	-3.9	-1.4	2.5	-10.7 ± 1.3	-12.0	-8.1	3.9	0.32	8	0.368

				δ18O‰				δ13C‰				covariance		
Specimen	**Species**	**Side**	**n**	**Mean**	**Min.**	**Max.**	**A**	**Mean**	**Min.**	**Max.**	**A**	**Pearson's R**	**df**	**p**
IG226	OA	R	12	-2.1 ± 1.2	-3.5	-0.3	3.2	-11 ± 1.1	-12.1	-8.7	3.4	0.90	10	**0.000**
IG233	OA	R	10	-3 ± 1.4	-4.8	-1.1	3.7	-11.3 ± 2.4	-13.3	-6.8	6.5	0.50	8	0.145
IG239	OA	L	11	-1.1 ± 1.7	-3.3	1.2	4.5	-11.7 ± 0.5	-12.4	-11.1	1.3	0.84	9	**0.001**
Pokrovnik (Danilo)														
PK54	CA	R	11	-1 ± 1.6	-3.1	1.3	4.4	-11.8 ± 0.3	-12.1	-11.2	0.9	0.18	9	0.606
PK87	CA	R	10	-1 ± 0.9	-2.6	0.2	2.8	-10.6 ± 2.2	-14.8	-8.5	6.3	0.17	8	0.648
PK88	OC	R	7	-0.2 ± 1.4	-2.5	1.4	3.8	-11.8 ± 0.4	-12.3	-11.3	0.9	0.74	5	0.055
PK89	OC	R	10	-2.4 ± 2	-4.5	0.7	5.2	-12.1 ± 0.9	-13.3	-11.1	2.2	0.93	8	**0.000**
PK95	CA	L	10	-1.8 ± 0.5	-2.8	-0.9	1.9	-12.5 ± 1.2	-14.2	-11.1	3.1	0.91	8	**0.000**
PK97	CA	L	8	-3.6 ± 1.6	-5.1	-1.0	4.1	-12.2 ± 0.6	-12.9	-11.3	1.6	0.81	6	**0.016**
Smilčić (Danilo)														
SMI130	OC	L	14	-2 ± 1.4	-3.7	0.1	3.8	-11.8 ± 0.9	-12.7	-9.1	3.5	0.14	12	0.627
SMI360	OA	R	10	-2 ± 1.5	-3.9	0.2	4.1	-11.6 ± 0.6	-12.3	-10.7	1.6	0.90	8	**0.000**
SMI421	OC	L	10	-1.4 ± 1.3	-2.6	0.7	3.3	-11.5 ± 1.5	-12.8	-9.0	3.8	0.92	8	**0.000**
SMI435	OA	R	11	-1.4 ± 1.6	-3.9	0.9	4.8	-10.9 ± 0.9	-11.9	-9.4	2.5	0.91	9	**0.000**
Zemunik Donji (Danilo)														
ZD10	CA	L	11	-1.8 ± 1.6	-4.1	0.1	4.2	-11.5 ± 1.2	-12.8	-9.7	3.1	0.94	9	**0.000**
ZD11	OA	L	10	-0.9 ± 1	-2.8	0.2	3.0	-10.1 ± 1	-11.7	-9.0	2.7	0.88	8	**0.001**
ZD13	OA	R	6	-1.7 ± 1.4	-3.6	-0.3	3.3	-10.3 ± 1.6	-12.2	-8.5	3.7	0.93	4	**0.007**
ZD14	OA	R	10	-1.4 ± 1.3	-3.7	0.1	3.7	-10.8 ± 1.1	-12.3	-9.4	2.8	0.74	8	**0.014**
ZD16	OC	R	11	-1.7 ± 1	-3.3	-0.3	3.0	-11.1 ± 1.1	-12.3	-9.2	3.1	0.71	9	**0.014**

				δ18O‰				δ13C‰				covariance		
Specimen	**Species**	**Side**	**n**	**Mean**	**Min.**	**Max.**	**A**	**Mean**	**Min.**	**Max.**	**A**	**Pearson's R**	**df**	**p**
ZD297	OC	L	10	-1.1 ± 1.5	-3.7	0.6	4.2	-10.1 ± 1.3	-12.7	-8.6	4.1	0.92	8	**0.000**
ZD298	CA	L	11	-0.9 ± 1.5	-3.7	0.7	4.4	-10.6 ± 1.7	-12.6	-8.1	4.5	0.88	9	**0.000**
Islam Grčki (Hvar)														
IG468	CA	R	12	-0.9 ± 1.5	-2.9	1.2	4.1	-11.1 ± 1.3	-12.7	-9.1	3.6	0.67	10	**0.017**
IG475	OC	R	10	-3.3 ± 0.8	-4.5	-1.9	2.5	-11 ± 0.4	-11.4	-10.1	1.3	0.53	8	0.114
IG476	OC	R	12	-2.8 ± 1.3	-4.2	-0.7	3.5	-11.6 ± 1.1	-12.8	-9.3	3.5	0.74	10	**0.006**
IG477	OA	R	10	-1.2 ± 1.2	-3.3	0.1	3.5	-10.8 ± 0.7	-12.0	-10.0	2.0	0.77	8	**0.009**
IG478	OA	R	10	-2.7 ± 1.8	-5.6	-0.6	5.1	-11 ± 1.1	-12.3	-9.2	3.1	0.63	8	0.052
IG479	OA	L	11	-4.2 ± 1.3	-5.8	-1.7	4.2	-11.3 ± 1.6	-12.7	-7.5	5.2	0.89	9	**0.000**
Velištak (Hvar)														
VEL28	OC	R	8	-2.9 ± 1.3	-4.8	-1.1	3.7	-10.3 ± 1.5	-13.3	-8.5	4.7	0.31	6	0.462
VEL29	OC	L	11	-1.9 ± 1	-3.6	-0.9	2.7	-10.8 ± 0.8	-12.3	-9.6	2.8	0.07	9	0.838
VEL32	OA	R	10	-1.6 ± 0.6	-2.4	-0.6	1.8	-10 ± 1.6	-11.5	-7.7	3.8	0.87	8	**0.001**
VEL34	OA	R	5	-1.1 ± 1	-2.7	0.0	2.7	-11.5 ± 0.4	-11.9	-11.0	0.9	0.02	3	0.973
VEL37	CA	L	7	-1.7 ± 0.7	-2.8	-0.8	2.0	-10.4 ± 0.5	-11.0	-9.7	1.3	0.31	5	0.498
Dinara (modern)														
DIN5	OA	R	6	-6.4 ± 1.4	-7.8	-4.3	3.5	-12.2 ± 2.1	-16.3	-10.7	5.6	0.07	4	0.901
DIN6	OA	R	3	-6 ± 1	-6.8	-5.0	1.8	-9.9 ± 1.2	-10.9	-8.5	2.4	1.00	1	**0.040**
DIN7	OA	R	9	-6.5 ± 0.7	-7.3	-5.3	2.0	-11.9 ± 1.1	-14.3	-11.0	3.2	0.53	7	0.139
Vrlika (modern)														
VRL481	OA	L	10	-5.7 ± 1	-7.0	-4.0	3.0	-13 ± 0.2	-13.2	-12.6	0.6	0.59	8	0.074

Table 8.6 Mean, minimum, maximum, and mean amplitude of variation of intra-tooth $\delta^{18}O_{apa}$ and $\delta^{13}C_{apa}$ values by period and site.

		$\delta^{18}O‰_{VPDB}$			$\delta^{13}C‰_{VPDB}$		
Site	**n**	**Mean**	**min/max**	**Mean Amp.**	**Mean**	**min/max**	**Mean Amp.**
Impresso							
Crno Vrilo	11	-1.5 ± 0.8	-4.3 / 1.7	3.2	-11.6 ± 0.9	-13.6 / -9.5	2.0
Pokrovnik	8	-1.7 ± 0.7	-4.2 / 0.8	2.9	-12.1 ± 0.4	-14.2 / -10.1	2.0
Smilčić	6	-1.8 ± 0.6	-4.4 / 1.4	3.9	-11.4 ± 0.9	-13.1 / -1.3	3.1
Total	**25**	**-1.6 ± 0.7**	**-4.4 / 1.7**	**3.3**	**-11.7 ± 0.8**	**-14.2 / -1.3**	**2.3**
Danilo							
Pokrovnik	6	-1.7 ± 1.2	-5.1 / 1.4	3.7	-11.8 ± 0.7	-14.8 / -8.5	2.5
Smilčić	4	-1.7 ± 0.4	-3.9 / 0.9	4.0	-11.5 ± 0.4	-12.8 / -9.0	2.9
Benkovac-Barice	6	-2.0 ± 1.0	-4.9 / 0.7	3.7	-11.5 ± 0.6	-13.5 / -5.9	3.1
Islam Grčki	6	-2.1 ± 0.7	-4.8 / 1.2	3.4	-11.1 ± 0.4	-13.3 / -6.8	3.6
Zemunik Donji	7	-1.4 ± 0.4	-4.1 / 0.7	3.7	-10.6 ± 0.5	-12.8 / -8.1	3.4
Total	**29**	**-1.8 ± 0.8**	**-5.1 / 1.4**	**3.7**	**-11.3 ± 0.7**	**-14.8 / -5.9**	**3.1**
Hvar							
Islam Grčki	6	-2.5 ± 1.3	-5.8 / 1.2	3.8	-11.1 ± 0.3	-12.8 / -7.5	3.1
Velištak	5	-1.9 ± 0.6	-4.8 / 0.0	2.6	-10.6 ± 0.6	-13.3 / -7.7	2.7
Total	**11**	**-2.2 ± 1.0**	**-5.8 / 1.2**	**3.3**	**-10.9 ± 0.5**	**-13.3 / -7.5**	**2.9**

		$\delta^{18}O‰_{VPDB}$			$\delta^{13}C‰_{VPDB}$		
Site	**n**	**Mean**	**min/max**	**Mean Amp.**	**Mean**	**min/max**	**Mean Amp.**
				Modern			
Dinara	3	-6.3 ± 0.2	-7.8 / -4.3	2.4	-11.3 ± 1.3	-16.3 / -8.5	3.7
Vrlika	1	-5.7	-7.0 / -4.0	3.0	-13.0	-13.2 / -12.6	0.6
Total	**4**	**-6.1 ± 0.4**	**-7.8 / -4.0**	**2.6**	**-11.8 ± 1.3**	**-16.3 / -8.5**	**3.0**

Table 8.7. Results of Dunn's Kruskal-Wallis multiple comparisons test between Impresso/Early (EN), Danilo/Middle (MN), and Hvar/Late Neolithic (LN) caprine specimens. Only variables where significant differences were found are reported. Bold text indicates significance at 95% confidence.

variable	Periods	Z	p-value (unadjusted)	Adjusted p-value
Max. $\delta^{13}C$	**EN - LN**	-3.322	**0.001**	**0.002**
	EN - MN	-3.620	**0.000**	**0.001**
	LN - MN	0.604	0.546	0.546
Mean $\delta^{13}C$	**EN - LN**	-3.574	**0.000**	**0.001**
	EN - MN	-2.703	**0.007**	**0.014**
	LN - MN	1.569	0.117	0.117
Amp. $\delta^{13}C$	EN - LN	-1.822	0.069	0.137
	EN - MN	-2.680	**0.007**	**0.022**
	LN - MN	-0.205	0.838	0.838
Mid-Range. $\delta^{13}C$	**EN - LN**	-3.255	**0.001**	**0.003**
	EN - MN	-3.020	**0.003**	**0.005**
	LN - MN	0.998	0.318	0.318

2. Oxygen Isotope Ratios

For the entire archaeological sample $\delta^{18}O_{apa}$ values range from -5.8 to 1.7‰. The mid-range (max + min / 2) is from -3.8 to -0.1‰. One isotope sample from Islam Grčki, IG219-2 exhibited an anomalously high $\delta^{18}O$ value of 31.4‰ and was omitted from statistical comparisons and model fitting. Amplitude of variation (max - min) ranges from 0.98 to 5.2‰. Average $\delta^{18}O_{apa}$ is similar for goats (-1.6 ± 0.9‰, n=20), sheep (-1.9 ± 0.8‰, n=31), and ovicaprids (-1.8 ±0.9‰, n=14). The range and amplitude for each tooth sampled are plotted in Figure 8.9.

Grouping results by period, the mean $\delta^{18}O$ values of Late Neolithic teeth (-2.2 ± 1.0‰) were lower relative to Impresso/Early (-1.6 ± 0.7‰) and Danilo/Middle Neolithic (-1.8 ± 0.8‰) specimens (Figure 8.9D). The $\delta^{18}O_{apa}$ range for Impresso specimens is from -4.4

to 1.7‰, mid-ranges vary between -2.8 and -0.1‰, and amplitudes between 0.98 and 4.98‰. The $\delta^{18}O_{apa}$ of the Danilo specimens range from -5.1 to 1.4 ‰, mid-ranges are from -3.1 to -0.6‰, and amplitudes from 1.9 to 5.2‰. For the Hvar/Late Neolithic specimens, intra-tooth $\delta^{18}O_{apa}$ ranges from -5.8 to 1.2‰, mid-ranges are from -3.8 to -0.8‰ and amplitudes from 1.8 to 5.1‰. Mean amplitude of variation is slightly higher in the Middle Neolithic (3.7 ± 0.8‰) than the Early (3.3 ± 1.0‰) and Late Neolithic (3.3 ± 1.0‰). Mean $\delta^{18}O$ values of teeth are more similar among Impresso and Hvar specimens compared to Danilo, even when outliers are excluded (p-value by Shapiro-Wilk test of mean $\delta^{18}O$: Impresso p=0.65; Danilo p=0.13; Hvar p=0.56). Amplitudes of variation are normally distributed for the entire archaeological group (Shapiro-Wilk test for normality $p > 0.05$). Otherwise, the amplitude of variation is slightly more variable among Impresso specimens (Shapiro-Wilk test for normality of amplitude: Impresso p=0.474; Danilo p=0.753; Hvar p = 0.848). A Kruskal-Wallis rank sum test revealed no statistically significant differences when mean, minimum, maximum, mid-range, and amplitude of variation of $\delta^{18}O$ values of teeth were compared by period.

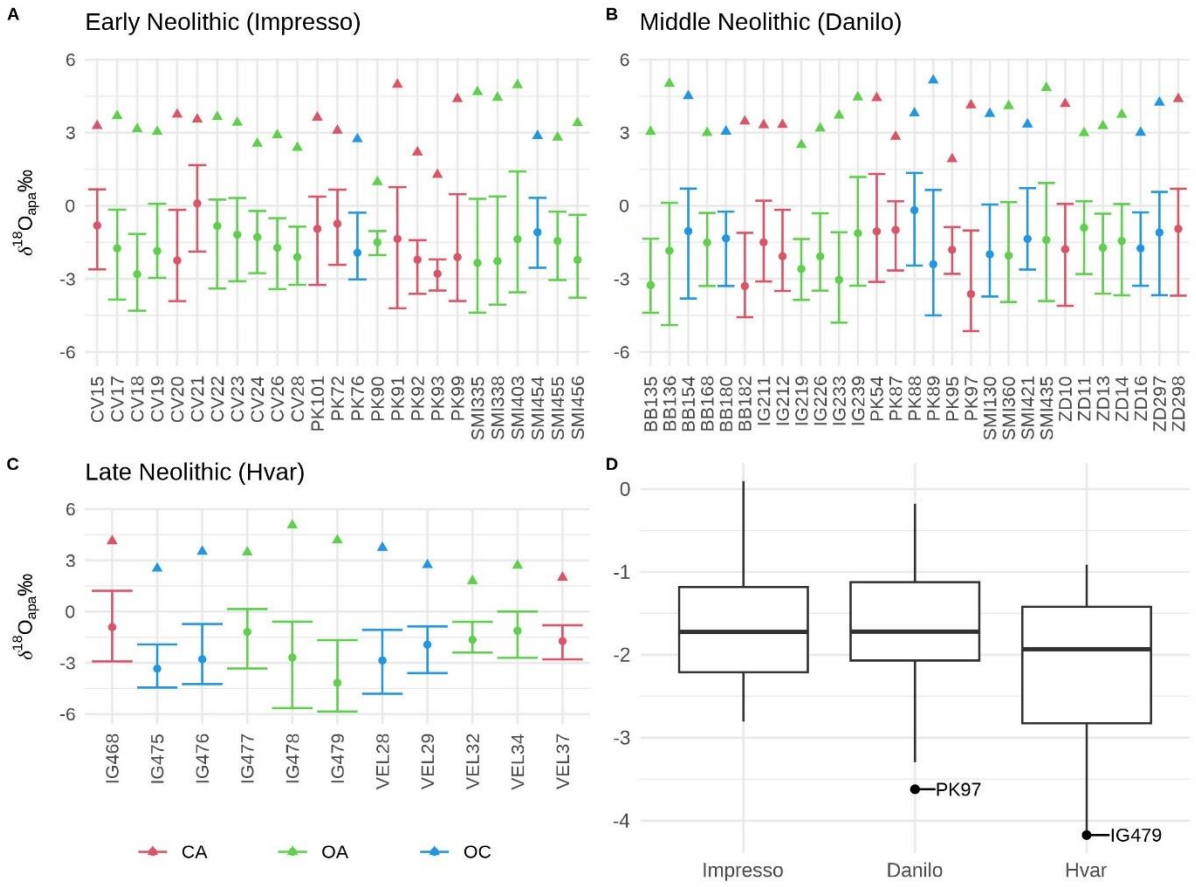

Figure 8.9 Comparison $\delta^{18}O_{apa}$ range (vertical lines), mean (dots), and amplitudes (triangles) for each specimen by period: (A) Early Neolithic – Impresso; (B) Middle Neolithic – Danilo; (C) Late Neolithic – Hvar. (D) Intra-tooth mean $\delta^{18}O_{apa}$ by period. Colors in A-C correspond to goat (CA), sheep (OA), and ovicaprid (OC). Site and sample numbers in Table 8.5.

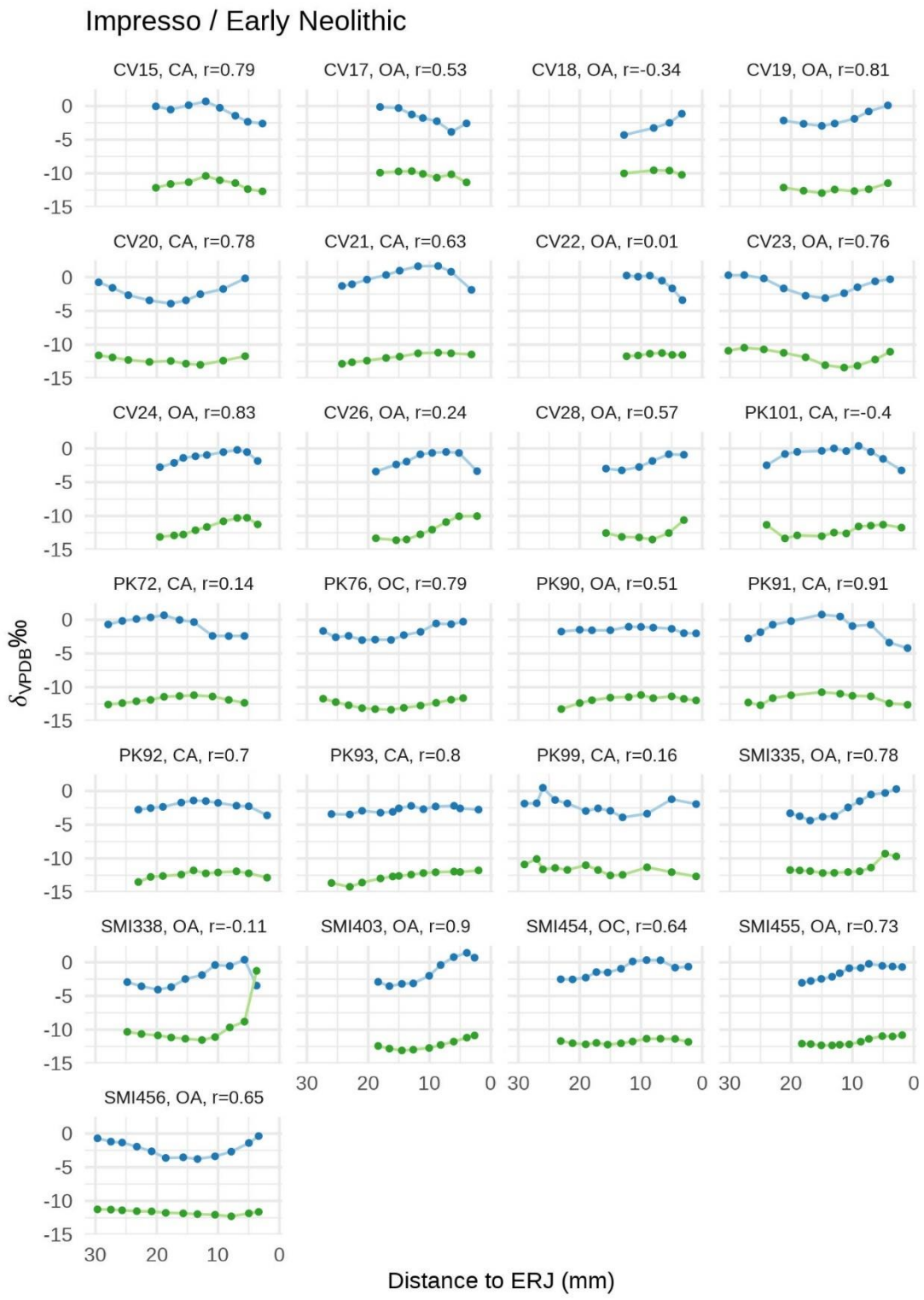

Figure 8.10. Plots of $\delta^{18}O_{apa}$ (blue) and $\delta^{13}C_{apa}$ (green) for Early Neolithic specimens. Plot titles include specimen number, species (goat (CA), sheep (OA), and ovicaprid (OC)), and Pearson's correlation coefficient calculated between $\delta^{13}C_{apa}$ and $\delta^{18}O_{apa}$ values.

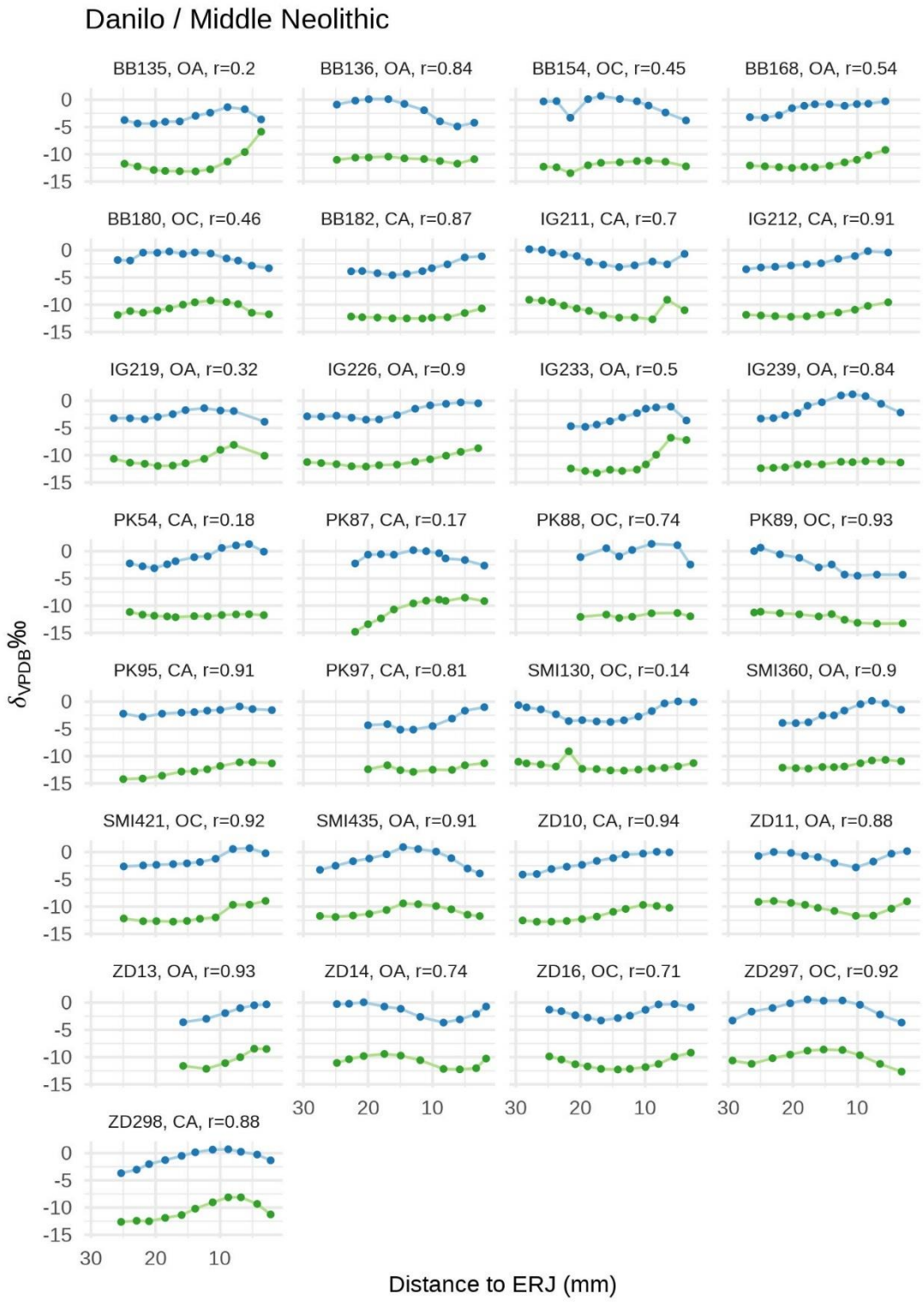

Figure 8.11. Plots of $\delta^{18}O_{apa}$ (blue) and $\delta^{13}C_{apa}$ (green) for Middle Neolithic specimens. Plot titles include specimen number, species (goat (CA), sheep (OA), and ovicaprid (OC)), and Pearson's correlation coefficient calculated between $\delta^{13}C_{apa}$ and $\delta^{18}O_{apa}$ values.

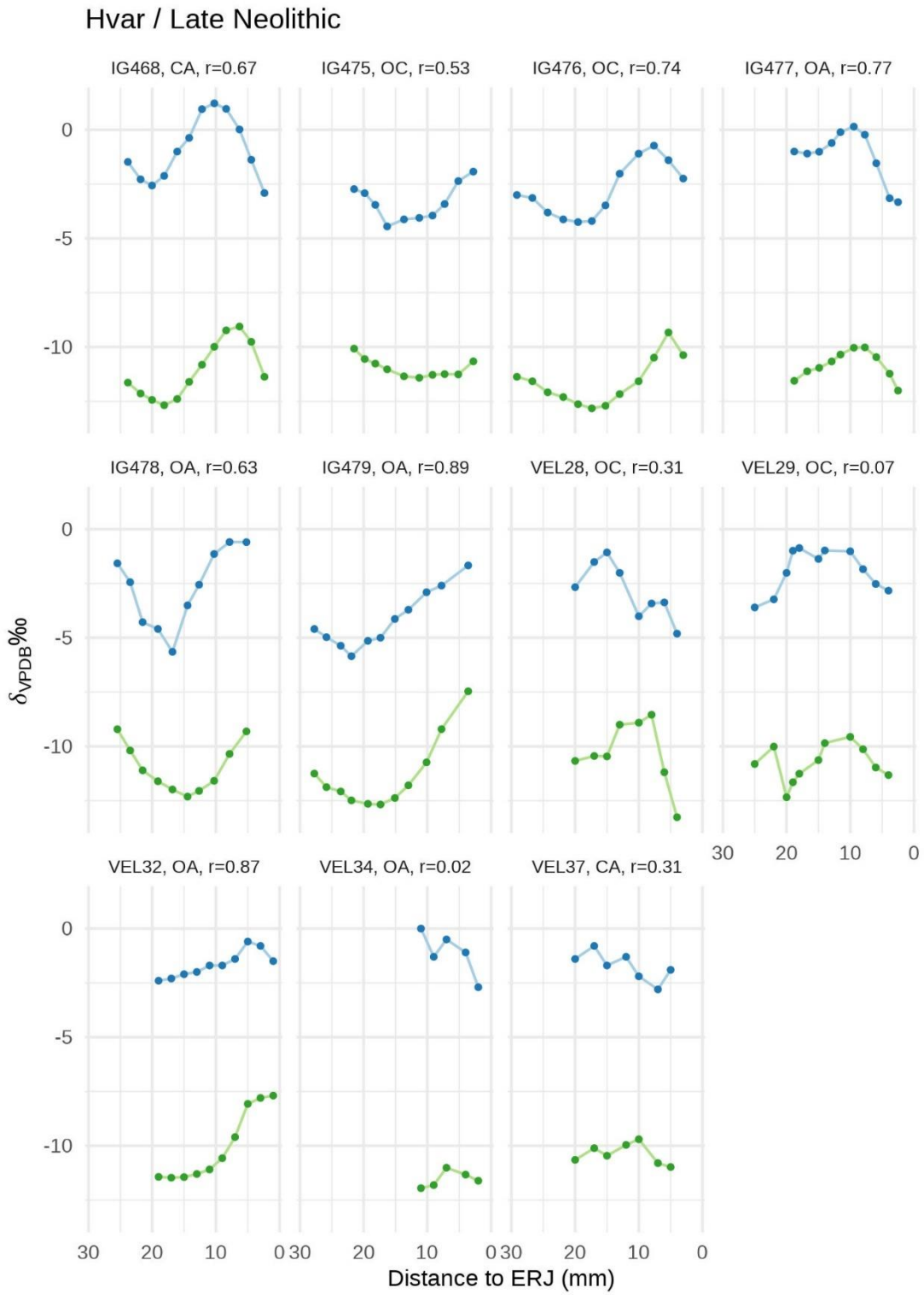

Figure 8.12. Plots of $\delta^{18}O_{apa}$ (blue) and $\delta^{13}C_{apa}$ (green) for Late Neolithic specimens. Plot titles include specimen number, species (goat (CA), sheep (OA), and ovicaprid (OC)), and Pearson's correlation coefficient calculated between $\delta^{13}C_{apa}$ and $\delta^{18}O_{apa}$ values.

3. Reconstructing diet spaces from enamel $\delta^{13}C$ and $\delta^{18}O$ data

The constitution of caprine diet becomes increasingly enriched in ^{13}C over the Neolithic (Figure 8.8; Table 8.7). While no major differences in mean $\delta^{18}O_{apa}$ were detected when comparing specimens by period (Figure 8.9), grouping the data this way obscures inter-site and inter-individual variation. Figure 8.13 illustrates the dietary space of sheep and goats as convex hull polygons that encompass the amplitude and mid-range of $\delta^{13}C_{apa}$ of specimens from the same site and period. Larger polygons reflect greater diversity in plant types consumed by the herd. Lower carbon isotope profile amplitudes reflect the homogenized $\delta^{13}C$ values of a variety of plants whereas high amplitude profiles are a product of seasonal variation of a more restricted range of plant types. Reduced variation in $\delta^{13}C_{apa}$ mid-ranges, producing smaller polygons, would be expected to result from lower variation in the types of grazing habitats herders exploited. The convex hulls in Figure 8.14 encompass the variation of amplitude and mid-range $\delta^{18}O_{apa}$. Larger polygons are formed by the presence of individuals with both high and low amplitude $\delta^{18}O_{apa}$ profiles, resulting from higher and lower degrees of mobility, respectively. Smaller polygons reflect reduced variation in terms of the spatial range of grazing areas exploited by herders. Inter-individual variation in mean $\delta^{13}C_{apa}$ and $\delta^{18}O_{apa}$ is illustrated for each site as box plots in Figure 8.15.

The limited intra-tooth $\delta^{13}C_{apa}$ range among Early Neolithic specimens relative to later periods (Figure 8.8) echoes the overlapping diet spaces inferred by $\delta^{13}C_{apa}$ amplitudes and mid-ranges of specimens from the three Impresso sites (Figure 8.13). Mean $\delta^{13}C_{apa}$ is also broadly consistent between Impresso sites although reduced inter-individual variation is shown among specimens from Early Neolithic Smilčić (Figure 8.15A). Similar degrees of inter-individual variation in mean $\delta^{18}O_{apa}$ are also observed between the Impresso period sites

(Figure 8.15B). Most Impresso specimens exhibit covariation between their $\delta^{13}C_{apa}$ and $\delta^{18}O_{apa}$ sequences suggesting husbandry activities were generally carried out close to the settlement. This interpretation applies to specimens from Crno Vrilo and Smilčić but to a lesser extent Pokrovnik. Low amplitude oxygen isotope profiles observed among specimens from Pokrovnik (i.e., PK90, PK92, and PK93) has the effect of enlarging the convex hull polygon shown in Figure 8.14. Dampened intra-tooth $\delta^{18}O_{apa}$ variation could result from vertical transhumance (Britton et al. 2009; Pellegrini et al. 2008) or residence near a buffered water source (Henton 2012; Henton et al. 2014), both of which imply the exploitation of potentially non-local environments (see Chapter Nine).

By comparison, considerable inter-site variation in how sheep and goat diet was managed is evident from the Danilo specimens. For example, the dietary space of herds at Zemunik Donji and at Danilo Smilčić appears to have been more restricted considering the tight distribution of $\delta^{13}C_{apa}$ and $\delta^{18}O_{apa}$ amplitudes and mid-ranges of specimens from these two sites (Figure 8.13 and Figure 8.14). Strong covariation between seasonally fluctuating carbon and oxygen isotope ratios has been shown for all Zemunik Donji specimens and most individuals from Smilčić which most likely indicates herds were kept close to the settlement. In comparison, a wider variety of plants is implied by the distribution of $\delta^{13}C_{apa}$ amplitudes and mid-ranges of specimens from Benkovac-Barice and Islam Grčki, which encompass specimens from both Zemunik Donji and Smilčić (Figure 8.13).

At Pokrovnik, Danilo-period herders engaged in a form of husbandry that can be clearly distinguished from herding practices at contemporary sites. Caprine diet at Pokrovnik was ^{13}C-depleted relative to herds at other Danilo period sites (Figure 8.15A), signaling a distinct dietary space (Figure 8.13). The exploitation of non-local environments by

Pokrovnik herders is implied by the distribution of $\delta^{18}O_{apa}$ amplitudes and mid-ranges, which nearly encompasses all other Middle Neolithic sites (Figure 8.14). Furthermore, inter-individual variation in mean $\delta^{18}O_{apa}$ is far greater among Danilo Pokrovnik specimens than what is seen at other sites (Figure 8.15B).

The intra-tooth sequences for the Pokrovnik specimens show considerable variety in how animals were managed during both the Early and Middle Neolithic relative to contemporary villages. For example, two specimens each from Impresso (PK76, PK91) and Danilo (PK89, PK97) contexts were found to have $\delta^{18}O_{apa}$ sequences recording a seasonal signal and covariation with $\delta^{13}C_{apa}$ with significant positive correlation. Most specimens sampled from Pokrovnik were identified as goat (Impresso: n=7; Danilo: n=4). Intra-tooth variation in these specimens may reflect the extreme dietary flexibility of goats relative to sheep (Leppard and Birch 2016).

Inter-individual differences in the $\delta^{13}C_{apa}$ and $\delta^{18}O_{apa}$ sequences are less pronounced among the Late Neolithic specimens from Islam Grčki compared to specimens from Velištak (Figure 8.12). Apart from VEL32, none of the Velištak specimens exhibit a strong positive correlation between intra-tooth carbon and oxygen isotope ratios and present lower intra-tooth $\delta^{18}O_{apa}$ amplitudes and mid-ranges (Figure 8.14) compared to Islam Grčki. This pattern supports a more mobile form of husbandry by Velištak herders.

Comparing the results of Danilo and Hvar specimens from Islam Grčki indicates roughly similar caprine management styles through time. Intra-individual differences can be seen among the Danilo period specimens suggesting human intervention in the diet of some individuals. IG239 for example has the smallest amplitude of $\delta^{13}C_{apa}$ variation but the highest $\delta^{18}O_{apa}$ amplitude relative to the other specimens from this site which may be related to a diet

with a substantial fodder component. Inverse trends in intra-tooth oxygen and carbon isotope ratios are also observed in IG211, IG219, and IG233 at loci representing more recently formed enamel (Figure 8.11) suggesting some change in diet or grazing environment occurred in the months leading up to the slaughter of these individuals. By comparison, positive correlations between carbon and oxygen isotope ratios are shown for all Hvar period specimens from Islam Grčki (Table 8.5) and a seasonal signal is shown in both $\delta^{18}O_{apa}$ and $\delta^{13}C_{apa}$ profiles. While inter-individual variation points to greater mobility of herds from Velištak, Late Neolithic Islam Grčki herders appear to have managed flocks intensively. Overall, however, husbandry at Islam Grčki appears to be relatively stable from Danilo to Hvar period, despite differences in herd culling strategies (see Chapter Five). In summary, herding in the Late Neolithic appears to have been largely intensive at Islam Grčki and potentially extensive at Velištak.

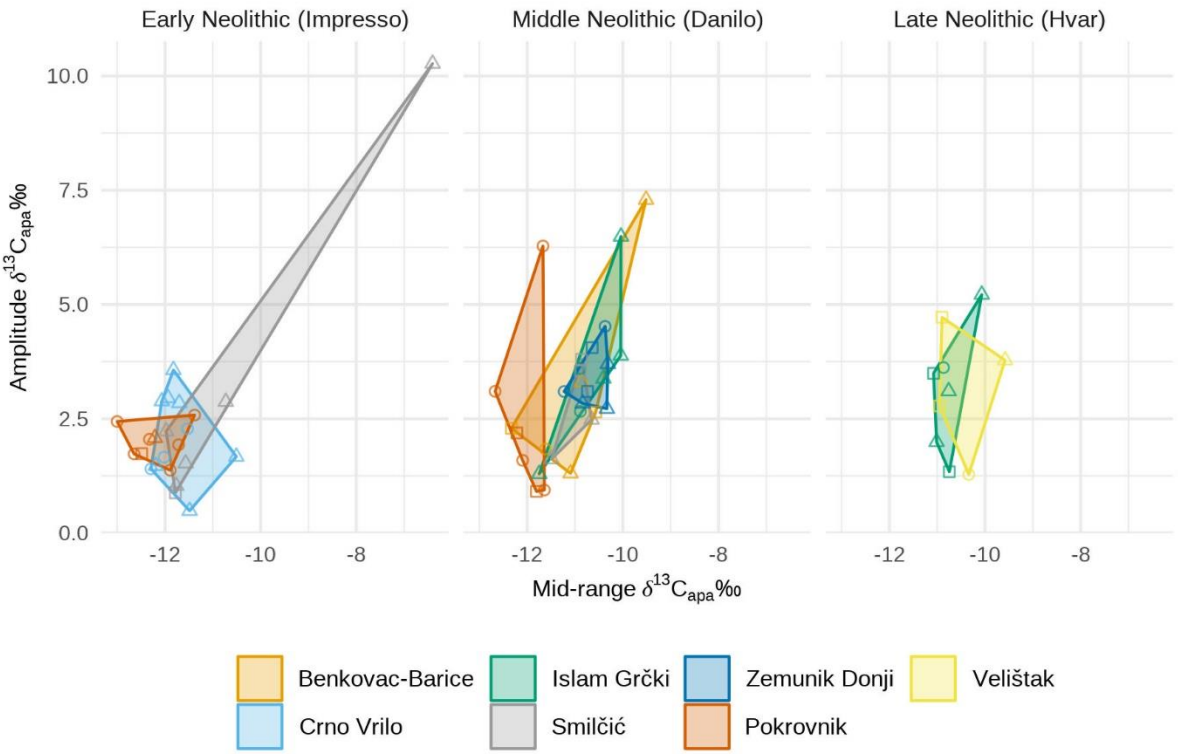

Figure 8.13. Dietary space of caprines represented by convex hull polygons encompassing the amplitude and mid-range of $\delta^{13}C_{apa}$ of groups of specimens from the same site for the Early (Impresso), Middle (Danilo), and Late Neolithic (Hvar). Larger polygons indicate greater diversity in overall herd diet. Circles, triangles, and squares symbolize goats, sheep, and ovicaprids, respectively. Data omits specimens with less than six intra-tooth samples.

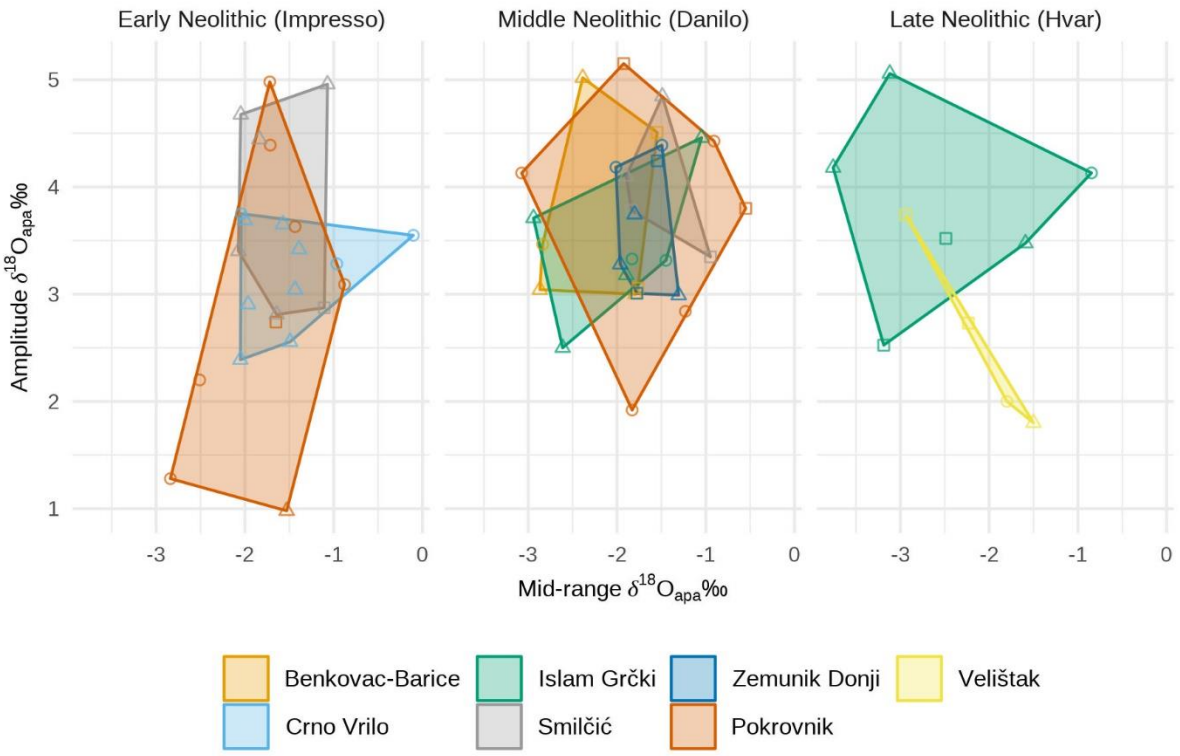

Figure 8.14. Environmental range of caprines represented by convex hull polygons encompassing the amplitude and mid-range of $\delta^{18}O_{apa}$ of groups of specimens from the same site for the Early (Impresso), Middle (Danilo), and Late Neolithic (Hvar). Larger polygons indicate higher mobility. Circles, triangles, and squares symbolize goats, sheep, and ovicaprids, respectively. Data omits specimens with less than 6 intra-tooth samples.

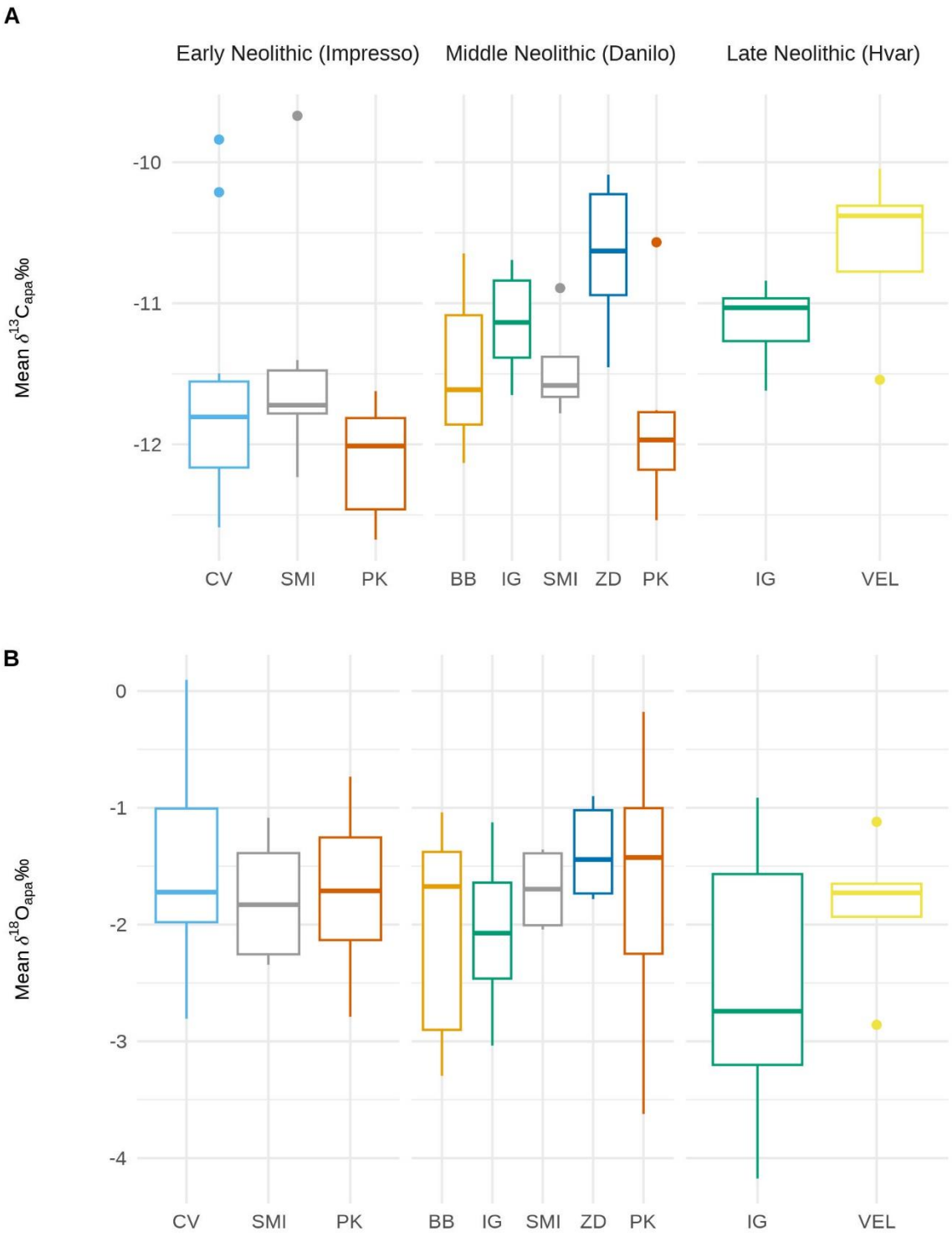

Figure 8.15. Box plots showing inter-individual variation in (A) mean $\delta^{13}C_{apa}$ and (B) mean $\delta^{18}O_{apa}$ by site for Early (Impresso), Middle (Danilo) and Late Neolithic (Hvar) specimens. Site abbreviations on x-axis: CV = Crno Vrilo; SMI = Smilčić; PK = Pokrovnik; BB = Benkovac-Barice; IG = Islam Grčki; ZD = Zemunik Donji; VEL = Velištak.

D. Implications of Stable Isotope Data for Livestock Diet Reconstruction

The bone collagen and enamel bioapatite stable isotope data presented in this chapter provide compelling insights into how herders managed livestock diet during the Neolithic in Dalmatia. First, based on the results of stable isotope analysis of bone collagen, sheep and goat diet were statistically indistinguishable during both the Impresso (Early Neolithic) and Danilo (Middle Neolithic) phases. Furthermore, during the Early and Middle Neolithic, goats intra-tooth mean $\delta^{13}C_{apa}$ values were similar to sheep. This is somewhat unsurprising as it was expected that sheep and goats were herded together, as mixed herds during both the Impresso and Danilo periods of the Neolithic in Dalmatia. Second, neither Early nor Middle Neolithic caprine diet can be distinguished from cattle diet. Together, these first two points indicate that for the first half of the Neolithic (c. 8000-7000 cal. BP) herders did not treat caprines different from cattle in terms of what these animals ultimately ate.

The third insight is that significant dietary changes in both cattle and caprines are evident from the Impresso to the Danilo period based on comparison of $\delta^{13}C$ and $\delta^{15}N$ values of bone collagen. Impresso cattle diet was significantly depleted in ^{13}C and slightly more enriched in ^{15}N relative to the diet of Danilo period cattle in Northern Dalmatia. Additionally, the comparisons of domestic and wild large-bodied herbivores revealed that Impresso cattle shared a diet space with roe deer and consumed vegetation more enriched in ^{15}N than red deer (Figure 8.6B). In the Middle Neolithic, Danilo herders managed cattle diet differently than how Impresso herders did, such that consumed vegetation that was more enriched in ^{13}C than both roe and red deer, while the degree of ^{15}N-enrichment remained higher than red deer diet (Figure 8.6C and Figure 8.6D).

Furthermore, Impresso period caprines, and especially goats, consumed a diet that led

to significantly higher $\delta^{15}N$ values relative to Danilo period caprines while the $\delta^{13}C$ values of bone collagen remained unchanged (Figure 8.4). However, a change in the enrichment of sheep and goat diet in ^{13}C was detected in enamel bioapatite as significantly higher intra-tooth $\delta^{13}C_{apa}$ mean, amplitude, and maximum values among the Danilo caprines over the Impresso specimens (Table 8.7). The higher amplitudes of $\delta^{13}C_{apa}$ variation shown for Danilo sheep and goats effectively reflects the consumption of plants with a wider range of $\delta^{13}C$ relative to the diet of Impresso phase animals. This may indicate that Danilo herders diversified the browsing and grazing resources used to feed their sheep and goats.

Moreover, higher mean and maximum $\delta^{13}C_{apa}$ points to a diet that was generally more ^{13}C-enriched relative to Impresso sheep and goat diet. Since the amplitude of $\delta^{13}C_{apa}$ variation reflects the variety of plants an individual consumed within a single year, higher amplitudes shown for Danilo specimens could be the result of a herding strategy that entailed greater mobility. If herds were more mobile, they might have consumed fewer quantities of fodder grown locally in manure-improved soils. Reduced mobility, on the other hand might result in higher $\delta^{15}N$ values in bone collagen, particularly if animals were contributing manure to fields on which they were penned. Indeed, Impresso caprine diet was significantly more enriched in ^{15}N than wild cervids, suggesting consumption of vegetation grown in soils improved with manure. During this time, caprine diet was similar to wild cervids in terms of ^{13}C enrichment, indicating Impresso herders grazed their animals in—or collected fodder from—roe and red deer habitats. In the Middle Neolithic, sheep and goat diet was less ^{15}N-enriched and became more like that of wild roe deer in terms of both ^{13}C and ^{15}N. While cattle diet moves out of the dietary space of roe and red deer from the Impresso to the Danilo periods, sheep and goat diet appears to do the opposite.

While not statistically significant, caprine diet is generally more enriched in ^{15}N relative to both Impresso and Danilo cattle diet. The number of cattle raised by individual households was much smaller than the number of sheep and goats kept in coastal areas during the Neolithic (Orton et al 2016). Impresso and Danilo faunal assemblages in Dalmatia are dominated by sheep and goat bones, while cattle occur in much smaller proportions (McClure and Podrug 2016). High stocking density and manuring has been found to increase $\delta^{15}N$ values of plant, soil, and livestock tissues (Bogaard et al. 2007; Kriszan et al. 2014; Schwertl et al. 2005; Szpak 2014). One possible explanation for the higher mean $\delta^{15}N$ in sheep and goats could be related to higher stocking density compared to cattle, which require more space, food, and water. Keeping only a few cattle would make sense if grazing or fodder resources needed to also be allocated to relatively larger herds of sheep and goats.

The fourth insight is that strategies varied from one Impresso period community to the next. Based on comparisons of stable isotope values of caprine bone collagen from three Early Neolithic period sites (i.e., Crno Vrilo, Pokrovnik, and Zemunica Cave), at least three distinct husbandry strategies were in use by farmers living contemporaneously. Recent work using ZooMS has demonstrated that sheep constituted the majority of caprine herds at Crno Vrilo and Tinj, while birth seasonality and culling strategies appear to be fairly consistent between the two Early Neolithic sites in Dalmatia (Sierra et al. 2023). The bone collagen stable isotope data presented here suggest that Crno Vrilo, Pokrovnik, and Zemunica Cave practiced distinct husbandry approaches. At Crno Vrilo, sheep and goats were likely grazing in cultivated areas and/or provisioned with fodder grown in soils improved by manure and grazed in ^{13}C-depleted habitats such as forests or were routinely provisioned with collected forest vegetation. Pokrovnik sheep and goats were also provided with ^{15}N-rich plants but

higher $\delta^{13}C$ relative to the Crno Vrilo caprine specimens suggests Pokrovnik herders may have exploited increasingly open habitats. The data from Zemunica Cave shows more positive $\delta^{13}C$ values and more negative $\delta^{15}N$ values among sheep and goats relative to samples representing the open-air sites at Crno Vrilo and Pokrovnik. This suggests Zemunica Cave herders potentially exploited non-forested areas, perhaps as part of a more mobile strategy which resulted in sheep and goats consuming plants relatively enriched in ^{13}C and on plants that were not grown in nitrogen-rich soils. Moreover, this would be consistent with the observations made above, that higher $\delta^{13}C_{apa}$ in the Danilo period could be a result of sheep and goat herders exploiting increasingly open habitats.

While the collagen data provide a view of animal diet over multiple years, the enamel bioapatite data shed light on herder decisions that impacted livestock diet in the near-term. For example, most intra-tooth $\delta^{18}O_{apa}$ sequences exhibit a full or partial signal of seasonal variation in meteoric water $\delta^{18}O$ for which covariation with $\delta^{13}C_{apa}$ sequences is significant. With few exceptions, fluctuating intra-tooth $\delta^{18}O_{apa}$ values of individuals in this group coincide with variation of $\delta^{13}C_{apa}$ (i.e., increasing and decreasing $\delta^{18}O_{apa}$ corresponds to increasing and decreasing $\delta^{13}C_{apa}$). This relationship is best explained by a diet in which body water was primarily obtained via leaf water in C_3 plants whose ^{13}C-enrichment fluctuated in step with seasonal variation in meteoric water $\delta^{18}O$. Individuals exhibiting a high degree of synchronization in seasonally fluctuating $\delta^{13}C_{apa}$ and $\delta^{18}O_{apa}$ values were likely grazing on naturally occurring flora within a restricted geographic range and possibly foddered with byproducts of in-season crops (Chase et al. 2014; Knockaert et al. 2018). Based on these observations, sheep and goat management was largely focused nearby settlements and herders maximized the availability of natural pastures whenever possible.

Disruptions to expected seasonal signals in either or both oxygen and carbon isotope profiles likely reflect herder decisions that impacted the isotopic composition of grazing and browsing resources and sources of ingested water. For example, multiple specimens exhibit seasonal $\delta^{18}O_{apa}$ signatures that covary with $\delta^{13}C_{apa}$ sequences but with moderate or weak correlation caused by dampened, irregular, or non-seasonal $\delta^{18}O_{apa}$ or $\delta^{13}C_{apa}$ sequences. Other individuals show aberrant values in otherwise seasonal sequences or exhibit very irregular intra-tooth variation in the isotopic composition of the enamel bioapatite. Special attention must be paid to these specimens whose intra-tooth $\delta^{18}O_{apa}$ and $\delta^{13}C_{apa}$ sequences deviate from expected seasonal variation. Such examples offer compelling insight into how risk was mitigated either through use of alternative local or non-local grazing and browsing resources or strategic provisioning of fodder crops.

Five specimens exhibit sharp increases in $\delta^{13}C_{apa}$ where $\delta^{18}O_{apa}$ is low (Impresso: SMI338; Danilo: BB135, IG211, IG233, and SMI130; Figure 8.10 and Figure 8.11). In C_3 plants $\delta^{13}C$ increases with temperature and aridity (Kohn 2010; Stewart et al. 1995) but in these specimens, sections of enamel bioapatite with high $\delta^{13}C_{apa}$ have low $\delta^{18}O_{apa}$ values. Low $\delta^{18}O_{apa}$ typically reflects the ingestion of ^{18}O-depleted water associated with low precipitation $\delta^{18}O$ in cold temperatures (Gat 1980; 1996). Therefore, the elevated $\delta^{13}C_{apa}$ values reflect plants that these animals consumed during colder months.

However, in seasonal environments $\delta^{13}C$ is the highest at the end of summer while minimum $\delta^{13}C$ values are observed at the end of winter in C_3 plants (Smedley et al. 1991). An explanation for this recurrent pattern in these five specimens is that herders collected or cultivated fodder during the growing season to feed animals in colder months. This practice could disrupt the signal of seasonal variation in $\delta^{13}C$ in plants resulting in more positive

winter $\delta^{13}C$ values (Berthon et al. 2018). The collection of leafy vegetation from forests to provision livestock over the winter is a known strategy used by herders in Europe (Gillis et al. 2013; Halstead 1998a; Halstead et al. 1998; Rasmussen 1989). In these specimens, $\delta^{13}C_{apa}$ values range from -9.1 to -1.3‰ where $\delta^{18}O_{apa}$ is low. Accounting for the 14‰ enrichment factor from diet to enamel bioapatite (Cerling and Harris 1999), the winter diet of these individuals consisted of plants whose $\delta^{13}C$ values ranged from -23.1 to -15.3‰. This range is above the -31.5‰ threshold suggested for discriminating understory forest vegetation from plants growing in open environments (Kohn 2010). It is therefore likely that in the winter, these individuals were provisioned with plants grown in open environments, such as leafy or grassy hay that was collected during warmer months. The collection of hay during the summer for overwintering was also proposed to explain similar disruptions to seasonal variation of intra-tooth $\delta^{13}C_{apa}$ observed in Bronze Age caprines in the Pyrenees (Knockaert et al. 2018). In recent history Plikáti herders preferentially harvested leaf-fodder from beech and deciduous oak trees during the summer to over-winter sheep and goats because the leaves of these species are more durable and store better than other species (Halstead 1998a). This practice likely explains the out-of-season spikes in $\delta^{13}C_{apa}$ shown in these specimens.

For some of these specimens (SMI338, BB135, and IG233) the disrupted seasonal $\delta^{13}C_{apa}$ signal is characterized by maximum $\delta^{13}C_{apa}$ values that exceed the range expected from a purely C_3 diet (Figure 8.8). These elevated $\delta^{13}C_{apa}$ values are most likely the result of consuming substantial quantities of C_4 plants, which are more ^{13}C-enriched than C_3 plants. Native C_4 plants comprise less than 1% of vascular plants found in the Eastern Adriatic region including Dalmatia (Collins and Jones 1985). Evidence for the cultivation of millet (*Panicum miliaceum*), a C_4 crop typically sowed in the spring and harvested in the summer,

is rare but has been suggested for Danilo period contexts at Pokrovnik (Moore et al. 2019; 2007a). However, the results presented here provide compelling indirect evidence for the use of C_4 plants as fodder. Two Impresso period specimens from Smilčić (SMI335 and SMI338) and multiple Danilo and Hvar period specimens exhibit maximum $\delta^{13}C_{apa}$ values beyond the upper range of most C_3 plants (Figure 8.8). The possibility that millet was used as fodder during the Neolithic, as suggested by these data is potentially significant considering the limited available archaeobotanical evidence of the cultivation of this crop prior to the Bronze Age in this part of the world (Reed 2017). Future work employing Bayesian mixing models may be able to resolve what proportion of the diet, if any, was comprised of C_4 plants (Makarewicz and Pederzani 2017).

While $\delta^{13}C$ varies on a seasonal basis in C_3 plants (Smedley et al. 1991), the appearance of aberrant $\delta^{13}C_{apa}$ values within an otherwise seasonal sequence may signal a substantial change in diet. A simultaneous decrease in $\delta^{13}C_{apa}$ and $\delta^{18}O_{apa}$ is observed close to the tooth crown of specimen BB154 (Figure 8.11). This pattern may be explained by a change from an open to a closed grazing environment. Lower temperatures and reduced exposure to sunlight due to canopy cover in forests may lead to lower rates of evapotranspiration and result in relatively depleted isotopic compositions of leaf water (Flanagan and Ehleringer 1991). A similar disruption in the carbon and oxygen isotope ratios is also seen in IG219 but as this event occurs close to the ERJ, the trajectory of the signal is unclear so the above interpretation must be applied with caution.

Among the six individuals with flattened intra-tooth $\delta^{13}C_{apa}$ sequences identified based on low amplitude signals, only SMI454, SMI456 (Figure 8.10), and PK54 (Figure 8.11) preserve a seasonal signal in their corresponding $\delta^{18}O_{apa}$ sequences. A similar

dampening effect, due to a diet consisting of both natural graze and fodder is shown in modern specimen VRL481 (See Chapter Nine, Figure 9.4), whose intra-tooth $\delta^{13}C_{apa}$ amplitude was 0.6‰. Individuals SMI335 and SMI338 also exhibit flattened $\delta^{13}C_{apa}$ sequences corresponding to low $\delta^{18}O_{apa}$ which indicates the consumption of a mixed diet during the winter (Figure 8.10).

Foddering can obscure covariance of carbon and oxygen isotope ratios in enamel bioapatite (Dufour et al. 2014; Makarewicz and Pederzani 2017) because mixing different sources of fodder may reduce the range of intra-tooth $\delta^{13}C_{apa}$ (Chase et al. 2014; Zazzo et al. 2010). The foddering strategies described for modern Plikáti sheep and goat herders in northwest Greece (Halstead 1998a; Halstead et al. 1998) and in Sweden during the 19th century (Slotte 2001) entail the collection of grassy hay during the summer and leafy hay during the autumn that is either consumed immediately or reserved for over-wintering. Leafy branches of various drought-resistant tree species typical for sub-montane environments (e.g., *Fagus*, *Abies alba*) as well as deciduous oak species (e.g., *Quercus sp.*) that grow at lower altitudes used by the Plikáti (Halstead et al. 1998) were not only present during the Neolithic (Horvat et al. 1974), they continue to be a major component of modern sheep and goat diet in Dalmatia today (Rogosic et al. 2006). Overwintering with shrubby vegetation collected during the summer may explain why sections of the $\delta^{13}C_{apa}$ sequences corresponding to winter signals are dampened in several of the Impresso period Smilčić specimens (i.e., SMI335, SMI338, SMI454, and SMI456). Meanwhile, foddering more regularly throughout the year may explain low-amplitude carbon isotope profiles paired with seasonal oxygen sequences in other specimens (e.g., PK72, PK54, PK88, IG475, and IG477).

The Benkovac-Barice specimens also demonstrate diversity in how intensive

husbandry was employed by Danilo herders. Covariance and significant positive correlation between the carbon and oxygen isotope values and a clear seasonal signal in the $\delta^{18}O_{apa}$ profile is shown only for BB136 and BB182 (Table 8.5; Figure 8.11). BB154 exhibits an aberrant decrease in both $\delta^{18}O$ and $\delta^{13}C$ in the early section of the sequence, just before the peak $\delta^{18}O_{apa}$ value is reached, corresponding to the warmest period of the annual cycle. While a swift vertical change in grazing area could account for the abrupt decrease in $\delta^{18}O_{apa}$, this seems unlikely as a corresponding but lower magnitude increase in $\delta^{13}C_{apa}$ of would be expected as plants become more ^{13}C-enriched with increasing altitude (Körner et al. 1988). It is more likely that the oxygen and carbon patterns shown for BB154 resulted from ingestion of water from some type of buffered source (e.g., stream or spring) and the consumption of ^{13}C-depleted vegetation such as understory forest plants.

The case for the collection of fodder from forest environments by herders at Benkovac-Barice is strengthened when the data from BB135, BB168, and BB180 are considered. In each case an inverse relationship between changes in $\delta^{18}O_{apa}$ and changes in $\delta^{13}C_{apa}$ can be seen. This inverse relationship, most clearly seen for BB135 suggests a diet depleted in ^{13}C was consumed during a point in the annual cycle when temperatures began to rise and increasing $\delta^{13}C_{apa}$ corresponds with peak $\delta^{18}O_{apa}$. The patterning is consistent with a diet supplemented by forest vegetation depleted in ^{13}C. However, wet conditions can also result in more negative $\delta^{13}C$ values in C_3 plants, while the reverse has been shown for arid conditions (Kohn 2010; Smedley et al. 1991; Stewart et al. 1995). Precipitation depleted in ^{18}O may be expected due to rainout processes and the amount effect (Gat 1981b). In Dalmatia, a pluvial period from 7600 to 6900 cal. BP (Ilijanić et al. 2018) may have created wetter conditions at various points during the later Early though Middle Neolithic. It is

therefore possible that dampened environmental signals in $\delta^{18}O_{apa}$ and weak correlation with $\delta^{13}C_{apa}$ is a product of wetter climate while the management of these animals was intensive in nature (i.e., restricted grazing and minimal fodder), resembling the management of herds represented by BB136 and BB182.

E. Summary of Evidence Pertaining to Neolithic Livestock Diet

The above discussion can be distilled into six main points. First, similar $\delta^{13}C$ and $\delta^{15}N$ values for sheep and goat suggest these species were managed together as mixed herds by Impresso and Danilo herders. However, during the Danilo period the mid-range of intra-tooth $\delta^{13}C_{apa}$ of sheep is significantly higher than that of goats. This likely reflects differences in the feeding behaviors of sheep and goats. Sheep consume higher amounts of grasses growing in exposed areas while the more flexible browsing behaviors of goats (Leppard and Birch 2016) may result in greater contributions of understory vegetation characterized by low $\delta^{13}C$ values due to the canopy effect (van der Merwe and Medina 1991).

Second, caprine diet approximates that of cattle within the Impresso and Danilo periods of the Neolithic but is slightly more enriched in ^{15}N than cattle for both periods. Stocking higher densities of sheep and goats than cattle could lead to the enrichment in ^{15}N of plants and elevate caprine bone collagen $\delta^{15}N$ values if cattle were let free to graze in less intensively cultivated fields or open pastures (Kriszan et al. 2014; Szpak 2014).

Third, lower $\delta^{13}C$ values for Impresso cattle relative to Danilo cattle were obtained from bone collagen samples. The ^{13}C-depleted diet for Impresso period cattle may be the result of consuming understory vegetation. During the Danilo period cattle diet moves outside of wild roe deer diet space, perhaps involving grazing in more open environments

where vegetation is more enriched in ^{13}C.

Fourth, Impresso sheep and goat diet was more ^{15}N-enriched than in the Danilo period. Although no difference in $\delta^{13}C$ was shown for bone collagen, mean intra-tooth $\delta^{13}C_{apa}$ is significantly higher for Danilo sheep and goats, and specimens exhibit higher amplitudes of variation and maximum values. Additionally, there is greater inter-individual variability of $\delta^{13}C_{apa}$ among Danilo period specimens and this trend continues into the Hvar period. Overall, these patterns suggest greater herding mobility in the Danilo and Hvar periods than the Impresso period.

Fifth, inter-site variation in caprine bone collagen $\delta^{13}C$ and $\delta^{15}N$ values between Impresso Crno Vrilo, Pokrovnik, and Zemunica Cave suggests alternative herding strategies. Specifically, high $\delta^{15}N$ values of Crno Vrilo samples suggests herders supplemented sheep and goat diet with fodder crops grown in manure-improved soils while the low $\delta^{13}C$ values suggest consumption of vegetation potentially obtained from closed habitats. In comparison, Zemunica Cave samples had the lowest $\delta^{15}N$ values of the three sites suggesting fodder crops—if at all provisioned—were not likely grown in manured soils. Zemunica Cave samples also exhibited similar $\delta^{13}C$ values to the Pokrovnik group which were also significantly higher than the Crno Vrilo specimens. It is therefore reasonable to conclude that Zemunica Cave and Pokrovnik herders exploited browsing/grazing habitats that were more open while Crno Vrilo herders frequented forested areas with their herds or collected vegetation from these areas for use as fodder. Furthermore, Pokrovnik caprine diet was significantly less enriched in ^{15}N than Crno Vrilo which may be explained by consumption of fodder grown in or collected from unimproved soils and possibly lower stocking densities.

The differences between domesticated caprine diet at Pokrovnik and Crno Vrilo

shown in the bone collagen data are less apparent when average intra-tooth $\delta^{13}C_{apa}$ and $\delta^{18}O_{apa}$ are compared. The interpretation that Impresso Pokrovnik herders exploited more open habitats than Crno Vrilo herders based on significantly higher $\delta^{13}C$ values in Pokrovnik bone collagen samples is not reflected in the comparison of mean $\delta^{13}C_{apa}$ (Figure 8.15A). However, the exploitation of different grazing habitats is reinforced by the comparative differences in dietary space reconstructed from the amplitudes of variation and midranges of intra-tooth $\delta^{13}C_{apa}$ and $\delta^{18}O_{apa}$ (Figure 8.13 and Figure 8.14). Specifically, greater mobility is implied by the relatively larger convex hull joining $\delta^{18}O_{apa}$ amplitudes and mid-ranges of Impresso Pokrovnik specimens. Meanwhile, the restricted range of intra-tooth $\delta^{13}C_{apa}$ values for Early Neolithic Pokrovnik specimens likely reflects the consumption of a wider range of plants (Chase et al. 2014; Zazzo et al. 2010). Collectively, these data suggest that Crno Vrilo caprine management was focused close to the settlement and that herds may have been tightly corralled on fields whose soils were subsequently enriched by excrement. Rotating herds between these fields may have enabled Crno Vrilo residents to obtain higher yields of crops for human consumption or specifically for use as fodder while the ^{15}N-enriched stubble remaining after harvest would be a reliable source of grazing.

Finally, intra-tooth stable isotope analysis of enamel bioapatite revealed that by and large, herds were kept close to villages. However, inter-individual variation in diet is observed in the form of attenuation of or discontinuities within the seasonal signal preserved in $\delta^{13}C_{apa}$ and/or $\delta^{18}O_{apa}$ of some specimen's profiles. Explanations for recurrent patterns include the collection of out-of-season fodder for overwintering, abruptly shifting from open to closed-canopy environments, provisioning of C_4 fodder crops (i.e., millet), and movement of herd to areas featuring buffered sources of water. These strategies are interpreted as ways

herders minimized the risk of failing to meet the dietary needs of their animals and were variably employed throughout the Early, Middle, and Late Neolithic.

F. Conclusion

If we are to assume that intensive sheep and goat management entailed high stocking densities and/or grazing on or foddering with crops grown in manured soils, then the initial expectation, that animal husbandry intensified during the Danilo period is not supported by the bone collagen data. But the expectation that intensification of livestock production should be associated with a ^{15}N-enriched diet resulting, in part, from improving crop yields with manure may be misguided. Intensification can entail a combination of strategies. For example, the collection of wild fodder resources for overwintering is evident in the $\delta^{13}C_{apa}$ profiles of multiple Impresso and Danilo period tooth specimens examined. Stockpiling fodder resources for the winter could have been a crucial investment of time if the goal was to minimize the risk of pregnant females miscarrying due to poor quality diet (Halstead 1996; 1998b).

Additionally, the higher mean and amplitudes of $\delta^{13}C_{apa}$ intra-tooth variation in Middle Neolithic specimens suggests that Danilo period herders may have offered herds a broader diversity of plant species, including those found in wild cervid habitats. However, the different trends borne in the caprine bone collagen and enamel bioapatite $\delta^{13}C$ from the Early to Middle Neolithic is remarkable for another reason. Bone remodels continuously over the course of an animal's life so $\delta^{13}C$ values obtained from collagen samples reflect an animal's diet spanning several years or more. Conversely, intra-tooth $\delta^{13}C_{apa}$ values obtained from enamel bioapatite provide much higher temporal resolution of an individual's diet but

insight into herd management is restricted to the 12-18 months of life in sheep and goats. It is therefore possible trends shown by inter-site comparison of caprine bone collagen $\delta^{13}C$ values are not echoed in similar comparisons of intra-tooth $\delta^{13}C_{apa}$ values due to herders employing strategies that result in adults consuming different plants in different habitats than young animals.

Separating herds according to age or sex can enable more effective use of scarce resources by allowing animals with higher caloric needs (e.g., females) to have preferential access to the best pastures or nutrient-rich fodder plants (Halstead 1996: 25). For example, on the Greek island of Amorgos, modern agropastoralists grazed breeding cows, milking goats, and fattening calves on pulses growing *in situ* and collected ripened seeds of barley and oat to fodder working animals (Halstead and Jones 1989: 48). It has also been reported that preventing lambs and kids from grazing prior to slaughter by confining them to pens or caves yields the best rennet use for making cheese (Miracle 2006: 74). Comparable intra-tooth mean $\delta^{13}C_{apa}$ between Impresso period Pokrovnik and Crno Vrilo specimens may therefore reflect similar treatment of young animals with diverging $\delta^{13}C$ and $\delta^{15}N$ bone collagen values arising from distinct management tactics of adult animals.

Higher $\delta^{13}C$ values in bone collagen would be expected for Middle Neolithic specimens if Danilo period herders routinely provided sheep and goats access to vegetation more enriched in ^{13}C than vegetation consumed by Impresso herds. But this is not the case. Instead, the trend of significantly higher mean $\delta^{13}C_{apa}$ shown from the Early to the Middle to the Late Neolithic likely reflects short-term interventions in sheep and goat diet. From this point of view, Danilo period herders may have adopted a unique risk minimization strategy which entailed provisioning young animals with ^{13}C-enriched crops (e.g., millet), or

alternatively moving herds to coastlines to graze on seagrasses. Seagrass $\delta^{13}C$ values range from -23‰ to -3‰ but generally hover around -10‰ (Hemminga and Mateo 1996; Lepoint et al. 2004). Seagrass and seaweed deposited on the shoreline by storm activity in the Adriatic or exposed during low tide could have served as a valuable source of collectible fodder or an important grazing habitat when pasture resources were scarce. This practice has been observed among herders in Iceland, the British Isles, and Brittany (Chapman and Chapman 1980; Hallson 1964; Hansen et al. 2003), and could lead to $\delta^{13}C_{apa}$ values occurring outside and above the range expected from a purely terrestrial diet of C_3 plants (Balasse et al. 2005; 2009; 2019).

The exploitation of a broader array of grazing habitats including more open environments or exploitation of marine environments would be consistent with a strategy of extensively grazing livestock. This approach is better suited to managing large herds than intensive husbandry (Halstead 1996) and is not the only indication that Middle Neolithic subsistence was focused more heavily on livestock breeding. For example, the introduction of dairy fermentation technology as well as culling profiles recreated from zooarchaeological remains point towards an emphasis on milk in the Middle Neolithic (McClure et al. 2018; 2022). However, inter-site comparisons of sheep and goat dietary signatures indicate that extensive herding might not be an exclusively Danilo period strategy. Instead, extensive grazing was likely one of several viable alternative strategies available to Neolithic agriculturalists to meet their subsistence needs. In the next chapter, I explore the question of mobility in greater depth and consider whether vertical transhumance during the Neolithic in Dalmatia is supported by the evidence from stable isotope analysis of enamel bioapatite.

IX. Transhumance

A. Preface

Until as recently as the mid-20th century sheep and goat pastoralism was the backbone of Dalmatia's economy. Each year, communities in Dalmatia organized the movement of their sheep and goat herds to high-quality grassland and sources of water in the Velebit and Dinara mountain ranges (Belaj 2004; Forenbaher 2007; Marković 1975; 1980; 1987; Nimac 1940; Perišić 1940; Vinšćak 1981). Movements from the Ravni Kotari were scheduled to avoid the arid summer conditions that limit water and pasturage in the lowlands (Chapman et al. 1996; Marković 1975; Nimac 1940). Pastures on the coastal face of the Velebit are found above 1,000 m dispersed throughout depressions in the karstic terrain with the best grassland located above 1400 m (Marković 1980; Vinšćak 1981). Dinara pastures are also distributed variably between 1200 and 1400 m (Marković 1987). This type of herding system, in which livestock are moved between upland and lowland pastures on a seasonal basis is termed *vertical transhumance*. Visitation of summer mountain pastures by transhumant herders from Dalmatia dates to the Roman period but archaeological deposits in caves in the Velebit range testify to earlier use of these sites by Bronze and Iron Age herders (Forenbaher 2007).

There is good reason to suspect that Neolithic herders in Dalmatia engaged in vertical

transhumance. Velebit cave use during the Neolithic is demonstrated at several sites including Vaganačka peć (720 masl; Forenbaher and Pavle 1985), Stolačka peć (900 masl; Forenbaher and Vranjican 1990), and Pećina u Pazjanicama (320 masl; Forenbaher and Vranjican 1982) and caves in the Učka mountains such as Pupićina Cave (220 masl; Miracle and Forenbaher 2005) and Vela peć Cave (Forenbaher et al. 2006). Neolithic use of mountain caves for seasonal sheep and goat herding activities such as breeding has been recognized for the Mediterranean (Martín and Tornero 2023), but linking the use of Velebit mountain caves to transhumant pastoralism remains speculative without any direct connections to open-air sites on the Ravni Kotari coastal plain (Forenbaher 2007; 2022). In this chapter, I discuss the results of intra-tooth stable isotope analysis of enamel bioapatite and consider whether vertical transhumance during the Neolithic in Northern Dalmatia is supported by the data.

B. Modeling the Environmental Signals of Vertical Transhumance in the Eastern Adriatic

A detailed explanation of the relationship between meteoric water $\delta^{18}O$, temperature, and altitude is provided in Chapter Seven. To briefly recapitulate, this relationship is highly predictable and can be leveraged to identify seasonal herding practices such as vertical transhumance via stable isotope analysis of $\delta^{18}O$ values of enamel bioapatite (Pederzani and Britton 2019). Precipitation $\delta^{18}O$ varies seasonally largely due to the temperature dependent fractionation of oxygen isotopes in meteoric water (Rozanski et al. 1992). Meteoric water $\delta^{18}O$ is also inversely related to altitude. At lower elevations, precipitation $\delta^{18}O$ tends to be more positive because warmer temperatures enable more water molecules with the heavier oxygen isotopes (^{18}O) to evaporate from water bodies; these heavier water molecules are

preferentially and progressively removed through rain out as cloud masses move away from the coast (i.e., the rainout effect; Gat 1996; Rozanski et al. 1993; Yang et al. 2019; Yurtsever and Gat 1981). As a result of progressive rainout of ^{18}O-enriched water and low air temperatures at higher elevations, precipitation in mountain areas tend to be more depleted in ^{18}O relative to coastal zones which receive ^{18}O-enriched precipitation (Gonfiantini et al. 2001; Poage and Chamberlain 2001; Roller-Lutz et al. 2013). Herding animals during the summer from low to high elevation environments can therefore lead to the incorporation of meteoric water with lower $\delta^{18}O_{ew}$ values (Daniel Bryant et al. 1996b; Daniel Bryant and Froelich 1995; Fricke and O'Neil 1996; Kohn et al. 1996; 1998) into skeletal tissues.

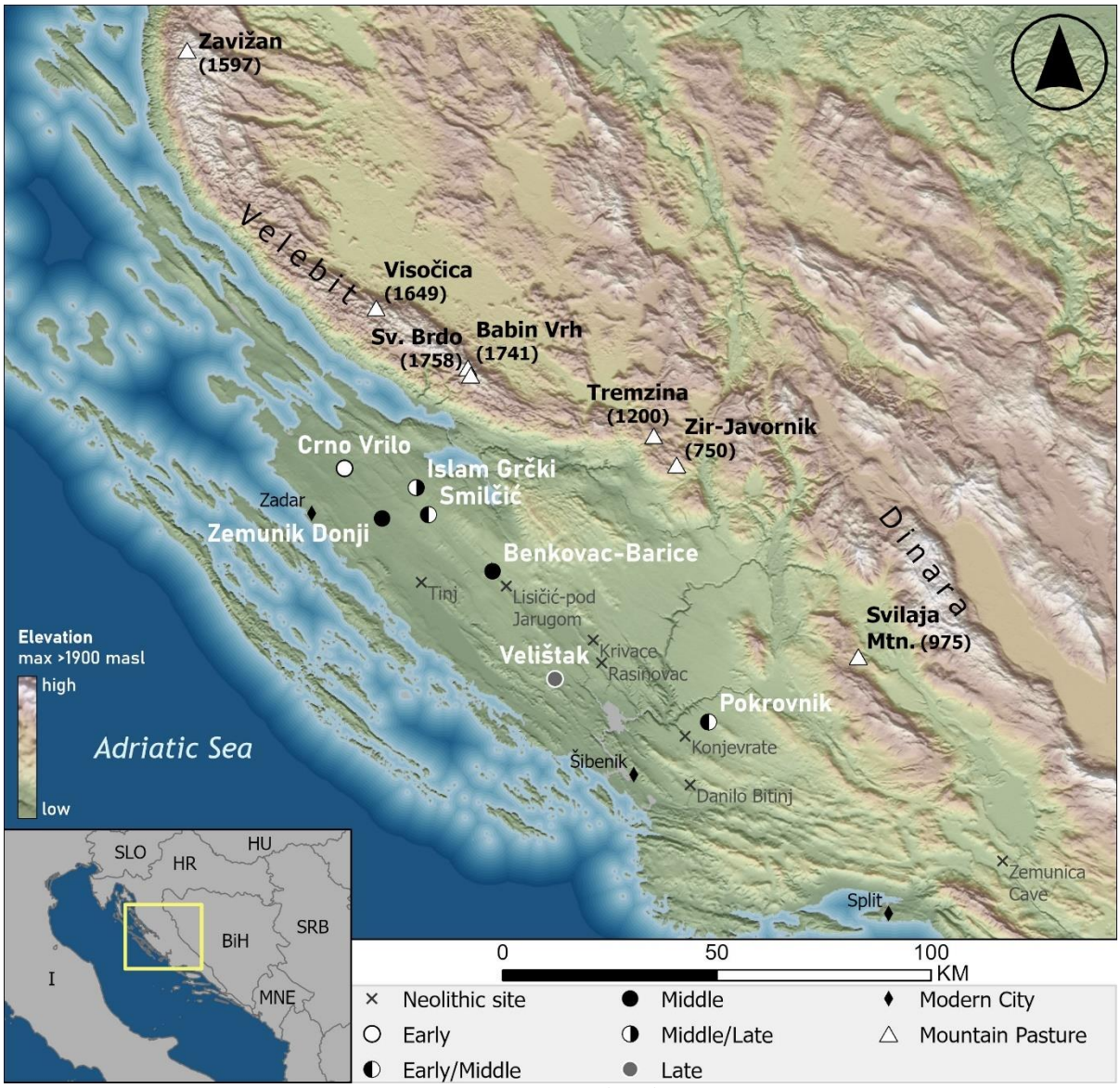

Figure 9.1. Map of mountain pasture locations visited by 19th-20th century sheep and goat herders in Dalmatia (Marković 1980) and archaeological sites discussed.

Stable isotope analysis of enamel bioapatite serially sampled from the lower M2 molar of sheep and goats, which forms completely in the first year of life (Milhaud and Nezit 1991; Upex and Dobney 2012; Weinreb and Sharav 1964; Zazzo et al. 2010), provides an intra-annual record of changes to the main source of body water primarily derived from meteoric water by small herbivores in the form of leaf water (Balasse 2002; Bernard et al. 2009; Henton 2012; Pederzani et al. 2021; Podlesak et al. 2008). Intra-tooth oxygen isotope

profiles of non-migratory animals should have high amplitudes of variation with sinusoidal undulations corresponding to seasonal precipitation $\delta^{18}O$ (Henton 2012; Henton et al. 2014; Julien et al. 2012) as illustrated in Figure 7.1. However, a weakened contrast between summer and winter signals is expected for livestock that moved to high elevation habitats in the summer because precipitation $\delta^{18}O$ at high altitudes is relatively lower. Migration patterns along altitude gradients should attenuate the differences between high and low elevation precipitation $\delta^{18}O$ and result in flattened intra-tooth $\delta^{18}O_{apa}$ profiles (Britton et al. 2008; Pellegrini et al. 2008; Pilaar Birch et al. 2016).

In non-migratory caprids the amplitudes of intra-tooth $\delta^{18}O_{apa}$ variation may range from 2 to 4‰ (Balasse et al. 2002) but could be as low as 1‰ for migratory species or livestock herded between high and low elevation pastures (Britton et al. 2009). On the other hand, modern transhumant ewes grazing on summer pastures at 1500-2000 masl in the western Pyrenees exhibited amplitudes of $\delta^{18}O_{apa}$ variation from 4.7 to 5.3‰ (Knockaert et al. 2018). Some have argued that rapid changes in elevation should be detectable as "change points" whereas slower migrations would entail longer-term averaging of isotopic signals along an altitude gradient and render a flattened intra-tooth $\delta^{18}O_{apa}$ profile (Hermes et al. 2017). Importantly, attenuation of the environmental signal can also result from residing in areas where groundwater is fed by rivers or other buffered water sources whose isotopic compositions are stable throughout the year (Henton et al. 2014). Given seasonal fluctuations in the enrichment of rainfall in ^{18}O and the divergence between high and low elevation locations in precipitation $\delta^{18}O$, expectations for intra-tooth $\delta^{18}O_{apa}$ variation resulting from intensive husbandry and vertical transhumance can be modeled.

The Online Isotopes in Precipitation Calculator (OIPC; Bowen 2024; Bowen et al.

2005; Bowen and Revenaugh 2003; IAEA/WMO 2015) was used to obtain monthly precipitation $\delta^{18}O_{VSMOW}$ estimates at weather stations in Zadar (5 masl) and at Zavižan peak (1594 masl) in the Velebit mountains (Figure 9.1) to estimate the difference in the enrichment of meteoric water in ^{18}O at low and high elevations, respectively (Figure 9.2). Estimated average monthly precipitation $\delta^{18}O_{VSMOW}$ for these two locations show precipitation in the Ravni Kotari lowlands surrounding Zadar is enriched in ^{18}O by approximately 3.5‰$_{VSMOW}$ relative to precipitation in the Velebit range. This is consistent with a gradient of -0.24‰$_{VSMOW}$ per 100 m increase in elevation described for the Adriatic coast based on monthly measurements of precipitation $\delta^{18}O_{VSMOW}$ in the study area (Roller-Lutz et al. 2013; Vreča et al. 2006). At the Velebit station on Zavižan, average annual precipitation $\delta^{18}O_{VSMOW}$ is estimated to be -10.2 ± 0.4‰$_{VSMOW}$, and -6.3 ± 0.2‰$_{VSMOW}$ (OIPC; Bowen and Revenaugh 2003).

Following Hermes et al. (2017), I substituted OIPC precipitation $\delta^{18}O$ values of summer months in Zadar with the corresponding values for Zavižan to model monthly variation in meteoric water $\delta^{18}O$ that animals would be exposed to while moving from the lowland area to the mountain pastures in the summer. In other words, the model shown in the right panels of Figure 9.2 combines OIPC estimates for Zavižan's summer months (June-September) and monthly autumn, winter, and spring estimates for Zadar.

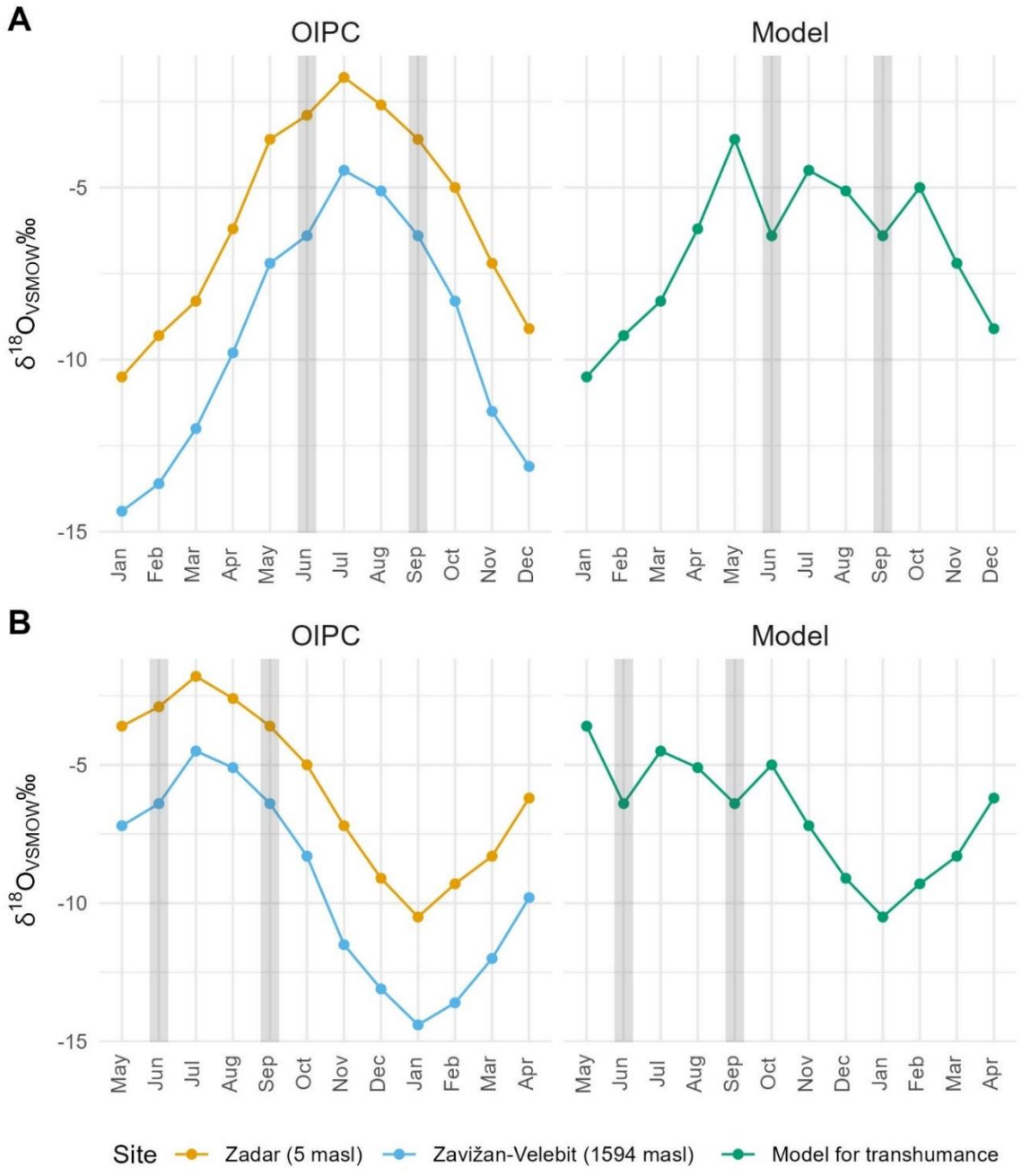

Figure 9.2. (A) left panel: Precipitation $\delta^{18}O_{VSMOW}$ values estimated for Zadar and Zavižan; right panel: modeled $\delta^{18}O_{VSMOW}$ values of meteoric water an animal would be exposed to by relocating to pastures near Zavižan in the Velebit mountains in June and returning to Zadar to in September. Migration periods highlighted in grey shaded areas. (B) Same data but shifted with series beginning in May to simulate a 5-month delay in enamel mineralization for sheep and goats. With this shift, the values in May would correspond to δ18Oapa values preserved in the earliest mineralized sections of enamel. Precipitation δ18OVSMOW values were estimated using the OIPC (Bowen 2024; Bowen et al. 2005; Bowen and Revenaugh 2003; IAEA/WMO 2015).

Herds that moved upland to the Velebit or Dinara mountains above 1500 masl from June to September would be grazing in pastures where rainfall is approximately 2.9‰$_{VSMOW}$ depleted in ^{18}O relative to precipitation in the lowlands. The vertical shift in grazing area, which occurred in as little as six days (Nimac 1940), corresponds to a -2.8‰$_{VSMOW}$ difference in ^{18}O-enrichment.

The abrupt change in altitude is reflected in the modeled sequence of precipitation $\delta^{18}O_{VSMOW}$ as a reversal of the gradual ^{18}O-enrichment of lowland precipitation from January to May (Figure 9.2A). Maximum precipitation $\delta^{18}O_{VSMOW}$ values are achieved in July at Zadar and Zavižan but in the modeled series, the maximum occurs in May while the mid-summer peak $\delta^{18}O_{VSMOW}$ value is achieved after a sharp decrease associated with the rapid elevation gain of 1500 m. In the model, precipitation $\delta^{18}O_{VSMOW}$ in July becomes the second of three peaks in the yearly cycle, whereas in both upland and lowland settings, after peaking in July, precipitation $\delta^{18}O_{VSMOW}$ gradually descends into the autumn and winter months. This descent is interrupted by another reversal of the slope as the downward progression of precipitation $\delta^{18}O_{VSMOW}$ from July reverses course in September when herds return to the lowlands coinciding with the onset of Dalmatia's generous autumnal rainfall (see Chapter 2, Figure 3.2A). The reversal associated with the modeled descent creates a third peak in precipitation $\delta^{18}O_{VSMOW}$ achieved in October, well after herds historically returned to graze in the lowlands (Nimac 1940; Perišić 1940). Based on these simulations, the amplitude of intra-tooth $\delta^{18}O_{apa}$ variation in transhumant animals would be 6.9‰$_{VSMOW}$ and 8.7‰$_{VSMOW}$ in stationary herds exposed to the full cycle of lowland precipitation.

Given the 5-6 month delay in enamel mineralization for sheep (Balasse et al. 2012b; Blaise and Balasse 2011) a series of $\delta^{18}O_{apa}$ values representing 12 months would begin when

sheep were approximately 6 months old. The series in Figure 9.2B beginning in May reflects the early winter lambing season modeled for sheep raised by Impresso herders at Crno Vrilo (Sierra et al. 2023). Notably, the May and June values in these figures would correspond to enamel bioapatite samples recovered from sections of the tooth crown closest to the occlusal surface. In heavily worn teeth, these potentially diagnostic isotopic signals may not be observable in $\delta^{18}O_{apa}$ series obtained from older individuals. For example, if occlusal wear removed sections of enamel that mineralized in the first two months, the amplitude of variation would be even lower for transhumant animals but unchanged for stationary herds. Furthermore, the section of the modeled curve from October to May is indistinguishable from the corresponding section of the Zadar monthly estimates. As an aside, this observation highlights the importance of screening samples to avoid heavily worn teeth.

To refine the model presented in Figure 9.2, I consulted ethnographic research on transhumant pastoralists in Dalmatia for whom several varieties of transhumance have been described involving seasonal use of pastures in the Dinaric Alps (Belaj 2004; Forenbaher 2007; Marković 1975; 1980; 1987; Nimac 1940; Perišić 1940). For transhumant communities based in the Ravni Kotari, Bukovica, and Primorje regions, two systems particularly relevant for the present study are distinguished by the timing of movements within the calendar year and the length of time spent in pastures at different elevations (Figure 9.1). I refer to these two systems using the terms *rapid* and *stepwise* (Figure 9.3 A and B, respectively) to distinguish the models according to differences in the pace of seasonal movements between lowland and upland pastures.

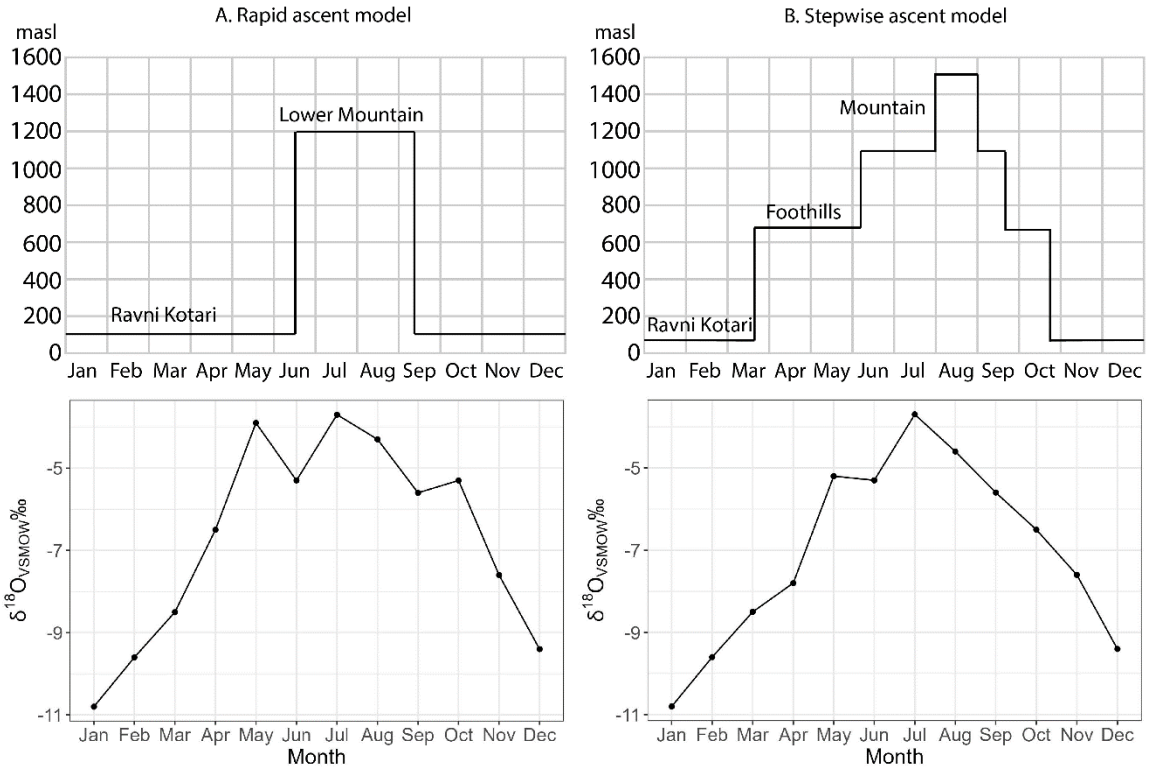

Figure 9.3. Schedule of elevation changes associated with the "rapid" (top panel, A) and "stepwise" ascent models (top panel B) and the modeled precipitation $\delta^{18}O_{VSMOW}$ estimates (bottom panels). Diagrams in the top two panels based on Markovic (Figure 3, 1980). Precipitation $\delta^{18}O_{VSMOW}$ values estimated using the OIPC (Bowen 2024; Bowen and Revenaugh 2003; IAEA/WMO 2015). Coordinates used to estimate monthly isotopes in precipitation data provided in Appendix I.

The *rapid* movement model refers to the system Marković (1980) described for the shepherds from Ravni Kotari and Bukovica that used Velebit pastures but the schedule is similar to the timing of Zagorje shepherd movements into pastures in the Dinara mountains (Nimac 1940). Travel from coastal lowlands to Velebit and Dinara mountain pastures typically began on 13 June, the feast day of Sveti Anton (Forenbaher 2007; Marković 1980; Perišić 1940). Communities from the Drniš and Šibenik areas including the modern villages of Pokrovnik (260 masl), Konjevrate (200 masl), and Danilo (150 masl) completed the journey to Šator mountain pastures (1500-1800 masl) of the Dinara range in five to six days (Nimac 1940). Villages on the Ravni Kotari and in Bukovica, including Smilčić (175 masl),

and Benkovac (175 masl), moved sheep into elevations between 1000 and 1400 masl in the southern Velebit mountains. The return to lowlands was completed in only three days and progressed in two waves to keep lambs separated from the lactating ewes to maximize milk availability (Nimac 1940). Lambs returned to the lowlands in mid-August, followed by the remaining herds of adult animals on or after September 8 (Nimac 1940). This system is characterized by swift and substantial changes in elevation (i.e., >1000 m elevation change in 3-6 days) and is illustrated in Figure 9.3A.

The second version of transhumance involved *stepwise* ascents and descents between Dalmatia and pastures at staggered elevations in the Velebit mountain range and was mainly practiced in the littoral zone (Marković 1980). During the winter (i.e., from November to mid-March) herds were kept near villages on the coast, only slightly above sea level. In the spring, herds were moved to the Velebit foothills to graze in pastures at around 750 masl from March to early June. Another move to grasslands in even higher elevations (around 1250 masl) occurred in the early summer. In August some shepherds moved flocks to the highest Velebit pastures near Visočica (1649 masl), Sveto Brdo (1758 masl), and Babin Vrh (1741 masl; Figure 9.1). In September herds returned to pastures at 1250 masl for part of the month before returning to the 750 masl zone. By mid-October herds were again at the low elevation coastal zone (Marković 1980; Figure 9.3B).

Monthly estimates of precipitation $\delta^{18}O$ were obtained via the OIPC for locations of Velebit pastures used by Dalmatian herders in the recent past (Marković 1980) to calibrate the model to reflect the schedules and altitude changes of the rapid and stepwise versions of transhumance described above (bottom panels of Figure 9.3; see Appendix I). The rapid model simulates the transition between Benkovac (175 masl) and the Tremzina pasture (1200

masl). The stepwise model involves movements from Benkovac to Javornik (750 masl), then to Tremzina, and finally to Sveti Brdo (1441 masl) and back, in reverse order (Figure 9.1). As shown in Figure 9.3A, only the curve simulated in the rapid model exhibits potentially diagnostic features.

The amplitude of $\delta^{18}O_{apa}$ variation resulting from both simulated transhumance routes is 7.1‰$_{VSMOW}$. Further dampening of the environmental signal in $\delta^{18}O_{apa}$ is expected due to the delay in enamel mineralization (Passey and Cerling 2002), estimated for small ruminants such as sheep and goats to be less than 10% (Kohn 2004). This is in addition to the 10% dampening of the signal resulting from residence time of the isotope in the animal (Kohn et al. 2002). The modeled amplitudes of $\delta^{18}O_{apa}$ variation for herds moving from Zadar to Zavižan was 6.9‰ and 7.1‰ for the rapid and stepwise models. If herds remained in Zadar or Benkovac the amplitudes would be around 8.8‰. Thus, the difference in amplitudes for stationary versus transhumant animals would be approximately 1.7 - 1.9‰. The attenuation factors associated with the delay in enamel mineralization and residence time of body water totaling to 20% could therefore reduce these differences to 1.3‰ to 1.5‰.

Based on these models, a series of $\delta^{18}O_{apa}$ values obtained from archaeological caprine tooth specimens should reflect maximum and minimum precipitation $\delta^{18}O_{VSMOW}$ for the Ravni Kotari if herding was focused close to settlements year-round. This seasonal signal may be weakened by around 1.5‰ if pastures in the Velebit or Dinara were visited during the summer or further obscured if herding was centered close to a source of buffered water (Henton et al. 2014). Ingestion of isotopically distinct water sources following swift transitions between different pastures separated by 1000-1500 m in altitude may be reflected as abrupt shifts between $\delta^{18}O_{apa}$ values corresponding to changes in elevation (Hermes et al.

2017).

Distinguishing between vertical transhumance and averaging effects of buffered groundwater remains challenging when intra-tooth $\delta^{18}O_{apa}$ sequences are used in isolation. However, leveraging expectations of seasonal changes in plant $\delta^{13}C$ to assess whether intra-tooth $\delta^{18}O_{apa}$ fluctuations correspond to $\delta^{13}C_{apa}$ can help resolve these confounding effects (Fraser et al. 2008; Lazzerini et al. 2021; Makarewicz et al. 2017; Tornero et al. 2016; 2018). Anti-covariance was proposed as a potentially useful indication of vertical transhumance by Lazzerini et al. (2021) although intra-tooth $\delta^{18}O_{apa}$ sequences of mobile caprines in their study exhibited seasonal variation. However, increasing altitude is associated with lower meteoric water $\delta^{18}O$ (Gat 1980; Roller-Lutz et al. 2013) and more positive $\delta^{13}C$ in C_3 plants (Körner et al. 1988; 1991). As temperatures began to rise in the lowlands during the months leading up to the move to pastures in the Dinarides, immature enamel would be incorporating body water obtained from meteoric water increasingly enriched in ^{18}O. Once higher elevation pastures were reached, the enamel would begin to incorporate the relatively ^{18}O-depleted meteoric water expected in higher altitudes.

The dampening of this environmental signal due to a combination of the delay in mineralization and sampling through multiple enamel layers (Kohn 2004; Passey and Cerling 2002) might only subdue these increases rather than result in a reversal of the direction of $\delta^{18}O_{apa}$ towards more negative values. Additionally, in the Velebit mountains summer precipitation can be as ^{18}O-enriched as precipitation on the Ravni Kotari during the winter and autumn (Vreča et al. 2006), which could result in very low-amplitude $\delta^{18}O_{apa}$. In other words, because intra-tooth $\delta^{18}O_{apa}$ variation is attenuated by sampling, delayed mineralization, and change in elevation, carbon and oxygen profiles of individuals that were

moved into the mountains may not necessarily exhibit an inverse relationship. Therefore, vertical transhumance could result in covariance between $\delta^{13}C_{apa}$ and $\delta^{18}O_{apa}$ expressed as a weakly or moderately positive correlation.

C. Evaluating the Stable Oxygen Isotope Results for Evidence of Vertical Transhumance in the Neolithic

A total of 65 out of 73 archaeological specimens passed FTIR quality control assessments (Appendix F). Of these 65 specimens sampled for isotope analysis, 20 goats and 31 sheep were identified using established criteria (Zeder and Pilaar 2010); only 14 specimens were assigned to a catch-all, "ovicaprid" group. Additionally, four modern tooth specimens were sampled, including three that were extracted from mandibles collected from unspecified pastures in the Dinara mountain range (DIN5, DIN6, and DIN7) and one specimen (VRL481) was obtained from a sheep raised near Svilaja mountain (Figure 9.1).

Identifying vertical transhumance from intra-tooth stable isotope measurements can be challenging in absence of modern reference data (Knockaert et al. 2018; Lazzerini et al. 2021). Migratory behavior has been shown to lead to reduced intra-tooth $\delta^{18}O_{apa}$ variation (Britton et al. 2009; Pellegrini et al. 2008). Based on the models discussed in the previous section, amplitudes of $\delta^{18}O_{apa}$ variation for transhumant animals should be approximately 1.3 to 1.5‰ less than that of stationary animals. Others suggest rapid changes in elevation could be detected as change-points within a sequence (Hermes et al. 2017). Transhumance may also result in greater inter-individual variability in $\delta^{18}O_{apa}$ as animals have access to a non-local source of water (Mashkour 2003). Strong positive correlations between $\delta^{13}C_{apa}$ and $\delta^{18}O_{apa}$ may result from remaining in the same area year-round whereas anti-covariation

between the two profiles has been interpreted as potentially indicating migratory behavior (Knockaert et al. 2018; Lazzerini et al. 2021; Tejedor-Rodríguez et al. 2021). In the following section I present insights from the intra-tooth stable isotope data obtained for the four modern specimens before describing the methods used to isolate the archaeological samples whose $\delta^{18}O_{apa}$ or $\delta^{13}C_{apa}$ deviate from expected signals of seasonal variation potentially related to vertical transhumance.

D. Modern Specimens

The results of stable isotope analysis of enamel bioapatite of the modern specimens (excluding DIN6, for which too few samples were collected) offer useful insight into the expected patterns of intra-tooth $\delta^{18}O_{apa}$ and $\delta^{13}C_{apa}$ arising from foddering and mobility. Details on the provenience of the three specimens recovered from unspecified pastures in the Dinara mountains are limited (see Chapter Seven). Whether DIN5 and DIN7 were raised under a vertical transhumant strategy cannot be verified but VRL481 did move between lowlands and higher elevations on a seasonal basis. Nonetheless, these animals certainly spent some portion of their lives in the Dinara mountains.

The seasonal signal within the $\delta^{18}O_{apa}$ sequences of the modern specimens is weak relative to the archaeological specimens. For example, the amplitudes of $\delta^{18}O_{apa}$ variation among the archaeological specimens range from 1.0 to 5.2‰ and the range for modern specimens is 2.0 to 3.5‰-. The mean $\delta^{18}O_{apa}$ amplitude for the modern specimens is 2.8‰, compared to 3.3‰, 3.7‰, and 3.3‰ for the Impresso, Danilo, and Hvar groups, respectively.

Excluding DIN6, none of the modern specimens exhibit significant anti-covariation or significant covariation between $\delta^{13}C_{apa}$ and $\delta^{18}O_{apa}$ profiles (Table 8.5). The weakest

correlation between modern intra-tooth carbon and oxygen ratios is seen in DIN5, as the trajectories of these values are clearly divergent along the entire length of the tooth (Figure 9.4). $\delta^{18}O_{apa}$ mid-ranges ((max + min) / 2) for DIN5 and DIN7 are similar (-6.0‰ and -6.4‰, respectively) but the amplitude of $\delta^{18}O_{apa}$ variation is larger for DIN5 (3.5‰) relative to DIN7 (2.0‰) which shows a weaker environmental signal. VRL481 grazed in pastures between 975 and 750 masl yet also shows a weak environmental signal in the $\delta^{18}O_{apa}$ sequence with an amplitude of variation of 3.0‰. Additionally, the $\delta^{13}C_{apa}$ sequences in the Dinara specimens have a downward parabola shape suggesting that the ^{13}C-enrichment of these individuals' diet likely varied seasonally, leading to amplitudes of $\delta^{13}C_{apa}$ variation of 5.6‰ and 3.2‰ in DIN5 and DIN7, respectively. The amplitude of $\delta^{13}C_{apa}$ variation for VRL481 is comparatively very low 0.6‰. This individual's diet consisted of primarily natural pasture grasses in the summer but supplemented with oats, barley, and maize (a C_4 crop) in the winter. The dampening effects of a foddering on intra-tooth $\delta^{13}C_{apa}$ variation (e.g., Chase et al. 2014) is clear in VRL481.

Given the lack of information available about how these modern specimens were managed, their utility for direct comparison to archaeological samples is somewhat limited. However, assuming the Dinara specimens were indeed moved seasonally between the mountains and the Dalmatian lowlands, the modern samples demonstrate four key insights:

1. As suggested by the carbon and oxygen profiles of DIN5, vertical transhumance may lead to an inverse relationship between the two series of isotope ratios but anti-covariation may not be so severe as to result in a negative correlation.
2. Based on the comparison of the amplitudes of $\delta^{18}O_{apa}$ variation for DIN7 (2.0‰) and VRL481 (3.0‰), vertical transhumance may result in more significant dampening of

the environmental signal in oxygen isotope sequences for individuals that experienced greater changes in elevation.

3. While it cannot be ruled out that the diet of DIN5 and DIN7 was supplemented by fodder, vertical transhumance may potentially result in noticeably higher amplitudes of $\delta^{13}C_{apa}$ variation than individuals whose diet consisted of fodder on a semi-annual basis (i.e., VRL481).

4. VRL481 demonstrates how a combination of natural grasses and fodder consisting of a variety of plant types can virtually erase a seasonal signal in a $\delta^{13}C_{apa}$ sequence.

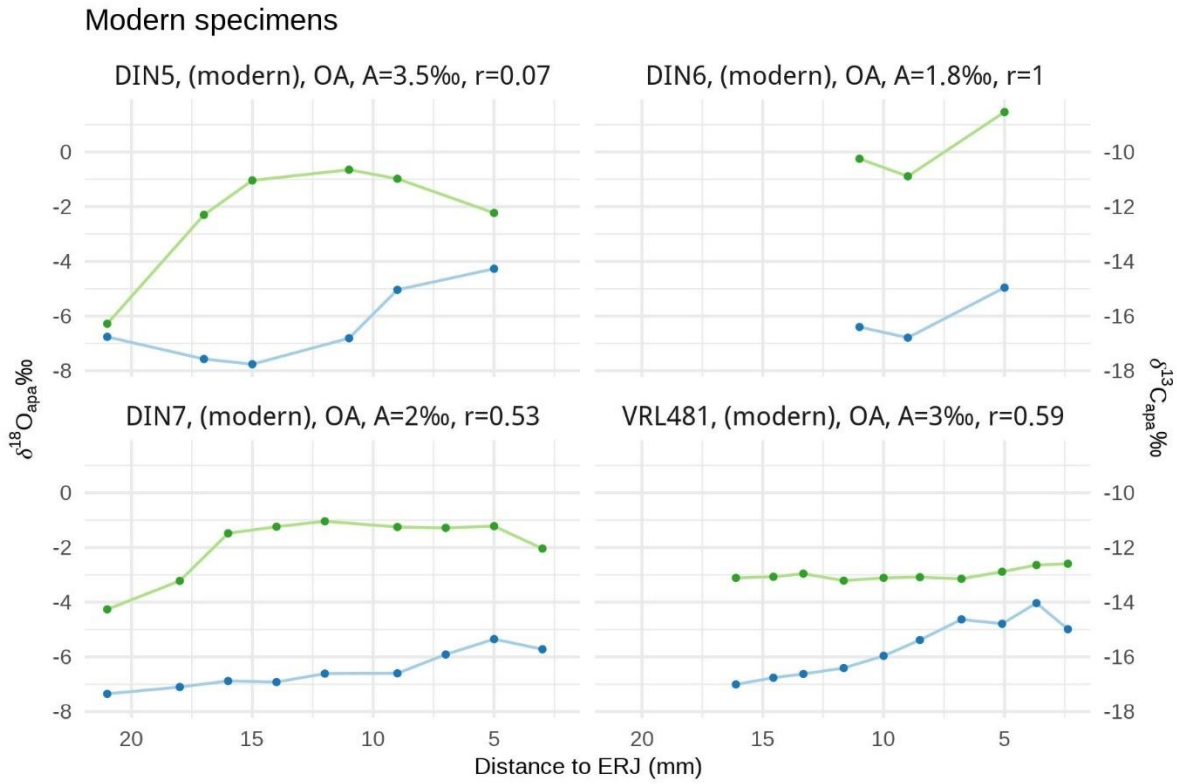

Figure 9.4. Plots of $\delta^{18}O_{apa}$ (blue) and $\delta^{13}C_{apa}$ (green) for modern sheep specimens from Dinara (DIN5, DIN6, DIN7) and Vrlika (VRL481).

E. Assessing inter-individual and intra-tooth variation

Visual inspection of the plotted $\delta^{18}O_{apa}$ sequences was a vital first step towards identifying patterns that deviated from expected seasonal variation. Except for those whose sequences are truncated (i.e., CV18, CV22, ZD13, and VEL34), specimens exhibit sinusoidal, parabolic, flattened, or irregular patterns in the plotted $\delta^{18}O_{apa}$ sequences (Table 9.1). Sinusoidal and parabolic shaped $\delta^{18}O_{apa}$ sequences reflect seasonal cycling in the ^{18}O-enrichment of ingested water (Figure 6.1). Parabolic sequences are defined here as profiles in which either the minimum or maximum value is observed in a trough or peak, respectively. For sequences shaped as parabola opening downward (e.g., CV21 and PK91 in Figure 8.10), peak values likely reflect the environmental signal of ^{18}O-enriched precipitation associated with high summer temperatures. Sequences shaped as upward-opening parabola (e.g., CV20, and SMI456 in Figure 8.10), capture only the winter precipitation signal. Sinusoidally-shaped profiles record most clearly the full year of seasonal variation with winter and summer environmental signals captured in the troughs and peaks of $\delta^{18}O_{apa}$ sequences (e.g., BB136 and IG219 in Figure 8.11).

The lower 10th percentile of the amplitude of $\delta^{18}O_{apa}$ variation (max - min) of the archaeological specimens was used to distinguish specimens with flattened sequences from those exhibiting variation expected to arise from seasonal enrichment of precipitation $\delta^{18}O$ (i.e., intra-tooth $\delta^{18}O_{apa}$ amplitude $\leq$ 2.4‰). According to this criteria, four Impresso specimens (CV28, PK90, PK92 and PK93), one Danilo specimen (PK95), and two Hvar individuals from Veliš̌tak (VEL32 and VEL37) have dampened $\delta^{18}O_{apa}$ sequences relative to all other archaeological specimens. For the Pokrovnik specimens and for VEL32, attenuation of the oxygen isotope profile is easily observed when the data are plotted (Figure 9.5). In

comparison, intra-tooth $\delta^{18}O_{apa}$ variation in CV28 exhibits a sinusoidal shape while the profile of VEL37 is more erratic.

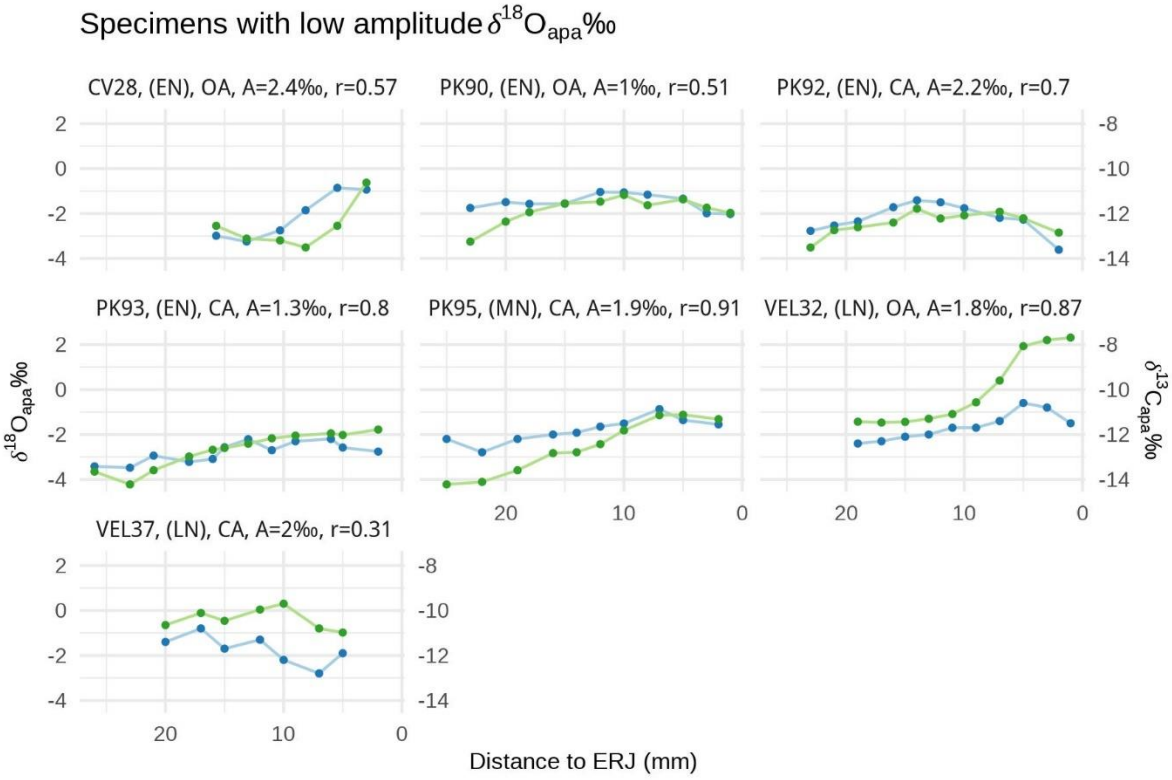

Figure 9.5. Intra-tooth $\delta^{18}O_{apa}$ (blue) and $\delta^{13}C_{apa}$ (green) sequences of individuals with low amplitudes of $\delta^{18}O_{apa}$ variation (max - min). Low amplitudes were defined as values below the 10th percentile (2.4‰). Individual plot titles identify the specimen, period (EN=Impresso/Early Neolithic; MN=Danilo/Middle Neolithic; LN=Hvar/Late Neolithic), species (OA=sheep; CA=goat), amplitude of $\delta^{18}O_{apa}$ variation (A), and Pearson's correlation coefficient (r) calculating covariance between the carbon and oxygen sequences.

The same filtering criteria was applied to the amplitude of variation in the $\delta^{13}C_{apa}$ sequences (i.e., intra-tooth $\delta^{13}C_{apa}$ amplitude ≤ 1.1‰) to distinguish specimens with flattened carbon isotope sequences. This group includes Impresso specimens CV18, CV22, SMI454, and SMI456, Danilo individuals PK54 and PK88, and VEL34 from Hvar-period Velištak (Figure 9.6). With fewer than six stable isotope values, the carbon and oxygen profiles for CV18 and VEL34 are truncated so it is unclear if a seasonal signal is preserved in the sequences. However, CV22, PK54, PK88, SMI454, and SMI456 exhibit flattened $\delta^{13}C_{apa}$

relative to undulating $\delta^{18}O_{apa}$ profiles.

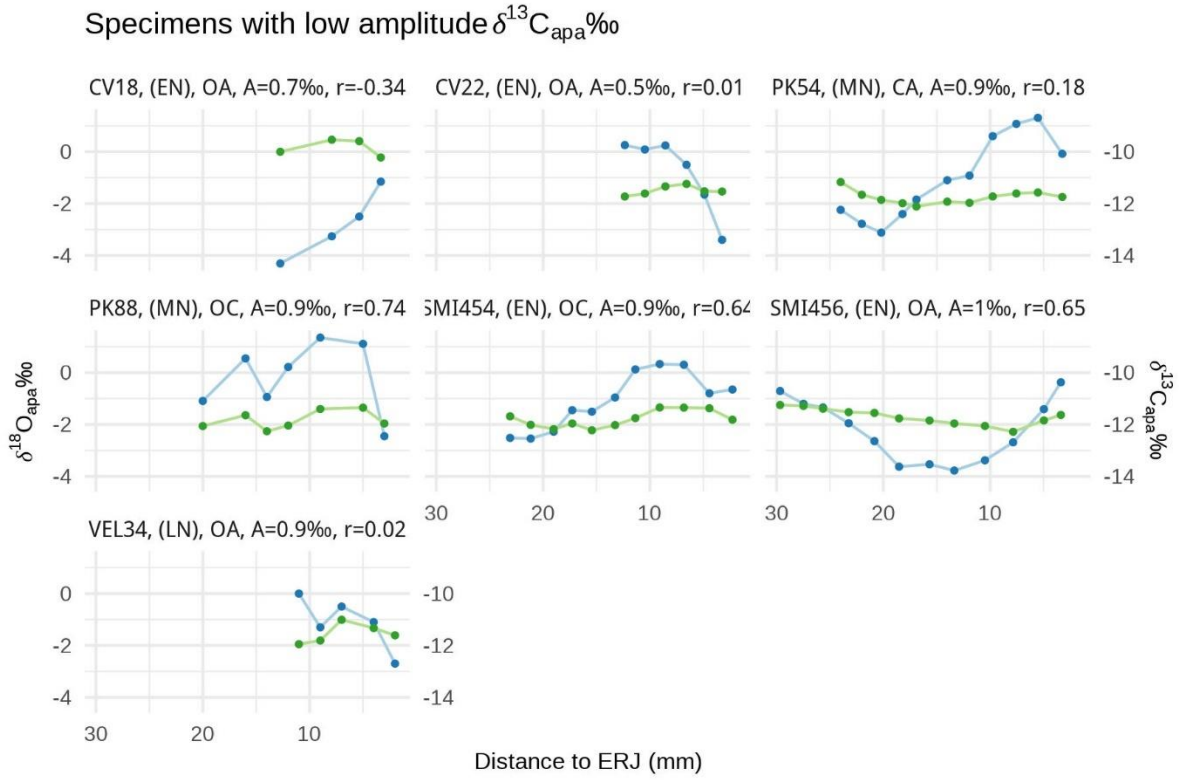

Figure 9.6. Intra-tooth $\delta^{18}O_{apa}$ (blue) and $\delta^{13}C_{apa}$ (green) sequences of individuals with low amplitudes of $\delta^{13}C_{apa}$ variation (max - min). Low amplitudes were defined as values below the 10th percentile (1.1‰). Individual plot titles identify the specimen, period (EN=Impresso/Early Neolithic; MN=Danilo/Middle Neolithic; LN=Hvar/Late Neolithic), species (OA=sheep; CA=goat; OC=ovicaprid), amplitude of $\delta^{13}C_{apa}$ variation (A), and Pearson's correlation coefficient (r) calculating covariance between the carbon and oxygen sequences.

Several of the sequences exhibit one or more sharp changes in $\delta^{18}O_{apa}$ from one point on the tooth to the next. Although these sequences can be easily (albeit subjectively) identified by visually inspecting plotted $\delta^{18}O_{apa}$ values, they are also distinguishable quantitatively. The first derivative of a function *f*, denoted as *f'*(*x*), represents the rate of change of that function with respect to its independent variable, *x*. Here, the first derivative was calculated to quantify the rate of change in $\delta^{18}O_{apa}$ from one measurement to the next along each specimen's tooth (the first derivative of $\delta^{18}O_{apa} = \delta^{18}O_{apa}'(erj)$). Assuming each

specimen's $\delta^{18}O_{apa}$ sequence is a representation of meteoric water $\delta^{18}O$, identifying unusually dramatic changes within a sequence should reflect rapid shifts in the ^{18}O-enrichment of body water and, by extension, rapid movements between grazing areas potentially in different elevations. To this end, the variance (s^2) of $\delta^{18}O_{apa}$'(*erj*) for each specimen was calculated. Outlier detection was based on whether the variance of an individual's first derivative fell outside of the 25% and 75% quantiles. Four outliers (Impresso: PK99 and SMI338; Danilo: PK88 and BB154) were identified among tooth specimens for which at least six stable isotope measurements were available (Figure 9.7).

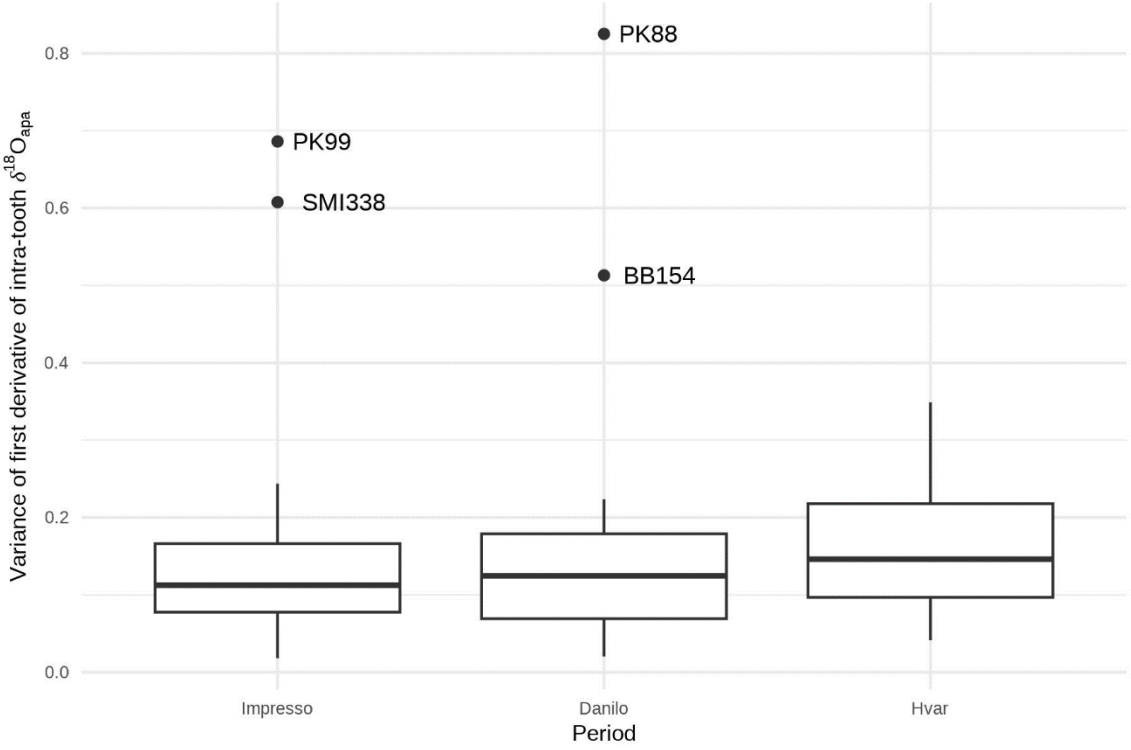

Figure 9.7. Box plot showing variance (s^2) of the first derivative of intra-tooth $\delta^{18}O_{apa}$ sequences. Outliers exhibit s^2 greater than the 75% quantile of tooth specimens with at least six stable isotope measurements. These individuals exhibit dramatic shifts in the oxygen isotope profiles, possibly related to rapid movements between environments characterized by different precipitation $\delta^{18}O$ values.

The irregularity of the $\delta^{18}O_{apa}$ sequences for these four specimens can be seen in Figure 9.8 as either erratic intra-tooth $\delta^{18}O_{apa}$ profiles (i.e., PK88 and PK 99) or as a shift in

$\delta^{18}O_{apa}$ > 3‰ somewhere in the sequence (i.e., SMI338 and BB154). Specimens SMI338 and BB154 have $\delta^{18}O_{apa}$ sequences that resemble expected seasonal variation in precipitation $\delta^{18}O$ but each individual features an abrupt decrease in $\delta^{18}O_{apa}$ leading to unusually high $s^2_{\delta 18O\text{-}apa'(erj)}$. SMI338 exhibits a sharp decrease late in the tooth's enamel formation as the $\delta^{18}O_{apa}$ value at 5.69 mm drops from 0.4‰ to -3.5‰ at 3.71 mm from the ERJ. This shift in $\delta^{18}O_{apa}$ coincides with a sharp increase in $\delta^{13}C_{apa}$. For BB154, a rapid decrease in $\delta^{18}O_{apa}$ interrupts an otherwise seasonal sequence and occurs closer to the crown (relative to SMI338) as the $\delta^{18}O_{apa}$ value at 23.7 mm from the ERJ drops from -0.3‰ to -3.3‰ at 21.57 mm from the ERJ. The abrupt change in $\delta^{18}O_{apa}$ coincides with a less extreme but noticeable decrease in $\delta^{13}C_{apa}$.

Pearson's correlation coefficient was calculated for each specimen's paired $\delta^{13}C_{apa}$ and $\delta^{18}O_{apa}$ sequences to evaluate the degree of covariation between intra-tooth carbon and oxygen isotope ratios. Among the 65 archaeological specimens, 62 individuals exhibit covariation in intra-tooth carbon and oxygen stable isotope and there is a significant ($p < 0.05$) positive correlation for 38 of these individuals (Table 8.5). Covariation with significant positive correlations was found between the carbon and oxygen isotope sequences of four specimens with attenuated intra-tooth $\delta^{18}O_{apa}$ variation (PK92, PK93, PK95, and VEL 32; Figure 9.5; Table 8.5). Three Early Neolithic specimens (CV18, PK101, and SMI338) exhibit anti-covariation (i.e., Pearson's $r < 0$) between their $\delta^{13}C_{apa}$ and $\delta^{18}O_{apa}$ values. The sequence for CV18 is limited to four samples and may be disregarded because a seasonal signal is not observable when there are too few data points. Specimens for which Pearson's r is below the 20% quantile ($r < 0.286$) represent negative or weakly positive correlations include BB135, CV26, PK72, PK87, PK101, SMI130, and VEL29 (Figure 9.9), in addition to three

specimens with low amplitudes of $\delta^{13}C_{apa}$ (CV22, PK54, VEL34; Figure 9.6) and $\delta^{18}O_{apa}$ variation (PK99, SMI338; Figure 9.8).

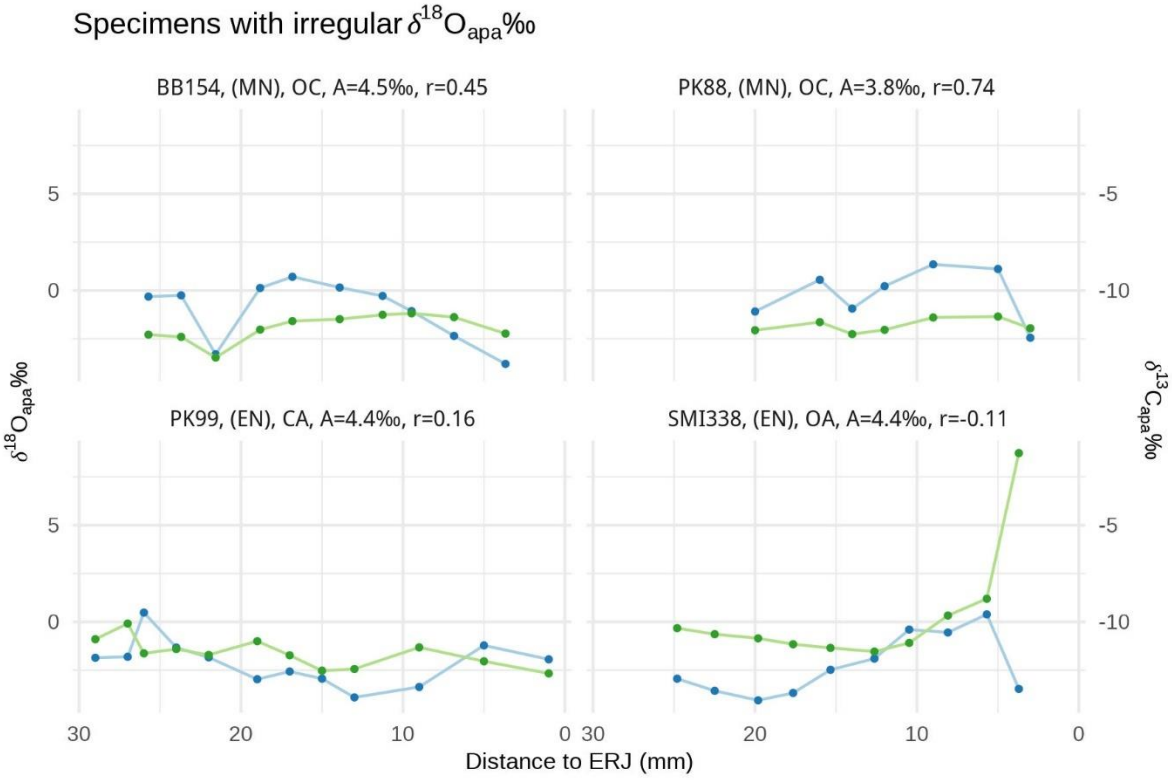

Figure 9.8. Intra-tooth $\delta^{18}O_{apa}$ (blue) and $\delta^{13}C_{apa}$ (green) sequences of individuals with irregular $\delta^{18}O_{apa}$ sequences. The variance of the first derivative of the oxygen isotope profiles for these specimens is greater than the 75% quantile of the variance calculated for tooth specimens with at least six stable isotope measurements. Individual plot titles identify the specimen, period (EN=Impresso/Early Neolithic; MN=Danilo/Middle Neolithic), species (OA=sheep; CA=goat; OC=ovicaprid), amplitude of $\delta^{18}O_{apa}$ variation (A), and Pearson's correlation coefficient (r) calculating covariance between the carbon and oxygen sequences.

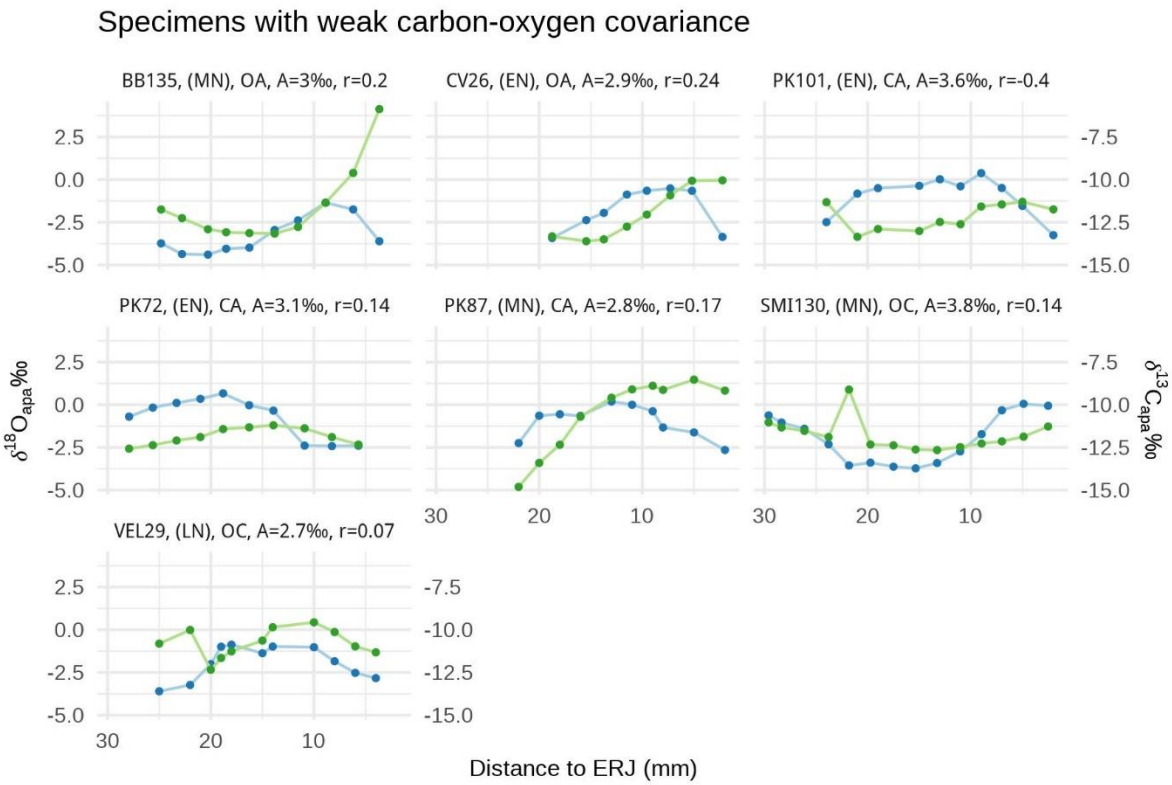

Figure 9.9. Intra-tooth $\delta^{18}O_{apa}$ (blue) and $\delta^{13}C_{apa}$ (green) sequences of individuals with weak positive or negative correlation between the carbon and oxygen isotope profiles. The Pearson's r correlation coefficient for these individuals is below the 20% quantile ($r < 0.286$). Other specimens included in this group are CV18, CV22, PK54, VEL34 (Figure 9.6), PK99, and SMI338 (Figure 9.8). Individual plot titles identify the specimen, period (EN=Impresso/Early Neolithic; MN=Danilo/Middle Neolithic; LN=Hvar/Late Neolithic), species (OA=sheep; CA=goat; OC=ovicaprid), amplitude of $\delta^{13}C_{apa}$ variation (A), and Pearson's correlation coefficient (r) calculating covariance between the carbon and oxygen sequences.

*Table 9.1 Description of $\delta^{18}O_{apa}$ profiles. *FTIR analysis suggested diagenetic alteration of specimen, omitted from further analysis.*

Curve Pattern	Description	Specimens	Mean $\delta^{18}O_{apa}$ Amplitude
Sinusoidal	Curves are relatively smooth and contain at least one peak and one trough	CV15, CV17, CV23, CV28, PK72, SMI338, SMI403, SMI454, BB135, BB136, BB168, IG212, IG219, IG226, IG233, PK54, PK89, PK98*, SMI130, SMI360, SMI421, ZD10, ZD11, ZD14, ZD16, IG468, IG476	3.6‰
Parabolic	U-shaped curves where minimum and maximum values are located in the trough (for parabola opening upwards) or peak (for parabola opening downward), respectively.	CV19, CV20, CV21, CV24, CV26, PK100*, PK101, PK76, PK91, PK92, SMI335, SMI455, SMI456, BB180, BB182, IG211, IG239, PK87, PK97, SMI435, ZD297, ZD298, IG475, IG477, IG478, IG479, VEL29, VEL30*	3.6‰
Flattened	Series may show upward or downward trend but no clear peaks or troughs are visible.	PK104*, PK90, PK93, PK95, VEL32	1.4‰
Irregular	Series may have aberrant values in sequence, abrupt changes in slope, and/or multiple peaks.	PK102*, PK99, BB154, PK88, PK94*, PK96*, SMI338, VEL28, VEL31*, VEL37	4.8‰
Truncated	No peak or trough visible in plot	CV18, CV22, ZD13, VEL34	3.2‰

F. Weighing Evidence for Vertical Transhumance in the Archaeological Data

The discussion of diet space in the previous chapter alluded to the implication of inter-individual variability shown among the specimens from Pokrovnik and Velištak could be the result of a more mobile herding strategy (Julien et al. 2012). In the previous section, I discussed three ways that vertical transhumance could be observed in intra-tooth stable isotope data: (1) attenuation of intra-tooth $\delta^{18}O_{apa}$ variation, (2) unusually erratic shifts within the series of $\delta^{18}O_{apa}$ values, and (3) anti-covariation between $\delta^{18}O_{apa}$ and $\delta^{13}C_{apa}$; and

described the quantitative approaches I used to identify specimens whose intra-tooth stable isotope sequences fit these criteria. Indeed, most of the specimens identified as having been potentially herded into higher elevation pastures are associated with Pokrovnik or Velištak. Before reviewing the Pokrovnik and Velištak examples that offer the strongest evidence of vertical transhumance during the Neolithic, I assess the intra-tooth carbon and oxygen sequences of individuals representing other sites which were likely managed quite differently.

The group of specimens with attenuated $\delta^{18}O_{apa}$ profiles exhibit amplitudes of variation ranging from 1‰ to 2.4‰ (Figure 9.5). Based on monthly precipitation $\delta^{18}O$ values obtained via the OIPC (Figure 9.2), the difference between modeled amplitudes of intra-tooth $\delta^{18}O_{apa}$ variation of stationary versus transhumant animals was estimated to be between 1.3‰ and 1.5‰. The difference between the amplitude of $\delta^{18}O_{apa}$ variation of CV28 and the mean site amplitude for Crno Vrilo (3.2‰) is 0.8‰ (Table 8.6). By this criteria, vertical transhumance may not explain the low $\delta^{18}O_{apa}$ amplitude shown for this individual. A seasonal signal is retained in the sinusoidal oxygen isotope profile of CV28 and the $\delta^{13}C_{apa}$ series for this specimen increases as the $\delta^{18}O_{apa}$ values peak. The convergence of high carbon and oxygen isotope ratios shown for CV28 is likely a reflection of the individual ingesting ^{18}O-enriched meteoric water via plants with higher $\delta^{13}C$ values during the summer's hot, arid conditions (Gat 1996; Kohn 2010; Stewart et al. 1995).

BB154 and SMI338 were two specimens determined to have irregular $\delta^{18}O_{apa}$ sequences on the basis of variation of the first derivative function of the oxygen isotope profile (Figure 9.7). A moderate positive correlation exists between the carbon and oxygen isotope profiles of BB154 (Table 8.5). The simultaneous decreases in $\delta^{18}O_{apa}$ and $\delta^{13}C_{apa}$

shown in BB154 were interpreted as a rapid change from an open to closed environment and ingestion of ^{18}O-depleted water from a buffered source such as a spring (see Chapter Eight). The negative correlation between $\delta^{13}C_{apa}$ and $\delta^{18}O_{apa}$ of SMI338 is due to the dampened $\delta^{13}C_{apa}$ variation spanning a trough in the $\delta^{18}O_{apa}$ series and the sharp divergence of these values in the most recently formed enamel (Figure 8.10). The $\delta^{13}C_{apa}$ value (-1.3‰) in the most recently formed enamel exceeds the range expected from a diet of purely C_3 plants (Figure 8.8). SMI338 was therefore not likely to have been part of a migratory herd but instead was foddered with a variety of C_3 plants and towards the end of life, consumed a highly ^{13}C-enriched diet, possibly including C_4 plants or seagrasses. This foddering strategy likely explains the sequences of SMI130 and BB135 which exhibit sharp increases in $\delta^{13}C_{apa}$ corresponding with low $\delta^{18}O_{apa}$ values (Figure 9.9).

1. Pokrovnik

Inter-individual variation in $\delta^{18}O_{apa}$ among the Impresso and Danilo period specimens from Pokrovnik suggests herders engaged in a more mobile strategy (Julien et al. 2012) than herders at other contemporary sites (see Chapter Eight). Several specimens from Pokrovnik exhibit attenuated intra-tooth $\delta^{18}O_{apa}$ profiles (Impresso: PK90, PK92, PK93; Danilo: PK95). Two individuals were identified as outliers with high variance of the rate of change within intra-tooth $\delta^{18}O_{apa}$ (Impresso PK99 and Danilo PK88). Anti-covariation was found between the carbon and oxygen isotope sequences of Impresso PK101 and weak positive correlations found for Impresso PK72 and Danilo PK87 (Figure 9.10 and Figure 9.11).

The oxygen isotope profiles for four Pokrovnik specimens are clearly dampened relative to others from the same period (see PK90, PK92, and PK93 in Figure 9.10; see PK95 in Figure 9.11). The amplitudes of variation of $\delta^{18}O_{apa}$ of PK90, PK92, and PK93 are 0.7‰

to 1.8‰ lower than the mean amplitude for Impresso Pokrovnik (2.9‰) and the amplitude of PK95 is 1.8‰ lower than the Danilo Pokrovnik average (3.7‰; Table 8.6). Considering the modeled difference in $\delta^{18}O_{apa}$ amplitude for stationary versus transhumant animals (i.e., 1.3-1.5‰; Figure 9.2), the low-amplitude environmental signals in the $\delta^{18}O_{apa}$ profiles of PK90, PK93, and PK95 may reflect seasonal movements between Pokrovnik (265 masl) and pastures in the nearby Dinara mountains (1200-1500 masl).

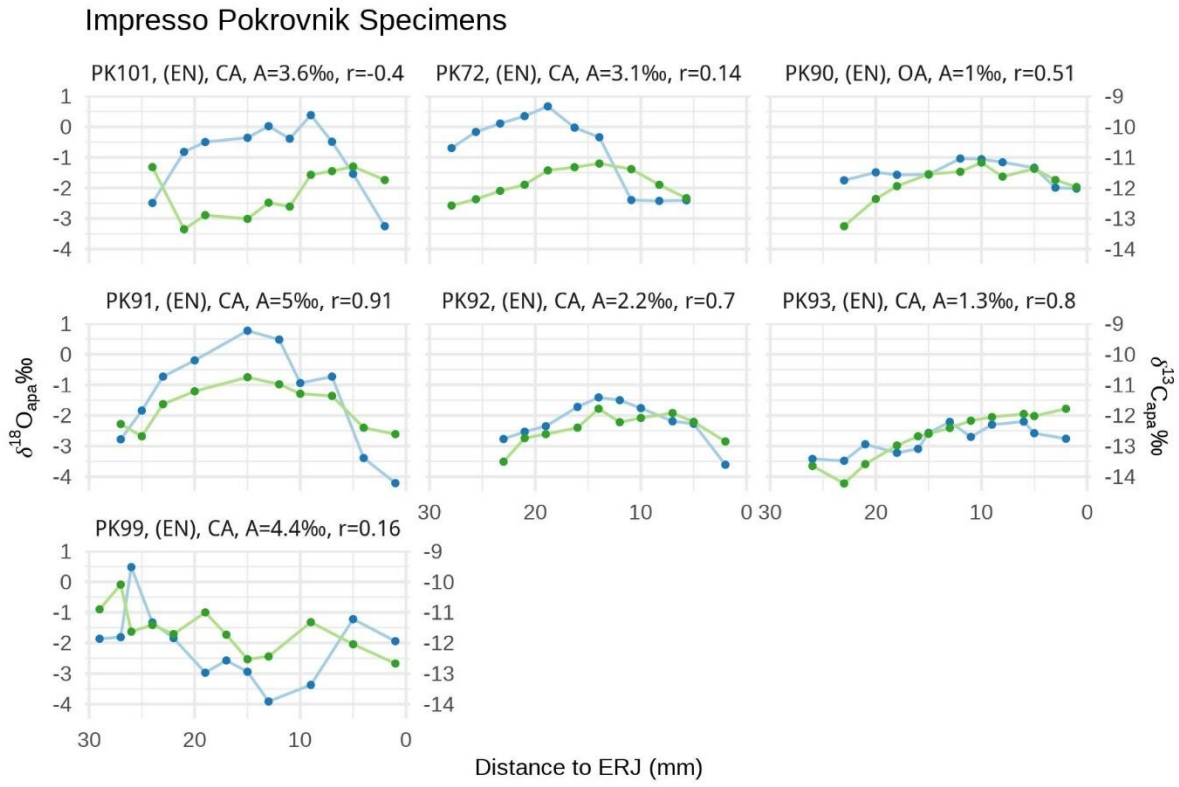

Figure 9.10. Intra-tooth $\delta^{18}O_{apa}$ (blue) and $\delta^{13}C_{apa}$ (green) sequences of Impresso individuals from Pokrovnik. Individual plot titles identify the specimen, period (EN=Impresso/Early Neolithic), species (OA=sheep; CA=goat; OC=ovicaprid), amplitude of $\delta^{18}O_{apa}$ variation (A), and Pearson's correlation coefficient (r) calculating covariance between the carbon and oxygen sequences.

However, a moderate positive correlation is shown for the carbon and oxygen isotope values of PK90 and significant positive correlations shown for PK92, PK93, and PK95 (Table 8.6). Oxygen isotope profiles that are sinusoidal and covary with the $\delta^{13}C_{apa}$ series are

indicative of restricted mobility as animals consume plants whose variation in $\delta^{13}C$ and $\delta^{18}O$ in leaf water varied seasonally (Lazzerini et al. 2021). But variation within oxygen isotope profiles of these individuals is attenuated, and the seasonal signal in $\delta^{18}O_{apa}$ may have been extinguished as result of being herded between low and high altitude environments (Britton et al. 2009; Pellegrini et al. 2008) or ingestion of buffered water sources (Henton et al. 2014). An alternative explanation for the positive correlation between the oxygen and carbon isotope ratios for PK92, PK93, and PK95 is that these animals grazed on pastures within a restricted range of elevation near buffered water sources (Henton et al. 2014; Pellegrini et al. 2008). This could explain dampened intra-tooth $\delta^{18}O_{apa}$ variation if body water was obtained from a buffered source of water such as a spring, pond, or stream which are mainly recharged by groundwater in karst environments (Bonacci et al. 2019). Indeed, excavators suggest that the village at Pokrovnik was established in its location to take advantage of the bountiful Pećina spring adjacent to the site (Moore et al. 2019: 19).

The isotopic composition of meteoric groundwater typically mirrors mean precipitation $\delta^{18}O$ over the catchment area. However, selection effects (i.e., the preferential movement or retention of heavier or lighter isotopes within the groundwater system due to evaporation, recharge, biological activity, and rock-water interaction) can lead to the enrichment or depletion in ^{18}O of groundwater relative to mean precipitation $\delta^{18}O$ (Gat 1981a: 223–224). In temperate climates, the depletion of groundwater relative to precipitation and the extinguishing of seasonal variation has been attributed to selection in favor of winter rainfall (Gat 1981a: 225). This situation could explain the more negative $\delta^{18}O_{apa}$ values observed for PK92, PK93, and PK95 relative to Pokrovnik individuals from the same period. The positive correlation between the carbon and oxygen isotope series of

PK90 is of moderate strength (Pearson's r = 0.51). As was the case for modern specimen DIN7 (Figure 9.4), the oxygen isotope profile of PK90 is flattened but a weak environmental signal is shown in the carbon isotope profile. The gradual increase in $\delta^{13}C_{apa}$ values of approximately 2‰ from the earliest formed enamel to the peak value of -11.2‰ at 10 mm from the ERJ (Figure 9.10) may potentially be attributed to ^{13}C-enrichment in C_3 plants of approximately 1.2‰ per 1000 m gain in elevation (Körner et al. 1988; 1991). While vertical transhumance is a somewhat tenuous explanation for the attenuated variation of intra-tooth $\delta^{18}O_{apa}$ in PK92, PK93, and PK95, it is more tenable for PK90.

Two Impresso (PK72 and PK99) and two Danilo Pokrovnik (PK54 and PK87) specimens feature carbon and oxygen isotope profiles with weak positive correlation. Impresso specimen PK72 exhibits seasonal $\delta^{18}O_{apa}$ variation but weakly positive correlation with $\delta^{13}C_{apa}$. A gradual increase in the $\delta^{18}O_{apa}$ values is observed in the earliest enamel formed for PK72 but after achieving a peak value of 0.7‰ at 18.81 mm from the ERJ, the series begins to decrease, reaching a minimum at 10.91 mm. This 3.1‰ drop in the $\delta^{18}O_{apa}$ occurs swiftly relative to the gradual decrease in $\delta^{13}C_{apa}$, a trend which continues as corresponding $\delta^{18}O_{apa}$ stabilizes around -2.4‰ (Figure 9.10). The plateauing of low $\delta^{18}O_{apa}$ in the most recently formed enamel corresponds with decreasing $\delta^{13}C_{apa}$; the seasonal signal in the carbon isotope profile in this region of the tooth is associated with an extinguished seasonal signal in the oxygen isotope profile. This pattern suggests that PK72 was herded around a buffered water source characterized by lower $\delta^{18}O_{apa}$ values.

The patterns of PK99's intra-tooth $\delta^{18}O_{apa}$ and $\delta^{13}C_{apa}$ are unique from the other Impresso specimens (Figure 9.10). In addition to weak correlation in carbon and oxygen isotope sequences, PK99 was also identified as having an outlier based on the rate of change

in the intra-tooth $\delta^{18}O_{apa}$ series. The disrupted seasonal signal in the $\delta^{18}O_{apa}$ sequence of PK99 is manifested as a sharp, 2.3‰ increase in $\delta^{18}O_{apa}$, followed by a rapid decrease of 1.8‰ as the sequence gradually descends to the minimum value of -3.9‰ at around 13 mm from the ERJ. This peak, reflecting a rapid increase in meteoric water ^{18}O-enrichment occurs at 26 mm from the ERJ, relatively early in this individual's life. This pattern reflects movements between environments characterized by very different precipitation regimes. The undulating and sometimes inversely related trajectories of $\delta^{18}O_{apa}$ and $\delta^{13}C_{apa}$ are difficult to explain. However, the oxygen isotope profile exhibits a similar pattern to the progression of precipitation $\delta^{18}O$ modeled for the rapid vertical transhumance strategy (Figure 9.3).

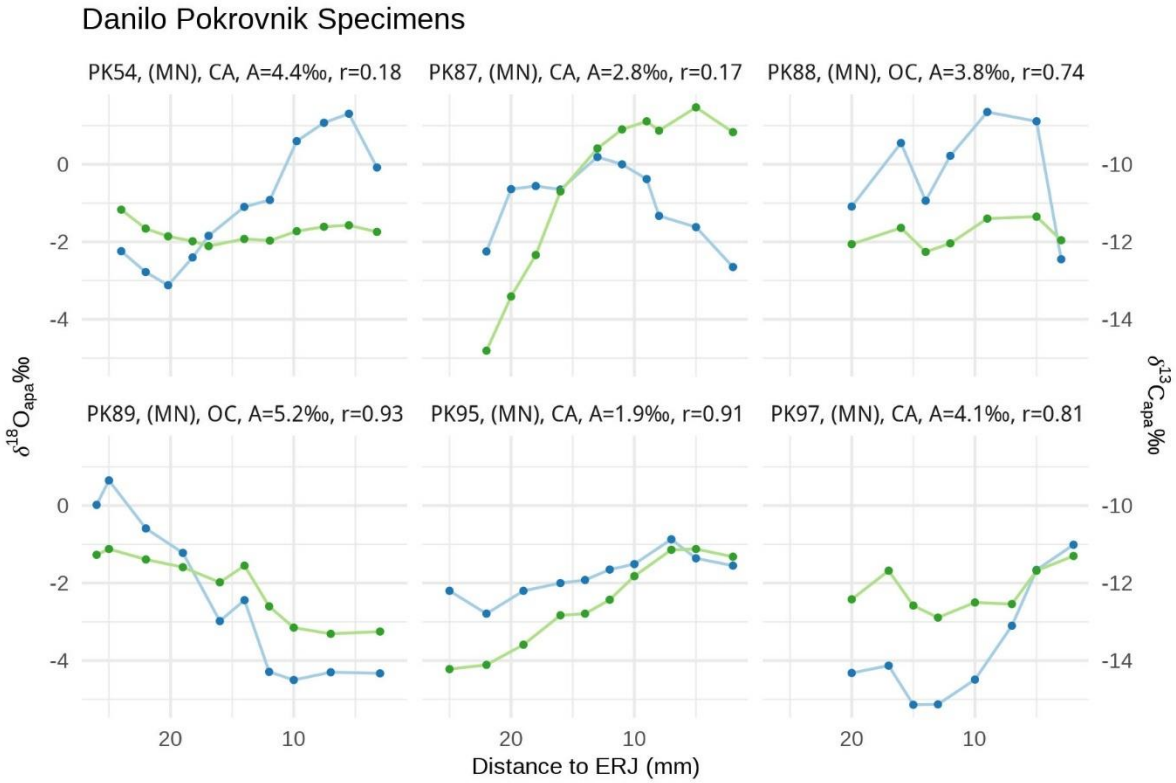

Figure 9.11. Intra-tooth $\delta^{18}O_{apa}$ (blue) and $\delta^{13}C_{apa}$ (green) sequences of Danilo individuals from Pokrovnik. Individual plot titles identify the specimen, period (MN=Danilo/Middle Neolithic), species (OA=sheep; CA=goat; OC=ovicaprid), amplitude of $\delta^{18}O_{apa}$ variation (A), and Pearson's correlation coefficient (r) calculating covariance between the carbon and oxygen sequences.

Danilo specimens PK54 and PK87 (Figure 9.11) also exhibit weak positive correlation between oxygen and carbon isotope ratios (Table 8.5). For PK54 the intra-tooth $\delta^{13}C_{apa}$ sequence does follow the seasonal signal reflected by the sinusoidal pattern of $\delta^{18}O_{apa}$ values. Meanwhile, a weak seasonal signal is recorded in the $\delta^{18}O_{apa}$ values for PK87 while the range of $\delta^{13}C_{apa}$ for this specimen is larger relative to other Danilo specimens (Figure 8.8D). PK89 also shows a plateau in its oxygen profile which begins at 12 mm from the ERJ, where $\delta^{18}O_{apa}$ ranges from -4.3 to -4.5‰ along the last 9 mm of enamel sampled (Figure 9.10). However, the values in the plateaued section of the oxygen isotope profile overlap with the range of minimum $\delta^{18}O_{apa}$ observed in PK97 which exhibits a seasonal signal in their intra-tooth $\delta^{18}O_{apa}$. This suggests that there may have been buffered source of water not far from the settlement at Pokrovnik that was occasionally exploited by herders. Additionally, based on the above observation, one might suggest that the sections of enamel closest to the ERJ in these specimens were formed in the late autumn during the onset of colder weather leading up to the winter. If true, disruptions in the preceding oxygen isotope profile may reflect feeding behaviors during the late spring and summer, which is when transhumant herders in Dalmatia utilized pastures in the Dinara mountains (Marković 1975; 1987; Nimac 1940).

Transhumant pastoralists in Dalmatia preferred mountain pastures that feature springs or lakes where animals can access water (Marković 1975; 1987; Nimac 1940). These water sources are expected to be the most depleted in ^{18}O due to the subdued strength of evaporation in colder climates and the preferential removal of heavier oxygen isotopes during rain out as cloud masses move inland (Gat 1980). Additionally, spring water is generally more depleted than open surface waters which are not shielded from evaporation even at high

altitudes (Brkić et al. 2020; Gat 1981a). This is corroborated by samples collected from the source spring of Lake Šator and the lake itself in the Dinara mountains at 1437 masl (Appendix D). It is therefore possible that rapid decreases in $\delta^{18}O_{apa}$ observed in PK88 and PK89 reflect differences between lowland elevation precipitation $\delta^{18}O$ and high elevation spring water $\delta^{18}O$. However, carbon and oxygen isotope profiles in PK88 and PK89 covary with strong positive correlations (Table 8.5) suggesting a more stationary herd management strategy.

In PK101, the directionality of intra-tooth changes in $\delta^{13}C_{apa}$ and $\delta^{18}O_{apa}$ diverge along the length of this specimen's tooth (Figure 9.10); high $\delta^{18}O_{apa}$ corresponds with low $\delta^{13}C_{apa}$, which could reflect a ^{13}C-depleted diet during the summer. One explanation for the inversely related changes in oxygen and carbon compositions in PK101 is that fodder consisting of winter crop by-products and possibly other ^{13}C-depleted vegetation (e.g., understory plants collected from forested areas during the winter) was provisioned during the summer. Herders will sometimes retain surplus winter crop byproducts to use as fodder in response to low summer pasture productivity (Halstead 1998a). However, this strategy would require the collection and storage of immense quantities of winter fodder to sustain even a small herd throughout the summer. Smaller volumes of fodder could be sufficient to feed lambs and kids but herders might then opt to slaughter young animals early to allow reproductive females to fatten in the months leading up to the autumn mating season. Additionally, the ability for a herd to recover after losses due to starvation would be less impacted by slaughtering lambs and kids at higher rates than reproductive animals that were properly fed during a summer drought. Moreover, unless herds exclusively consumed ^{13}C-depleted winter fodder during the summertime, consumption of a combination of winter

fodder and naturally occurring plants with seasonally high $\delta^{13}C$ would be expected to dampen intra-tooth $\delta^{13}C_{apa}$ variation (Chase et al. 2014; Zazzo et al. 2010). But the carbon isotope profile of PK101 exhibits a seasonal signal and the amplitude of intra-tooth $\delta^{13}C$ variation (2.0‰) is equal to the mean amplitude of the Impresso Pokrovnik samples. Therefore, the contribution of fodder to this individual's diet was likely negligible.

An alternative interpretation of the inversely related carbon and oxygen profiles for PK101 is that the high $\delta^{18}O_{apa}$ values reflect water ingested in the lowlands, and low $\delta^{18}O$ precipitation was incorporated through a diet consumed at high elevations. The amplitude of $\delta^{18}O_{apa}$ variation for PK101 is 1.4‰ lower than that of PK91, whose oxygen isotope profile exhibits a seasonal signal, covaries with the carbon isotope profile (Figure 9.10) and indicates limited mobility. If typical seasonal variation in precipitation $\delta^{18}O$ and plant $\delta^{13}C$ at Pokrovnik is reflected in the PK91 carbon and oxygen profiles, then vertical transhumance may explain the anti-covariation of $\delta^{18}O_{apa}$ and $\delta^{13}C_{apa}$ of PK101.

Wetter conditions are associated with more negative $\delta^{13}C$ values in C_3 plants (Kohn 2010; Smedley et al. 1991; Stewart et al. 1995) and the highest levels of rainfall occur in Dalmatia from September through January (Figure 3.2). It is possible that low $\delta^{13}C_{apa}$ in PK101 is a result of higher levels of precipitation experienced during the autumn and early winter. Additionally, increasing altitude is associated with ^{13}C-enrichment in C_3 plants (Körner et al. 1988; 1991) and higher $\delta^{13}C_{apa}$ values are only observed where this individual's $\delta^{18}O_{apa}$ decreases. The onset of higher summer temperatures, drier conditions, and associated ^{13}C-enrichment of C_3 plants $\delta^{13}C$ increases (Tieszen 1991) could be reflected in the gradual increase of $\delta^{13}C_{apa}$ values in PK101, from -12.6‰ beginning at 11 mm from the ERJ (Figure 9.10). Thereafter, $\delta^{13}C_{apa}$ values increase at a very slow rate, potentially

reflecting the modest 1.2‰ $\delta^{13}C$ increase in C_3 plants per 1000 m elevation gain (Körner et al. 1988; 1991). In this scenario, the low $\delta^{18}O_{apa}$ in the most recently formed enamel (i.e., from 10 to 0 mm from the ERJ) would then reflect the ingestion of ^{18}O-depleted water via grazing in Dinara mountain pastures.

Anti-covariation of carbon and oxygen isotope profiles seen in studies of ancient caprine management has been proposed as a means for identifying vertical transhumance (Chase et al. 2014; Lazzerini et al. 2021; Makarewicz and Pederzani 2017). Vertical transhumance was proposed to explain similar patterns of diverging carbon and oxygen isotope ratios observed in sequentially sampled enamel of caprines from archaeological contexts in Jordan (Makarewicz 2017), central Anatolia (Makarewicz et al. 2017), and the Central Pyrenees (Tejedor-Rodríguez et al. 2021). The carbon and oxygen isotope sequences of PK101 fits well with these patterns which can therefore be reasonably interpreted as having arisen from vertical transhumance.

2. Velištak

The differences between the amplitudes of $\delta^{18}O_{apa}$ variation of VEL32 and VEL37 and the mean site amplitude for Velištak (2.6‰) is 0.8‰ and 0.6‰, respectively (Table 8.6). The intra-tooth oxygen isotope profile of VEL37 is roughly similar in shape to the modeled $\delta^{18}O$ of precipitation for an individual moving from Zadar to Zavižan (Figure 9.2B). Furthermore, covariance but with a weak positive correlation was detected between the $\delta^{13}C_{apa}$ and $\delta^{18}O_{apa}$ of VEL37 which as explained earlier might be associated with dampening of the environmental signal as individuals move through different precipitation $\delta^{18}O$ regimes (Pellegrini et al 2008). It is therefore possible that this individual was rapidly herded from Velištak (95 masl) to upland pastures in the Dinara. On the other hand, the carbon and

oxygen isotope profile of VEL37 is limited to only 7 measurements so it is unclear whether the environmental signal is truncated or reflects a full year of seasonal variation in meteoric water $\delta^{18}O$. Meanwhile, peak $\delta^{18}O_{apa}$ values in VEL32 coincide with $\delta^{13}C_{apa}$ values exceeding -9.5‰ which was defined as the upper limit of a purely C_3 diet in enamel bioapatite after accounting for c. 14‰ enrichment (Cerling and Harris 1999; Passey et al. 2005; Zazzo et al. 2010). Since C_4 plants are in very low abundance in southeastern Europe (Collins and Jones 1985; Pyankov et al. 2010) it is likely that VEL32 was foddered with C_4 plants such as millet during the summertime.

Each Velištak specimen is unique, and only in VEL32 is there a significant correlation between the carbon profile and the low-amplitude oxygen profile (Figure 9.12). VEL29 exhibits a seasonal $\delta^{18}O$ signal but out-of-season contributions to the diet are reflected in the earliest formed enamel where $\delta^{13}C_{apa}$ deviates from the expected seasonal pattern. The weak positively correlated carbon and oxygen profiles seen in the remaining specimens from Velištak is difficult to explain (i.e., VEL28, VEL29, and VEL37) as both isotope ratio sequences are highly irregular. On the one hand, irregularity of $\delta^{18}O_{apa}$ values seen in VEL28 and VEL37 indicates changes in the ^{18}O-enrichment of imbibed water. This irregularity may be contrasted with low-amplitude $\delta^{13}C_{apa}$ sequences observed in other specimens which was attributed to a homogenized diet characteristic of mixed fodder crops and forage.

The inter-individual differences observed among Velištak teeth may have been driven by the exploitation of a wider variety of dietary resources as well as fairly regular horizontal or vertical movements across the landscape (Julien et al. 2012). The irregularity observed in VEL28 and VEL37 also bears some resemblance to the modeled exposure to precipitation

$\delta^{18}O$ presented in Figure 9.2. It is not unreasonable to suspect that intra-tooth variation observed in the Veliš̌tak data reflects vertical transhumance. However, these conclusions must remain unverified until they can be compared with a more robust comparative dataset generated from modern specimens whose movements are more carefully monitored than the modern teeth used here.

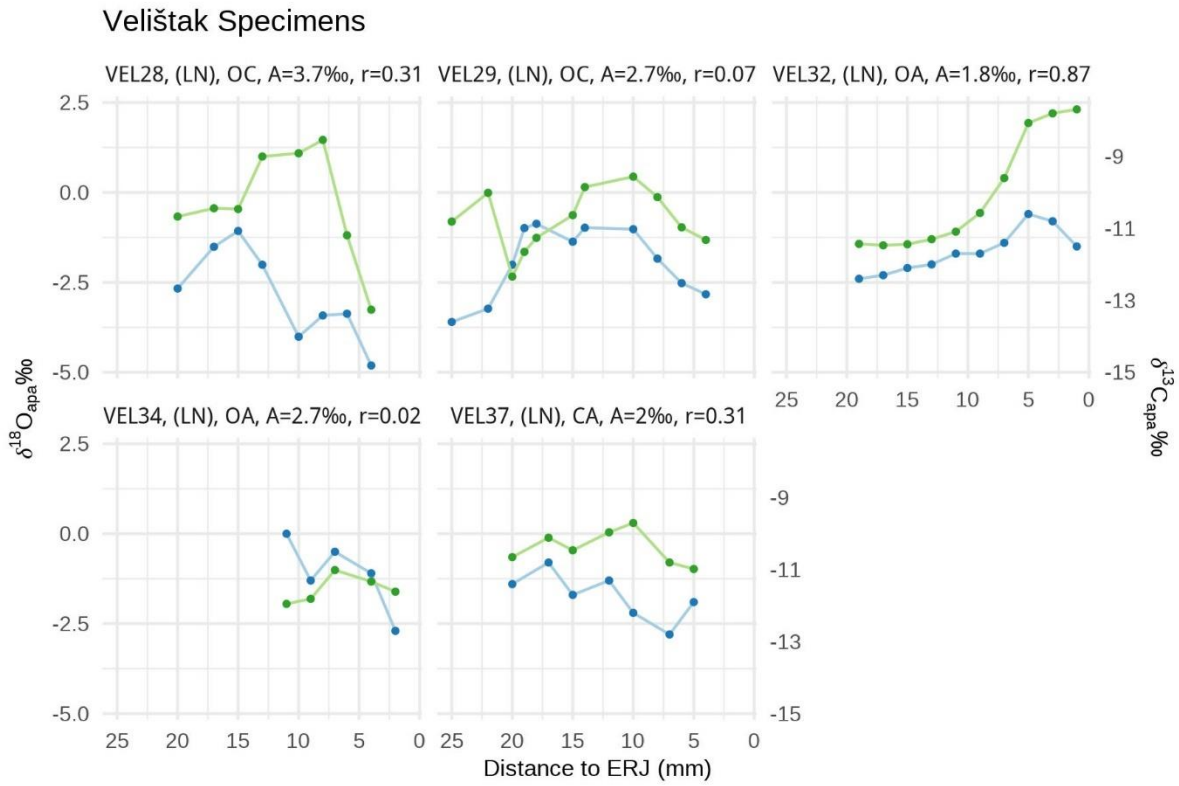

Figure 9.12. Intra-tooth $\delta^{18}O_{apa}$ (blue) and $\delta^{13}C_{apa}$ (green) sequences of Hvar individuals from Veliš̌tak. Individual plot titles identify the specimen, period (LN=Hvar/Late Neolithic), species (OA=sheep; CA=goat; OC=ovicaprid), amplitude of $\delta^{18}O_{apa}$ variation (A), and Pearson's correlation coefficient (r) calculating covariance between the carbon and oxygen sequences.

G. Summary

Distinct patterns of herd management emerge via the analysis of archaeological intra-tooth $\delta^{18}O_{apa}$ and $\delta^{13}C_{apa}$ profiles. Some specimens from Pokrovnik and Veliš̌tak provide compelling evidence of mobile herding. The strongest evidence that Impresso period herders

utilized summer pastures in the Dinara mountains is shown in PK101. Anti-covariation is expressed as the inverse trajectories of carbon and oxygen isotope profiles—a pattern shared with modern and archaeological specimens that has been interpreted to be a result of a vertical transhumant herding strategy (Chase et al. 2014; Lazzerini et al. 2021; Makarewicz 2017; Makarewicz et al. 2017; Makarewicz and Pederzani 2017).

Attenuated intra-tooth $\delta^{18}O_{apa}$ variation in several other specimens from the Impresso (PK90, PK92, and PK93) and Danilo periods (PK95) is possibly due to movements between Pokrovnik and higher-elevation pastures. Dampened oxygen isotope profiles observed in sequential enamel bioapatite samples has been interpreted as evidence for migratory behaviors in wild (Britton et al. 2009; Pellegrini et al. 2008) and managed species (Henton et al. 2014). Specimen PK99, on the other hand, shows a disrupted seasonal signal in $\delta^{18}O_{apa}$, indicating abrupt environmental changes likely associated with movements between regions with different precipitation regimes. Further observations in specimens PK54, PK72, PK87, and PK89 suggest the presence of localized water sources, potentially indicating stationary herd management centralized near the village settlement at Pokrovnik. Overall, the inter-individual variability among the Pokrovnik specimens indicates that a variety of herding strategies, likely involving horizontal or vertical mobility were practiced throughout the Impresso and Danilo periods.

With respect to the rather limited Velištak dataset, specimens VEL32 and VEL37 reveal intra-tooth isotopic patterns that might indicate rapid movements to upland pastures. The weak seasonal signal in the $\delta^{18}O_{apa}$ sequence of VEL32 could indicate movements through environments characterized by different levels of precipitation ^{18}O-enrichment while high $\delta^{13}C_{apa}$ values point to the consumption of C_4 plants, possibly including millet.

Meanwhile, VEL37 exhibits an irregular and disrupted intra-tooth $\delta^{18}O_{apa}$ sequence that resembles the monthly $\delta^{18}O$ precipitation modeled for rapid transitions between low and high-altitude pastures (i.e., the rapid transhumance model; Figure 9.3). However, irregular $\delta^{18}O_{apa}$ sequences and weak correlations with $\delta^{13}C_{apa}$ in other specimens (e.g., VEL28, VEL29, and VEL37) hint at complex movement patterns, possibly involving both horizontal and vertical transhumance.

The Pokrovnik and Veliš̌tak data point to diverse and dynamic herding practices, with some individuals showing clear signs of transhumance that manifest as different patterns of intra-tooth $\delta^{13}C_{apa}$ and $\delta^{18}O_{apa}$ profiles. If herders only engaged in strategies that exploited strictly localized pastures and forage, intra-individual variation would likely be reduced (Julien et al. 2012). Both datasets are characterized by inter-individual variability which may therefore be interpreted as distinct herding strategies. It is important to note that the strongest evidence for vertical transhumance is limited to only a few individuals from Pokrovnik. Since the modern comparative dataset presented here is limited, it is unclear precisely how vertical transhumance between the Ravni Kotari and Velebit pastures would be imprinted in intra-tooth carbon and oxygen isotope profiles. However, the oxygen isotope profiles for multiple specimens closely resemble the modeled fluctuations in meteoric water $\delta^{18}O$ for the rapid transhumance model.

At a minimum, the research presented in this chapter demonstrates that vertical transhumance was likely an important strategy that herders employed to a limited extent. Seasonal visitation of mountain pastures would have minimized the risk of reduced herd productivity and herd losses during summer drought conditions. Future research should focus on expanding the sample size for Pokrovnik and improving the quality of the modern

comparative data by obtaining samples from herds with well-documented movement and dietary patterns. Lastly, this sort of analysis should be completed on samples recovered from Neolithic deposits in Velebit cave sites to understand whether or not these sites were utilized as part of a transhumant strategy as has long been suspected (Forenbaher 2007; 2022; Forenbaher and Miracle 2014).

X. Lambing and Kidding Seasonality in Neolithic Dalmatia

A. Preface

The preceding chapters focus on the viability of herds under different culling regimes (Chapter Six), how the dietary needs of herds were met (Chapter Eight), and the extent of mobility in Neolithic herding in Dalmatia (Chapter Nine). This chapter examines one final aspect of livestock husbandry: birth seasonality. Among some mammalian species adapted to environments where seasonal variation in climate influences the abundance and quality of dietary resources, reproductive cycles are synchronized to climatic cues to metabolically prepare females for pregnancy (Bronson and Heideman 1994). For goats and sheep, the onset and duration of breeding cycles respond to seasonal changes in photoperiod (i.e. daylength) and temperature (Chemineau et al. 1992; Hafez 1952; Paranhos da Costa et al. 1992; Rosa and Bryant 2003; Yeates 1949). Although the duration of the reproductive season varies between breeds, ewes and does enter estrous when daylength begins to decrease and end estrus when daylength increases (Thimonier 1981). Due to the high metabolic costs of lactation and pregnancy (Clutton-Brock et al. 1989), the nutritional status of reproductive ewes and does is a key variable affecting the survival of lamb and kid neonates (Dwyer et al. 2016).

In the Mediterranean, including the Eastern Adriatic, precipitation levels are highest

during the autumn and spring (Figure 3.2), so dry summers lead to low autumn and high spring forage availability. In middle and high latitudes, including temperate Europe and parts of the Mediterranean, daylength decreases during the autumn, and the birthing season in sheep and goats accordingly coincides with the spring (Hafez 1952). The seasonality of sheep and goat reproduction has practical implications for the scheduling of agropastoral activities and constrains the availability of animal products throughout the year. For example, access to fresh milk would begin with the onset of the lambing/kidding season in the spring. Herders would also need to incorporate milking into daily routines from the time that lambs and kids are weaned to the end of lactation. This period typically lasts 3-4 months (Dahl and Hjort 1976) but some pastoral communities rely on a milking season of 6 months duration (Nitsiakos 1985).

Strategies to extend the duration of the milking season may have developed among early herding systems that relied heavily on diary production. The slaughter of male and surplus female kids and lambs of pre-weaning age is meant to increase the availability of milk for human consumption (Payne 1973). Breaking the infant-mother bond prematurely can lead to lactational cessation in cattle but the flow of milk in sheep and goats is less dependent on the secretion of oxytocin initiated by infant suckling than stimulation of udders during milking (Marnet and McKusick 2001). Dependency on the presence of infants for continued lactation is therefore less of a concern for dairy production in sheep and goat husbandry than it is for cattle management (Balasse 2003). Nonetheless, steps must be taken to ensure that the flow of milk from nursing females is sustained. Some herding communities delay the slaughter of suckling young until warmer weather brings better quality pasture, leading to greater volumes of more nutritious milk (Halstead 1998b). Additionally,

staggering herd reproduction by separating herds can allow herders to schedule early and late lambing seasons, thereby increasing the periodicity of access to milk or tender meat via the slaughter of infants without risk to the milk supply (Halstead 1998b: 8).

The main birthing season tends to be the spring among sheep and goat breeds originating from latitudes north of 40° but some modern sheep production systems in the Mediterranean manipulate reproductive cycles to exploit the capacity of some breeds for autumn lambing (Balasse et al. 2023; Todaro et al. 2015). Aseasonal breeding primarily relies on the "ram effect" (Watson and Radford 1960) which entails separation of flocks and carefully scheduled introduction of rams to anestrous ewes (Todaro et al. 2015). This strategy has been shown to advance the breeding period by 4-6 weeks, induce early first ovulation in young females, and in some cases extend the breeding season by three weeks (Rosa and Bryant 2002). While the term "ram effect" is primarily used to describe manipulation of sheep breeding cycles, the acute reproductive responses of females to the exposure of males has been shown in other species including goats (e.g., Amoah and Bryant 1984; Walkden-Brown and Restall 1993). Recent work has shown that the ram effect can be effective among sheep breeds that tend to lamb during the spring, suggesting that this strategy could have been used during the Neolithic to manipulate the reproductive seasonality of unimproved sheep breeds (Balasse et al. 2023; Fabre et al. 2023).

In terms of production and in the context of Neolithic agropastoral subsistence economies, there are clear advantages to manipulating the reproductive behavior of sheep and goats. Among them are extending the duration or increasing the periodicity of milking seasons and availability of tender meat via slaughter of young animals. Previous research has demonstrated that the primary lambing season of sheep raised by Impresso period herders at

two sites in Northern Dalmatia, Crno Vrilo and Tinj, was early winter (Sierra et al. 2023) which is typically associated with a second period of lambing in the autumn in the Western Mediterranean (Tejedor-Rodríguez et al. 2021; Tornero et al. 2020). In this chapter, the results of incremental stable isotope analysis of enamel bioapatite samples recovered from Impresso, Danilo, and Hvar-period archaeological sites in Dalmatia are used to model season of birth. Examining birth seasonality on a diachronic scale provides insight into developments within early agropastoral subsistence systems. In the following sections I provide an overview of how birth season is estimated by modeling intra-tooth $\delta^{18}O_{apa}$ series and comparison with modern reference sets. I then describe the results, followed by a discussion of the implications for managing risk within Neolithic agropastoral subsistence economies.

B. Modelling Season of Birth

In sheep and goats, the lower M2 molar forms completely during the first year of life (Kierdorf et al. 2012; Milhaud and Nezit 1991; Weinreb and Sharav 1964; Zazzo et al. 2010). During this time, seasonal variation in the ^{18}O-enrichment of meteoric water ($\delta^{18}O_{ew}$) is recorded in the isotopic composition of the enamel bioapatite as it incorporates body water (Fry and Arnold 1982). Since the timing of tooth eruption and mineralization is fixed within species and similar for goats and sheep, the positions of peaks and troughs within intra-tooth $\delta^{18}O_{apa}$ profiles should correspond among individuals born during the same time of the year (Balasse et al. 2012b; Tornero et al. 2016: 812). The M2 is preferable for reconstructing birth seasonality (Tornero et al. 2013) as the M3 exhibits greater inter-individual variability in the timing of tooth formation (Blaise and Balasse 2011; Zazzo et al. 2010). Nonetheless, it is

necessary to normalize the data to the periodic cycle in the measured $\delta^{18}O$ values of M2 molars to account for potential variability in tooth size and different rates of enamel maturation from one individual to the next (Balasse et al. 2012b; 2020; Blaise and Balasse 2011; Zazzo et al. 2010).

Intra-tooth $\delta^{18}O_{apa}$ series of the archaeological specimens were modeled using an equation derived from a cosine function (Balasse et al. 2012b). The cosine model predicts the mean (*M*) and amplitude (*A*) of the environmental signal in the $\delta^{18}O$ series, in addition to the position on the tooth with the maximum $\delta^{18}O_{apa}$ value (x_0), and the period of the cycle (*X*) which refers to the length of the tooth where a full annual cycle is represented in the measured $\delta^{18}O_{apa}$ values (Balasse et al. 2012b; 2020). Eliminating inter-individual variation in tooth size is achieved by normalizing x_0 to the length of the tooth potentially formed in one year as the ratio x_0/X, which gives a reference for the individual's birth date (Balasse et al. 2012b; 2020; 2023). The model is as follows:

$$\delta^{18}O_m = A \times e^{\left(\frac{x-x_B}{x_A}\right)} \times \cos\left(2\pi\frac{x-x_0}{X+bx}\right) + M + px \quad (10.1)$$

where $\delta^{18}O_m$ is the modeled $\delta^{18}O$ value and *x* is the distance from the enamel-root junction (ERJ). Parameters *p* (the slope of the mean in ‰ mm^{-1}), *b* (gradation of the period, unit-less), x_A (the severity of the amplitude of variation in mm), and x_B (the lateral shift in mm) were omitted because they were found to have negligible influence over the modeled $\delta^{18}O$ values for M2 molars (Balasse et al. 2012b). The modified model is thus defined in Equation 10.2 as:

$$\delta^{18}O_m = A \times \cos\left(2\pi\frac{(x-x_0)}{X}\right) + M \qquad (10.2)$$

where variables, *X* (the height of the tooth crown in mm potentially formed over one year,

referred to as the period), *A* (the amplitude of isotopic variation in ‰), *M* (the mean in ‰), and x_0 (the distance from the ERJ in mm giving the highest $\delta^{18}O$ value) are free to vary as the model is fitted to the data via an iterative least squares procedure (Balasse et al. 2012b).

x_0/X ratios fall between 0 and 1, referring to the point in the annual cycle when an individual was born. The annual cycle begins in January and ends in December; when the ratio reaches 1, it also reaches 0 (Balasse et al. 2012b). The ratio is corrected by subtracting or adding 1 when $x_0/X > 1$ or $x_0/X < 0$, respectively. For example, the corrected x_0/X ratio of -0.02 becomes 0.98, corresponding to a late December birth. The length of time over which a sub-set of individuals were born can be estimated by range of x_0/X ratios. For instance, the duration of a lambing season represented by two individuals with x_0/X ratios of 0.96 and 0.04 would be 0.08 year, estimated as 0.08*365 days, or 29 days. It is important to note that x_0/X ratios are reference values for dates of birth and do not necessarily correspond precisely to months. But on a seasonal scale, incorrectly attributing summer births to the winter is unlikely when x_0/X ratios are far enough apart in the annual cycle (Balasse et al. 2023).

Comparison of archaeological x_0/X ratios with ratios of modern reference sheep for which date of birth is known contextualizes the modeled ratios within seasons (Balasse et al. 2012b; 2020). Since x_0/X ratios reflect different points within an annual cycle, the values are plotted on circular graphs to aid interpretation (Balasse et al. 2020). To define the primary period of birth, 66% confidence intervals were calculated around the mean x_0/X ratios for each site and period and individuals with ratios falling outside the 95% confidence interval are considered outliers (Balasse et al. 2020).

A shortcoming of this approach is that the model can only be applied to $\delta^{18}O_{apa}$ sequences where minimum and maximum values are well-identified (Balasse et al. 2012b;

Hadjikoumis et al. 2019). This caveat unfortunately introduces bias against older individuals since occlusal wear reduces the length of the tooth thus limiting the number of samples that can be obtained, potentially resulting the exclusion of animals born in certain seasons (Chazin 2021; Chazin et al. 2019). Additionally, the extent of the parameter space for X, x_0, M, and A must be defined by the researcher, which may lead to unrealistic estimations of X, defined as the length of the tooth formed in one year (Chazin et al. 2019). An alternative method has been developed known as the splitting coalescence estimation method (SCEM) which has been shown to be effective for modeling season of birth using $\delta^{18}O_{apa}$ series that partially capture intra-annual variation in the seasonal signal (Chazin et al. 2019). However, the implementation of the cosine model presented here utilizes bootstrapped parameter estimations thereby producing probability distributions for the x_0/X ratios modeled for each individual (Hermes et al. 2022).

The cosine model shown as Equation 10.2 was fitted to $\delta^{18}O_{apa}$ sequences of archaeological and modern M2 tooth specimens using an adaptation of code published by Hermes et al. (2022) executed in R Statistical Software v4.3.1 (R Core Team 2023). The procedure uses bootstrapped re-sampling of the best fit parameter values to generate probability distributions for the modeled $\delta^{18}O_{apa}$ values and derived x_0/X ratios for each specimen. Model performance was assessed using Pearson's R correlation coefficient with strong positive correlations (>0.91) between observed and predicted $\delta^{18}O$ values (i.e., $\delta^{18}O_m$) indicating closeness of fit.

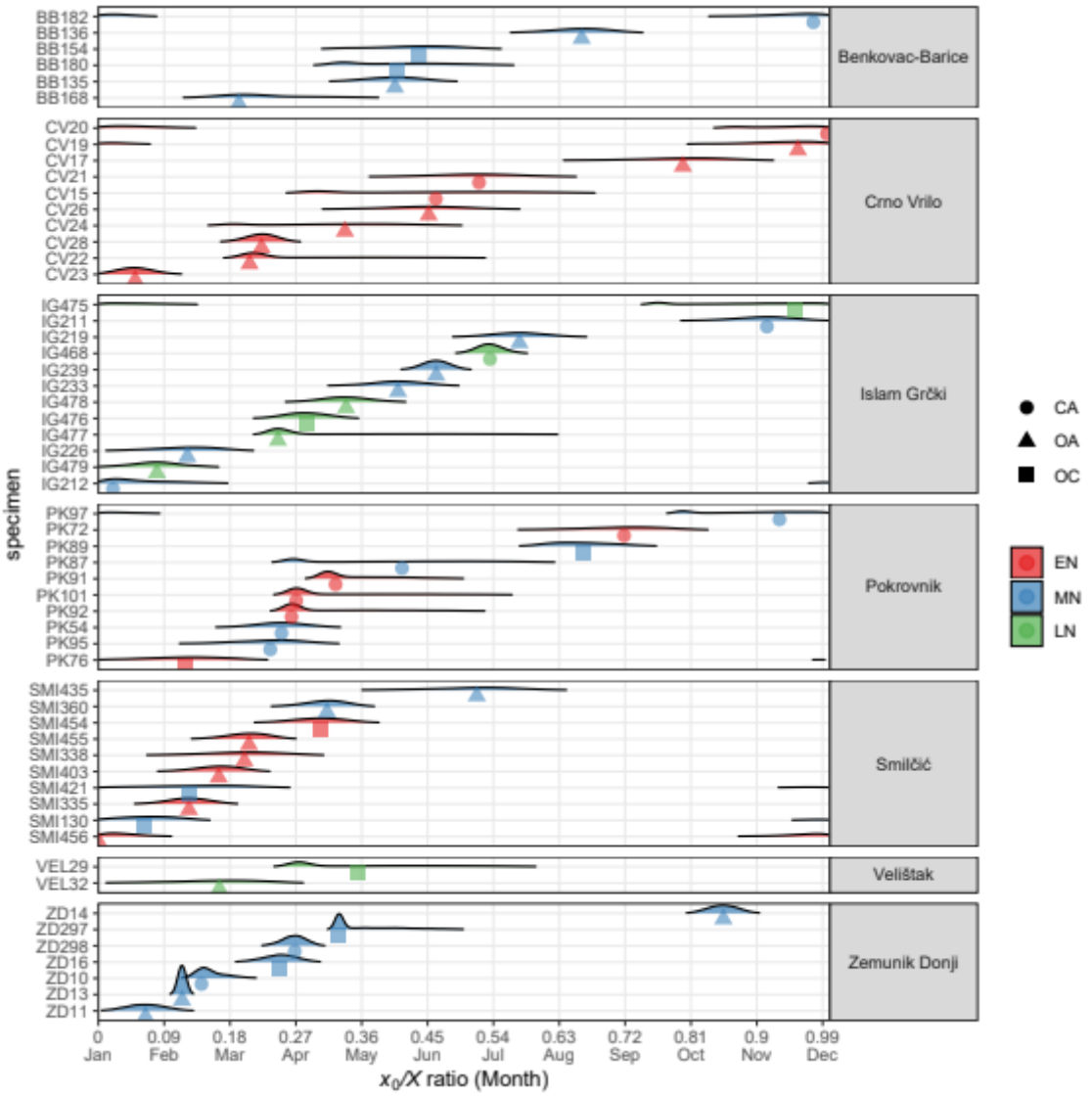

Figure 10.1. Distribution of births and probability distributions of modeled x_0/X ratios generated by bootstrapped sampling of parameter values used in cosine model. Taxon abbreviations are for goats (CA), sheep (OA), and ovicaprid (OC). Period is color-coded to reflect Impresso (EN), Danilo (MN), and Hvar (LN). Figure produced using modified scripting procedures published by Hermes et al (2020). Correspondence between x0/X ratios and months are approximate (Balasse et al. 2020).

C. Birth Seasonality Results

Results of modeling season of birth are provided in Table 10.1 and summarized by site in Table 10.2. Two specimens could not be modeled because the sequences were truncated (CV18 and DIN6). Omitting problematic values within an $\delta^{18}O_{apa}$ series is a common workaround to avoid mischaracterizing season of birth for individuals whose

oxygen isotope profiles exhibit erratic changes at the start or end of a sequence (Balasse et al. 2023). Therefore, the last three subsamples of BB154 (i.e., three samples closest to the occlusal surface) and the first subsample of SMI338 were omitted from modeling because at least one of the values in the sequences interrupted otherwise clear seasonal fluctuations in the oxygen isotope profile.

In this study three reference sets of sequential $\delta^{18}O$ values obtained from M2 molars of modern sheep are used to elucidate more precisely the season of birth of the Neolithic specimens. The reference sets include sheep from Collet-Redon in southeastern France born in the winter and autumn (Blaise and Balasse 2011), sheep born in the spring on Rousay Island in Scotland's Orkney archipelago (Balasse et al. 2012b), and sheep born in October on Corsica (Fabre et al. 2023). The reproduced and previously reported model parameters for the modern reference sets are provided in Appendix J.

Model performance was assessed using Pearson's correlation coefficient to assess goodness of fit of modeled and observed $\delta^{18}O_{apa}$ with Pearson's $r > 0.91$ indicating satisfactory results. The results are considered unreliable for seven specimens that failed to meet this criterion which was likely due to non-sinusoidal (PK88, VEL28, VEL34, and VEL37) or very low amplitude sequences (PK90, PK92, and PK93). The results and discussion focus on the estimated season of birth for the remaining 57 specimens.

The parameter estimates of A, M, x_0, and X generated by the cosine function for the modern reference sheep from Rousay were nearly identical to those reported by Balasse et al. (2012b; Appendix J). The position of the highest $\delta^{18}O_m$ value (i.e., x_0) for ROU 04 was over-estimated by 33.5 mm resulting in an x_0/X ratio of 1.19. Correcting the reproduced x_0/X ratio for ROU 04 by subtracting 1 yields an identical x_0/X ratio to the one reported for this

specimen by Balasse et al. (2012b). This correction procedure was performed on other specimens for which $x_0/X > 1$. For two of the modern Corsica sheep, COR Ovis 4 and COR Ovis 5, model parameters were slightly different from those reported by Fabre et al. (2023) resulting in x_0/X ratios that were underestimated by 0.02 year (or 7 days) and overestimated by 0.01 year (or 4 days), respectively (Appendix J). Greater differences were observed between the reproduced x_0/X ratios for the Carmejane reference set and those reported by Tornero et al. (2013), with the most extreme deviations shown for Ovis 0522 (delta = 0.20 year) and Ovis 1511 (delta = 0.28 year; Appendix J). The reason for these inconsistencies could not be determined. Although there was good agreement between the $\delta^{18}O_{apa}$ of Carmejane sheep and modeled values (Pearson's $r \geq 0.97$; Appendix J), the x_0/X ratios reported by Tornero et al. (2013) are employed to elucidate season of birth of the 57 archaeological specimens. Otherwise, season of birth estimates corresponded to reported values for modern specimens, lending confidence to the reliability of the model's performance when applied to the present dataset.

The annual cycle period (X) is represented by the length of the tooth in mm. The mean of the modeled cycle period for the archaeological specimens is 31.9 mm and a standard deviation of 9.6 mm indicating inter-individual variability in tooth size. This high standard deviation highlights the importance of normalizing the modeled position of the maximum $\delta^{18}O_{apa}$ value (x_0) to the annual cycle period (Balasse et al. 2012b). Modeled seasons of birth for the archaeological specimens are shown in Figure 10.1 with probability distributions of the x_0/X ratios obtained via bootstrapped estimations of parameters X and x_0 (Hermes et al. 2022). Following Balasse et al. (2020), the 66% confidence interval is used to define the main birthing period for each group of specimens (Table 10.2) and outliers

identified using the 95% confidence interval (shown as an 'x' in Figure 10.2). Given the small sample sizes, 66% confidence intervals were obtained via bootstrap re-sampling (n=500) of the x_0/X ratios. The 66% confidence intervals are illustrated alongside x_0/X ratios plotted on circular graphs for each site and period in Figure 10.2.

For the Crno Vrilo specimens the mean period (X) is 29.0 ± 9.6 mm (n=10) and modeled x_0/X ratios are between -0.04 (or 0.96) and 0.80 year (Figure 10.2). Although the main breeding period defined by the 66% confidence interval is 0.13 to 0.27 year, all but two of the modeled x_0/X ratios fall within this range. Three individuals present x_0/X ratios between -0.04 (or 0.96) and 0.15, spanning 0.19 year, or c. 70 days. This range reflects the part of the annual cycle corresponding to the early winter, and was determined to be the main breeding period for this site by Sierra et al. (2023). However, the x_0/X ratios of three other specimens plot opposite to the early winter births and between the ranges of spring-born sheep from Rousay and September-born sheep from Carmejane suggesting these individuals were born in the late spring or summer (Figure 10.2). Additionally, three specimens exhibit x_0/X ratios within the range of the Rousay sheep born in April and May. The x_0/X ratio of CV17 corresponds to the range of October-born sheep from Corsica but a maximum $\delta^{18}O_{apa}$ value is not well-defined in this individual's oxygen isotope profile (Figure 8.10) so the significance of this result remains unclear. Aside from this (rather unlikely) autumn birth, this distribution of births is not dissimilar from what has previously been reported but the concentration of births in the early winter at Crno Vrilo (Sierra et al. 2023) is not demonstrated by these results. This inconsistency may be due to the small sample size in this study since late spring births are also observed in the minority of specimens considered by Sierra et al. (2023).

Mean annual cycle period (X) for Impresso period Pokrovnik specimens (n=6) is 41.8 ± 10.5 mm. The large standard deviation of 10.5 mm suggests considerable inter-individual variability in the timing of M2 growth. In other words, the estimated length of M2 molar growth in one year is highly variable within the Impresso specimens. This is likely due to the model over-estimating the annual cycle period of three specimens (i.e., PK101, PK91 and PK92) for which minimum $\delta^{18}O_{apa}$ values are not clearly identifiable in the downward parabolic profiles of these individuals (Figure 9.10; Table 10.1). The range of x_0/X ratios for the Impresso specimens from Pokrovnik varies between 0.12 and 0.72 year. The main lambing/kidding season was calculated as 0.24 to 0.43 year which spans 0.19 year, or approximately 70 days. The beginning of the main birth season corresponds to the middle of the range of spring births for modern Rousay sheep (Balasse et al. 2012b; Figure 10.2). Notably, the x_0/X ratio for PK72 is 0.72, which falls within the range of modern Carmejane sheep born in the autumn.

The Danilo period specimens from Pokrovnik show less inter-individual variability in the estimated cycle period (mean X = 32.7 ± 5.4 mm) than the Impresso group. The x_0/X ratios for these Middle Neolithic specimens range from -0.07 (or 0.93) to 0.66 year. The main breeding period was calculated as the period from 0.21 to 0.40 year, again overlapping with the range of spring-born sheep from Rousay (Figure 10.3). Modeled x_0/X ratios of two individuals fall outside of this estimated springtime breeding period: one early winter birth (PK97) and one autumn birth (PK89) corresponding to the birth seasons of modern sheep from Corsica and Carmejane, respectively (Figure 10.2).

At Smilčić, modeled X values for Impresso period are the most homogeneous of the various groupings of archaeological specimens (mean X = 27.1 ± 2.5 mm; n=6) and x_0/X

ratios vary between 0 and 0.30 year indicating all individuals were born within a period of approximately 110 days in the late winter-early spring. The main birthing period was determined to be from 0.12 to 0.20 year lasting approximately 30 days. This lambing/kidding period falls between the range of the x_0/X ratios obtained from modern sheep from Carmejane born in February and sheep born in April-May from Rousay, indicating the main period was in the early spring (Figure 10.2).

Specimens from Danilo period Smilčić also exhibit relatively similar rates of tooth growth (mean X = 29.0 ± 4.1 mm; n=4). While x_0/X ratios range from 0.06 to 0.52, the main breeding period was calculated to be from 0.16 to 0.35, corresponding with sheep from Rousay born in the spring (Figure 10.2). Two out-of-season births were observed in late winter (Figure 10.3). The distribution of Danilo births at Smilčić is wider than for the Impresso group, potentially reflecting an extended lambing/kidding season during the Middle Neolithic. Additionally, the main lambing/kidding season appears to begin later in the annual cycle for the Danilo relative to Impresso specimens, but it should be noted that the small sample size limits the reliability of this interpretation.

The mean cycle period (X) is 35.6 ± 10.6 mm for the six Danilo period specimens from Benkovac-Barice (Table 10.2). Modeled x_0/X ratios vary between -0.02 (or 0.98) and 0.66 year while the main lambing period was calculated to be from 0.23 to 0.42 year, spanning roughly two months in the spring. Two out-of-season births are observed: one early winter birth (BB182) and one late summer or early autumn birth (BB136) which is in the range of the modern sheep from Carmejane born in September and the Corsica sheep born in October.

At Zemunik Donji, the mean cycle period is 33.0 ± 12.9 mm (n=7). The main

breeding period was calculated as 0.10 to 0.20, overlapping with the modern sheep from Carmejane born in January and February. However, most individuals exhibit x_0/X ratios from 0.06 to 0.33 year, spanning approximately 3 months, and the x_0/X ratios of three individuals correspond with the modern sheep from Rousay born in April and May. One out-of-season x_0/X ratio (ZD14) coincides with the range of autumn born sheep from Corsica (Figure 10.3).

The results of modeling season of birth for the six Danilo period specimens from Graduša Lokve at Islam Grčki exhibit mean cycle period of 30.8 ± 11.1 mm with two groups of x_0/X ratios occupying opposite ranges of the annual cycle. Estimated season of birth for three specimens (IG211, IG212, and IG226) correspond to the late autumn through winter. The other three specimens (IG219, IG233, and IG239) fall between the ranges of modern spring-born sheep from Rousay and autumn-born sheep from Carmejane, pointing to a late-spring and summer breeding period. None of these births occur within the main breeding period defined by the 66% confidence interval of 0.16 to 0.35 year (Figure 10.3).

In contrast, three of the six specimens (IG476, IG477, and IG478) recovered from the Hvar/Late Neolithic component of the Islam Grčki site exhibit x_0/X ratios falling within the range of modern sheep from Rousay which spans the two-month main breeding period calculated as 0.17 to 0.30 year (Figure 10.2). Out-of-season births include two specimens (IG475 and IG479) that fall between modern sheep from Corsica born in October and the Carmejane sheep born in January and February, indicating winter births, and one individual (IG468) with an x_0/X ratio falling between the range of Rousay spring births and Carmejane September births, suggesting a late-summer or early autumn birth.

Only two of the five Velištak specimens could be modeled (VEL29 and VEL32) as the oxygen isotope profiles of the remaining three were either truncated (VEL34) or lack a

clear seasonal signal (VEL28 and VEL37; Figure 9.12). The mean cycle period of the two viable Hvar-period specimens from Velištak is 32.1 ± 9.1 mm. The main breeding period was calculated as 0.17 to 0.35 year, overlapping with the ranges of modern sheep from Rousay born April and May (Figure 10.2).

Based on the 66% confidence intervals x_0/X ratio distributions, the main lambing/kidding seasons at Neolithic sites in northern Dalmatia generally correspond to the late winter and spring (Figure 10.3). However, this metric may not adequately describe the breeding strategy observed at sites where births are distributed broadly across the annual cycle and for sites with small sample sizes (e.g., Velištak and Danilo Smilčić). For example, the 66% confidence interval for Crno Vrilo corresponds to early spring while a majority of specimens fall outside of this range (Figure 10.2). Additionally, no specimens from Danilo period Islam Grčki have x_0/X ratios corresponding to the spring, which was determined to be the main birthing season (Figure 10.2).

Table 10.1. Results of birth season modeling, reporting number of stable isotope measurements (n), modeled amplitude of variation (A), mean $\delta^{18}O_m$ (M), location of highest $\delta^{18}O_m$ value (x0), and period of tooth growth in one annual cycle in mm (X). Table includes only specimens for which Pearson's r ≥ 0.91, indicating satisfactory fitting of modeled $\delta^{18}O_m$ to observed $\delta^{18}O_{apa}$. Species abbreviations are CA – Capra hircus (goat); OA – Ovis aries (sheep); OC – ovicaprid (sheep or goat). Specimen and site details provided in Table 8.5.

Specimen	Species	n	A	M	x_0	X	Pearson's r	x_0/X
Crno Vrilo (Impresso)								
CV15	CA	8	1.8	-1.5	14.8	32.0	0.939	0.46
CV17	OA	7	1.6	-1.6	16.8	21.0	0.959	0.80
CV19	OA	7	2.0	-0.9	33.4	35.0	0.995	0.96
CV20	CA	9	2.3	-1.5	36.9	37.0	0.992	1.00
CV21	CA	9	1.6	0.3	11.8	22.7	0.933	0.52
CV22	OA	6	10.0	-9.6	10.2	49.5	0.990	0.21
CV23	OA	10	1.7	-1.3	1.4	27.3	0.991	0.05
CV24	OA	9	1.4	-1.8	9.1	27.1	0.937	0.34
CV26	OA	8	1.6	-1.9	8.9	19.7	0.951	0.45
CV28	OA	6	1.3	-2.1	4.1	18.5	0.998	0.22
Pokrovnik (Impresso)								
PK101	CA	10	3.5	-3.3	13.5	50.0	0.935	0.27
PK72	CA	10	1.6	-1.0	20.8	28.9	0.968	0.72
PK76	OC	11	1.4	-1.7	35.5	31.7	0.975	0.12
PK91	CA	10	3.8	-3.1	15.6	48.2	0.971	0.32
PK92	CA	10	2.2	-3.7	13.2	50.0	0.960	0.26
Smilčić (Impresso)								
SMI335	OA	10	2.2	-2.0	3.2	26.1	0.994	0.12
SMI338	OA	10	2.0	-1.8	5.8	29.0	0.984	0.20
SMI403	OA	9	2.4	-1.3	26.7	22.9	0.992	0.16
SMI454	OC	11	1.4	-1.2	35.6	27.3	0.967	0.30
SMI455	OA	11	1.4	-1.7	5.6	27.4	0.989	0.21
SMI456	OA	12	1.6	-2.2	30.1	30.1	0.973	0.00

Specimen	Species	n	A	M	x_0	X	Pearson's r	x_0/X
Benkovac-Barice (Danilo)								
BB135	OA	10	1.4	-3.2	9.1	22.4	0.953	0.41
BB136	OA	9	2.5	-2.1	19.3	29.2	0.987	0.66
BB154	OC	10	2.8	-2.3	16.0	36.6	0.997	0.44
BB168	OA	11	1.9	-2.4	9.6	50.0	0.938	0.19
BB180	OC	12	2.0	-2.2	16.6	40.8	0.966	0.41
BB182	CA	10	1.9	-2.6	34.5	35.3	0.989	0.98
Islam Grčki (Danilo)								
IG211	CA	12	1.6	-1.4	-2.7	31.0	0.966	0.91
IG212	CA	10	1.7	-1.6	1.0	50.0	0.981	0.02
IG219	OA	11	1.1	-2.5	12.4	21.5	0.968	0.58
IG226	OA	12	1.5	-1.9	40.8	36.4	0.972	0.12
IG233	OA	10	1.8	-3.1	29.7	21.1	0.963	0.41
IG239	OA	11	2.2	-1.1	11.4	24.6	0.994	0.46
Pokrovnik (Danilo)								
PK54	CA	11	1.9	-1.0	34.1	27.3	0.976	0.25
PK87	CA	10	1.7	-1.7	13.4	32.2	0.932	0.42
PK89	OC	10	2.5	-2.1	27.3	41.2	0.978	0.66
PK95	CA	10	0.7	-1.8	6.8	29.0	0.936	0.23
PK97	CA	8	2.5	-2.6	-2.3	33.9	0.972	0.93
Smilčić (Danilo)								
SMI130	OC	14	2.0	-1.9	2.0	31.2	0.980	0.06
SMI360	OA	10	1.9	-2.1	31.7	24.1	0.985	0.31
SMI421	OC	10	1.5	-1.2	4.2	33.4	0.941	0.12
SMI435	OA	11	2.1	-1.4	14.1	27.2	0.959	0.52
Zemunik Donji (Danilo)								
ZD10	CA	11	2.1	-2.1	7.0	50.0	0.996	0.14
ZD11	OA	10	1.4	-1.2	1.3	20.0	0.973	0.06
ZD13	OA	6	1.6	-2.0	2.9	25.8	1.000	0.11
ZD14	OA	10	1.8	-1.6	-3.6	24.5	0.974	0.85
ZD16	OC	11	1.4	-1.8	5.6	22.6	0.984	0.25
ZD297	OC	10	3.7	-3.2	16.4	50.0	0.987	0.33
ZD298	CA	11	2.4	-1.8	10.2	38.1	0.996	0.27

Specimen	Species	n	A	M	x_0	X	Pearson's r	x_0/X
Islam Grčki (Hvar)								
IG468	CA	12	2.0	-0.7	29.8	19.4	0.988	0.54
IG475	OC	10	1.5	-2.8	28.1	29.5	0.967	0.95
IG476	OC	12	1.7	-2.8	34.9	27.2	0.965	0.28
IG477	OA	10	4.8	-5.0	12.3	50.0	0.911	0.25
IG478	OA	10	2.4	-2.7	28.9	21.6	0.981	0.34
IG479	OA	11	1.8	-3.6	40.8	37.8	0.990	0.08
Velištak (Hvar)								
VEL29	OC	11	2.2	-3.1	13.6	38.6	0.922	0.35
VEL32	OA	10	0.7	-1.7	4.2	25.7	0.918	0.17
Dinara (modern)								
DIN5	OA	6	1.8	-6.0	4.0	24.6	0.978	0.16
DIN7	OA	9	1.0	-6.2	-3.7	50.0	0.949	0.93
Vrlika (modern)								
VRL481	OA	10	1.2	-5.7	4.3	21.4	0.973	0.20

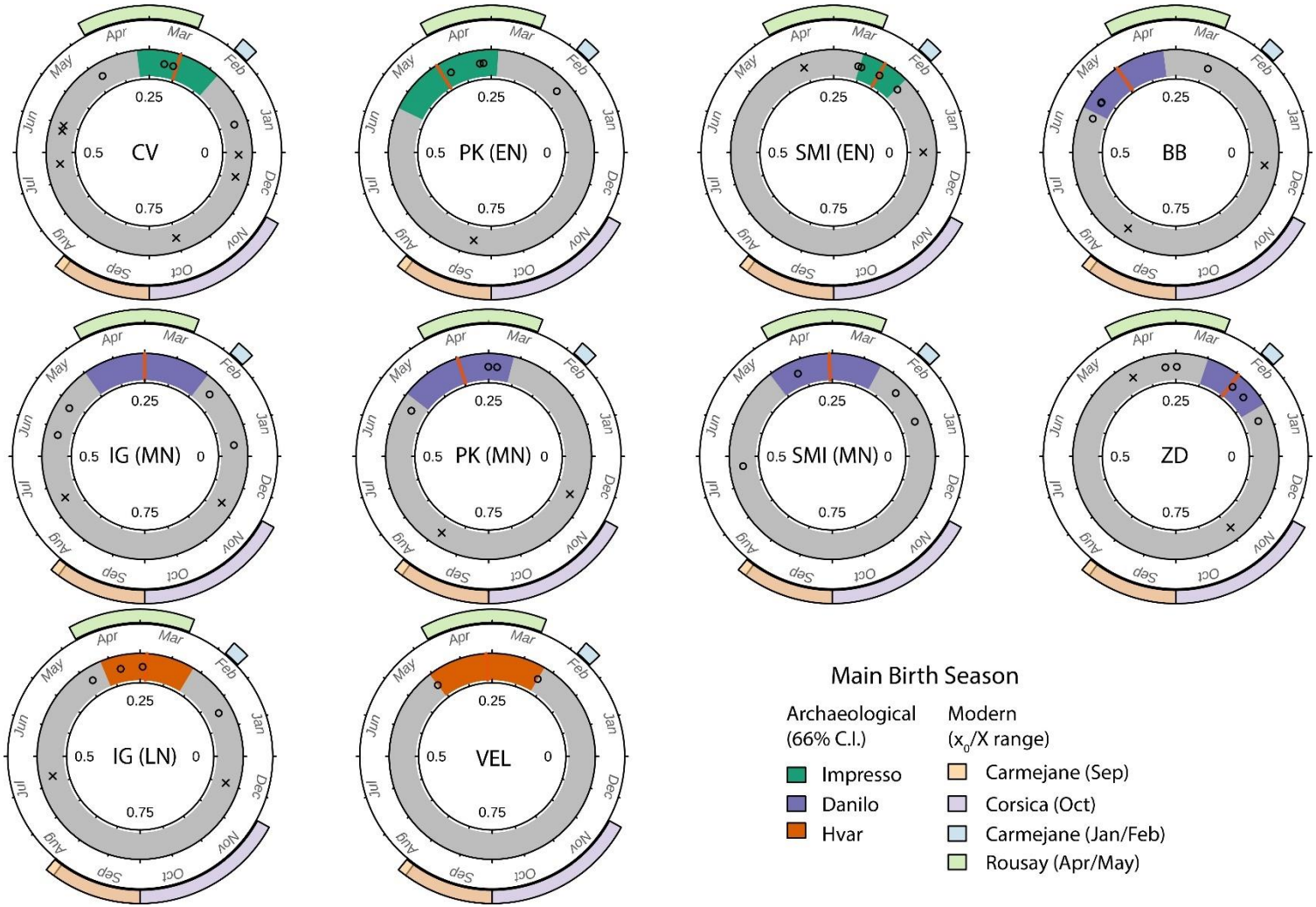

Figure 10.2. Circle plots of x_0/X ratios by site and period with highlighted region signifying the 66% confidence interval. x_0/X ratios falling outside the 95% confidence interval are symbolized with an "x". Red line marks the mean x_0/X ratio. Exterior bands show x0/X ranges of modern reference sheep from Carmejane (Blaise and Balasse 2011; Tornero et al. 2013), Corsica (Fabre et al. 2023), and Rousay (Balasse et al. 2012b).

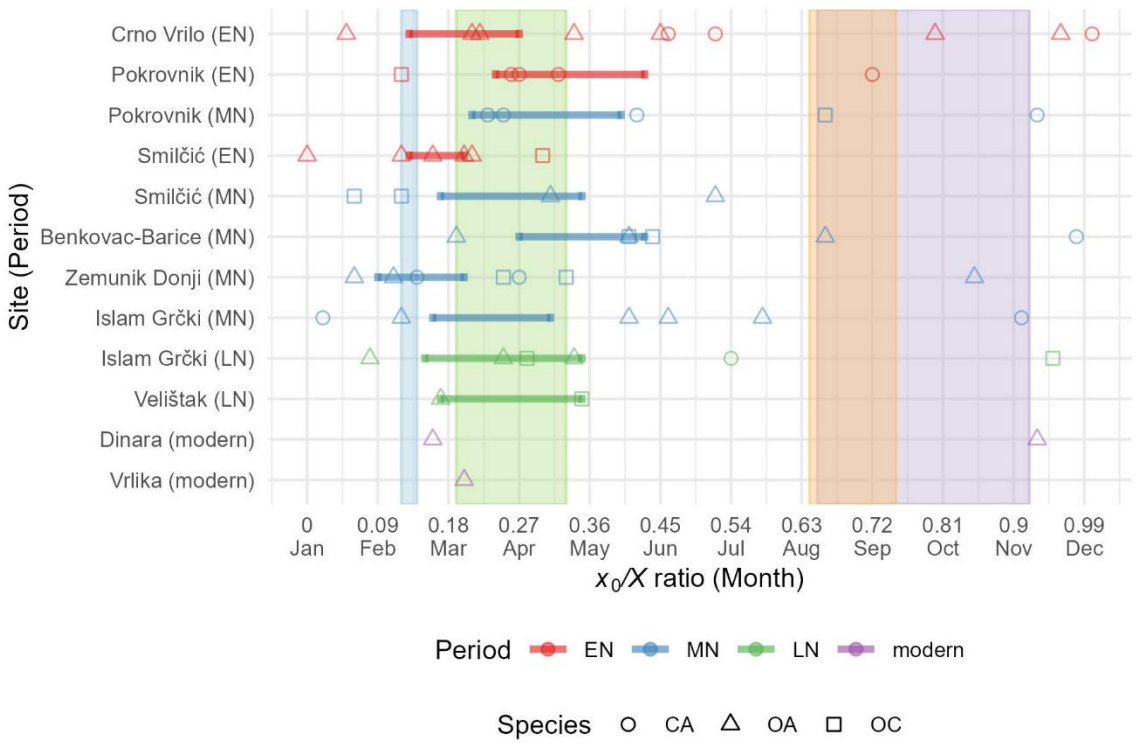

Figure 10.3. Distribution of x_0/X ratios representing modeled season of birth for goats (circle), sheep (triangle), and ovicaprids (square) from each site by period (EN=Impresso; MN=Danilo, LN=Hvar). Horizontal bars indicate main lambing/kidding season determined by bootstrapped 66% confidence interval. Light blue, green, orange, and magenta shaded areas represent range of x0/X ratios of modern reference sheep from Carmejane (February births), Rousay (April/May births), Carmejane (September births), and Corsica (October births), respectively (Balasse et al. 2012b; Blaise and Balasse 2011; Fabre et al. 2023; Tornero et al. 2013). Correspondence between x0/X ratio and calendar month is approximated.

Table 10.2. Summary of modeled birth seasons. Main breeding season values are the 66% confidence intervals calculated by bootstrapped resampling (n=500). Mean X (mm) refers to the mean length of the second molar. Based on models developed/described by Balasse et al. (Balasse et al. 2012b).

Site	n	Mean X (mm)	min x_0/X	max x_0/X	Main Birthing Season
Impresso					
Crno Vrilo	10	29.0 ± 9.6	-0.20	0.52	0.13 to 0.27
Pokrovnik	5	41.8 ± 10.5	0.12	0.72	0.24 to 0.43
Smilčić	6	27.1 ± 2.5	0.00	0.30	0.13 to 0.2
Danilo					
Benkovac-Barice	6	35.7 ± 9.5	-0.02	0.66	0.27 to 0.43
Islam Grčki	6	30.8 ± 11.1	-0.09	0.58	0.16 to 0.31
Pokrovnik	5	32.7 ± 5.4	-0.07	0.66	0.21 to 0.4
Smilčić	4	29.0 ± 4.1	0.06	0.52	0.17 to 0.35
Zemunik Donji	7	33.0 ± 12.9	-0.15	0.33	0.09 to 0.2
Hvar					
Islam Grčki	6	30.9 ± 11.4	-0.05	0.54	0.15 to 0.35
Velištak	2	32.1 ± 9.1	0.17	0.35	0.17 to 0.35
modern					
Dinara	2	37.3 ± 18.0	-0.07	0.16	-
Vrlika	1	21.4	0.20	0.20	-

D. Manipulation of Sheep and Goat Reproduction Rhythms

The modeling results for the three Impresso period sites demonstrate variation in the onset, length, and duration of the breeding season. The modeled seasons of birth for Crno Vrilo specimens are distributed from early winter through late spring but are restricted to the spring among Smilčić and Pokrovnik specimens (Figure 10.3). Sierra et al. (2023) completed

a similar study focusing only on Impresso period herding practices using materials from Tinj and Crno Vrilo. That study used M3 molars and determined that the main breeding period for sheep at both sites was early winter which can be distinguished from late winter/spring birthing seasons observed elsewhere in Neolithic Europe (Sierra et al. 2023).

Apart from CV17, whose x_0/X ratio corresponds with modern sheep born in the autumn (Figure 10.2), the distribution of births in the present study is similar to that presented by Sierra et al. (2023). However the x_0/X ratios of most Crno Vrilo specimens presented here fall outside of the early winter range of 0.98 to 0.15 cited as the main breeding period for this site (Sierra et al. 2023). The inconsistency could be related to differences in how the model estimates x_0 and X for the M3 versus the M2. As indicated in Equation 10.1, additional parameters (b, p, x_A, and x_B) are required to calibrate the model to account for inter-individual differences in the timing of M3 growth, whereas M2 growth is more consistent allowing for the omission of these parameters (Equation 10.2; Balasse et al. 2012b; Blaise and Balasse 2011; Hermes et al. 2022; Tornero et al. 2013; Zazzo et al. 2010). Alternatively, the broader range of x_0/X ratios could reflect deliberate attempts by Crno Vrilo herders to stagger breeding to extend the milking season (Halstead 1998b).

By comparison, Impresso specimen births at Pokrovnik and Smilčić are not as widely distributed across the annual cycle as are the births at Crno Vrilo (Figure 10.3). The main birthing season at Pokrovnik is estimated to have been mid- to late-spring, lasting approximately 70 days (i.e., 66% confidence interval range 0.24 to 0.43 year spans 0.19 year; 0.19*365 = 69.4 days). There is little difference between the duration and distribution of Impresso and Danilo period births at Pokrovnik; the main lambing/kidding season during

both the Early and Neolithic lasts approximately 70 days in mid- to late-spring (Figure 10.3).

Impresso period Smilčić births are concentrated between 0 and 0.30 year with the main lambing period lasting approximately 0.07 year, or 26 days in the late-winter or early spring (Table 10.2). At Danilo period Smilčić the onset of the birthing season is later and lasts about twice as long as the Impresso period, potentially reflecting practices performed in the autumn to extend the length of the breeding season. This would result in a longer lambing/kidding season which may have enabled herders to exploit herds for milk for a longer period and potentially provide a surplus of very young animals available for slaughter (Halstead 1998b). This assumption would be consistent with the shift in herd culling observed at Smilčić from the Early to the Middle Neolithic, marked by an increase in the mortality rate of pre-weaning animals in the Danilo period (Figure 5.2).

An earlier, short-lived lambing/kidding season might have implications for slaughtering regimes. For example, the only site for which the main lambing/kidding season is earlier than Impresso Smilčić is Zemunik Donji. The main birthing season at Danilo period Zemunik Donji was determined to be from 0.09 to 0.20 year, lasting approximately 40 days (Table 10.2) and here as well, a very low mortality rate of pre-weaning animals was observed (Figure 5.2). Herders at Zemunik Donji likely avoided culling very young animals to maximize milk availability within a relatively short lambing/kidding season.

Relative to Zemunik Donji and Impresso Smilčić, the onset of the spring birthing season was delayed at other Danilo sites including Smilčić, Pokrovnik, and Benkovac-Barice (Figure 10.3). A late-spring lambing season is proposed for Benkovac-Barice based on the distribution of modeled x_0/X ratios falling between 0.27 and 0.43 year, lasting approximately

59 days. Based on the mortality profile of caprines from Benkovac-Barice herders preferentially slaughtered lambs and kids between 2 and 6 months of age but an extended birthing season could have allowed for the culling of pre-weaned animals (see Chapter Five, Figure 5.2). With spring as the main birthing season at Benkovac-Barice most young animals were likely slaughtered in early autumn while pre-weaning animals could be removed before the milking season was complete. This strategy of keeping some young animals alive long enough to sustain the quantity of milk produced by nursing females may be effective for extending the milking season (Halstead 1998b). Additionally, the x_0/X of two individuals, BB136 and BB182, correspond to the autumn and early-winter, respectively which may represent a second breeding season timed to coincide with the end of the lambing/kidding season. This could be achieved by keeping herds separated and timing the introduction of males to females who recently gave birth or failed to carry pregnancies to term (Balasse et al. 2023; Rosa and Bryant 2002).

It is also remarkable that two clusters of births corresponding to winter and late spring are observed among Danilo period specimens from Islam Grčki (Figure 10.2). At this site, the difference between mean x_0/X ratios of winter births (0.02 year) and spring births (0.48 year) is 0.46 year, or approximately 168 days. The interval between births can be as low as 160 days for sheep and 170 days for goats but can be as high as 260 and 300 days, respectively, depending on grazing conditions among other things (Dahl and Hjort 1976). The distribution of births shown for this site may reflect intensified reproduction achieved by decreasing the inter-birth interval of females in the herd. Both sheep and goats are capable of giving birth twice per year when grazing conditions are favorable but the demands of nursing

may restrict a females capacity to do so (Dahl and Hjort 1976). The high mortality rate of pre-weaning infants younger than two months old shown in the Danilo period assemblage from Islam Grčki (Chapter Five, Figure 5.2) may be associated with efforts by herders to facilitate re-impregnation of females in the herd shortly after lambing.

Although there is a small number of Hvar period specimens from which season of birth could be estimated (n=6), most specimens from Late Neolithic Islam Grčki were born in the spring (Figure 10.2). The season of birth of one individual, IG468 occurs in the middle of the annual cycle ($x_0/X = 0.54$), which coincides with the series of late births shown among Danilo period specimens from Islam Grčki. It is possible that Hvar herders at this site extended the fall breeding season as suggested for Danilo breeding management but further sampling is required to assess whether this reflects a late impregnation or a second lambing/kidding season. The x_0/X ratios of the two specimens from Velištak that could be modeled fall within the range of the main lambing/kidding season determined for Hvar period Islam Grčki, and correspond with spring-born sheep from Rousay (Blaise and Balasse 2011).

Overall, the results presented in this chapter show most animals were born in the spring. This agrees with the dominant pattern of sheep breeding at middle-latitude (42°-46° N) Neolithic Europe sites (Balasse et al. 2017; 2020). However, several autumnal births were identified based on comparison of the modeled season of birth with x_0/X ratios of modern reference sheep born in September from Carmejane and in October from Corsica (Figure 10.3). These include one Impresso specimen from Pokrovnik (PK72), and five Danilo individuals (BB136, IG211, IG219, PK89, and ZD14). Sheep reproduction can be

manipulated by herders to schedule births in the autumn by introducing rams into the herd in the spring to induce females into ovulation (Rosa and Bryant 2002), and evidence points to the occasional implementation of this strategy by Mediterranean herders during the Neolithic (Balasse et al. 2023; Fabre et al. 2023; Hadjikoumis et al. 2019; Tornero et al. 2020). Alternatively, in non-segregated flocks autumn births could occur naturally among ewes that, either failed to mate in their first year or stopped lactating after losing a lamb, were impregnated in the spring (Balasse et al. 2023). The low occurrence of autumn births shown for the Dalmatian sites suggests herders were not deliberately timing reproduction for the autumn but echoes observations of the capacity of Mediterranean sheep breeds to reproduce out-of-season (Todaro et al. 2015). Evidence for extended breeding and birthing seasons is suggested for the Danilo period at Benkovac-Barice, Pokrovnik, and Islam Grčki. However, further sampling is needed to determine whether reproductive rhythms were deliberately manipulated or if the wide distribution of births throughout the annual cycle was a result of a more casual approach to breeding.

XI. Conclusion

In the introductory chapter of this dissertation, I established the motivation behind this research by highlighting the possibility that significant advancements in animal husbandry during the Neolithic period within the study area may have remained undetected. This observation stems from a comprehensive review of existing literature, which suggests that the evolution of animal management practices in this region could hold valuable insights into early agricultural societies. By delving into this potentially overlooked aspect, this research aims to illuminate the nuances of Neolithic subsistence across time and space. Current archaeological research focusing on the Neolithic period of the Dalmatian Coast in Croatia indicates that sheep and goat husbandry was a significant and enduring aspect of subsistence (Legge and Moore 2011; McClure et al. 2022; Radović 2011; Schwartz 1988).

Technological developments and stable isotope analysis of animal bones indicate significant changes to food production during the Impresso-Danilo transition beginning c. 7500 cal. BP in Northern Dalmatia (Mazzucco et al. 2018; McClure et al. 2018; Zavodny et al. 2014; 2015). These findings prompted me to hypothesize that novel food production strategies spurred changes to the subsistence value of livestock and consequently drove Neolithic herders to experiment with various strategies to minimize the risk of failing to sustain the nutritional needs of their herds. Chapters Four through Nine each featured a

unique approach to investigating some combination of these assumptions, and the concluding remarks were topical. In this final chapter, I summarize and interweave the most important findings presented above and highlight the main contributions of my work to the body of research about the Neolithic in the Eastern Adriatic.

In the preceding chapters I presented a series of inter-related studies that aimed to address three thematic assumptions about risk minimization within Neolithic herding systems.

1. . Sheep and goat herding decisions were sensitive to changes in herd size and demography. Herders employed alternative breeding and slaughtering regimes to minimize the risk of failing to meet subsistence needs.

Integrating the reconstructed mortality profiles, simulations of population dynamics, and modeled season of birth provided important insight into breeding and slaughtering decisions. The simulations revealed the demographic implications of various real and theoretical age-based survivorship probabilities associated with livestock production. In the short term, the decision to curtail the culling of females may come at the expense of returns from meat, and reducing infant culling rates may inhibit the maximization of milk production (Halstead 1998b). Overall, while both milk and meat were central to Neolithic sheep and goat husbandry in Northern Dalmatia, strategies for optimizing the production of these products evolved over time and varied from one site to the next.

A significant finding from the newly constructed mortality profiles is the emergence of three distinct strategies. This conclusion is based on a comparison of caprine season of birth with herder culling strategies during the Danilo period at the sites of Smilčić,

Benkovac-Barice, Zemunik Donji, and Islam Grčki. Namely, the culling strategies appear to correspond with differences in the onset and duration of lambing/kidding seasons. For example, the mortality profiles for Impresso period Smilčić and Danilo-period Zemunik Donji indicate herders delayed the slaughter of lambs and kids younger than two months, reflecting milk production and a preference for tender meat. Notably, these two contexts exhibit the shortest duration and the earliest onset of the main lambing/kidding seasons, corresponding to late winter/early spring (Figure 10.3). The concentration of births could be a result of high fertility, and the earlier onset of the season may indicate that herders were not intervening to delay breeding (Sierra et al. 2023).

The primary birthing season calculated for Impresso, Danilo, and Hvar period samples is winter/spring, which resembles the dominant pattern for Neolithic Europe (Balasse et al. 2020). However, several examples of out-of-season births corresponding with modern sheep born during autumn months are among Danilo period specimens from Pokrovnik, Benkovac-Barice, Zemunik Donji, and Islam Grčki. Further sampling from these sites is necessary to assess the significance of autumnal birthing seasons. However, it is possible that the Impresso herders at Smilčić and Danilo herders at Zemunik Donji strategically restricted out-of-season mating to avoid overlapping the intensive labor demands of dairying with other essential subsistence activities. This careful timing ensures that the herders can manage their agricultural tasks without jeopardizing their livestock care and dairy production (Halstead 2006: 47).

When milk production is a primary production goal, separating young animals from their mothers is an important but labor-intensive aspect of herding. This is particularly true

when herders postpone the slaughter of lambs and kids, as they must allocate extra resources for the survival of the young (Dahl and Hjort 1976; Halstead 1998b). According to the mortality profiles for Danilo Smilčić and Zemunik Donji, herders delayed slaughtering lambs and kids until they were 2-6 months old. However, population projection simulations show that the high mortality rate of this age group at Impresso Smilčić likely had a negative impact on herd survival. By contrast, population projection modeling demonstrated that the culling strategy at Zemunik Donji, in which post-weaning animals had a slightly higher survival probability than at Impresso Smilčić, was sustainable.

The change in culling strategies from the Impresso period to the Danilo period at Smilčić resulted in a significant increase in the survival rates of post-weaning lambs and kids aged 2 to 6 months. This approach is similar to that of Benkovac-Barice and facilitated rapid herd growth. Meanwhile, the main seasons of birth for both Benkovac-Barice and Danilo Smilčić began later and lasted longer than at Impresso Smilčić and Danilo Zemunik Donji (Figure 10.3). Further sampling is needed to confirm whether herders staggered breeding to achieve two lambing/kidding seasons, but an extended birthing season is also suggested for Danilo Pokrovnik and Islam Grčki, where the distribution of births appears to be bi-modal. However, the slaughter of lambs born in late spring, during warm weather, may not have negatively affected milk production since higher pasture quality could support ewe lactation even without nursing infants (Halstead 1998b: 6).

Examining the Pokrovnik and Smilčić results brings to light contrasts in sheep and goat management that may be related to alternative goals of livestock production. Recall that the inferred economic goals based on mortality profiles point to a focus on meat at Impresso

period Pokrovnik but in the Middle Neolithic, herd culling appears oriented towards optimizing milk production (McClure et al. 2022). Both meat and dairy were exploited by Impresso and Danilo herders at Smilčić but were realized via markedly different culling strategies: mortality for 1-2 year old animals at Smilčić in the Danilo period was nearly twice that of the Impresso period. Compared to the Impresso period, dietary spaces and environmental ranges expand for Pokrovnik herds but contracts for Smilčić herds (Figure 8.13 and Figure 8.14). The intensification of dairy production by Danilo Pokrovnik herders could have entailed a more mobile strategy, potentially involving the separation of herds, which might explain the two autumn births (Rosa and Bryant 2002; Todaro et al. 2015). For Impresso Smilčić, delaying slaughter would be compatible with a somewhat more mobile herding strategy as herders would be unburdened by early removal of infants. Meanwhile, the contraction of the environmental range suggested for Smilčić during the Danilo period, could be related to higher labor demands of an extended milking season paired with an increase in the culling rate of pre-weaning infants.

The culling strategy at Danilo period Islam Grčki is characterized by high pre-weaning mortality. This pattern may reflect seasonal site use since the high rate of infants being slaughtered could be problematic for maintaining herd size (Vigne and Helmer 2007). However, as suggested by population projection simulations, high survival probabilities of reproductive aged females likely compensated for the high infant harvest rate, demonstrating that herd size could be sustained in the long-term.

The integration of mortality profiles, population simulations, and birth seasonality presented here provides a nuanced view of how herders employed diverse strategies over

time, both within and between sites. Neolithic herders in Dalmatia balanced the demands of dairy and meat production with the long-term survival of their herds. Delaying slaughter until post-weaning was an adaptation to optimize herd growth while minimizing the risk of reduced milk production. Variations between periods and Neolithic villages are most clearly recognized when mortality profiles are paired with trends in season of birth. These findings underscore the dynamic nature of livestock management during the Neolithic in Dalmatia. Namely, herders adapted their strategies to production goals in various ways such that short-term subsistence was ensured while maintaining viability of herds in the long-term.

2. Herders employed a variety of strategies to ensure the nutritional requirements of herds were met, not limited to the incorporation of fodder into animal diet.

Major contributions to our current knowledge of Neolithic economies in Dalmatia derive from traditional zooarchaeological methods (McClure et al. 2022; Radović 2011; Schwartz 1988), lithic analysis (Mazzucco et al. 2018), ceramic typological, radiometric, (McClure et al. 2014; Spataro 2002), geochemical sourcing (Teoh et al. 2014), and functional analyses (McClure et al. 2018). Stable isotope analysis of livestock bone collagen (Guiry et al. 2017; Lightfoot et al. 2011; Zavodny et al. 2014; 2015) and enamel bioapatite (Sierra et al. 2023) has also been instrumental in examining developments in Neolithic animal husbandry in this region. Chapter Eight broadened the current base of knowledge pertaining to how herders managed the nutritional needs of their animals. That chapter presented stable isotope data from 65 individual tooth specimens and 147 bone samples from 12 unique contexts spanning a 2,000-year period. Similar studies focused on developments within

Neolithic sheep and goat husbandry present and compare stable isotope data of individual animals representing one or a few different sites and contexts (e.g., Fabre et al. 2023; Henton et al. 2010; Hermes et al. 2022; Makarewicz 2017; Sierra et al. 2023; Tornero et al. 2018). The broad sampling strategy implemented here was designed to assess how sheep and goat husbandry developed through time in consideration of what is currently understood about Neolithic economies in Dalmatia.

Overall, the bone collagen data indicate foddering was an important aspect of Impresso animal husbandry. But the enamel bioapatite stable isotope data refines this interpretation, demonstrating it was not necessarily the rule. This is supported by inter-individual variation in the strength of intra-tooth oxygen and carbon isotope covariation, the constrained range of intra-tooth $\delta^{13}C_{apa}$ values relative to later periods, and the existence of some specimens, mainly from Pokrovnik whose $\delta^{18}O_{apa}$ sequences deviate from the expected seasonal pattern.

Focusing on the Danilo period, the broad dietary space of sheep and goats from Benkovac-Barice, Pokrovnik, and Islam Grčki may reflect herder initiatives to minimize the risk of starvation. Several specimens from these sites exhibit aberrant values within their respective sequences of intra-tooth oxygen and carbon isotope ratios that were attributed to provisioning out-of-season fodder or ingesting water that was uncharacteristically enriched or depleted in ^{18}O. Provisioning of fodder to females that were pregnant or had just given birth would be an effective strategy for ensuring the survival of offspring as well as improving the quality of milk (Dahl and Hjort 1976). The dairy-focused herding activities that occurred at Pokrovnik produced a dietary space similar in size to Benkovac-Barice and Islam Grčki

(Figure 8.13) but with greater inter-individual variation in intra-tooth $\delta^{18}O_{apa}$ amplitudes and mid-ranges (Figure 8.14). In contrast, dairy-focused livestock management Zemunik Donji appears to have been centered near the settlement as suggested by the close correspondence of $\delta^{13}C_{apa}$ and $\delta^{18}O_{apa}$ profiles and tight clustering of amplitudes and mid-ranges (Figure 8.13 and Figure 8.14).

Additionally, the suitability of the Dalmatian lowlands for raising sheep and goats is reflected by covariance of carbon and oxygen isotope profiles observed in a majority of archaeological specimens. However, inter-individual differences in the degree of covariation and unique patterns within intra-tooth $\delta^{13}C_{apa}$ and $\delta^{18}O_{apa}$ series of some specimens reveal several risk minimization strategies. For example, collection of vegetation during the summer for overwintering animals is demonstrated in the carbon and oxygen isotope profiles of numerous specimens from Danilo period Smilčić and Benkovac-Barice. For economies that rely on intensive caprine dairying, the winter is a critical period because herders aim to fatten pregnant females in preparation for the upcoming spring milking season (Nitsiakos 1985). Modern agropastoralists in Dalmatia and Greece harvested hay from summer pastures to provision to their animals during the winter to ensure the quality and volume of milk produced (Belaj 2004; Halstead 1998a; Halstead et al. 1998; Marković 1980). Neolithic herders at Smilčić and Benkovac-Barice likely employed a similar risk-minimization strategy, which may be a reflection of intensified dairying during the Danilo period.

High $\delta^{13}C_{apa}$ values shown among multiple Danilo tooth specimens suggest herders periodically intervened in the diet of their animals. Moreover, differing trends in $\delta^{13}C$ values between bone collagen and enamel bioapatite of Impresso and Danilo period specimens

indicate short-term changes in diet, rather than consistent consumption of ^{13}C-enriched vegetation. This pattern may reflect a newly introduced risk herding strategy associated with the arrival of the Danilo culture to the Dalmatian Coast of Croatia in which herders exploited C_4 crops like millet or visited marine environments to access ^{13}C-enriched seagrasses (Balasse et al. 2005; 2009) as supplementary fodder during times of scarcity.

The small intra-tooth ranges of $\delta^{13}C_{apa}$ shown amongst many Impresso period specimens, however suggests fodder was routinely provisioned (Chase et al. 2014; Knockaert et al. 2018). This finding is consistent with the stable isotope results of caprine bone collagen from sites in Dalmatia including Crno Vrilo, Pokrovnik, and Smilčić, which indicate Impresso herders supplemented sheep and goat diet with ^{15}N-enriched vegetation such as fodder cultivated with manure. Although significant differences were found between the $\delta^{13}C$ values of caprine bone collagen from Crno Vrilo and Impresso Pokrovnik, this was not the case for $\delta^{13}C_{apa}$. Additionally, limited inter-site comparisons of Impresso phase stable isotope analyses of bone collagen data indicate herders adapted foddering and grazing strategies to optimize their individual farming systems. Crno Vrilo herders, who focused mainly on sheep husbandry (Sierra et al. 2023), may have penned their animals on arable land, which would have maintained soil fertility by concentrating the deposition of dung to cultivated areas. This strategy was practiced by modern agropastoralists in Greece and the Asturias, who employed preventative grazing to reduce the risk of lodging resulting from excessive crop growth (Halstead 2006). The revelation of alternative Impresso herd diet management strategies reflects different forms of food production among sites in the same bioregion (Gaastra et al. 2019).

One aim of this research was to assess whether stable isotope analysis of enamel bioapatite could shed light on how livestock management strategies developed throughout the Neolithic. My initial prediction was that variation in livestock feeding strategies during the Impresso and Danilo phases of the Neolithic would be observed as clear and significant differences in the enrichment of livestock bone collagen in ^{13}C and/or ^{15}N. The bone collagen data demonstrate shifts in how cattle and caprine diet was managed and identifies variation in Impresso period husbandry strategies. Furthermore, at the outset of this research I aimed to assess whether innovations to food production that accompanied the arrival of the Danilo culture to Northern Dalmatia (i.e., specialized lithic blades and dairy fermentation) might be associated with changes to livestock feeding strategies. Although a direct link between the apparent livestock diets and Danilo technological innovations cannot be clearly established, both the bone collagen and enamel bioapatite stable isotope data suggest that Middle Neolithic management strategies for cattle, sheep and goats were different from those used by Early Neolithic Impresso period herders.

Shifting priorities of livestock management from Impresso to Danilo to Hvar phases of the Neolithic in Northern Dalmatia resonate primarily as inter-site differences in sheep and goat husbandry. The clearest evidence for broad changes in sheep and goat husbandry generated by this research is the progressive increase in $\delta^{13}C_{apa}$ values through time while $\delta^{13}C$ values of bone collagen remain stable. The nature of this change in herding strategy most likely stems from novel risk minimization strategies associated with the Danilo period as the $\delta^{13}C_{apa}$ data reflect short-term shifts in diet.

3. Exploitation of non-local pastures via vertical transhumance (i.e., seasonal movement between high and low altitude pastures) was effective towards minimizing risk within small-scale intensive herding systems.

Stable isotope analyses of enamel bioapatite present compelling evidence that transhumance was a strategy used on a small scale by some of the earliest herders to settle Northern Dalmatia. Inter-individual variation in carbon isotope profiles is greater at some sites than others and inter-site variability may be linked to different degrees of herding mobility. For example, seasonal signals in intra-tooth $\delta^{18}O_{apa}$ and homogeneous $\delta^{13}C_{apa}$ amplitudes and means shown among Zemunik Donji specimens indicates that herd forage resources near the settlement were both abundant and predictable. This situation can be contrasted with other Danilo sites, particularly Benkovac-Barice and both Impresso and Danilo phase Pokrovnik where high inter-individual variability in $\delta^{13}C_{apa}$ suggests grazing and browsing habitats and sources of water may have been accessed across a wide spatial range (Julien et al. 2012; Mashkour 2003), possibly including the exploitation of grazing areas close to the Adriatic coastline.

Inter-individual variability observed at Pokrovnik suggests that herders frequently adapted husbandry strategies, either to minimize risk or to accommodate changes to the goals of production. In particular, the dampened oxygen isotope profiles observed in several of the Pokrovnik specimens offer compelling evidence that vertical transhumance may indeed have been practiced on a small scale, perhaps as early as the Impresso period in Dalmatia. If reduced inter-individual variation is expected from non-migratory behaviors (Julien et al. 2012), then the large amount of variation shown for Pokrovnik herds likely reflects a strategy

involving a greater degree of mobility (Mashkour 2003) than strategies used at contemporary villages.

Overgrazing, seasonal changes in resource availability, and certain varieties of dairying production are a few reasons why herders might increase the spatial range of herding activities. An important aspect of moving herds between lowland Dalmatia and pastures in the Dinaric alps was the staggered return of lambs and lactating ewes to the lowlands (Nimac 1940). During the 20-day delay of the descent from mountain pastures, milking sheep would regain weight while being separated from lambs which reportedly increased the quality of the milk (Nimac 1940). Separating herds in this way could involve a spatial range large enough that would provide animals with access to a greater variety of plants and sources of water. At Pokrovnik, a similar strategy involving separation of herds with the aim of improving the quality of milk could explain differences in dietary space and environmental range associated with a dairy versus a meat focused operation and explain the pronounced inter-individual variation observed at the site.

A. Broader relevance to the study of the Neolithic

The shifts evident in how Neolithic herders managed sheep and goat dietary needs speak to the adaptability of pioneering agropastoral communities in the Eastern Adriatic. However, attempting to link nascent risk minimization strategies to broader social and economic trends occurring over 2,000 years may oversimplify the ecological effects of the introduction of domesticated animals into coastal regions of southeastern Europe. Once introduced to new environments, the capacity of domesticated herds to restructure local

ecologies was integral to the establishment and spread of early agricultural economies into Europe (McClure 2015).

Viewed as invasive species, the feeding ecology of sheep and particularly goats has been suggested to have devastated the biodiversity of endemic plant species of Mediterranean islands once they were introduced by pioneering Early Neolithic farmers (Leppard and Birch 2016). Palynological records show declining levels of deciduous tree pollens in the Eastern Adriatic attributed to the 8.2 kya event led to the opening of forests (Combourieu-Nebout et al. 2013). The onset of rapid cooling oscillations roughly coincides with the arrival of farming and domesticated animals to Dalmatia (Kačar 2021). It is conceivable that the introduction of sheep and goats exacerbated climate-induced changes to vulnerable plant communities, perhaps by increasing the rate of forest clearance. In addition to aiding in the creation of agricultural fields, intensive browsing could also have a negative effect on the abundance and regrowth of understory vegetation (Leppard and Birch 2016; McClure 2015) which tends to be depleted in ^{13}C due to reduced solar irradiance (van der Merwe and Medina 1991).

The effects of the arrival of mixed farming activities on the spatial distribution and biodiversity of forage and grazing resources in Dalmatia by 8000 cal. BP may have played a role in shaping herder strategies in the long term. The data presented here show that Impresso period herders were intensively managing mixed-species herds, potentially implementing a crop-fallow rotational cycle much like modern agropastoralists in the Andes (Orlove and Godoy 1986) and Greece (Halstead and Jones 1989). If the assumption that the agricultural complement of Early Neolithic subsistence was also intensive (Bogaard 2005; Halstead

1996) is true, such a grazing strategy would have improved local biodiversity and pasture productivity (Anderson et al. 2012). Moreover, restricting the spatial scale of subsistence activities would have required herders maintain a balance between herd size and the grazing capacity of fallow fields. Absent a market economy, Neolithic herders would have little incentive to maximize the size of their herds for the purposes of selling surplus animal products and could therefore allocate more time to cultivating and hunting (McClure et al. 2022).

This situation appears to have changed following the arrival of new food production technologies during the Danilo period, which facilitated intensification of farming and pastoral activities. Although Impresso period herders throughout the Adriatic oriented production towards both meat and milk (Gillis et al. 2016), the advantages of processing dairy foods may have incentivized Danilo herders to maintain larger numbers of sheep, goats, and cattle. Accordingly, one potential explanation for the ^{13}C-enrichment of sheep and goat enamel bioapatite shown through time relates to the long-term effects of livestock feeding ecology in novel environments that manifested as changes in the spatial distribution and density of grazing and browsing habitats. The rapid forest clearance by Impresso period herding may have reduced the quality of grazing and browsing resources in these habitats. Danilo herders appear to have adapted to periodic shortages in pasture by broadening the diet of their animals to include a vegetation characterized by high $\delta^{13}C$ values. In other words, resource availability shaped by herding in turn shaped strategies used by successive generations of herders in the long-term.

Compared to the development of contemporary Neolithic Vinča and LBK cultures

emanating from the Central Balkans, intensified dairying and milk processing (Gillis et al. 2017) developed within an agropastoral system that was reconfigured to deprioritize sheep and goats and focus on cattle (Orton et al. 2016), as an adaptation to colder conditions in temperate Europe (Ivanova et al. 2018). The exploitation of livestock for milk production and processing occurred at different times in different regions of Europe during the Neolithic, which is most likely due to the ways in which both environmental and cultural factors shape animal husbandry strategies (Debono Spiteri et al. 2016). The question of whether the adoption of innovative technologies associated with agricultural intensification (i.e., improved crop harvesting blades and ceramics for dairy fermentation) during the Danilo phase of the Neolithic might be related to changes in livestock husbandry remains a compelling avenue for continued research in this study area.

In conclusion, this work contributes a nuanced understanding of Neolithic livestock management in the Eastern Adriatic. The earliest farming societies to settle to the Dalmatian coast of Croatia adapted to the challenges of raising livestock in a novel environment. Subsequent generations navigated shifting production priorities and unpredictable changes in resource distribution by adapting traditional herding practices to local ecological conditions. This dissertation has demonstrated the complexity and variability of ancient herding strategies via a combination of conventional zooarchaeological methods, demographic modeling, radiometric dating, and stable isotope analysis and reveals how these practices were shaped by both ecological factors and alternative production goals. Additionally, the holistic approach implemented here contextualizes the information implicit in various types of archaeological data. The findings presented here underscore the importance of considering

the constraints and opportunities of agropastoral decision making. Future research should carry on the exploration of these themes and dedicate special attention to investigating potential links between technological innovations and changes in livestock management. Going forward, drawing on archaeological data recovered from both open-air and cave sites will be vital to furthering our understanding of the development and dispersal of early agricultural economies in this region.

Appendix A. Mandibular Tooth Wear

This appendix contains the results of ovicaprid mandibular tooth wear analysis used to construct mortality profiles and survivorship curves for Benkovac-Barice, Smilčić, Islam Grčki, and Zemunik Donji. These data are presented in Chapter Five and Chapter Six.

.

Table A.1. Results of ovicaprid mandibular tooth wear analysis used to construct mortality profiles presented in Chapter Five and survivorship probabilities evaluated in Chapter Six. Values in "wear" column reflect Zeder's (2006) revised tooth wear classification system. Age group attributed according Zeder's revision of Payne's (1973) classification system: A = 0-2 months; B = 2-6 months; C = 6-12 months; D = 1-2 years; E = 2-3 years; F = 3-4 years; G = 4-6 years; H = 6-8 years; I = 8-10 years. Tooth abbreviations: d = deciduous; P = pre-molar; M = molar. Species abbreviations: CA = Capra hircus (goat); OA = Ovis aries (sheep); OC = ovicaprid (goat/sheep).

Bone ID	Isotope Specimen	Species*	Side	dP2	dP3	dP4	P2	P3	P4	M1	M2	M3	Payne's Age Class
Benkovac-Barice - Danilo													
BB.A1..SJ49.209		OA	R						20	18	17	15	F
BB.A2..SJ27.208		OA	R						20				G
BB.A2..SJ6.146		CA	L	7	9	12							A
BB.A2..SJ6.147		OA	L						20				G
BB.A2..SJ6.148		CA	R						17	17			E
BB.A2..SJ6.149		CA	L						19	25			G
BB.A2..SJ6.327		CA	L							11	7		D
BB.A3..SJ21.151		OA	L			1							
BB.B1..SJ12.206		OC	R								17	15	E
BB.B1..SJ12.207		CA	R						20	20	17		G
BB.B1..SJ49.133		OC	L			17		1		14			D
BB.B1..SJ49.134		OA	L						23	20	17	17	G
BB.B1..SJ49.135	BB135	OA	L							17	17		E, F
BB.B1..SJ49.136	BB136	OA	R						14	17	16		D
BB.B1..SJ49.137		OC	R									9	D, E
BB.B1..SJ49.154	BB154	OC	L							17	17		E, F
BB.B1..SJ6.142		OA	L		13	15							B

Bone ID	Isotope Specimen	Species*	Side	dP2	dP3	dP4	P2	P3	P4	M1	M2	M3	Payne's Age Class
BB.B1..SJ6.143		OC	R	16	18								D
BB.B1..SJ6.144		OA	L										
BB.B1..SJ6.145		OC	L		18	13							B
BB.B1..SJ6.181		OC	R										
BB.B1..SJ6.182	BB182	CA	L				4		20	17	16	1	F
BB.B1..SJ6.183		OC	L						20				F, G
BB.B1..SJ6.184		OC	L							22	17	17	G
BB.B1..SJ6.185		OC	L							17	1	16	E, F
BB.B1..SJ6.186		CA	L						20	25	17		G
BB.B1..SJ6.187		OC	R						14	17	16		D
BB.B1..SJ6.188		OC	R						17	11			E, F, G
BB.B2..SJ26.190		OC	L						17		1		E, F, G
BB.B2..SJ26.191		CA	R				1		18				E
BB.B2..SJ26.192		OA	R						20	19			G
BB.B2..SJ49.138		OC	L						16	18	17		F
BB.B2..SJ49.139		OC	R						20		17	17	F, G
BB.B2..SJ49.160		OC	L							1	17		E, F, G
BB.B2..SJ49.161		OC	L							17	16		D, E
BB.B2..SJ49.162		OC	R	1	20	17							B
BB.B2..SJ49.163		CA	R		20	20				16	5		D
BB.B2..SJ49.164		OC	L				1	1	1	1			

Bone ID	Isotope Specimen	Species*	Side	dP2	dP3	dP4	P2	P3	P4	M1	M2	M3	Payne's Age Class
BB.B2..SJ49.165		CA	L						25	22	17		H
BB.B2..SJ49.166		OC	R			20				14			D
BB.B2..SJ6.153		OA	R			17				5			B
BB.B3..SJ13.170		OA	L						16	20	17	17	G
BB.B3..SJ49.167		CA	R		16	13							B
BB.B3..SJ49.168	BB168	OA	R		25	25				17	16		D
BB.B3..SJ49.169		CA	L	1	13	12							B
BB.B3..SJ6.152		OA	L			20				18			D
BB.C1..SJ13.155		OC	R							16	9		D
BB.C1..SJ13.156		OC	R			19							C, D
BB.C1..SJ13.157		CA	L				3	7	10				D
BB.C1..SJ13.158		CA	R							17	17	7	D
BB.C1..SJ13.159		OC	R						1	17	13		D
BB.C1..SJ2.150		OC	L							17	17		E, F
BB.C1..SJ49.189		OC	R								19	17	H
BB.C1..SJ49.193		OC	L			1		1			14		D
BB.C1..SJ49.194		OA	R						20	22	17		G
BB.C1..SJ49.195		OC	R			20				14			D
BB.C1..SJ51.175		OC	L		1	17	1			1			B, C, D
BB.C1..SJ51.176		OC	R			19				14	10		D
BB.C1.PODNICA_2A.SJ35.205		OC	R							17	17	16	E

Bone ID	Isotope Specimen	Species*	Side	dP2	dP3	dP4	P2	P3	P4	M1	M2	M3	Payne's Age Class
BB.C1.ZEMLJA_POD_2A_3A.SJ49.203		OA	R						20				G
BB.C1.ZEMLJA_POD_2A_3A.SJ49.204		OC	R								17	10	E
BB.C2..SJ13.140		OA	L						20				G
BB.C2..SJ26.172		OC	R										
BB.C2..SJ26.173		OA	L						20				G
BB.C2..SJ26.174		OC	R		17						4		B
BB.C2..SJ49.177		OC	L							20	17	17	G
BB.C2..SJ49.178		OC	L			20				16			D
BB.C2..SJ49.179		OA	L	16	18	19							C
BB.C2..SJ49.180	BB180	OC	L							17	17		E, F
BB.C2..SJ49.281		BT	L									13	
BB.C2..SJ6.196		OC	L							17	11		D
BB.C2..SJ6.197		OC	L								16	1	D, E
BB.C2..SJ6.198		OA	R		20	17				14			D
BB.C2..SJ6.199		OA	R						20				G
BB.C2..SJ6.200		OC	R		20	19							D
BB.C2..SJ6.201		CA	L						20	22	17	16	G
BB.C3..SJ2.141		CA	L						20				F, G, H
BB.IZBACENA_ZEMLJA..SJ6.202		OC	R								17	16	E
		Islam Grčki - Danilo											
IG.A.mix..236		OC	L	5	7	9							A

Bone ID	Isotope Specimen	Species*	Side	dP2	dP3	dP4	P2	P3	P4	M1	M2	M3	Payne's Age Class
IG.A.SJ15.NW.235		CA	R			21				14			C
IG.A.SJ16B..224		CA	R						17	13	14		D
IG.A.SJ25.SWX.240		OC	L		7	11							A
IG.A.SJ25.SWX.241		OC	R			1				11			C, D
IG.A.SJ25.SWX.242		OC	R						1	1	1	1	
IG.A.SJ25.SWX.243		OA	L	4	6	5							A
IG.A.SJ25.SWX.244		OA	L							26	25	20	I
IG.A.SJ25.SWX.245		OA	R			20				14	4		D
IG.A.SJ25_SWX.1.239	IG239	OA	L						20	18	15	15	F
IG.A.SJ27..237		OA	R						20	22	17		G
IG.A.SJ27..238		OC	R			20				14	4		D
IG.A.SJ29..246		OA	R						25	25	22	17	H
IG.A.SJ3..230		OC	R							18	17	10	E
IG.A.SJ3..231		OC	R					1					
IG.A.SJ3..232		CA	L						11	1	13	9	D
IG.A.SJ32..228		OC	R						16	1			D, E
IG.A.SJ32..229		OC	R										
IG.A.SJ36.2.225		OA	L										
IG.A.SJ4..211	IG211	CA	L				4	5	7	17	14	7	D
IG.A.SJ4..227		OA	R						20	20	17		G
IG.A.SJ4..233	IG233	OA	R						17	18	17	16	F

Bone ID	Isotope Specimen	Species*	Side	dP2	dP3	dP4	P2	P3	P4	M1	M2	M3	Payne's Age Class
IG.A.SJ4.2.226	IG226	OA	R						11	17	14	4	D
IG.A.SJ4.2.234		CA	R			19				11			C
IG.A.SJ4.5/6.210		CA	R			19				9			C
IG.A.SJ44.1.213		OA	R			19							C
IG.A.SJ44.1.214		OA	R					25	25				I
IG.A.SJ45..222		OA	L	4	7	11				3			A
IG.A.SJ45..223		CA	R			11							A
IG.A.SJ47..212	IG212	CA	L				7	7	9	17	17	4	D
IG.A.SJ47..215		OC	L					25	21	25			G
IG.A.SJ47..216		OC	R										
IG.A.SJ47..217		OA	L				4						D
IG.A.SJ47..218		OA	R			11	4						A
IG.A.SJ47..219	IG219	OA	L						16	17	16	11	E
IG.A.SJ47..220		OC	L									9	D, E
IG.A.SJ47..221		OC	R							25	17	16	G
		Islam Grčki - Hvar											
IG.B..11.467		BOS	L						12	15		1	
IG.B..11.471		BOS	L						11	15	15		
IG.B..11.472		OC	R					1	25				H, I
IG.B..11.473		OC	R								17	15	E
IG.B..11.474		CA	R						20	19			G

Bone ID	Isotope Specimen	Species*	Side	dP2	dP3	dP4	P2	P3	P4	M1	M2	M3	Payne's Age Class
IG.B..20.468	IG468	CA	R						18	19	17	16	G
IG.B..20.475	IG475	OC	R								17	15	E
IG.B..22.476	IG476	OC	R								14	7	D
IG.B..22.477	IG477	OA	R						20	17	17	15	F
IG.B..29.478	IG478	OA	R						20	17	17	13	F
IG.B..29.479	IG479	OA	L					7	5	17	14		D
IG.B..31.480		OA	L						11	17			D
			Smilčić - Danilo										
SMI.15...113		CA	R						20	20	17	18	G
SMI.15...114		CA	R				7		10				D
SMI.15...115		OA	R						16				D, E
SMI.15...116		CA	R						16	17	14		D
SMI.15...117		CA	R						11				D
SMI.15...118		OA	R						17	18	17		F
SMI.15...119		CA	R						16	17	17		D
SMI.15...120		OA	R						20	25	18		G
SMI.15...121		CA	R						18		17	10	E
SMI.15...122		OC	L						18				F, G
SMI.15...123		CA	L		16	16	1						D
SMI.15...124		OC	L		11	14	1						B
SMI.15...125		CA	L						1	1	1		

Bone ID	Isotope Specimen	Species*	Side	dP2	dP3	dP4	P2	P3	P4	M1	M2	M3	Payne's Age Class
SMI.15...126		OA	L						22	26	1	1	H
SMI.15...127		OC	L			17				12			D
SMI.15...128		OC	L									15	E, F, G
SMI.15...129		OC	L			17			3				B, C, D
SMI.15...130	SMI130	OC	L								11		D
SMI.15...131		CA	L						20	25	17	17	G
SMI.15...132		OA	L						20	25	17		G
SMI.C..41.349		CA	R		20	19				14	11		D
SMI.C..41.350		BOS	R							16	15		
SMI.C.O10.41.364		OA	L		20	17							D
SMI.C.O10.41.365		OC	R	14	16	19				11			C
SMI.C.O10.41.366		OC	R					3	1	14	11		D
SMI.C.O10.41B.358		OC	L									17	F, G, H, I
SMI.C.O10.41B.359		OA	L	17	25	19				11			C
SMI.C.P10.41.360	SMI360	OA	R					20	17	18	17	17	F
SMI.C.P10.41.361		OA	R				1	22	22	25	17	17	H
SMI.C.P10.41.362		OC	R							16	9		D
SMI.C.P10.41.363		OC	R			21				17			D
SMI.C.P9.41.355		OC	R						17				E, F, G
SMI.C.P9.41.356		OC	L						7	17	11		D
SMI.C.P9.41.357		OA	L				10	16	20	18			F

Bone ID	Isotope Specimen	Species*	Side	dP2	dP3	dP4	P2	P3	P4	M1	M2	M3	Payne's Age Class
SMI.C.P9.41A.351		CA	L				4	5	7	17			D
SMI.C.P9.41A.352		OA	R	12	16	17				10	3		B
SMI.C.P9.41A.353		OC	L			17				14			D
SMI.C.P9.41A.354		CA	R				7	17	14	17	17		D
SMI.D.L6.56.405		OA	L						20	19	17	17	G
SMI.D.L6.56.406		OC	R						25	25			I
SMI.D.L6.56.407		OC	R						25	25	19	17	H
SMI.D.L6.56.408		OA	R		24	19				16	13		D
SMI.D.L6.56.409		OC	R			19							C, D
SMI.D.L7.56.410		OA	L						20		18		G
SMI.D.L7.56.411		OC	R						17	20	18		G
SMI.D.M7.56.419		OC	R		10	13							A
SMI.D.M7.56.420		OC	R		14	19				11			D
SMI.D.M7.56.421	SMI421	OC	L							17	16	10	D
SMI.D.M7.56/1.446		OA	R						26	25	20	18	H
SMI.D.M7.56A.444		OC	L				1	1	20				G
SMI.D.M7.56A.445		OA	R					8	9	17			D
SMI.D.M8.56.441		OC	L	1	17	17							B
SMI.D.N7.56.434		OA	R						20	22		17	G
SMI.D.N7.56.435	SMI435	OA	R						14	17	13		D
SMI.D.N7.56.436		OC	R	12	14	18				7			B

Bone ID	Isotope Specimen	Species*	Side	dP2	dP3	dP4	P2	P3	P4	M1	M2	M3	Payne's Age Class
SMI.D.N7.56.437		OC	L		17	20							D
SMI.D.N7.56.438		OA	L						20	17	17	12	F
SMI.D.N7.56A.439		OC	R		16	19				16			D
SMI.D.N7.56A.440		OC	L			19				14	4		C
		Smilčić - Impresso											
SMI.B.M1.21.333		CA	L					12	10	17	14		D
SMI.B.M1.21.334		CA	L				20	24	20	18	17	16	H
SMI.B.N2.22.338	SMI338	OA	L						20	17	17	16	F
SMI.B.N2/M2.22.335	SMI335	OA	L					20	20	17	17		F
SMI.D..JAMA_17.403	SMI403	OA	L						20	19	17		G
SMI.D..JAMA_17.404		OC	L	10	14	19				11			B
SMI.D.M5.54.412		OC	L	5	12	12							B
SMI.D.M5.54.413		OC	L	14	18	19							C
SMI.D.M5.54.414		OC	R						16				D, E
SMI.D.M5.54.415		OC	R	8	10	12				5			B
SMI.D.M5.54.416		OA	R		19	19				7			B
SMI.D.M5.54.417		CA	R		17	19				10	4		C
SMI.D.M5.54.418		OC	L			1				16	11		D
SMI.D.M5/6.58.442		OA	R		16	16				7			B
SMI.D.M6.58.422		OC	R	1	1	19				13	3		C
SMI.D.M6.58.423		OC	R		22	20				16			D

Bone ID	Isotope Specimen	Species*	Side	dP2	dP3	dP4	P2	P3	P4	M1	M2	M3	Payne's Age Class
SMI.D.M6.58.424		OC	R		10	1				9			B
SMI.D.M6.58.425		OA	L						14				D
SMI.D.M6.58.426		OA	L	9	14	19							B
SMI.D.M6.58.427		OC	L								11		D
SMI.D.M6.58.428		OC	L	12	16	12				7			B
SMI.D.M6.58.429		OC	L		22	19				13			D
SMI.D.M6.58.430		OC	L		20	19							D
SMI.D.M6.58.431		OC	L	9	14	19				5			B
SMI.D.M6.58.432		OC	L		22	20				11	4		D
SMI.D.M6.58.433		OA	L	10	14	19				11			B
SMI.D.M6.58A.447		CA	L	17	17	17				9			C
SMI.D.M6.58A.448		CA	L	10	16	17				14			C
SMI.D.M6.58A.449		OC	R							1	4		C
SMI.D.M6.JAMA_17.457		OA	L		17	18				16			D
SMI.D.M6.JAMA_17.458		OC	L			20				13	10		D
SMI.D.M6.JAMA_17.459		OC	L		20	21							D
SMI.D.M6.JAMA_17.460		OC	R							17	10		D
SMI.D.M6.JAMA_17.461		OC	R							14	4		D
SMI.D.M6.JAMA_17.462		OC	R		20	12				3			B
SMI.D.M6.JAMA_17.463		OA	L	14	16	18							B
SMI.D.N5.50.443		OA	R						17	19	17	17	G

Bone ID	Isotope Specimen	Species*	Side	dP2	dP3	dP4	P2	P3	P4	M1	M2	M3	Payne's Age Class
SMI.D.N6.52.450		OC	L							17	13		D
SMI.D.N6.52.451		OA	L	19	20	19							C
SMI.D.N6.52.452		OA	L					6	7	17	14	15	E
SMI.D.N6.52.453		OA	L				7	16	17	17	17		E
SMI.D.N6.52.454	SMI454	OC	L			26				17	17		D
SMI.D.N6.52.455	SMI455	OA	R						17	18	17		F
SMI.D.N6.52.456	SMI456	OA	R				5	7	9	17	14		D
		Zemunik Donji - Danilo											
ZD.KV10.sj42..299		OC	R						9				D
ZD.KV10.sj43A..14	ZD10	CA	L								11		C, D
ZD.KV10.sj43A..16	ZD16	OC	R								16		D, E
ZD.KV10.sj43A..300		OC	R						11				D
ZD.KV10.sj43A..301		OC	R			17				9			B
ZD.KV9.sj43A..291		OA	R		25	16				4			B
ZD.KV9.sj43A..292		CA	L		25	17							C
ZD.KV9.sj43A..293		CA	R									12	F
ZD.KV9.sj43A..294		OC	L			18				13	3		D
ZD.KV9.sj43A..295		OC	R			12				10			B
ZD.KV9.sj43A..296		OA	R		20	19				14			D
ZD.KV9.sj43A..297	ZD297	OC	L								16		D, E
ZD.KV9.sj43A..298	ZD298	CA	L						17	17	17		E

Bone ID	Isotope Specimen	Species*	Side	dP2	dP3	dP4	P2	P3	P4	M1	M2	M3	Payne's Age Class
ZD.KV9.sj43A..48	ZD11	OA	L						19	17	16		F
ZD.KV9.sj43A..49		OA	L						16	22	17		G
ZD.KV9.sj43A..50		CA	L			1				17	11		D
ZD.KV9.sj43A..51		OA	L						20	17	17		F
ZD.KV9/8.sj47..302		OC	R				4						B, C, D
ZD.KV9/8.sj47..303		OA	R						20	18			F
ZD.KV9/8.sj47..304		CA	L	1	20	19				7			C
ZD.KV9/8.sj47..305		OA	L		25	24				17			D
ZD.KV9/8.sj47..306		OC	R					5	10				D
ZD.KV9/8.sj47..307		OA	L		20	20				13	3		C
ZD.KV9/8.sj47..308		CA	R						16	17			D
ZD.KV9/8.sj47..309		OC	L				4						B, C, D
ZD.KV9/8.sj47..310		CA	L	16	14	19				13			D
ZD.KV9/8.sj47..311		OA	L						20	18			F
ZD.KV9/8.sj47..312		OC	R	17	1	19							D
ZD.KV9/8.sj47..313		OC	R						9				D
ZD.KV9/8.sj47..314		OA	R		17	14							B
ZD.KV9/8.sj47..315		CA	L			16				4			B
ZD.KV9/8.sj47..64	ZD13	OA	R								10	10	D
ZD.KV9/8.sj47..65	ZD14	OA	R						20	18	17		F

*OA: *Ovis aries*; CA: *Capra hircus*; OC: Ovicaprid

Appendix B. Construction of Mortality Profiles from Tooth Wear Data

This appendix details the procedures for constructing mortality profiles from the data provided in Appendix A. The results are presented in Chapter Five.

Construction of Ovicaprid Mortality Profiles from Tooth Wear Analysis

Nicholas Triozzi

2023-11-17

Introduction

This document outlines the procedures used to generate mortality profiles from age-at-death estimates based on mandibular tooth wear analysis. The results and implications of the analyses completed here are the focus of Chapter Five of Nicholas Triozzi's PhD Dissertation. The code here is executed in R (R Core Team 2023) and generates Figure 5.2 and Table 5.1.

Step 1. Read in data

The primary data set used here is Appendix A which is read into R as a .csv file named "Dalmatia_Wear_pivot.csv". The table contains Payne's (1973) Age classes for each individual mandible analyzed (including isotope samples).

This code chunk reads in that file and creates a new *data.frame* called *wear.df*. *wear.df* is then reformatted to group all caprine species (including goats, sheep, and "ovicaprids") into the "ovicaprid" genus, and filtered to remove non-caprine data, modern tooth wear data, and data associated with Iron Age samples. The last line of code summarizes the number of mandibles per site/period.

```
#-- read in data
wear.df = read.csv("../../data/Dalmatia_Wear_pivot.csv")
str(wear.df)
```

```
## 'data.frame':    309 obs. of  18 variables:
##  $ Column1           : int  138 139 77 78 79 80 211 82 136 137 ...
##  $ Site              : chr  "Benkovac-Barice" "Benkovac-Barice" "Benko
vac-Barice" "Benkovac-Barice" ...
##  $ Period            : chr  "MN" "MN" "MN" "MN" ...
##  $ BoneID            : chr  "BB.A1..SJ49.209" "BB.A2..SJ27.208" "BB.A2
..SJ6.146" "BB.A2..SJ6.147" ...
##  $ IsotopeSampleNumber: chr  "" "" "" "" ...
##  $ Species           : chr  "OA" "OA" "CA" "OA" ...
##  $ Side              : chr  "R" "R" "L" "L" ...
##  $ dP2               : int  NA NA 7 NA NA NA NA NA NA NA ...
##  $ dP3               : int  NA NA 9 NA NA NA NA NA NA NA ...
##  $ dP4               : int  NA NA 12 NA NA NA NA 1 NA NA ...
##  $ P2                : int  NA NA NA NA NA NA NA NA NA NA ...
##  $ P3                : int  NA NA NA NA NA NA NA NA NA NA ...
```

```
##  $ P4                : int  20 20 NA 20 17 19 NA NA NA 20 ...
##  $ M1                : int  18 NA NA NA 17 25 11 NA NA 20 ...
##  $ M2                : int  17 NA NA NA NA NA 7 NA 17 17 ...
##  $ M3                : int  15 NA NA NA NA NA NA NA 15 NA ...
##  $ Zeder_Group       : chr  "VII" "VII, VIII, IX" "I" "VII, VIII, IX"
...
##  $ Payne.Group       : chr  "F" "G" "A" "G" ...
```

```
#-- drop unused columns, reclassify species as "OC", filter for ovicaprids
from Neolithic sites.
# colnames(wear.df)
wear.df = wear.df %>%
  select( Site:Side, contains( "Group" ) ) %>%
  mutate(
    Genus = case_when(
      Species == "OA" ~ "OC",
      Species == "CA" ~ "OC",
      .default = Species )
    ) %>%
  filter(
    Genus == "OC" & Site != "MOD" & Site !="IA" ) # drop modern and iron a
ge data

#-- quick summary of age groups
wear.df %>% group_by(Site, Period) %>% summarise(n())
```

```
## `summarise()` has grouped output by 'Site'. You can override using the
## `.groups` argument.

## # A tibble: 10 × 3
## # Groups:   Site [8]
##    Site            Period `n()`
##    <chr>           <chr>  <int>
##  1 Benkovac-Barice MN        77
##  2 Crno Vrilo      EN        25
##  3 Islam Grčki     LN        10
##  4 Islam Grčki     MN        37
##  5 Lisicic         MN         2
##  6 Smilčić         EN        44
##  7 Smilčić         MN        58
##  8 Vrcevo          IA        13
##  9 Vrlika          MOD        2
## 10 Zemunik Donji   MN        33
```

Read in data for other sites

This chunk reads an excel worksheet that contains age classifications of OC mandibles for Pokrovnik and Velištak (McClure et al. 2022) and Crno Vrilo (Sierra et al. 2023). These data are discussed in the dissertation but not included in figures or tables.

```
#-- Crno Vrilo - Sierra et al (2023)
cv = readxl::read_xlsx("../../data/OtherSites_Age_at_death.xlsx", sheet =
"Sierra_et_al_2023") %>% filter(grepl( 'CV', Samples ))
#-- reformat for rbind with ages.df
cv = cv %>%
  reframe(Site="Crno Vrilo (Sierra)", Period="EN", BoneID=paste(Samples, "
(Sierra)"),
          IsotopeSampleNumber = Samples, Species=SP, Side=NA,
          Zeder_Group=NA, Payne.Group = `Payne' class`, Genus="OC" )

wear.df = rbind.data.frame(wear.df, cv)
```

Step 2. Define function for computing number of individuals in each age class

This chunk defines the function `correct.counts()` which performs two tasks.

First, the function reads as input `a` which is the column containing Payne's (1973) Age group assignments as capital letters A through I. A tally of the number of individuals in each age group is created. If there is more than one age group assigned to a specimen, the function proportionally allocates that individual to each age group. For example, if Individual 1 was assigned to age groups E, F, and G, and Individual 2 was assigned to age group E, the resulting tally would be E: 1.33, F: 0.33, G: 0.33.

Next, the function includes an option to calculate the relative frequencies following Brochier (2013). If set to `TRUE`, the function will calculate the relative frequencies following Price, Wolfhagen, and Otárola-Castillo (2016) and multiply the frequency density by the bin width of each age class.

In the `correct.counts` function, the following age classes and bin widths are used:

Table B.1. Age classes and bin widths

Age.Class	Bin.width.over.12.months
A (0-2m)	1/6
B (2-6m)	1/3
C (6-12m)	1/2
D (1-2y)	1
EF (2-4y)	2

Age.Class	Bin.width.over.12.months
G (4-6y)	2
HI (6-10y)	4

This code chunk shows the *correct.couunts()* function.

```
source("../../R/correct_counts.R")

correct.counts = function( a, probability.correction = FALSE ){
  # vector of groups (A through I)
  v = LETTERS[ 1:9 ]
  # table to store counts
  t = data.frame( v = v, n = 0 )

  for( i in 1:length( a ) ){ # iterate through rows
    if( nchar( a[ i ] ) == 0 ){  # if blank, do nothing
      next
    }
    if( nchar( a[ i ]) == 1 ){  # if group is valid add one to count
      t$n[ t$v == a[ i ] ] = t$n[ t$v == a[ i ] ] + 1
    }
    if( nchar( a[ i ]) > 1 ){   # if multiple groups, parse and add to cou
nt for each group proportionally
      g = str_match( a[ i ], v ) # collect age classes
      g = g[ ,1 ][ !is.na( g ) ]   # create vector, dropping NA's from mat
ch fun
      f = 1 / length( g )        # calculate fraction
      for( l in 1:length( g ) ){ # add fraction to table for each letter r
epresented in age class
        t$n[ t$v == g[ l ] ] = t$n[ t$v == g[ l ] ] + f
      }
    }
  }

  # function for computing relative frequencies
  rel.freq = function( x ) {
    tot = sum( x )
    q = vector()
    for ( i in 1 : length( x ) ) {
      q[ i ] = x[ i ] / tot
    }
    q
  }

  # if probability.correction parameter set to "TRUE", groups age classes
EF and HI before multiplying groups by bin widths
  if( probability.correction ){
```

```
    t2 = data.frame( v = t$v[ 1:4 ], n = t$n[ 1:4 ])
    t2 = rbind.data.frame(
      t2,
      data.frame(
        v = c( "EF", "G", "HI" ),
        n = c( t$n[ 5 ] + t$n[ 6 ], t$n[ 7 ], t$n[ 8 ] + t$n[ 9 ] )
        )
      )

    # relative frequencies
    t2$qx = rel.freq( t2$n )

    #-- probability corrections after Vigne and Helmer 2007:
    #-- for age groups A,   B,   C,  D, EF,   G,   HI
    #-- probability   1/6, 1/3, 1/2, 1,   2,  2,   4
    t2$fd = t2$qx * c(  6,   3,   2, 1, 0.5, 0.5, 0.25 ) # 1/p correction

    t = t2

  }

  return( as.data.frame( t ) )
}
```

Step 3. Compute corrected counts for age groups

In this chunk the corrected counts of age group occurrences for each site/period grouping are calculated. Then the percent of the frequency density is determined. Finally, the output is formatted and saved as *`ages.df.correct`*.

```
#-- create list for each site/period
wear.df.list = wear.df %>%
  group_by( Site, Period ) %>%
  group_split( .keep = T )

#-- get names
l.names = wear.df %>%
  group_by( Site, Period ) %>%
  group_keys() %>%
  reframe( name = paste( Site, Period ) )
names( wear.df.list ) = l.names$name # assign names to list

#-- run correct.counts function, get relative frequencies
ages.list = lapply( wear.df.list, function( a ){
  counts = correct.counts( a$Payne.Group, probability.correction = TRUE )
  # counts
```

```
  df = counts
  df$Qx = cumsum( df$qx )
  df$lx = 1-df$Qx # survivorship probability (Price et al 2016)
  df
})

names( ages.list ) = l.names$name # names

#-- return to data.frame for plotting
ages.df.correct = bind_rows( ages.list, .id = "Site_Period" )

#-- format data.frame
ages.df.correct = ages.df.correct %>%
  mutate(
    Freq.Dens = fd,
    Age = case_when(    # add ages in months to age classes
      v == "A" ~ "0-2m",
      v == "B" ~ "2-6m",
      v == "C" ~ "6-12m",
      v == "D" ~ "12-24m",
      v == "EF" ~ "24-48m",
      v == "G" ~ "48-72m",
      v == "HI" ~ ">72m"
      ) ) %>%
  mutate(
    Age = paste0( v, " (", Age, ")" )
    ) %>%
  group_by( Site_Period ) %>%
  mutate(
    # calculate percent of cumulative frequency density
    fd.percent = Freq.Dens / sum( Freq.Dens )
    ) %>%
  mutate(
    # factor site-period field
    Site_Period = factor(
      Site_Period,
      levels = c(
        # "Crno Vrilo (Sierra) EN",
        "Smilčić EN" , "Smilčić MN", "Benkovac-Barice MN",
        "Zemunik Donji MN", "Islam Grčki MN", "Islam Grčki LN" ) ,
      labels = c(
        # "Crno Vrilo (Impresso)",
        "Smilčić (Impresso)", "Smilčić (Danilo)", "Benkovac-Barice (Danilo
)",
        "Zemunik Donji (Danilo)", "Islam Grčki (Danilo)", "Islam Grčki (Hv
ar)" )))
# ages.df.correct
```

Table B.2. Corrected counts, frequency densities and percent of frequency density for Benkovac-Barice

Site_Period	Age	n	Freq.Dens	fd.percent
Benkovac-Barice (Danilo)	A (0-2m)	1.000000	0.0833333	0.0820046
Benkovac-Barice (Danilo)	B (2-6m)	7.333333	0.3055556	0.3006834
Benkovac-Barice (Danilo)	C (6-12m)	1.833333	0.0509259	0.0501139
Benkovac-Barice (Danilo)	D (12-24m)	22.333333	0.3101852	0.3052392
Benkovac-Barice (Danilo)	EF (24-48m)	18.833333	0.1307870	0.1287016
Benkovac-Barice (Danilo)	G (48-72m)	18.333333	0.1273148	0.1252847
Benkovac-Barice (Danilo)	HI (>72m)	2.333333	0.0081019	0.0079727

Step 4. Plots mortality profiles

Now the frequency densities and percentages can be plotted as mortality profiles (Chapter 5, Figure 5.2).

```
Mort.Profiles =
  left_join(ages.df.correct, strip.labeller) %>%
  filter(!is.na(Site_Period)) %>%
  ggplot(aes(x = Age, y = fd.percent)) +
  geom_col(
    alpha=0.8,
    ) +
  geom_text(aes(label = paste0(round(fd.percent*100), "%")), size = 3, vju
st = -0.5) +
  ylim(c(0, 0.7)) +
  ylab("Percent Cumulative Frequency Distribution") + xlab("Age Class") +
  theme_minimal() +
  theme(
    axis.text.x = element_text(angle = 45, hjust = 1, size = 6),
    strip.background = element_rect(fill = "#d9d9d980")
    ) +
  # facet_wrap(~ strat.lab)
  facet_wrap(~ Site_Period, labeller = strip_labeller)

## Joining with `by = join_by(Site_Period)`

## Warning: The `labeller` API has been updated. Labellers taking `variabl
e` and `value`
## arguments are now deprecated.
## ℹ See labellers documentation.

Mort.Profiles
```

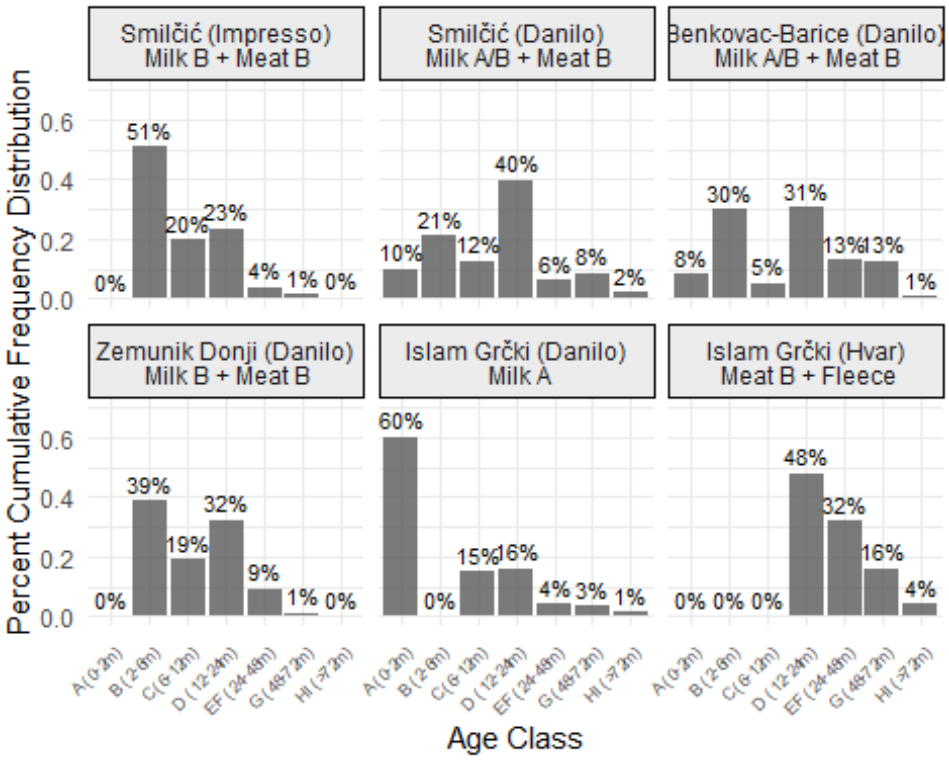


```
# ggsave("../../Figures/Fig4_2_MortalityProfiles.jpg", Mort.Profiles, widt
h = 6, height = 4)
```

Step 5. Create Table 5.1

Table 5.1 is created from the `ages.df.correct` data.frame.

Age Class	A (0-2m)	B (2-6m)	C (6-12m)	D (12-24m)	EF (24-48m)	G (48-72m)	HI (>72m)
Benkovac-Barice (Danilo)							
n	1.00	7.33	1.83	22.33	18.83	18.33	2.33
Rel. Freq.	0.01	0.10	0.03	0.31	0.26	0.25	0.03
Freq. Density	0.08	0.31	0.05	0.31	0.13	0.13	0.01
Proportion Freq. Density	0.08	0.30	0.05	0.31	0.13	0.13	0.01

Age Class	A (0-2m)	B (2-6m)	C (6-12m)	D (12-24m)	EF (24-48m)	G (48-72m)	HI (>72m)
Islam Grčki (Hvar)							
n	0.00	0.00	0.00	3.00	4.00	2.00	1.00
Rel. Freq.	0.00	0.00	0.00	0.30	0.40	0.20	0.10
Freq. Density	0.00	0.00	0.00	0.30	0.20	0.10	0.02
Proportion Freq. Density	0.00	0.00	0.00	0.48	0.32	0.16	0.04
Islam Grčki (Danilo)							
n	6.00	0.00	4.50	9.50	5.00	4.00	3.00
Rel. Freq.	0.19	0.00	0.14	0.30	0.16	0.12	0.09
Freq. Density	1.12	0.00	0.28	0.30	0.08	0.06	0.02
Proportion Freq. Density	0.60	0.00	0.15	0.16	0.04	0.03	0.01
Smilčić (Impresso)							
n	0.00	12.00	7.00	16.50	5.50	2.00	1.00
Rel. Freq.	0.00	0.27	0.16	0.38	0.12	0.05	0.02
Freq. Density	0.00	0.82	0.32	0.38	0.06	0.02	0.01
Proportion Freq. Density	0.00	0.51	0.20	0.23	0.04	0.01	0.00
Smilčić (Danilo)							
n	1.00	4.33	3.83	24.33	7.58	10.42	5.50
Rel. Freq.	0.02	0.08	0.07	0.43	0.13	0.18	0.10
Freq. Density	0.11	0.23	0.13	0.43	0.07	0.09	0.02
Proportion Freq. Density	0.10	0.21	0.12	0.40	0.06	0.08	0.02
Zemunik Donji (Danilo)							
n	0.00	5.67	4.17	14.17	8.00	1.00	0.00
Rel. Freq.	0.00	0.17	0.13	0.43	0.24	0.03	0.00
Freq. Density	0.00	0.52	0.25	0.43	0.12	0.02	0.00
Proportion Freq. Density	0.00	0.39	0.19	0.32	0.09	0.01	0.00

References

Brochier, J. É. 2013. “The use and abuse of culling profiles in recent zooarchaeological studies: Some methodological comments on "frequency correction" and its consequences.” *Journal of Archaeological Science* 40 (2): 1416–20. https://doi.org/10.1016/j.jas.2012.09.028.

McClure, Sarah B., Emil Podrug, Jelena Jović, Shayla Monroe, Hugh D. Radde, Nicholas Triozzi, Martin H. Welker, and Emily Zavodny. 2022. “The Zooarchaeology of Neolithic farmers: Herding and hunting on the Dalmatian coast of Croatia.” *Quaternary International* 634 (October): 27–37. https://doi.org/10.1016/j.quaint.2022.06.013.

Payne, Sebastian. 1973. “Kill-off Patterns in Sheep and Goats: The Mandibles from Aşvan Kale.” *Anatolian Studies* 23 (September): 281–303. https://doi.org/10.2307/3642547.

Price, Max, Jesse Wolfhagen, and Erik Otárola-Castillo. 2016. “Confidence Intervals in the Analysis of Mortality and Survivorship Curves in Zooarchaeology.” *American Antiquity* 81 (1): 157–73. https://doi.org/10.7183/0002-7316.81.1.157.

R Core Team. 2023. *R: A Language and Environment for Statistical Computing*. Vienna, Austria: R Foundation for Statistical Computing. https://www.R-project.org/.

Sierra, A., M. Balasse, S. Radović, D. Orton, D. Fiorillo, and S. Presslee. 2023. “Early Dalmatian farmers specialized in sheep husbandry.” *Scientific Reports* 13 (1): 10355. https://doi.org/10.1038/s41598-023-37516-z.

Appendix C. Modeling Herd Demography under Various Management Strategies

This appendix provides the step-by-step modeling procedures used to simulate ovicaprid herd demography under various culling strategies. The procedure is presented as an RMarkdown file. Underlying scripts can be obtained by visiting the repository at github.com/penguinnick. Also included is Table C.6, which provides the studies used to model lamb and kid mortality rates.

Livestock Population Dynamics and Optimziation of Culling Rates

Introduction

This document outlines the procedures for simulating goat and sheep herd dynamics and using the resulting models in a stochastic dynamic program that will identify the optimal culling strategy and herd reproduction parameters. The code here is executed in R (R Core Team 2023) and generates all figures and tables in Chapter Six of Nicholas Triozzi's PhD Dissertation.

Overview

The population projection model presented here uses customized code that draws on functions within the mmage package (Lesnoff 2024a). Certain procedures described in the mmage reference manual have been consolidated into functions such as "build_tcla", and "build.param".

```
source("../R/build_tcla.R")
source("../R/buildparam.R")
```

Part I - Parameters

Below, a Lefkovitch population projection model (Lefkovitch 1965) is used to project sheep and goat herd population dynamics. The probability of survival and fecundity are influenced by the competing risks of intrinsic mortality and offtake (i.e., slaugther). The transition matrix is created using published data on fecundity, intrinsic mortality, and offtake rates which are derived from theoretical culling profiles in archaeological literature (See Chapter Six).

Age Classes

The first step is to establish age classes for the simulation. Since the goal is to evaluate whether theoretical culling profiles allow herd sizes to be be maintained given intrinsic mortality and the reproductive biology of sheep and goats, the age classes and lengths (or widths) of each age class are informed by studies focusing on culling profiles. For example, Payne's (1973) work separates ages into classes A through I and Grant's (1982) work distinguishes age by month. Synthesized mandible ontogenic stages provided by Vigne and Helmer (2007) demonstrate theses groupings and their corresponding ages in years. Although Payne's (1973) Age class grouping is the most common implementation Marom and Bar-Oz (2009) compare 10 different the culling profiles by restructuring age groups to nine age classes ranging from 0.17 to 8 years.

Table C.1. Age classes and widths

Age.Class	months	years
A (0-2m)	2	0.17
B (2-6m)	4	0.33
C (6-12m)	6	0.50
D (1-2y)	12	1.00
E (2-3y)	12	1.00
F (3-4y)	12	1.00
G (4-6y)	12	1.00
H (6-8y)	12	1.00
I (>8y)	Inf	Inf

The model presented here is an "untruncated" model since the final age class includes animals 6 years old and up, with no terminal age specified for old animals. In this chunk, variable *lclass* is created as a vector of integers corresponding to the width of each age class in months. Here, an "untruncated" model is used which does not specify a terminal age for individuals in the oldest age class so the last value in *lclass* is set to *Inf*.

```
# Payne's Class
ageClasses = c("", "A (0-2m)",  "B (2-6m)", "C (6-12m)", "D (1-2y)", "E (2
-3y)", "F (3-4y)", "G (4-6y)", "H (6-8y)", "I (>8y)")

#-- Age classes in years
ages = c(  0.17,  0.5,   1, 2, 3, 4, 5, 6, 7)

#-- length of each age class
# lclass = c(0.17, 0.33, 0.5, 1, 1,   1, 1, 1, Inf ) # in years
lclass = c( 2,   4,    6, 12, 12, 12, 12, 12, Inf) # in months
```

Once the age classes are set, the function *build_tcla()* uses the *mmage::fclass* function to create the data.frame *tcla*. Parameter *nbphase* is set to either 1 or 12 to indicate whether the model will eventually be run to project herd size change on a yearly or monthly basis. The *tcla* table includes for each age group, the length of each group (i.e., 2 months, 4 months, 6 months, 12 months, etc.), and the minimum and maximum ages of the group. This procedure is streamlined by the customized *build_tcla* function which is designed to adjust the values provided as input (lclass) according to *nbphase*, and recognize whether *lclass* is formatted for a "truncated" or "untruncated" model. Since the *lclass* variable has already been set up to track age in months, *nbphase* is set to 1.

```
#-- load tcla function
source("../R/mmagefclass.R")

nbphase = 1
tcla = build_tcla(female.ages = lclass, male.ages = lclass, nbphase = nbph
```

```
ase)

flextable(tcla) %>%
  theme_vanilla() %>%
  autofit() %>%
  set_caption( "Table C.2. Initiated age and sex table (tcla), containing
age classes, lengths, and minimum and maximum ages in months for each age
class." )
```

Table C.2. Initiated age and sex table (tcla), containing age classes, lengths, and minimum and maximum ages in months for each age class.

sex	class	lclass	cellmin	cellmax
F	0	1	0	0
F	1	2	1	2
F	2	4	3	6
F	3	6	7	12
F	4	12	13	24
F	5	12	25	36
F	6	12	37	48
F	7	12	49	60
F	8	12	61	72
F	9	Inf	73	Inf
M	0	1	0	0
M	1	2	1	2
M	2	4	3	6
M	3	6	7	12
M	4	12	13	24
M	5	12	25	36
M	6	12	37	48
M	7	12	49	60
M	8	12	61	72

sex	class	lclass	cellmin	cellmax
M	9	Inf	73	Inf

Herd Culling Strategies

In this step a list of different harvest profiles for various herd management goals is defined. These include Redding's (1981) **Energy** and **Security**, Payne's (1973) **Meat**, **Milk**, and **Wool** strategies, and Vigne and Helmer's (2007) Meat and Milk types A and B (**MeatA**, **MeatB**, **MilkA**, **MilkB**) and **Fleece** strategies. Marom and Bar-Oz (2009) provide survivorship probabilities standardized across nine age classes. From these data, a list (*`offtake.models`*) is created which will be converted to offtake probabilities of death to reflect the proportion of individuals in each age class removed from the herd.

The offtake rates given here are generated from zooarchaeological research which does not account for sex-based differences in culling practices. But these offtake rates are often interpreted on the level of the herd regardless of sex. Here they are used to model the offtake rates of males. These rates are downscaled for females as described later.

Table C.3. The theoretical culling rates in Table 6.2 in Chapter 6 standardized by Marom and Bar-Oz (2009).

Age	Energy[a]	Security[a]	Meat[b]	Milk[b]	Wool[b]	Meat A[c]	Meat B[c]	Milk A[c]	Milk B[c]	Fleece[c]
0.17	90.4	90.4	85	47	85	81	86	22	83	69
0.50	90.4	90.4	75	42	75	34	68	11	50	35
1.00	77.6	64.5	70	39	65	11	28	4	36	24
2.00	47.6	38.0	50	35	63	7	6	3	18	17
3.00	25.0	25.0	30	28	57	7	6	3	18	17
4.00	23.9	23.9	22	23	50	3	1	2	6	6
5.00	18.2	18.2	19	18	43	1	1	1	1	1
6.00	16.1	16.1	19	18	43	1	1	1	1	1
7.00	11.8	11.8	10	10	20	1	1	1	1	1

[a]Redding (1981); [b]Payne (1973); [c]Vigne and Helmer (2007);

Age-at-death data from four Neolithic sites

Age-at-death data for sheep and goat mandibles collected from **Benkovac-Barice**, **Islam Grčki**, **Smilčić**, and **Zemunik Donji** is used to create survivorship probabilities for each age class. The process was described in Appendix B. First, the data is called from *`age_at_death_data.csv`*. The data has already been formatted and filtered, combining all goats and sheep as ovicaprids, and dropping Late Neolithic Islam Grcki, for which there are

only 10 mandibles. The absolute frequencies are calculated using a special function, `correct.counts()` (see Appendix B) that accounts for mandibles that were assigned multiple age classes. Then the survivorship probabilities are calculated following Price et al. (2016), using the function `survivorship()` (see Appendix B). Lastly, the data is formatted as a list, similar to the `offtake.models` list created previously.

Table C.4. The empirical culling rates in Table 6.3 in Chapter 6 standardized into age groups used by Marom and Bar-Oz (2009).

Age (years)	Smilčić EN	Smilčić MN	Benkovac-Barice MN	Islam Grčki MN	Zemunik Donji MN
0.2	100.0	98.2	98.6	81.2	100.0
0.5	72.7	90.6	88.4	81.2	82.8
1.0	56.8	83.9	85.9	67.2	70.2
2.0	19.3	41.2	54.9	37.5	27.3
3.0	13.6	37.4	39.6	28.1	21.2
4.0	6.8	27.9	28.7	21.9	3.0
5.0	2.3	9.6	3.2	9.4	0.0
6.0	0.0	2.2	0.0	6.2	0.0
7.0	0.0	0.0	0.0	0.0	0.0

Plot survivorship curves

The data in Tables C.2 and C.3 can now be visualized as survivorship curves.

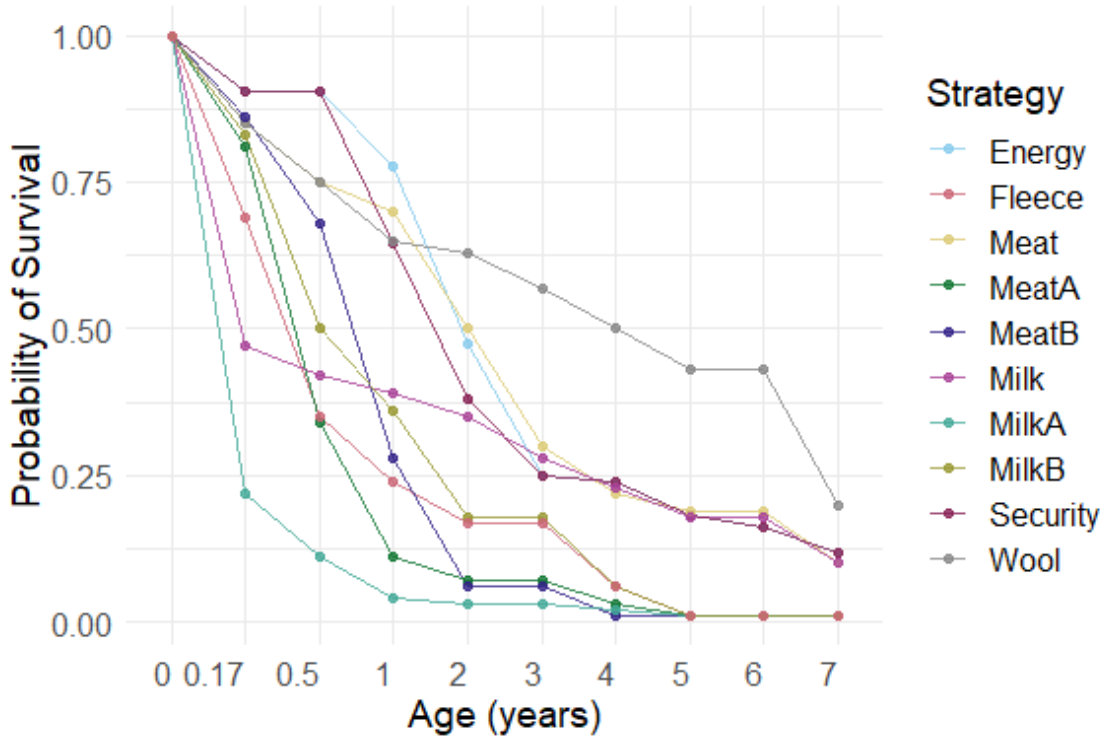

Figure C.1. Survivorship curves for threoretical harvest strategies as shown in Figure 5.1 in Chapter 5.

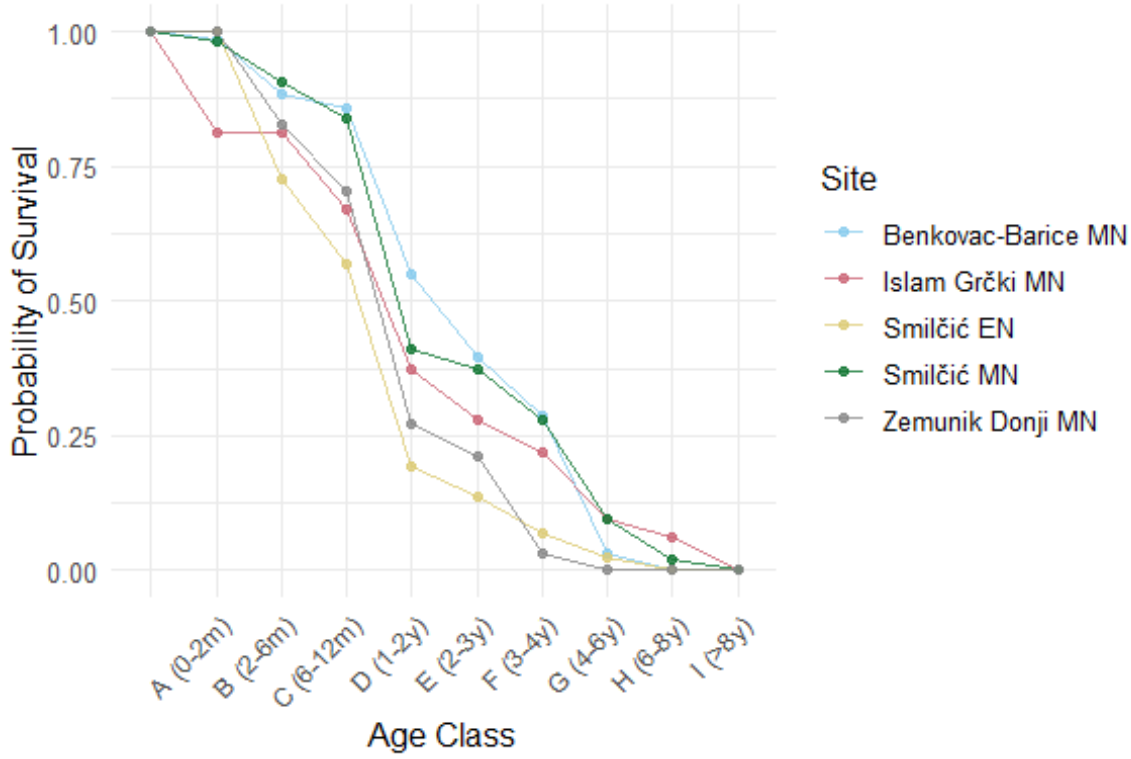

Figure. C.2. Survivorship curves of empirical culling data as shown in Figure 6.1 in Chapter 6

Herd Population Growth Parameters

Offtake represents the number of animals slaughtered in each age group. These numbers will affect herd size changes by restricting the number of animals available to reproduce. Two other important parameters are *intrinsic mortality* and *fertility*.

Mortality

The probability that an animal will survive from one time step to the next is affected by the competing risks of being slaughtered (i.e., offtake) and intrinsic mortality. We set intrinsic mortality for males and females separately. According to Redding (1981), there is no conclusive evidence that there is a difference in mortality between male and female lambs and kids. Redding applies a mortality rate of 32% for lambs and 45% for kids in the first year of life. These rates can be proportionally allocated to the first three age classes which include animals under 1 year. Redding (1981) assigns ewe and doe mortality from ages 1-9 to 18% per year; 10% for rams and 15% for bucks aged 1 to 2 years, 5% for both species ages 2-6 years and 100% for ages six and up. Male mortality is modeled slightly lower than female mortality since rams and bucks selected for breeding should be more robust and have better resistance to disease, whereas this artificial selection should be weaker for females. We simulate this by making females in their later years much more susceptible to natural deaths than males.

In this program age classes for males and females may be specified separately. However, culling profiles constructed from archaeological remains cannot distinguish male from female mandibles. Therefore, offtake rates modeled here will be applied to the entire herd while intrinsic mortality rates will be defined separately for males and females.

Fertility - Reproduction Parameters

Several parameters are important regarding the reproductive biology of goats and sheep. `pfbirth` specifies probability of giving birth to a female. This value is set as 0.5 by default in the code generating the parameter table. `part.age` specifies the age of first parturition. , as an index corresponding to the age classes defined by `lclassf` and `lclassm`. By setting this variable to 4, we set the age of first parturition to 1 year. `parturition` specifies the number of parturitions per female per year. Redding (1981) models a breeding rate of once per year but notes that under conditions of very good pasturage goats may breed twice per year (1981:59). Parturition rate is also referred to as the annual reproductive rate (ARR) and is calculated by Equation 6.13 in Chapter 6:

$$ARR = \frac{l * 365}{i}$$

where l is the litter size (i.e., prolificacy rate) multiplied by the number of days in the year and i is the parturition interval (Upton 1984; R. T. Wilson, Peacock, and Sayers 1984). To keep variation in fertility consistent, parturition varies from year to year, depending on the prolificacy rates, which are generated as described below. *parturitionInterval* is set to 300 days, reflecting a mean of 10 months for bot goats and sheep (R. T. Wilson 1989).

prolificacy specifies the prolificacy rate, defined as the number of live offspring per parturition per year. Goats are capable of giving birth to twins, triplets, and quadruplets, while kidding rates increase with age up to five or six years (Redding, 1981:70). To simulate stochastic inter-annual variation in fertility, a function is used to sample prolificacy rates from a normal distribution given mean kidding and lambing rates obtained from the literature. The *prolificacy.csv* file contains this data.

The net fecundity rate is the product of the parturition and net prolificacy rates. The parturition rate is calculated differently for birth-pulse (all births occur at the same time) and birth-flow models (births occur continuously over the time interval (t, t+1)). The Parturition rate *vpar* is dependent on the number of individuals removed from the herd, or *ptot* which is the sum of natural death rates and offtake rates:

$$vpar = \frac{1 - ptot}{2} * hpar$$

where *hpar* is the number of parturitions expected per female-time unit.

Using the mortality and prolificacy data called in the previous chunk two lists are created (one for goats, one for sheep) containing the fertility and mortality parameters used to compute **lambda** (λ), reproductive values, and project herd growth. The function *generate_ProlificacyRates()* is used to vary inter-annual fertility values.

```
generate_ProlificacyRates <- function( meanPro = MeanProlificacy, sdPro =
sdProlificacy,  n = length( part.age.Ind : len.fclass )) {

  s = seq( 1 : n )
  p.order = c( s[ s %% 2 == 1 ], rev( s[ s %% 2 != 1 ] ))
  # Generate n values from a normal distribution
  # values <- rnorm(n, meanPro, sdPro)
  values <- rnorm(mean = meanPro, sd = sdPro, n = 100)
  value.sample = sample(values, n)
  # Sort the values
  # sv <- sort( abs( values ) )
  sv <- sort( abs( value.sample ) )
  # Arrange values so that peak values are in the middle
  arranged_values = sv[ p.order ]

  return(abs( arranged_values) )
}
```

The above function is used in this chunk to generate a series of prolificacy rates based on fertility data. Also defined is the function `Part.rate` which calculates ARR (Equation 6.13 in Chapter 6). The resulting parameters are given in Table 6.1 in Chapter 6.

```
param.dat$Age = ages

#-- function for auto-generating prolificacy rates, used in build param fu
nction when prolificacyRate="auto"
source("../R/generate_prolificacy.R")
NetPro = pro.dat %>% group_by(Taxon) %>% reframe(mn.pro = mean(LitterSize)
, sd.pro = sd(LitterSize))
NetPro

## # A tibble: 2 × 3
##   Taxon mn.pro sd.pro
##   <chr>  <dbl>  <dbl>
## 1 Goats   1.49  0.275
## 2 Sheep   1.15  0.122

#-- example prolificacy rates for goats
replicate(n = 3, generate_ProlificacyRates(meanPro = NetPro$mn.pro[1], sdP
ro = NetPro$sd.pro[1], n = 6), simplify = "array")

##          [,1]     [,2]     [,3]
## [1,] 1.029077 1.378644 1.240943
## [2,] 1.214532 1.605681 1.436950
## [3,] 1.459105 1.695911 1.688528
## [4,] 1.509029 1.836180 1.767070
## [5,] 1.354119 1.633225 1.576335
## [6,] 1.177719 1.567068 1.375748

#-- Ages, parturition rate, and age of first parturition set here
ages = unique(param.dat$Age)

#-- parturition rate calculation
Part.rate = function( mean.Litter, part.interval){
  (mean.Litter * 365) / part.interval
}

parturition.Interval = 300
#-- age of first parturition set to animals in the 1-2 year age class
part.age = 2

#-- get vector of age structured mortality rates for male and female goats
goat.mort.f = param.dat %>% filter(Taxon == "Goat" & Sex == "Female") %>%
select(Mortality)
goat.mort.m = param.dat %>% filter(Taxon == "Goat" & Sex == "Male") %>% se
lect(Mortality)
```

```r
#-- get vector of age structured mortality rates for male and female sheep
sheep.mort.f = param.dat %>% filter(Taxon == "Sheep" & Sex == "Female") %>
% select(Mortality)
sheep.mort.m = param.dat %>% filter(Taxon == "Sheep" & Sex == "Male") %>%
select(Mortality)

#-- create parms lists
goat.parms = list(
  ages = ages,
  parturition = Part.rate(NetPro$mn.pro[1], parturition.Interval),
  parturition.Interval = 300,
  part.age = part.age,
  MeanProlificacy = NetPro$mn.pro[1],
  sdProlificacy = NetPro$sd.pro[1],
  f.mortality = as.vector(goat.mort.f$Mortality),
  m.mortality = as.vector(goat.mort.m$Mortality)
)

sheep.parms = list(
  ages = ages,
  parturition = Part.rate(NetPro$mn.pro[2], parturition.Interval),
  parturition.Interval = 300,
  part.age = part.age,
  MeanProlificacy = NetPro$mn.pro[2],
  sdProlificacy = NetPro$sd.pro[2],
  f.mortality = as.vector(sheep.mort.f$Mortality),
  m.mortality = as.vector(sheep.mort.m$Mortality)
)

#-- clean up
rm( goat.mort.m, goat.mort.f, sheep.mort.m, sheep.mort.f, pro.dat)
```

Build Lefkovitch matrix

Now that the mortality, offtake, and fertility parameters have been defined, it's time to create the Lefkovitch matrix. The first step is to convert the survivorship percentages to mortality probabilities. This is done by dividing each value by 100 and subtracting from 1. A **Baseline** strategy is also created to track herd population dynamics free from the offtake constraint by setting survivorship probability to 100% which translates to an offtake rate of 0 for each age group.

In the chunk below, `Baseline.offtake` is created as a list of 100% survivorship for all age classes to model herd growth with no offtake. The list is appended to the list of all offtake models to be run in the subsequent projections.

```
#-- put all harvest strategies into a single list
Baseline.offtake = list(rep(100, length(offtake.models$Energy)))
names(Baseline.offtake) = "Baseline"
all.offtake = append(offtake.models, culling.profiles)
all.offtake = append(all.offtake, Baseline.offtake)

#-- convert survivorship to mortality
offtake.mortality = lapply(all.offtake, function(x){1-(x/100)})
```

Next, a list variable containing all the parameters defined above, the original *tcla* table, *nbphase*, and a female offtake modifier, *female.offtake* is created and named *param.props*. This list is supplied to the *build.param* function which streamlines the creation of the hazards table and Lefkovitch matrix used by mmage to project population changes. The variable *female.offtake* is supplied (or not, if set to *NULL*). This value adjusts the female offtake rate, setting the female offtake probabilities to a product of offtake, female mortality, and *female.offtake*. Setting this value to 0 implies that females exit the herd acording to female mortality probabilities. Since those values are global, setting *female.offtake* to 0 eliminates all variation between different offtake models with respect to herd growth and defeats the purpose of this experiment. *female.offtake* is therefore set to *15* reflecting a culling rate of females due to infertility reported by Malher et al. (2001).

```
#-- This number is used to account for culling of females due to infertili
ty. If Null, no female offtake assumed.
female.offtake = 15

sheep.param.props = list(
  tcla = tcla, parms = sheep.parms, nbphase = nbphase, female.offtake = fe
male.offtake, truncated = FALSE)

goat.param.props = list(
  tcla = tcla, parms = goat.parms, nbphase = nbphase, female.offtake = fem
ale.offtake, truncated = FALSE)

param.props = list(goat = goat.param.props, sheep = sheep.param.props)
```

This chunk shows the definition of the *vary.fert.mort()* function, which is used to generate a new set of prolificacy and fertility rates based on mean and standard deviations provided in *parms*.

```
#-- function to vary prolificacy and mortality
# source("../R/varyFertMort.R")
#-- function to vary prolificacy and mortality
vary.fert.mort = function( parms, n = 6 ){
  source("../R/generate_prolificacy.R")
  parms$prolificacy = generate_ProlificacyRates(
    meanPro = parms$MeanProlificacy,#$mn.pro,
    sdPro = parms$sdProlificacy,#$sd.pro,
```

```
    n = n)

  #-- vary parturition rate
  parms$parturition = (mean(parms$prolificacy)*365)/parms$parturition.Inte
rval

  generate_InfantMortalityRates <- function( Mort = f.mortality, n = 3) {
    inf.mort = Mort[1:3]
    sort( generate_ProlificacyRates( meanPro = mean( inf.mort ), sdPro = s
d( inf.mort ), n = 3), decreasing = TRUE )
    # sort( generate_ProlificacyRates( meanPro = sum( inf.mort ), sdPro =
sd( inf.mort ), n = 3), decreasing = TRUE )
  }

  generate_AdultMortalityRates <- function( Mort = f.mortality, n = 6) {
    adult.mort = Mort[4:length(Mort)]
    sort( generate_ProlificacyRates( meanPro = mean( adult.mort ), sdPro =
sd( adult.mort ), n = 6), decreasing = FALSE )
    # sort( generate_ProlificacyRates( meanPro = sum( inf.mort ), sdPro =
sd( inf.mort ), n = 3), decreasing = TRUE )
  }

  # parms$f.mortality[1:3] = c(generate_InfantMortalityRates( parms$f.mort
ality ), generate_AdultMortalityRates(parms$f.mortality))
  parms$f.mortality = c(generate_InfantMortalityRates( parms$f.mortality )
, generate_AdultMortalityRates(parms$f.mortality))
  parms$m.mortality = c(generate_InfantMortalityRates( parms$m.mortality )
, generate_AdultMortalityRates(parms$m.mortality))
  # parms$m.mortality[1:3] = parms$f.mortality[1:3]
  return(parms)
}
```

Here a single param table is created for each survivorship profile in **two steps**.

First, the parms object is updated with prolificacy and infant mortality rates generated by sampling from a normal distribution using the `vary.fert.mort()` function defined above.

Second, build.param function is run which creates a table that contains offtake, mortality, fecundity, and survival probabilities for each age class

```
param = lapply(param.props, function( p ) {
  p$parms = vary.fert.mort( p$parms )
  lapply( offtake.mortality, function( o ) {
    with( p , {
      build.param( tcla, parms, nbphase, female.offtake,  truncated = trun
cated, correctionfec = TRUE, offtake = o)
    })
  })
```

```
  })

str(param$goat$Energy$param)

## 'data.frame':    20 obs. of  11 variables:
##  $ sex    : chr  "F" "F" "F" "F" ...
##  $ class  : int  0 1 2 3 4 5 6 7 8 9 ...
##  $ lclass : num  1 2 4 6 12 ...
##  $ cellmin: num  0 1 3 7 13 25 37 49 61 73 ...
##  $ cellmax: num  0 2 6 12 24 ...
##  $ nupar  : num  0 0 0 0.136 1.648 ...
##  $ ff     : num  0 0 0 0.0857 1.0448 ...
##  $ fm     : num  0 0 0 0.0857 1.0448 ...
##  $ pdea   : num  0.0897 0.1594 0.1222 0.1016 0.0403 ...
##  $ poff   : num  0.00685 0.01312 0.01561 0.03474 0.07529 ...
##  $ g      : num  1 0.4528 0.1974 0.112 0.0388 ...

rm(sheep.param.props, goat.param.props, Baseline.offtake)
# param$goat$Energy$param
```

Part II - Simulating Environmental Variation

In the previous chunk, the function *build.param()* was run to produce a parameter set using auto-generated prolificacy rates and infant mortality rates using mean and standard deviation for each taxon.

In this chunk, environmental variation is simulated by creating a new *param* table for each time-step containing unique sets of fertility and mortality parameters using the *vary.fert.mort()* function described above. This is done using the *make.listpar()* function which has the *vary.fert.mort()* function built into it. The function simulates a single environment with unique fertility and mortality rates while keeping the offtake rates defined earlier constant. The environment is called *listpar*. The number of years over which the simulation will run is specified by *nbcycle*.

```
source("../R/makeListpar.R")

nbcycle = 200
p0 = 150

#-- uncomment lines below to re-create simulation environment or use exist
ing by loading from data folder
listpar = lapply(param.props, function(p){
  make.listpar(
    param.props = p,
    nbcycle = nbcycle,
    offtake.mortality = offtake.mortality
```

```
    )
  })

# save(listpar, file = "../data/listpar.RData")
# load(file = "../data/listpar.RData")
```

Basic Herd structure and growth

With the fertility and mortality rates have been established the next step is to extract the structure of the herd, lambda, and the proportion of male to females for each model. To do this, an initial herd size, *p0* is set to *150*. In the following chunk, these traits are calculated for comparison of the impacts of culling strategies on herd demography.

While lambda can be computed from a single *param* table, the herd multiplication rate will change from one time-step to the next as fertility and mortality rates change. To estimate lambda given this variation a bootstrapping procedure is used.

Using the list of mortality and fertility parameters created in the previous chunk, the custom function *getLambda()* is run using *lapply* to obtain lambda, sex proportion, and number of individuals in each age class for the initial population. This function is a wrapper function that uses functions in the *mmage* package to obtain the dominant eigenvalue (lambda) to get the multiplication rate for the population.

With the environment simulated as *listpar*, the chunk below calculates lambda and proportion of females for each year under each offtake strategy.

```
#-- a function that gets lambda, sex proportion, and herd structure.
source("../R/getLambda.R")

#-- wrapper function to get demography information from every listpar tabl
e
wrapper.repro = function( listpar, out = c("lambda", "sex") ){
  out <- match.arg(out)
  lapply(seq_along(listpar), function(l) {
  p = listpar[[l]]
  lapply(p, function(s){
    sapply(s, function(x){
      r = getLambda(x, tcla=tcla, lclass = lclass, p0=p0) #$lambda
      if(out=="lambda"){
        return(r$lambda)
      } else {
        if(out=="sex"){
          return(r$sex.proportion[1,2])
        }
      }
      })
    })
```

```
  })
}

#-- put all lambda and female proportions in lists
lambda.list = wrapper.repro(listpar, out = "lambda")
sex.prop.list = wrapper.repro(listpar, out = "sex")

names(lambda.list) = names(listpar)
names(sex.prop.list) = names(listpar)

lambda.list = unlist(lambda.list, recursive = F)
sex.prop.list = unlist(sex.prop.list, recursive = F)
```

Bootstrap lambda and sex proportions

This chunk defines the function used in the bootstrap estimation of mean λ (λ_{boot}) and proportion of females. The bootstrap is replicated 1000 times. The output is *repro.boot.df*.

```
#-- Define function to calculate the mean
mean_function <- function(data, indices) {
  # This function will be applied to resampled data
  return(mean(data[indices]))
}

#-- function to compute bootstrapped mean and 95% confidence intervals
boot.fun = function( s, n ){
  # Perform bootstrapping
  bootstrap_results = boot(data = s, statistic = mean_function, R = n )
  # Obtain bootstrapped confidence interval
  boot_conf_interval = boot.ci(bootstrap_results, type = "perc")
  #-- returns mean, lower and upper ci
  return(data.frame(t0 = boot_conf_interval$t0, low = boot_conf_interval$p
ercent[4], up = boot_conf_interval$percent[5]))
}

#-- set number of bootstrap replicates
n.boot = 1000

lambda.boot.df = do.call(rbind.data.frame, lapply(lambda.list, FUN = boot.
fun, n = n.boot))
sex.prop.boot.df = do.call(rbind.data.frame, lapply(sex.prop.list, FUN = b
oot.fun, n = n.boot))

#-- create taxon and strategy columns
taxon.strat = str_split(rownames(lambda.boot.df), "\\.", simplify = T)

#-- bind columns from each bootstrapped results table
```

```
repro.boot.df = cbind.data.frame(
  lambda.boot.df %>% reframe(Taxon = taxon.strat[,1], strategy = taxon.str
at[,2], Lambda = t0, low.lambda = low, up.lambda = up),
  sex.prop.boot.df %>% reframe("Proportion.Female" = t0, "Proportion.Male"
= 1 - t0, low.sex.F = low, up.sex.F = up)
  )

# head(repro.boot.df)
# write.table(repro.boot.df, file = "../data/reproboot.csv", sep = ",")

# rm(lambda.list, sex.prop.list, sex.prop.boot.df)
```

In this chunk, λ_{boot} and proportion of females in the herd are plotted to show the negative correlation between these two values.

```
#-- check correlation between lambda and sex proportions
repro.boot.df %>% filter(strategy!="Baseline") %>% with(cor.test( Lambda,
`Proportion Female` ))

##
##  Pearson's product-moment correlation
##
## data:  Lambda and Proportion Female
## t = -11.07, df = 28, p-value = 9.741e-12
## alternative hypothesis: true correlation is not equal to 0
## 95 percent confidence interval:
##  -0.9527957 -0.8029552
## sample estimates:
##        cor
## -0.9022279
```

Herd Structure

This chunk calculates herd structure which is used to produce Figure 6.2 in Chapter 6.

```
#-- set initial population size
p0 = 150

#-- call function getLambda to extract reproduction traits
repro = lapply(listpar, function(l){
  lapply(l, function(x){
    getLambda(x[[1]], tcla=tcla, lclass = lclass, p0=p0)
  })
})

#-- wrapper function to get a dataframe with herd structure from repro obj
ect
```

```r
xini.to.data.frame = function( repro, ageClasses, ages ) {
  xini.list = lapply(repro, function( r ) {  # given repro, a list of repr
oductive params for n species,
    lapply( r, function( x ) {
      with(x, {
        # summarize initial herds (total males and females for each age cl
ass)
        xini = initial.herd %>%
          group_by( class ) %>%
          reframe( n = as.integer( sum( xini ) ) )
        })
      })
    })
  xini.list = unlist( xini.list, recursive = F ) # unlist species grouping
s
  taxon.strat = str_split( names( xini.list ), "\\." ) # create list of sp
ecies and strategies
  # create Taxon, strategy, and AgeClass fields for each df in xini.list
  for ( i in 1: length( xini.list ) ) {
    ts = taxon.strat[[ i ]]
    taxon = rep( unlist( ts )[ 1 ], 9 )
    strat = rep( unlist( ts )[ 2 ], 9 )
    xini.list[[ i ]]$Taxon = taxon
    xini.list[[ i ]]$strategy = strat
    xini.list[[ i ]]$AgeClass = ageClasses[ -1 ]
    xini.list[[ i ]]$Age = as.character(ages)
  }
  # call all dataframes into a single df
  xini.df = do.call( rbind.data.frame, xini.list )
  # make strategy field a factor
  xini.df$strategy = factor( xini.df$strategy, levels = c(  names(offtake.
mortality) ))
  xini.df$AgeClass = factor( xini.df$AgeClass, levels = ageClasses[-1] )
  return( xini.df )
}

xini.df = xini.to.data.frame(repro, ageClasses = ageClasses, ages = ages)
head(xini.df)
```

```
## # A tibble: 6 × 6
##   class     n Taxon strategy AgeClass  Age
##   <int> <int> <chr> <fct>    <fct>     <chr>
## 1     1    55 goat  Energy   A (0-2m)  0.17
## 2     2    51 goat  Energy   B (2-6m)  0.5
## 3     3    27 goat  Energy   C (6-12m) 1
## 4     4    13 goat  Energy   D (1-2y)  2
```

```
## 5     5     2 goat  Energy   E (2-3y)  3
## 6     6     0 goat  Energy   F (3-4y)  4
```

Part III - Population Projection

The next step is to simulate herd demographic change through time given the parameters defined above and the reproductive traits calculated for each model and culling profile. The initial herd size was established already as *p0* and the simulated environment as *listpar*. The number of times-teps is equal to the length of *listpar*.

The projection is run using the script "projectHerd2.R". This function takes fewer inputs than the *projectHerd()* function. First, *listpar* is created using the makeListpar.R function. This function simulates environmental variation of one herd under inter-annual variation in mortality and fertility. One herd, multiple offtake strategies can be assessed this way. Results are in the same format as projectHerd.R. This function is a wrapper function that streamlines the herd projection procedure described in the mmage documentation (Lesnoff 2024b) but is used when the environment is predefined. The alternative function *projectHerd* has additional functionality such as varying environments from one step to the next. This is useful when there is only one *param* table but environmental variation is generated for each time-step. This process is explained in another document.

The output of the projection is saves as *results*. When the projection is run for every strategy using the mortality and fertility rates for each taxon using *lapply*, the output is a list of length n.strategies * n.taxa.

```
#-- load projectHerd function
source("../R/projectHerd2.R")

listpar = unlist(listpar, recursive = F)
results = lapply(listpar, function(l) { projectHerd2( listpar = l, p0 = p0
) } )
```

Output Metrics

Here summary statistics of interest are calculated to compare how the different models perform (i.e., values that will be used to compare differences in herd size, etc.).

First, a wrapper function is defined as *pop.summary*, which takes the results list (*results*) and creates a list of data.frames each containing two columns: the time step (*time*) and the number of animals in the herd (*pop*). Then another wrapper function, *res.to.df* is used to create a single data.frame of all results which is used for plotting.

```
#-- function to summarize dynamics of the total population through time
source("../R/popsummary.R")
```

```r
tot.pop.res = lapply(results, function(r){pop.summary(r, sex = FALSE, inte
rval = "year")})
# tot.pop.res.sex = lapply(results, function(r){pop.summary(r, sex = TRUE,
interval = "year")})

# function to gather results into a single dataframe
res.to.df = function(tot.pop.res){
  df = do.call(rbind.data.frame, args=c(tot.pop.res, make.row.names=FALSE)
)
  strats = names(tot.pop.res)
  df$strategy = unlist(lapply(strats, FUN=rep, (nrow(df)/length(strats))))
  ts = str_split(df$strategy, "\\.", simplify = T)
  df$Taxon = ts[, 1]
  df$strategy = ts[, 2]
  return(df)
}
tot.pop.df = res.to.df(tot.pop.res)
# tot.pop.df.sex = res.to.df(tot.pop.res.sex)
head(tot.pop.df)

##   time      pop strategy Taxon
## 1    1 150.0000   Energy  goat
## 2    2 160.2489   Energy  goat
## 3    3 170.1196   Energy  goat
## 4    4 178.5106   Energy  goat
## 5    5 171.2988   Energy  goat
## 6    6 155.1515   Energy  goat

# head(tot.pop.df.sex)
```

Figure. C.3. Plots showing the change in sheep and goat herd sizes through time under the various survivorship profiles used as shown in Figure 6.3 in Chapter 6.

Stochastic variation

Since there is an element of stochastic variation, it is useful to examine multiple iterations of the simulation. Here *nbrep* is set as the number of simulations to replicate. A wrapper function is created, *stochastic.rep* which combines *make.listpar*, *projectHerd2*, and *pop.summary* functions. Then, the simulation is replicated *nbrep* times. Results are combined into a data.frame for plotting.

```
#-- function to replicate
stochastic.rep = function( p0, param.props, offtake.mortality, nbcycle){
  lp = make.listpar(param.props = param.props, nbcycle = nbcycle, offtake.
mortality = list(offtake.mortality))
  result = projectHerd2( listpar = unlist(lp, recursive = F) , p0 = p0 )
  pop.summary(result, sex = FALSE, interval = "year")$pop
}

#-- set number
nbrep = 10
nbcycle = nbcycle

#-- run simulation for all strategies
```

```
stochastic.sim.res = replicate(
  n = nbrep,
  lapply(param.props, function( p ){
    lapply(offtake.mortality, function( o ){
      r = stochastic.rep(p0 = p0, param.props = p, offtake.mortality = o,
nbcycle = nbcycle)
      })
    }),
  simplify = "array"
  )

#-- create df from matrix output of replicated stochastic.rep func
matrix.to.df = function( mat ){
  df = as.data.frame(mat)
  df$time = as.numeric(str_replace_all(rownames(df), "[:alpha:]|[:punct:]"
, ""))
  df$strategy = str_replace_all(rownames(df), "[:digit:]", "")
  df %>% pivot_longer( cols = c(-time, -strategy) )
}

#-- function to transform lists into matrix
list.to.mat = function( l ){
  n.col = length( l )
  l.mat = matrix( unlist( l ), ncol = n.col)
  rownames(l.mat) = unique(names(unlist(l)))
  l.mat
}

#-- create matrix, then df from results
sto.res.mat = apply(stochastic.sim.res, 1, FUN = list.to.mat, simplify = F
)
sto.res.df = lapply(sto.res.mat, FUN = matrix.to.df)

#-- set taxon fields
sto.res.df$goat$taxon = "goat"
sto.res.df$sheep$taxon = "sheep"

#-- combine into one df
sto.res.df = do.call(rbind.data.frame, sto.res.df)
sto.res.df$strategy = factor(sto.res.df$strategy, levels = c(names(offtake
.mortality)))

## Scale for colour is already present.
## Adding another scale for colour, which will replace the existing scale.
```

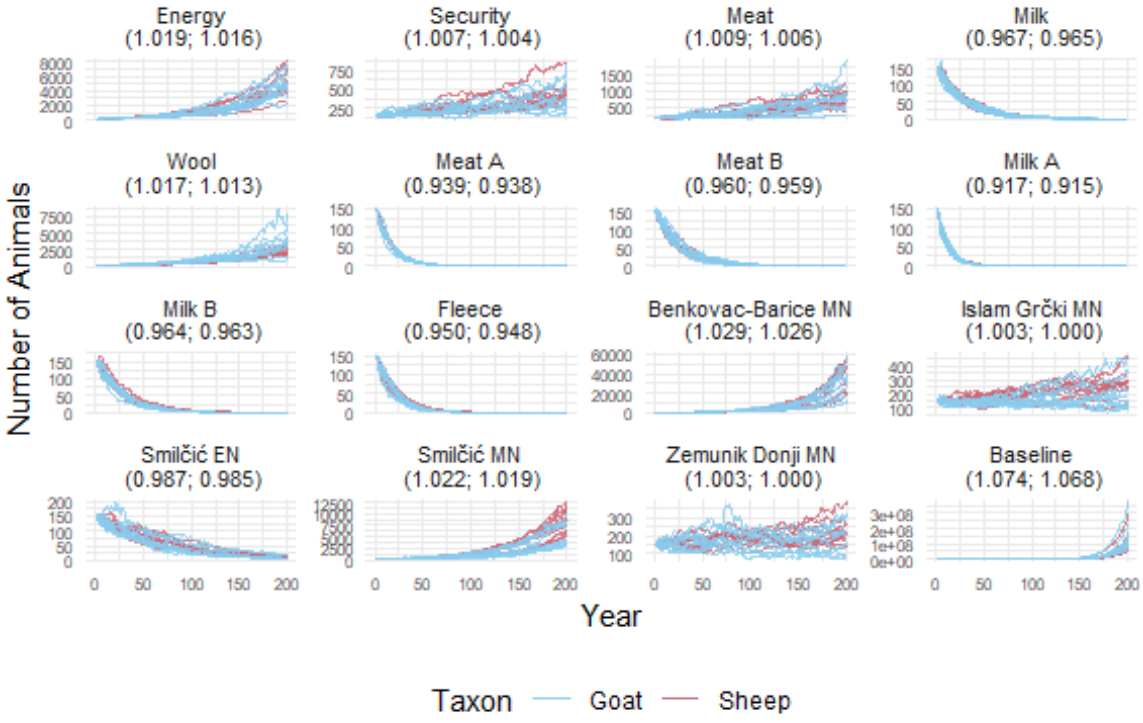

Figure. C.4. Plots showing results of replicated projections of change in sheep and goat herd sizes through time under the various survivorship profiles used as shown in Figure 6.4 in Chapter 6.

Part IV - Optimizing offtake

Modification of offtake rates may allow for herd size to remain stable. An optimization routine is needed to determine the factor, φ, by which female offtake needs to be adjusted to maintain herd size. The goal is to achieve a steady state multiplication rate under stochastic changes in fertility and mortality. The first step is to determine the multiplication rate of the herd from one timestep to the next. This is done using the modified `mmage::fm` function, `mmagefm()`. In this chunk, a dataframe, `lambda.df` is created by obtaining the multiplication rate from the results of the herd projection which used the `listpar` object that simulates inter-annual variation in fertility and mortality.

After creating `lambda.df`, an index of the years with lowest lambda is created. This index will be used to determine `phi` (φ) in a later step.

Adjust offtake function

In this chunk, a function is defined that will take as input a `param` table from the list of params associated with the worst years for herd growth and return a value of $(\lambda - m)^2$,

which should be close to 0. This function will be used in the optimization routine in the subsequent chunk.

```
#-- function to adjust offtake based on poff in param table
get.off.adjust.poff = function( phi, param.ref, m = 1 ){
  u = param.ref
  zf = u$poff[ u$sex == "F" ]
  zm = u$poff[ u$sex == "M" ]
  u$poff = c( phi * zf, zm )
  Lf = length( u$sex[ u$sex == "F" ]) - 1
  Lm = length( u$sex[ u$sex == "M" ]) - 1
  param = u
  A = fmat( param, Lf, Lm )$A
  ( feig( A )$lambda - m ) ^ 2
}
```

Optimize

In this chunk, the function defined above is optimized to find φ_{opt}, which is the value that will be used to adjust female offtake in a new projection.

```
#-- optimize to find the value that minimizes (lambda-m)^2 (i.e., differen
ce between projected herd growth rate and objective growth)
#-- an example of optimized phi
optimize(f=get.off.adjust.poff, param.ref = listpar$goat.Energy[[1]], inte
rval = c(0,5))$minimum
```

```
## [1] 2.470137
```

```
#-- optimize for all
optimize.res = lapply( listpar$goat.Energy, function( b ){
  optimize( f = get.off.adjust.poff, param.ref = b, interval = c(0,5))$min
imum
  })

#-- phi
optimize.res[1:5]
```

```
## [[1]]
## [1] 2.470137
##
## [[2]]
## [1] 1.897497
##
## [[3]]
## [1] 1.630349
##
```

```
## [[4]]
## [1] 0.5165457
##
## [[5]]
## [1] 0.5977545
```

Now that the optimization procedure has been demonstrated for one set of parameters, a function is defined that will adjust offtake rates by φ_{opt} when $< $ *low.threshold* or $$ *high.threshold*.

Dynamic optimization function

Here a function is defined that will multiply female offtake probabilities by φ_{opt} if λ falls outside of the defined thresholds. This will run inside of the project herd wrapper function and return a new *param* table for every cycle

```
#-- function for adjusting p. female offtake
adjust.offtake = function( in.param, low.threshold, high.threshold, p0 = 1
50 ){
  #-- calculate phi.opt
  phi.opt = optimize(f = get.off.adjust.poff, param.ref = in.param, interv
al = c(0,5))$minimum

  #-- get unadjusted female offtake
  f.off = in.param$poff[ in.param$sex == "F" & in.param$class > 0 ]

  #-- extract tcla
  tcla1 = in.param[ , c( 1:5 ) ]

  #-- extract lclass
  lclass1 = in.param$lclass[ in.param$sex=="F" & in.param$class > 0 ]

  #-- get lambda
  lambda = getLambda( param = in.param,  tcla = tcla1, lclass = lclass1, p
0 = p0)$lambda

  #-- compare lambda to threshold value
  if( lambda < low.threshold | lambda >= high.threshold ){
    #-- if lambda below threshold, adjust female offtake
    in.param$poff[in.param$sex=="F" & in.param$class > 0] = f.off * phi.op
t
  } else {
    in.param$poff[in.param$sex=="F" & in.param$class > 0] = f.off
  }
  return(in.param)
}
```

Reproject herd with optimal offtake adjustments

Now the simulation is run after setting the upper and lower thresholds as the 25% and 75% quantiles of λ_{boot} stored in in *repro.boot.df*.

Based on λ_{boot} estimates, the optimization function will adjust offtake if λ is below 0.954 or above 1.017. After optimizing, the original projection results are combined with the new results and can be plotted.

```
#-- reproject with optimization
new.results = lapply( listpar, function( l ) {
  l = lapply( l,
              FUN = adjust.offtake,
              low.threshold = Lambda.threshold.low,
              high.threshold = Lambda.threshold.high )
  projectHerd2( listpar = l, p0 = p0 )
  })

#-- send results to df
new.tot.pop.res = lapply(new.results, function(r){pop.summary(r, interval
= "year")})
new.pop.res.df = res.to.df(new.tot.pop.res)

#-- create column for offtake adjustment
tot.pop.df$offtake = "unadjusted"
new.pop.res.df$offtake = "adjusted"

#-- merge into a single data.frame
all.res.df = rbind.data.frame(tot.pop.df, new.pop.res.df)
```

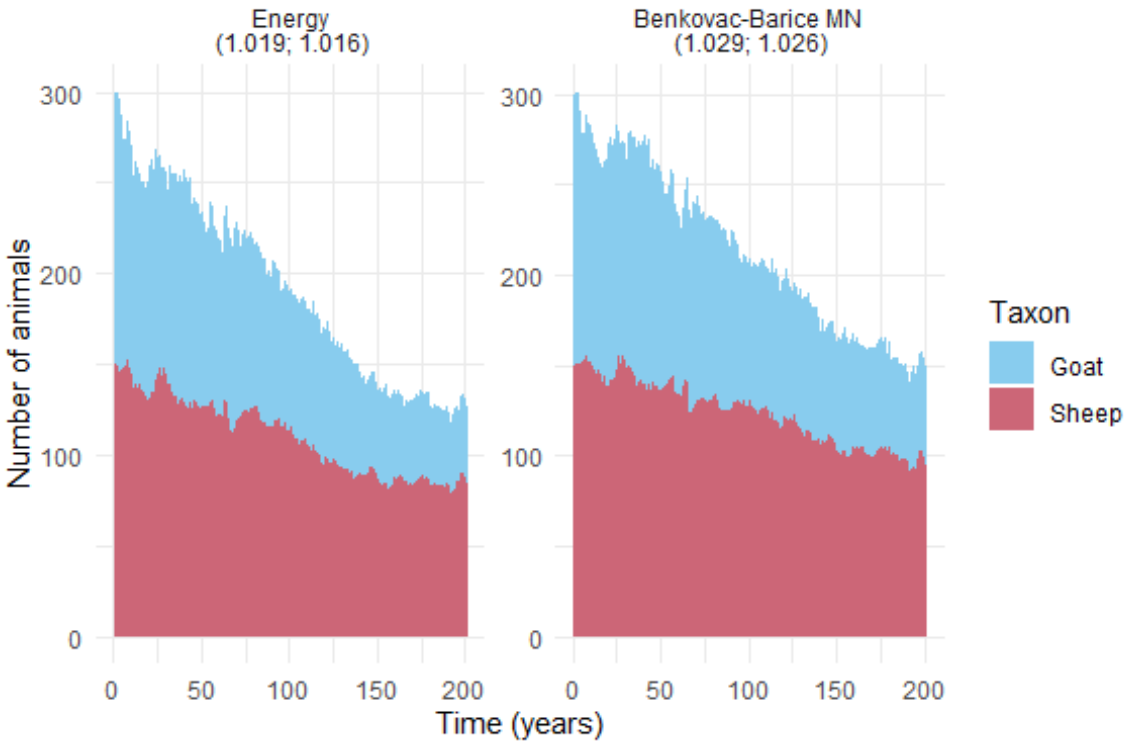

Figure C.5. Projected sheep and goat populations after applying optimized offtake procedure for the Energy and Benkovac-Barice strategies.

Part V - Evaluate optimization results

This chunk uses `fprod()` function from the `mmage` package (Lesnoff 2024b) to calculate mean herd size as shown in Figure 6.6 in Chapter 6.

```
source("../R/mmagefprod.R")
new.vprod = do.call(rbind.data.frame, lapply(new.results, function(l){ fpr
od(formula = ~ 1, l$vecprod)  }))
new.vprod$Taxon = str_split_i(rownames(new.vprod), "\\.", i = 1)
new.vprod$strategy = str_split_i(rownames(new.vprod), "\\.", i = 2)
new.vprod = new.vprod %>%
  mutate(
    strategy = factor( strategy,
      levels = rev(names(offtake.mortality)),
      labels = rev(c(
        names(offtake.mortality)[1:5],
        "Meat A", "Meat B", "Milk A", "Milk B",
        names(offtake.mortality)[10:16])
```

```
        )),
    Taxon = factor(Taxon, levels = c( "goat", "sheep")))
```

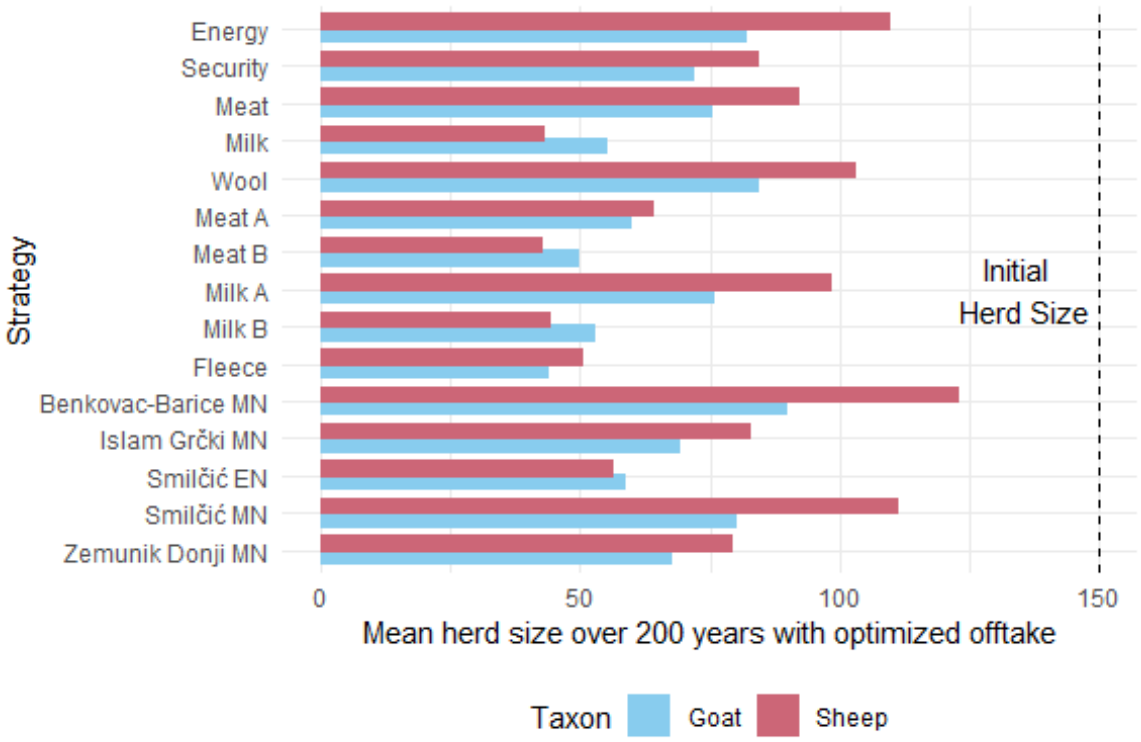

Figure C.6. Mean herd size after optimized culling rates applied, as shown in Figure 6.6 in Chapter 6.

This chunk uses a modified version of the *`fm()`* function in the *`mmage`* package to obtain the annual multiplication rates of the optimized offtake (adjusted) and unadjusted simulations.

```
#-- modified mmage function to get multiplication rate of the herd
source("../R/mmagefm.R")

#-- summarize multiplication rate for old and new results
m.df = lapply( results, function( r ){
  o = mmage.fm( formula = ~ cycle , vecprod = r$vecprod ); return( data.fr
ame( cycle = o$cycle, m = o$m ))
  })
m.df = res.to.df(m.df)

new.m.df = lapply(new.results, function(r){
  o = mmage.fm( formula = ~ cycle , vecprod = r$vecprod ); return( data.fr
ame( cycle = o$cycle, m = o$m ))
  })
new.m.df = res.to.df(new.m.df)
```

```
#-- create column for offtake adjustment
m.df$offtake = "unadjusted"
new.m.df$offtake = "adjusted"

#-- merge into a single data.frame
all.m.df = rbind.data.frame(m.df, new.m.df)
```

10-year moving averages of the multiplication rates were calculated to simplify illustration. This chunk defines functions to calculate the moving averages and detect detect maximum and minimum multiplication rates. These functions are used to produce Figures 6.7 and 6.8 in Chapter 6.

```
# Function to calculate moving average
calculate_moving_average <- function(time_series, window_size, type = c("s
imple", "exponential"), alpha = 0.1) {
  type <- match.arg(type)

  if (type == "simple") {
    # Calculate simple moving average
    moving_average <- rollmean(time_series, k = window_size, fill = NA, al
ign = "right")
  } else if (type == "exponential") {
    # Calculate exponential moving average
    moving_average <- zoo::rollapply(time_series, width = window_size, FUN
= function(x) {
      n <- length(x)
      weights <- (1 - alpha)^(n:1)
      sum(weights * x) / sum(weights)
    }, fill = NA, align = "right")
  }

  return(moving_average)
}


# Function to detect peaks
detect_peaks <- function(x, span = 3) {
  z <- embed(x, span)
  s <- span %/% 2
  v <- max.col(z, ties.method = "first") == 1 + s
  c(rep(FALSE, s), v, rep(FALSE, s))
}

# Function to detect valleys
detect_valleys <- function(x, span = 3) {
  z <- embed(x, span)
  s <- span %/% 2
```

```
  v <- apply(z, 1, which.min) == 1 + s
  c(rep(FALSE, s), v, rep(FALSE, s))
}
```

This section performs a Levene's Test for Equality of variances between the herd multiplication rate after offtake was optimized and the predicted λ value (i.e., unadjusted rates). The output is used to create Table 6.6 in Chapter 6.

```
all.m.list = all.m.df %>%
  mutate(strategy = factor(strategy, levels = names(offtake.mortality),
                           labels = c(names(offtake.mortality)[1:5], "Meat
A", "Meat B", "Milk A", "Milk B",
                                      names(offtake.mortality)[10:16]))) %
>%
  group_by(strategy, Taxon) %>%
  group_split()

m.lev.res = lapply(all.m.list, function(l){
  lev.res = l %>% with(leveneTest(m, offtake))
  data.frame(strategy = first(l$strategy), Taxon = first(l$Taxon), F.value
= lev.res$`F value`[1], p = lev.res$`Pr(>F)`[1])
})

lev.res.df = do.call(rbind.data.frame, m.lev.res)
head(lev.res.df)

##   strategy Taxon  F.value           p
## 1   Energy  goat 5.558744 0.018871758
## 2   Energy sheep 7.170969 0.007716038
## 3 Security  goat 3.068269 0.080604651
## 4 Security sheep 5.199702 0.023118889
## 5     Meat  goat 3.747102 0.053607027
## 6     Meat sheep 7.214736 0.007533441
```

Now offtake and productions are compared using a modified version of the *mmage* package function *fprod()*. Here I create survivorship curves using the total number of animals that died (including natural deaths and slaughtered animals) for the unadjusted offtake and optimized simulations. This figure is not included in Chapter Six but this graphical comparison illustrates how that optimization of offtake rates will likely go undetected when the data are visualized as survivorship curves.

```
source("../R/mmagefprod.R")
#-- function for caclulating annual production values
class.prod = function( x ){
  vecprod = x$vecprod
  res = fprod(formula =  ~ class , vecprod )
  res[res$class > 0, ]
}
```

```
class.df = do.call(rbind.data.frame, lapply(results, FUN = class.prod))
# nrow(class.df)
class.df = rbind.data.frame(class.df, do.call(rbind.data.frame, lapply(new
.results, FUN = class.prod)) )
class.df$Taxon = str_split_fixed( rownames(class.df ), "\\.", 3 )[,1]
class.df$strategy = str_split_fixed( rownames(class.df ), "\\.", 3 )[,2]
class.df$offtake = c(rep("unadjusted", 288), rep("adjusted", 288))
```

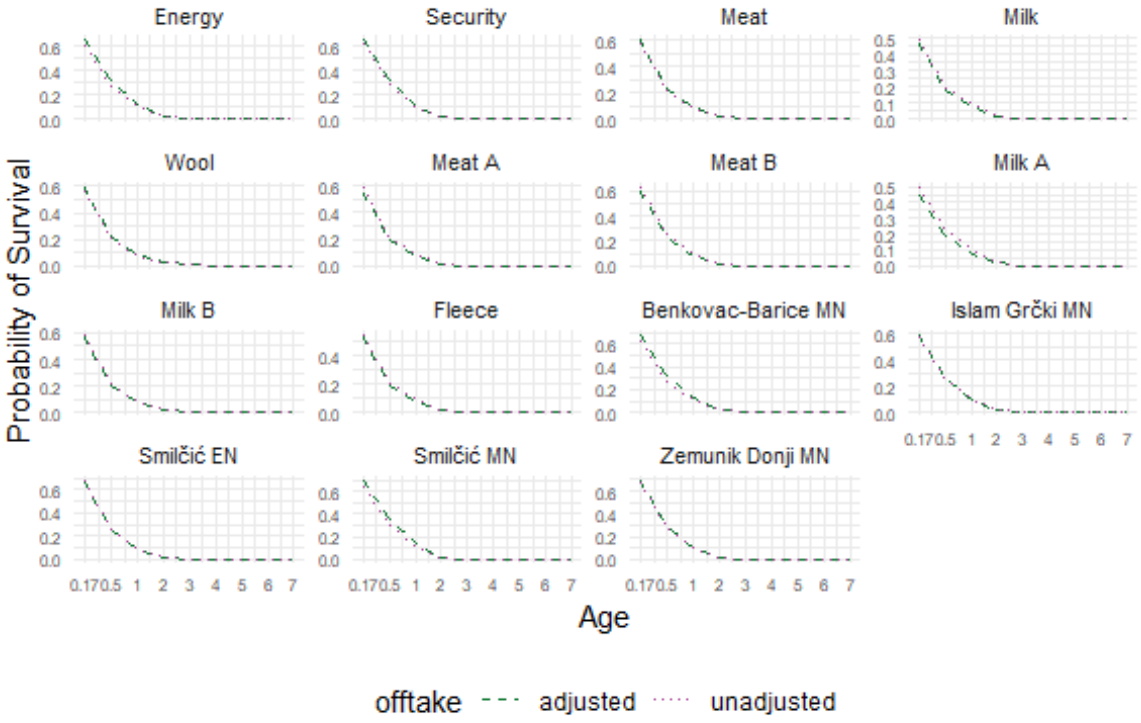

Figure C.7. Commparison of survivorship curves resulting from projections with unadjusted and optimized offtake rates

This chunk uses a Kolmogorov-Smirnov Test to compare the survival probabilities associated with each strategy's results. Are the strategies statistically indistinguishable? This test is not included in Chapter 6 but will be useful for future publication of this work.

```
off.df = do.call(cbind.data.frame, args=c(all.offtake[-16]))
off.df2 = off.df

p.list = sapply(1:ncol(off.df2), function(j){
  sapply(1:ncol(off.df), function(i){
    ks = ks.test(as.vector(off.df[,i]), as.vector(off.df2[,j]), exact = TR
UE, B=2000)
    return(paste0("D=", ks$statistic, ", ", round(ks$p.value, 3)))
    }, simplify = TRUE)
```

```
})

#-- rename rows and columns
rownames(p.list) = colnames(p.list) = names(offtake.mortality)[-16]
```

Table C.5. Results of Kolmogorov-Smirnov Test comparing each strategy's offtake rates

Energy	Security	Meat	Milk	Wool	MeatA	MeatB	MilkA	MilkB	Fleece	Benkovac-Barice MN	Islam Grčki MN	Smilčić EN	Smilčić MN	Zemunik Donji MN
D=0, 1	D=0.1, 1	D=0.2, 0.994	D=0.4, 0.397	D=0.4, 0.418	D=0.7, 0.012	D=0.6, 0.052	D=0.8, 0.002	D=0.4, 0.418	D=0.4, 0.418	D=0.3, 0.787	D=0.3, 0.732	D=0.4, 0.397	D=0.3, 0.763	D=0.4, 0.397
D=0.1, 1	D=0, 1	D=0.2, 0.994	D=0.3, 0.763	D=0.5, 0.168	D=0.7, 0.012	D=0.6, 0.052	D=0.8, 0.002	D=0.4, 0.418	D=0.4, 0.418	D=0.3, 0.787	D=0.3, 0.732	D=0.4, 0.397	D=0.3, 0.763	D=0.4, 0.397
D=0.2, 0.994	D=0.2, 0.994	D=0, 1	D=0.4, 0.418	D=0.4, 0.418	D=0.6, 0.052	D=0.6, 0.045	D=0.7, 0.012	D=0.5, 0.153	D=0.5, 0.168	D=0.3, 0.763	D=0.3, 0.763	D=0.4, 0.418	D=0.3, 0.763	D=0.4, 0.393
D=0.4, 0.397	D=0.3, 0.763	D=0.4, 0.418	D=0, 1	D=0.7, 0.012	D=0.6, 0.052	D=0.6, 0.045	D=0.7, 0.012	D=0.4, 0.354	D=0.5, 0.153	D=0.4, 0.418	D=0.3, 0.737	D=0.4, 0.418	D=0.3, 0.763	D=0.4, 0.393
D=0.4, 0.418	D=0.5, 0.168	D=0.4, 0.418	D=0.7, 0.012	D=0, 1	D=0.7, 0.012	D=0.6, 0.052	D=0.8, 0.002	D=0.6, 0.052	D=0.7, 0.012	D=0.4, 0.418	D=0.5, 0.168	D=0.6, 0.045	D=0.5, 0.168	D=0.5, 0.168
D=0.7, 0.012	D=0.7, 0.012	D=0.6, 0.052	D=0.6, 0.052	D=0.7, 0.012	D=0, 1	D=0.2, 0.976	D=0.3, 0.693	D=0.3, 0.693	D=0.3, 0.693	D=0.4, 0.37	D=0.4, 0.418	D=0.3, 0.737	D=0.4, 0.418	D=0.3, 0.737
D=0.6, 0.052	D=0.6, 0.052	D=0.6, 0.045	D=0.6, 0.045	D=0.6, 0.052	D=0.2, 0.976	D=0, 1	D=0.3, 0.693	D=0.2, 0.964	D=0.2, 0.964	D=0.4, 0.37	D=0.5, 0.168	D=0.3, 0.724	D=0.4, 0.397	D=0.3, 0.737
D=0.8, 0.002	D=0.8, 0.002	D=0.7, 0.012	D=0.7, 0.012	D=0.8, 0.002	D=0.3, 0.693	D=0.3, 0.693	D=0, 1	D=0.4, 0.37	D=0.4, 0.37	D=0.6, 0.052	D=0.6, 0.048	D=0.4, 0.37	D=0.6, 0.052	D=0.4, 0.37
D=0.4, 0.418	D=0.4, 0.418	D=0.5, 0.153	D=0.4, 0.354	D=0.6, 0.052	D=0.3, 0.693	D=0.2, 0.964	D=0.4, 0.37	D=0, 1	D=0.2, 0.986	D=0.3, 0.763	D=0.3, 0.763	D=0.2, 0.981	D=0.3, 0.763	D=0.3, 0.737
D=0.4, 0.418	D=0.4, 0.418	D=0.5, 0.168	D=0.5, 0.153	D=0.7, 0.012	D=0.3, 0.693	D=0.2, 0.964	D=0.4, 0.37	D=0.2, 0.986	D=0, 1	D=0.4, 0.37	D=0.3, 0.737	D=0.2, 0.981	D=0.4, 0.393	D=0.3, 0.737
D=0.3, 0.787	D=0.3, 0.787	D=0.3, 0.763	D=0.4, 0.418	D=0.4, 0.418	D=0.4, 0.37	D=0.4, 0.37	D=0.6, 0.052	D=0.3, 0.763	D=0.4, 0.37	D=0, 1	D=0.3, 0.787	D=0.3, 0.763	D=0.1, 1	D=0.3, 0.763
D=0.3,	D=0.3,	D=0.3,	D=0.3,	D=0.5,	D=0.4,	D=0.5,	D=0.6,	D=0.3,	D=0.3,	D=0.3, 0.787	D=0, 1	D=0.3,	D=0.3,	D=0.3,

Energy	Security	Meat	Milk	Wool	MeatA	MeatB	MilkA	MilkB	Fleece	Benkovac-Barice MN	Islam Grčki MN	Smilčić EN	Smilčić MN	Zemunik Donji MN
0.732	0.732	0.763	0.737	0.168	0.418	0.168	0.048	0.763	0.737			0.787	0.787	0.737
D=0.4, 0.397	D=0.4, 0.397	D=0.4, 0.418	D=0.4, 0.418	D=0.6, 0.045	D=0.3, 0.737	D=0.3, 0.724	D=0.4, 0.37	D=0.2, 0.981	D=0.2, 0.981	D=0.3, 0.763	D=0.3, 0.787	D=0, 1	D=0.3, 0.787	D=0.2, 0.979
D=0.3, 0.763	D=0.3, 0.763	D=0.3, 0.763	D=0.3, 0.763	D=0.5, 0.168	D=0.4, 0.418	D=0.4, 0.397	D=0.6, 0.052	D=0.3, 0.763	D=0.4, 0.393	D=0.1, 1	D=0.3, 0.787	D=0.3, 0.787	D=0, 1	D=0.3, 0.763
D=0.4, 0.397	D=0.4, 0.397	D=0.4, 0.393	D=0.4, 0.393	D=0.5, 0.168	D=0.3, 0.737	D=0.3, 0.737	D=0.4, 0.37	D=0.3, 0.737	D=0.3, 0.737	D=0.3, 0.763	D=0.3, 0.737	D=0.2, 0.979	D=0.3, 0.763	D=0, 1

Table C.6. Studies of lamb and kid mortality rates discussed in Chapter Five.

Study[a]	Breed	Weaning Age	Age (months)	Mortality (%): Total	Male	Female
		Taxon: Goat				
Al-Barakeh et al (2024)	Baladi	2 months	0-12	14.50		
Debele et al (2011; 2013)	Arsi-Bale	3 months	0-12	22.40	7.28	15.12
Talore et al (2014)			0-3	12.59	4.44	8.15
Ebozoje and Ngere (1995)	West African Dwarf	1 month	0-1	5.30		
			0-3	23.00	44.00	30.00
			0-5	28.90	18.00	35.00
			0-5	28.90	18.00	15.00
			2-3	19.00		
	West African Dwarf-Red Sokoto cross		0-1	5.30		
			0-3	17.00	6.00	27.00
			0-5	23.00	14.00	33.00
			0-5	23.00	14.00	11.00
			2-3	19.00		
Gachuiri et al. (1986)*	Small East African	5 months	0-5	18.00		
Gatongi (1995)*			0-5	17.00		
Hailu et al (2016)	Borana and Arsi-Bale		0-12	31.00	33.00	29.00
Mourad (1993)	French Alpine	3 months	0-3	16.00		
	Zairabi		0-3	13.00		
Singh (2008)	Jamunapari		0-1	11.00		
			0-3	17.75	18.29	14.71

Study[a]	Breed	Weaning Age	Age (months)	Mortality (%): Total	Male	Female
			1-2	3.00		
			2-3	3.00		
Wilson et al (1985)	Masai	5 months	0-5	28.60		
Angwenyi and Bebe (1989)*	NA	4 months	0-4	19.00		
Carles et al. (1987) Isiolo research station*		5 months	0-5	15.00		
Carles et al. (1987) Marasbit research station*			0-5	24.00		
Herren (1991)*		6 months	0-6	39.00		
Maina (1996)*		4 months	0-4	34.00		
Njanja (1991)*		5 months	0-5	11.00		
Skea et al. (1990)		4-5 months	0-5	3.00		
	Taxon: Sheep					
Abdelqader et al (2017)	Awassi	2 months	0-2	18.60	19.40	17.70
Al-Barakeh et al (2024)			0-12	7.70		
Green and Morgan (1993)	Poll Dorset, Suffolk, Mule cross breeds	5-7 weeks	0-2	9.70		
Mandal et al (2007)	Muzaffarnagari	3 months	0-12	12.60	13.52	7.64
			0-2	6.43	7.02	5.85
			0-3	7.50	7.39	2.71
			3-6	2.70		
			6-9	1.60		
			9-12	1.20		

Study[a]	Breed	Weaning Age	Age (months)	Mortality (%): Total	Male	Female
Mukasa-Mugerwa et al (2000)	Horro and Menz		0-12	44.00	49.10	38.60
			0-2	15.90	16.30	13.50
			0-3	20.00	18.60	15.60
			3-6	18.00		
			6-9	10.00		
			9-12	5.00		
Talore et al (2014)	Adilo		0-3	14.84	5.81	9.03
Wilson et al (1985)	Red Masai	5 months	0-5	32.10		
Yappi et al (1990)	Dorset, Finnsheep, Lincoln, Rambouillet, Suffolk, Targhee and crosses	2 months	0-2	25.90		
Gatongi (1995)*	NA	5 months	0-5	17.00		
Herren (1991)*		6 months	0-6	29.00		
Maina (1996)*		4 months	0-4	23.00		
Njanja (1991)*		5-7 months	0-5	5.00		

[a]* study reported in Peeler and Wanyangu (Table 1; 1998)

References

Grant, Annie. 1982. “The Use of Tooth Wear as a Guide to the Age of Domestic Ungulates.” In *Ageing and Sexing Animal Bones from Archaeological Sites - British Archaeological Records International Series 109.*, edited by Bob Wilson, Caroline Grigson, and Sebastian Payne, 91–108. Oxford: Archaeopress.

Lefkovitch, L. P. 1965. “The study of population growth in organisms grouped by stages.” *Biometrics* 21 (1): 1–18.

Lesnoff, Matthieu. 2024b. *Mmage: A r Package for Sex-and-Age Population Matrix Models*.

———. 2024a. *mmage: A R package for sex-and-age population matrix models*.

Malher, X., H. Seegers, and F. Beaudeau. 2001. “Culling and mortality in large dairy goat herds managed under intensive conditions in western France.” *Livestock Production Science* 71 (1): 75–86. https://doi.org/10.1016/S0301-6226(01)00242-1.

Marom, Nimrod, and Guy Bar-Oz. 2009. “Culling profiles: the indeterminacy of archaeozoological data to survivorship curve modelling of sheep and goat herd maintenance strategies.” *Journal of Archaeological Science* 36 (5): 1184–87. https://doi.org/10.1016/j.jas.2009.01.007.

Payne, Sebastian. 1973. “Kill-off Patterns in Sheep and Goats: The Mandibles from Aşvan Kale.” *Anatolian Studies* 23 (September): 281–303. https://doi.org/10.2307/3642547.

Price, Max, Jesse Wolfhagen, and Erik Otárola-Castillo. 2016. “Confidence Intervals in the Analysis of Mortality and Survivorship Curves in Zooarchaeology.” *American Antiquity* 81 (1): 157–73. https://doi.org/10.7183/0002-7316.81.1.157.

R Core Team. 2023. *R: A Language and Environment for Statistical Computing*. Vienna, Austria: R Foundation for Statistical Computing. https://www.R-project.org/.

Redding, Richard William. 1981. “Decision making in subsistence herding of sheep and goats in the Middle East.” Doctoral Dissertation, University of Michigan.

Upton, Martin. 1984. “Models of improved production systems for small ruminants.” In *Proceedings of the Workshop on Small Ruminant Production Systems in the Humid Zone of West Africa*, edited by J. E. Sumberg and K. Cassaday, 55–67. Ibadan, Nigeria: International Livestock Centre for Africa. https://api.semanticscholar.org/CorpusID:131461953.

Vigne, Jean-Denis, and Daniel Helmer. 2007. “Was milk a ‘secondary product’ in the Old World Neolithisation process? Its role in the domestication of cattle, sheep and goats.” *Anthropozoologica* 42 (2): 9–40.

Wilson, R T. 1989. “Reproductive performance of African indigenous small ruminants under various management systems: a review.” *Animal Reproduction Science* 20 (4): 265–86.

Wilson, R. T., Christie Peacock, and A. R. Sayers. 1984. “Aspects of reproduction in goats and sheep in south-central Kenya.” *Animal Science* 38 (3): 463–67. https://doi.org/10.1017/S0003356100041660.

Appendix D. Water Samples Collected from Northern Dalmatia

This appendix provides background on water samples collected from the study area which are used to infer altitudinal gradients of precipitation $\delta^{18}O$.

Water samples were collected from springs, wells, ponds, rivers, and streams in the study area in July of 2016 (Figure D.1, Table D.1). The data presented in Figure D.2 demonstrate how ponds, wells, and streams in low-altitude areas (i.e., below 500 masl), which are sourced primarily from groundwater in karst environments (Bonacci et al. 2019) tend to be more ^{18}O-enriched than river water. The $\delta^{18}O$ values of water samples collected from springs that discharge water from subterranean aquifers exhibit a negative relationship with altitude (Figure D.2). Three river water samples, whose water sources may be located at a considerable distance from where the samples were collected are depleted in ^{18}O relative to springs, wells, and ponds at similar altitudes (Figure D.2).

One river sample (DWS8) exhibits a high $\delta^{18}O_{VSMOW}$ relative to other river samples at similar altitudes. DWS8 was collected from the Čikola River near the Ružić hydrological station, downstream from the source spring located at Čikola cave which has extremely low discharge rates between May and October (Bonacci et al. 2019). Discharged water is pooled in the catchment area of the Čikola cave spring until it spills over a dam before it reaches Ružić station. At that point, the discharge is so significant that contributions from other springs feeding the Čikola river are negligible (Bonacci et al. 2019). It is therefore likely that the high $\delta^{18}O_{VSMOW}$ value from this site is a result of the unique hydrological situation there, in which preferential evaporation of lighter oxygen isotopes while the water was accumulating in the spring basin resulted in the collection of a water sample that was more enriched in ^{18}O.

Figure D.2 also shows three samples taken from Šator Jezero, a lake located at 1437

masl in the Dinara mountains: one from the source spring (-9.4‰), and two samples from deep (-7.63‰) and shallow (-7.56‰) sections of the lake. The main water body of Šator Jezero is enriched in ^{18}O by approximately 1.8‰ relative to the source spring, likely a result of preferential evaporation of the lighter oxygen isotope in cooler, high-elevation temperatures.

The $\delta^{18}O$ values of pond, stream, and well samples are 1.3 to 1.8‰ more negative than the mean $\delta^{18}O$ of precipitation recorded at the Zadar station at 5 masl (Figure D.3) but deviate from estimated annual $\delta^{18}O$ for their respective altitudes by 0.0 to 0.3‰ (Table D.1; Bowen 2024; Bowen and Revenaugh 2003; IAEA/WMO 2015). In contrast, the water samples taken from rivers are between 1.7 and 2.1‰ more negative than estimated annual $\delta^{18}O$ values, indicating that even during the summer, river water will tend to be more depleted in ^{18}O relative to precipitation.

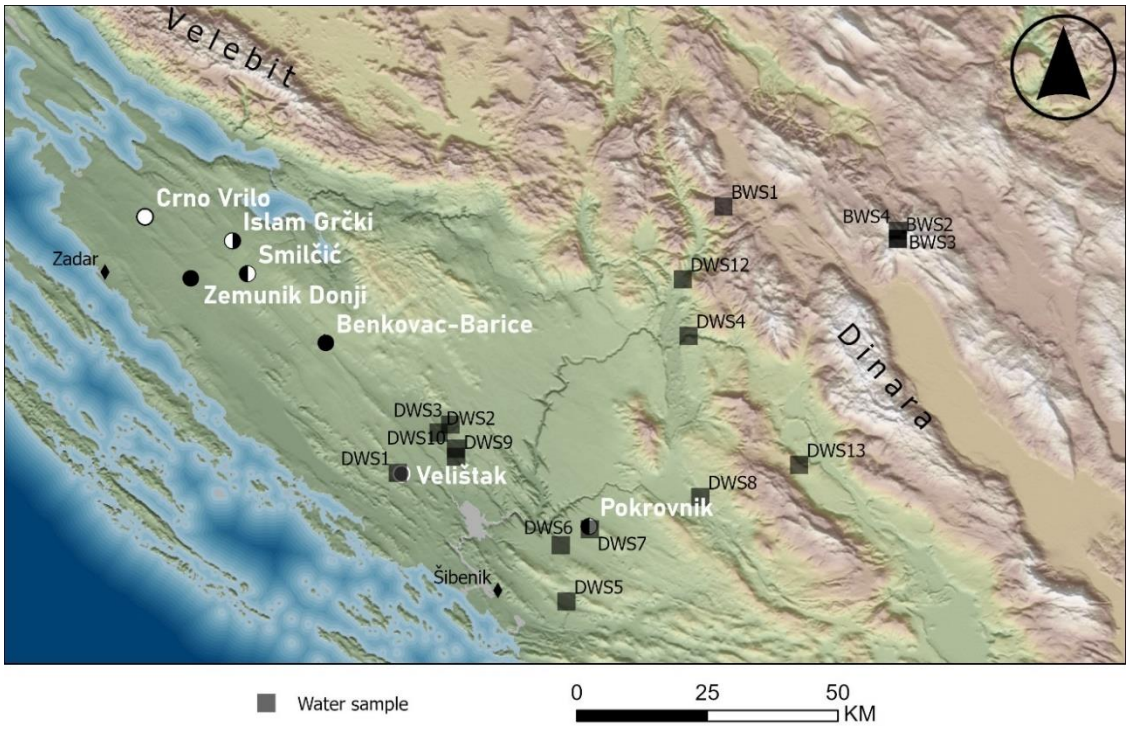

Figure D.1. Locations of water samples listed in Table D.1 and Neolithic sites discussed in this dissertation.

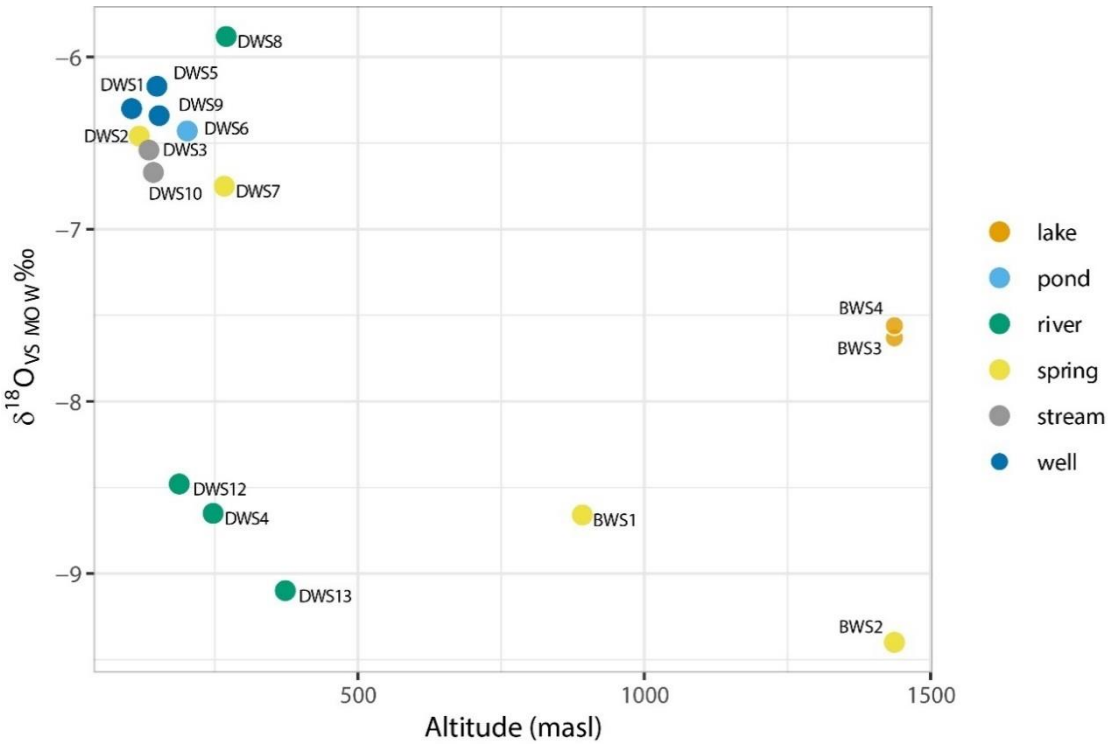

Figure D.2. $\delta^{18}O$ values of water samples collected in the study area presented by source type and elevation. See Table D.1 for sample information and Figure D.1 for location.

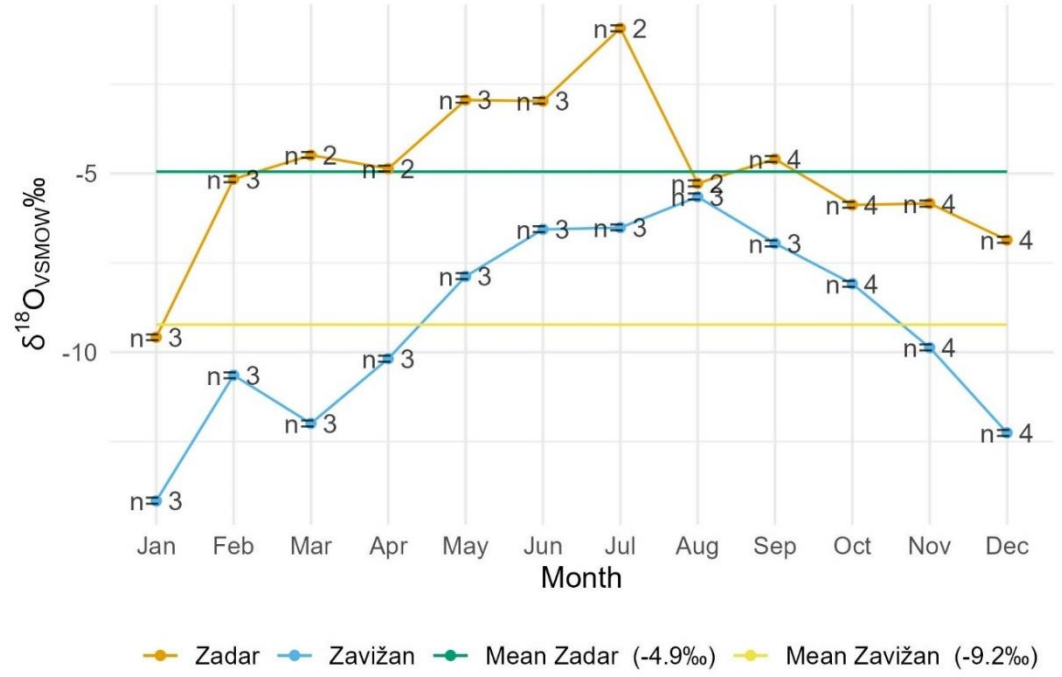

Figure D.3. Monthly $\delta^{18}O_{VSMOW}$ of precipitation from the Global Network for Isotopes in Precipitation (GNIP; IAEA/WMO 2015) for Zadar and Zavižan, number of samples, and averages for each site for the period Sept. 2000 to Dec. 2003.

Table D.1. Water samples from northern Dalmatia.

Sample ID	Site	Source Type	Lat.	Long.	Altitude (masl)	$\delta^{18}O$ (‰$_{VSMOW}$)	OIPC Annual Estimate ($\delta^{18}O$ ‰$_{VSMOW}$)	95% CI	delta
DWS1	Velištak	well	43.87	15.74	105	-6.30	-6.4	0.2	0.1
DWS2	Vrbica	spring	43.92	15.81	118	-6.46	-6.5	0.2	0.0
DWS3	Krivače	stream	43.93	15.83	135	-6.54	-6.5	0.2	0.0
DWS4	Krka	river	44.04	16.24	247	-8.65	-6.9	0.1	1.8
DWS5	Danilo	well	43.71	16.03	149	-6.17	-6.4	0.2	0.2
DWS6	Konjevrate	pond	43.78	16.02	202	-6.43	-6.6	0.2	0.2
DWS7	Pokrovnik	spring	43.80	16.07	267	-6.75	-6.7	0.2	0.0
DWS8	Čikola River	river	43.84	16.26	270	-5.88	-6.7	0.2	0.8
DWS9	Rašinovac	well	43.89	15.84	153	-6.34	-6.6	0.2	0.3
DWS10	Mokrice	stream	43.90	15.84	143	-6.67	-6.5	0.2	0.2
DWS12	Bustiča River	river	44.11	16.23	188	-8.48	-6.8	0.1	1.7
DWS13	Cetina Spring	river	43.88	16.43	373	-9.10	-7.0	0.2	2.1
BWS1	Lemića Vrelo	spring	44.20	16.30	892	-8.66	-8.4	0.2	0.3
BWS2	Šator Jezero	spring	44.16	16.60	1,437	-9.40	-9.6	0.5	0.2
BWS3	Šator Jezero	lake	44.16	16.60	1,437	-7.63	-9.6	0.5	2.0
BWS4	Šator Jezero	lake	44.17	16.60	1,437	-7.56	-9.6	0.5	2.0

Appendix E. Tooth Enamel Specimen Information

This appendix provides details for the tooth specimens sampled for stable isotope analysis of enamel bioapatite as described in Chapter Seven.

Table E.1. Specimen information for teeth sampled for stable isotope analysis of enamel bioapatite. [a]EN = Early Neolithic/Impresso, MN = Middle Neolithic/Danilo, LN = Late Neolithic/Hvar; [b]CA = goat, OA = sheep, OC = ovicaprid; [c]Age and wear based on Zeder's (2006) revision of Payne's (1973) tooth wear classification method.

Specimen	Period[a]	Provenience	Species[b]	Max. Crown Height (mm)	Side	Wear	n samples	Payne's Age Class	Revised Age[c]
CV15	EN	C / IX / 2	CA	25.49	R	16	8	G	4-5y
CV17	EN	C / V / 1	OA	26.50	L	09	7	D	12-18m
CV18	EN	C / I / 1	OA	28.30	L	05	4	D	12-18m
CV19	EN	C / I / 1	OA	25.91	L	17	7	F	3-4y
CV20	EN	C / I / 1	CA	32.08	L	14	9	D	12-18m
CV21	EN	A / IIIb / 2	CA	27.84	L	16	9	G	4-5y
CV22	EN	A / IIIb / 2	OA	14.09	R	18	6	H	6-8y
CV23	EN	A / IIIb / 2	OA	33.69	R	16	10	F	3-4y
CV24	EN	A / IIIb / 2	OA	23.64	R	17	9	G	4-5y
CV26	EN	C / IV / zdravica	OA	20.38	R	17	8	F	3-4y
CV28	EN	A / IIa / zdravica	OA	23.95	R	17	6	F	3-4y
PK100	EN	D/11	CA	30.00	L	17	11		
PK101	EN	D/11	CA	29.40	L	16	10		
PK102	EN	D/21	CA	28.70	L	14	10		
PK104	EN	D/22	CA	27.00	L	14	10		
PK72	EN		CA	27.92	L		10		
PK76	EN		OC	27.36	R		11		
PK90	EN	D/21	OA	28.10	R	16	10		
PK91	EN	D/22	CA	24.90	L	N/A	10		
PK92	EN	D/23	CA	33.70	R	14	10		

Specimen	Period[a]	Provenience	Species[b]	Max. Crown Height (mm)	Side	Wear	n samples	Payne's Age Class	Revised Age[c]
PK93	EN	D/23	CA	30.40	R	16	12		
PK99	EN	D/11	CA	37.60	L	14	12		
SMI335	EN	B / N2/M2 / 22	OA	22.64	L	17	10	F	3-4y
SMI338	EN	B / N2 / 22	OA	27.85	L	17	10	F	3-4y
SMI403	EN	D / JAMA 17	OA	21.00	L	17	9	G	4-5y
SMI454	EN	D / N6 / 52	OC	26.09	L	17	11	D	18-24m
SMI455	EN	D / N6 / 52	OA	21.92	R	17	11	F	3-4y
SMI456	EN	D / N6 / 52	OA	31.86	R	14	12	D	18-24m
BB135	MN	B1 / SJ49	OA	27.50	L	17	10	E, F	2-4y
BB136	MN	B1 / SJ49	OA	30.96	R	16	9	D	18-24m
BB154	MN	B1 / SJ49	OC	29.19	L	17	10	E, F	2-4y
BB168	MN	B3 / SJ49	OA	30.95	R	16	11	D	12-18m
BB180	MN	C2 / SJ49	OC	28.24	L	17	12	E, F	2-4y
BB182	MN	B1 / SJ6	CA	26.58	L	16	10	F	3-4y
IG211	MN	A / SJ4	CA	30.94	L	14	12	D	12-18m
IG212	MN	A / SJ47	CA	30.94	L	17	10	D	18-24m
IG219	MN	A / SJ47	OA	28.91	L	16	11	E	2-3y
IG226	MN	A / SJ4 / 2	OA	32.32	R	14	12	D	18-24m
IG233	MN	A / SJ4	OA	24.35	R	17	10	F	3-4y
IG239	MN	A / SJ25_SWX / 1	OA	27.55	L	15	11	F	3-4y
PK54	MN		CA	26.88	R		11		
PK87	MN	D/9	CA	22.30	R	16	10		

Specimen	Period[a]	Provenience	Species[b]	Max. Crown Height (mm)	Side	Wear	n samples	Payne's Age Class	Revised Age[c]
PK88	MN	D/10	OC	28.00	R	14	7		
PK89	MN	D/10	OC	25.80	R	9	10		
PK94	MN	D/3	CA	30.50	R	16	11		
PK95	MN	D/3	CA	24.70	L	16	10		
PK96	MN	D/3	CA	31.30	L	N/A	12		
PK97	MN	D/10	CA	30.30	L	17	8		
PK98	MN	D/10	OA	27.30	L	N/A	12		
SMI130	MN	15	OC	34.32	L	11	14	D	12-18m
SMI360	MN	C / P10 / 41	OA	23.88	R	17	10	F	3-4y
SMI421	MN	D / M7 / 56	OC	28.01	L	16	10	D	18-24m
SMI435	MN	D / N7 / 56	OA	32.02	R	13	11	D	18-24m
ZD10	MN	KV10 / sj43A	CA	23.87	L	11	11	C, D	
ZD11	MN	KV9 / sj43A	OA	26.43	L	16	10	F	3-4y
ZD13	MN	KV9/8 / sj47	OA	27.04	R	10	6	D	18-24m
ZD14	MN	KV9/8 / sj47	OA	27.72	R	17	10	F	3-4y
ZD16	MN	KV10 / sj43A	OC	28.53	R	16	11	D, E	18m-3y
ZD297	MN	KV9 / sj43A	OC	35.49	L	16	10	D, E	18m-3y
ZD298	MN	KV9 / sj43A	CA	27.42	L	17	11	E	2-3y
IG468	LN	B / SJ20	CA	26.44	R	17	12	G	4-5y
IG475	LN	B / SJ20	OC	22.91	R	17	10	E	2-3y
IG476	LN	B / SJ22	OC	31.76	R	14	12	D	18-24m
IG477	LN	B / SJ22	OA	21.53	R	17	10	F	3-4y

Specimen	Period[a]	Provenience	Species[b]	Max. Crown Height (mm)	Side	Wear	n samples	Payne's Age Class	Revised Age[c]
IG478	LN	B / SJ29	OA	28.08	R	17	10	F	3-4y
IG479	LN	B / SJ29	OA	30.11	L	14	11	D	18-24m
VEL28	LN	A/3	OC	27.80	R	N/A	8		
VEL29	LN	A/3	OC	31.60	L	N/A	11		
VEL30	LN	E/3	CA	34.70	L	16	10		
VEL31	LN	F/3	CA	25.60	L	16	8		
VEL32	LN	B-E/105-1 DO 1-5-6	OA	24.80	R	17	10		
VEL34	LN	F/3	OA	17.40	R	17	5		
VEL37	LN	CD/41-1	CA	27.51	L	17	7		
DIN5	modern		OA	27.85	R		6		
DIN6	modern		OA	18.51	R		3		
DIN7	modern		OA	29.13	R		9		
VRL481	modern	MOD / 1	OA	18.59	L	17	10	G	5-6y

[a]EN = Early Neolithic/Impresso; MN = Middle Neolithic/Danilo; LN = Late Neolithic/Hvar

[b]OA = *Ovis aries*; CA = *Capra hircus;* OC = ovicaprid

[c]Estimated according to conversion of Payne's (1973) age classes as described by Zeder (2006)

Appendix F. FTIR Analysis for Assessment of Diagenetic Alteration of Enamel Bioapatite Samples

This appendix describes the application and results of Fourier Transform Infrared spectroscopy analysis of archaeological and modern tooth enamel samples to test for diagenesis of bioapatite.

Due to higher crystallinity, enamel is generally more resistant to diagenesis than bone (Gage et al. 1989). However, subtle alteration of isotopic signatures does occur as a result of exogenous carbonate incorporation, endogenous carbonate loss, or endogenous carbonate reorganization (Sponheimer and Lee-Thorpe 1999). Additionally, some sample pretreatment protocols intending to remove organics from samples such as the addition of hydrogen peroxide (H_2O_2) have been shown to decrease $\delta^{13}C$ values in enamel bioapatite samples while the effects on $\delta^{18}O$ are unclear (Pellegrini and Snoeck 2016). Therefore, it is necessary to ensure the accuracy of paleoenvironmental inferences using stable isotope analyses of enamel bioapatite the integrity of samples and assess the extent to which sample pretreatment protocols could have impacted a sample's isotopic composition (Ventresca Miller et al. 2018). Various methods exist to identify diagenesis in bioapatite samples (Madupalli et al. 2017). Fourier Transform infrared spectroscopy (FTIR) is used to obtain the information about the chemical composition and crystallinity of a material (Trueman et al. 2008). Instruments equipped with an Attenuated Total Reflection unit (i.e., FTIR-ATR) enhance the sensitivity of the FTIR measurements and is a practical option because it is fast, relatively low-cost, requires a very small amount of sample which requires minimal preparation (Hollund et al. 2013).

FTIR analysis subjects samples to infrared radiation that is absorbed at frequencies corresponding to specific molecular groups. Peaks attributed to specific compounds such as phosphate (PO_4^{3-}), carbonate (CO_3^{2-}), and hydroxyl (OH^-) within FTIR spectra obtained from archaeological (or fossil) enamel samples are evaluated to determine if the sample experienced structural or chemical modifications or was contaminated by external carbonates (Sponheimer and Lee-Thorp 1999). This is achieved by computing peak height ratios from

intensity of infrared absorbance at certain wavelengths to produce indices that are compared with modern samples. The most common indices are the phosphate crystallinity index (PCI; also known as InfraRed Splitting Factor, IRSF), ratios of A-site and B-site carbonates to phosphate peaks (API and BPI), carbonate-phosphate ratio (C/P), and carbonate-carbonate ratio (C/C) (Table F.1). Among these, PCI (ISRF) and C/P have been suggested to be the most useful for identifying preservation status of enamel bioapatite (France et al. 2020).

FTIR was performed on one to three subsamples of each archaeological and modern tooth discussed in this study using a Thermo Nicolet is10 FTIR Spectrometer equipped with a Smart Diamond ATR accessory at the Materials Research Laboratory at UC Santa Barbara. Each sample was scanned 64 times. A new background scan was completed to account for noise after scanning 10 samples. Attenuated Total Reflectance (ATR) corrections were performed using OMNIC spectroscopy software. Spectral data was exported as comma separated value (i.e., ".csv") files. Individual files were imported using the ChemoSpec package v6.1.10 (Hanson 2024) in R Statistical Software v4.3.1 (R Core Team 2023).

A custom scripting procedure was written to compute the indexes shown in Table S5 by obtaining intensities at band positions corresponding to the functional groups Water-Amide (1650 cm^{-1}), A-site carbonates (1545 cm^{-1}, and 1455 cm^{-1}), B-site carbonates (1450 cm^{-1} and 1415 cm^{-1}), V_3 phosphate (1035 cm^{-1}), and V_4 phosphates (565 cm^{-1}, 590 cm^{-1}, and 605 cm^{-1}). The computed indexes of teeth for which IR spectra from multiple subsamples was obtained were averaged. The indexes are provided in Table F.2.

Well preserved enamel samples that have been chemically pre-treated can be distinguished from poorly preserved samples primarily by C/P ratios that fall between 0.08 and 0.2, as well as PCI (or IRSF) values between 3.1 and 4.0, although PCI up to 4.5 may

also be acceptable (France et al. 2020; Hopkins et al. 2016). The nine modern samples exhibit C/P ratios between 0.11 and 0.2 and PCI ranging from 3.2 to 3.9, indicating good preservation. Four subsamples of specimen IG219 that were not chemically pre-treated (UIG219 in Table F.2) exhibit PCI and C/P values expected from well-preserved untreated samples (France et al. 2020). The archaeological samples that were pretreated exhibit C/P ratios that range from 0.08 to 0.46 and PCI values that vary between 2.6 and 4.2.

Seven specimens (PK100, PK102, PK104, PK96, PK98, VEL30, and VEL31) exhibit C/P ratios greater than 0.2 and PCI values below 3.1 (Table F.2). BPI values for PK98, PK104 and VEL30 are above the upper recommended boundary for well-preserved enamel. API values for PK98 and PK104 are also above the acceptable range. Based on these results the seven specimens are poorly preserved and that the associated stable isotope data should be evaluated with caution or excluded from analysis.

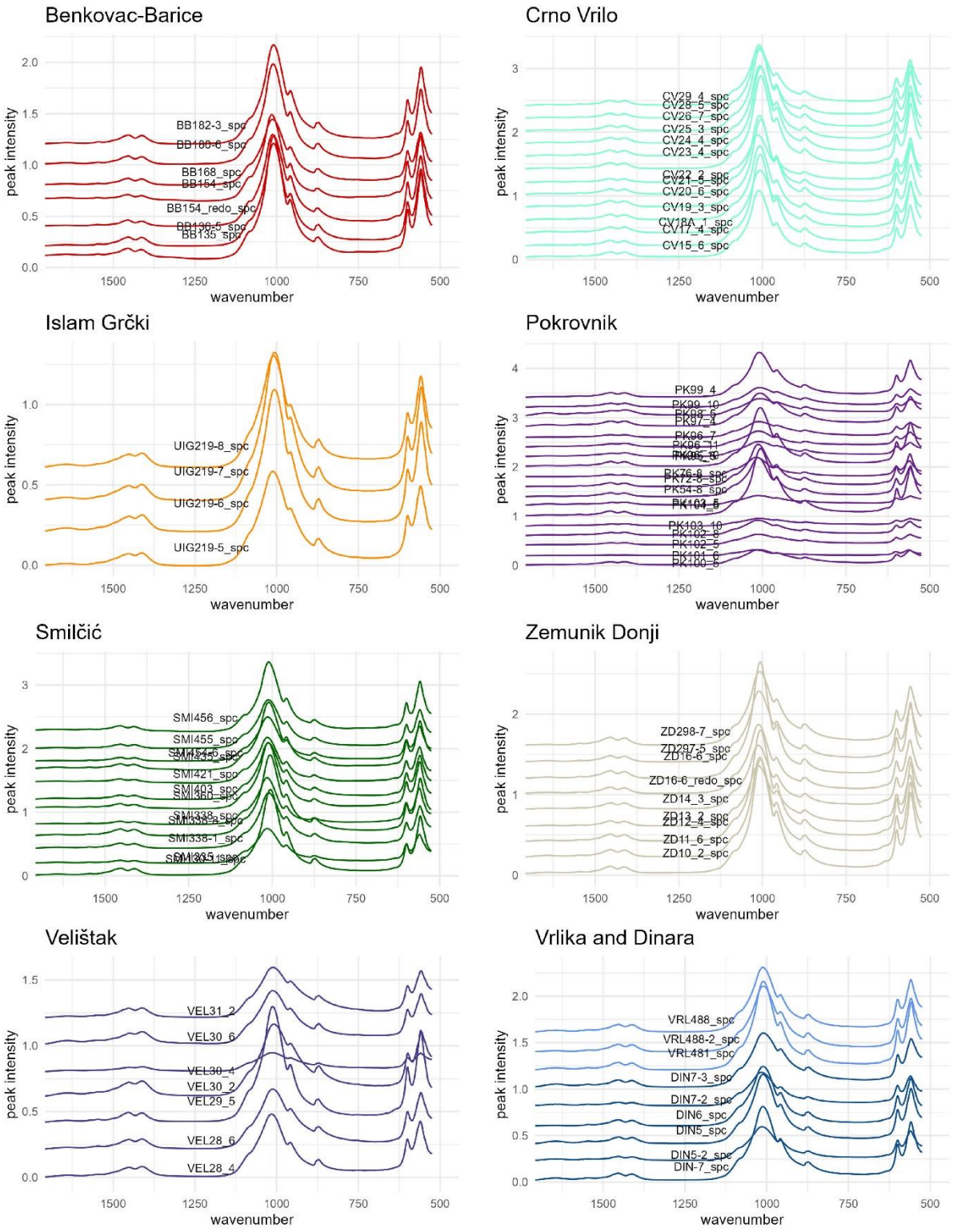

Figure F.1. FTIR spectra of enamel samples, produced using ChemoSpec package v6.1.10 (Hanson 2024) in R Statistical Software v4.3.1 (R Core Team 2023).

Table F.1. Indexes used for assessing preservation status of enamel bioapatite based on FTIR-ATR data.

Index	Formula	References	Range for adequately preserved enamel
PCI (Phosphate Crystallinity Index) other names: CI-IR (Crystallinity Index - InfraRed) ISRF (InfraRed Splitting Factor)	$\frac{B(605) + B(565)}{V(590)}$	Sponheimer and Lee-Thorp (1999); Shemesh (1990); Weiner and Bar-Yosef (1990)	3.1 - 4.0 (4.5)
C/P (B-type carbonate to V3 phosphate)	$\frac{B(1415)}{B(1035)}$	France et al. (2020)	0.08 - 0.2
C/C (A-type carbonate to B-type carbonate)	$\frac{B(1455)}{B(1415)}$	Snoeck et al. (2014)	0.9 - 1.1 (1.27)
BPI (B-site carbonate on Phosphate Index)	$\frac{B(1415)}{B(605)}$	LeGeros (1991)	0.13 - 0.35
API (A-site carbonate on Phosphate Index)	$\frac{B(1545)}{B(605)}$	Sponheimer and Lee-Thorp (1999)	0.04 - 0.2
BAI (relative amount of B- to A-site carbonate)	$\frac{B(1415)}{B(1540)}$	Sponheimer (1999); Sponheimer and Lee-Thorp (1999)	n/a
WAMPI (Water-Amide on Phosphate Index)	$\frac{B(1650)}{B(605)}$	Roche et al. (2010)	n/a
CO3/PO4 Index	$\frac{B(1450) + B(1415)}{B(605) + B(565)}$	Puceat et al. (2004)	n/a
CO3 weight (%)	10 * BPI + 0.7	LeGeros (1991)	n/a
PO4RF (PO4 Resolution Factor)	$\frac{AV(590)}{AV(590) + V(590)}$	Rey et al. (1990)	n/a

B: height of band; V: height of valley; AV: height of "above valley"

Table F.2. Results of FTIR analysis.

Specimen	n	CP	PCI	CC	BPI	API	BAI	CO_3/PO_4	WAMPI	CO_3 (% weight)	Index Flag
Dinara (modern)											
DIN5	2	0.16	3.4	1.1	0.25	0.15	1.68	0.20	0.15	3.2	
DIN6	1	0.12	3.7	1.1	0.19	0.06	3.25	0.16	0.03	2.6	
DIN7	3	0.16	3.4	1.1	0.23	0.14	1.69	0.19	0.14	3.0	
Vrlika (modern)											
VRL481	1	0.11	3.9	1.1	0.19	0.07	2.60	0.15	0.07	2.6	
VRL488	2	0.14	3.5	1.1	0.23	0.08	2.94	0.18	0.06	3.1	
Benkovac-Barice											
BB135	1	0.19	3.7	1.1	0.31	0.23	1.34	0.25	0.23	3.8	API
BB136	1	0.12	3.8	1.0	0.21	0.07	3.15	0.16	0.05	2.8	
BB154	2	0.10	4.0	1.2	0.17	0.12	1.96	0.14	0.10	2.5	
BB168	1	0.12	3.6	1.1	0.19	0.06	2.94	0.16	0.05	2.6	
BB180	1	0.11	4.0	1.1	0.19	0.06	3.00	0.14	0.05	2.6	
BB182	1	0.12	3.9	1.1	0.20	0.06	3.51	0.15	0.04	2.7	
Crno Vrilo											
CV15	1	0.14	3.8	1.0	0.23	0.12	1.92	0.18	0.11	3.0	
CV17	1	0.10	4.2	1.1	0.17	0.07	2.44	0.13	0.06	2.4	
CV18	1	0.15	3.5	1.0	0.24	0.10	2.48	0.18	0.09	3.1	
CV19	1	0.13	3.8	1.1	0.21	0.09	2.30	0.16	0.08	2.8	
CV20	1	0.14	3.9	1.0	0.22	0.09	2.42	0.16	0.08	2.9	
CV21	1	0.12	4.0	1.1	0.20	0.09	2.22	0.15	0.08	2.7	

CV22	1	0.10	3.8	1.1	0.17	0.07	2.41	0.13	0.06	2.4	
CV23	1	0.13	4.0	1.1	0.20	0.09	2.39	0.15	0.07	2.7	
CV24	1	0.13	3.9	1.1	0.20	0.09	2.27	0.15	0.08	2.7	
CV25	1	0.13	3.8	1.1	0.21	0.09	2.25	0.16	0.08	2.8	
CV26	1	0.12	3.9	1.1	0.19	0.08	2.40	0.14	0.07	2.6	
CV28	1	0.10	4.0	1.1	0.18	0.08	2.16	0.14	0.07	2.5	
CV29	1	0.13	3.7	1.1	0.21	0.09	2.23	0.17	0.08	2.8	
Islam Grčki											
IG211	3	0.12	3.7	1.1	0.19	0.08	2.44	0.15	0.07	2.6	
IG212	1	0.17	3.8	1.1	0.27	0.20	1.38	0.22	0.20	3.4	
IG219	1	0.16	3.8	1.1	0.27	0.19	1.41	0.22	0.19	3.4	
IG226	1	0.16	3.8	1.1	0.26	0.17	1.48	0.21	0.17	3.3	
IG233	1	0.14	3.4	1.0	0.22	0.07	3.11	0.18	0.07	2.9	
IG239	1	0.16	3.8	1.1	0.28	0.20	1.38	0.22	0.20	3.5	
IG468	1	0.11	3.9	1.1	0.19	0.06	3.24	0.15	0.03	2.6	
IG475	4	0.22	3.3	1.1	0.33	0.20	1.93	0.28	0.20	4.0	API
IG476	1	0.15	3.7	1.1	0.25	0.17	1.45	0.21	0.17	3.2	
IG477	2	0.12	3.8	1.1	0.20	0.08	2.67	0.16	0.08	2.7	
IG478	1	0.16	3.7	1.1	0.27	0.18	1.46	0.21	0.18	3.4	
IG479	1	0.17	3.8	1.1	0.27	0.20	1.39	0.22	0.19	3.4	
Pokrovnik											
PK100	1	0.26	2.9	1.0	0.34	0.14	2.38	0.28	0.10	4.1	PCI/CP
PK101	1	0.13	3.5	1.0	0.18	0.07	2.52	0.16	0.05	2.5	

PK102	2	0.26	2.9	1.0	0.35	0.16	2.18	0.30	0.13	4.2	PCI/CP
PK103	2	0.22	3.4	1.0	0.28	0.12	2.29	0.24	0.11	3.6	
PK104	1	0.42	2.6	0.9	0.51	0.31	1.65	0.45	0.31	5.8	PCI/CP
PK54	1	0.11	3.9	1.1	0.20	0.05	4.23	0.16	0.02	2.7	
PK72	1	0.11	4.0	1.1	0.18	0.05	3.46	0.15	0.02	2.5	
PK76	1	0.12	3.7	1.1	0.20	0.07	3.07	0.17	0.03	2.7	
PK95	1	0.13	3.9	1.0	0.21	0.08	2.66	0.16	0.06	2.8	
PK96	3	0.26	2.9	0.9	0.35	0.13	2.80	0.28	0.10	4.2	PCI/CP
PK97	1	0.23	3.2	1.0	0.32	0.16	1.96	0.26	0.14	3.9	
PK98	1	0.46	2.6	0.9	0.56	0.34	1.66	0.47	0.35	6.3	PCI/CP
PK99	2	0.20	3.3	1.0	0.29	0.12	2.42	0.23	0.08	3.6	
Smilčić											
SMI130	1	0.13	4.0	1.1	0.22	0.07	3.21	0.16	0.05	2.9	
SMI335	1	0.08	3.8	1.2	0.12	0.04	2.82	0.11	0.04	1.9	BPI
SMI338	3	0.13	3.8	1.1	0.21	0.10	2.10	0.17	0.09	2.8	
SMI360	1	0.15	4.0	1.1	0.25	0.18	1.37	0.20	0.18	3.2	
SMI403	1	0.09	3.9	1.1	0.15	0.05	2.91	0.12	0.05	2.2	
SMI421	1	0.17	3.7	1.1	0.28	0.22	1.25	0.23	0.21	3.4	API
SMI435	1	0.18	3.8	1.1	0.30	0.21	1.40	0.23	0.21	3.6	API
SMI454	1	0.09	3.9	1.1	0.16	0.05	3.11	0.13	0.04	2.3	
SMI455	1	0.10	3.9	1.1	0.16	0.05	2.98	0.13	0.04	2.3	
SMI456	1	0.17	3.9	1.1	0.28	0.21	1.35	0.22	0.20	3.5	API
Islam Grčki											

UIG219	4	0.16	3.3	0.9	0.27	0.08	3.40	0.20	0.06	3.4	
Velištak											
VEL28	2	0.20	3.3	1.0	0.29	0.10	2.94	0.23	0.08	3.6	
VEL29	1	0.12	3.8	1.1	0.21	0.09	2.18	0.16	0.07	2.8	
VEL30	3	0.29	3.0	0.9	0.38	0.15	2.56	0.31	0.13	4.5	PCI/CP
VEL31	1	0.25	3.0	1.0	0.34	0.13	2.59	0.28	0.10	4.1	PCI/CP
Zemunik Donji											
ZD10	1	0.11	4.1	1.1	0.18	0.08	2.35	0.14	0.06	2.5	
ZD11	1	0.13	3.9	1.1	0.21	0.09	2.24	0.16	0.09	2.8	
ZD12	1	0.12	4.0	1.1	0.19	0.08	2.47	0.14	0.06	2.6	
ZD13	1	0.11	3.7	1.1	0.17	0.06	2.83	0.14	0.04	2.4	
ZD14	1	0.14	3.6	1.0	0.23	0.09	2.52	0.18	0.08	3.0	
ZD16	2	0.11	4.0	1.1	0.18	0.06	2.96	0.14	0.06	2.6	
ZD297	1	0.11	3.8	1.1	0.18	0.06	2.97	0.15	0.05	2.5	
ZD298	1	0.15	3.7	1.1	0.24	0.08	2.79	0.19	0.06	3.1	

Appendix G. Stable Isotope Results of Enamel Bioapatite Samples

This appendix provides the stable carbon and oxygen isotope values for each enamel bioapatite increment analyzed for each arcaheological and modern tooth specimen. Table is organized by specimen, identified in bold in the center of each table. This identifier corresponds to the "Isotope Specimen" column in Table A.1 in Appendix A and the "Specimen" column in Table E.1 in Appendix E.

Sample	$\delta^{18}O‰_{VPDB}$	$\delta^{13}C‰_{VPDB}$	Distance to ERJ (mm)
BB135			
BB135 M2 1	-3.6	-5.9	3.66
BB135 M2 2	-1.7	-9.6	6.20
BB135 M2 3	-1.3	-11.4	8.87
BB135 M2 4	-2.4	-12.8	11.55
BB135 M2 5	-3.0	-13.2	13.81
BB135 M2 6	-4.0	-13.1	16.26
BB135 M2 7	-4.0	-13.1	18.51
BB135 M2 8	-4.4	-12.9	20.28
BB135 M2 9	-4.4	-12.3	22.79
BB135 M2 10	-3.7	-11.7	24.82
BB136			
BB136 M2 1	-4.2	-10.9	3.56
BB136 M2 2	-4.9	-11.7	6.17
BB136 M2 3	-4.0	-11.2	8.87
BB136 M2 4	-1.9	-10.9	11.33
BB136 M2 5	-0.8	-10.8	14.37
BB136 M2 6	0.1	-10.4	16.85
BB136 M2 7	0.1	-10.6	19.89
BB136 M2 8	-0.2	-10.6	21.97
BB136 M2 9	-0.9	-11.0	24.83
BB154			
BB154 M2 1	-3.8	-12.2	3.67
BB154 M2 2	-2.4	-11.4	6.85
BB154 M2 3	-1.1	-11.2	9.47
BB154 M2 4	-0.3	-11.3	11.26
BB154 M2 5	0.2	-11.5	13.91
BB154 M2 6	0.7	-11.6	16.83
BB154 M2 7	0.1	-12.0	18.82
BB154 M2 8	-3.3	-13.5	21.57
BB154 M2 9	-0.3	-12.4	23.70
BB154 M2 10	-0.3	-12.3	25.72

Sample	$\delta^{18}O‰_{VPDB}$	$\delta^{13}C‰_{VPDB}$	Distance to ERJ (mm)
BB168			
BB168 M2 1	-0.3	-9.2	5.69
BB168 M2 2	-0.7	-10.2	8.32
BB168 M2 3	-0.8	-11.0	10.09
BB168 M2 4	-1.1	-11.5	12.00
BB168 M2 5	-0.8	-12.1	14.32
BB168 M2 6	-0.8	-12.4	16.60
BB168 M2 7	-1.1	-12.3	18.24
BB168 M2 8	-1.5	-12.5	20.14
BB168 M2 9	-2.8	-12.4	22.15
BB168 M2 10	-3.3	-12.2	24.33
BB168 M2 11	-3.2	-12.1	26.65
BB180			
BB180 M2 1	-3.3	-11.8	2.46
BB180 M2 2	-2.8	-11.5	5.12
BB180 M2 3	-1.9	-9.9	7.23
BB180 M2 4	-1.5	-9.5	9.02
BB180 M2 5	-0.6	-9.2	11.47
BB180 M2 6	-0.4	-9.6	13.92
BB180 M2 7	-0.7	-10.0	15.77
BB180 M2 8	-0.2	-10.7	17.87
BB180 M2 9	-0.5	-11.1	19.73
BB180 M2 10	-0.4	-11.5	21.94
BB180 M2 11	-1.9	-11.2	23.93
BB180 M2 12	-1.8	-11.9	25.87

Sample	$\delta^{18}O‰_{VPDB}$	$\delta^{13}C‰_{VPDB}$	Distance to ERJ (mm)
BB182			
BB182 M2 1	-1.1	-10.7	2.40
BB182 M2 2	-1.3	-11.5	5.03
BB182 M2 3	-2.6	-12.3	7.71
BB182 M2 4	-3.3	-12.4	10.13
BB182 M2 5	-3.8	-12.5	11.58
BB182 M2 6	-4.3	-12.5	14.00
BB182 M2 7	-4.6	-12.5	16.22
BB182 M2 8	-4.2	-12.4	18.54
BB182 M2 9	-3.8	-12.3	20.90
BB182 M2 10	-3.9	-12.2	22.62
CV15			
CV15 M2 1	-2.6	-12.7	2.75
CV15 M2 2	-2.3	-12.3	5.16
CV15 M2 3	-1.4	-11.4	7.19
CV15 M2 4	-0.3	-11.0	9.72
CV15 M2 5	0.7	-10.4	12.01
CV15 M2 6	0.1	-11.3	14.79
CV15 M2 7	-0.5	-11.6	17.74
CV15 M2 8	-0.1	-12.1	20.15
CV17			
CV17 M2 1	-2.6	-11.3	3.96
CV17 M2 2	-3.8	-10.1	6.44
CV17 M2 3	-2.3	-10.6	8.80
CV17 M2 4	-1.8	-10.1	11.09
CV17 M2 5	-1.3	-9.7	12.90
CV17 M2 6	-0.3	-9.7	15.05
CV17 M2 7	-0.2	-9.9	18.06
CV18			
CV18 M2 1	-1.2	-10.2	3.33
CV18 M2 2	-2.5	-9.6	5.35
CV18 M2 3	-3.3	-9.5	7.92
CV18 M2 5	-4.3	-10.0	12.75

Sample	$\delta^{18}O‰_{VPDB}$	$\delta^{13}C‰_{VPDB}$	Distance to ERJ (mm)
		CV19	
CV19 M2 2	0.1	-11.5	4.21
CV19 M2 3	-0.8	-12.3	7.34
CV19 M2 4	-1.9	-12.6	9.68
CV19 M2 5	-2.6	-12.4	12.89
CV19 M2 6	-3.0	-12.9	14.99
CV19 M2 7	-2.6	-12.6	17.96
CV19 M2 8	-2.2	-12.1	21.23
		CV20	
CV20 M2 1	-0.2	-11.7	5.58
CV20 M2 2	-1.7	-12.4	9.16
CV20 M2 3	-2.5	-13.0	12.89
CV20 M2 4	-3.4	-12.8	15.24
CV20 M2 5	-3.9	-12.4	17.71
CV20 M2 6	-3.4	-12.6	21.19
CV20 M2 7	-2.7	-12.3	24.64
CV20 M2 8	-1.6	-11.9	27.22
CV20 M2 9	-0.8	-11.6	29.48
		CV21	
CV21 M2 1	-1.9	-11.5	3.15
CV21 M2 2	0.8	-11.3	6.48
CV21 M2 3	1.7	-11.2	8.60
CV21 M2 4	1.6	-11.3	11.87
CV21 M2 5	1.0	-11.8	14.87
CV21 M2 6	0.3	-12.0	17.08
CV21 M2 7	-0.3	-12.4	20.20
CV21 M2 8	-1.0	-12.6	22.64
CV21 M2 9	-1.3	-12.8	24.28

Sample	$\delta^{18}O‰_{VPDB}$	$\delta^{13}C‰_{VPDB}$	Distance to ERJ (mm)
		CV22	
CV22 M2 1	-3.4	-11.5	3.24
CV22 M2 2	-1.7	-11.5	4.90
CV22 M2 3	-0.5	-11.2	6.57
CV22 M2 4	0.2	-11.3	8.55
CV22 M2 5	0.1	-11.6	10.47
CV22 M2 6	0.3	-11.7	12.35
		CV23	
CV23 M2 1	-0.3	-11.1	3.85
CV23 M2 2	-0.6	-12.2	6.29
CV23 M2 3	-1.5	-13.1	9.17
CV23 M2 4	-2.4	-13.4	11.35
CV23 M2 5	-3.1	-13.0	14.44
CV23 M2 6	-2.7	-11.9	17.64
CV23 M2 7	-1.7	-11.2	21.21
CV23 M2 8	-0.2	-10.7	24.45
CV23 M2 9	0.3	-10.5	27.64
CV23 M2 10	0.3	-10.9	30.24
		CV24	
CV24 M2 0	-1.9	-11.3	3.53
CV24 M2 1	-0.5	-10.3	5.28
CV24 M2 2	-0.2	-10.3	6.87
CV24 M2 3	-0.5	-10.8	9.13
CV24 M2 4	-1.0	-11.6	11.82
CV24 M2 5	-1.2	-12.1	13.68
CV24 M2 6	-1.4	-12.8	15.67
CV24 M2 7	-2.1	-12.9	17.17
CV24 M2 8	-2.8	-13.1	19.49

Sample	$\delta^{18}O‰_{VPDB}$	$\delta^{13}C‰_{VPDB}$	Distance to ERJ (mm)
		CV26	
CV26 M2 1	-3.4	-10.0	2.24
CV26 M2 2	-0.7	-10.1	5.19
CV26 M2 3	-0.5	-10.9	7.30
CV26 M2 4	-0.7	-12.0	9.57
CV26 M2 5	-0.9	-12.7	11.50
CV26 M2 6	-1.9	-13.5	13.74
CV26 M2 7	-2.4	-13.6	15.44
CV26 M2 8	-3.4	-13.3	18.75
		CV28	
CV28 M2 1	-0.9	-10.6	3.00
CV28 M2 2	-0.9	-12.5	5.46
CV28 M2 3	-1.9	-13.5	8.14
CV28 M2 4	-2.7	-13.2	10.30
CV28 M2 5	-3.2	-13.1	13.13
CV28 M2 6	-3.0	-12.5	15.71
		DIN5	
DIN5 M2 1	-4.3	-12.2	5.00
DIN5 M2 3	-5.0	-11.0	9.00
DIN5 M2 4	-6.8	-10.6	11.00
DIN5 M2 5	-7.8	-11.0	15.00
DIN5 M2 6	-7.6	-12.3	17.00
DIN5 M2 7	-6.8	-16.3	21.00
		DIN6	
DIN6 M2 3	-5.0	-8.5	5.00
DIN6 M2 5	-6.8	-10.9	9.00
DIN6 M2 6	-6.4	-10.2	11.00

Sample	$\delta^{18}O‰_{VPDB}$	$\delta^{13}C‰_{VPDB}$	Distance to ERJ (mm)
DIN7			
DIN7 M2 2	-5.7	-12.0	3.00
DIN7 M2 3	-5.3	-11.2	5.00
DIN7 M2 4	-5.9	-11.3	7.00
DIN7 M2 5	-6.6	-11.2	9.00
DIN7 M2 6	-6.6	-11.0	12.00
DIN7 M2 7	-6.9	-11.2	14.00
DIN7 M2 8	-6.9	-11.5	16.00
DIN7 M2 9	-7.1	-13.2	18.00
DIN7 M2 10	-7.3	-14.3	21.00
IG211			
IG211 M2 1	-0.7	-11.0	3.89
IG211 M2 2	-2.6	-9.1	6.58
IG211 M2 3	-2.1	-12.7	8.85
IG211 M2 4	-2.8	-12.3	11.62
IG211 M2 5	-3.1	-12.4	14.01
IG211 M2 6	-2.6	-11.9	16.48
IG211 M2 7	-2.2	-11.1	18.69
IG211 M2 8	-1.1	-10.7	20.57
IG211 M2 9	-0.8	-10.2	22.56
IG211 M2 10	-0.4	-9.5	24.40
IG211 M2 11	0.1	-9.3	25.96
IG211 M2 12	0.2	-9.1	27.93

Sample	$\delta^{18}O‰_{VPDB}$	$\delta^{13}C‰_{VPDB}$	Distance to ERJ (mm)
IG212			
IG212 M2 1	-0.4	-9.6	5.25
IG212 M2 2	-0.2	-10.2	8.39
IG212 M2 3	-1.1	-10.9	10.40
IG212 M2 4	-1.6	-11.5	12.99
IG212 M2 5	-2.4	-11.8	15.63
IG212 M2 6	-2.6	-12.1	17.85
IG212 M2 7	-2.8	-12.2	20.30
IG212 M2 8	-3.0	-12.1	22.74
IG212 M2 9	-3.2	-12.0	24.95
IG212 M2 10	-3.5	-11.9	27.23
IG219			
IG219 M2 1	-3.9	-10.1	3.14
IG219 M2 3	-1.9	-8.1	7.90
IG219 M2 4	-1.8	-9.0	9.97
IG219 M2 5	-1.4	-10.7	12.47
IG219 M2 6	-1.7	-11.5	15.37
IG219 M2 7	-2.5	-11.9	17.34
IG219 M2 8	-3.0	-12.0	19.66
IG219 M2 9	-3.4	-11.6	21.68
IG219 M2 10	-3.2	-11.4	23.96
IG219 M2 11	-3.2	-10.7	26.47

Sample	$\delta^{18}O‰_{VPDB}$	$\delta^{13}C‰_{VPDB}$	Distance to ERJ (mm)
IG226			
IG226 M2 1	-0.5	-8.7	2.95
IG226 M2 2	-0.3	-9.4	5.65
IG226 M2 3	-0.6	-10.1	7.92
IG226 M2 4	-0.8	-10.7	10.38
IG226 M2 5	-1.5	-11.2	12.70
IG226 M2 6	-2.6	-11.7	15.52
IG226 M2 7	-3.4	-11.8	18.29
IG226 M2 8	-3.5	-12.1	20.31
IG226 M2 9	-3.1	-12.0	22.55
IG226 M2 10	-2.8	-11.7	24.88
IG226 M2 11	-2.9	-11.4	27.25
IG226 M2 12	-2.9	-11.3	29.42
IG233			
IG233 M2 1	-3.6	-7.2	3.60
IG233 M2 2	-1.1	-6.8	6.02
IG233 M2 3	-1.2	-9.9	8.28
IG233 M2 4	-1.5	-11.7	9.87
IG233 M2 5	-2.3	-12.7	11.26
IG233 M2 6	-3.1	-12.9	13.54
IG233 M2 7	-3.8	-12.7	15.42
IG233 M2 8	-4.4	-13.3	17.48
IG233 M2 9	-4.8	-12.9	19.26
IG233 M2 10	-4.7	-12.4	21.49

Sample	$\delta^{18}O‰_{VPDB}$	$\delta^{13}C‰_{VPDB}$	Distance to ERJ (mm)
IG239			
IG239 M2 1	-2.2	-11.4	3.35
IG239 M2 2	-0.6	-11.2	6.36
IG239 M2 3	0.8	-11.1	8.76
IG239 M2 4	1.2	-11.3	10.77
IG239 M2 5	1.0	-11.2	12.55
IG239 M2 6	-0.3	-11.7	15.51
IG239 M2 7	-0.9	-11.6	17.73
IG239 M2 8	-2.3	-11.8	19.30
IG239 M2 9	-2.7	-12.2	21.21
IG239 M2 10	-3.2	-12.3	23.02
IG239 M2 11	-3.3	-12.4	24.96
IG468			
IG468 M2 1	-2.9	-11.4	2.38
IG468 M2 2	-1.4	-9.8	4.45
IG468 M2 3	0.0	-9.1	6.30
IG468 M2 4	1.0	-9.2	8.39
IG468 M2 5	1.2	-10.0	10.25
IG468 M2 6	0.9	-10.8	12.19
IG468 M2 7	-0.4	-11.6	14.20
IG468 M2 8	-1.0	-12.4	16.07
IG468 M2 9	-2.1	-12.7	18.12
IG468 M2 10	-2.6	-12.4	20.03
IG468 M2 11	-2.3	-12.1	21.83
IG468 M2 12	-1.5	-11.6	23.82

Sample	$\delta^{18}O‰_{VPDB}$	$\delta^{13}C‰_{VPDB}$	Distance to ERJ (mm)
IG475			
IG475 M2 1	-1.9	-10.7	2.79
IG475 M2 2	-2.4	-11.3	5.15
IG475 M2 3	-3.4	-11.2	7.29
IG475 M2 4	-3.9	-11.3	9.19
IG475 M2 5	-4.1	-11.4	11.27
IG475 M2 6	-4.1	-11.3	13.67
IG475 M2 7	-4.5	-11.0	16.31
IG475 M2 8	-3.5	-10.8	18.17
IG475 M2 9	-2.9	-10.6	19.84
IG475 M2 10	-2.7	-10.1	21.51
IG476			
IG476 M2 1	-2.2	-10.4	3.03
IG476 M2 2	-1.4	-9.3	5.35
IG476 M2 3	-0.7	-10.5	7.62
IG476 M2 4	-1.1	-11.6	10.03
IG476 M2 5	-2.0	-12.2	13.00
IG476 M2 6	-3.5	-12.7	15.23
IG476 M2 7	-4.2	-12.8	17.38
IG476 M2 8	-4.2	-12.6	19.54
IG476 M2 9	-4.1	-12.3	21.86
IG476 M2 10	-3.8	-12.1	24.30
IG476 M2 11	-3.1	-11.6	26.71
IG476 M2 12	-3.0	-11.4	29.14

Sample	$\delta^{18}O‰_{VPDB}$	$\delta^{13}C‰_{VPDB}$	Distance to ERJ (mm)
		IG477	
IG477 M2 1	-3.3	-12.0	2.50
IG477 M2 2	-3.1	-11.2	3.83
IG477 M2 3	-1.5	-10.5	5.91
IG477 M2 4	-0.2	-10.0	7.71
IG477 M2 5	0.1	-10.0	9.44
IG477 M2 6	-0.1	-10.3	11.54
IG477 M2 7	-0.6	-10.7	12.92
IG477 M2 8	-1.0	-11.0	14.88
IG477 M2 9	-1.1	-11.1	16.76
IG477 M2 10	-1.0	-11.6	18.80
		IG478	
IG478 M2 1	-0.6	-9.3	5.21
IG478 M2 2	-0.6	-10.3	7.86
IG478 M2 3	-1.1	-11.6	10.28
IG478 M2 4	-2.6	-12.0	12.64
IG478 M2 5	-3.5	-12.3	14.45
IG478 M2 6	-5.6	-12.0	16.82
IG478 M2 7	-4.6	-11.6	19.10
IG478 M2 8	-4.3	-11.1	21.50
IG478 M2 9	-2.4	-10.2	23.46
IG478 M2 10	-1.6	-9.2	25.47

Sample	$\delta^{18}O‰_{VPDB}$	$\delta^{13}C‰_{VPDB}$	Distance to ERJ (mm)
IG479			
IG479 M2 1	-1.7	-7.5	3.59
IG479 M2 3	-2.6	-9.2	7.78
IG479 M2 4	-2.9	-10.7	10.13
IG479 M2 5	-3.7	-11.8	12.98
IG479 M2 6	-4.1	-12.4	15.10
IG479 M2 7	-5.0	-12.7	17.36
IG479 M2 8	-5.1	-12.6	19.33
IG479 M2 9	-5.8	-12.5	21.92
IG479 M2 10	-5.4	-12.1	23.60
IG479 M2 11	-5.0	-11.9	25.84
IG479 M2 12	-4.6	-11.3	27.74
PK100*			
PK100 M2 1	-4.0	-12.5	3.00
PK100 M2 2	-2.8	-12.3	6.00
PK100 M2 3	-1.1	-12.0	7.50
PK100 M2 4	0.6	-11.2	9.00
PK100 M2 5	-0.1	-12.0	11.00
PK100 M2 6	-0.8	-12.2	13.00
PK100 M2 7	-0.7	-12.4	16.00
PK100 M2 8	-1.6	-12.7	18.00
PK100 M2 9	-3.1	-13.2	22.00
PK100 M2 10	-4.0	-12.9	24.00
PK100 M2 11	-3.9	-13.3	25.00

Sample	$\delta^{18}O‰_{VPDB}$	$\delta^{13}C‰_{VPDB}$	Distance to ERJ (mm)
PK101			
PK101 M2 1	-3.2	-11.7	2.00
PK101 M2 2	-1.5	-11.3	5.00
PK101 M2 3	-0.5	-11.4	7.00
PK101 M2 4	0.4	-11.6	9.00
PK101 M2 5	-0.4	-12.6	11.00
PK101 M2 6	0.0	-12.5	13.00
PK101 M2 7	-0.4	-13.0	15.00
PK101 M2 8	-0.5	-12.9	19.00
PK101 M2 9	-0.8	-13.3	21.00
PK101 M2 10	-2.5	-11.3	24.00
PK102*			
PK102 M2 1	-1.8	-11.9	2.00
PK102 M2 2	-1.1	-11.7	4.00
PK102 M2 3	-1.7	-11.7	8.00
PK102 M2 4	0.4	-11.1	10.00
PK102 M2 5	0.9	-11.0	13.00
PK102 M2 6	-2.5	-11.1	15.00
PK102 M2 7	-2.1	-11.3	18.00
PK102 M2 8	-2.2	-10.4	20.00
PK102 M2 9	-2.5	-12.1	22.00
PK102 M2 10	-3.8	-11.2	25.00
PK104*			
PK104 M2 1	-3.1	-11.3	1.00
PK104 M2 2	-2.6	-11.0	4.00
PK104 M2 3	-2.8	-11.2	6.00
PK104 M2 4	-2.3	-11.0	8.00
PK104 M2 5	-2.3	-11.5	11.00
PK104 M2 6	-2.8	-11.1	14.00
PK104 M2 7	-2.8	-11.1	16.00
PK104 M2 8	-2.3	-11.2	19.00
PK104 M2 9	-2.1	-11.4	22.00
PK104 M2 10	-2.8	-11.6	25.00

Sample	$\delta^{18}O‰_{VPDB}$	$\delta^{13}C‰_{VPDB}$	Distance to ERJ (mm)
PK54			
PK54 M2 1	-0.1	-11.7	3.25
PK54 M2 2	1.3	-11.6	5.53
PK54 M2 3	1.1	-11.6	7.55
PK54 M2 4	0.6	-11.7	9.76
PK54 M2 5	-0.9	-12.0	11.94
PK54 M2 6	-1.1	-11.9	14.02
PK54 M2 7	-1.8	-12.1	16.91
PK54 M2 8	-2.4	-12.0	18.21
PK54 M2 9	-3.1	-11.9	20.20
PK54 M2 10	-2.8	-11.7	22.02
PK54 M2 11	-2.2	-11.2	24.00
PK72			
PK72 M2 1	-2.4	-12.3	5.69
PK72 M2 2	-2.4	-11.9	8.26
PK72 M2 3	-2.4	-11.4	10.91
PK72 M2 4	-0.3	-11.2	13.93
PK72 M2 5	-0.0	-11.3	16.28
PK72 M2 6	0.7	-11.4	18.81
PK72 M2 7	0.3	-11.9	21.01
PK72 M2 8	0.1	-12.1	23.32
PK72 M2 9	-0.2	-12.4	25.62
PK72 M2 10	-0.7	-12.6	27.92

Sample	$\delta^{18}O‰_{VPDB}$	$\delta^{13}C‰_{VPDB}$	Distance to ERJ (mm)
		PK76	
PK76 M2 1	-0.3	-11.6	4.51
PK76 M2 2	-0.7	-11.9	6.47
PK76 M2 3	-0.6	-12.3	8.92
PK76 M2 4	-1.8	-12.7	11.46
PK76 M2 5	-2.3	-13.1	14.19
PK76 M2 6	-3.0	-13.4	16.27
PK76 M2 7	-2.9	-13.3	18.86
PK76 M2 8	-3.0	-13.1	21.00
PK76 M2 9	-2.4	-12.7	23.19
PK76 M2 10	-2.6	-12.2	25.30
PK76 M2 11	-1.7	-11.7	27.36
		PK87	
PK87 M2 1	-2.6	-9.2	2.00
PK87 M2 2	-1.6	-8.5	5.00
PK87 M2 3	-1.3	-9.1	8.00
PK87 M2 4	-0.4	-8.9	9.00
PK87 M2 5	0.0	-9.1	11.00
PK87 M2 6	0.2	-9.6	13.00
PK87 M2 7	-0.6	-10.7	16.00
PK87 M2 8	-0.6	-12.3	18.00
PK87 M2 9	-0.6	-13.4	20.00
PK87 M2 10	-2.2	-14.8	22.00
		PK88	
PK88 M2 1	-2.4	-12.0	3.00
PK88 M2 2	1.1	-11.3	5.00
PK88 M2 3	1.4	-11.4	9.00
PK88 M2 4	0.2	-12.0	12.00
PK88 M2 5	-0.9	-12.3	14.00
PK88 M2 6	0.6	-11.6	16.00
PK88 M2 7	-1.1	-12.1	20.00

Sample	$\delta^{18}O‰_{VPDB}$	$\delta^{13}C‰_{VPDB}$	Distance to ERJ (mm)
		PK89	
PK89 M2 1	-4.3	-13.2	3.00
PK89 M2 2	-4.3	-13.3	7.00
PK89 M2 3	-4.5	-13.2	10.00
PK89 M2 4	-4.3	-12.6	12.00
PK89 M2 5	-2.4	-11.6	14.00
PK89 M2 6	-3.0	-12.0	16.00
PK89 M2 7	-1.2	-11.6	19.00
PK89 M2 8	-0.6	-11.4	22.00
PK89 M2 9	0.6	-11.1	25.00
PK89 M2 10	0.0	-11.3	26.00
		PK90	
PK90 M2 1	-2.0	-12.0	1.00
PK90 M2 2	-2.0	-11.7	3.00
PK90 M2 3	-1.3	-11.4	5.00
PK90 M2 4	-1.2	-11.6	8.00
PK90 M2 5	-1.1	-11.2	10.00
PK90 M2 6	-1.0	-11.5	12.00
PK90 M2 7	-1.6	-11.6	15.00
PK90 M2 8	-1.6	-11.9	18.00
PK90 M2 9	-1.5	-12.4	20.00
PK90 M2 10	-1.8	-13.2	23.00
		PK91	
PK91 M2 1	-4.2	-12.6	1.00
PK91 M2 2	-3.4	-12.4	4.00
PK91 M2 3	-0.7	-11.4	7.00
PK91 M2 4	-0.9	-11.3	10.00
PK91 M2 5	0.5	-11.0	12.00
PK91 M2 6	0.8	-10.8	15.00
PK91 M2 7	-0.2	-11.2	20.00
PK91 M2 8	-0.7	-11.6	23.00
PK91 M2 9	-1.8	-12.7	25.00
PK91 M2 10	-2.8	-12.3	27.00

Sample	$\delta^{18}O‰_{VPDB}$	$\delta^{13}C‰_{VPDB}$	Distance to ERJ (mm)
		PK92	
PK92 M2 1	-3.6	-12.8	2.00
PK92 M2 2	-2.3	-12.2	5.00
PK92 M2 3	-2.2	-11.9	7.00
PK92 M2 4	-1.8	-12.1	10.00
PK92 M2 5	-1.5	-12.2	12.00
PK92 M2 6	-1.4	-11.8	14.00
PK92 M2 7	-1.7	-12.4	16.00
PK92 M2 8	-2.4	-12.6	19.00
PK92 M2 9	-2.5	-12.7	21.00
PK92 M2 10	-2.8	-13.5	23.00
		PK93	
PK93 M2 1	-2.8	-11.8	2.00
PK93 M2 2	-2.6	-12.0	5.00
PK93 M2 3	-2.2	-11.9	6.00
PK93 M2 4	-2.3	-12.1	9.00
PK93 M2 5	-2.7	-12.2	11.00
PK93 M2 6	-2.2	-12.4	13.00
PK93 M2 7	-2.6	-12.6	15.00
PK93 M2 8	-3.1	-12.7	16.00
PK93 M2 9	-3.2	-13.0	18.00
PK93 M2 10	-2.9	-13.6	21.00
PK93 M2 11	-3.5	-14.2	23.00
PK93 M2 12	-3.4	-13.6	26.00

Sample	$\delta^{18}O‰_{VPDB}$	$\delta^{13}C‰_{VPDB}$	Distance to ERJ (mm)
		PK94*	
PK94 M2 1	-5.2	-12.8	3.00
PK94 M2 2	-5.0	-10.3	5.00
PK94 M2 3	-4.9	-11.2	8.00
PK94 M2 4	-7.3	-10.3	10.00
PK94 M2 5	-3.2	-11.4	14.00
PK94 M2 6	-3.1	-11.0	16.00
PK94 M2 7	-1.3	-10.5	19.00
PK94 M2 8	-3.6	-10.6	22.00
PK94 M2 9	-1.7	-11.2	24.00
PK94 M2 10	-10.0	-10.7	27.00
PK94 M2 11	-2.1	-10.9	29.00
		PK95	
PK95 M2 1	-1.6	-11.3	2.00
PK95 M2 2	-1.4	-11.1	5.00
PK95 M2 3	-0.9	-11.1	7.00
PK95 M2 4	-1.5	-11.8	10.00
PK95 M2 5	-1.6	-12.4	12.00
PK95 M2 6	-1.9	-12.8	14.00
PK95 M2 7	-2.0	-12.8	16.00
PK95 M2 8	-2.2	-13.6	19.00
PK95 M2 9	-2.8	-14.1	22.00
PK95 M2 10	-2.2	-14.2	25.00

Sample	$\delta^{18}O‰_{VPDB}$	$\delta^{13}C‰_{VPDB}$	Distance to ERJ (mm)
		PK96*	
PK96 M2 1	-4.4	-11.0	2.00
PK96 M2 2	-4.4	-10.4	4.00
PK96 M2 3	-0.9	-12.2	6.00
PK96 M2 4	-2.3	-12.5	7.00
PK96 M2 5	-1.8	-12.8	9.00
PK96 M2 6	-1.6	-12.6	13.00
PK96 M2 7	-2.0	-13.0	15.00
PK96 M2 8	-3.7	-11.6	17.00
PK96 M2 9	-2.8	-11.7	20.00
PK96 M2 10	-9.6	-11.1	23.00
PK96 M2 11	-5.1	-11.2	25.00
PK96 M2 12	-4.0	-11.1	27.00
		PK97	
PK97 M2 1	-1.0	-11.3	2.00
PK97 M2 2	-1.7	-11.7	5.00
PK97 M2 3	-3.1	-12.5	7.00
PK97 M2 4	-4.5	-12.5	10.00
PK97 M2 5	-5.1	-12.9	13.00
PK97 M2 6	-5.1	-12.6	15.00
PK97 M2 7	-4.1	-11.7	17.00
PK97 M2 8	-4.3	-12.4	20.00

Sample	$\delta^{18}O‰_{VPDB}$	$\delta^{13}C‰_{VPDB}$	Distance to ERJ (mm)
		PK98*	
PK98 M2 1	-1.8	-10.9	2.00
PK98 M2 2	-0.9	-11.1	3.00
PK98 M2 3	-1.8	-11.7	5.00
PK98 M2 4	-2.4	-11.6	8.00
PK98 M2 5	-3.5	-12.1	10.00
PK98 M2 6	-4.0	-12.3	12.00
PK98 M2 7	-4.1	-12.5	14.00
PK98 M2 8	-4.5	-12.5	16.00
PK98 M2 9	-4.3	-12.2	20.00
PK98 M2 10	-4.0	-12.3	22.00
PK98 M2 11	-4.0	-11.8	25.00
PK98 M2 12	-3.3	-11.5	27.00
		PK99	
PK99 M2 1	-1.9	-12.7	1.00
PK99 M2 2	-1.2	-12.0	5.00
PK99 M2 3	-3.4	-11.3	9.00
PK99 M2 4	-3.9	-12.4	13.00
PK99 M2 5	-2.9	-12.5	15.00
PK99 M2 6	-2.6	-11.7	17.00
PK99 M2 7	-3.0	-11.0	19.00
PK99 M2 8	-1.8	-11.7	22.00
PK99 M2 9	-1.3	-11.4	24.00
PK99 M2 10	0.5	-11.6	26.00
PK99 M2 11	-1.8	-10.1	27.00
PK99 M2 12	-1.9	-10.9	29.00

Sample	$\delta^{18}O‰_{VPDB}$	$\delta^{13}C‰_{VPDB}$	Distance to ERJ (mm)
SMI130			
SMI130 M2 1	-0.1	-11.3	2.51
SMI130 M2 2	0.1	-11.9	4.89
SMI130 M2 3	-0.3	-12.1	6.99
SMI130 M2 4	-1.7	-12.3	8.96
SMI130 M2 5	-2.7	-12.5	11.03
SMI130 M2 6	-3.4	-12.7	13.27
SMI130 M2 7	-3.7	-12.6	15.35
SMI130 M2 8	-3.6	-12.4	17.50
SMI130 M2 9	-3.4	-12.3	19.73
SMI130 M2 10	-3.6	-9.1	21.81
SMI130 M2 11	-2.3	-11.9	23.79
SMI130 M2 12	-1.4	-11.5	26.13
SMI130 M2 13	-1.0	-11.3	28.35
SMI130 M2 14	-0.6	-11.0	29.60
SMI335			
SMI335 M2 1	0.3	-9.7	2.84
SMI335 M2 2	-0.3	-9.3	4.66
SMI335 M2 3	-0.5	-11.4	6.98
SMI335 M2 4	-1.5	-11.9	8.82
SMI335 M2 5	-2.4	-12.0	10.71
SMI335 M2 6	-3.7	-12.1	12.95
SMI335 M2 7	-3.8	-12.2	14.84
SMI335 M2 8	-4.4	-11.9	16.90
SMI335 M2 9	-3.7	-11.8	18.60
SMI335 M2 10	-3.3	-11.7	20.17

Sample	$\delta^{18}O‰_{VPDB}$	$\delta^{13}C‰_{VPDB}$	Distance to ERJ (mm)
SMI338			
SMI338 M2 1	-3.5	-1.3	3.71
SMI338 M2 2	0.4	-8.8	5.69
SMI338 M2 3	-0.6	-9.7	8.09
SMI338 M2 4	-0.4	-11.1	10.48
SMI338 M2 5	-1.9	-11.5	12.63
SMI338 M2 6	-2.5	-11.3	15.34
SMI338 M2 7	-3.7	-11.2	17.65
SMI338 M2 8	-4.1	-10.9	19.81
SMI338 M2 9	-3.6	-10.6	22.49
SMI338 M2 10	-2.9	-10.3	24.81
SMI360			
SMI360 M2 1	-1.5	-10.9	3.25
SMI360 M2 2	-0.3	-10.7	5.67
SMI360 M2 3	0.2	-10.8	7.77
SMI360 M2 4	-0.5	-11.3	9.54
SMI360 M2 5	-1.6	-11.9	12.04
SMI360 M2 6	-2.5	-12.0	13.64
SMI360 M2 7	-2.5	-12.0	15.42
SMI360 M2 8	-3.8	-12.3	17.60
SMI360 M2 9	-3.9	-12.2	19.55
SMI360 M2 10	-3.9	-12.1	21.61
SMI403			
SMI403 M2 0	0.7	-10.9	2.65
SMI403 M2 1	1.4	-11.2	3.91
SMI403 M2 2	0.8	-11.8	6.05
SMI403 M2 3	-0.4	-12.3	8.18
SMI403 M2 4	-2.0	-12.7	10.05
SMI403 M2 5	-3.1	-13.0	12.65
SMI403 M2 6	-3.2	-13.1	14.51
SMI403 M2 7	-3.5	-12.8	16.55
SMI403 M2 8	-2.9	-12.4	18.38

Sample	$\delta^{18}O‰_{VPDB}$	$\delta^{13}C‰_{VPDB}$	Distance to ERJ (mm)
SMI421			
SMI421 M2 1	-0.2	-9.0	2.98
SMI421 M2 2	0.7	-9.6	5.45
SMI421 M2 3	0.6	-9.7	8.04
SMI421 M2 4	-1.2	-12.0	10.71
SMI421 M2 5	-1.8	-12.2	13.13
SMI421 M2 6	-2.1	-12.6	15.14
SMI421 M2 7	-2.2	-12.8	17.28
SMI421 M2 8	-2.3	-12.7	19.88
SMI421 M2 9	-2.4	-12.7	21.93
SMI421 M2 10	-2.6	-12.2	24.93
SMI435			
SMI435 M2 1	-3.9	-11.7	2.71
SMI435 M2 2	-3.0	-11.5	4.60
SMI435 M2 3	-1.1	-10.5	7.11
SMI435 M2 4	0.1	-9.9	9.47
SMI435 M2 5	0.6	-9.6	12.24
SMI435 M2 6	0.9	-9.4	14.57
SMI435 M2 7	-0.4	-10.6	17.13
SMI435 M2 8	-1.2	-11.3	19.80
SMI435 M2 9	-1.7	-11.6	22.32
SMI435 M2 10	-2.5	-11.9	25.03
SMI435 M2 11	-3.3	-11.7	27.44

Sample	$\delta^{18}O‰_{VPDB}$	$\delta^{13}C‰_{VPDB}$	Distance to ERJ (mm)
SMI454			
SMI454 M2 1	-0.7	-11.8	2.27
SMI454 M2 2	-0.8	-11.4	4.43
SMI454 M2 3	0.3	-11.3	6.82
SMI454 M2 4	0.3	-11.3	9.08
SMI454 M2 5	0.1	-11.8	11.36
SMI454 M2 6	-1.0	-12.0	13.26
SMI454 M2 7	-1.5	-12.2	15.43
SMI454 M2 8	-1.4	-12.0	17.27
SMI454 M2 9	-2.3	-12.2	19.01
SMI454 M2 10	-2.5	-12.0	21.16
SMI454 M2 11	-2.5	-11.7	23.09
SMI455			
SMI455 M2 1	-0.7	-10.8	1.88
SMI455 M2 2	-0.6	-11.0	3.46
SMI455 M2 3	-0.5	-11.0	5.13
SMI455 M2 4	-0.2	-11.4	7.31
SMI455 M2 5	-0.8	-11.8	8.64
SMI455 M2 6	-0.9	-12.2	10.51
SMI455 M2 7	-1.6	-12.2	12.07
SMI455 M2 8	-2.1	-12.3	13.32
SMI455 M2 9	-2.5	-12.3	15.07
SMI455 M2 10	-2.8	-12.1	16.79
SMI455 M2 11	-3.0	-12.1	18.25

Sample	$\delta^{18}O‰_{VPDB}$	$\delta^{13}C‰_{VPDB}$	Distance to ERJ (mm)
SMI456			
SMI456 M2 0	-0.4	-11.6	3.38
SMI456 M2 1	-1.4	-11.8	4.97
SMI456 M2 2	-2.7	-12.3	7.85
SMI456 M2 3	-3.4	-12.1	10.49
SMI456 M2 4	-3.8	-12.0	13.36
SMI456 M2 5	-3.5	-11.8	15.68
SMI456 M2 6	-3.6	-11.8	18.53
SMI456 M2 7	-2.6	-11.6	20.84
SMI456 M2 8	-1.9	-11.5	23.25
SMI456 M2 9	-1.3	-11.4	25.65
SMI456 M2 10	-1.2	-11.3	27.48
SMI456 M2 11	-0.7	-11.2	29.67
VEL28			
VEL28 M2 1	-4.8	-13.3	4.00
VEL28 M2 2	-3.4	-11.2	6.00
VEL28 M2 3	-3.4	-8.5	8.00
VEL28 M2 4	-4.0	-8.9	10.00
VEL28 M2 5	-2.0	-9.0	13.00
VEL28 M2 6	-1.1	-10.5	15.00
VEL28 M2 7	-1.5	-10.4	17.00
VEL28 M2 8	-2.7	-10.7	20.00

Sample	$\delta^{18}O‰_{VPDB}$	$\delta^{13}C‰_{VPDB}$	Distance to ERJ (mm)
VEL29			
VEL29 M2 1	-2.8	-11.3	4.00
VEL29 M2 2	-2.5	-11.0	6.00
VEL29 M2 3	-1.8	-10.1	8.00
VEL29 M2 4	-1.0	-9.6	10.00
VEL29 M2 5	-1.0	-9.8	14.00
VEL29 M2 6	-1.4	-10.6	15.00
VEL29 M2 7	-0.9	-11.3	18.00
VEL29 M2 8	-1.0	-11.6	19.00
VEL29 M2 9	-2.0	-12.3	20.00
VEL29 M2 10	-3.2	-10.0	22.00
VEL29 M2 11	-3.6	-10.8	25.00
VEL30*			
VEL30 M2 1	-3.0	-8.7	2.00
VEL30 M2 2	-4.4	-10.6	4.00
VEL30 M2 3	-4.4	-11.3	5.00
VEL30 M2 4	-5.0	-3.7	8.00
VEL30 M2 5	-4.4	-11.0	11.00
VEL30 M2 6	-4.6	-9.7	13.00
VEL30 M2 7	-3.3	-7.8	15.00
VEL30 M2 8	-3.5	-8.3	17.00
VEL30 M2 9	-2.9	-7.9	19.00
VEL30 M2 10	-3.3	-8.3	20.00
VEL31*			
VEL31 M2 1	-1.7	-8.4	2.00
VEL31 M2 2	-3.5	-9.5	5.00
VEL31 M2 3	-2.5	-11.5	7.00
VEL31 M2 4	-2.9	-11.4	9.00
VEL31 M2 5	-3.0	-10.8	11.00
VEL31 M2 6	-0.9	-10.1	15.00
VEL31 M2 7	-3.8	-12.1	18.00
VEL31 M2 8	-2.4	-13.1	20.00

Sample	$\delta^{18}O‰_{VPDB}$	$\delta^{13}C‰_{VPDB}$	Distance to ERJ (mm)
		VEL32	
VEL32 M2 1	-1.5	-7.7	1.00
VEL32 M2 2	-0.8	-7.8	3.00
VEL32 M2 3	-0.6	-8.1	5.00
VEL32 M2 4	-1.4	-9.6	7.00
VEL32 M2 5	-1.7	-10.6	9.00
VEL32 M2 6	-1.7	-11.1	11.00
VEL32 M2 7	-2.0	-11.3	13.00
VEL32 M2 8	-2.1	-11.4	15.00
VEL32 M2 9	-2.3	-11.5	17.00
VEL32 M2 10	-2.4	-11.4	19.00
		VEL34	
VEL34 M2 1	-2.7	-11.6	2.00
VEL34 M2 2	-1.1	-11.3	4.00
VEL34 M2 3	-0.5	-11.0	7.00
VEL34 M2 4	-1.3	-11.8	9.00
VEL34 M2 5	0.0	-11.9	11.00
		VEL37	
VEL37 M2 2	-1.9	-11.0	5.00
VEL37 M2 3	-2.8	-10.8	7.00
VEL37 M2 4	-2.2	-9.7	10.00
VEL37 M2 5	-1.3	-10.0	12.00
VEL37 M2 6	-1.7	-10.5	15.00
VEL37 M2 7	-0.8	-10.1	17.00
VEL37 M2 8	-1.4	-10.6	20.00

Sample	$\delta^{18}O‰_{VPDB}$	$\delta^{13}C‰_{VPDB}$	Distance to ERJ (mm)
VRL481			
VRL481 M2 1	-5.0	-12.6	2.38
VRL481 M2 2	-4.0	-12.6	3.68
VRL481 M2 3	-4.8	-12.9	5.10
VRL481 M2 4	-4.6	-13.1	6.78
VRL481 M2 5	-5.4	-13.1	8.50
VRL481 M2 6	-6.0	-13.1	10.00
VRL481 M2 7	-6.4	-13.2	11.65
VRL481 M2 8	-6.6	-13.0	13.32
VRL481 M2 9	-6.8	-13.1	14.56
VRL481 M2 10	-7.0	-13.1	16.11
ZD10			
ZD10 M2 0	-0.0	-10.2	6.24
ZD10 M2 1	0.1	-9.9	8.19
ZD10 M2 2	-0.3	-9.7	10.32
ZD10 M2 3	-0.5	-10.4	13.00
ZD10 M2 4	-1.1	-11.0	14.94
ZD10 M2 5	-1.6	-11.8	17.47
ZD10 M2 6	-2.3	-12.3	19.76
ZD10 M2 7	-2.7	-12.6	22.12
ZD10 M2 8	-3.1	-12.8	24.50
ZD10 M2 9	-4.0	-12.8	26.75
ZD10 M2 10	-4.1	-12.5	28.95

Sample	$\delta^{18}O‰_{VPDB}$	$\delta^{13}C‰_{VPDB}$	Distance to ERJ (mm)
ZD11			
ZD11 M2 1	0.2	-9.0	2.33
ZD11 M2 2	-0.3	-10.4	4.75
ZD11 M2 3	-1.7	-11.7	7.56
ZD11 M2 4	-2.8	-11.7	10.25
ZD11 M2 5	-2.0	-10.8	13.58
ZD11 M2 6	-0.9	-10.2	16.13
ZD11 M2 7	-0.7	-9.7	18.12
ZD11 M2 8	-0.1	-9.3	20.29
ZD11 M2 9	0.0	-9.0	22.96
ZD11 M2 10	-0.7	-9.1	25.34
ZD13			
ZD13 M2 1	-0.3	-8.5	2.84
ZD13 M2 2	-0.5	-8.5	4.73
ZD13 M2 3	-1.0	-10.0	6.91
ZD13 M2 4	-1.9	-11.1	9.23
ZD13 M2 5	-3.0	-12.2	12.15
ZD13 M2 6	-3.6	-11.6	15.73
ZD14			
ZD14 M2 1	-0.7	-10.3	1.73
ZD14 M2 2	-2.1	-12.0	3.26
ZD14 M2 3	-3.1	-12.3	5.80
ZD14 M2 4	-3.7	-12.2	8.32
ZD14 M2 5	-2.6	-10.6	11.92
ZD14 M2 6	-1.1	-9.7	14.94
ZD14 M2 7	-0.7	-9.4	17.47
ZD14 M2 8	0.1	-9.8	20.67
ZD14 M2 9	-0.2	-10.4	22.94
ZD14 M2 10	-0.3	-11.1	24.82

Sample	$\delta^{18}O‰_{VPDB}$	$\delta^{13}C‰_{VPDB}$	Distance to ERJ (mm)
ZD16			
ZD16 M2 1	-0.8	-9.2	2.92
ZD16 M2 2	-0.3	-9.9	5.45
ZD16 M2 3	-0.3	-11.3	7.92
ZD16 M2 4	-1.3	-11.8	9.93
ZD16 M2 5	-2.4	-12.2	12.35
ZD16 M2 6	-2.8	-12.3	14.21
ZD16 M2 7	-3.3	-12.2	16.82
ZD16 M2 8	-2.8	-11.7	18.90
ZD16 M2 9	-2.3	-11.3	20.80
ZD16 M2 10	-1.6	-10.5	22.95
ZD16 M2 11	-1.3	-9.9	24.82
ZD297			
ZD297 M2 1	-3.7	-12.7	3.18
ZD297 M2 2	-2.2	-11.3	6.51
ZD297 M2 3	-0.4	-9.7	9.62
ZD297 M2 4	0.4	-8.7	12.33
ZD297 M2 5	0.3	-8.6	15.25
ZD297 M2 6	0.6	-8.8	17.74
ZD297 M2 7	-0.1	-9.5	20.42
ZD297 M2 8	-1.0	-10.2	23.15
ZD297 M2 9	-1.7	-11.2	26.39
ZD297 M2 10	-3.3	-10.6	29.35

Sample	$\delta^{18}O‰_{VPDB}$	$\delta^{13}C‰_{VPDB}$	Distance to ERJ (mm)
		ZD298	
ZD298 M2 1	-1.3	-11.3	2.20
ZD298 M2 2	-0.3	-9.3	4.28
ZD298 M2 3	0.2	-8.1	6.80
ZD298 M2 4	0.7	-8.1	8.76
ZD298 M2 5	0.6	-9.0	11.17
ZD298 M2 6	0.2	-10.2	13.86
ZD298 M2 7	-0.5	-11.4	15.97
ZD298 M2 8	-1.3	-11.9	18.51
ZD298 M2 9	-2.0	-12.5	21.01
ZD298 M2 10	-3.0	-12.4	22.94
ZD298 M2 11	-3.7	-12.6	25.34

*Failed FTIR quality control

Appendix H. Specimen Details and $\delta^{13}C$ and $\delta^{15}N$ Values for Bone Collagen Samples

This appendix provides sample information for new and previously reported bone collagen samples discussed in Chapter Seven and Chapter Eight.

Table H.1. Results of stable isotope analysis of bone collagen samples. Includes new and previously reported data (Zavodny et al. 2014)

Sample ID	Species	Element	$\delta^{13}C$ (‰$_{VPDB}$)	$\delta^{15}N$ (‰$_{AIR}$)	%C	%N	C:N
Crno Vrilo (Impresso)							
CV1	*Ovis aries*	humerus	-20.1	7.4	43.5	15.7	3.23
CV10	*Capra hircus*	humerus	-20.0	7.3	41.2	14.8	3.25
CV11	*Ovis aries*	humerus	-20.7	6.9	39.0	14.2	3.20
CV12	*Ovis aries*	humerus	-20.6	7.2	44.4	16.0	3.24
CV13	*Capra hircus*	humerus	-20.1	6.4	43.6	15.6	3.26
CV14	*Bos sp.*	metacarpal	-20.3	5.6	42.7	15.2	3.28
CV2	*Ovis aries*	humerus	-21.6	6.6	45.1	16.4	3.21
CV3	*Ovis aries*	humerus	-21.1	7.0	43.7	15.8	3.23
CV4	Ovicaprid	humerus	-20.1	7.0	44.1	16.1	3.20
CV5	*Capra hircus*	humerus	-21.4	8.0	44.5	16.0	3.24
CV6	*Ovis aries*	humerus	-20.4	8.3	40.7	14.9	3.19
CV7	*Ovis aries*	humerus	-20.5	6.2	43.6	16.0	3.18
CV8	*Capra hircus*	metatarsal	-20.0	6.8	41.7	15.1	3.22
Konjevrate (Impresso)							
KON-1*	*Bos sp.*	1st phalanx	-21.8	5.4	14.0	4.1	4.00
KON-2†	*Ovis aries*	tibia	-19.8	4.8	40.9	14.7	3.24
KON-4†	*Ovis aries*	tibia	-19.4	6.4	42.6	15.5	3.20
KON-5†	*Bos sp.*	1st phalanx	-20.3	6.2	42.0	15.0	3.26
KON-8	*Bos sp.*	mandible	-19.7	6.9	44.8	16.0	3.26
KON-10	*Capra hircus*	femur	-20.6	7.7	47.2	16.7	3.29
KON-11B	*Ovis aries*	mandible w/ teeth	-19.3	6.3	41.8	15.3	3.18

Sample ID	Species	Element	$\delta^{13}C$ (‰$_{VPDB}$)	$\delta^{15}N$ (‰$_{AIR}$)	%C	%N	C:N
Pokrovnik (Impresso)							
PK-15†	*Ovis aries*	humerus	-20.1	5.3	42.4	15.6	3.17
PK-19†	*Ovis aries*	humerus	-19.7	5.6	42.6	15.7	3.17
PK-21†	*Ovis aries*	humerus	-20.4	5.2	43.5	16.0	3.18
PK-22†	*Ovis aries*	humerus	-20.6	5.5	40.2	14.8	3.17
PK-24	Ovicaprid	M2 molar	-20.2	7.4	43.9	16.2	3.16
PK-25	Ovicaprid	deciduous pre-molar 4	-20.6	8.5	42.0	15.4	3.18
PK-37†	*Bos sp.*	2nd phalanx	-20.0	5.3	43.5	16.0	3.17
PK-4†	*Ovis aries*	humerus	-19.8	5.7	45.8	16.9	3.16
PK-45	*Bos sp.*	metacarpal	-20.6	6.0	43.5	16.5	3.08
PK-5†	*Ovis aries*	humerus	-20.4	6.0	43.3	15.9	3.18
PK50	*Bos sp.*	metacarpal	-19.9	6.5	53.1	18.8	3.29
PK-62B	*Ovis aries*	mandible w/ teeth	-19.7	7.6	49.4	17.7	3.27
PK-63B	*Capra hircus*	mandible w/ teeth	-19.6	6.3	28.1	10.1	3.24
PK-64	*Ovis aries*	mandible w/ teeth	-19.7	5.8	42.0	14.8	3.32
PK-65	Ovicaprid	mandible w/ teeth	-19.9	5.5	42.6	14.9	3.32
PK-66	Ovicaprid	mandible w/ teeth	-20.4	6.7	40.3	14.0	3.35
PK-67	*Capra hircus*	mandible w/ teeth	-19.7	5.6	43.4	15.5	3.27
PK-68	Ovicaprid	mandible w/ teeth	-20.0	5.9	42.2	14.9	3.30
PK-69	Ovicaprid	mandible w/ teeth	-20.4	6.3	50.0	17.2	3.39
PK-7†	*Bos sp.*	femur	-20.4	4.3	44.5	16.4	3.16
PK-70	Ovicaprid	mandible w/ teeth	-20.2	6.3	46.8	16.4	3.32
PK-71	*Capra hircus*	mandible w/ teeth	-20.4	6.0	49.0	17.7	3.24
PK-72	*Capra hircus*	mandible w/ teeth	-20.1	6.2	52.1	18.7	3.26
PK-73	*Capra hircus*	mandible w/ teeth	-19.9	5.5	48.5	17.3	3.26
PK-74	Ovicaprid	mandible w/ teeth	-18.1	6.7	44.3	15.8	3.28
PK-75	*Capra hircus*	mandible w/ teeth	-20.6	5.3	48.7	17.1	3.33
PK-76	Ovicaprid	mandible w/ teeth	-20.5	5.9	49.7	17.7	3.28
PK-77	*Capra hircus*	mandible w/ teeth	-20.3	5.7	44.4	15.8	3.27
PK-78	*Ovis aries*	mandible w/ teeth	-20.1	6.6	43.6	15.4	3.31
PK79	*Capreolus capreolus*	tibia	-20.4	6.3	48.2	17.0	3.31

Sample ID	Species	Element	$\delta^{13}C$ (‰$_{VPDB}$)	$\delta^{15}N$ (‰$_{AIR}$)	%C	%N	C:N
PK80	*Capreolus capreolus*	tibia	-20.1	5.7	45.1	16.1	3.26
PK81	*Cervus elaphus*	humerus	-20.7	5.5	52.8	18.3	3.38
PK85	*Capreolus capreolus*	humerus	-19.8	5.7	46.8	16.4	3.34
PK86	*Capreolus capreolus*	humerus	-19.9	5.6	62.3	22.0	3.30
PK-3†	*Ovis aries*		-20.6	5.7			
Rašinovac (Impresso)							
RAS-1	*Bos sp.*	humerus	-20.1	6.3	44.6	16.2	3.22
RAS-2	Ovicaprid	radius	-19.8	7.1	41.1	15.1	3.17
RAS-3	*Capra hircus*	thoracic vertebra	-19.8	9.1	44.4	15.8	3.28
RAS-5	Ovicaprid	metapodial	-19.5	9.2	44.9	15.9	3.30
RAS-6	*Capra hircus*	astragalus	-19.6	7.4	42.8	15.2	3.30
RAS-7	*Lepus europaeus*	calcaneus	-20.9	6.8	43.8	15.6	3.28
Smilčić (Impresso)							
SMI337	*Capra hircus*	humerus	-20.0	6.9	42.7	16.1	3.09
SMI382	*Capra hircus*	humerus	-20.5	6.2	42.9	16.7	3.00
Benkovac-Barice (Danilo)							
BB249	*Ovis aries*	humerus	-19.9	5.7	41.6	16.3	2.98
BB260	*Capra hircus*	humerus	-19.4	6.3	39.1	14.0	3.26
Danilo-bitnj (Danilo)							
DA-4*	*Bos sp.*	1st phalanx	-21.0	4.6	18.8	5.9	3.74
DA-5*	*Bos sp.*	radius	-21.1	4.2	14.2	4.1	4.07
DA-6†	*Ovis aries*	humerus	-19.0	5.7	43.3	15.7	3.21
DA-13†	*Ovis aries*	humerus	-17.4	5.3	42.9	15.6	3.21
DA-14*	*Bos sp.*	scapula	-21.8	5.4	14.0	4.1	4.00
DA-16	*Capra hircus*	astragalus	-20.3	4.9	6.4	2.2	3.46
DA21B	Ovicaprid		-19.8	4.8	7.3	2.6	3.23
DA22	*Cervus elaphus*		-21.0	4.1	48.5	17.5	3.24
Islam Grčki (Danilo)							
IG483	*Bos sp.*	radius	-19.9	6.9	42.8	16.4	3.04
IG485	*Ovis aries*	humerus	-19.5	7.3	46.0	18.0	2.98

Sample ID	Species	Element	$\delta^{13}C$ (‰$_{VPDB}$)	$\delta^{15}N$ (‰$_{AIR}$)	%C	%N	C:N
Krivače (Danilo)							
KRI-1†	Ovicaprid	tibia	-19.3	6.3	41.8	15.3	3.19
KRI-2†	*Sus scrofa*	astragalus	-20.5	5.7	41.5	14.6	3.32
KRI-3†	*Bos sp.*	1st phalanx	-20.4	4.0	47.7	17.8	3.13
KRI-9†	*Ovis aries*	1st phalanx	-21.4	6.1	44.2	16.3	3.18
KRI-10†	*Bos sp.*	1st phalanx	-19.9	4.6	45.3	16.7	3.16
KRI-11†	*Bos sp.*	calcaneus	-20.3	4.9	44.4	16.4	3.16
KRI-12	Ovicaprid	2nd phalanx	-20.3	4.9	44.4	16.4	3.16
KRI-13	Ovicaprid	2nd phalanx	-20.5	5.2	41.3	14.5	3.32
KRI-14	*Sus sp.*	3rd phalanx	-18.7	5.7	46.0	16.2	3.31
KRI-15	*Capra hircus*	tibia	-20.1	6.0	44.3	15.6	3.32
KRI-16	*Capra hircus*	1st phalanx	-19.9	4.8	48.0	17.2	3.27
KRI-17B	*Bos sp.*	femur	-20.1	4.6	44.9	16.5	3.17
KRI-18B	*Bos sp.*	tibia	-20.0	5.0	46.5	17.2	3.15
KRI-19	*Bos sp.*	1st phalanx	-20.6	4.6	47.5	17.0	3.26
KRI-20	*Bos sp.*	tibia	-18.4	5.7	44.8	16.0	3.27
KRI-21	*Ovis aries*	2nd phalanx	-20.1	5.8	44.4	15.6	3.32
KRI-22	*Ovis aries*	metacarpal	-20.5	5.3	45.4	16.1	3.29
KRI-23	*Lepus europaeus*	scapula	-22.4	4.4	43.6	14.7	3.46
KRI-24	*Capreolus capreolus*	pelvis	-20.6	6.1	44.3	15.6	3.31
KRI26	*Capreolus capreolus*	femur	-18.2	7.9	29.7	10.6	3.28
KRI27	*Cervus elaphus*	metapodial	-21.6	5.7	44.4	15.4	3.36
Lisičić (Danilo)							
LS273	*Ovis aries*	humerus	-20.6	7.2	44.1	16.8	3.06
LS275	*Bos sp.*	calcaneus	-18.9	5.9	42.6	16.6	2.99

Sample ID	Species	Element	$\delta^{13}C$ (‰$_{VPDB}$)	$\delta^{15}N$ (‰$_{AIR}$)	%C	%N	C:N
Pokrovnik (Danilo)							
PK-14†	*Bos sp.*	metapodial	-19.7	5.6	45.2	16.3	3.23
PK-27†	*Sus sp.*	upper M3 molar	-19.9	6.5	43.5	15.5	3.28
PK-31†	*Ovis aries*	humerus	-20.5	6.0	46.2	16.6	3.25
PK-36†	*Bos sp.*	metacarpal	-18.9	5.5	42.4	16.4	3.02
PK-39†	*Bos sp.*	rib	-19.7	5.9	44.9	16.4	3.20
PK-44	*Bos sp.*	metacarpal	-18.9	4.2	44.2	16.8	3.07
PK-46	Ovicaprid	humerus	-20.2	6.9	25.7	8.9	3.35
PK-47	*Bos sp.*	1st phalanx	-19.6	6.6	30.6	11.1	3.22
PK-49	*Bos sp.*	1st phalanx	-20.2	5.9	28.7	10.6	3.16
PK-54B	*Capra hircus*	mandible w/ teeth	-19.7	5.0	29.2	10.5	3.26
PK-55B	*Capra hircus*	mandible w/ teeth	-19.0	6.3	26.8	9.5	3.28
PK-56	*Capreolus capreolus*	mandible w/ teeth	-19.7	5.2	53.0	18.8	3.30
PK-57	*Capreolus capreolus*	mandible w/ teeth	-21.1	4.4	31.3	11.2	3.26
PK-58	*Ovis aries*	mandible	-19.8	4.3	47.2	16.5	3.34
PK-59B	*Ovis aries*	mandible w/ teeth	-20.0	5.7	22.5	8.2	3.19
PK-60	*Ovis aries*	mandible w/ teeth	-20.2	5.6	41.6	14.7	3.29
PK-61	*Sus sp.*	skull	-20.3	4.8	52.2	18.6	3.28
PK82	*Cervus elaphus*	tibia	-20.3	6.1	26.9	9.5	3.30
PK83	*Capreolus capreolus*	tibia	-20.8	5.6	48.5	16.2	3.50
PK84	*Capreolus capreolus*	tibia	-20.1	6.6	46.4	16.2	3.34
Smilčić (Danilo)							
SMI342	*Capra hircus*	humerus	-20.4	4.9	44.0	16.9	3.04
SMI376	*Ovis aries*	humerus	-19.7	6.6	38.4	14.2	3.15

Sample ID	Species	Element	$\delta^{13}C$ (‰$_{VPDB}$)	$\delta^{15}N$ (‰$_{AIR}$)	%C	%N	C:N
Zemunik Donji (Danilo)							
ZD2	*Ovis aries*	humerus	-20.8	8.4	41.7	15.1	3.22
ZD3	*Ovis aries*	humerus	-19.2	6.8	41.0	14.7	3.25
ZD4	*Bos sp.*	metatarsal	-19.9	7.1	40.5	14.7	3.21
ZD5	Ovicaprid	humerus	-20.4	6.3	39.4	14.3	3.21
ZD6	*Capreolus capreolus*	metatarsal	-18.5	6.4	44.8	16.2	3.23
ZD7	*Ovis aries*	humerus	-20.8	5.8	43.0	15.7	3.20
ZD8	*Ovis aries*	humerus	-20.3	7.3	41.9	15.1	3.24
ZD9	*Capra hircus*	metacarpal	-20.2	6.9	42.1	15.3	3.21
Islam Grčki (Hvar)							
IG464	*Bos sp.*	metacarpal	-19.0	6.1	44.8	17.3	3.02
IG466	*Bos sp.*	metapodial	-17.6	5.3	41.6	16.1	3.01
Velištak (Hvar)							
CMV-1[†]	*Sus scrofa*	maxilla	-20.6	5.4	42.0	15.4	3.19
CMV-2[†]	*Bos sp.*	1st phalanx	-19.5	6.3	55.2	20.2	3.19
CMV-28[†]	*Capra hircus*		-20.0	5.0	45.6	16.5	3.21
CMV-38[†]	*Capra hircus*		-19.9	5.0	42.4	15.3	3.23
CMV-3A[†]	*Bos sp.*	metacarpal	-18.8	5.8	47.1	17.5	3.14
CMV-4[†]	*Sus scrofa*	astragalus	-20.4	5.9	39.7	14.4	3.22
CMV-5[†]	*Ovis aries*	humerus	-20.8	4.8	48.5	17.8	3.17
CMV-6[†]	*Sus scrofa*	maxilla	-19.8	7.0	41.7	15.3	3.19
CMV-7[†]	*Bos sp.*	metatarsal	-20.0	4.8	45.7	16.9	3.15
VEL14B	*Capreolus capreolus*	humerus	-19.3	6.6	48.8	17.2	3.31
VEL15	*Cervus elaphus*	femur	-19.7	5.5	47.7	16.6	3.35
VEL16	*Cervus elaphus*	metacarpal	-17.1	7.8	52.7	18.9	3.26
VEL17	*Sus sp.*	ulna	-21.2	6.3	36.4	13.0	3.26
VEL18	*Sus sp.*	scapula	-19.8	7.0	41.1	14.4	3.33
VEL19	*Sus scrofa*	scapula	-20.3	7.4	37.7	13.3	3.31
VEL20	*Lepus europaeus*	tibia	-23.5	5.7	43.2	15.3	3.29
VEL21	*Lepus europaeus*	tibia	-20.9	4.9	17.2	6.2	3.23

[†]Zavodny et al. (2014); [*]Omitted from analysis based on C:N ratio;

Appendix I. Mountain Pasture Locations and OIPC Data

This appendix provides estimated $\delta^{18}O$ values for locations used to model precipitation regimes. The locations provided in Table I.1 are shown in Figure 9.1 in Chapter Nine and reference known villages and pastures visited by transhumant pastoralists in Dalmatia from the 19th to 20th centuries (Marković 1975; 1980; 1987). Figure I.1. shows the monthly estimates of precipitation $\delta^{18}O$ at these sites and the modeled variation expected when animals were herded under the "Rapid" and "Stepwise" scenarios discussed in Chapter Nine. The estimated $\delta^{18}O$ values were obtained via the Online Isotopes in Precipitation Calculator (Bowen 2024; Bowen and Revenaugh 2003; Bowen and Wilkinson 2002).

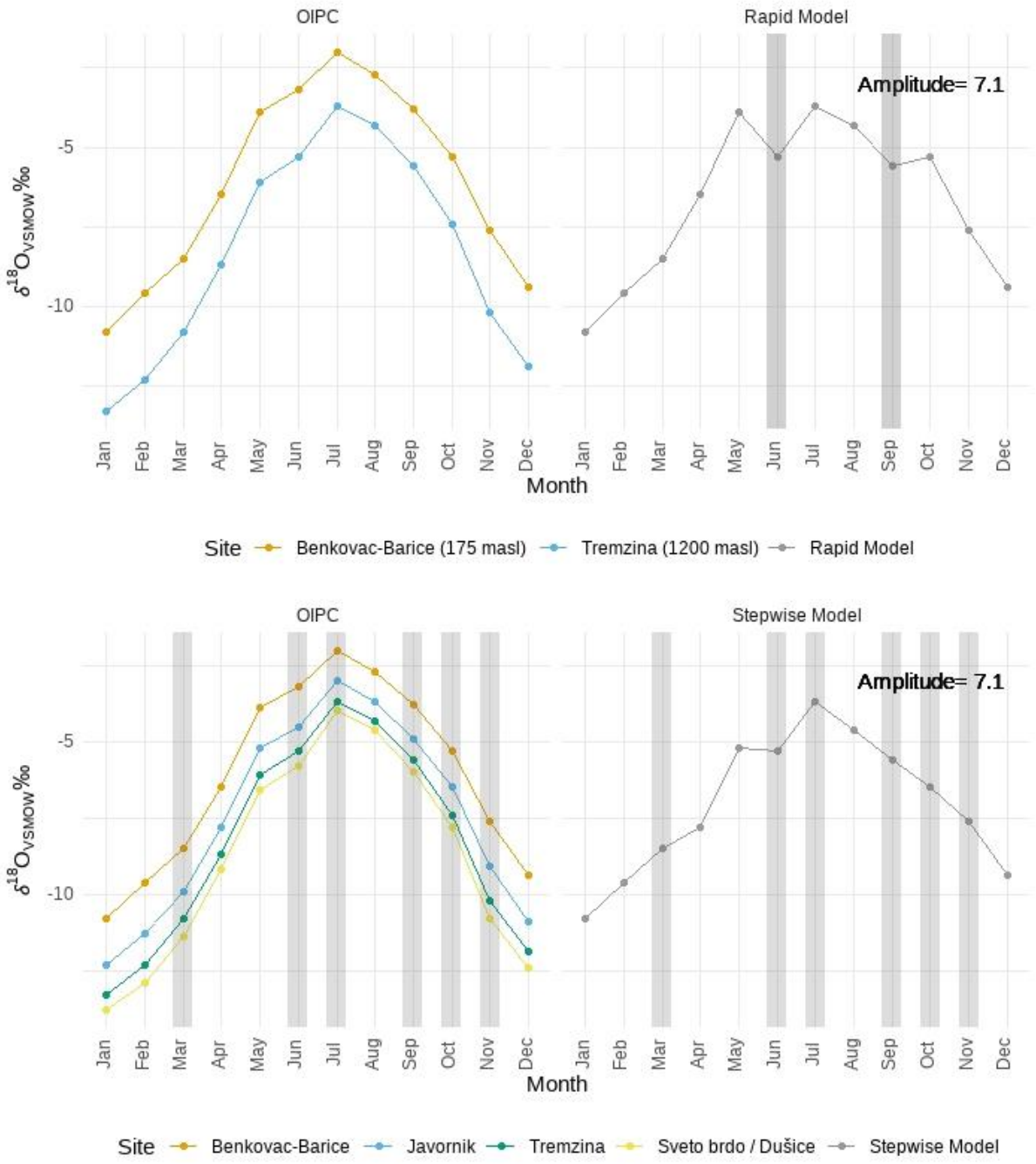

Figure I.1. Modeled environmental signals of rapid and stepwise transhumance models using Online Isotopes in Precipitation Calculator (Bowen 2024; Bowen et al. 2005) precipitation $\delta^{18}O_{VSMOW}$ values. Grey shaded regions correspond to movements to different elevations. See Table I.1. for coordinates and data used for plots.

Table I.1. Monthly Online Isotopes in Precipitation Calculator *(Bowen 2024; Bowen et al. 2005) estimates for mountain pastures used to model precipitation regimes of two variations of transhumance on the Dalmatian Coast of Croatia* (Marković 1980).

Pasture Lat/Long/Alt.	Zone	Month	$\delta^{18}O‰_{VSMOW}$
	Stepwise		
Benkovac-Barice :	Bukovica/Ravni Kotari	Jan	-10.8
44.03, 15.62, 175 masl		Feb	-9.6
		Mar	-8.5
Javornik :	Pod	Apr	-7.8
44.19, 16.0, 750 masl		May	-5.2
Tremzina :	Nadgorje	Jun	-5.3
44.24, 15.96, 1200 masl		Jul	-3.7
Sveto brdo / Dušice: 44.33, 15.57, 1441 masl	Vrgorje	Aug	-4.6
Tremzina: 44.24, 15.96, 1200 masl	Nadgorje	Sep	-5.6
Javornik : 44.19, 16.0, 750 masl	Pod	Oct	-6.5
Benkovac-Barice:	Bukovica/Ravni Kotari	Nov	-7.6
44.03, 15.62, 175 masl		Dec	-9.4
	Rapid		
Benkovac-Barice : 44.03, 15.62, 175 masl	Bukovica/Ravni Kotari	Jan	-10.8
		Feb	-9.6
		Mar	-8.5
		Apr	-6.5
		May	-3.9
Tremzina: 44.24, 15.96, 1200 masl	Nadgorje	Jun	-5.3
		Jul	-3.7
		Aug	-4.3
		Sep	-5.6
Benkovac-Barice: 44.03, 15.62, 175 masl	Bukovica/Ravni Kotari	Oct	-5.3
		Nov	-7.6
		Dec	-9.4

Appendix J. Modern Reference Data for Determining Birth Seasonality

This appendix provides replicated results of modeled season of birth of modern sheep tooth specimens for comparison with reported results. Table J.1 contains the published and replicated results of best fit values for the model derived from a cosine function used to estimate birth seasonality of sheep from intra-tooth $\delta^{18}O$ values (Balasse et al. 2012b). The left panel gives the reported amplitude (A), mean (M), position of the highest $\delta^{18}O_m$ value (x_0), the modeled length of the tooth formed in one annual cycle (X), and the reference value for the specimen's birth date within the annual cycle (x_0/X) for modern sheep from Rousay (Balasse et al. 2012b), Carmejane (Blaise and Balasse 2011; Tornero et al. 2013), and Corsica (Fabre et al. 2023). The right panel gives the results of replicating the modeling procedure on these specimens and the difference between reported and replicated x_0/X ratios (column delta).

Table J.1. Model results for modern reference sheep. Reported parameters (left panel) reflect model results associated with respective studies. Cosine function parameters (right panel) are the model results found in this study. Delta value is the difference between reported and replicated x_0/X ratios.

Rousay sheep – Balasse et al. (2012b)

	reported parameters						Cosine function (this study)						
Specimen	**A (‰)**	**M (‰)**	**x0 (mm)**	**X (mm)**	**x0/X**	**r Pearson**	**A (‰)**	**M (‰)**	**x0 (mm)**	**X (mm)**	**x0/X**	**r Pearson**	**delta**
ROU 01	1.9	-4.3	8.9	31.7	0.28		1.9	-4.3	8.9	31.7	0.28	0.998	**0.00**
ROU 04	2.0	-4.4	6.3	33.5	0.19		2.0	-4.4	39.8	33.6	1.19	0.998	**0.00**
ROU 06	1.5	-4.2	10.6	34.6	0.31		1.5	-4.2	10.6	34.6	0.31	0.989	**0.00**
ROU 07	1.3	-3.2	10.4	31.7	0.33		1.3	-3.2	10.4	31.6	0.33	0.994	**0.00**
ROU 08	1.2	-3.4	11.6	37.3	0.31		1.2	-3.4	11.6	37.3	0.31	0.988	**0.00**
ROU 09	1.8	-4.4	9	39	0.23		1.8	-4.4	9.1	39.0	0.23	0.989	**0.00**
ROU 11	1.9	-4.4	10.7	38.3	0.28		1.9	-4.4	10.7	38.3	0.28	0.994	**0.00**
ROU 16	1.8	-4.5	10.9	38.7	0.28		1.8	-4.5	10.9	38.8	0.28	0.994	**0.00**
ROU 17	1.8	-4.1	9.5	38.6	0.25		1.8	-4.1	9.6	38.6	0.25	0.998	**0.00**
ROU 18	1.3	-3.7	11.2	30.7	0.37		1.3	-3.7	11.2	30.7	0.37	0.988	**0.00**
min	-	-	-	-	-	-	-	-	-	-	-	-	**0**
max	-	-	-	-	-	-	-	-	-	-	-	-	**0**
mean	-	-	-	-	-	-	-	-	-	-	-	-	**0**

Carmejane sheep - Blaise and Balasse (2012); Tornero et al. (2013)

	reported parameters						Cosine function (this study)						
Specimen	**A (‰)**	**M (‰)**	**x0 (mm)**	**X (mm)**	**x0/X**	**r Pearson**	**A (‰)**	**M (‰)**	**x0 (mm)**	**X (mm)**	**x0/X**	**r Pearson**	**delta**
Ovis 0026	3.3	-3.4	3.2	27	0.12	0.989	3.1	-3.4	1.1	35.0	0.03	0.997	**0.09**
Ovis 0522	2	-3.7	24	32	0.75	0.992	1.9	-3.6	-1.1	23.6	-0.05	0.989	**0.20**
Ovis 0562	2	-3.3	21	27.5	0.76	0.957	2.1	-3.3	-3.8	25.6	-0.15	0.986	**0.09**
Ovis 1216	2	-4.3	5	35	0.14	0.96	2.0	-4.3	37.3	31.7	1.18	0.969	**0.04**
Ovis 1511	2.4	-2.7	18.3	28.5	0.64	0.971	4.3	-4.9	18.1	50.0	0.36	0.998	**0.28**
Ovis 9470	-	-	-	-	-	-	3.3	-2.2	-2.3	25.0	-0.09	0.994	**-**
min	-	-	-	-	-	-	-	-	-	-	-	-	**0.04**
max	-	-	-	-	-	-	-	-	-	-	-	-	**0.28**
mean	-	-	-	-	-	-	-	-	-	-	-	-	**0.14**

Corsica sheep - Fabre et al. (2023)													
	reported parameters						Cosine function (this study)						
Specimen	**A (‰)**	**M (‰)**	**x0 (mm)**	**X (mm)**	**x0/X**	**r Pearson**	**A (‰)**	**M (‰)**	**x0 (mm)**	**X (mm)**	**x0/X**	**r Pearson**	**delta**
COR Ovis 1 M2	1.18	-5.27	22.67	35.12	0.65	0.982	1.18	-5.27	22.67	35.12	0.65	0.982	**0.00**
COR Ovis 3 M2	1.10	-3.78	20.25	28.76	0.70	0.981	1.10	-3.78	20.25	28.76	0.70	0.981	**0.00**
COR Ovis 4 M2	0.93	-3.25	23.10	25.01	0.92	0.974	0.89	-3.23	-2.70	26.31	-0.10	0.958	**-0.02**
COR Ovis 5 M2	0.68	-3.71	20.48	24.01	0.85	0.935	0.78	-3.75	-3.25	23.66	-0.14	0.926	**0.01**
min	-	-	-	-	-	-	-	-	-	-	-	-	**-0.02**
max	-	-	-	-	-	-	-	-	-	-	-	-	**0.01**
mean	-	-	-	-	-	-	-	-	-	-	-	-	**0.01**

References

Abdelqader, A., Irshaid, R., Tabbaa, M. J., Abuajamieh, M., Titi, H. and Al-Fataftah, A.-R. (2017). Factors influencing Awassi lambs survivorship under fields conditions. *Livest. Sci.* **199**: 1–6.

Adserias-Garriga, J. and Visnapuu, V. (2019). The neonatal line as evidence of live birth. *Age Estimation*, Elsevier, pp.161–168.

Allan, J. H. (1967). Maturation of enamel. *Struct. Chem. Organ. teeth* **1**: 467–494.

Ambrose, S. H. and Norr, L. (1993). Experimental Evidence for the Relationship of the Carbon Isotope Ratios of Whole Diet and Dietary Protein to Those of Bone Collagen and Carbonate. In J. B. Lambert and G. Grupe (eds.), *Prehistoric Human Bone*, Springer Berlin Heidelberg, Berlin, Heidelberg, pp.1–37.

Amoah, E. A. and Bryant, M. J. (1984). A note on the effect of contact with male goats on occurrence of puberty in female goat kids. *Anim. Sci.* **38**: 141–144.

Amundson, R., Austin, A. T., Schuur, E. A. G., Yoo, K., Matzek, V., Kendall, C., Uebersax, A., Brenner, D. and Baisden, W. T. (2003). Global patterns of the isotopic composition of soil and plant nitrogen. *Global Biogeochem. Cycles* **17**:.

Anderson, D. M., Fredrickson, E. L. and Estell, R. E. (2012). Managing livestock using animal behavior: mixed-species stocking and flerds. *Animal* **6**: 1339–1349.

Aranibar, J. N., Otter, L., Macko, S. A., Feral, C. J. W., Epstein, H. E., Dowty, P. R., Eckardt, F., Shugart, H. H. and Swap, R. J. (2004). Nitrogen cycling in the soil-plant system along a precipitation gradient in the Kalahari sands. *Glob. Chang. Biol.* **10**: 359–373.

Arnold, E. R. and Greenfield, H. J. (2006). *The origins of transhumant pastoralism in temperate southeastern Europe : a zooarchaeological perspective from the central Balkans*, Archaeopress, Oxford.

Austin, A. T. and Vitousek, P. M. (1998). Nutrient Dynamics on a Precipitation Gradient in Hawai'i. *Oecologia* **113**: 519–529.

Awemu, E. M., Nwakalor, L. N. and Abubakar, B. Y. (1999). Environmental influences on preweaning mortality and reproductive performance of Red Sokoto does. *Small Rumin. Res.* **34**: 161–165.

Bakrač, K., Ilijanić, N., Miko, S. and Hasan, O. (2018). Evidence of sapropel S1 formation from Holocene lacustrine sequences in Lake Vrana in Dalmatia (Croatia). *Quat. Int.* **494**: 5–18.

Balasse, M. (2002). Reconstructing dietary and environmental history from enamel isotopic analysis: time resolution of intra-tooth sequential sampling. *Int. J. Osteoarchaeol.* **12**: 155–165.

Balasse, M. (2003). Keeping the young alive to stimulate milk production? Differences between cattle and small stock. *Anthropozoologica* **37**: 3–10.

Balasse, M., Ambrose, S. H., Smith, A. B. and Price, T. D. (2002). The Seasonal Mobility Model for Prehistoric Herders in the South-western Cape of South Africa Assessed by Isotopic Analysis of Sheep Tooth Enamel. *J. Archaeol. Sci.* **29**: 917–932.

Balasse, M., Bălăşescu, A., Janzen, A., Ughetto-Monfrin, J., Mirea, P. and Andreescu, R. (2013). Early herding at Măgura-Boldul lui Moş Ivănuş (early sixth millennium BC, Romania): environments and seasonality from stable isotope analysis. *Eur. J. Archaeol.* **16**: 221–246.

Balasse, M., Boury, L., Ughetto-Monfrin, J. and Tresset, A. (2012a). Stable isotope insights (δ18O, δ13C) into cattle and sheep husbandry at Bercy (Paris, France, 4th millennium BC): birth seasonality and winter leaf foddering. *Environ. Archaeol.* **17**: 29–44.

Balasse, M., Chemineau, P., Parisot, S., Fiorillo, D. and Keller, M. (2023). Experimental Data from Lacaune and Merino Sheep Provide New Methodological and Theoretical Grounds to Investigate Autumn Lambing in Past Husbandries. *J. Archaeol. Method Theory*.

Balasse, M., Mainland, I. and Richards, M. P. (2009). Stable isotope evidence for seasonal consumption of marine seaweed by modern and archaeological sheep in the Orkney archipelago (Scotland). *Environ. Archaeol.* **14**: 1–14.

Balasse, M., Obein, G., Ughetto-Monfrin, J. and Mainland, I. (2012b). Investigating seasonality and season of birth in past herds: a reference set of sheep enamel stable oxygen isotope ratios. *Archaeometry* **54**: 349–368.

Balasse, M., Renault-Fabregon, L., Gandois, H., Fiorillo, D., Gorczyk, J., Bacvarov, K. and Ivanova, M. (2020). Neolithic sheep birth distribution: Results from Nova Nadezhda (sixth millennium BC, Bulgaria) and a reassessment of European data with a new modern reference set including upper and lower molars. *J. Archaeol. Sci.* **118**: 105139.

Balasse, M., Smith, A. B., Ambrose, S. H. and Leigh, S. R. (2003). Determining Sheep Birth Seasonality by Analysis of Tooth Enamel Oxygen Isotope Ratios: The Late Stone Age Site of Kasteelberg (South Africa). *J. Archaeol. Sci.* **30**: 205–215.

Balasse, M., Tresset, A., Bălăşescu, A., Blaise, E., Tornero, C., Gandois, H., Fiorillo, D., Nyerges, É. Á., Frémondeau, D., Banffy, E. and Ivanova, M. (2017). Animal Board Invited Review: Sheep birth distribution in past herds: a review for prehistoric Europe (6th to 3rd millennia BC). *Animal* **11**: 2229–2236.

Balasse, M., Tresset, A., Dobney, K. and Ambrose, S. H. (2005). The use of isotope ratios to test for seaweed eating in sheep. *J. Zool.* **266**: 283–291.

Balasse, M., Tresset, A., Obein, G., Fiorillo, D. and Gandois, H. (2019). Seaweed-eating sheep and the adaptation of husbandry in Neolithic Orkney: new insights from Skara Brae. *Antiquity* **93**: 919–932.

Barlow, K. R. (2006). A formal model for predicting agriculture among the Fremont. In D. J. Kennett and B. Winterhalder (eds.), *Behavioral Ecology and the Transition to Agriculture*, University of California Press, Berkeley, pp.87–102.

Bartosiewicz, L. (2005). Plain talk: animals, environment and culture in the Neolithic of the Carpathian Basin and adjacent areas. In D. W. Bailey A. W. R. Whittle and V.

Cummings (eds.), *(Un)Settling the Neolithic*, Oxbow Books, Oxford, pp.51–63.

Bartosiewicz, L. and Greenfield, H. J. (1999). *Transhumant pastoralism in Southern Europe : recent perspectives from archaeology, history and ethnology / edited by László Bartosiewicz and Haskel J. Greenfield.*, Archaeolingua, Budapest.

Bass, B. (1998). Early Neolithic Offshore Accounts: Remote Islands, Maritime Exploitations, and the Trans-Adriatic Cultural Network. *J. Mediterr. Archaeol.* **11**: 190.

Batović, S. (1985). Prapovijesni ostatci u Islamu Grčkom. *Zadar. Rev.* **XXXIV**: 283–308.

Batović, S. (1987). Islam Grčki- nalazi od paleolitika do ranog brončanog doba. *Poročilo o raziskovanju Paleolit. Neolit. Eneolit. v Slov.* **XV**: 11–107.

Batović, Š. (1958). Neolitske kultne posude iz Smilčića. *Arheol. Vestn.* **9**–**10**: 79–93.

Batović, Š. (1963). Neolitsko nalazište Smilčić. *Radovi Instituta Jugoslavenske Akademije u Zadru*, Zadar, pp.89–138.

Batović, Š. (1966). *Stariji neolit u Dalmaciji*, Zadar.

Batović, Š. (1970). Brončani mač iz Islama Grčkog. *Adriat. Praehist. Antiq.* **zbornik po**: 173–188.

Batović, Š. (1974). *Prapovijesni ostaci na Zadarskom otočju*, Narodni muzej.

Batović, Š. (1979). Jadranska zona. In A. Benac (ed.), *Praistorija Jugoslovenskih Zemalja Vol. 2: Neolitsko Doba*, Svetlost, Sarajevo, pp.473–635.

Batović, Š. (1990). Benkovački kraj u prapovijesti. *Rad. Filoz. Fak. u Zadru, Razdio Povij. Znan.* **29**: 5–142.

Battaglia, V., Fornarino, S., Al-Zahery, N., Olivieri, A., Pala, M., Myres, N. M., King, R. J., Rootsi, S., Marjanovic, D., Primorac, D., Hadziselimovic, R., Vidovic, S., Drobnic, K., Durmishi, N., Torroni, A., Santachiara-Benerecetti, A. S., Underhill, P. A. and Semino, O. (2009). Y-chromosomal evidence of the cultural diffusion of agriculture in southeast Europe. *Eur. J. Hum. Genet.* **17**: 820–830.

Bayliss-Smith, T. (1982). *The ecology of agricultural systems*, Cambridge , Cambridge .

Belaj, V. (2004). Tradicijsko planinsko stočarstvo na Velebitu i bunjevačka etnogeneza. *Stud. Ethnol. Croat.* **16**: 5–31.

Bentley, J. W. (1987). Economic and Ecological Approaches to Land Fragmentation: In Defense of a Much-Maligned Phenomenon. *Annu. Rev. Anthropol.* **16**: 31–67.

Berger, J.-F. and Guilaine, J. (2009). The 8200calBP abrupt environmental change and the Neolithic transition: A Mediterranean perspective. *Quat. Int.* **200**: 31–49.

Berhan, A. and Van Arendonk, J. (2006). Reproductive performance and mortality rate in Menz and Horro sheep following controlled breeding in Ethiopia. *Small Rumin. Res.* **63**: 297–303.

Bernard, A., Daux, V., Lécuyer, C., Brugal, J. P., Genty, D., Wainer, K., Gardien, V., Fourel, F. and Jaubert, J. (2009). Pleistocene seasonal temperature variations recorded in the δ18O of Bison priscus teeth. *Earth Planet. Sci. Lett.* **283**: 133–143.

Berthon, R., Kovačiková, L., Tresset, A. and Balasse, M. (2018). Integration of Linearbandkeramik cattle husbandry in the forested landscape of the mid-Holocene climate optimum: Seasonal-scale investigations in Bohemia. *J. Anthropol. Archaeol.* **51**: 16–27.

Bettinger, R. L. (2009). Hunter-gatherer foraging: five simple models. ISD.

Bettinger, R. L., Garvey, R. and Tushingham, S. (2015). *Hunter-Gatherers*, Springer US, Boston, MA.

Biagi, P. (2003). The rhyton of the balkan peninsula: chronology, origin, dispersion and function of a neolithic "Cult" vessel. *J. Prehist. Relig.* **XVI**–**XVII**: 16–26.

Biagi, P., Shennan, S. and Spataro, M. (2005). Rapid Rivers and slow seas? New data for the radiocarbon chronology of the Balkan peninsula. *RPRP* **006**–**007**: 41//50.

Biagi, P. and Spataro, M. (2001). Plotting the evidence: some aspects of the radiocarbon chronology of the Mesolithic-Neolithic transition in the Mediterranean basin. *Atti della Soc. la Preist. e Protostoria della Reg. Friuli-Venezia Giulia* **12**: 15–54.

Binder, D., Lanos, P., Angeli, L., Gomart, L., Guilaine, J., Manen, C., Maggi, R., Muntoni, I. M., Panelli, C., Radi, G., Tozzi, C., Arobba, D., Battentier, J., Brandaglia, M., Bouby, L., Briois, F., Carré, A., Delhon, C., Gourichon, L., Marinval, P., Nisbet, R., Rossi, S., Rowley-Conwy, P. and Thiébault, S. (2017). Modelling the earliest north-western dispersal of Mediterranean Impressed Wares: new dates and Bayesian chronological model. *Doc. Praehist.* **44**: 54–77.

Bindi, L. ed. (2022). *Grazing Communities: Pastoralism on the Move and Biocultural Heritage Frictions*, Berghahn Books.

Bird, D. W., Bird, R. B. and Codding, B. F. (2009). In Pursuit of Mobile Prey: Martu Hunting Strategies and Archaeofaunal Interpretation. *Am. Antiq.* **74**: 3–29.

Bird, D. W. and O'Connell, J. F. (2006). Behavioral ecology and archaeology. *J. Archaeol. Res.* **14**: 143–188.

Blaise, E. and Balasse, M. (2011). Seasonality and season of birth of modern and late Neolithic sheep from south-eastern France using tooth enamel δ18O analysis. *J. Archaeol. Sci.* **38**: 3085–3093.

Bocherens, H., Hofman-Kamińska, E., Drucker, D. G., Schmölcke, U. and Kowalczyk, R. (2015). European Bison as a Refugee Species? Evidence from Isotopic Data on Early Holocene Bison and Other Large Herbivores in Northern Europe. *PLoS One* **10**: e0115090.

Bocquet-Appel, J.-P. and Naji, S. (2006). Testing the Hypothesis of a Worldwide Neolithic Demographic Transition Corroboration from American Cemeteries. *Curr. Anthropol.* **47**: 341–365.

Bocquet-Appel, J.-P., Naji, S., Linden, M. Vander and Kozlowski, J. K. (2009). Detection of diffusion and contact zones of early farming in Europe from the space-time distribution of 14C dates. *J. Archaeol. Sci.* **36**: 807–820.

Bogaard, A. (2004). The nature of early farming in Central and South-east Europe. *Doc.*

Praehist. **31**: 49–58.

Bogaard, A. (2005). 'Garden agriculture' and the nature of early farming in Europe and the Near East. *World Archaeol.* **37**: 177–196.

Bogaard, A., Arbogast, R.-M., Ebersbach, R., Fraser, R. A., Knipper, C., Krahn, C., Schäfer, M., Styring, A. K. and Krause, R. (2016). The Bandkeramik settlement of Vaihingen an der Enz, Kreis Ludwigsburg (Baden-Württemberg): an integrated perspective on land use, economy and diet.

Bogaard, A., Fraser, R., Heaton, T. H. E., Wallace, M., Vaiglova, P., Charles, M., Jones, G., Evershed, R. P., Styring, A. K., Andersen, N. H., Arbogast, R. and Bartosiewicz, L. (2013). Crop manuring and intensive land management by Europe's first farmers. *Proc. Natl. Acad. Sci.* **110**: 12589–12594.

Bogaard, A. and Halstead, P. (2015). Subsistence Practices and Social Routine in Neolithic Southern Europe. In C. Fowler J. Harding and D. Hofmann (eds.), *The Oxford Handbook of Neolithic Europe*, Oxford University Press, pp.386–415.

Bogaard, A., Heaton, T. H. E., Poulton, P. and Merbach, I. (2007). The impact of manuring on nitrogen isotope ratios in cereals: archaeological implications for reconstruction of diet and crop management practices. *J. Archaeol. Sci.* **34**: 335–343.

Bogucki, P. I. (1984). Ceramic Sieves of the Linear Pottery Culture and their Economic Implications. *Oxford J. Archaeol.* **3**: 15–30.

Bonacci, Terzić, Roje-Bonacci and Frangen (2019). An Intermittent Karst River: The Case of the Čikola River (Dinaric Karst, Croatia). *Water* **11**: 2415.

Bonafini, M., Pellegrini, M., Ditchfield, P. and Pollard, A. M. (2013). Investigation of the 'canopy effect'in the isotope ecology of temperate woodlands. *J. Archaeol. Sci.* **40**: 3926–3935.

Bonsall, C. (2007). When was the Neolithic transition in the Iron Gates? In M. Spataro and P. Biagi (eds.), *A Short Walk through the Balkans: The First Farmers of the Carpathian Basin and Adjacent Regions. Proceedings of t He Conference Held at the Institute of Archaeology UCL on June 20th - 22nd, 2005. Società Preistoria Protostoria Friuli-V.G., Trieste, Quade*, pp.53–66.

Bowen, G. J. (2024). The Online Isotopes in Precipitation Calculator. Version 3.1.

Bowen, G. J. and Revenaugh, J. (2003). Interpolating the isotopic composition of modern meteoric precipitation. *Water Resour. Res.* **39**:.

Bowen, G. J., Wassenaar, L. I. and Hobson, K. A. (2005). Global application of stable hydrogen and oxygen isotopes to wildlife forensics. *Oecologia* **143**: 337–348.

Bowen, G. J. and Wilkinson, B. (2002). Spatial distribution of δ18O in meteoric precipitation. *Geology* **30**: 315–318.

Bradburd, D. (1982). Volatility of Animal Wealth among Southwest Asian Pastoralists. *Hum. Ecol.* **10**: 85–106.

Bradburd, D. A. (1980). Never Give a Shepherd an Even Break: Class and Labor among the

Komachi. *Am. Ethnol.* **7**: 603–620.

Britton, K., Grimes, V., Dau, J. and Richards, M. P. (2009). Reconstructing faunal migrations using intra-tooth sampling and strontium and oxygen isotope analyses: a case study of modern caribou (Rangifer tarandus granti). *J. Archaeol. Sci.* **36**: 1163–1172.

Britton, K., Müldner, G. and Bell, M. (2008). Stable isotope evidence for salt-marsh grazing in the Bronze Age Severn Estuary, UK: implications for palaeodietary analysis at coastal sites. *J. Archaeol. Sci.* **35**: 2111–2118.

Brkić, Ž., Kuhta, M., Hunjak, T. and Larva, O. (2020). Regional Isotopic Signatures of Groundwater in Croatia. *Water* **12**: 1983.

Broadmeadow, M. S. J., Griffiths, H., Maxwell, C. and Borland, A. M. (1992). The carbon isotope ratio of plant organic material reflects temporal and spatial variations in CO_2 within tropical forest formations in Trinidad. *Oecologia* 435–441.

Brochier, J. É. (2013). The use and abuse of culling profiles in recent zooarchaeological studies: Some methodological comments on "frequency correction" and its consequences. *J. Archaeol. Sci.* **40**: 1416–1420.

Bronk Ramsey, C. (2009). Bayesian Analysis of Radiocarbon Dates. *Radiocarbon* **51**: 337–360.

Bronson, F. H. and Heideman, P. (1994). Seasonal regulation of reproduction in mammals. *Physiol. Reprod.* 541–584.

Broodbank, C. and Strasser, T. F. (1991). Migrant farmers and the Neolithic colonization of Crete. *Antiquity* **65**: 233–245.

Broughton, J. M., Cannon, M. D., Bayham, F. E. and Byers, D. A. (2011). Prey Body Size and Ranking in Zooarchaeology: Theory, Empirical Evidence, and Applications from the Northern Great Basin. *Am. Antiq.* **76**: 403–428.

Browman, D. L. (1987). Agro-pastoral risk management in the Central Andes. *Res. Econ. Anthropol.* **8**: 171–200.

Browman, D. L. (1997). Pastoral Risk Perception and Risk Definition for Altiplano Herders. *Nomad. People.* **1**: 22–36.

Brown, T. A., Nelson, D. E., Vogel, J. S. and Southon, J. R. (1988). Improved Collagen Extraction by Modified Longin Method. *Radiocarbon* **30**: 171–177.

Brush, S. B. (1976). Man's Use of an Andean Ecosystem. *Hum. Ecol.* **4**: 147–166.

Brush, S. B. (1982). The Natural and Human Environment of the Central Andes. *Mt. Res. Dev.* **2**: 19.

Brusić, Z. (1979). Pokrovnik, Drniš - naselje impresso i danilske faze neolitika. *Arheol. Pregl.* **21**: 19–20.

Brusić, Z. (2008). *Pokrovnik naselje iz neolitika*, Muzej Grada Šibenika, Šibenik.

Budja, M. (2013). Neolithic transition to farming in Northern Adriatic. Lactose tolerance, dairying and lipid biomarkers on pottery. *Archaeol. Adriat.* **7**: 53–75.

Burger, J., Kirchner, M., Bramanti, B., Haak, W. and Thomas, M. G. (2007). Absence of the lactase-persistence-associated allele in early Neolithic Europeans. *Proc. Natl. Acad. Sci.* **104**: 3736–3741.

Burr, D. B. (2002). The contribution of the organic matrix to bone's material properties. *Bone* **31**: 8–11.

Capelli, C., Starnini, E., Cabella, R. and Piazza, M. (2017). The circulation of Early Neolithic pottery in the Mediterranean: A synthesis of new archaeometric data from the Impressed Ware culture of Liguria (north-west Italy). *J. Archaeol. Sci. Reports* **16**: 532–541.

Caraco, T. (1981). Energy Budgets, Risk and Foraging Preferences in Dark-Eyed Juncos (Junco hyemalis). *Behav. Ecol. Sociobiol.* **8**: 213–217.

Caraco, T. (1982). Aspects of risk-aversion in foraging white-crowned sparrows. *Anim. Behav.* **30**: 719–727.

Caraco, T., Martindale, S. and Whittam, T. S. (1980). An Empirical Demonstration of Risk-Sensitive Foraging. *Anim. Behav.* 820–830.

Della Casa, P., Bass, B., Katunarić, T., Kirigin, B. and Radić, D. (2009). An overview of prehistoric and early historic settlement, topography, and maritime connections on Lastovo Island, Croatia. In S. Forenbaher (ed.), *A Connecting Sea: Maritime Interaction in Adriatic Prehistory*, Archaeopress, Oxford, pp.113–136.

Cashdan, E. A. (1985). Coping with Risk: Reciprocity Among the Basarwa of Northern Botswana. *Man* **20**: 454.

Cashdan, E. A. (1990). *Risk and uncertainty in tribal and peasant economies*, Westview Press, Boulder.

Caswell, H. (2001). Matrix population models : construction, analysis, and interpretation.

Čelhar, M. and Borzić, I. (2016). Gradina u Zemuniku Donjem, nalazi željeznog i rimskog doba. *Zemunik u Prost. i Vrem.* 68–117.

Cerling, T. E. and Harris, J. M. (1999). Carbon isotope fractionation between diet and bioapatite in ungulate mammals and implications for ecological and paleoecological studies. *Oecologia* **120**: 347–363.

Chang, C. (1993). Pastoral Transhumance in the Southern Balkans as a Social Ideology: Ethnoarcheological Research in Northern Greece. *Am. Anthropol.* **95**: 687–703.

Chapman, J. (1981). *The Vinča culture of south-east Europe : studies in chronology, economy and society*, British Archaeological Reports, Oxford SE - 167 pages.

Chapman, J., Shiel, R. and Batović, S. (1996). *The changing face of Dalmatia : archaeological and ecological studies in a Mediterranean landscape*, Leicester University Press in assoc. with the Society of Antiquaries of London, London.

Chapman, V. J. and Chapman, D. J. (1980). Seaweed as Animal Fodder, Manure and for Energy BT - Seaweeds and their Uses. In V. J. Chapman and D. J. Chapman (eds.), Springer Netherlands, Dordrecht, pp.30–61.

Charnov, E. L. (1976). Optimal foraging theory: the marginal value theorem. *Theor. Popul.*

Biol. **9**: 129–136.

Chase, B., Meiggs, D., Ajithprasad, P. and Slater, P. A. (2014). Pastoral land-use of the Indus Civilization in Gujarat: faunal analyses and biogenic isotopes at Bagasra. *J. Archaeol. Sci.* **50**: 1–15.

Chazin, H. (2021). Multi-Season Reproduction and Pastoralist Production Strategies: New Approaches to Birth Seasonality from the South Caucasus Region. *J. F. Archaeol.* **46**: 448–460.

Chazin, H., Deb, S., Falk, J. and Srinivasan, A. (2019). New Statistical Approaches to Intra-individual Isotopic Analysis and Modelling of Birth Seasonality in Studies of Herd Animals. *Archaeometry* **61**: 478–493.

Chemineau, P., Malpaux, B., Delgadillo, J. A., Guérin, Y., Ravault, J. P., Thimonier, J. and Pelletier, J. (1992). Control of sheep and goat reproduction: Use of light and melatonin. *Anim. Reprod. Sci.* **30**: 157–184.

Choi, W.-J., Ro, H.-M. and Hobbie, E. A. (2003). Patterns of natural 15N in soils and plants from chemically and organically fertilized uplands. *Soil Biol. Biochem.* **35**: 1493–1500.

Clutton-Brock, T. H., Albon, S. D. and Guinness, F. E. (1989). Fitness costs of gestation and lactation in wild mammals. *Nature* **337**: 260.

Codding, B. F. and Bird, D. W. (2015). Behavioral ecology and the future of archaeological science. *J. Archaeol. Sci.* **56**: 9–20.

Collins, R. P. and Jones, M. B. (1985). The influence of climatic factors on the distribution of C4 species in Europe. *Vegetatio* **64**: 121–129.

Combourieu-Nebout, N., Peyron, O., Bout-Roumazeilles, V., Goring, S., Dormoy, L., Joannin, S., Sadori, L., Siani, G. and Maguy, M. (2013). Holocene vegetation and climate changes in the central Mediterranean inferred from a high-resolution marine pollen record (Adriatic Sea). *Clim. Past* **9**: 2023–2042.

Cook, G. C. and Al-Torki, M. T. (1975). High intestinal lactase concentrations in adult Arbs in Saudi Arabia. *Br. Med. J.* **3**: 135–6.

Copley, M. S., Jim, S., Jones, V., Rose, P., Clapham, A., Edwards, D. N., Horton, M., Rowley-Conwy, P. and Evershed, R. P. (2004). Short- and long-term foraging and foddering strategies of domesticated animals from Qasr Ibrim, Egypt. *J. Archaeol. Sci.* **31**: 1273–1286.

Coughenour, M. B., Ellis, J. E., Swift, D. M., Coppock, D. L., Galvin, K., McCabe, J. T. and Hart, T. C. (1985). Energy Extraction and Use in a Nomadic Pastoral Ecosystem. *Science (80-.).* **230**: 619–625.

Craig, O. E., Chapman, J., Heron, C., Willis, L. H., Bartosiewicz, L., Taylor, G., Whittle, A. and Collins, M. (2005). Did the first farmers of central and eastern Europe produce dairy foods? *Antiquity* **79**: 882–894.

Crate, S. A. (2008). "Eating Hay": The Ecology, Economy and Culture of Viliui Sakha Smallholders of Northeastern Siberia. *Hum. Ecol.* **36**: 161–174.

Crouse, D. T., Crowder, L. B. and Caswell, H. (1987). A Stage-Based Population Model for Loggerhead Sea Turtles and Implications for Conservation. *Ecology* **68**: 1412–1423.

Cummings, V. and Morris, J. (2022). Neolithic Explanations Revisited: Modelling the Arrival and Spread of Domesticated Cattle into Neolithic Britain. *Environ. Archaeol.* **27**: 20–30.

Dahl, G. and Hjort, A. (1976). *Having herds : pastoral herd growth and household economy*, Dept. of Social Anthropology, University of Stockholm, Stockholm.

Daniel Bryant, J. and Froelich, P. N. (1995). A model of oxygen isotope fractionation in body water of large mammals. *Geochim. Cosmochim. Acta* **59**: 4523–4537.

Daniel Bryant, J., Froelich, P. N., Showers, W. J. and Genna, B. J. (1996a). Biologic and climatic signals in the oxygen isotopic composition of Eocene-Oligocene equid enamel phosphate. *Palaeogeogr. Palaeoclimatol. Palaeoecol.* **126**: 75–89.

Daniel Bryant, J., Koch, P. L., Froelich, P. N., Showers, W. J. and Genna, B. J. (1996b). Oxygen isotope partitioning between phosphate and carbonate in mammalian apatite. *Geochim. Cosmochim. Acta* **60**: 5145–5148.

Dansgaard, W. (1964). Stable isotopes in precipitation. Tellus 16, 436e468.

Dean, M. C. (1987). Growth layers and incremental markings in hard tissues; a review of the literature and some preliminary observations about enamel structure in Paranthropus boisei. *J. Hum. Evol.* **16**: 157–172.

Debbarma, A. and Sarkar, D. (2021). Non-genetic factors affecting mortality in goat kids under intensive housing system.

Debele, G. and Duguma, M. (2013). Study on major causes of kid mortality in Adami Tulu Jido Kombolcha District of Oromia, Ethiopia. *Agric. Biol. J. North Am.* **4**: 110–115.

Debele, G., Duguma, M. and Hundessa, F. (2011). Effect of different factors on mortality rate of Arsi- Bale kids in mid rift valley of Ethiopia. *Glob. Vet.* **6**: 56–60.

Debono Spiteri, C., Gillis, R. E., Roffet-Salque, M., Castells Navarro, L., Guilaine, J., Manen, C., Muntoni, I. M., Saña Segui, M., Urem-Kotsou, D., Whelton, H. L., Craig, O. E., Vigne, J.-D. and Evershed, R. P. (2016). Regional asynchronicity in dairy production and processing in early farming communities of the northern Mediterranean. *Proc. Natl. Acad. Sci.* **113**: 13594–13599.

von den Driesch, A. (1976). *A guide to the measurement of animal bones from archaeological sites*, Peabody Museum of Archaeology and Ethnology, Harvard University, Cambridge, Mass.

DeNiro, M. J. (1985). Postmortem preservation and alteration of in vivo bone collagen isotope ratios in relation to palaeodietary reconstruction. *Nature* **317**: 806–809.

DeNiro, M. J. and Epstein, S. (1978). Influence of diet on the distribution of carbon isotopes in animals. *Geochim. Cosmochim. Acta* **42**: 495–506.

DeNiro, M. J. and Epstein, S. (1981). Influence of diet on the distribution of nitrogen isotopes in animals. *Geochim. Cosmochim. Acta* **45**: 341–351.

Diaz-Maroto, P., Rey-Iglesia, A., Cartajena, I., Núñez, L., Westbury, M. V, Varas, V., Moraga, M., Campos, P. F., Orozco-terWengel, P., Marin, J. C. and Hansen, A. J. (2021). Ancient DNA reveals the lost domestication history of South American camelids in Northern Chile and across the Andes. *Elife* **10**:.

Dolukhanov, P., Shukurov, A., Gronenborn, D., Sokoloff, D., Timofeev, V. and Zaitseva, G. (2005). The chronology of Neolithic dispersal in Central and Eastern Europe. *J. Archaeol. Sci.* **32**: 1441–1458.

Doppler, T., Gerling, C., Heyd, V., Knipper, C., Kuhn, T., Lehmann, M. F., Pike, A. W. G. and Schibler, J. (2017). Landscape opening and herding strategies: Carbon isotope analyses of herbivore bone collagen from the Neolithic and Bronze Age lakeshore site of Zurich-Mozartstrasse, Switzerland. *Quat. Int.* **436**: 18–28.

Drucker, D. G., Bridault, A., Hobson, K. A., Szuma, E. and Bocherens, H. (2008). Can carbon-13 in large herbivores reflect the canopy effect in temperate and boreal ecosystems? Evidence from modern and ancient ungulates. *Palaeogeogr. Palaeoclimatol. Palaeoecol.* **266**: 69–82.

Dufour, E., Goepfert, N., Gutiérrez Léon, B., Chauchat, C., Franco Jordán, R. and Sánchez, S. V. (2014). Pastoralism in Northern Peru during Pre-Hispanic Times: Insights from the Mochica Period (100–800 AD) Based on Stable Isotopic Analysis of Domestic Camelids. *PLoS One* **9**: e87559.

Dunson, W. (1974). Some aspects of salt and water balance of feral goats from arid islands. *Am. J. Physiol. Content* **226**: 662–669.

Dwyer, C. M., Conington, J., Corbiere, F., Holmøy, I. H., Muri, K., Nowak, R., Rooke, J., Vipond, J. and Gautier, J.-M. (2016). Invited review: Improving neonatal survival in small ruminants: science into practice. *Animal* **10**: 449–459.

Dyson-Hudson, R. (1980). Toward a General Theory of Pastoralism And Social Stratification. *Nomad. People.* 1–7.

Dyson-Hudson, R. and Dyson-Hudson, N. (1969). Subsistence Herding in Uganda. *Sci. Am.* **220**: 76–89.

Dyson-Hudson, R. and Dyson-Hudson, N. (1980). Nomadic Pastoralism. *Annu. Rev. Anthropol.* **9**: 15–61.

Dyson-Hudson, R. and McCabe, J. T. (1985). South Turkana Nomadism: Coping With An Unpredictably Varying Environment.

Dyson-Hudson, R. and Smith, E. A. (1978). Human territoriality : an ecological reassessment. *Am. Anthropol.* **80**: 21–41.

Ebozoje, M. O. and Ngere, L. O. (1995). Incidence of Preweaning Mortality in West African Dward Goats and their Red Sokoto Halfbreds. *Niger. J. Anim. Prod.* **22**: 93–98.

Elliott, J. C. (2002). Calcium Phosphate Biominerals. *Rev. Mineral. Geochemistry* **48**: 427–453.

Erasmus, J. A., Fourie, A. J. and Venter, J. J. (1985). Influence of age on reproductive performance of the Improved Boer goat doe. *S. Afr. J. Anim. Sci.* **15**: 5–7.

Eriksen, E. F. (2010). Cellular mechanisms of bone remodeling. *Rev. Endocr. Metab. Disord.* **11**: 219–227.

Evershed, R. P., Payne, S., Sherratt, A. G., Copley, M. S., Coolidge, J., Urem-Kotsu, D., Kotsakis, K., Özdoğan, M., Özdoğan, A. E., Nieuwenhuyse, O., Akkermans, P. M. M. G., Bailey, D., Andeescu, R.-R., Campbell, S., Farid, S., Hodder, I., Yalman, N., Özbaşaran, M., Bıçakcı, E., Garfinkel, Y., Levy, T. and Burton, M. M. (2008). Earliest date for milk use in the Near East and southeastern Europe linked to cattle herding. *Nature* **455**: 528–531.

Fabre, M., Forest, V., Ranché, C., Fiorillo, D., Casabianca, F., Vigne, J.-D. and Balasse, M. (2023). Milk and meat exploitation, autumn lambing and use of forest resources in Neolithic Corsican sheep farming systems (fifth to third millennia cal BC). *J. Archaeol. Sci. Reports* **50**: 104037.

Fahy, G. E., Deter, C., Pitfield, R., Miszkiewicz, J. J. and Mahoney, P. (2017). Bone deep: Variation in stable isotope ratios and histomorphometric measurements of bone remodelling within adult humans. *J. Archaeol. Sci.* **87**: 10–16.

Farquhar, G. D., Ehleringer, J. R. and Hubick, K. T. (1989). Carbon Isotope Discrimination and Photosynthesis. *Annu. Rev. Plant Physiol. Plant Mol. Biol.* **40**: 503–537.

Fernández, E., Pérez-Pérez, A., Gamba, C., Prats, E., Cuesta, P., Anfruns, J., Molist, M., Arroyo-Pardo, E. and Turbón, D. (2014). Ancient DNA Analysis of 8000 B.C. Near Eastern Farmers Supports an Early Neolithic Pioneer Maritime Colonization of Mainland Europe through Cyprus and the Aegean Islands. *PLoS Genet.* **10**: e1004401.

Feulner, F., Gerbault, P., Gillis, R., Hollund, H., Howcroft, R., Leonardi, M., Liebert, A., Raghavan, M., Salque, M., Sverrisdóttir, O., Teasdale, M., van Doorn, N. and Wright, C. (2012). *May contain traces of milk : investigating the role of dairy farming and milk consumption in the European neolithic*, The University of York, Heslington.

Flanagan, L. B. and Ehleringer, J. R. (1991). Stable Isotope Composition of Stem and Leaf Water: Applications to the Study of Plant Water Use. *Funct. Ecol.* **5**: 270.

Flannery, K. V. (1969). Origins and ecological effects of early domestication in Iran and the Near East. In P. J. Ucko and G. W. Dimbleby (eds.), *The Domestication and Exploitation of Plants and Animals*, Duckworth, London.

Flannery, K. V (2002). The Origins of the Village Revisited : From Nuclear to Extended Households. *Am. Antiq.* **67**: 417–433.

Foley, R. (1985). Optimality Theory in Anthropology. *Man* **20**: 222–242.

Forenbaher, S. (2007). Shepherds of a coastal range : the archaeological potential of the Velebit mountain range (Eastern Adriatic). In M. van Leusen G. Pizziolo and L. Sarti (eds.), *Hidden Lanscapes of Mediterranean Europe: Cultural and Methodological Biases in Pre- and Protohistoric Landscape Studies*, Siena, Italy, pp.113–122.

Forenbaher, S. (2022). Početak sezonskog stočarstva u Dalmaciji. *Archaeol. Adriat.* **15**:.

Forenbaher, S. and Kaiser, T. (2000). Grapčeva spilja i apsolutno datiranje istočnojadranskog neolitika. *Vjesn. za Arheol. i Hist. Dalm.* **92**: 9–34.

Forenbaher, S. and Kaiser, T. (2006). The pottery of Pupićina Cave. In P. T. Miracle and S. Forenbaher (eds.), *Prehistoric Herders of Northern Istria: The Archaeology of Pupićina Cave, Vol. 1*, Pula, pp.163–223.

Forenbaher, S., Kaiser, T. and Miracle, P. (2004). Pupićina Cave pottery and the Neolithic sequence in northeastern Adriatic. *Atti della Soc. la Preist. e Protostoria della Reg. Friuli-Venezia Giulia* **14**: 61–102.

Forenbaher, S., Kaiser, T. and Miracle, P. T. (2013). Dating the East Adriatic Neolithic. *Eur. J. Archaeol.* **16**: 589–609.

Forenbaher, S. and Miracle, P. (2006). Pupićina Cave and the Spread of Farming in the Eastern Adriatic. In P. T. Miracle and S. Forenbaher (eds.), *Prehistoric Herders of Northern Istria: The Archaeology of Pupićina Cave, Vol. 1*, Pula, pp.483–523.

Forenbaher, S. and Miracle, P. T. (2005). The spread of farming in the eastern Adriatic. *Antiquity* **79**: 514–528.

Forenbaher, S. and Miracle, P. T. (2014). Transition to farming in the Adriatic: A view from the eastern shore. In C. Manen T. Perrin and J. Guilaine (eds.), *La Transition Néolithique En Méditerranée*, Editions Errance, pp.233–241.

Forenbaher, S. and Pavle, V. (1985). Vaganačka pećina. *Opvscvla Archaeol.* **10**: 1–21.

Forenbaher, S., Rajić Šikanjić, P. and Miracle, P. T. (2006). Lončarija iz Vele peći kod Vranje (Istra). *Histria Archaeol.* **37**: 5–44.

Forenbaher, S. and Vranjican, P. (1982). Pećina u Pazjanicama, Velika Paklenica: Prilog pretpovijesti Hrvatskog primorja. *Senj. Zb.* **9**: 5–14.

Forenbaher, S. and Vranjican, P. (1990). Velebit: Rekognosciranje speleoloških objekata. *Arheol. Pregl.* 237–239.

France, C. A. M., Sugiyama, N. and Aguayo, E. (2020). Establishing a preservation index for bone, dentin, and enamel bioapatite mineral using ATR-FTIR. *J. Archaeol. Sci. Reports* **33**: 102551.

Fraser, R. A., Grün, R., Privat, K. and Gagan, M. K. (2008). Stable-isotope microprofiling of wombat tooth enamel records seasonal changes in vegetation and environmental conditions in eastern Australia. *Palaeogeogr. Palaeoclimatol. Palaeoecol.* **269**: 66–77.

Freyer, H. D. and Belacy, N. (1983). 13C/12C records in northern hemispheric trees during the past 500 years—anthropogenic impact and climatic superpositions. *J. Geophys. Res. Ocean.* **88**: 6844–6852.

Fricke, H. C. and O'Neil, J. R. (1996). Inter- and intra-tooth variation in the oxygen isotope composition of mammalian tooth enamel phosphate: implications for palaeoclimatological and palaeobiological research. *Palaeogeogr. Palaeoclimatol. Palaeoecol.* **126**: 91–99.

Fritz, P. (1981). River Waters. In J. R. Gat and R. Gonfiantini (eds.), *Stable Isotope Hydrology Deuterium and Oxygen-18 in the Water Cycle*, International Atomic Energy Agency (IAEA): IAEA, pp.177–202.

Fry, B. and Arnold, C. (1982). Rapid 13 C/12 C turnover during growth of brown shrimp (Penaeus aztecus). *Oecologia* **54**: 200–204.

Gaastra, J. S. and Vander Linden, M. (2018). Farming data: Testing climatic and palaeoenvironmental effect on Neolithic Adriatic stockbreeding and hunting through zooarchaeological meta-analysis. *The Holocene* **28**: 1181–1196.

Gaastra, J. S., de Vareilles, A. and Vander Linden, M. (2019). Bones and Seeds: An Integrated Approach to Understanding the Spread of Farming across the Western Balkans. *Environ. Archaeol.* 1–17.

Gage, J. P., Francis, M. J. O. and Triffit, J. T. (1989). *Collagen and dental matrices*, Butterworth-Heinemann.

Galaty, J. (2021). Pastoralism in Eastern Africa. *Oxford Research Encyclopedia of African History*, Oxford University Press.

Galina, M. A., Silva, E., Morales, R. and Lopez, B. (1995). Reproductive performance of Mexican dairy goats under various management systems. *Small Rumin. Res.* **18**: 249–253.

Gamba, C., Jones, E. R., Teasdale, M. D., McLaughlin, R. L., Gonzalez-Fortes, G., Mattiangeli, V., Domboróczki, L., Kővári, I., Pap, I., Anders, A., Whittle, A., Dani, J., Raczky, P., Higham, T. F. G., Hofreiter, M., Bradley, D. G. and Pinhasi, R. (2014). Genome flux and stasis in a five millennium transect of European prehistory. *Nat. Commun.* **5**: 5257.

Gat, J. R. (1980). *The isotopes of hydrogen and oxygen in precipitation*, Elsevier, Netherlands.

Gat, J. R. (1981a). Groundwaters. In J. R. Gat and R. Gonfiantini (eds.), *Stable Isotope Hydrology Deuterium and Oxygen-18 in the Water Cycle1*, International Atomic Energy Agency (IAEA): IAEA, pp.223–240.

Gat, J. R. (1981b). *Stable isotope hydrology Deuterium and oxygen-18 in the water cycle*, J. R. Gat and R. Gonfiantini (eds.), IAEA, International Atomic Energy Agency (IAEA).

Gat, J. R. (1996). Oxygen and Hydrogen Isotopes in the Hydrologic Cycle. *Annu. Rev. Earth Planet. Sci.* **24**: 225–262.

Gebert, C. and Verheyden-Tixier, H. (2001). Variations of diet composition of Red Deer (Cervus elaphus L.) in Europe. *Mamm. Rev.* **31**: 189–201.

Gerbault, P., Liebert, A., Itan, Y., Powell, A., Currat, M., Burger, J., Swallow, D. M. and Thomas, M. G. (2011). Evolution of lactase persistence: an example of human niche construction. *Philos. Trans. R. Soc. B Biol. Sci.* **366**: 863–877.

Gidarakou, I. and Apostolopoulos, C. (1995). The productive system of itinerant stockfarming in Greece. *Medit* **3**: 56–63.

Gillis, R., Bréhard, S., Bălăşescu, A., Ughetto-Monfrin, J., Popovici, D., Vigne, J.-D. and Balasse, M. (2013). Sophisticated cattle dairy husbandry at Borduşani-Popină (Romania, fifth millennium BC): the evidence from complementary analysis of mortality profiles and stable isotopes. *World Archaeol.* **45**: 447–472.

Gillis, R., Carrère, I., Saña Seguí, M., Radi, G. and Vigne, J. (2016). Neonatal Mortality, Young Calf Slaughter and Milk Production during the Early Neolithic of North Western Mediterranean. *Int. J. Osteoarchaeol.* **26**: 303–313.

Gillis, R. E., Kovačiková, L., Bréhard, S., Guthmann, E., Vostrovská, I., Nohálová, H., Arbogast, R.-M., Domboróczki, L., Pechtl, J., Anders, A., Marciniak, A., Tresset, A. and Vigne, J.-D. (2017). The evolution of dual meat and milk cattle husbandry in Linearbandkeramik societies. *Proc. R. Soc. B Biol. Sci.* **284**: 20170905.

Goland, C. (1993a). Agricultural Risk Management Through Diversity: Field Scattering in Cuyo Cuyo, Peru. *Cult. Agric.* 8–13.

Goland, C. (1993b). Field Scattering as Agricultural Risk Management: A Case Study from Cuyo Cuyo, Department of Puno, Peru. *Mt. Res. Dev.* **13**: 317–338.

Gonfiantini, R., Roche, M.-A., Olivry, J.-C., Fontes, J.-C. and Zuppi, G. M. (2001). The altitude effect on the isotopic composition of tropical rains. *Chem. Geol.* **181**: 147–167.

Grafen, A. (1984). Natural selection, kin selection and group selection. In J. R. Krebs and N. B. Davies (eds.), *Behavioral Ecology: An Evolutionary Approach*, Blackwell Scientific, Oxford, pp.62–84.

Grant, A. (1982). The Use of Tooth Wear as a Guide to the Age of Domestic Ungulates. In B. Wilson C. Grigson and S. Payne (eds.), *Ageing and Sexing Animal Bones from Archaeological Sites - British Archaeological Records International Series 109.*, Archaeopress, Oxford, pp.91–108.

Green, L. E. and Morgan, K. L. (1993). Mortality in early born, housed lambs in south-west England. *Prev. Vet. Med.* **17**: 251–261.

Greenfield, H. J. (1999). The advent of transhumant pastoralism in the temperate southeast Europe: a zooarchaeological perspective from the Central Balkans. In L. Bartosiewicz and H. J. Greenfield (eds.), *Transhumant Pastoralism in Southern Europe: Recent Perspectives from Archaeology, History and Ethnology*, Archaeolingua, Budapest, pp.15–36.

Greenfield, H. J. (2005). A reconsideration of the secondary products revolution in southeastern Europe: on the origins and use of domestic animal milk, wool, and traction in the central Balkans. In J. Mulville and A. K. Outram (eds.), *The Zooarchaeology of Fats, Oils, Milk and Dairying.*, Oxbow Books, pp.14–31.

Greenfield, H. J. (2010). The secondary products revolution: The past, the present and the future. *World Archaeol.* **42**: 29–54.

Greenfield, H. J. (2014). The origins of secondary product exploitation and the zooarchaeology of the Late Neolithic, Eneolithic and Middle Bronze Ages at Vinča-Belo Brdo, Serbia: the 1982 excavations. In H. J. Greenfield (ed.), *Animal Secondary Products: Domestic Animal Exploitation in Prehistoric Europe, the Near East and the Far East*, Oxbow Books, Oxford, pp.274–334.

Gronenborn, D. (1999). A Variation on a Basic Theme: The Transition to Farming in Southern Central Europe. *J. World Prehistory* **13**: 123–210.

Gronenborn, D. and Dolukhanov, P. (2013). Early Neolithic Manifestations in Central and Eastern Europe. In C. Fowler J. Harding and D. Hoffman (eds.), *The Oxford Handbook of Neolithic Europe*, Oxford University Press.

Grüger, E. (1996). Vegetational Change. In J. C. Chapman R. Shiel and Š. Batović (eds.), *The Changing Face of Dalmatia*, Leicester University Press in assoc. with the Society of Antiquaries of London, London, pp.34–43.

Guillet, D. (1981). Agrarian Ecology and Peasant Production in the Central Andes. *Mt. Res. Dev.* **1**: 19.

Guillet, D. (1987). Agricultural Intensification and Deintensification in Lari, Colca Valley, Southern Peru. *Res. Econ. Anthropol.* **8**: 201–224.

Guiry, E., Karavanić, I., Klindžić, R. Š., Talamo, S., Radović, S. and Richards, M. P. (2017). Stable Isotope Palaeodietary and Radiocarbon Evidence from the Early Neolithic Site of Zemunica, Dalmatia, Croatia. *Eur. J. Archaeol.* **20**: 235–256.

Hadjigeorgiou, I. (2011). Past, present and future of pastoralism in Greece. *Pastor. Res. Policy Pract.* **1**: 24.

Hadjikoumis, A. (2017). Age-at-death in traditional Cypriot sheep and goat husbandry: In P. Rowley-Conwy D. Serjeanston and P. Halstead (eds.), *Economic Zooarchaeology*, Oxbow Books.

Hadjikoumis, A., Vigne, J.-D., Simmons, A., Guilaine, J., Fiorillo, D. and Balasse, M. (2019). Autumn/winter births in traditional and Pre-Pottery Neolithic caprine husbandry in Cyprus: Evidence from ethnography and stable isotopes. *J. Anthropol. Archaeol.* **53**: 102–111.

Hafez, E. S. E. (1952). Studies on the breeding season and reproduction of the ewe Part III. The breeding season and artificial light Part IV. Studies on the reproduction of the ewe Part V. Mating behaviour and pregnancy diagnosis. *J. Agric. Sci.* **42**: 232–265.

Hailu, D., Mieso, G., Nigatu, A., Fufa, D. and Gamada, D. (2006). The effect of environmental factors on preweaning survival rate of Borana and Arsi-Bale kids. *Small Rumin. Res.* **66**: 291–294.

Hajek-Tadesse, V., Ilijanić, N., Miko, S. and Hasan, O. (2018). Holocene Ostracoda (Crustacea) from the shallow Lake Vrana (Dalmatia, Croatia) and their paleoenvironmental significance. *Quat. Int.* **494**: 80–91.

Hallson, S. V. (1964). The uses of seaweeds in Iceland. *Proceedings of the Fourth International Seaweeds Symposium, Biarritz 1961*, Pergamon Press, Oxford.

Halstead, P. (1987). Traditional and ancient rural economy in Mediterranean Europe: plus ça change? *J. Hell. Stud.* **107**: 77–87.

Halstead, P. (1989). Like rising damp? An ecological approach to the spread of farming in southeast and central Europe. In A. Milles D. Williams and N. Gardner (eds.), *The Beginnings of Agriculture*, Oxford, pp.23–53.

Halstead, P. (1990). Waste not, want not: traditional responses to crop failure in Greece. *Rural Hist.* **1**: 147–164.

Halstead, P. (1996). Pastoralism or Household Herding? Problems of Scale and Specialization in Early Greek Animal Husbandry. *World Archaeol.* **28**: 20–42.

Halstead, P. (1998a). Ask the Fellows who Lop the Hay Leaf-Fodder in the Mountains of Northwest Greece. *Rural Hist.* **9**: 211–234.

Halstead, P. (1998b). Mortality models and milking: problems of uniformitarianism, optimality and equifinality reconsidered. *Anthropozoologica* **27**: 3–20.

Halstead, P. (2006). Sheep in the garden: the integration of crop and livestock husbandry in early farming regimes of Greece and southern Europe. In D. Serjeantson and D. Field (eds.), *Animals in the Neolithic of Britain and Europe*, Oxbow Books, Oxford, pp.42–55.

Halstead, P. (2024). Zooarchaeological evidence for livestock management in (earlier) Neolithic Europe: Outstanding questions and some limitations of current approaches. *Quat. Int.* **683**–**684**: 42–50.

Halstead, P. and Jones, G. (1989). Agrarian Ecology in the Greek Islands: Time Stress, Scale and Risk. *J. Hell. Stud.* **109**: 41–55.

Halstead, P. and O'Shea, J. (1989). Bad Year Economics.

Halstead, P., Tierney, J., Butler, S. and Mulder, Y. (1998). Leafy hay: an ethnoarchaeological study in NW Greece. *Environ. Archaeol.* **1**: 71–80.

Hansen, H. ., Hector, B. . and Feldmann, J. (2003). A qualitative and quantitative evaluation of the seaweed diet of North Ronaldsay sheep. *Anim. Feed Sci. Technol.* **105**: 21–28.

Hanson, B. A. (2024). ChemoSpec: Exploratory Chemometrics for Spectroscopy.

Hartman, G. and Danin, A. (2010). Isotopic values of plants in relation to water availability in the Eastern Mediterranean region. *Oecologia* **162**: 837–852.

Hatcher, S., Eppleston, J., Graham, R. P., McDonald, J., Schlunke, S., Watt, B. and Thornberry, K. J. (2008). Higher weaning weight improves postweaning growth and survival in young Merino sheep. *Aust. J. Exp. Agric.* **48**: 966.

Hawkes, K., Hill, K. and O 'Connell, J. F. (1982). Why Hunters Gather: Optimal Foraging and the Aché of Eastern Paraguay optimal foraging and the Ache of eastern Paraguay. *Source Am. Ethnol.* **9**: 379–398.

Hedges, R. E. M., Clement, J. G., Thomas, C. D. L. and O'Connell, T. C. (2007). Collagen turnover in the adult femoral mid-shaft: Modeled from anthropogenic radiocarbon tracer measurements. *Am. J. Phys. Anthropol.* **133**: 808–816.

Hedges, R. E. M. and Reynard, L. M. (2007). Nitrogen isotopes and the trophic level of humans in archaeology. *J. Archaeol. Sci.* **34**: 1240–1251.

Helliker, B. R. and Ehleringer, J. R. (2000). Establishing a grassland signature in veins: 18 O in the leaf water of C 3 and C 4 grasses. *Proc. Natl. Acad. Sci.* **97**: 7894–7898.

Helmer, D., Gourichon, L. and Vila, E. (2007). The development of the exploitation of products from Capra and Ovis (meat, milk and fleece) from the PPNB to the Early Bronze in the northern Near East (8700 to 2000 BC cal.). *Anthropozoologica* **2**: 41–69.

Helmer, D. and Vigne, J.-D. (2004). La gestion des cheptels de caprinés au Néolithique dans le midi de la France. *Approch. Fonct. en Préhistoire* 397–407.

Hemminga, M. A. and Mateo, M. A. (1996). Stable carbon isotopes in seagrasses: variability in ratios and use in ecological studies. *Mar. Ecol. Prog. Ser.* **140**: 285–298.

Henrich, J. and McElreath, R. (2002). Are Peasants Risk-Averse Decision Makers? *Curr. Anthropol.* **43**: 172–181.

Henton, E. (2012). The combined use of oxygen isotopes and microwear in sheep teeth to elucidate seasonal management of domestic herds: The case study of Çatalhöyük, central Anatolia. *J. Archaeol. Sci.* **39**: 3264–3276.

Henton, E., MCorriston, J., Martin, L. and Oches, E. A. (2014). Seasonal aggregation and ritual slaughter: Isotopic and dental microwear evidence for cattle herder mobility in the Arabian Neolithic. *J. Anthropol. Archaeol.* **33**: 119–131.

Henton, E., Meier-Augenstein, W. and Kemp, H. F. (2010). The use of oxygen isotopes in sheep molars to investigate past herding practices at the Neolithic settlement of Çatalhöyük, central Anatolia. *Archaeometry* **52**: 429–449.

Hermes, T., Pederzani, S. and Makarewicz, C. A. (2017). Ahead of the curve?: Implications for isolating vertical transhumance in seasonal montane environments using sequential oxygen isotope analyses of tooth enamel. *Isot. Investig. Pastor. Prehistory* 57–76.

Hermes, T. R., Frachetti, M. D., Doumani Dupuy, P. N., Mar'yashev, A., Nebel, A. and Makarewicz, C. A. (2019). Early integration of pastoralism and millet cultivation in Bronze Age Eurasia. *Proc. R. Soc. B Biol. Sci.* **286**: 20191273.

Hermes, T. R., Schmid, C., Tabaldiev, K. and Motuzaite Matuzeviciute, G. (2022). Carbon and oxygen stable isotopic evidence for diverse sheep and goat husbandry strategies amid a Final Bronze Age farming milieu in the Kyrgyz Tian Shan. *Int. J. Osteoarchaeol.* **32**: 792–803.

Herring, D. A., Saunders, S. R. and Katzenberg, M. A. (1998). Investigating the weaning process in past populations. *Am. J. Phys. Anthropol.* **105**: 425–439.

Hillson, S. (1986). Archaeology and the study of teeth. *Endeavour* **10**: 145–149.

Hoffman, J. M. and Valencak, T. G. (2020). A short life on the farm: aging and longevity in agricultural, large-bodied mammals. *GeroScience* **42**: 909–922.

Hofman-Kamińska, E., Bocherens, H., Borowik, T., Drucker, D. G. and Kowalczyk, R. (2018). Stable isotope signatures of large herbivore foraging habitats across Europe. *PLoS One* **13**: e0190723.

Hofmanová, Z., Kreutzer, S., Hellenthal, G., Sell, C., Diekmann, Y., Díez-del-Molino, D., van Dorp, L., López, S., Kousathanas, A., Link, V., Kirsanow, K., Cassidy, L. M., Martiniano, R., Strobel, M., Scheu, A., Kotsakis, K., Halstead, P., Triantaphyllou, S., Kyparissi-Apostolika, N., Urem-Kotsou, D., Ziota, C., Adaktylou, F., Gopalan, S., Bobo, D. M., Winkelbach, L., Blöcher, J., Unterländer, M., Leuenberger, C., Çilingiroğlu, Ç., Horejs, B., Gerritsen, F., Shennan, S. J., Bradley, D. G., Currat, M., Veeramah, K. R., Wegmann, D., Thomas, M. G., Papageorgopoulou, C. and Burger, J.

(2016). Early farmers from across Europe directly descended from Neolithic Aegeans. *Proc. Natl. Acad. Sci.* **113**: 6886–6891.

Hogg, R. (1987). Development in Kenya: Drought, Desertification and Food Scarcity. *Afr. Aff. (Lond).* **86**: 47–58.

Hollund, H. I., Ariese, F., Fernandes, R., Jans, M. M. E. and Kars, H. (2013). Testing an alternative high-throughput tool for investigating bone diagenesis: FTIR in Attenuated Total Reflection (ATR) mode. *Archaeometry* **55**: 507–532.

Holm, S. (1979). A Simple Sequentially Rejective Multiple Test Procedure. *Scand. J. Stat.* **6**: 65–70.

Hopkins, R. J. A., Snoeck, C. and Higham, T. F. G. (2016). When Dental Enamel is Put to the Acid Test: Pretreatment Effects and Radiocarbon Dating. *Radiocarbon* **58**: 893–904.

Hoppe, K. A., Stover, S. M., Pascoe, J. R. and Amundson, R. (2004). Tooth enamel biomineralization in extant horses: implications for isotopic microsampling. *Palaeogeogr. Palaeoclimatol. Palaeoecol.* **206**: 355–365.

Horejs, B., Milić, B., Ostmann, F., Thanheiser, U., Weninger, B. and Galik, A. (2015). The Aegean in the Early 7th Millennium BC: Maritime Networks and Colonization. *J. World Prehistory* **28**: 289–330.

Horvat, I., Glavac, V. and Ellenberg, H. (1974). *Vegetation Südosteuropas*, G. Fischer.

Horvat, K. (2017). Ambijentalne Osnove Razvoja Neolitičkih Zajednica Istočnog Jadrana-Primjer Benkovačkog Područja, University of Zadar.

Horvat, K. and Vujević, D. (2017). Pokrovnik – materijalna kultura neolitičkog naselja. *Pril. Instituta za Arheol. u Zagreb.* **34**: 45–82.

Horvat Oštrić, K. and Triozzi, N. (2024a). Neolitičko nalazište Pod Jarugom. *situ* **1**: 72–76.

Horvat Oštrić, K. and Triozzi, N. (2024b). Probna istraživanja neolitičkog nalazišta u Islamu Grčkom. *situ* **1**: 46–51.

Horvat Oštrić, K., Triozzi, N., McClure, S. B., Reed, K. and Vidas, D. (forthcoming). Rezultati Probnog Arheološkog Istraživanja Neolitičkog Nalazišta Pod Jarugom. *Archeol. Adriat.* **19**:.

Houston, A., Clark, C., McNamara, J. and Mangel, M. (1988). Dynamic models in behavioural and evolutionary ecology. *Nature* **332**: 29–34.

Howland, M. R., Corr, L. T., Young, S. M. M., Jones, V., Jim, S., van der Merwe, N. J., Mitchell, A. D. and Evershed, R. P. (2003). Expression of the dietary isotope signal in the compound-specific δ 13 C values of pig bone lipids and amino acids. *Int. J. Osteoarchaeol.* **13**: 54–65.

IAEA/WMO (2015). Global Network of Isotopes in Precipitation (consulted https://nucleus.iaea.org/wiser).

Ilijanić, N., Miko, S., Hasan, O. and Bakrač, K. (2018). Holocene environmental record from lake sediments in the Bokanjačko blato karst polje (Dalmatia, Croatia). *Quat. Int.* **494**: 66–79.

Isaakidou, V., Halstead, P., Stroud, E., Sarpaki, A., Hatzaki, E., Nitsch, E. and Bogaard, A. (2022). Changing Land Use and Political Economy at Neolithic and Bronze Age Knossos, Crete: Stable Carbon (δ 13 C) and Nitrogen (δ 15 N) Isotope Analysis of Charred Crop Grains and Faunal Bone Collagen. *Proc. Prehist. Soc.* **88**: 155–191.

Isaakidou, V., Styring, A., Halstead, P., Nitsch, E., Stroud, E., le Roux, P., Lee-Thorp, J. and Bogaard, A. (2019). From texts to teeth: A multi-isotope study of sheep and goat herding practices in the Late Bronze Age ('Mycenaean') polity of Knossos, Crete. *J. Archaeol. Sci. Reports* **23**: 36–56.

Itan, Y., Powell, A., Beaumont, M. A., Burger, J. and Thomas, M. G. (2009). The Origins of Lactase Persistence in Europe. *PLoS Comput. Biol.* **5**: e1000491.

Ivanova, M., De Cupere, B., Ethier, J. and Marinova, E. (2018). Pioneer farming in southeast Europe during the early sixth millennium BC: Climate-related adaptations in the exploitation of plants and animals. *PLoS One* **13**: e0197225.

Jahns, S. and van den Bogaard, C. (1998). New palynological and tephrostratigraphical investigations of two salt lagoons on the island of Mljet, south Dalmatia, Croatia. *Veg. Hist. Archaeobot.* **7**: 219–234.

Jakucs, J., Bánffy, E., Oross, K., Voicsek, V., Bronk Ramsey, C., Dunbar, E., Kromer, B., Bayliss, A., Hofmann, D., Marshall, P. and Whittle, A. (2016). Between the Vinča and Linearbandkeramik Worlds: The Diversity of Practices and Identities in the 54th–53rd Centuries cal BC in Southwest Hungary and Beyond. *J. World Prehistory* **29**: 267–336.

Janković, I., Marijanović, B., Čavka, M., Carić, M. and Novak, M. (2020). A case of probable interpersonal violence from the Early Neolithic site at Smilčić, Croatia. *Int. J. Osteoarchaeol.* 1–6.

Jim, S., Ambrose, S. H. and Evershed, R. P. (2004). Stable carbon isotopic evidence for differences in the dietary origin of bone cholesterol, collagen and apatite: implications for their use in palaeodietary reconstruction. *Geochim. Cosmochim. Acta* **68**: 61–72.

Johnson, D. L. (1993). Nomadism and desertification in Africa and the Middle East. *GeoJournal* **31**: 51–66.

Johnston, K. J. (2003). The intensification of pre-industrial cereal agriculture in the tropics: Boserup, cultivation lengthening, and the Classic Maya. *J. Anthropol. Archaeol.* **22**: 126–161.

Jones, G. (2005). Garden cultivation of staple crops and its implications for settlement location and continuity. *World Archaeol.* **37**: 164–176.

Jones, G. and Halstead, P. (1995). Maslins, Mixtures and Monocrops: on the Interpretation of Archaeobotanical Crop Samples of Heterogeneous Composition. *J. Archaeol. Sci.* **22**: 103–114.

Jones, G., Wardle, K., Halstead, P. and Wardle, D. (1986). Crop Storage at Assiros. *Sci. Am.* **254**: 96–103.

Jones, J. R. and Mulville, J. A. (2018). Norse Animal Husbandry in Liminal Environments: Stable Isotope Evidence from the Scottish North Atlantic Islands. *Environ. Archaeol.*

23: 338–351.

Julien, M.-A., Bocherens, H., Burke, A., Drucker, D. G., Patou-Mathis, M., Krotova, O. and Péan, S. (2012). Were European steppe bison migratory? 18O, 13C and Sr intra-tooth isotopic variations applied to a palaeoethological reconstruction. *Quat. Int.* **271**: 106–119.

Kačar, S. (2019). Impressed Ware blade production of Northern Dalmatia (Eastern Adriatic, Croatia) in the context of Neolithisation. *Doc. Praehist.* **46**: 352–374.

Kačar, S. (2021). The Neolithisation of the Adriatic: Contrasting Regional Patterns and Interactions Along and Across the Shores. *Open Archaeol.* **7**: 798–814.

Kačar, S. and Philibert, S. (2022). Early Neolithic Large Blades from Crno Vrilo (Dalmatia, Croatia): Preliminary Techno-Functional Analysis. *Open Archaeol.* **8**: 256–272.

Kanstrup, M., Thomsen, I. K., Andersen, A. J., Bogaard, A. and Christensen, B. T. (2011). Abundance of13C and15N in emmer, spelt and naked barley grown on differently manured soils: Towards a method for identifying past manuring practice. *Rapid Commun. Mass Spectrom.* **25**: 2879–2887.

Karg, S. and Müller, J. (1990). Neolithische Getreidefunde aus Pokrovnik, Dalmatien. *Archäologisches Korrespondenzblatt* **20**: 373–386.

Kennett, D. J., Plog, S., George, R. J., Culleton, B. J., Watson, A. S., Skoglund, P., Rohland, N., Mallick, S., Stewardson, K., Kistler, L., LeBlanc, S. A., Whiteley, P. M., Reich, D. and Perry, G. H. (2017). Archaeogenomic evidence reveals prehistoric matrilineal dynasty. *Nat. Commun.* **8**: 14115.

Kennett, D. J. and Winterhalder, B. (2006). *Behavioral ecology and the transition to agriculture*, University of California Press, Berkeley.

Kerslake, J., Everett-Hincks, J. and Campbell, A. (2005). Lamb survival: a new examination of an old problem. *Proceedings of the New Zealand Society of Animal Production*, New Zealand Society of Animal Production, Christchurch.

Kierdorf, H., Kierdorf, U., Frölich, K. and Witzel, C. (2013). Lines of Evidence–Incremental Markings in Molar Enamel of Soay Sheep as Revealed by a Fluorochrome Labeling and Backscattered Electron Imaging Study. *PLoS One* **8**: e74597.

Kierdorf, H., Witzel, C., Upex, B., Dobney, K. and Kierdorf, U. (2012). Enamel hypoplasia in molars of sheep and goats, and its relationship to the pattern of tooth crown growth. *J. Anat.* **220**: 484–495.

van Klinken, G. J. (1999). Bone Collagen Quality Indicators for Palaeodietary and Radiocarbon Measurements. *J. Archaeol. Sci.* **26**: 687–695.

Knockaert, J., Balasse, M., Rendu, C., Burens, A., Campmajo, P., Carozza, L., Bousquet, D., Fiorillo, D. and Vigne, J.-D. (2018). Mountain adaptation of caprine herding in the eastern Pyrenees during the Bronze Age: A stable oxygen and carbon isotope analysis of teeth. *Quat. Int.* **484**: 60–74.

Kohn, M. J. (2004). Comment: Tooth Enamel Mineralization in Ungulates: Implications for Recovering a Primary Isotopic Time-Series, by B. H. Passey and T. E. Cerling (2002).

Geochim. Cosmochim. Acta **68**: 403–405.

Kohn, M. J. (2010). Carbon isotope compositions of terrestrial C3 plants as indicators of (paleo)ecology and (paleo)climate. *Proc. Natl. Acad. Sci.* **107**: 19691–19695.

Kohn, M. J., Miselis, J. L. and Fremd, T. J. (2002). Oxygen isotope evidence for progressive uplift of the Cascade Range, Oregon. *Earth Planet. Sci. Lett.* **204**: 151–165.

Kohn, M. J., Schoeninger, M. J. and Valley, J. W. (1996). Herbivore tooth oxygen isotope compositions: Effects of diet and physiology. *Geochim. Cosmochim. Acta* **60**: 3889–3896.

Kohn, M. J., Schoeninger, M. J. and Valley, J. W. (1998). Variability in oxygen isotope compositions of herbivore teeth: reflections of seasonality or developmental physiology? *Chem. Geol.* **152**: 97–112.

Kohn, M. J. and Welker, J. M. (2005). On the temperature correlation of δ18O in modern precipitation. *Earth Planet. Sci. Lett.* **231**: 87–96.

Komšo, D. (2006). Kargadur- eine Seidlung aus dem frühen- und mittleren Neolithikum Istriens. *Mitteilungen der Berliner Gesellschaft für Anthropol. Ethnol. und Urgeschichte* **27**: 111–118.

Korić, M. and Horvat, K. (2018). Tipološke i stilske karakteristike keramičkih nalaza ranog neolitika iz Konjevrata/the typological and stylistic characteristics of the early Neolithic pottery found in Konjevrate. *Diadora* **32**: 7–34.

Körner, C., Farquhar, G. D. and Roksandic, Z. (1988). A global survey of carbon isotope discrimination in plants from high altitude. *Oecologia* **74**: 623–632.

Körner, C., Farquhar, G. D. and Wong, S. C. (1991). Carbon isotope discrimination by plants follows latitudinal and altitudinal trends. *Oecologia* **88**: 30–40.

Korošec, J. (1952). Nova neolitska kulturna grupa na području Dalmacije. *Vjesn. za Arheol. i Hist. Dalm.* **54**: 91–119.

Korošec, J. (1958). *Neolitska naseobina u Danilu Bitinju: rezultati istraživanja u 1953. godini*, Jugoslavenska akademija znanosti i umjetnosti, Odjel za filozofiju i društvene nauke, Zagreb.

Korošec, J. and Korošec, P. (1974). Bribir i njegova okolica u prapovijesno doba. *Diadora* **7**: 5–33.

Koster, H. A. (1977). The ecology of pastoralism in relation to changing patterns of land use in the Northeast Peloponnese, Ph.D. dissertation, University of Pennsylvania.

Kotsakis, K. (2014). Domesticating the periphery New research into the Neolithic of Greece.

Krauß, R., Marinova, E., De Brue, H. and Weninger, B. (2018). The rapid spread of early farming from the Aegean into the Balkans via the Sub-Mediterranean-Aegean Vegetation Zone. *Quat. Int.* **496**: 24–41.

Krebs, J. R. and Davies, N. B. (1997). *Behavioural ecology : an evolutionary approach*, 4th ed, Blackwell Pub., Malden, MA SE - viii, 456 pages : illustrations ; 25 cm.

Kriszan, M., Schellberg, J., Amelung, W., Gebbing, T., Pötsch, E. M. and Kühbauch, W. (2014). Revealing N management intensity on grassland farms based on natural δ15N abundance. *Agric. Ecosyst. Environ.* **184**: 158–167.

Kuznar, L. A. (1991). Transhumant Goat Pastoralism in the High Sierra of the South Central Andes: Human Responses to Environmental and Social Uncertainty. *Nomad. People.* 93–104.

Kuznar, L. A. (2001). Risk Sensitivity and Value among Andean Pastoralists: Measures, Models, and Empirical Tests. *Curr. Anthropol.* **42**: 432–440.

Lacan, M., Keyser, C., Ricaut, F.-X., Brucato, N., Duranthon, F., Guilaine, J., Crubézy, E. and Ludes, B. (2011). Ancient DNA reveals male diffusion through the Neolithic Mediterranean route. *Proc. Natl. Acad. Sci.* **108**: 9788–9791.

Larson, G., Albarella, U., Dobney, K., Rowley-Conwy, P., Schibler, J., Tresset, A., Vigne, J.-D., Edwards, C. J., Schlumbaum, A., Dinu, A., Balacsescu, A., Dolman, G., Tagliacozzo, A., Manaseryan, N., Miracle, P., Van Wijngaarden-Bakker, L., Masseti, M., Bradley, D. G. and Cooper, A. (2007). Ancient DNA, pig domestication, and the spread of the Neolithic into Europe. *Proc. Natl. Acad. Sci.* **104**: 15276–15281.

Lawrimore, J. H., Ray, R., Applequist, S., Korzeniewski, B. and Menne, M. J. (2016). Global Summary of the Month, Version 1.0., Split Marijan, Zavižan, Zadar, HR 1948-2023 (consulted https://www.ncei.noaa.gov/data/global-summary-of-the-month/).

Lazzerini, N., Coulon, A., Simon, L., Marchina, C., Fiorillo, D., Turbat, T., Bayarkhuu, N., Noûs, C., Lepetz, S. and Zazzo, A. (2021). The isotope record (δ13C, δ18O) of vertical mobility in incremental tissues (tooth enamel, hair) of modern livestock: A reference set from the Mongolian Altai. *Quat. Int.* **595**: 128–144.

Lee-Thorp, J. A. and van der Merwe, N. J. (1991). Aspects of the chemistry of modern and fossil biological apatites. *J. Archaeol. Sci.* **18**: 343–354.

Lefkovitch, L. P. (1965). The study of population growth in organisms grouped by stages. *Biometrics* **21**: 1–18.

LeGeros, R. Z. (1991). Calcium phosphates in oral biology and medicine. *Monogr. Oral Sci.* **15**: 1–201.

Legge, A. J. and Moore, A. M. T. (2011). Clutching at straw: the Early Neolithic of Croatia and the dispersal of agriculture. In A. Hadjikoumis E. Robinson and S. Viner (eds.), *The Dynamics of Neolithisation in Europe : Studies in Honour of Andrew Sherratt*, Oxbow Books, Oxford; Oakville, Conn, pp.176–195.

Lelli, R., Allen, R., Biondi, G., Calattini, M., Barbaro, C. C., Gorgoglione, M. A., Manfredini, A., Martı, C., Radina, F., Silvestrini, M., Tozzi, C., Rickards, O., Craig, O. E., Vergata, R. T. and Sapienza, L. (2012). Examining Dietary Variability of the Earliest Farmers of. **390**: 380–390.

Lepoint, G., Dauby, P. and Gobert, S. (2004). Applications of C and N stable isotopes to ecological and environmental studies in seagrass ecosystems. *Mar. Pollut. Bull.* **49**: 887–891.

Leppard, T. and Birch, S. (2016). The insular ecology and palaeoenvironmental impacts of the domestic goat (Capra hircus) in Mediterranean Neolithization. pp.47–56.

Leslie, P. H. (1945). On the Use of Matrices in Certain Population Mathematics. *Biometrika* **33**: 183.

Lesnoff, M. (1999). Dynamics of a sheep population in a Sahelian area (Ndiagne district in Senegal). *Agric. Syst.* **61**: 207–221.

Lesnoff, M. (2024). mmage: A R package for sex-and-age population matrix models.

Lesnoff, M., Lancelot, R., Moulin, C.-H., Messad, S., Juanès, X. and Sahut, C. (2014). *Calculation of Demographic Parameters in Tropical Livestock Herds*, Springer Netherlands, Dordrecht.

Lesnoff, M., Lancelot, R., Tillard, E. and Dohoo, I. R. (2000). A steady-state approach of benefit–cost analysis with a periodic Leslie-matrix model. *Prev. Vet. Med.* **46**: 113–128.

Lespez, L., Tsirtsoni, Z., Darcque, P., Koukouli-Chryssanthaki, H., Malamidou, D., Treuil, R., Davidson, R., Kourtessi-Philippakis, G. and Oberlin, C. (2013). The lowest levels at Dikili Tash, northern Greece: a missing link in the Early Neolithic of Europe. *Antiquity* **87**: 30–45.

Lightfoot, E., Boneva, B., Miracle, P. T., Šlaus, M. and O'Connell, T. C. (2011). Exploring the Mesolithic and Neolithic transition in Croatia through isotopic investigations. *Antiquity* **85**: 73–86.

Lightfoot, E., Šlaus, M., Šikanjić, P. R. and O'Connell, T. C. (2015). Metals and millets: Bronze and Iron Age diet in inland and coastal Croatia seen through stable isotope analysis. *Archaeol. Anthropol. Sci.* **7**: 375–386.

Lomer, M. C. E., Parkes, G. C. and Sanderson, J. D. (2007). Review article: lactose intolerance in clinical practice - myths and realities. *Aliment. Pharmacol. Ther.* **27**: 93–103.

Longin, R. (1971). New Method of Collagen Extraction for Radiocarbon Dating. *Nature* **230**: 241–242.

Longinelli, A. (1984). Oxygen isotopes in mammal bone phosphate: A new tool for paleohydrological and paleoclimatological research? *Geochim. Cosmochim. Acta* **48**: 385–390.

López-i-Gelats, F., Contreras Paco, J. L., Huilcas Huayra, R., Siguas Robles, O. D., Quispe Peña, E. C. and Bartolomé Filella, J. (2015). Adaptation Strategies of Andean Pastoralist Households to Both Climate and Non-Climate Changes. *Hum. Ecol.* **43**: 267–282.

Luz, B., Barkan, E., Yam, R. and Shemesh, A. (2009). Fractionation of oxygen and hydrogen isotopes in evaporating water. *Geochim. Cosmochim. Acta* **73**: 6697–6703.

Luz, B., Kolodny, Y. and Horowitz, M. (1984). Fractionation of oxygen isotopes between mammalian bone-phosphate and environmental drinking water. *Geochim. Cosmochim. Acta* **48**: 1689–1693.

Macarthur, R. H. and Pianka, E. R. (1966). On Optimal Use of a Patchy Environment. *Am.*

Nat. **100**: 603–609.

Mace, R. (1990). Pastoralist herd compositions in unpredictable environments: A comparison of model predictions and data from camel-keeping groups. *Agric. Syst.* **33**: 1–11.

Mace, R. (1993a). Transitions between Cultivation and Pastoralism in Sub-Saharan Africa. *Curr. Anthropol.* **34**: 363–382.

Mace, R. (1993b). Nomadic Pastoralists Adopt Subsistence Strategies That Maximise Long-Term Household Survival. *Behav. Ecol. Sociobiol.* **33**: 329–334.

Mace, R. and Houston, A. (1989). Pastoralist Strategies for Survival in Unpredictable Environments : A Model of Herd Composition that Maximises Household Viability. *Agric. Syst.* **31**: 185–204.

Madupalli, H., Pavan, B. and Tecklenburg, M. M. J. (2017). Carbonate substitution in the mineral component of bone: Discriminating the structural changes, simultaneously imposed by carbonate in A and B sites of apatite. *J. Solid State Chem.* **255**: 27–35.

Makarewicz, C. A. (2014). Winter pasturing practices and variable fodder provisioning detected in nitrogen (δ15N) and carbon (δ13C) isotopes in sheep dentinal collagen. *J. Archaeol. Sci.* **41**: 502–510.

Makarewicz, C. A. (2017). Sequential δ13C and δ18O analyses of early Holocene bovid tooth enamel: Resolving vertical transhumance in Neolithic domesticated sheep and goats. *Palaeogeogr. Palaeoclimatol. Palaeoecol.* **485**: 16–29.

Makarewicz, C. A., Arbuckle, B. S. and Öztan, A. (2017). Vertical transhumance of sheep and goats identified by intra-tooth sequential carbon (δ13C) and oxygen (δ18O) isotopic analyses: Evidence from Chalcolithic Köşk Höyük, central Turkey. *J. Archaeol. Sci.* **86**: 68–80.

Makarewicz, C. A. and Pederzani, S. (2017). Oxygen (δ18O) and carbon (δ13C) isotopic distinction in sequentially sampled tooth enamel of co-localized wild and domesticated caprines: Complications to establishing seasonality and mobility in herbivores. *Palaeogeogr. Palaeoclimatol. Palaeoecol.* **485**: 1–15.

Makarewicz, C. and Tuross, N. (2006). Foddering by Mongolian pastoralists is recorded in the stable carbon (δ13C) and nitrogen (δ15N) isotopes of caprine dentinal collagen. *J. Archaeol. Sci.* **33**: 862–870.

Makarewicz, C. and Tuross, N. (2012). Finding Fodder and Tracking Transhumance: Isotopic Detection of Goat Domestication Processes in the Near East. *Curr. Anthropol.* **53**: 495–505.

Malher, X., Seegers, H. and Beaudeau, F. (2001). Culling and mortality in large dairy goat herds managed under intensive conditions in western France. *Livest. Prod. Sci.* **71**: 75–86.

Mandal, A., Prasad, H., Kumar, A., Roy, R. and Sharma, N. (2007). Factors associated with lamb mortalities in Muzaffarnagari sheep. *Small Rumin. Res.* **71**: 273–279.

Manen, C., Perrin, T., Guilaine, J., Bouby, L., Bréhard, S., Briois, F., Durand, F., Marinval, P. and Vigne, J.-D. (2019). The Neolithic Transition in the Western Mediterranean: a

Complex and Non-Linear Diffusion Process—The Radiocarbon Record Revisited. *Radiocarbon* **61**: 531–571.

Manning, K., Downey, S. S., Colledge, S., Conolly, J., Stopp, B., Dobney, K. and Shennan, S. (2013). The origins and spread of stock-keeping: the role of cultural and environmental influences on early Neolithic animal exploitation in Europe. *Antiquity* **87**: 1046–1059.

Manolagas, S. C. (2000). Birth and Death of Bone Cells: Basic Regulatory Mechanisms and Implications for the Pathogenesis and Treatment of Osteoporosis*. *Endocr. Rev.* **21**: 115–137.

Marciniak, S. and Perry, G. H. (2017). Harnessing ancient genomes to study the history of human adaptation. *Nat. Rev. Genet.* **18**: 659–674.

Marijanović, B. (1993). Neki aspekti pokapanja u neolitiku Dalmacije. *Rad. Razdio Povij. Znan. Svezak 33, Br. 20*.

Marijanović, B. (2009a). *Crno vrilo. 1*, Sveučilište u Zadru, Zadar.

Marijanović, B. (2009b). *Crno vrilo 2*, Sveučilište u Zadru, Zadar.

Marijanović, B. (2012). Barice – Settlement of the Danilo Culture in Benkovac. *Archaeol. Adriat.* **VI**: 1–30.

Marijanović, B. (2017). Pokrovnik – primjer ograđenoga neolitičkog naselja. *Pril. Instituta za Arheol. u Zagreb.* **34**: 5–44.

Marijanović, B. (2022). *Neolitičko Nalazište Barice u Smilčiću: istraživanje 2016./2017.*, Sveučilište u Zadru, Zadar.

Marijanović, B. and Horvat, K. (2016). Početci naseljavanja na području Zemunika. In J. Faričić and Z. Dundović (eds.), *Zemunik u Prostoru i Vremenu*, Svučilište u Zadru, Zadar, pp.48–67.

Marijanović, B. and Vujević, D. (2013). Lokalitet: Zemunik Donji – Gradina. *Hrvatski Arheološki Godišnjak 11/2014*, pp.534–537.

Mark, B. G., Bury, J., McKenzie, J. M., French, A. and Baraer, M. (2010). Climate Change and Tropical Andean Glacier Recession: Evaluating Hydrologic Changes and Livelihood Vulnerability in the Cordillera Blanca, Peru. *Ann. Assoc. Am. Geogr.* **100**: 794–805.

Marković, M. (1975). Sezonska stočarska naselja na Dinarskim planinama. *Zb. za Nar. život i običaje* **46**: 253–296.

Marković, M. (1980). Narodni život i običaji sezonskih stočara na Velebitu. *Zb. za Nar. život i običaje* **48**: 5–139.

Marković, M. (1987). Stočarstvo na Dinari . *Stočarstvo* **41**: 257–273.

Marnet, P. G. and McKusick, B. C. (2001). Regulation of milk ejection and milkability in small ruminants. *Livest. Prod. Sci.* **70**: 125–133.

Marom, N. and Bar-Oz, G. (2009). Culling profiles: the indeterminacy of archaeozoological

data to survivorship curve modelling of sheep and goat herd maintenance strategies. *J. Archaeol. Sci.* **36**: 1184–1187.

Marston, J. M. (2011). Archaeological markers of agricultural risk management. *J. Anthropol. Archaeol.* **30**: 190–205.

Marston, J. M. (2021). Archaeological Approaches to Agricultural Economies. *J. Archaeol. Res.*

Marston, J. M. and Miller, N. F. (2014). Intensive agriculture and land use at Roman Gordion, central Turkey. *Veg. Hist. Archaeobot.* **23**: 761–773.

Martin, H., Schmid, C., Knitter, D. and Tietze, C. (2021). oxcAAR: Interface to "OxCal" Radiocarbon Calibration.

Martín, P. and Tornero, C. (2023). Sheepfold caves under study: A review of zooarchaeological approaches to old and new-fashioned research questions. *Quat. Int.*

Martin, T. J. and Seeman, E. (2008). Bone remodelling: its local regulation and the emergence of bone fragility. *Best Pract. Res. Clin. Endocrinol. Metab.* **22**: 701–722.

Martinelli, L. A., Piccolo, M. C., Townsend, A. R., Vitousek, P. M., Cuevas, E., McDowell, W., Robertson, G. P., Santos, O. C. and Treseder, K. (1999). Nitrogen stable isotopic composition of leaves and soil: Tropical versus temperate forests. *Biogeochemistry* **46**: 45–65.

Martins-Noguerol, R., Moreno-Pérez, A. J., Pedroche, J., Gallego-Tévar, B., Cambrollé, J., Matías, L., Fernández-Rebollo, P., Martínez-Force, E. and Pérez-Ramos, I. M. (2023). Climate change alters pasture productivity and quality: Impact on fatty acids and amino acids in Mediterranean silvopastoral ecosystems. *Agric. Ecosyst. Environ.* **358**: 108703.

Mashkour, M. (2003). Tracing Ancient "Nomads": Isotopic Research on the Origins of Vertical "Transhumance" in the Zagros Region. *Nomad. People.* **7**: 36–47.

Maynard Smith, J. (1978). Optimization Theory in Evolution. *Annu. Rev. Ecol. Syst.* **9**: 31–56.

Mazzucco, N., Guilbeau, D., Kačar, S., Podrug, E., Forenbaher, S., Radić, D. and Moore, A. M. T. (2018). The time is ripe for a change. The evolution of harvesting technologies in Central Dalmatia during the Neolithic period (6th millennium cal BC). *J. Anthropol. Archaeol.* **51**: 88–103.

McAlvay, A. C., DiPaola, A., D'Andrea, A. C., Ruelle, M. L., Mosulishvili, M., Halstead, P. and Power, A. G. (2022). Cereal species mixtures: an ancient practice with potential for climate resilience. A review. *Agron. Sustain. Dev.* **42**: 100.

McCabe, J. T. (1987). Drought and Recovery: Livestock Dynamics among the Ngisonyoka Turkana of Kenya. *Hum. Ecol.* **15**: 371–389.

McCloskey, D. N. (1976). English Open Fields as Behavior towards Risk. *Res. Econ. Hist.* **1**: 124–170.

McCloskey, D. N. (1991). The Prudent Peasant: New Findings on Open Fields. *J. Econ. Hist.* **51**: 343–355.

McClure, S. B. (2013). Domesticated animals and biodiversity: Early agriculture at the gates of Europe and long-term ecological consequences. *Anthropocene* **4**: 57–68.

McClure, S. B. (2015). The Pastoral Effect. *Curr. Anthropol.* **56**: 901–910.

McClure, S. B., Magill, C., Podrug, E., Moore, A. M. T., Harper, T. K., Culleton, B. J., Kennett, D. J. and Freeman, K. H. (2018). Fatty acid specific δ 13 C values reveal earliest Mediterranean cheese production 7,200 years ago. 1–15.

McClure, S. B. and Podrug, E. (2016). Villages, Landscapes, and Early Farming in Northern Dalmatia. In K. T. Lillios and M. Chazan (eds.), *Fresh Fields and Pastures New'*, Sidestone Press, Leiden, pp.117–144.

McClure, S. B., Podrug, E., Jović, J., Monroe, S., Radde, H. D., Triozzi, N., Welker, M. H. and Zavodny, E. (2022). The Zooarchaeology of Neolithic farmers: Herding and hunting on the Dalmatian coast of Croatia. *Quat. Int.* **634**: 27–37.

McClure, S. B., Podrug, E., Moore, A. M. T., Culleton, B. J. and Kennett, D. J. (2014). AMS 14C Chronology and Ceramic Sequences of Early Farmers in the Eastern Adriatic. *Radiocarbon* **56**: 1019–1038.

McClure, S. B., Puchol, O. G. and Culleton, B. J. (2010). Ams Dating of Human Bone from Cova De La Pastora: New Evidence of Ritual Continuity in the Prehistory of Eastern Spain. *Radiocarbon* **52**: 25–32.

McGrory, S., Svensson, E. M., Götherström, A., Mulville, J., Powell, A. J., Collins, M. J. and O'Connor, T. P. (2012). A novel method for integrated age and sex determination from archaeological cattle mandibles. *J. Archaeol. Sci.* **39**: 3324–3330.

Mellado, M., Valdéz, R., García, J. E., López, R. and Rodríguez, A. (2006). Factors affecting the reproductive performance of goats under intensive conditions in a hot arid environment. *Small Rumin. Res.* **63**: 110–118.

Menđušić, M. (1988). Konjevrate - ranoneolitičko naselje / Konjevrate - Early Neolithic settlement. *Arheol. Pregl. 29* **46**: 22–25.

Menđušić, M. (1993). Danilo Gornje – zaštitno istraživanje. *Obavijesti - Hrvat. Arheol. društvo* **2**: 22–25.

Menđušić, M. (1998). Neolitička naselja na šibensko-drniškom području. *Izd. Hrvat. Arheol. društva* **19**: 47–62.

Menđušić, M. (1999). Konjevrate - istraživanje neolitičkoga naselja. *Obavijesti Hrvat. Arheol. društva* **3**: 52–54.

Menđušić, M. (2005). Pretpovijesna arheološka topografija prostora župa Konjevrate i Mirlović Zagora. *Konjevrate i Mirlović Zagora - Župe Šibenske Biskupije. Zbornik Radova Znanstvenog Skupa Sela Šibenskog Zaleđa Župa Konjevrate i Mirlović Zagora, u Prošlosti, Šibenik, Šibenik, 14.-16. Studenoga 2002*, Zagreb, pp.85–101.

van der Merwe, N. J. (1982). Carbon isotopes, photosynthesis, and archaeology: Different pathways of photosynthesis cause characteristic changes in carbon isotope ratios that make possible the study of prehistoric human diets. *Am. Sci.* **70**: 596–606.

van der Merwe, N. J. and Medina, E. (1991). The canopy effect, carbon isotope ratios and foodwebs in amazonia. *J. Archaeol. Sci.* **18**: 249–259.

van der Merwe, N. J. and Vogel, J. C. (1978). 13C content of human collagen as a measure of prehistoric diet in woodland North America. *Nature* **276**: 815–816.

Milhaud, G. and Nezit, J. (1991). Molar development in sheep: morphology, radiography, microhardness. *Rec. Med. Vet. Ec. Alfort.* **167**: 121–127.

Miracle, P. (2006). Neolithic shepherds and their herds in the Northern Adriatic Basin. *Anim. Neolit. Britain Eur.* 63–94.

Miracle, P. T. and Forenbaher, S. (2005). Neolithic and Bronze-Age Herders of Pupićina Cave, Croatia. *J. F. Archaeol.* **30**: 255–281.

Mlekuž, D. (2007). "Sheep are your mother" rhyta and the interspecies politics in the Neolithic of the eastern Adriatic. *Doc. Praehist.* **34**: 267–280.

Moore, A. M. T., Mendušić, M., Smith, J., Zaninović, J. and Podrug, E. (2007a). Project "Early Farming in Dalmatia: Pokrovnik 2006." *Vjesn. Arheol. muzeja u Zagreb.* **40**: 25–34.

Moore, A. and Menđušić, M. (2004). Development of Farming in the Adriatic basin: New Research at Danilo in Dalmatia. *Obavijesti - Hrvat. Arheol. društvo* **1**: 33–34.

Moore, A. and Menđušić, M. (2019). Early Farming in Dalmatia : Pokrovnik and Danilo Bitinj: Two Neolithic Villages in South-East Europe.

Moore, A., Menđušić, M., Brown, L., Colledge, S., Giegengack, R., Higham, T., Hršak, V., Legge, A., Marguš, D., McClure, S., Palmer, C., Podrug, E., Reed, K., Smith, J. and Zaninović, J. (2019). *Early Farming in Dalmatia*, Archaeopress.

Moore, A., Smith, J., Mendušić, M. and Podrug, E. (2007b). Project "Early Farming in Dalmatia": Danilo Bitinj 2004-2005. *Vjesn. Arheol. muzeja u Zagreb.* **40**: 15–24.

Moran, N. C. and O'Connor, T. P. (1994). Age attribution in domestic sheep by skeletal and dental maturation: A pilot study of available sources. *Int. J. Osteoarchaeol.* **4**: 267–285.

Moritz, M., Buffington, A., Yoak, A. J., Hamilton, I. M. and Garabed, R. (2017). No Magic Number: an Examination of the Herd-Size Threshold in Pastoral Systems Using Agent-Based Modeling. *Hum. Ecol.* **45**: 525–532.

Morrison, K. D. (1994). The intensification of production: Archaeological approaches. *J. Archaeol. Method Theory* **1**: 111–159.

Morrison, K. D. (1996). Typological schemes and agricultural change: Beyond Boserup in precolonial South India. *Curr. Anthropol.* **37**: 583–608.

Moudopoulos-Athanasiou, F., Bokas, T., Mikulić, A., Dimitrova, P., Karaivanov, K., Tubanović, A., Sayılgan, İ., Papadopoulou, K. and Banu, A. (2022). 'Around the hut': an archaeological ethnography around the experimental construction of a shepherd's hut in Konitsa, north-west Greece. *Post-Medieval Archaeol.* **56**: 97–115.

Mourad, M. (1993). Reproductive performance of Alpine and Zaraibi goats and growth of their first cross in Egypt. *Small Rumin. Res.* **12**: 379–384.

Mukasa-Mugerwa, E., Lahlou-Kassi, A., Anindo, D., Rege, J. E. ., Tembely, S., Tibbo, M. and Baker, R. . (2000). Between and within breed variation in lamb survival and the risk factors associated with major causes of mortality in indigenous Horro and Menz sheep in Ethiopia. *Small Rumin. Res.* **37**: 1–12.

Munro, N. D. and Stiner, M. C. (2015). Zooarchaeological Evidence for Early Neolithic Colonization at Franchthi Cave (Peloponnese, Greece). *Curr. Anthropol.* **56**: 596–603.

Munson, P. J. and Garniewicz, R. C. (2003). Age-mediated Survivorship of Ungulate Mandibles and Teeth in Canid-ravaged Faunal Assemblages. *J. Archaeol. Sci.* **30**: 405–416.

Nandris, J. G. (1999). Ethnoarchaeology and latinity in the mountains of the southern Velebit. In L. Bartosiewicz and H. J. Greenfield (eds.), *Transhumant Pastoralism in Southern Europe: Recent Perspectives from Archaeology, History and Ethnology*, Archaeolingua, Budapest, pp.111–131.

Negassa, A., Gebremedhin, B., Desta, S., Nigussie, K., Gebru, G., Shapiro, B., Dutilly-Diane, C. and Tegegne, A. (2015). Integrated bio-economic simulation model for goat production: Ex-ante evaluation of investment opportunities in Ethiopia. *Nairobi, Kenya Int. Livest. Res. Inst.* **LIVES Work**:

Nikitin, A. G., Stadler, P., Kotova, N., Teschler-Nicola, M., Price, T. D., Hoover, J., Kennett, D. J., Lazaridis, I., Rohland, N., Lipson, M. and Reich, D. (2019). Interactions between earliest Linearbandkeramik farmers and central European hunter gatherers at the dawn of European Neolithization. *Sci. Rep.* **9**: 19544.

Nimac, F. (1940). Čobanovanje. Život i tradicije pastira Dalmatinske zagore na bosanskim planinama. *Etnografska Istra Živanja i Građa*, Zagreb, pp.102–130.

Nitsiakos, V. (1985). A Vlach pastoral community in Greece, University of Cambridge.

Novak, G. (1955). *Prethistorijski Hvar, Grapčeva spilja*, Jugoslavenska Akademija Znanosti i Umjetnosti, Zagreb.

O'Brien, M. J. and Bentley, R. A. (2015). The role of food storage in human niche construction: An example from Neolithic Europe. *Environ. Archaeol.* **20**: 364–378.

O'Connell, J. F. and Hawkes, K. (1984). Food Choice and Foraging Sites among the Alyawara. *J. Anthropol. Res.* **40**: 504–535.

O'Leary, M. H. (1988). Carbon Isotopes in Photosynthesis. *Bioscience* **38**: 328–336.

Olalde, I., Schroeder, H., Sandoval-Velasco, M., Vinner, L., Lobón, I., Ramirez, O., Civit, S., García Borja, P., Salazar-García, D. C., Talamo, S., María Fullola, J., Xavier Oms, F., Pedro, M., Martínez, P., Sanz, M., Daura, J., Zilhão, J., Marquès-Bonet, T., Gilbert, M. T. P. and Lalueza-Fox, C. (2015). A Common Genetic Origin for Early Farmers from Mediterranean Cardial and Central European LBK Cultures. *Mol. Biol. Evol.* **32**: 3132–42.

Orlove, B. and Godoy, R. (1986). Sectoral Fallowing Systems in the Central Andes. *J. Ethnobiol.* **6**: 169–204.

Orton, D., Gaastra, J. and Linden, M. Vander (2016). Between the danube and the deep blue

sea: Zooarchaeological meta-analysis reveals variability in the spread and development of neolithic farming across the western balkans. *Open Quat.* **2**: 1–26.

Özdoğan, M. (2011). Archaeological Evidence on the Westward Expansion of Farming Communities from Eastern Anatolia to the Aegean and the Balkans. *Curr. Anthropol.* **52**: S415–S430.

Paranhos da Costa, M. J. R., da Silva, R. G. and de Souza, R. C. (1992). Effect of air temperature and humidity on ingestive behaviour of sheep. *Int. J. Biometeorol.* **36**: 218–222.

Passey, B. H. and Cerling, T. E. (2002). Tooth enamel mineralization in ungulates: implications for recovering a primary isotopic time-series. *Geochim. Cosmochim. Acta* **66**: 3225–3234.

Passey, B. H., Robinson, T. F., Ayliffe, L. K., Cerling, T. E., Sponheimer, M., Dearing, M. D., Roeder, B. L. and Ehleringer, J. R. (2005). Carbon isotope fractionation between diet, breath CO2, and bioapatite in different mammals. *J. Archaeol. Sci.* **32**: 1459–1470.

Payne, S. (1973). Kill-off Patterns in Sheep and Goats: The Mandibles from Aşvan Kale. *Anatol. Stud.* **23**: 281–303.

Pearson, J. A., Buitenhuis, H., Hedges, R. E. M., Martin, L., Russell, N. and Twiss, K. C. (2007). New light on early caprine herding strategies from isotope analysis: a case study from Neolithic Anatolia. *J. Archaeol. Sci.* **34**: 2170–2179.

Pearson, J. and Grove, M. (2013). Counting sheep: sample size and statistical inference in stable isotope analysis and palaeodietary reconstruction. *World Archaeol.* **45**: 373–387.

Pederzani, S., Aldeias, V., Dibble, H. L., Goldberg, P., Hublin, J.-J., Madelaine, S., McPherron, S. P., Sandgathe, D., Steele, T. E., Turq, A. and Britton, K. (2021). Reconstructing Late Pleistocene paleoclimate at the scale of human behavior: an example from the Neandertal occupation of La Ferrassie (France). *Sci. Rep.* **11**: 1419.

Pederzani, S. and Britton, K. (2019). Oxygen isotopes in bioarchaeology: Principles and applications, challenges and opportunities. *Earth-Science Rev.* **188**: 77–107.

Peeler, E. . and Wanyangu, S. . (1998). Infectious causes of small ruminant mortality in Kenya: A review. *Small Rumin. Res.* **29**: 1–11.

Pellegrini, M., Donahue, R. E., Chenery, C., Evans, J., Lee-Thorp, J., Montgomery, J. and Mussi, M. (2008). Faunal migration in late-glacial central Italy: implications for human resource exploitation. *Rapid Commun. Mass Spectrom.* **22**: 1714–1726.

Pellegrini, M. and Snoeck, C. (2016). Comparing bioapatite carbonate pre-treatments for isotopic measurements: Part 2 — Impact on carbon and oxygen isotope compositions. *Chem. Geol.* **420**: 88–96.

Perišić, I. (1940). *Prilozi o čobanovanju na šator-planini*, na, Zagreb.

Perles, C. (2003). An alternate (and old-fashioned) view of Neolithisation in Greece. *Doc. Praehist.* **30**: 99–113.

Perlès, C., Quiles, A. and Valladas, H. (2013). Early seventh-millennium AMS dates from

domestic seeds in the Initial Neolithic at Franchthi Cave (Argolid, Greece). *Antiquity* **87**: 1001–1015.

Peyron, O., Goring, S., Dormoy, I., Kotthoff, U., Pross, J., de Beaulieu, J.-L., Drescher-Schneider, R., Vannière, B. and Magny, M. (2011). Holocene seasonality changes in the central Mediterranean region reconstructed from the pollen sequences of Lake Accesa (Italy) and Tenaghi Philippon (Greece). *The Holocene* **21**: 131–146.

Pfeiffer, S., Crowder, C., Harrington, L. and Brown, M. (2006). Secondary osteon and Haversian canal dimensions as behavioral indicators. *Am. J. Phys. Anthropol.* **131**: 460–468.

Pilaar Birch, S. E. (2017). Neolithic subsistence at Vela Špilja on the island of Lošinj, Croatia. In P. Rowley-Conwy D. Serjeanston and P. Halstead (eds.), *Economic Zooarchaeology: Studies in Hunting, Herding and Early Agriculture*, Oxbow Books, Philadelphia.

Pilaar Birch, S. E. (2018). From the Aegean to the Adriatic: Exploring the Earliest Neolithic Island Fauna. *J. Isl. Coast. Archaeol.* **13**: 256–268.

Pilaar Birch, S. E., Atici, L. and Erdoğu, B. (2019). Spread of domestic animals across Neolithic western Anatolia: New stable isotope evidence from Uğurlu Höyük, the island of Gökçeada, Turkey. *PLoS One* **14**: e0222319.

Pilaar Birch, S. E., Miracle, P. T., Stevens, R. E. and O'Connell, T. C. (2016). Late Pleistocene/early Holocene migratory behavior of ungulates using isotopic analysis of tooth enamel and its effects on forager mobility. *PLoS One* **11**: 1–19.

Pluciennik, M. (1998). Radiocarbon Determinations and the Mesolithic-Neolithic Transition in Southern Italy. *J. Mediterr. Archaeol.* **10**: 115–150.

Poage, M. A. and Chamberlain, C. P. (2001). Empirical relationships between elevation and the stable isotope composition of precipitation and surface waters: Considerations for studies of paleoelevation change. *Am. J. Sci.* **301**: 1–15.

Podlesak, D. W., Torregrossa, A.-M., Ehleringer, J. R., Dearing, M. D., Passey, B. H. and Cerling, T. E. (2008). Turnover of oxygen and hydrogen isotopes in the body water, CO2, hair, and enamel of a small mammal. *Geochim. Cosmochim. Acta* **72**: 19–35.

Podrug, E. (2010). Čista Mala – Velištak : the first three excavation campaigns at a Hvar Culture site. *Diadora* **24**: 7–26.

Podrug, E. (2013). Neolitički nepokretni nalazi na šibenskom području. *Diadora* **26/27**: 185–212.

Podrug, E., B. Mcclure, S., Perhoč, Z., Kačar, S., Reed, K. and Zavodny, E. (2018). Rašinovac near Ždrapanj (northern Dalmatia) – An early neolithic site. *Archaeol. Adriat.* **12**: 47–97.

Podrug, E., McClure, S. B. and Solter, S. B. (2013). Lokalitet: Rašinovac. *Hrvat. Arheol. godišnjak* **10**: 532–533.

Price, M., Wolfhagen, J. and Otárola-Castillo, E. (2016). Confidence Intervals in the Analysis of Mortality and Survivorship Curves in Zooarchaeology. *Am. Antiq.* **81**: 157–

173.

Pucéat, E., Reynard, B. and Lécuyer, C. (2004). Can crystallinity be used to determine the degree of chemical alteration of biogenic apatites? *Chem. Geol.* **205**: 83–97.

Pyankov, V. I., Ziegler, H., Akhani, H., Deigele, C. and Lüttge, U. (2010). European plants with C4 photosynthesis: geographical and taxonomic distribution and relations to climate parameters. *Bot. J. Linn. Soc.* **163**: 283–304.

R Core Team (2023). R: A Language and Environment for Statistical Computing.

Raczky, P. (2015). Settlements in South-East Europe. In C. Fowler J. Harding and D. Hofmann (eds.), *The Oxford Handbook of Neolithic Europe*, Oxford University Press, pp.236–257.

Radović, S. (2009). Analiza ostataka faune sisavaca. In B. Marijanović (ed.), *Crno Vrilo. Vol 2*, Sveučilište u Zadru, Zadar, pp.53–66.

Radović, S. (2011). Ekonomija prvih stočara na istočnom Jadranu: značenje lova i stočarstva u prehrani neolitičkih ljudi.

Ragkos, A. (2022). Transhumance in Greece: Multifunctionality as an Asset for Sustainable Development. In L. Bindi (ed.), *Grazing Communities: Pastoralism on the Move and Biocultural Heritage Frictions*, Berghahn Books, New York, Oxford, pp.23–43.

Ramsey, C. B. (2008). Radiocarbon Dating: Revolutions in Understanding. *Archaeometry* **50**: 249–275.

Rasmussen, P. (1989). Leaf-foddering of Livestock in the Neolithic: Archaeobotanical Evidence from Weier, Switzerland. *J. Danish Archaeol.* **8**: 51–71.

Redden, R. and Thorne, J. W. (2020). Reproductive management of sheep and goats. *Animal Agriculture*, Elsevier, pp.211–230.

Redding, R. (1984). Theoretical determinants of a herder's decisions: Modeling variation in the sheep/goat ratio. In J. Clutton-Brock and C. Grigson (eds.), *Animals and Archaeology 3, Early Herders and Their Flocks*, British Archaeological Reports 202, pp.223–242.

Redding, R. W. (1981). Decision making in subsistence herding of sheep and goats in the Middle East, University of Michigan.

Reed, K. (2015). From the field to the hearth: plant remains from Neolithic Croatia (ca. 6000–4000 cal bc). *Veg. Hist. Archaeobot.* **24**: 601–619.

Reed, K. (2016). Archaeobotany in Croatia : An overview. *Vjesn. Arheol. muzeja u Zagreb.* **49**: 7–28.

Reed, K. (2017). Agricultural change in Copper Age Croatia (ca. 4500–2500 cal B.C)? *Archaeol. Anthropol. Sci.* **9**: 1745–1765.

Reed, K. and Colledge, S. (2016). Plant economies in the Neolithic eastern Adriatic: Archaeobotanical results from Danilo and Pokrovnik. **109**: 9–23.

Reed, K. and Podrug, E. (2016). Reconstructing late neolithic plant economies at the eastern

adriatic site of Velištak (5th millennium cal BC). *Doc. Praehist.* **43**: 399–412.

Reimer, P. J., Austin, W. E. N., Bard, E., Bayliss, A., Blackwell, P. G., Bronk Ramsey, C., Butzin, M., Cheng, H., Edwards, R. L., Friedrich, M., Grootes, P. M., Guilderson, T. P., Hajdas, I., Heaton, T. J., Hogg, A. G., Hughen, K. A., Kromer, B., Manning, S. W., Muscheler, R., Palmer, J. G., Pearson, C., van der Plicht, J., Reimer, R. W., Richards, D. A., Scott, E. M., Southon, J. R., Turney, C. S. M., Wacker, L., Adolphi, F., Büntgen, U., Capano, M., Fahrni, S. M., Fogtmann-Schulz, A., Friedrich, R., Köhler, P., Kudsk, S., Miyake, F., Olsen, J., Reinig, F., Sakamoto, M., Sookdeo, A. and Talamo, S. (2020). The IntCal20 Northern Hemisphere Radiocarbon Age Calibration Curve (0–55 cal kBP). *Radiocarbon* **62**: 725–757.

Reingruber, A. (2011). Early Neolithic settlement patterns and exchange networks in the Aegean. *Doc. Praehist.* **38**: 291–306.

Reitz, E. J. and Wing, E. S. (2008). *Zooarchaeology*, Cambridge University Press, Cambridge.

Rey, C., Renugopalakrishnany, V., Shimizu, M., Collins, B. and Glimcher, M. J. (1990). Resolution enhanced Fourier transform infrared study of the environment of the CO2−3 ion in enamel mineral during its formation and aging. *Calcif. Tissue Int*.

Richerson, P. J. and Boyd, R. (1992). Cultural Inheritance and Evolutionary Ecology. In E. A. Smith and B. Winterhalder (eds.), *Evolutionary Ecology and Human Behavior*, Routledge, New York, pp.61–92.

Rocha, R. A., Bresciani, K. D. S., Barros, T. F. M., Fernandes, L. H., Silva, M. B. and Amarante, A. F. T. (2008). Sheep and cattle grazing alternately: Nematode parasitism and pasture decontamination. *Small Rumin. Res.* **75**: 135–143.

Roche, D., Ségalen, L., Balan, E. and Delattre, S. (2010). Preservation assessment of Miocene–Pliocene tooth enamel from Tugen Hills (Kenyan Rift Valley) through FTIR, chemical and stable-isotope analyses. *J. Archaeol. Sci.* **37**: 1690–1699.

Rogosic, J., Pfister, J. A., Provenza, F. D. and Grbesa, D. (2006). Sheep and goat preference for and nutritional value of Mediterranean maquis shrubs. *Small Rumin. Res.* **64**: 169–179.

Roller-Lutz, Z., Mance, D., Hunjak, T. and Lutz, H. O. (2013). On the Isotopic Altitude Effect of Precipitation in the Northern Adriatic (Croatia). *Isot. Hydrol. Mar. Ecosyst. Clim. Change Stud. Vol Proc. Int. Symp.*

Rosa, H. J. . and Bryant, M. . (2003). Seasonality of reproduction in sheep. *Small Rumin. Res.* **48**: 155–171.

Rosa, H. J. D. and Bryant, M. J. (2002). The 'ram effect' as a way of modifying the reproductive activity in the ewe. *Small Rumin. Res.* **45**: 1–16.

Roumasset, J. A. (1979). Introduction and state of the arts. In J. A. Roumasset J.-M. Boussard and I. Singh (eds.), *Risk, Uncertainty, and Agricultural Development*, Southeast Asian Regional Center for Graduate Study and Research in Agriculture; Agricultural Development Council, College, Laguna, Philippines, New York, N.Y., pp.1–21.

Rowley-Conwy, P. (2011). Westward Ho! The Spread of Agriculturalism from Central Europe to the Atlantic. *Curr. Anthropol.* **52**: S431–S451.

Rozanski, K., Araguás-Araguás, L. and Gonfiantini, R. (1992). Relation Between Long-Term Trends of Oxygen-18 Isotope Composition of Precipitation and Climate. *Science (80-.).* **258**: 981–985.

Rozanski, K., Araguás-Araguás, L. and Gonfiantini, R. (1993). Isotopic Patterns in Modern Global Precipitation. *Geophys. Monogr. Ser. Clim. Chang. Cont. Isot. Rec.* **78**: 1–36.

Rozanski, K., Araguás-Araguás, L. and Gonfiantini, R. (2013). Isotopic Patterns in Modern Global Precipitation. pp.1–36.

Russell, K. W. (1988). *After Eden : the behavioral ecology of early food production in the Near East and North Africa*, Oxford, England : B.A.R., Oxford, England.

Ruxton, G. D. (2006). The unequal variance t-test is an underused alternative to Student's t-test and the Mann–Whitney U test. *Behav. Ecol.* **17**: 688–690.

Sadori, L., Jahns, S. and Peyron, O. (2011). Mid-Holocene vegetation history of the central Mediterranean. *The Holocene* **21**: 117–129.

Salque, M., Bogucki, P. I., Pyzel, J., Sobkowiak-Tabaka, I., Grygiel, R., Szmyt, M. and Evershed, R. P. (2013). Earliest evidence for cheese making in the sixth millennium bc in northern Europe. *Nature* **493**: 522–525.

Santos, G. M., Southon, J. R., Druffel-Rodriguez, K. C., Griffin, S. and Mazon, M. (2004). Magnesium Perchlorate as an Alternative Water Trap in AMS Graphite Sample Preparation: A Report On Sample Preparation at Kccams at the University of California, Irvine. *Radiocarbon* **46**: 165–173.

Scarry, C. M. and Scarry, J. F. (2005). Native American "Garden Agriculture" in Southeastern North America. *World Archaeol.* **37**: 259–274.

Schoeninger, M. J. and DeNiro, M. J. (1984). Nitrogen and carbon isotopic composition of bone collagen from marine and terrestrial animals. *Geochim. Cosmochim. Acta* **48**: 625–639.

Schutkowski, H. (2006). *Human Ecology: Biocultural Adaptations in Human Communities*, Springer Berlin Heidelberg.

Schwartz, C. (1988). The Neolithic animal husbandry of Smilčić and Nin. *Recent Developments in Yugoslav Archaeology*, BAR International Series 431, Oxford, pp.45–76.

Schwartz, C. (1996). The faunal remains. In J. Chapman R. Shiel and Š. Batović (eds.), *The Changing Face of Dalmatia*, Leicester University Press in assoc. with the Society of Antiquaries of London, London, pp.186–187.

Schwertl, M., Auerswald, K., Schäufele, R. and Schnyder, H. (2005). Carbon and nitrogen stable isotope composition of cattle hair: ecological fingerprints of production systems? *Agric. Ecosyst. Environ.* **109**: 153–165.

Şevketoğlu, M. (2008). Early settlements and precurement of raw materials - New evidence

based on research at Akanthou-Arkosykos (Tatlisu-Çiftlikdüzö), Northern Cyprus. *TUBA-AR* **11**: 63–72.

Sharp, Z. (2007). *Principles of Stable Isotope Geochemistry*, , 2nd ed.

Shemesh, A. (1990). Crystallinity and diagenesis of sedimentary apatites. *Geochim. Cosmochim. Acta* **54**: 2433–2438.

Sherratt, A. (1983). The secondary exploitation of animals in the Old World. *World Archaeol.* **15**: 90–104.

Sierra, A., Balasse, M., Radović, S., Orton, D., Fiorillo, D. and Presslee, S. (2023). Early Dalmatian farmers specialized in sheep husbandry. *Sci. Rep.* **13**: 10355.

Silanikove, N. (1987). Impact of shelter in hot Mediterranean climate on feed intake, feed utilization and body fluid distribution in sheep. *Appetite* **9**: 207–215.

Silva, E., Galina, M. A., Palma, J. M. and Valencia, J. (1998). Reproductive performance of Alpine dairy goats in a semi-arid environment of Mexico under a continuous breeding system. *Small Rumin. Res.* **27**: 79–84.

Simms, S. R. and Russell, K. W. (1997). Bedouin Hand Harvesting of ism associated with Petra. They perceived change as harmful to their limited ties to the tourist economy, Wheat and Barley: Implications and to maintain this aspect of their livelihood they held to traditional lands and practice. *Curr. Anthropol.* **38**: 696–702.

Singh, M. K., Rai, B. and Sharma, N. (2011). Factors affecting survivability of Jamunapari kids under semi-intensive management system. *Indian J. Anim. Sci.* **78**:.

Skeates, R. (1994). Towards an absolute chronology for the Neolithic in Central Italy. In R. Skeates and R. Whitehouse (eds.), *Radiocarbon Dating and Italian Prehistory*, Accordia Special Studies on Italy, 3, London, pp.61–72.

Sloat, L. L., Gerber, J. S., Samberg, L. H., Smith, W. K., Herrero, M., Ferreira, L. G., Godde, C. M. and West, P. C. (2018). Increasing importance of precipitation variability on global livestock grazing lands. *Nat. Clim. Chang.* **8**: 214–218.

Slotte, H. (2001). Harvesting of leaf-hay shaped the Swedish landscape. *Landsc. Ecol.* **16**: 691–702.

Smedley, M. P., Dawson, T. E., Comstock, J. P., Donovan, L. A., Sherrill, D. E., Cook, C. S. and Ehleringer, J. R. (1991). Seasonal carbon isotope discrimination in a grassland community. *Oecologia* **85**: 314–320.

Smith, E. A. and Winterhalder, B. (1992). *Evolutionary Ecology and Human Behavior*, Aldine Pub. Co., New York.

Snoeck, C., Lee-Thorp, J. A. and Schulting, R. J. (2014). From bone to ash: Compositional and structural changes in burned modern and archaeological bone. *Palaeogeogr. Palaeoclimatol. Palaeoecol.* **416**: 55–68.

Šošić-Klindžić, R., Radović, Š., Tezak-Gregl, T., Šlaus, M., Perhoč, Z., Altherr, R., Hulina, M., Gerometta, K., Boschian, G., Vukosavljević, N., Ahern, J. C. M., Janković, I., Richards, M. P. and Karavanić, I. (2015). Late Upper Paleolithic, early Mesolithic and

early Neolithic from the cave site Zemunica near Bisko (Dalmatia, Croatia).

Šoštarić, R. (2009). Karbonizirani ostatci žitarica -tragovi poljodjelstva. In B. Marijanović (ed.), *Crno Vrilo. Vol 2*, Sveučilište u Zadru, Zadar, pp.49–52.

Spataro, M. (2002). *The first farming communities of the Adriatic: pottery production and circulation in the Early and Middle Neolithic*, Italo Svevo.

Spataro, M. (2009). Cultural Diversities: The Early Neolithic in the Adriatic Region and Central Balkans. A pottery perspective. In G. Gheorghiu (ed.), *Early Farmers, Late Foragers, and Ceramic Traditions: On the Beginning of Pottery in the Near East and Europe*, Cambridge Scholars Publishing, Newcastle, pp.87–115.

Sponheimer, M. (1999). Isotopic paleoecology of the Makapansgat Limeworks fauna, Rutgers The State University of New Jersey.

Sponheimer, M. and Lee-Thorp, J. A. (1999). Alteration of Enamel Carbonate Environments during Fossilization. *J. Archaeol. Sci.* **26**: 143–150.

Stephens, D. W. (1987). On economically tracking a variable environment. *Theor. Popul. Biol.* **32**: 15–25.

Stephens, D. W. (1989). Variance and the Value of Information. *Am. Nat.* **134**: 128–140.

Stephens, D. W. and Charnov, E. L. (1982). Optimal foraging: some simple stochastic models. *Behav. Ecol. Sociobiol.* **10**: 251–263.

Stevens, R. E., Lister, A. M. and Hedges, R. E. M. (2006). Predicting diet, trophic level and palaeoecology from bone stable isotope analysis: a comparative study of five red deer populations. *Oecologia* **149**: 12–21.

Stewart, G., Turnbull, M., Schmidt, S. and Erskine, P. (1995). 13C Natural Abundance in Plant Communities Along a Rainfall Gradient: a Biological Integrator of Water Availability. *Funct. Plant Biol.* **22**: 51.

Stone, G. D. and Downum, C. E. (1999). Non-Boserupian Ecology and Agricultural Risk: Ethnic Politics and Land Control in the Arid Southwest. *Am. Anthropol.* **101**: 113–128.

Stuiver, M. and Polach, H. A. (1977). Discussion Reporting of 14 C Data. *Radiocarbon* **19**: 355–363.

Styring, A., Maier, U., Stephan, E., Schlichtherle, H. and Bogaard, A. (2016). Cultivation of choice: new insights into farming practices at Neolithic lakeshore sites. *Antiquity* **90**: 95–110.

Suga, S. (1982). Progressive mineralization pattern of developing enamel during the maturation stage. *J. Dent. Res.* **61**: 1532–1542.

Sykut, M., Pawełczyk, S., Borowik, T., Pokorny, B., Flajšman, K., Hunink, T. and Niedziałkowska, M. (2021). Environmental factors shaping stable isotope signatures of modern red deer (Cervus elaphus) inhabiting various habitats. *PLoS One* **16**: e0255398.

Szpak, P. (2014). Complexities of nitrogen isotope biogeochemistry in plant-soil systems: implications for the study of ancient agricultural and animal management practices. *Front. Plant Sci.* **5**:.

Szpak, P. and Chiou, K. L. (2020). A comparison of nitrogen isotope compositions of charred and desiccated botanical remains from northern Peru. *Veg. Hist. Archaeobot.* **29**: 527–538.

Tejedor-Rodríguez, C., Moreno-García, M., Tornero, C., Hoffmann, A., García-Martínez de Lagrán, Í., Arcusa-Magallón, H., Garrido-Pena, R., Royo-Guillén, J. I., Díaz-Navarro, S., Peña-Chocarro, L., Alt, K. W. and Rojo-Guerra, M. (2021). Investigating Neolithic caprine husbandry in the Central Pyrenees: Insights from a multi-proxy study at Els Trocs cave (Bisaurri, Spain). *PLoS One* **16**: e0244139.

Teoh, M. L., Mcclure, S. B. and Podrug, E. (2014). Macroscopic, petrographic and XRD analysis of Middle Neolithic figulina pottery from central Dalmatia. *J. Archaeol. Sci.* **50**: 350–358.

Thimonier, J. (1981). Control of seasonal reproduction in sheep and goats by light and hormones. *J. Reprod. Fertil. Suppl. TA - TT* - **30**: 33–45.

Thomas, D. H. (2008). When should a forager farm? *Native American Landscapes of St. Catherines Island, Georgia, I. The Theoretical Framework*, American Museum of Natural History, pp.198–210.

Thomas, F. R. (2014). Shellfish Gathering and Conservation on Low Coral Islands: Kiribati Perspectives. *J. Isl. Coast. Archaeol.* **9**: 203–218.

Tieszen, L. L. (1991). Natural variations in the carbon isotope values of plants: Implications for archaeology, ecology, and paleoecology. *J. Archaeol. Sci.* **18**: 227–248.

Tieszen, L. L. and Fagre, T. (1993). Effect of Diet Quality and Composition on the Isotopic Composition of Respiratory CO2, Bone Collagen, Bioapatite, and Soft Tissues. *Prehistoric Human Bone*, Springer Berlin Heidelberg, Berlin, Heidelberg, pp.121–155.

Tinbergen, N. (1963). On aims and methods of Ethology. *ETH Zeitschrift für Tierpsychologie* **20**: 410–433.

Tishkoff, S. A., Reed, F. A., Ranciaro, A., Voight, B. F., Babbitt, C. C., Silverman, J. S., Powell, K., Mortensen, H. M., Hirbo, J. B., Osman, M., Ibrahim, M., Omar, S. A., Lema, G., Nyambo, T. B., Ghori, J., Bumpstead, S., Pritchard, J. K., Wray, G. A. and Deloukas, P. (2007). Convergent adaptation of human lactase persistence in Africa and Europe. *Nat. Genet.* **39**: 31–40.

Todaro, M., Dattena, M., Acciaioli, A., Bonanno, A., Bruni, G., Caroprese, M., Mele, M., Sevi, A. and Marinucci, M. T. (2015). Aseasonal sheep and goat milk production in the Mediterranean area: Physiological and technical insights. *Small Rumin. Res.* **126**: 59–66.

Tornero, C., Aguilera, M., Ferrio, J. P., Arcusa, H., Moreno-García, M., Garcia-Reig, S. and Rojo-Guerra, M. (2018). Vertical sheep mobility along the altitudinal gradient through stable isotope analyses in tooth molar bioapatite, meteoric water and pastures: A reference from the Ebro valley to the Central Pyrenees. *Quat. Int.* **484**: 94–106.

Tornero, C., Bălăşescu, A., Ughetto-Monfrin, J., Voinea, V. and Balasse, M. (2013). Seasonality and season of birth in early Eneolithic sheep from Cheia (Romania): methodological advances and implications for animal economy. *J. Archaeol. Sci.* **40**: 4039–4055.

Tornero, C., Balasse, M., Bréhard, S., Carrère, I., Fiorillo, D., Guilaine, J., Vigne, J.-D. and Manen, C. (2020). Early evidence of sheep lambing de-seasoning in the Western Mediterranean in the sixth millennium BCE. *Sci. Rep.* **10**: 12798.

Tornero, C., Balasse, M., Molist, M. and Saña, M. (2016). Seasonal reproductive patterns of early domestic sheep at Tell Halula (PPNB, Middle Euphrates Valley): Evidence from sequential oxygen isotope analyses of tooth enamel. *J. Archaeol. Sci. Reports* **6**: 810–818.

Trayler, R. B. and Kohn, M. J. (2017). Tooth enamel maturation reequilibrates oxygen isotope compositions and supports simple sampling methods. *Geochim. Cosmochim. Acta* **198**: 32–47.

Trueman, C. N., Privat, K. and Field, J. (2008). Why do crystallinity values fail to predict the extent of diagenetic alteration of bone mineral? *Palaeogeogr. Palaeoclimatol. Palaeoecol.* **266**: 160–167.

Tucker, B. (2006). A Future Discounting Explanation for the Persistence of a Mixed Foraging-Horticulture Strategy among the Mikea of Madagascar. In D. J. Kennett and B. Winterhalder (eds.), *Behavioral Ecology and the Transition to Agriculture*, University of California Press, Berkely and Los Angeles, pp.22–40.

Upex, B. and Dobney, K. (2012). Dental enamel hypoplasia as indicators of seasonal environmental and physiological impacts in modern sheep populations: a model for interpreting the zooarchaeological record. *J. Zool.* **287**: 259–268.

Upton, M. (1984). Models of improved production systems for small ruminants. In J. E. Sumberg and K. Cassaday (eds.), *Proceedings of the Workshop on Small Ruminant Production Systems in the Humid Zone of West Africa*, International Livestock Centre for Africa, Ibadan, Nigeria.

Valdivia, C., Dunn, E. G. and Jetté, C. (1996). Diversification as a Risk Management Strategy in an Andean Agropastoral Community. *Am. J. Agric. Econ.* **78**: 1329–1334.

VanDerwarker, A. M., Marcoux, J. B. and Hollenbach, K. D. (2013). Farming and Foraging at the Crossroads: The Consequences of Cherokee and European Interaction Through the Late Eighteenth Century. *Am. Antiq.* **78**: 68–88.

Varkuleviciute, K., Gron, K. J., Patterson, W. P., Panelli, C., Rossi, S., Timsic, S., Gröcke, D. R., Maggi, R. and Rowley-Conwy, P. (2021). Transhumance in the Early Neolithic? Carbon and oxygen isotope insights into sheep husbandry at Arene Candide, Northern Italy. *J. Archaeol. Sci. Reports* **40**: 103240.

van der Veen, M. (2005). Gardens and Fields: The Intensity and Scale of Food Production. *World Archaeol.* **37**: 157–163.

Ventresca Miller, A., Fernandes, R., Janzen, A., Nayak, A., Swift, J., Zech, J., Boivin, N. and Roberts, P. (2018). Sampling and Pretreatment of Tooth Enamel Carbonate for Stable Carbon and Oxygen Isotope Analysis. *JoVE* e58002.

Ventresca Miller, A. R., Bragina, T. M., Abil, Y. A., Rulyova, M. M. and Makarewicz, C. A. (2019). Pasture usage by ancient pastoralists in the northern Kazakh steppe informed by carbon and nitrogen isoscapes of contemporary floral biomes. *Archaeol. Anthropol. Sci.*

11: 2151–2166.

Ventresca Miller, A. R., Haruda, A., Varfolomeev, V., Goryachev, A. and Makarewicz, C. A. (2020). Close management of sheep in ancient Central Asia: evidence for foddering, transhumance, and extended lambing seasons during the Bronze and Iron Ages. *Sci. Technol. Archaeol. Res.* **6**: 41–60.

Verzijl, A. and Quispe, S. G. (2013). The System Nobody Sees: Irrigated Wetland Management and Alpaca Herding in the Peruvian Andes. *Mt. Res. Dev.* **33**: 280.

Vigne, J.-D., Briois, F., Zazzo, A., Willcox, G., Cucchi, T., Thiébault, S., Carrère, I., Franel, Y., Touquet, R., Martin, C., Moreau, C., Comby, C. and Guilaine, J. (2012). First wave of cultivators spread to Cyprus at least 10,600 y ago. *Proc. Natl. Acad. Sci.* **109**: 8445–8449.

Vigne, J.-D. and Helmer, D. (2007). Was milk a "secondary product" in the Old World Neolithisation process? Its role in the domestication of cattle, sheep and goats. *Anthropozoologica* **42**: 9–40.

Vinšćak, T. (1981). Transhumantno stočarstvo na Velebitu. *Etnoloki Pregl.* **18**: 101–105.

Vogel, J. C. (1978). Isotopic Assessment of the Dietary Habits of Ungulates. *S. Afr. J. Sci.* **74**: 298–301.

Vostrý, L. and Milerski, M. (2013). Genetic and non-genetic effects influencing lamb survivability in the Czech Republic. *Small Rumin. Res.* **113**: 47–54.

Vreča, P., Bronić, I. K., Horvatinčić, N. and Barešić, J. (2006). Isotopic characteristics of precipitation in Slovenia and Croatia: Comparison of continental and maritime stations. *J. Hydrol.* **330**: 457–469.

Vujević, D. and Horvat, K. (2012). Cultural Image of the Danilo Culture Settlement in Barice. *Archaeol. Adriat.* **6**: 31–65.

Walkden-Brown, S. W. and Restall, B. J. (1993). The male effect in the Australian Cashmere goat. 1. Ovarian and behavioural response of seasonally anovulatory does following the introduction of bucks. *Anim. Reprod. Sci.* **32**: 41–53.

Walker, J. (1994). Multispecies grazing: The ecological advantage. *Sheep Res. Journal, Spec. Issue* 52–64.

Walker, T. S. and Jodha, N. S. (1986). How Small Farm Households Adapt to Risk. In P. B. R. Hazell C. Pomareda and A. Valdés (eds.), *Crop Insurance for Agricultural Development: Issues and Experience*, The Johns Hopkins University Press, Baltimore and London, pp.17–34.

Watson, R. H. and Radford, H. M. (1960). The influence of rams on onset of oestrus in Merino ewes in the spring. *Aust. J. Agric. Res.* **11**: 65–71.

Weiner, S. and Bar-Yosef, O. (1990). States of preservation of bones from prehistoric sites in the Near East: A survey. *J. Archaeol. Sci.* **17**: 187–196.

Weinreb, M. M. and Sharav, Y. (1964). Tooth Development in Sheep. *Am. J. Vet. Res.* **25**: 891–908.

Welker, M. H., Zavodny, E., Podrug, E., Jović, J., Triozzi, N., Kennett, D. J. and McClure, S. B. (2022). A wolf in sheep's clothing: The development of livestock guarding dogs in the Adriatic region of Croatia. *J. Archaeol. Sci. Reports* **42**: 103380.

Weninger, B., Alram-Stern, E., Bauer, E., Clare, L., Danzeglocke, U., Jöris, O., Kubatzki, C., Rollefson, G., Todorova, H. and van Andel, T. (2006). Climate Forcing Due to the 8200 Cal yr BP Event Observed at Early Neolithic Sites in the Eastern Mediterranean. *Quat. Res.* **66**: 401–420.

Weninger, B., Clare, L., Gerritsen, F., Horejs, B., Krauß, R., Linstädter, J., Özbal, R. and Rohling, E. J. (2014). Neolithisation of the Aegean and Southeast Europe during the 6600–6000 calBC period of Rapid Climate Change. *Doc. Praehist.* **41**: 1–31.

Weninger, B., Clare, L., Rohling, E. J., Bar-Yosef, O., Böhner, U., Budja, M., Bundschuh, M., Feurdean, A., Gebel, H. G., Jöris, O., Linstädter, J., Mayewski, P., Mühlenbruch, T., Reingruber, A., Rollefson, G., Schyle, D., Thissen, L., Todorova, H. and Zielhofer, C. (2009). The Impact of Rapid Climate Change on prehistoric societies during the Holocene in the Eastern Mediterranean. *Doc. Praehist.* **36**: 7–59.

Westreicher, C. A., Mérega, J. L. and Palmili, G. (2007). The Economics of Pastoralism: Study on Current Practices in South America. *Nomad. People.* **11**: 87–105.

Wheeler, J. (1995). Evolution and present situation of the South American camelidae. *Biol. J. Linn. Soc.* **54**: 271–295.

Whitehouse, R. (1970). The Neolithic Pottery Sequence in Southern Italy. *Proc. Prehist. Soc.* **35**: 267–310.

Whittle, A., Bartosiewicz, L., Boric, D., Pettitt, P. and Richards, M. (2005). New radiocarbon dates for the Early Neolithic in Northern Serbia ans South-.East Hungary. *Antaeus* **028**: 347//355.

Wilson, B., Grigson, C. and Payne, S. (1982). *Ageing and sexing animal bones from archaeological sites*, B.A.R., Oxford, England SE - 268 pages : illustrations ; 30 cm.

Wilson, R. T. (1978). Livestock Production on Masai Group Ranches. *East African Agric. For. J.* **43**: 193–199.

Wilson, R. T. (1985). Livestock production in central Mali: Reproductive aspects of sedentary cows. *Anim. Reprod. Sci.* **9**: 1–9.

Wilson, R. T. (1989). Reproductive performance of African indigenous small ruminants under various management systems: a review. *Anim. Reprod. Sci.* **20**: 265–286.

Wilson, R. T. and Durkin, J. W. (1983). Livestock production in central Mali: weight at first conception and ages at first and second parturitions in traditionally managed goats and sheep. *J. Agric. Sci.* **100**: 625–628.

Wilson, R. T., Peacock, C. P. and Sayers, A. R. (1985). Pre-weaning mortality and productivity indices for goats and sheep on a Masai group ranch in south-central Kenya. *Anim. Sci.* **41**: 201–206.

Wilson, R. T., Peacock, C. and Sayers, A. R. (1984). Aspects of reproduction in goats and sheep in south-central Kenya. *Anim. Sci.* **38**: 463–467.

Winterhalder, B. (1986). Diet Choice, Risk, and Food Sharing in a Stochastic Environment. *J. Anthropol. Archaeol.* **5**: 369–392.

Winterhalder, B. (1990). Open field, common pot: Harvest variability and risk a voidance in agricultural and foraging societies. In E. A. Cashdan (ed.), *Risk and Uncertainty in Tribal and Peasant EconomiesTribal and Peasant Economies*, Westview Press, Boulder, CO, pp.67–87.

Winterhalder, B. and Goland, C. (1997). An evolutionary ecology perspective on diet choice, risk, and plant domestication. In K. J. Gremillion (ed.), *People, Plands, and Landscapes: Studies in Paleoethnobotany*, University of Alabama Press, Tuscaloosa, pp.123–160.

Winterhalder, B. and Kennett, D. J. (2006). Behavioral Ecology and the transition from huntering and gathering to agriculture. *Behav. Ecol. Transit. to Agric.* 1–21.

Winterhalder, B., Larsen, R. and Thomas, R. (1974). Dung as an essential resource in a highland Peruvian community. *An Interdiscip. J.* **2**: 89–104.

Winterhalder, B., Lu, F. and Tucker, B. (1999). Risk-Sensitive Adaptive Tactics : Models and Evidence from Subsistence Studies in Biology and Anthropology. *J. Archaeol. Res.* **7**: 301–348.

Winterhalder, B. and Smith, E. A. (2000). Analyzing adaptive strategies: Human behavioral ecology at twenty-five. *Evol. Anthropol. Issues, News, Rev.* **9**: 51–72.

Wunsam, S., Schmidt, R. and Müller, J. (1999). Holocene lake development of two Dalmatian lagoons (Malo and Veliko Jezero, Isle of Mljet) in respect to changes in Adriatic sea level and climate. *Palaeogeogr. Palaeoclimatol. Palaeoecol.* **146**: 251–281.

Yang, Q., Mu, H., Guo, J., Bao, X. and Martín, J. D. (2019). Temperature and rainfall amount effects on hydrogen and oxygen stable isotope in precipitation. *Quat. Int.* **519**: 25–31.

Yapi, C. V, Boylan, W. J. and Robinson, R. A. (1990). Factors associated with causes of preweaning lamb mortality. *Prev. Vet. Med.* **10**: 145–152.

Yeates, N. T. M. (1949). The breeding season of the sheep with particular reference to its modification by artificial means using light. *J. Agric. Sci.* **39**: 1–43.

Yurtsever, Y. and Gat, J. R. (1981). Atmospheric waters. In J. R. Gat and R. Gonfiantini (eds.), *Stable Isotope Hydrology*, IAEA Technical Report Series 210, pp.103–142.

Zavodny, E., Culleton, B. J., McClure, S. B., Kennett, D. J. and Balen, J. (2017). Minimizing risk on the margins: Insights on Iron Age agriculture from stable isotope analyses in central Croatia. *J. Anthropol. Archaeol.* **48**: 250–261.

Zavodny, E., McClure, S. B., Culleton, B. J., Podrug, E., Balen, J., Drnić, I. and Kennett, D. J. (2022). Investigating Past Livestock Mobility Using δ34S Stable Isotopes: Three Preliminary Case Studies From Prehistoric Croatia. *Open Quat.* **8**:.

Zavodny, E., McClure, S. B., Culleton, B. J., Podrug, E. and Kennett, D. J. (2014). Neolithic animal management practices and stable isotope studies in the Adriatic. *Environ. Archaeol.* **19**: 184–195.

Zavodny, E., McClure, S. B., Culleton, B. J., Podrug, E. and Kennett, D. J. (2015). Identifying neolithic animal management practices in the Adriatic using stable isotopes. *Doc. Praehistorica. Porocilo o raziskovanju Paleolit. Neolit. Eneolit. v Slov. Neolit. Stud. = Neolit. Stud.* **42**: 261–274.

Zavodny, E., Mcclure, S. B., Welker, M. H., Culleton, B. J., Balen, J. and Kennett, D. J. (2019). Scaling up : Stable isotope evidence for the intensification of animal husbandry in Bronze-Iron Age Lika, Croatia. *J. Archaeol. Sci. Reports* **23**: 1055–1065.

Zazzo, A., Balasse, M., Passey, B. H., Moloney, A. P., Monahan, F. J. and Schmidt, O. (2010). The isotope record of short- and long-term dietary changes in sheep tooth enamel: Implications for quantitative reconstruction of paleodiets. *Geochim. Cosmochim. Acta* **74**: 3571–3586.

Zazzo, A., Bendrey, R., Vella, D., Moloney, A. P., Monahan, F. J. and Schmidt, O. (2012). A refined sampling strategy for intra-tooth stable isotope analysis of mammalian enamel. *Geochim. Cosmochim. Acta* **84**: 1–13.

Zeder, M. (2006). Reconciling rates of long bone fusion and tooth eruption and wear in sheep (Ovis) and goat (capra). In D. Ruscillo (ed.), *Recent Advances in Ageing and Sexing Animal Bones. Proceedings of the 9th ICAZ Conference, Durham 2002*, pp.87–118.

Zeder, M. A. (2008). Domestication and early agriculture in the Mediterranean Basin: Origins, diffusion, and impact. *Proc. Natl. Acad. Sci.* **105**: 11597–11604.

Zeder, M. A. (2011). The Origins of Agriculture in the Near East. *Curr. Anthropol.* **52**: S221–S235.

Zeder, M. A. and Lapham, H. A. (2010). Assessing the reliability of criteria used to identify postcranial bones in sheep, Ovis, and goats, Capra. *J. Archaeol. Sci.* **37**: 2887–2905.

Zeder, M. A. and Pilaar, S. E. (2010). Assessing the reliability of criteria used to identify mandibles and mandibular teeth in sheep, Ovis, and goats, Capra. *J. Archaeol. Sci.* **37**: 225–242.

Zervas, G. (1998). Quantifying and optimizing grazing regimes in Greek mountain systems. *J. Appl. Ecol.* **35**: 983–986.

Zvelebil, M. (2001). The agricultural transition and the origins of Neolithic society in Europe. *Doc. Praehist.* **28**: 1–26.